
Evaluation of Macrotexture and Friction of Alternative Asphalt Surface Course Material



NCDOT Project 2024-12
FHWA/NC/2024-12
December 2024



B. Shane Underwood, Ph.D., et al.
Department of Civil, Construction, and
Environmental Engineering
North Carolina State University



**RESEARCH &
DEVELOPMENT**

This page is intentionally blank.

Technical Documentation Page

1. Report No. <i>FHWA/NC/2024-12</i>	2. Government Accession No. No	3. Recipient's Catalog No. ...	
4. Title and Subtitle Evaluation of Macrottexture and Friction of Alternative Asphalt Surface Course Material		5. Report Date December, 2024	
		6. Performing Organization Code	
7. Author(s) B. Shane Underwood, Ph.D., Cassie Castorena, Ph.D., Boris Goenaga, Ph.D., Jaime Preciado, and Paul Rogers, P.E.		8. Performing Organization Report No. None	
9. Performing Organization Name and Address Civil, Construction, and Environmental Engineering, North Carolina State University 915 Partners Way Raleigh NC 27606		10. Work Unit No. (TRAIS)	
		11. Contract or Grant No. NCDOT RP2024-12	
12. Sponsoring Agency Name and Address North Carolina Department of Transportation Research and Development Unit 104 Fayetteville Street Raleigh, North Carolina 27601		13. Type of Report and Period Covered August 1, 2023 – July 31, 2024	
		14. Sponsoring Agency Code NCDOT RP2024-12	
Supplementary Notes:			
16. Abstract Low macrottexture may contribute to reduced pavement skid resistance. Revising the existing North Carolina DOT (NCDOT) asphalt mixture categories to address these problems has some practical constraints due to contractor practices, familiarity with mixture designs, and unintended consequences to durability. On the other hand, a preliminary evaluation of the surface mixture guidelines used in neighboring states shows important differences with the NCDOT current practice. This study was instigated to evaluate and understand the effectiveness of these alternative surface course materials, namely stone matrix asphalt (SMA) and microsurfacing, but others as well. There are two primary goals of the research reported herein; 1) characterizing friction and texture performance of alternative surface mixtures designs from other states and 2) identifying alternative structural mixture designs that could be used in North Carolina. A set of pavements with different traffic volumes, ages, and spatial locations were selected from two neighboring states. On each pavement, friction and texture observations were collected and these observations were used to update the model coefficients of the performance models proposed in the FHWA/NC 2022-5 project. Additionally, the crash history of each pavement was collected and a 'before-after' safety evaluation was conducted to compare the safety performance of the alternative surface course materials with respect to the performance of pavements using only dense-graded surface course materials. For this evaluation, the pavements selected have the same surface type in the 'before' and 'after' periods. The 'after' period crash frequency was compared with the frequency in the 'before' period by computing the % <i>change</i> , defined as the percent difference in the number of crashes in the 'after' period with respect to the crashes in the 'before' period. The surfaces that were evaluated in this work seem to experience lower crash frequencies than the pavements with a normal dense-graded surface mixture. Finally, if one considers the traffic exposure, then the surface type with the lowest crash rates are the SMA mixtures. However, the microsurfacing was the surface type with the lowest 'after' crash rate. A performance evaluation of SMAs used in two neighboring states compared to North Carolina's dense-graded mixtures was conducted through linear viscoelastic characterization and pavement performance simulations. The results showed that SMAs have cracking performance most similar to North Carolina's B and C mixes, but are softer and more viscous (higher phase angle) than the D mixes. They also exhibit superior resistance to permanent deformation compared to B and C designs, but lower resistance than D designs. Lastly, a life-cycle cost analysis was conducted. The investment was defined as the additional cost required to build a specific surface treatment compared to constructing a pavement with a regular dense-graded surface. The crash cost reductions expected from the reduction in crash rates were computed and the analysis indicated that crash cost reductions of the alternative surface studied were greater than the investments. While this analysis provides a preliminary estimate of the viability of the alternative surface course materials, there are many factors, including engineering familiarity with the techniques, user cost impacts, material supply limitations, and others that the cost analysis could not fully account for.			
17. Key Words Pavement friction, macrottexture, highway safety, surface treatments, rehabilitation		18. Distribution Statement	
19. Security Classif. (of this report) Unclassified	20. Security Classif. (of this page) Unclassified	21. No. of Pages 260	22. Price

Disclaimer

The contents of this report reflect the views of the author who is responsible for the facts and the accuracy of the data presented herein. The contents of the report do not reflect the official views or policies of the North Carolina Department of Transportation. This report does not constitute a standard, specification, or regulation.”

Acknowledgments

The research team would like to express their gratitude and appreciation to the North Carolina Department of Transportation (NCDOT) for the provided funding needed to conclude this research study.

TABLE OF CONTENTS

Table of Contents	i
List of Figures	iii
List of Tables	ix
Executive Summary	1
1. Introduction.....	3
1.1. Overview.....	3
1.2. Connection of the Research to Previous Efforts	3
1.3. Status of the Literature.....	4
1.3.1. Asphalt Mixture Design for Improved Surface Characteristics.....	5
1.3.2. Ultrathin Bounded Wearing Course (UTBWC).....	6
1.3.3. Open-Graded Friction Course (OGFC).....	6
1.3.4. Stone Matrix Asphalt (SMA).....	6
1.3.5. Other Treatment Types	7
1.3.6. Knowledge Gaps and Conclusions	8
1.4. Report Organization.....	8
2. Data Processing.....	9
2.1. Friction and Texture Measurements	10
2.1.1. Equipment.....	10
2.1.2. Representative Friction and Texture Values.....	11
2.2. Crash Information	14
3. Pavement Friction and Texture Performance Modeling.....	15
3.1. Friction.....	15
3.1.1. Friction in RWP at 40-mph.....	17
3.1.2. Friction in RWP at 60-mph.....	17
3.2. Calibration of Friction Performance Models.....	17
3.2.1. Friction Performance Models in FHWA/NC 2022-5.....	17
3.2.2. Updated Friction Performance Models for Alternative Surfaces.....	19
3.3. Macrotexture.....	23
3.3.1. High-Speed Texture – RWP	23
3.3.2. Static Measurements	25
3.4. Calibration of Texture Performance Models	25
3.4.1. Texture Performance Models in FHWA/NC 2022-5.....	25
3.4.2. Updated Texture Performance Models for Alternative Surfaces.....	26
3.5. Future work.....	31
3.6. Conclusions.....	31
4. Performance Comparison of Alternative Surface Treatments	33
4.1. Overview.....	33
4.2. Experimental test results.....	33
4.2.1. Dynamic Modulus Test Results	33
4.2.2. Uniaxial Cyclic Fatigue Test Results.....	35
4.2.3. IDT-CT Results.....	36
4.2.4. Stress Sweep Rutting Test Results.....	37
4.3. Pavement Performance Simulations	38
4.4. Conclusions.....	41

5. Evaluation of the Effect of Alternative Asphalt Surfaces on Safety	43
5.1. Methodology	44
5.1.1. Analysis 1: Aggregated Crash Analysis	44
5.1.2. Analysis 2: Individual Crash Analysis	45
5.1.3. Analysis 3: ‘Before’ and ‘After’ Crash Rate Comparison	45
5.2. Results	45
5.2.1. Aggregated Crash Analysis	45
5.2.2. Individual Crash Analysis	47
5.2.3. ‘Before’ and ‘After’ Crash Rate Comparison	49
5.3. Conclusions	49
6. Life-cycle Cost Comparison	51
6.1. Methodology	51
6.2. Conclusions	53
6.3. Limitations	54
7. Conclusions and Recommendations	57
7.1. Conclusions	57
7.2. Recommendations	58
7.2.1. Pavement Friction Management Program Recommendations	58
7.2.2. Future Research Recommendations	58
8. Implementation and Technology Transfer Plan	59
9. References	61
Appendix A. Detailed Literature Review	69
Appendix B. Friction and Texture Measurements – Complementary Analysis	115
Appendix C. Performance Models Calibration Details	117
Appendix D. Static Texture Measurements	136
Appendix E. Specification Draft for the Implementation of SMA Surface Mix in North Carolina	184
Appendix F. Supplementary Information on Asphalt Concrete Experiments and Analyses	193
Appendix G. Supplementary Information on Pavement Simulations	202
Appendix H. Supplementary Information on Life-Cycle Cost Analysis	210

LIST OF FIGURES

Figure 1. Including friction in the mix design.	5
Figure 2. Data inventory for the research project.	9
Figure 3. Example of the friction measurement processing collected in: (a) RWP at 40-mph, (b) RWP at 60-mph, and (c) CL at 60-mph. The site shown is a Dense-I surface type.	12
Figure 4. Example of the <i>MPD</i> measurement processing collected in: (a) RWP and (b) CL. The site shown is a Dense-I surface type.	12
Figure 5. Distribution of the friction measurements made in the RWP at 40-mph for each surface type.	15
Figure 6. Distribution of the friction measurements made in the RWP at 60-mph for each surface type.	16
Figure 7. Graphical comparison of the friction performance models.	21
Figure 8. Points in time at which the OGFC reaches the Non-Interchange investigatory threshold.	23
Figure 9. Distribution of the <i>MPD</i> measurements made in the RWP for each surface type.	24
Figure 10. OGFCs proposed <i>MPD</i> performance curve (Co: Coastal, Pi: Piedmont, Mo: Mountains).	28
Figure 11. OGFCs proposed <i>MPD</i> performance curve when the AADT = 5,000 vpd (Co: Coastal, Pi: Piedmont, Mo: Mountains).	28
Figure 12. Number of years required to reach the texture investigatory threshold for: (a) sites in the coastal plain region and (b) sites in the piedmont and mountains.	29
Figure 13. Dynamic modulus and phase angle results for SMAs and surface mixtures from the NC Piedmont region: (a) dynamic modulus master curve log-log plot, (b) dynamic modulus master curve semi-log plot, and (c) phase angle master curve.	35
Figure 14. Cyclic fatigue test results for SMAs and surface mixtures: (a) damage characteristic curve, (b) failure criteria plot, and (c) S_{app} results.	36
Figure 15. IDT-CT test results for SMAs and surface mixtures from the NC Piedmont region. The asterisk denotes the mixtures evaluated in the FHWA/NC 2023-3 project. The error bars indicate CT_{Index} variability plus/minus one standard deviation.	37
Figure 16. SSR test results for SMAs and surface mixtures from the NC Piedmont region: (a) ϵ_{vp} at 29°C, (b) ϵ_{vp} at 51°C, and (c) RSI results for Garner (NC).	38
Figure 17. Pavement performance simulation results for NC Piedmont region and ABC structures: (a) total percent damage - thin structure, (b) total rutting - thin structure, (c) total percent damage - intermediate structure, (d) total rutting damage – intermediate structure, (e) total percent damage – thick structure, and (f) total rutting – thick structure.	40
Figure 18. Example of life extension for Intermediate-DS structure using an SMA as a surface layer: (a) SMA-1A and (b) SMA-3.	41
Figure 19. Graphic comparison of the ‘before’ and ‘after’ crashes/month/mile.	47
Figure 20. Summary of the % <i>change</i> computed for individual sites.	47
Figure 21. Summary of the number of crashes/month/mile in the ‘before’ and ‘after’ period.	48
Figure 22. Summary of the crash rates in the ‘before’ and ‘after’ period.	49
Figure 23. Life-cycle costs input.	51
Figure A-1. Maximum density lines on FHWA 0.45 power gradation curves.	70
Figure A-2. Gradation Control Zone of different NMA: (a) NMA = 25.0 mm, (b) NMA = 19.0 mm, (c) NMA = 12.5 mm, and (d) NMA = 9.5 mm.	71

Figure A-3. Variation of the percent passing Sieve #8 (2.36 mm) in 9.5 mm mixes used by KTDOT.....	78
Figure A-4. Comparison of the different state requirements on the percent passing Sieve #8 (2.36 mm).....	83
Figure A-5. Comparison of the number of gyrations (N_d).....	83
Figure A-6. Comparison of the VFA.....	84
Figure A-7. Comparison of the VMA.....	84
Figure A-8. SMA usage in the United States (11).....	85
Figure A-9. The structure of SMA versus conventional HMA (54).....	87
Figure A-10. Percent passing limits in Sieve #4 (4.75 mm) for SMA mixtures: (a) 9.5 mm and (b) 12.5 mm NMAS.....	90
Figure A-11. Percent passing limits in Sieve #8 (2.36 mm) for SMA mixtures: (a) 9.5 mm and (b) 12.5 mm NMAS.....	90
Figure A-12. A schematic of UTBWC (59).....	91
Figure A-13. Comparison of the percent passing Sieve #4 (4.75 mm) for UTBWC mixes: (a) 9.5 mm and (b) 12.5 mm.....	95
Figure A-14. Comparison of the percent passing Sieve #8 (2.36 mm) for UTBWC mixes: (a) 9.5 mm and (b) 12.5 mm.....	95
Figure A-15. OGFC mean texture depth comparison; where, E9A: 9.5 mm OGFC; E9B: 12.5 mm OGFC with synthetic fiber; E10: 12.5 mm GTR modified OGFC mix (65).....	97
Figure A-16. Comparison of the percent passing by sieves: (a) 4.75 mm and (b) 2.36 mm.	99
Figure A-17. Method for obtaining OAC for Microsurfacing mixtures.....	106
Figure A-18. (a) Single layer and (b) double layer chip seal application scheme (5).	108
Figure A-19. North Carolina's surface mix gradations.	111
Figure A-20. Distribution of the counties where the mix is produced.....	112
Figure A-21. Distribution of 12.5 mm Superpave mix that were received and approved by the NCDOT during years 2011-2017.....	112
Figure B-1. Distribution of the friction measurements made in the CL at 60-mph for each surface type.....	115
Figure B-2. Distribution of the <i>MPD</i> measurements made in the CL for each surface type.....	116
Figure C-1. Variation of OGFC friction values at 60-mph with respect to: (a) age and (b) cumulative traffic.....	117
Figure C-2. Variation of UTBWC friction values at 60-mph with respect to: (a) age and (b) cumulative traffic.....	118
Figure C-3. Variation of North Carolina's Microsurfacing friction values at 60-mph with respect to: (a) age and (b) cumulative traffic.	119
Figure C-4. Variation of Microsurfacing-Alt friction values at 60-mph with respect to: (a) age and (b) cumulative traffic.....	120
Figure C-5. Variation of the Dense-I/II friction values at 60-mph with respect to: (a) age and (b) cumulative traffic.....	120
Figure C-6. Variation of the SMA-1 friction values at 60-mph with respect to: (a) age and (b) cumulative traffic.....	121
Figure C-7. Variation of the SMA-2 friction values at 60-mph with respect to: (a) age and (b) cumulative traffic.....	122
Figure C-8. Variation of the SMA-3A friction values at 60-mph with respect to: (a) age and (b) cumulative traffic.....	123

Figure C-9. Variation of OGFC <i>MPD</i> values in the RWP with respect to: (a) age and (b) cumulative traffic.	124
Figure C-10. Calibration of texture performance model for the OGFCs in the Coastal climate region.	125
Figure C-11. Calibration of texture performance model for the OGFCs in the Piedmont climate region.	126
Figure C-12. Calibration of texture performance model for the OGFCs in the Mountains climate region.	126
Figure C-13. OGFC performance models graphical comparison.	127
Figure C-14. Variation of UTBWC <i>MPD</i> values in the RWP with respect to: (a) age and (b) cumulative traffic.	127
Figure C-15. Calibration of texture performance model for the UTBWCs in the Coastal climate region.	128
Figure C-16. Calibration of texture performance model for the UTBWCs in the Piedmont climate region.	129
Figure C-17. Calibration of texture performance model for the UTBWCs in the Mountains climate region.	129
Figure C-18. UTBWC performance models graphical comparison.	130
Figure C-19. Variation of North Carolina’s Microsurfacing <i>MPD</i> values with respect to: (a) age and (b) cumulative traffic.	130
Figure C-20. Variation of Microsurfacing-Alt <i>MPD</i> values with respect to: (a) age and (b) cumulative traffic.	131
Figure C-21. Variation of Dense-I/II <i>MPD</i> values with respect to: (a) age and (b) cumulative traffic.	131
Figure C-22. Dense I/II and Microsurfacing performance models graphical comparison.	132
Figure C-23. Variation of SMA-1 <i>MPD</i> values with respect to: (a) age and (b) cumulative traffic.	133
Figure C-24. Variation of SMA-2 <i>MPD</i> values with respect to: (a) age and (b) cumulative traffic.	133
Figure C-25. Variation of the SMA-3A <i>MPD</i> values with respect to: (a) age and (b) cumulative traffic.	134
Figure C-26. SMA performance models graphical comparison.	135
Figure D-1. Average <i>MPD</i> of the surface scans for North Carolina’s Microsurfacing.	136
Figure D-2. Average <i>MPD</i> of the surface scans for North Carolina’s OGFC.	136
Figure D-3. Average <i>MPD</i> of the surface scans for Dense-II.	137
Figure D-4. Average <i>MPD</i> of the surface scans for SMA-2 and SMA-1.	137
Figure D-5. Average <i>MPD</i> of the surface scans for the Microsurfacing-Alt.	137
Figure D-6. Average <i>RMSD</i> of the surface scans for North Carolina’s Microsurfacing.	138
Figure D-7. Average <i>RMSD</i> of the surface scans for North Carolina’s OGFC.	138
Figure D-8. Average <i>RMSD</i> of the surface scans for Dense-II.	139
Figure D-9. Average <i>RMSD</i> of the surface scans for SMA-2 and SMA-1.	139
Figure D-10. Average <i>RMSD</i> of the surface scans for the Microsurfacing-Alt.	139
Figure D-11. Average <i>Rsk</i> of the surface scans for North Carolina’s Microsurfacing.	140
Figure D-12. Average <i>Rsk</i> of the surface scans for North Carolina’s OGFC.	140
Figure D-13. Average <i>Rsk</i> of the surface scans for Dense-II.	141
Figure D-14. Average <i>Rsk</i> of the surface scans for SMA-2 and SMA-1.	141

Figure D-15. Average <i>Rsk</i> of the surface scans for the Microsurfacing-Alt.	141
Figure D-16. Average <i>Rku</i> of the surface scans for North Carolina’s Microsurfacing.	142
Figure D-17. Average <i>Rku</i> of the surface scans for North Carolina’s OGFC.	142
Figure D-18. Average <i>Rku</i> of the surface scans for Dense-II.	142
Figure D-19. Average <i>Rku</i> of the surface scans for SMA-2 and SMA-1.	143
Figure D-20. Average <i>Rku</i> of the surface scans for the Microsurfacing-Alt.	143
Figure D-21. Microsurfacing surface scan 1.....	144
Figure D-22. Microsurfacing surface scan 2.....	144
Figure D-23. Microsurfacing surface scan 3.....	145
Figure D-24. Microsurfacing surface scan 4.....	145
Figure D-25. Microsurfacing surface scan 5.....	146
Figure D-26. Microsurfacing surface scan 6.....	146
Figure D-27. Microsurfacing surface scan 7.....	147
Figure D-28. Microsurfacing surface scan 8.....	147
Figure D-29. Microsurfacing surface scan 9.....	148
Figure D-30. Microsurfacing surface scan 10.....	148
Figure D-31. Microsurfacing surface scan 11.....	149
Figure D-32. Microsurfacing surface scan 12.....	149
Figure D-33. Microsurfacing surface scan 13.....	150
Figure D-34. Microsurfacing surface scan 14.....	150
Figure D-35. Microsurfacing surface scan 15.....	151
Figure D-36. Microsurfacing surface scan 16.....	151
Figure D-37. Microsurfacing surface scan 17.....	152
Figure D-38. Microsurfacing surface scan 18.....	152
Figure D-39. Microsurfacing surface scan 19.....	153
Figure D-40. OGFC surface scan 21.....	153
Figure D-41. OGFC surface scan 22.....	154
Figure D-42. OGFC surface scan 23.....	154
Figure D-43. OGFC surface scan 24.....	155
Figure D-44. OGFC surface scan 25.....	155
Figure D-45. OGFC surface scan 26.....	156
Figure D-46. OGFC surface scan 27.....	156
Figure D-47. OGFC surface scan 28.....	157
Figure D-48. OGFC surface scan 29.....	157
Figure D-49. OGFC surface scan 30.....	158
Figure D-50. OGFC surface scan 31.....	158
Figure D-51. OGFC surface scan 32.....	159
Figure D-52. OGFC surface scan 33.....	159
Figure D-53. OGFC surface scan 34.....	160
Figure D-54. OGFC surface scan 35.....	160
Figure D-55. OGFC surface scan 36.....	161
Figure D-56. OGFC surface scan 37.....	161
Figure D-57. OGFC surface scan 38.....	162
Figure D-58. OGFC surface scan 39.....	162
Figure D-59. OGFC surface scan 40.....	163
Figure D-60. OGFC surface scan 41.....	163

Figure D-61. OGFC surface scan 42.....	164
Figure D-62. Dense-II surface scan 44.	164
Figure D-63. Dense-II surface scan 45.	165
Figure D-64. Dense-II surface scan 46.	165
Figure D-65. Dense-II surface scan 47.	166
Figure D-66. Dense-II surface scan 48.	166
Figure D-67. Dense-II surface scan 49.	167
Figure D-68. Dense-II surface scan 50.	167
Figure D-69. Dense-II surface scan 51.	168
Figure D-70. Dense-II surface scan 52.	168
Figure D-71. Dense-II surface scan 53.	169
Figure D-72. Dense-II surface scan 54.	169
Figure D-73. Dense-II surface scan 55.	170
Figure D-74. Dense-II surface scan 56.	170
Figure D-75. Dense-II surface scan 57.	171
Figure D-76. Dense-II surface scan 58.	171
Figure D-77. Dense-II surface scan 59.	172
Figure D-78. SMA-2B surface scan 61.....	172
Figure D-79. SMA-2B surface scan 62.....	173
Figure D-80. SMA-2B surface scan 63.....	173
Figure D-81. SMA-2B surface scan 64.....	174
Figure D-82. SMA-2A surface scan 66.	174
Figure D-83. SMA-2A surface scan 67.	175
Figure D-84. SMA-2A surface scan 68.	175
Figure D-85. SMA-2A surface scan 69.	176
Figure D-86. SMA-1B surface scan 71.....	176
Figure D-87. SMA-1B surface scan 72.....	177
Figure D-88. SMA-1B surface scan 73.....	177
Figure D-89. SMA-1B surface scan 74.....	178
Figure D-90. Microsurfacing-Alt surface scan 76.	178
Figure D-91. Microsurfacing-Alt surface scan 77.	179
Figure D-92. Microsurfacing-Alt surface scan 78.	179
Figure D-93. Microsurfacing-Alt surface scan 79.	180
Figure D-94. Microsurfacing-Alt surface scan 80.	180
Figure D-95. Microsurfacing-Alt surface scan 81.	181
Figure D-96. Microsurfacing-Alt surface scan 82.	181
Figure D-97. Microsurfacing-Alt surface scan 83.	182
Figure D-98. Microsurfacing-Alt surface scan 84.	182
Figure D-99. Microsurfacing-Alt surface scan 85.	183
Figure F-2. Dynamic modulus and phase angle results for SMAs and surface mixtures from the Mountain region: (a) dynamic modulus master curve log-log plot, (b) dynamic modulus master curve semi-log plot, and (c) phase angle master curve.	197
Figure F-3. Cyclic fatigue test results for SMAs and surface mixtures: (a) damage characteristic curve for Coastal region, (b) failure criteria plot for Coastal region, (c) damage characteristic curve for Mountain region, and (d) failure criteria plot for Mountain region.	198
Figure F-4. RSI results for SMA and dense-graded mixtures.	200

Figure G-2. Pavement performance simulation results for NC Piedmont region and DS structures: (a) total percent damage - thin structure, (b) total rutting - thin structure, (c) total percent damage - intermediate structure, (d) total rutting damage – intermediate structure, (e) total percent damage – thick structure, and (f) total rutting – thick structure.....	203
Figure G-3. Pavement performance simulation results for NC Coastal region and FDA structures: (a) total percent damage - thin structure, (b) total rutting - thin structure, (c) total percent damage - intermediate structure, (d) total rutting damage – intermediate structure, (e) total percent damage – thick structure, and (f) total rutting – thick structure.....	204
Figure G-4. Pavement performance simulation results for NC Coastal region and ABC structures: (a) total percent damage - thin structure, (b) total rutting - thin structure, (c) total percent damage - intermediate structure, (d) total rutting damage – intermediate structure, (e) total percent damage – thick structure, and (f) total rutting – thick structure.....	205
Figure G-5. Pavement performance simulation results for NC Coastal region and DS structures: (a) total percent damage - thin structure, (b) total rutting - thin structure, (c) total percent damage - intermediate structure, (d) total rutting damage – intermediate structure, (e) total percent damage – thick structure, and (f) total rutting – thick structure.....	206
Figure G-6. Pavement performance simulation results for NC Mountain region and FDA structures: (a) total percent damage - thin structure, (b) total rutting - thin structure, (c) total percent damage - intermediate structure, (d) total rutting damage – intermediate structure, (e) total percent damage – thick structure, and (f) total rutting – thick structure.....	207
Figure G-7. Pavement performance simulation results for NC Mountain region and ABC structures: (a) total percent damage - thin structure, (b) total rutting - thin structure, (c) total percent damage - intermediate structure, (d) total rutting damage – intermediate structure, (e) total percent damage – thick structure, and (f) total rutting – thick structure.....	208
Figure G-8. Pavement performance simulation results for NC Mountain region and DS structures: (a) total percent damage - thin structure, (b) total rutting - thin structure, (c) total percent damage - intermediate structure, (d) total rutting damage – intermediate structure, (e) total percent damage – thick structure, and (f) total rutting – thick structure.....	209
Figure H-1. Crash risk – friction relationship.....	224
Figure H-2. Crash risk – MPD relationship.....	225

LIST OF TABLES

Table 1. Total number of sites available for analysis in North Carolina.	10
Table 2. Number of sites studied in neighboring states.	10
Table 3. Summary of the site characteristics tested in all the research efforts.	13
Table 4. Summary of the number of friction and texture measurements collected in all the research efforts.	14
Table 5. Number of 3D surface scans collected for this project.	14
Table 6. Recommended friction investigatory and intervention thresholds.	16
Table 7. Summary of friction statistics computed for each surface type.	16
Table 8. Average value of the parameters of the friction model for each surface type.	19
Table 9. Friction model coefficients for alternative surfaces.	20
Table 10. AADT and age of the sites used to update the friction model coefficients.	20
Table 11. Estimated number of years needed to reach the investigatory friction Non-Interchange investigatory threshold when friction is increasing.	22
Table 12. Estimated number of years needed to reach the investigatory friction Non-Interchange investigatory threshold when friction is decreasing.	22
Table 13. Recommended <i>MPD</i> investigatory and intervention thresholds.	24
Table 14. Summary of <i>MPD</i> statistics computed for each surface type.	24
Table 15. Random effect coefficients for the <i>MPD</i> rate of change.	26
Table 16. The average value of the intercept random effect coefficient.	26
Table 17. Texture model coefficients for alternative surfaces.	27
Table 18. Estimated number of years needed to reach the investigatory texture threshold.	30
Table 19. Mix design information of SMAs and surface mixtures evaluated in FHWA/NC 2019-20.	34
Table 20. Matrix of performance simulation inputs.	39
Table 21. Pavement structures used in performance simulations.	39
Table 22. Summary of the aggregated crash analysis.	46
Table 23. Maintenance schedule defined for dense-graded surfaces.	52
Table A-1. Aggregate gradation control points.	71
Table A-2. Gradation classification.	72
Table A-3. Summary of the NCDOT mixture designs and volumetric factors in 2012 (48).	73
Table A-4. NCDOT aggregate gradation criteria in 2012 Specifications (48).	73
Table A-5. Summary of the NCDOT mixture designs and volumetric factors in 2016 (49).	73
Table A-6. NCDOT aggregate gradation criteria in 2016 specifications (49).	74
Table A-7. Summary of NCDOT mixture designs and volumetric factors for 2018-2023 (50, 51).	74
Table A-8. NCDOT aggregate gradation criteria for 2018-2023 specifications (50, 51).	74
Table A-9. Mix designation for flexible pavements in Virginia.	75
Table A-10. Specialized pavement locations.	75
Table A-11. Percentage by weight passing sieve sizes.	75
Table A-12. VDOT VMA and VFA requirements for Superpave mixtures.	75
Table A-13. GDOT gradation limits (% passing) for Superpave mixes.	76
Table A-14. GDOT VMA criteria for Superpave mixes.	76
Table A-15. GDOT VFA criteria for Superpave mixes.	76
Table A-16. SCDOT gradation and design requirements for Superpave mixes.	77

Table A-17. TDOT gradation criteria for Superpave mixes.	77
Table A-18. TDOT criteria for mineral aggregate and asphalt cement proportions.	78
Table A-19. KTDOT traffic categorization for pavement design.	78
Table A-20. ALDOT criteria for gradations for Superpave mixes.	79
Table A-21. ALDOT criteria voids in mineral aggregate (VMA) specifications.	79
Table A-22. ALDOT criteria for asphalt binder content (AC%).	79
Table A-23. Gradation specifications for Superpave mixtures.	81
Table A-24. AASHTO M325-18 SMA Coarse Aggregate quality Requirements.	86
Table A-25. SMA Mixture Design Procedures for state DOTs (10, 11).	87
Table A-26. Gradation specification for SMA design for state DOTs.	89
Table A-27. UTBWC mix design specification for state DOTs.	94
Table A-28. FHWA gradation specifications for OGFC mixes (70).	97
Table A-29. NCDOT OGFC gradation criteria (NCDOT 2012 specifications, Table 650-1).	98
Table A-30. NCDOT OGFC mix design criteria (NCDOT 2012 specifications, Table 650-2)...	98
Table A-31. OGFC mix design specifications for state DOTs (68).	100
Table A-32. Friction for different aggregate types used in HFST (77).	102
Table A-33. Physical property requirements for HFST resin binder materials (78).	103
Table A-34. Physical property requirements for HFST aggregate materials (78).	104
Table A-35. Friction metrics used by State DOTs for quality assurance of HFST (80).	104
Table A-36. Microsurfacing aggregate gradations requirements (25, 95–97).	107
Table A-37. Tolerance limits for aggregate gradation (25, 95–97).	107
Table A-38. Tolerance limits for residual asphalt content.	107
Table A-39. Summary of the pros and cons of alternative surface treatments.	109
Table C-1. Updated friction model coefficients for the OGFCs.	118
Table C-2. Updated friction model coefficients for the UTBWCs.	119
Table C-3. Microsurfacing friction model coefficients.	120
Table C-4. Updated friction model coefficients for the Dense-I/II.	121
Table C-5. Updated friction model coefficients for the SMA-1.	122
Table C-6. Updated friction model coefficients for the SMA-2.	123
Table C-7. Texture model coefficients for OGFC surfaces.	125
Table C-8. Texture model coefficients for UTBWC surfaces.	128
Table C-9. Texture model coefficients for Microsurfacing.	131
Table C-10. Texture model coefficients for Dense-I/II.	132
Table C-11. Texture model coefficients for SMA-1.	133
Table C-12. Texture model coefficients for SMA-2.	134
Table C-13. Texture model coefficients for SMA-3A.	134
Table F-2. Dynamic modulus results.	196
Table F-3. Dynamic modulus results.	197
Table F-4. Linear viscoelastic and FlexPAVE™ S-VECD fatigue properties.	198
Table F-5. Detailed IDT-CT results.	199
Table F-6. Corrected CT_{Index} values.	199
Table F-8. Life extension of the SMA-1 versus RS9.5D.	201
Table H-5. Maintenance schedule defined for Microsurfacing-NC.	217
Table H-6. Maintenance schedule defined for Microsurfacing-Alt.	218
Table H-7. Material density used for unit cost calculation.	219
Table H-8. Unit cost as reported by the two neighboring states websites.	219

Table H-9. Material cost used for the life-cycle cost analysis.....	219
Table H-10. Summary of the maintenance cost NPV in 100,000 USD for a discount rate of 0.5%.	220
Table H-11. Summary of the maintenance cost NPV in 100,000 USD for a discount rate of 3.0%.	221
Table H-12. Summary of the maintenance cost NPV in 100,000 USD for a discount rate of 5.0%.	222
Table H-13. Summary of the maintenance cost NPV in 100,000 USD for a discount rate of 7.0%.	223
Table H-14. Parameters of the crash risk – friction relationship.	224
Table H-16. Summary of the Crash Cost NPV in 100,000 USD for North Carolina dense graded surface (Dense-NC).	226
Table H-17. Summary of the Crash Cost NPV in 100,000 USD for SMA-1.....	227
Table H-18. Summary of the Crash Cost NPV in 100,000 USD for SMA-3.....	228
Table H-19. Summary of the Crash Cost NPV in 100,000 USD for OGFC.	229
Table H-20. Summary of the Crash Cost NPV in 100,000 USD for UTBWC.....	230
Table H-21. Summary of the Crash Cost NPV in 100,000 USD for Microsurfacing-NC.	231
Table H-22. Summary of the Crash Cost NPV in 100,000 USD for Microsurfacing-Alt.....	232

This page is intentionally blank

EXECUTIVE SUMMARY

This research has built upon the work conducted under research projects FHWA/NC 2017-2, FHWA/NC 2020-11, and FHWA/NC 2022-5. The main goal of the current research is to identify alternative surface mixture designs that could be specified to ensure adequate friction and macrotexture in North Carolina. The alternative surface mixtures and treatments (hereafter referred to simply as surface treatments) included stone matrix asphalt (SMA) and microsurfacing. The former is not used in North Carolina, but the latter has been applied in specific locations to address skid resistance-related issues, though its effectiveness on high-speed facilities has not been evaluated. Two neighboring states were selected, and a set of pavements with varying ages, traffic volumes, and spatial locations, featuring either SMA or microsurfacing, were identified. For each pavement, friction and macrotexture measurements were collected. These observations were used to calibrate the model coefficients of the performance models proposed in the FHWA/NC 2022-5 research project for SMA and microsurfacing. Additionally, the dataset created in the FHWA/NC 2022-5 project for open-graded friction course (OGFC) and ultra-thin bonded wearing course (UTBWC) was expanded to include new sites with varying surface ages and locations in additional administrative divisions, thereby updating the model coefficients of the performance models.

The analysis confirmed the FHWA/NC 2022-5 project's hypothesis that site-specific models are needed to capture friction and texture performance variability. Further, the analysis provided initial estimates for various surface types and climate regions. Results showed that North Carolina microsurfacing surfaces generally have high friction and texture, with friction consistently above the investigatory threshold values proposed in FHWA/NC 2022-5, although macrotexture decreases with time. The dense-graded surfaces from neighboring states performed similarly to North Carolina's dense-graded surfaces but had higher macrotexture and exceeded the investigatory threshold more quickly. This study included SMA surfaces from two neighboring states and most were found to lie above the preliminary investigatory thresholds.

Loose SMA plant-mixed material was sampled from the two neighboring states. The samples were used to conduct a performance evaluation of the SMAs with respect to North Carolina's dense-graded mixtures. The evaluation consisted of linear viscoelastic characterization using the dynamic modulus test, cracking characterization using the uniaxial cyclic fatigue test and the indirect tensile asphalt cracking test (IDT-CT), and rutting characterization using the stress sweep rutting test. Additionally, pavement simulations were conducted using FlexPAVE v.2.2 to evaluate the potential differences in performance when using SMA designs from the neighboring states as surface mixtures in pavement structures in North Carolina.

The mixture-level assessment revealed that both SMA mixtures exhibit linear viscoelastic behavior like North Carolina's B and C mixes but are softer and more viscous (higher phase angle) than the D mix. Fatigue cracking performance via the cyclic fatigue test varied with one SMA showing better and another showing slightly worse performance than the D mixes. The IDT-CT tests rated the SMA better than the D mix. The laboratory tests suggested that rutting performance with the D design is better than the SMAs, though the SMAs displayed superior resistance to permanent deformation compared to B and C designs. This suggests that the SMA design benefits in resisting permanent deformation under repeated loading. Overall, pavement structural simulations support these experimental findings.

Afterwards, the crash history was obtained for each site where friction and texture were observed, and the wet lane departure crash frequency was used to conduct a safety evaluation that compared

the ‘before’ and ‘after’ periods when a surface treatment was applied. For this analysis, the pavements used in the analysis have the same surface type in the ‘before’ and ‘after’ period. Three separate analyses were conducted: i) an aggregated crash analysis, ii) an individual crash analysis, and iii) a before-after crash rate comparison. Three separate analyses were completed because the study conducted in the FHWA/NC 2022-5 evaluated the average trend of wet lane departure collisions. Hence, the analysis presented here refines the previous analysis and provides insights into the variation in crash frequency across sites with the same surface type. The aggregate crash analysis showed that the dense-graded surface had a %*change* of up to 400%, meaning the number of crashes/month/mile in the ‘after’ period was 400% higher than the number of crashes/month/mile in the ‘before’ period. By computing the %*change* for each site individually, it was observed that the dense-graded surfaces from neighboring states had similar %*change* variability. Except for the dense-graded surface, all the other surface types had an average %*change* closer to or below zero. Finally, if one considers the traffic exposure, then the surface type with the lowest crash rates is the SMAs in both the ‘before’ and ‘after’ period; however, the microsurfacing was the surface type with the lowest ‘after’ crash rate.

Lastly, a life-cycle cost (LCC) analysis was conducted. The investment was defined as the additional cost required to build a specific surface treatment compared to constructing a regular dense-graded pavement. Crash cost reductions were defined as the cost savings resulting from the lower crash frequencies expected from the alternative surfaces compared to dense-graded pavements. The results of the analysis indicated that the crash cost reductions of the alternative surfaces studied were approximately ten times greater than the investments, making all evaluated treatments financially viable. Even under a low discount rate of 0.5%, the net benefit remains positive, while a high discount rate of 7.0% reduces the net present value by about half. SMAs are estimated to require the lowest life-cycle investments, sometimes resulting in a net negative cost compared to dense-graded surfaces, especially at a 0.5% discount rate. Microsurfacing, particularly North Carolina’s material, follows with lower investment values, while OGFC and UTBWC have higher costs. SMAs and North Carolina’s microsurfacing both achieve significant crash cost reductions, with SMA-3 and North Carolina’s microsurfacing leading in this aspect. The current report differs from FHWA/NC 2022-5 as it focuses on a specific road segment, uses distinct friction/texture relationships for each surface type, and includes comprehensive maintenance costs and schedules.

The LCC analysis has some limitations. User costs were not considered, which could affect rankings as surfaces like microsurfacing, which have quicker installation times, might reduce delays and road closures. Mobilization and work zone delineation costs were also excluded. Environmental impacts were not assessed, and surfaces may rank differently if the overall carbon footprint of the surfaces based on maintenance and construction requirements is considered. Additionally, the technical challenges of the implementation of SMAs at a network level were not addressed, and the unfamiliarity of some contractors with SMA design and construction could lead to increased costs and adaptation challenges for the NCDOT.

The Traffic Safety Unit and Materials and Test Unit of the NCDOT will be the primary users of this product. The products of this research will be used by the NCDOT to decide whether pavement mixture design specifications from neighboring states can be implemented to improve friction and texture performance. The SMA mixture design specifications were adapted to the NCDOT design practices and can be evaluated for implementation. The SMA can be included as a new mixture category instead of replacing existing mixtures.

1. INTRODUCTION

1.1. Overview

Vehicle collisions and increases in collisions rates during wet conditions are one of the safety concerns for the NCDOT. Collision rates increase when the surface is wet because skid resistance reduces under these conditions. In recent years, the NCDOT has conducted different research efforts to characterize the friction and texture characteristics of North Carolina mixtures. Most recently, FHWA/NC 2020-11 quantified the impact of new asphalt overlays on friction and texture values and FHWA/NC 2022-5 proposed a set of preliminary friction and texture performance models. Both projects have evaluated the effect of mixture compositional factors on the short and long-term performance of both friction and macrotexture.

Low macrotexture may contribute to reduced wet surface skid resistance values in the field. Revising the existing asphalt mixture categories to solve these problems may result in many practical issues due to contractor practices, familiarity with mixture designs, and unintended consequences to durability. On the other hand, an evaluation of the surface mixture guidelines in South Carolina and Virginia shows important differences with the NCDOT current practice. Both state DOTs use coarser gradations for dense-graded surface mixtures and have SMA mixes as an option to use in roads with high traffic volumes and high friction demand. Considering these specifications and existing NCDOT mixture design practices, this research study was instigated to identify alternative surface mixture designs that could be specified to ensure adequate friction and macrotexture in North Carolina.

With respect to this need, the specific objectives of the research study described in this report are to;

- 1) characterize friction and texture performance of alternative surface mixture designs from other states, and
- 2) identify alternative structural mixture designs that can be specified to ensure adequate friction and texture performance in North Carolina.

1.2. Connection of the Research to Previous Efforts

This research has built upon but does not duplicate the work conducted under FHWA/NC 2017-2, FHWA/NC 2020-11, and FHWA/NC 2022-5. The FHWA/NC 2017-2 project: “Evaluation of Methods for Pavement Surface Friction, Testing on Non-Tangent Roadways and Segments” involved a small subset of North Carolina roadways and recommended that the NCDOT should consider characterizing both friction and macrotexture as part of its pavement friction measurement and management plan (1).

The follow-up to this study was FHWA/NC 2020-11: “Evolution of Pavement Friction and Texture after Asphalt Overlay” (2). The FHWA/NC 2020-11 had three main objectives: 1) identify whether the observations from the initial study were systemic and quantify on a larger basis the initial findings, 2) determine how long potential impacts may last after the overlay is applied and what, if any, asphalt mixture characteristics contribute to the effect and longevity, and 3) develop a strategy for how to best monitor and manage the friction and surface characteristics of NCDOT pavements.

Twenty-six recently overlaid projects across the state of North Carolina were identified to monitor friction and texture right after construction. A continuous friction measurement equipment

(CFME) and a high-speed laser profiler (HSLP) were used to characterize friction and texture, respectively. The friction and texture measurements were collected in the center of the lane (CL) as well as in the right wheel path (RWP). The first measurement was obtained as close as possible to the construction date after which sequential measurements were collected at each site over a time window that varied from half a year to almost two years. In addition, a set of field cores were acquired in 10 of the monitored sites and used to evaluate different test protocols for characterizing friction and texture in the laboratory. Descriptive statistics and regression techniques were used to identify mixture compositional factors that affect the initial friction and texture values and their posterior variation. The key findings of this study are summarized below.

- Strong evidence exists that texture, expressed in terms of the mean profile depth (*MPD*), systematically reduces after an asphalt overlay. The average reduction was 55% and observed to be as high as 73%.
- The effect of asphalt overlays on friction was not consistent and half of the sites showed an average reduction of 17%, whereas the other half showed an average increase of 19%.
- A correlation was found between the compositional factors from the Job Mix Formula (JMF) and the initial *MPD* of new overlays. In general, coarser gradations produce higher macrotexture.
- A correlation was found between the field friction measurements and the surface parameters measured in the lab. The models developed suggest that there is a potential for using field cores, such as the ones collected during construction for quality assurance of the in-place density, to monitor the friction and texture characteristics of the as-constructed surfaces.
- The time-wise friction measurements suggested that the average traffic required to reach the point of maximum friction was 15.5 million repetitions (with a range of 0.8 million to 58.2 million repetitions). These values were determined after correcting for seasonal effects on friction and by examining only those sites that showed a peak in the friction measurements over the study period.

Based on the findings of the FHWA/NC 2020-11 project, a second research effort was initiated, FHWA/NC 2022-5: “Development of Friction and Texture Performance Models” (3). This project had three main objectives; 1) characterize friction and texture performance models, 2) develop friction and texture performance thresholds, and 3) identify asphalt mixture compositional factors (gradation, asphalt content, presence of modified versus non-modified asphalt, etc.) that affect the as-constructed macrotexture and friction. To achieve these objectives, data on a new set of recently overlaid surfaces were collected to supplement the observations from FHWA/NC 2020-11 project. Additionally, more than 100 sites with historical observations were cataloged to describe the long-term friction and texture performance. The primary outcome of this project was an initial set of performance models that can be used to assess immediate and potentially long-term friction/macrotexture. The research also produced a set of candidate threshold limits for friction/macrotexture where investigatory and intervention steps could be taken to possibly improve safety. Finally, the research produced information on the mixture design factors that contribute to higher or lower friction/macrotexture.

1.3. Status of the Literature

A review of the literature pertaining to this project is presented in Appendix A, but a summary of the most relevant components of this review is presented below.

1.3.1. Asphalt Mixture Design for Improved Surface Characteristics

Pavement friction design is a relatively small component of the overall roadway design process but of great relevance considering pavement friction is critical to safety. Friction design requires a thorough understanding of the factors that influence friction and knowledge of the materials and construction techniques (4). It also requires an understanding of the economic and engineering tradeoffs associated with different materials and techniques, such as the costs/benefits of utilizing one friction strategy over another and how each strategy impacts structural design and other functional aspects (e.g., noise, splash/spray) (5). Studies that have tried to incorporate friction and texture in the mix design process followed the general process shown in Figure 1 (6, 7).

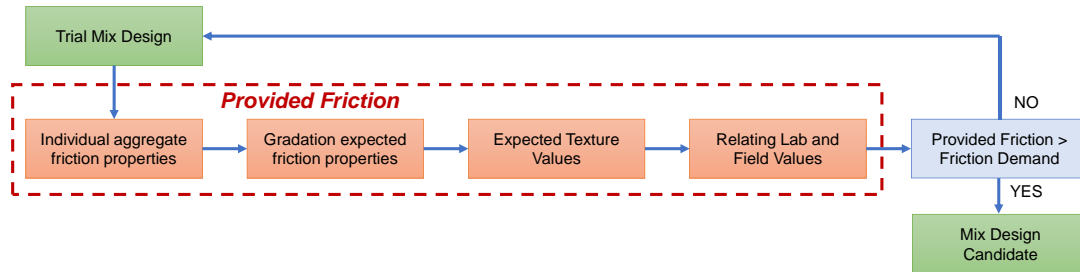


Figure 1. Including friction in the mix design.

The process starts with the selection of a trial mix design, which should comply with the Superpave specifications (or relevant alternative state specifications) and use aggregates that satisfy the properties described in NCHRP Document 108 (5). In brief, these properties include aggregate angularity (coarse and fine), abrasion/wear resistance, hardness, polish resistance, and soundness. Once the trial mix is established, the friction of individual aggregate fractions is defined, and the expected frictional properties of the surface provided with the proposed gradation is predicted. Afterwards, the gradation curve is translated to an expected texture depth. These studies have reported that coarse, open-graded, and gap-graded mixtures result in higher macrotexture values compared to the values obtained with a dense-graded mix. Also, texture analysis has shown that surface macrotexture indices (like *MPD*, *MTD*, etc.) are higher for sections with high RAP content (more than 50%) than those with low RAP content (less than 15%), while microtexture values are the same or slightly higher compared to a non-RAP mixture. It has also been reported that the texture durability is slightly worse for high RAP content (50%) sections than those of lower RAP content sections (8).

The FHWA/NC 2020-12 research project (9) found that North Carolina mixes have become finer over the last two decades. Furthermore, in 2018 the NCDOT introduced a modification in their mixture design procedures, in part to increase the asphalt content. A statistical analysis between the mixtures designed prior to and after the re-classification was conducted. The analysis also found (not unexpectedly) that most of the asphalt mixtures in North Carolina contain RAP. No substantial differences were found in the volumetric comparisons of the recycled mixtures before and after the re-classification.

Recent reports indicate that SMA mixes exhibit very good rutting and cracking resistance, resulting in longer service lives, and provide high macrotexture and microtexture characteristics compared to standard dense-graded asphalt mixtures, but the mixtures are more costly (10, 11). Approximately, 18 states currently have, or are working to implement, a methodology to use SMA mixes on Interstates and high-traffic roads. As mentioned above, the NCDOT does not currently permit SMA and restricts the Nominal Maximum Aggregate Size (NMAS) of surface mixtures to

9.5 mm. For the NCDOT, the ‘high friction’ surface courses include ultrathin bonded wearing course (UTBWC) and Open-Graded Friction Course (OGFC). A critical difference between these materials and SMA is that the SMA provides structural contribution. A brief discussion of these surface treatment strategies is provided below.

1.3.2. Ultrathin Bounded Wearing Course (UTBWC)

UTBWC involves applying a thin layer of asphalt over a prepared surface to extend the life of the existing pavement, improve skid resistance, and provide a smooth, durable driving surface. The thickness of the thin layer typically ranges from 0.5 to 0.75 inches (12.5 to 19 mm), a polymer modified asphalt emulsion is used to improve adhesion and durability and incorporates high-quality, durable aggregate to resist wear and provide a skid-resistant surface. This treatment can be applied quickly with minimal disruption to traffic, often allowing for same-day reopening of the roadway; therefore, is ideal for high-traffic urban roads, highways, and other pavements requiring quick maintenance with minimal traffic disruption. The primary purpose of UTBWC is to extend the life of the existing pavement, improve ride quality, and enhance overall surface durability and skid resistance. It acts as a preventive maintenance measure and improves the smoothness of the driving surface.

1.3.3. Open-Graded Friction Course (OGFC)

OGFC is a surface treatment where the void content is high and thus water can rapidly drain. These treatments can improve water management and reduce environmental impacts from runoff (7, 12). Because OGFC can help to manage stormwater runoff, it is considered a Low Impact Development (LID) practice. To do so, the fine aggregates are screened or reduced while the proportion of coarse aggregate increases. These changes lead to improved drainage and noise reduction because of the significant pore structure they impart (7). OGFC’s are designed to meet the special requirements of stone-on-stone contact and a high connected air void content. It is possible to obtain high macrotexture values (between 1.5 mm to 3.0 mm) with OGFC. While a typical OGFC has high initial friction, the long-term friction performance will depend on the aggregate abrasion and polishing resistance (5).

1.3.4. Stone Matrix Asphalt (SMA)

Stone matrix asphalt (SMA), also called stone mastic asphalt, is a tough and rut-resistant dense, gap-graded asphalt mixture with a stable stone-on-stone skeleton. The stone-on-stone skeleton can increase mixture strength while a rich mortar binder, coupled with stabilizing agents such as fibers and/or asphalt modifiers provides durability. SMA is comprised of 70 to 80 percent coarse aggregate, 8 to 12 percent filler, and 6 to 7 percent asphalt binder (11). SMA requires higher asphalt binder content compared to dense-graded mixtures, so there is a higher tendency for asphalt draindown during silo storage and transportation. To address draindown, a small amount of cellulose or mineral fibers (about 0.3 percent for cellulose and 0.3–0.4 percent for mineral fiber) is added to the mixture (13).

Historically, SMA mixtures have been placed on routes that must withstand heavy traffic such as State and Interstate routes, high-stress pavement areas, airfields, and racetracks. In terms of initial cost, a SMA mixture typically is more expensive than conventional mixtures, mainly because it requires higher asphalt contents, more durable aggregates, fibers, and a polymer-modified asphalt binder. There has been no consistent conclusion on comparing the long-term cost-effectiveness of SMA versus conventional dense-graded mixtures (11).

More than 18 state DOTs specify SMA as an option for sites with high friction demand. Four of NC's neighboring states; Georgia, Virginia, Maryland, and South Carolina, have technical provisions for the implementation and design of SMAs. Details relating to the specifications for these states as well as the documentation available from other states are provided in Appendix A. It is noted that SMA design guidance is given in terms of NMAS, percent passing control sieves, aggregate properties, and mix volumetrics.

A friction performance curve for SMA has not been presented in the literature. However different authors have reported that SMA mixes tend to have high friction values due to the high-quality aggregate used in their design/construction (5, 14). Because of the coarse gradation, the aggregates tend to be exposed to traffic wear. Woodward et al. (15) developed a laboratory method to quantify the surface wear of SMA samples under the action of traffic repetitions. No study has been shown to date that indicates the SMAs aggregate structure polish differently than a dense-graded or open-graded surface. In fact, Kowalski et al. (16) evaluated three different sections over four years, one with porous asphalt, one with SMA, and others with a dense-graded surface. The authors noted that little to no friction variation was observed on the SMA surface. Also, the raveling susceptibility of SMA is lower than OGFC because SMA consists of a full pavement layer (15, 17).

1.3.5. Other Treatment Types

The high friction surface treatment (HFST) has been used as one of the low-cost safety countermeasures to address high friction demand concerns on curved roadways. A HFST is specifically designed to significantly enhance the skid resistance and safety of road surfaces, particularly in areas where high friction is critical, such as curves, intersections, and steep grades. HFST share some similarities with UTBWC, but are more commonly used as spot treatments due to their cost.

It was developed in the 1960s in the U.K. by the Greater London Council and the Transport and Road Research Laboratory to restore friction on high-crash road sections (14). The aggregate used for this treatment type is calcinated bauxite. A properly constructed HFST on pavements in good condition typically maintains a high friction value throughout its expected life. Based on some studies, the typical HFST life ranges from 7 to 12 years, and the benefits surpass the cost when the HFST is more than 7 years (5, 14, 18). However, this treatment can fail earlier, and the main reported causes are in the form of delamination, aggregate loss (the most common), or cohesion failure (14).

Microsurfacing consists of spreading and applying a mixture of dense-graded aggregate, polymer-modified asphalt emulsion, water, and mineral fillers in a layer that is usually 10 to 12 mm thick (0.4 to 0.5 in.) over an existing pavement surface as preventive maintenance. The pavement life extension expected from this treatment, when applied as preventive maintenance before the onset of structural damage, generally ranges from 7 to 9 years (19, 20). Microsurfacing emulsions are formulated to break due to chemical interactions with aggregate shortly after placement. Consequently, microsurfacing can be placed at night and cure rapidly, allowing traffic to typically open as soon as one hour after application (19–21). The main benefits observed in the field when implementing microsurfacing are reduced rut depths, less traffic delays than conventional overlays, reduction in crash rates by improving skid resistance, and decreasing water infiltration (19, 22). Microsurfacing treatments do not contribute to the structural capacity of a pavement and are ideally applied only to pavements in good structural condition.

Chip seals are commonly used to improve skid resistance, prevent oxidation, seal small cracks, improve friction, and correct surface defects. Although it is most typically applied to the preservation of roads with low total traffic volumes and low truck volumes, the treatment may also be employed to prevent further deterioration on roads with high traffic volumes (23–25). If successfully executed on pavements in good structural condition, chip seal treatments can provide satisfactory friction for around five years, with skid numbers (*SN*) values generally ranging from 40 to 60. However, the occurrence of excessive chip loss and bleeding can negatively impact the performance of the surface in the first 12 months, leading to premature failure (23, 25).

1.3.6. Knowledge Gaps and Conclusions

Currently, the Superpave mixture design process does not consider friction/texture as a parameter during the design process. However, it does control for aggregate characteristics such as gradation, hardness, and mineralogy, which ultimately affect the surface micro and macro texture components. When the coarse aggregate content (aggregates larger than the primary control sieve) decreases, positive macrotexture is diminished and as a result, the macrotexture tends to decrease. This change may also increase the field air void content in the mixture, which can in turn reduce mix stability, increase aging, increase permeability, and reduce fatigue life (5). In other words, a change in the gradation and consequent aggregate packaging requires a holistic evaluation of the mixture stability and durability. Mix designs in North Carolina have shifted towards denser and finer configurations that result in lower macrotexture levels, characterized by a higher proportion of valleys (that contributes to water drainage and voids) than peaks (that contributes to friction hysteresis in the form of tire deformation).

The experience from different states has shown that coarse gradations, especially stone-based gradations like those of the SMA, produce better structural performance and higher macrotexture values. Therefore, research is needed to assess the implications of using coarser dense-graded mixtures and SMA in North Carolina by using texture observations of these mixtures in neighboring states. There is also a need to evaluate other, less typical surfacing materials like Microsurfacing, HFST, chips seals, and surfaces that have been shotblasted. This evaluation must consider short and long term functional and structural performance and the economic implications of these changes from the production, construction, and economy standpoints.

1.4. Report Organization

This report is organized into nine chapters and eight appendices as follows: first, an introductory chapter (this chapter) summarizes the research conducted to date. Chapter 2 presents the data collected and processing methods. Chapter 3 develops the friction and texture performance models of alternative asphalt surfaces. Chapter 4 contrasts the rutting and cracking performance of SMA materials from neighboring states against the expected performance of dense-graded mixtures in North Carolina. Chapter 5 conducts a macro-level safety assessment to quantify the effect of different surface types on highway safety. Chapter 6 provides a life-cycle comparison to evaluate the cost/benefit ratio of traditional surface treatments used in North Carolina to address friction issues, such as OGFC and UTBWC, against alternative surface treatments like SMAs and Microsurfacing. Chapters 7 and 8 present the main conclusions and the implementation and technology transfer plan, respectively. Finally, Chapter 9 lists the research references consulted in this project. Appendix A provides the detailed literature review; Appendices B, C, D, F, G, and H provide supplementary data and analysis; and Appendix E provides the draft SMA specification.

2. DATA PROCESSING

The primary data for this research was collected in three different states; North Carolina and two neighboring states. This primary information was complemented with the dataset acquired in the previous projects, FHWA/NC 2020-11 and FHWA/NC 2022-5. The pieces of information compiled for this project are summarized in Figure 2.

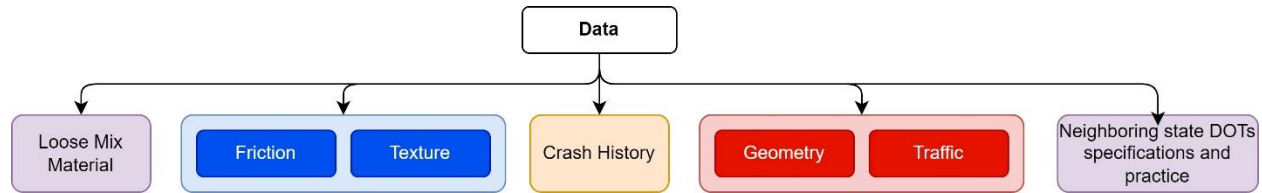


Figure 2. Data inventory for the research project.

As shown, the activities included sampling loose mix material to characterize SMA materials used in two neighboring states. For State 1, the material was sampled directly by the research team in November of 2023; whereas for State 2, the state agency sampled the materials at an indeterminate date in 2023. The loose material was used to prepare Superpave gyratory compacted asphalt samples to perform the material characterization.

In a parallel effort, friction and texture measurements were collected to characterize skid resistance of alternative asphalt surfaces. Friction measurements were collected using a continuous friction measurement equipment (CFME) whereas texture was characterized using a high-speed texture profiler (HSTP) and a static laser. Additionally, in collaboration with engineers from the two states, the crash history of all the sites was identified. Subsequently, using publicly available layers from the two states' geographic information systems it was possible to characterize the road geometry in terms of road setting (functional classification and speed limit) and the traffic volume (AADT). Finally, material and construction specifications for all the neighboring states, i.e., South Carolina, Kentucky, Virginia, Georgia, and Alabama were consulted and used as a guideline to propose a preliminary draft for the implementation of SMAs in North Carolina.

For the case of North Carolina, five surface treatments were of interest: 1) chip seals, 2) Microsurfacing, 3) HFST, 4) OGFC, and 5) UTWBC. Like in previous research projects, the measurements were collected on road sites specifically selected based on the surface type, age, functional classification, and speed limit. For this research, a 'site' is a road section that has the same traffic conditions, functional classification, operating conditions, age, and surface type. Most of the sites evaluated were controlled access, high-speed facilities with speed limits greater than or equal to 55-mph. The exception to this rule were the sites that had chip seals, Microsurfacing, and HFST because these treatments are typically applied on secondary roads that tend to have speed limits below 55-mph. Sites are grouped (NC G1 through NC G3) based on the project where data was primarily collected and a summary with the number of sites included in this project and the previous research efforts is included in Table 1.

In the two neighboring states where friction and texture were collected, three surface types were of interest; 1) Superpave mixes with a 12.5 mm NMAS, 2) SMA with a 9.5 mm and 12.5 mm NMAS, and 3) Microsurfacing. The total number of sites studied in the two neighboring states is presented in Table 2. Superpave and SMA surfaces with two different binder grades, PG 70-22 (identified with letter B at the end of the code name used in Table 2) and PG 76-22 (identified with letter A at the end of the code name used in Table 2), were included.

Table 1. Total number of sites available for analysis in North Carolina.

Surface Type	RP2020-11 and RP2022-5		RP2024-12	Total
	NC_G1	NC_G2	NC_G3	
Chip Seals	0	0	15	15
Microsurfacing	0	0	10	10
HFST	0	0	4	4
OGFC	2	19	19	40
UTBWC	3	21	14	38
Dense	31	68	0	99
Other	0	9	0	9
Total	36	117	62	215

Table 2. Number of sites studied in neighboring states.

Surface Type	Total
Dense-I ^{1,5}	11
Dense-II ¹	14
SMA-1A ^{1,3}	12
SMA-1B ^{1,4}	8
SMA-2A ^{2,3}	6
SMA-2B ^{2,4}	5
SMA-3A ^{2,4}	8
Microsurfacing-Alt	23
Total	87

¹ Surface mix with a 9.5 mm NMAS

² Surface mix with a 12.5 mm NMAS

³ PG 76-22

⁴ PG 70-22

⁵ Superpave mix

2.1. Friction and Texture Measurements

2.1.1. Equipment

The same Skiddometer BV-11 used in FHWA/NC 2020-11 and FHWA/NC 2022-5 was used to collect the friction data in this project. The device has a fixed 17% slip ratio using a smooth ASTM E1551 tire. For testing, a constant water film thickness of 1 mm was used, and all the testing was carried out under similar climatological conditions. Data was collected continuously and reported every 10 m (32.8 ft) on two locations, the right wheel path (RWP) and the center of the lane (CL), measurements were performed at 60-mph (96 km/h) and 40-mph (60 km/h) (only on certain sites in the RWP).

For texture, high-speed texture measurements were taken using the same AMES AccuTexture 100 laser used in FHWA/NC 2020-11 and FHWA/NC 2022-5. This laser is currently the highest-resolution highway-speed texture measurement device commercially available (26). A point laser was chosen for this purpose because such a laser has shown to be in 99% agreement with older static lasers such as the Circular Texture Meter (CTM) on asphalt pavements (27).

The laser chosen for this study was also the only high-speed measurement device among the group evaluated in the NCHRP 10-98 study to accurately measure texture across a wide range of speeds. In that study, other devices showed measurement degradation above 25 mph (28). Raw data

collected by the laser was filtered for spikes, dropouts, and outliers as recommended by the ISO 13473-19 standard. Measurements were reduced to a reported length of 32.8 ft (10 m). The filtered data was used to calculate the Mean Profile Depth (*MPD*). The *MPD* was ultimately selected for comparison since it is the texture parameter most used by practitioners (28). As with friction, measurements were collected in two locations, RWP and CL. The high-speed observations were complemented with a set of static measurements collected with the AMES 9500, which is a rapid laser texture scanner (rLTS) capable of collecting a pavement surface with more than 4,000,000 points.

2.1.2. Representative Friction and Texture Values

Once the measurements were collected, they were processed to remove potential outliers and to calculate a single value that represents the overall friction and texture of a given site. To do so, the authors followed the same procedure established in the previous two research projects, FHWA/NC 2020-11 and FHWA/NC 2022-5. In short, the observations are spatially divided in 0.1-mile increments, then the continuous friction and texture reading are summarized using two main statistics for each of these individual segments:

- For friction, the representative value is defined as the 2.5th percentile of the continuous reading.
- For texture, the representative value is set as the 50th percentile of the high-speed texture reading.

This process is illustrated in Figure 3 and Figure 4 for friction and texture, respectively, using the observations collected in a site with a Dense-I surface type. In the case of friction, the three friction measurements are plotted in Part (a) to (c), for the RWP at 40-mph, RWP at 60-mph, and CL at 60-mph, respectively. The black series represents the continuous friction reading, whereas the short red segments represent the 2.5th friction percentile computed every 0.1-mile, the dashed red line indicates the representative friction value defined as the average of the values of the short red segments. In this example, the representative friction in the RWP collected at 40-mph and 60-mph is 0.62 and 0.57, respectively, and the representative value for the CL at 60-mph is 0.70.

Likewise, for the *MPD* values depicted in Figure 4, panel (a) shows the RWP observation, and panel (b) shows the CL record. As with friction, the black data series indicates the raw *MPD* profile obtained with the high-speed texture laser, while the short red segments represent the 50th *MPD* percentile computed in 0.1-mile increments and the red dashed line is the representative *MPD* value defined as the average of the individual 0.1-mile segments. For the data shown, the representative value of the RWP and CL observations is 0.65 mm and 0.59 mm, respectively.

By computing the representative friction and texture values in this way, it is possible to account for the spatial variation of the observations and to capture a stable trend in the data without the effect of potential outliers like the high *MPD* value recorded between 0.3 to 0.4 miles and 1.6 to 1.7 miles in Figure 4. These high *MPD* observations correspond to a bridge in portland cement concrete pavement. This process was replicated in all the sites.

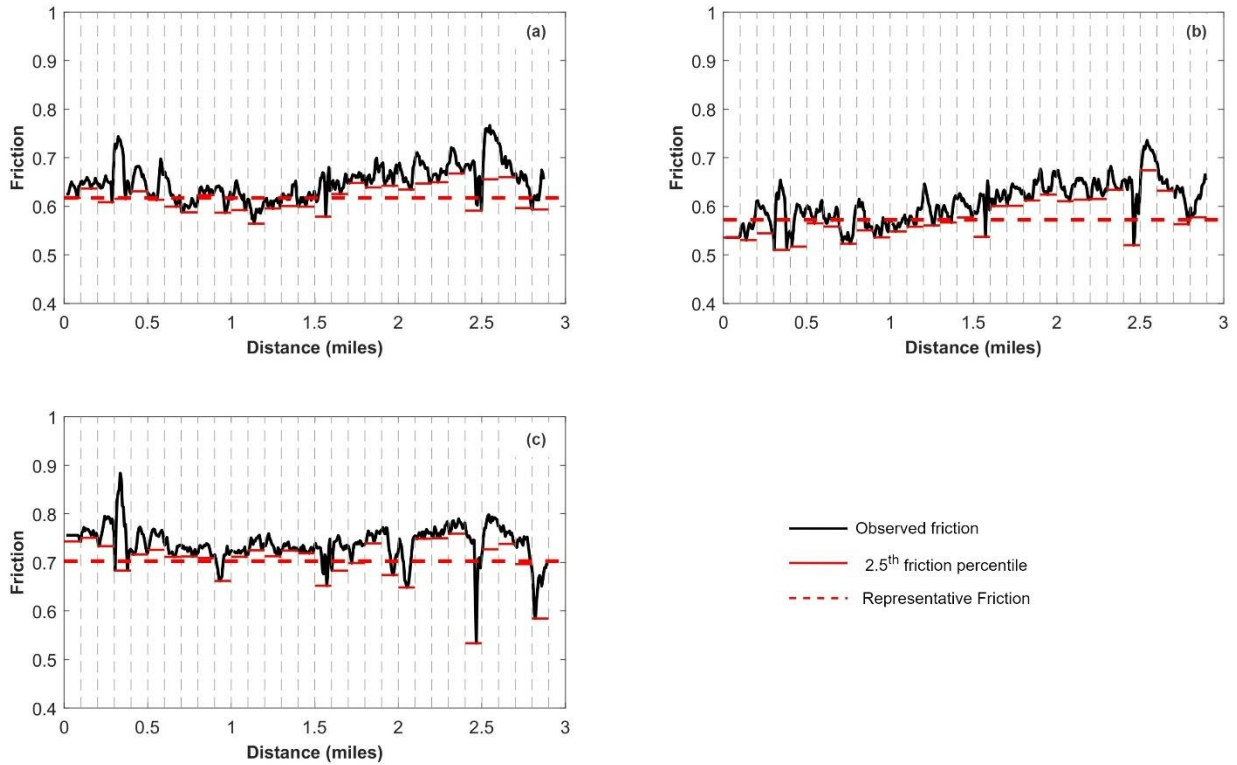


Figure 3. Example of the friction measurement processing collected in: (a) RWP at 40-mph, (b) RWP at 60-mph, and (c) CL at 60-mph. The site shown is a Dense-I surface type.

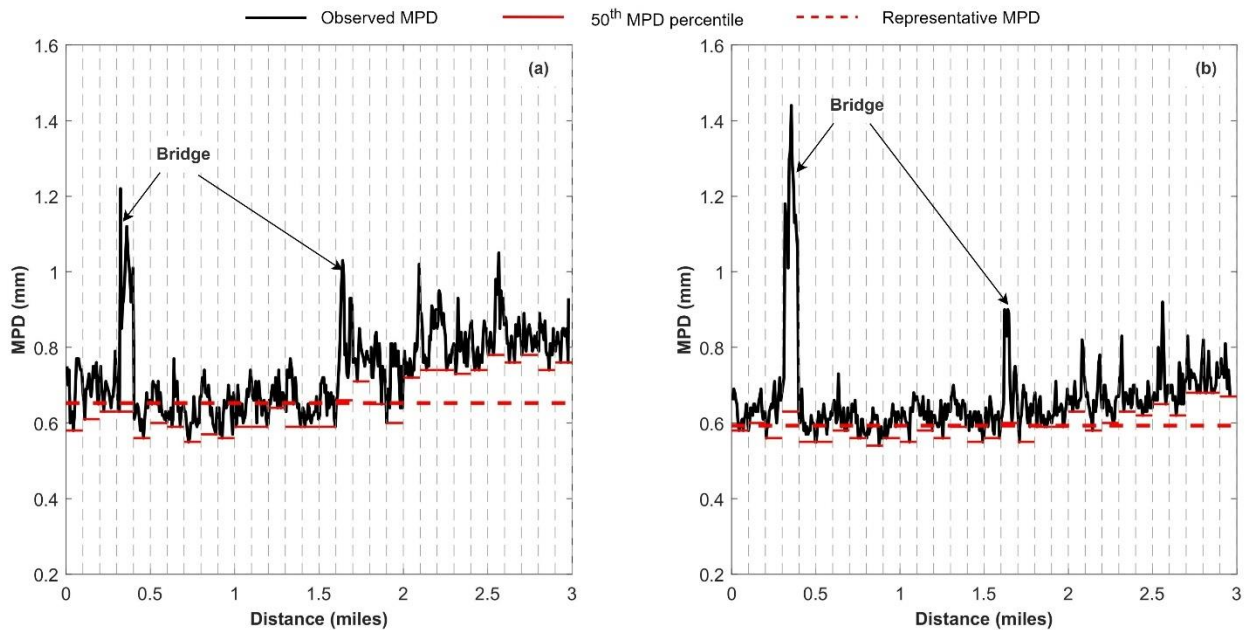


Figure 4. Example of the MPD measurement processing collected in: (a) RWP and (b) CL. The site shown is a Dense-I surface type.

A summary of the characteristics of the sites tested in the current research effort, data set NC G3 and the data collected in two neighboring states, as well as the characteristics of the sites tested in

the previous two research projects NC G1 and G2 is included in Table 3. As shown in the table, the sites tested encompassed a wide range of traffic volumes, speed limit, and surface age for all the surface types tested, except for the chip seals where all the sites tested had an age of 2.2 years.

Table 3. Summary of the site characteristics tested in all the research efforts.

Data Set	Surface Type	AADT (vpd ¹)			Speed Limit (mph)			Age		
		Min	Avg	Max	Min	Mode	Max	Min	Avg	Max
NC G1 ² and G2 ³	Dense	1,400	30,958	122,000	35	55	70	0.0	4.9	15.9
	OGFC	5,700	35,200	77,000	45	55	70	0.1	6.4	12.9
	UTBWC	8,900	48,475	82,000	35	70	70	0.0	6.3	13.0
	Other	5,000	54,611	138,000	55	55	70	3.0	6.1	8.0
NC G3 ⁴	Chip Seal	90	849	2,700	55	55	55	2.2	2.2	2.2
	Microsurfacing	150	4,350	21,000	55	55	60	0.6	1.4	7.9
	OGFC	5,000	24,668	105,000	55	55	70	0.6	3.6	10.5
	UTBWC	9,500	57,714	127,000	35	55	70	0.5	5.0	16.5
	HFST	400	4,725	13,000	35	35	45	3.3	5.5	7.0
Two Neighboring States ⁴	Microsurfacing-Alt	350	20,608	69,000	45	55	70	0.7	0.8	0.9
	Dense-I	2,300	16,345	40,000	55	55	70	1.4	4.8	7.7
	Dense-II	1,500	46,536	119,000	55	65	70	1.4	3.3	6.5
	SMA-3A	35,500	62,575	102,600	65	70	70	0.3	0.8	1.3
	SMA-2A	40,000	62,167	109,000	65	70	70	2.5	8.2	13.5
	SMA-2B	40,000	50,800	74,000	65	70	70	13.7	14.6	15.4
	SMA-1A	40,000	53,583	134,000	65	70	70	1.4	5.9	8.7
SMA-1B	45,000	48,125	56,000	70	70	70	1.9	7.1	15.7	

¹ Vehicles per day

² Sites tested in FHWA/NC 2020-11 research project

³ Sites tested in FHWA/NC 2022-5 research project

⁴ Sites tested in FHWA/NC 2024-12 research project

The number of friction and texture observations collected in the RWP and CL by surface type is presented in Table 4. As in the previous projects, a friction/texture observation is a measurement collected at a given site in a given traffic direction on a given location. For instance, a site with two traffic directions, e.g., NB and SB, if friction measurements were made in both directions at 40-mph and 60-mph in the RWP and CL, then this site will have a total of six friction measurements (four in the RWP, two at each speed, and two in the CL) and if texture was also collected it will have four texture values in total (two in the RWP and CL, respectively).

Lastly, in a subset of the North Carolina's G3 sites (see Table 1) and a subset of the sites tested in the two neighboring states (see Table 2) 3D surface scans were collected using the AMES 9500 laser. The number of surface scans obtained by surface type is summarized in Table 5. A total of 79 surface scans were collected, these scans were conducted either in the RWP or in the CL. By default, seven texture indexes are computed by the laser software: *MPD*, estimated texture depth (*EMTD*), root-mean square depth (*RMS*), profile mean elevation (*Ra*), profile root-mean square depth (*Ra*), Skewness (*Rsk*), and Kurtosis (*Rku*).

Table 4. Summary of the number of friction and texture measurements collected in all the research efforts.

Data Set	Surface Type	Friction No. Obs. ¹			Texture No. Obs.	
		RWP ₄₀	RWP ₆₀	CL ₆₀	RWP	CL
NC G1 and G2	Dense	219	563	337	486	258
	OGFC	32	55	12	66	4
	UTBWC	34	89	23	89	18
	Other	15	26	0	25	0
NC G3	Chip Seal	17	0	0	16	14
	Microsurfacing	11	8	4	11	11
	OGFC	19	21	8	22	22
	UTBWC	12	14	6	16	16
	HFST	6	0	0	7	4
Two Neighboring States	Microsurfacing-Alt	13	8	8	22	24
	Dense-I	11	10	10	14	12
	Dense-II	14	14	13	14	14
	SMA-3A	12	12	12	12	12
	SMA-2A	6	8	6	6	6
	SMA-2B	4	4	4	5	5
	SMA-1A	10	10	10	12	12
	SMA-1B	7	7	7	8	8

¹ RWP₄₀ = friction measured in the right wheel path (RWP) at 40-mph; RWP₆₀ = friction measured in the right wheel path (RWP) at 60-mph; and CL₆₀ = friction measured in the center of the lane (CL) at 60-mph.

Table 5. Number of 3D surface scans collected for this project.

Source	Surface Type	Number of scans
NC G3	Microsurfacing	19
	OGFC	22
Two Neighboring States	Dense-II	16
	SMA-2B	4
	SMA-2A	4
	SMA-1B	4
	Microsurfacing-Alt	10

2.2. Crash Information

The crash history of each of the sites listed for North Carolina and the two neighboring states was compiled and organized to conduct a macro-level safety analysis. In the case of North Carolina, NCDOT personnel helped the research team to get a query report that contains the number of crashes per road inventory direction coded as wet lane departure crashes for each location (from January 1, 2010 to December 31, 2023). For State 2, the research team consulted with personnel from the DOT who pointed to a public repository that contains the crash analysis tool developed by the traffic operations division. The crash history was downloaded for the sites tested in this state from January 1, 2015, to October 31, 2023. Similarly, for State 1, the research team consulted the DOT personnel to obtain the crash frequencies in the eight locations tested. A crash report that contained the number of collisions per traffic direction on each site from January 1, 2018, to September 30, 2023 was obtained. Because the analysis conducted in FHWA/NC 2022-5 focused on wet lane departure crashes, the fields included in the datasets from these two states were used to filter out the crash numbers that match the same crash type, i.e., wet lane departure crashes. Crashes of all types, from property damage only to fatality, were included in this data extraction.

3. PAVEMENT FRICTION AND TEXTURE PERFORMANCE MODELING

In the FHWA/NC 2022-5 project, a set of friction and texture performance models was proposed altogether with investigatory and intervention thresholds for the friction and texture measured with the BV-11 and the AMES Accu-Texture 100, respectively. Mixed effect (random/fixed) models were employed to describe the friction and texture evolution while accounting for the unobserved random heterogeneity. The random parameters accounted for individual initial friction/texture values and differences in the deterioration rate among pavements with the same surface type.

3.1. Friction

The RWP friction observations collected with the Moventor BV-11 in NC_G1 through NC_G3 as well as the sites measured outside North Carolina are compared graphically in Figure 5 and Figure 6 for the measurements made at 40-mph and 60-mph, respectively. The graphical comparison for the CL records is included in Appendix B. As indicated in Table 3, each surface type encompasses sites with different ages and traffic volumes, therefore Figure 5 and Figure 6 provides a general visualization of the friction values one could expect at these two measurement speeds over the entire performance curve for each surface type. For reference, the two investigatory thresholds proposed in FHWA/NC 2022-5 are included in both figures to visually identify the surface types that have friction values above the thresholds proposed in FHWA/NC 2022-5. These values, which were based on 60-mph, are also summarized, along with the proposed intervention thresholds, in Table 6. The dense-graded friction values from the North Carolina sites are included in Figure 5 and Figure 6 as a reference of comparison. Additionally, Table 7 was included with a summary of the three statistics computed for the friction values, i.e., the 25th and 75th friction percentile of all the sites with a given surface type.

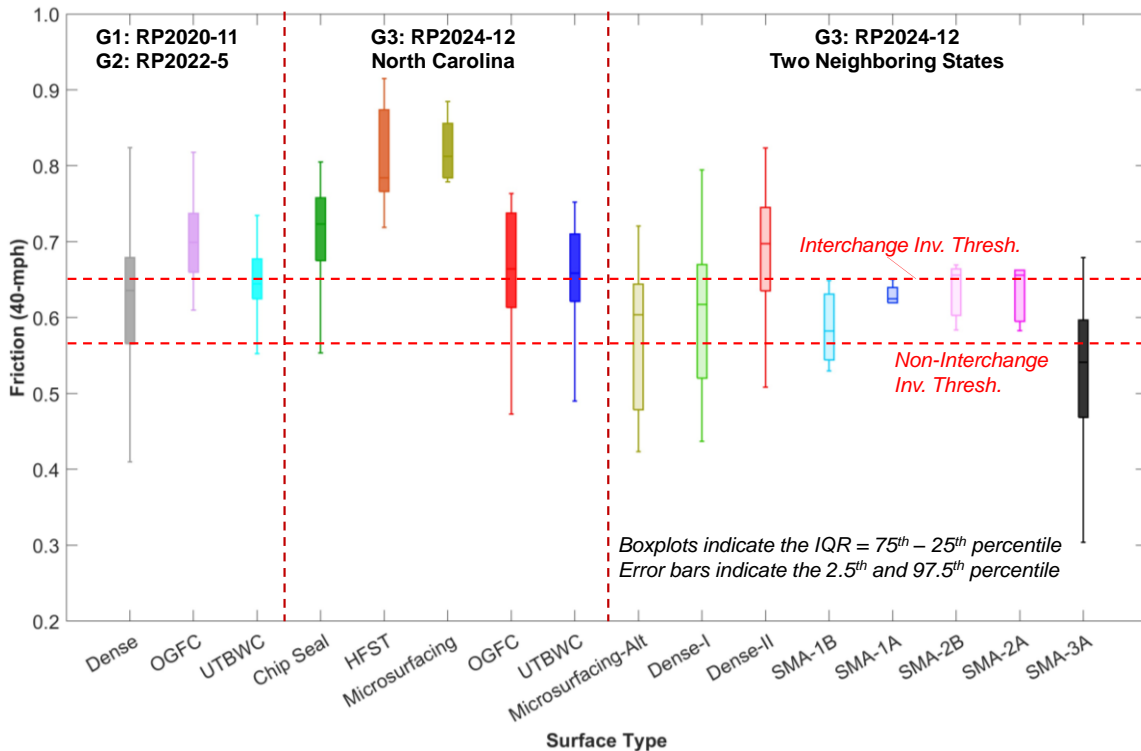


Figure 5. Distribution of the friction measurements made in the RWP at 40-mph for each surface type.

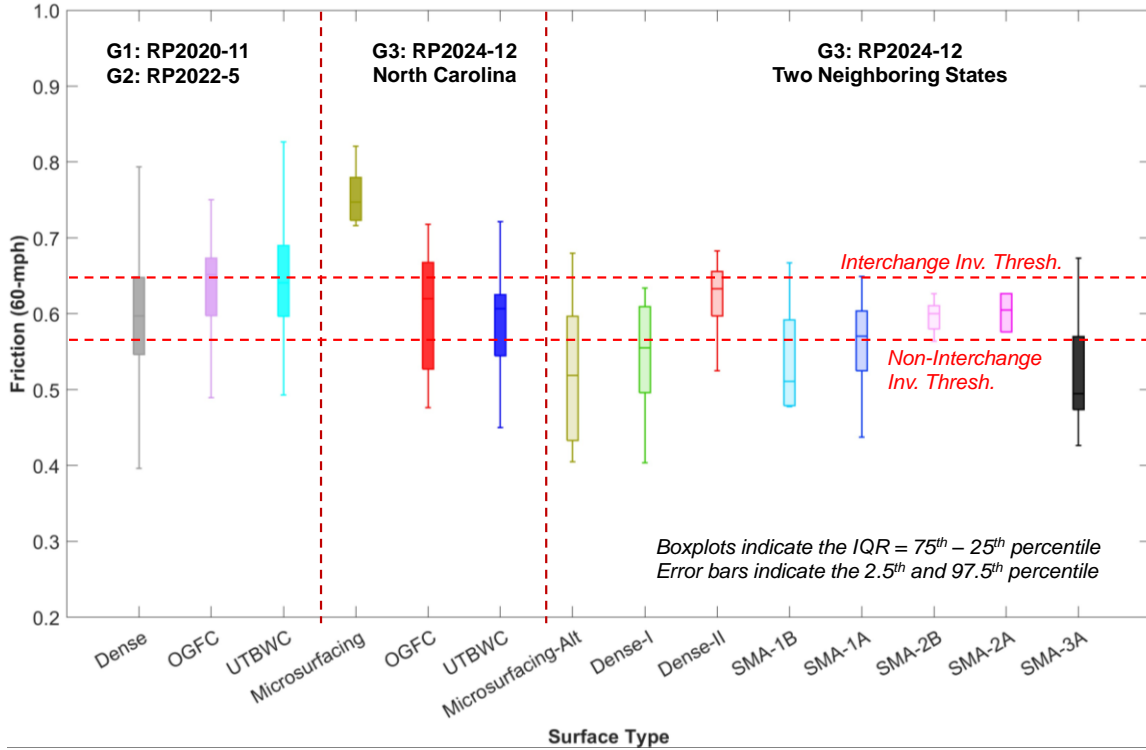


Figure 6. Distribution of the friction measurements made in the RWP at 60-mph for each surface type.

Table 6. Recommended friction investigatory and intervention thresholds.

Variable	Non-Interchanges	Interchanges
FN_{INV}	0.57	0.65
FN_{INT}	0.43	0.49

Table 7. Summary of friction statistics computed for each surface type.

Data Set	Surface Type	Friction RWP ₄₀			Friction RWP ₆₀		
		P ₂₅ ¹	P ₇₅ ²	Mean	P ₂₅ ¹	P ₇₅ ²	Mean
NC G1 and G2	Dense	0.57	0.68	0.64	0.55	0.65	0.60
	OGFC	0.66	0.74	0.70	0.60	0.67	0.65
	UTBWC	0.63	0.68	0.65	0.60	0.69	0.64
NC G3	Chip Seal	0.68	0.76	0.72	-	-	-
	Microsurfacing	0.79	0.86	0.82	0.72	0.78	0.75
	OGFC	0.61	0.74	0.66	0.53	0.67	0.62
	UTBWC	0.62	0.71	0.65	0.54	0.62	0.61
	HFST	0.77	0.88	0.79	-	-	-
Two Neighboring States	Microsurfacing-Alt	0.48	0.65	0.60	0.43	0.60	0.52
	Dense-I	0.52	0.67	0.62	0.49	0.61	0.55
	Dense-II	0.63	0.75	0.70	0.59	0.65	0.63
	SMA-2A	0.60	0.66	0.67	0.57	0.62	0.60
	SMA-2B	0.60	0.66	0.66	0.58	0.61	0.60
	SMA-1A	0.62	0.64	0.63	0.52	0.60	0.57
	SMA-1B	0.55	0.63	0.58	0.48	0.59	0.51
	SMA-3A	0.47	0.60	0.54	0.47	0.57	0.49

¹ 25th friction percentile

² 75th friction percentile

3.1.1. Friction in RWP at 40-mph

As indicated in Figure 5 and Table 7, the dense-graded surfaces, as well as SMA-1 and SMA-2, tend to have similar friction values, and the interquartile range of these surfaces lies between the Interchange and Non-Interchange investigatory thresholds (thresholds established for 60-mph measurements). SMA-3 has friction values lower than those of the North Carolina dense-graded surfaces. North Carolina Microsurfacing exhibits one of the highest friction values, like those of the HFST. In contrast, the friction of Microsurfacing-Alt is closer to that of North Carolina dense-graded pavements. The friction values of Dense-I are comparable to those of North Carolina dense-graded surfaces, but Dense-II shows a substantial difference, with friction values higher than the Interchange investigatory threshold. Lastly, the OGFC and UTBWC in the G3 dataset differ from the values in G1 and G2. This difference may be attributed to variations in average age: the OGFC tested in G1 and G2 sites were 6.4 years old, whereas those observed in G3 were only 3.6 years old. In contrast, the UTBWC tested in G1 and G2 sites had an age of 6.3 years, while the G3 sites had an age of 5.0 years.

3.1.2. Friction in RWP at 60-mph

The results for the 60-mph measurements are distributed like those at 40-mph. As shown in Figure 6 and Table 7, the friction of dense-graded surfaces tends to lie between the Interchange and Non-Interchange investigatory thresholds. The average friction of SMA-2 surfaces is comparable to that of North Carolina dense-graded pavements, whereas the average friction of SMA-1 surfaces is closer to the Non-Interchange threshold. SMA-3 has the lowest friction among the SMAs tested. North Carolina Microsurfacing exhibits one of the highest friction values, similar to those of the HFST. In contrast, the friction of Microsurfacing-Alt is lower than that of North Carolina dense-graded pavements. The friction values of Dense-I are comparable to those of Microsurfacing-Alt, but Dense-II shows a substantial difference, with average friction values closer to the Interchange investigatory threshold. Lastly, the OGFC and UTBWC in the G3 dataset differ from the values in G1 and G2. This difference may be attributed to variations in average age as discussed in the previous section.

3.2. Calibration of Friction Performance Models

In this section, the generalities of the friction performance models developed in FHWA/NC 2022-5 are shown first and then the model coefficients were updated for the OGFC, UTBWC, Microsurfacing, Dense-I and Dense-II, and SMA-1 to SMA-3. For the neighboring state where SMA-1 and SMA-2 observations were collected, the data was categorized into the three climate regions, although these regions correspond to North Carolina boundaries, it is assumed that the same climate variation prevails in this state, i.e., the vertical delineation of the polygons that delimits these regions in North Carolina also applies for the neighboring state.

3.2.1. Friction Performance Models in FHWA/NC 2022-5

In the FHWA/NC 2022-5 project, friction was modeled using a two-step approach. First, seasonality of friction measurements due to temperature and precipitation (expressed as the cumulative number of dry days between measurements) was described using a sigmoidal function that was calibrated using only CL observations under the assumption that the CL experience lower traffic repetitions and therefore the variability observed between measurements may be attributed to seasonality. Next, this seasonal model was employed to remove the seasonality from the RWP observations and in this way model the effect of traffic on friction observations. For the first model

regular non-linear regression was used, whereas for the second model a random effect structure was proposed to characterize both the individual initial friction and heterogeneity in the deterioration process.

After a series of statistical evaluations, it was concluded that only friction exhibited seasonality between measurements, therefore the seasonal model was calibrated only for friction. The proposed model is presented in Equation (1).

$$SF = \frac{Friction_{Seasonal}}{Friction_{Mean}} = 1.10 - 0.028 \times \sin\left(\frac{2\pi \times DoY}{365} + 1.59\right) - 0.0065 \times Temp - 0.0002 \times DD \quad (1)$$

where;

- SF = seasonal factor,
- $Obs_{Seasonal}$ = observed value at any given day of the year,
- Obs_{Mean} = mean value of friction or texture without seasonal effect,
- a_0 to a_4 = coefficients to be calibrated,
- DoY = Julian calendar days,
- $Temp$ = average 7-day mean temperature, Celsius degrees, and
- DD = number of dry days.

The mathematical expression proposed to describe the friction performance as a function of the cumulative traffic is included in Equation (2). This model has two distinct parts delineated by the traffic needed to reach the maximum friction; so, the first portion describes the expected friction increment after construction and the second part describes the deterioration process via an exponential function. The first part of the curve incorporates two random terms, one for the initial friction (Δa_{site}) and the other for the initial rate at which friction increases (Δb_{site}). Next, although a random structure was evaluated for both the intercept and the deterioration rate in the second portion of the model, it was found that only the intercept needed the random term (ΔA_{site}) to fully describe the process.

$$FN(T) = \begin{cases} (0.54 + \Delta a_{site}) + (0.0051 + \Delta b_{site}) \cdot T - 7.3 \times 10^{-5} \cdot T^2 \rightarrow \left[T \leq \frac{-0.0051 + \Delta b_{site}}{-14.6 \times 10^{-5}} \right] \\ (-0.44 + \Delta A_{site}) \cdot \exp[-3.7 \times 10^{-4} \cdot T] \rightarrow \left[T > \frac{-0.0051 + \Delta b_{site}}{-14.6 \times 10^{-5}} \right] \end{cases} \quad (2)$$

where;

- Δa_{site} = random effect of Phase-1 *Friction* intercept, one value per site,
- Δb_{site} = random effect of Phase-1 *Friction* rate of change, one value per site,
- ΔA_{site} = random effect of Phase-2 *Friction* intercept, one value per site, and
- T = cumulative traffic.

The random effects were estimated for each site; however, the average value of these coefficients was also estimated for each surface type evaluated as shown in Table 8.

Table 8. Average value of the parameters of the friction model for each surface type.

Surface Type	Parameters					
	<i>a</i>	<i>b</i>	<i>c</i>	T_{max}	<i>A</i>	<i>B</i>
S9.5B	0.54	0.0051	-7.27×10^{-5}	34.84	0.64	-3.70×10^{-4}
S9.5C	0.56	0.0051	-7.27×10^{-5}	35.13	0.64	-3.70×10^{-4}
S9.5D	0.56	0.0050	-7.27×10^{-5}	34.58	0.65	-3.70×10^{-4}
UTBWC	0.56	0.0050	-7.27×10^{-5}	34.61	0.66	-3.70×10^{-4}
OGFC	0.57	0.0050	-7.27×10^{-5}	34.46	0.67	-3.70×10^{-4}

The previous section discussed the variation of the friction values collected in the RWP at 40-mph and 60-mph (RWP₄₀ and RWP₆₀). A discussion with the variation observed in the CL at 60-mph (CL₆₀) is included in Appendix B. As described above, the performance models developed during FHWA/NC 2022-5 were derived using the RWP₆₀ observations and so the performance models for the alternative surface treatments were also derived using the RWP₆₀ records. Additionally, it must be noted that the friction performance model calibrated in FHWA/NC 2022-5 as shown in Equation (2) grouped the OGFC and UTBWC as a single category named ‘high friction course’ or HFC. This decision was made due to the limited sample size of these surface types in comparison to the dense-graded sites; hence, due to the new observations collected in this research effort separate models were derived for OGFCs and UTBWCs.

To calibrate Equation (2) from FHWA/NC 2022-5, the observations were first corrected for seasonality using Equation (1); however, this was not done in the analysis presented here because it was not possible to evaluate the temporal friction variation in this project on an individual basis because in this project a single record was collected per site. Hence, to avoid inducing more uncertainty in the dataset (i.e., the uncertainty associated with Equation (1)), the raw observations were used to describe friction performance without seasonal adjustment.

3.2.2. Updated Friction Performance Models for Alternative Surfaces

The details of the process followed to update the coefficients of the friction model are provided in Appendix C. A summary of the results is presented in Table 9 and Table 10. It must be noted that a performance model was not calibrated for chip seals. This treatment type is used in low traffic roads, typical of a residential or rural setting with an undivided road geometry, which differs from the facilities evaluated in FHWA/NC 2022-5. Additionally, most of the observations were in surfaces that were less than one year old with just a few observations on older pavements. As indicated in Table 9, the highest initial friction is obtained with the Microsurfacing and Microsurfacing-Alt, followed by the UTBWC. The OGFC has similar initial friction as the SMA-2 and the North Carolina’s dense-graded surface. The Dense-I/II and SMA-1 have almost the same initial friction. In terms of rate of change, the Microsurfacing-Alt and North Carolina’s Microsurfacing have the highest rate of deterioration (Parameter *B*), followed by the SMA-1 and UTBWC. Also, the fastest initial rate of change (Parameter *b*) is observed in the OGFC and SMA-1 and Dense-I/II. This finding indicates that even though the OGFC has lower friction than the UTBWC it can reach similar friction performance after some traffic repetitions.

As indicated in Table 10, the OGFC and UTBWC have similar age, but the former surface type is slightly older, 5.9 years old versus 5.3 years, respectively. The oldest sites evaluated were those with a SMA-2 surface type and the newest ones were those with a Microsurfacing surface. The sites with a Microsurfacing-Alt experienced higher traffic volumes than the ones located in North Carolina with a Microsurfacing, the former group on average has an AADT of 24,000 vpd, whereas the latter one has on average an AADT of 4,000 vpd.

Table 9. Friction model coefficients for alternative surfaces.

Surface	<i>a</i>	<i>b</i>	<i>c</i>	T_{max}	<i>A</i>	<i>B</i>
OGFC	0.56	0.0045	-7.30E-05	30.9	0.63	-4.00E-04
UTBWC	0.64	0.0007	-7.30E-05	5.0	0.65	-7.18E-04
Microsurfacing	-	-	-	-	0.75	-3.68E-02
SMA-2	0.56	0.0047	-7.30E-05	32.2	0.64	-1.94E-04
SMA-1	0.44	0.0063	-7.30E-05	43.1	0.61	-9.79E-04
Dense-I/II	0.46	0.0066	-7.30E-05	44.9	0.63	-7.10E-04
Microsurfacing-Alt	-	-	-	-	0.70	-0.15

Table 10. AADT and age of the sites used to update the friction model coefficients.

Surface	AADT			Avg Age
	Avg	Min	Max	
OGFC	31,944	5,900	115,000	5.9
UTBWC	48,451	8,900	148,000	5.3
Microsurfacing	3,911	200	30,000	1.0
Microsurfacing-Alt	24,075	2,900	57,000	0.9
Dense-I/II	33,396	1,500	109,000	4.0
SMA-2	55,583	40,000	109,000	11.1
SMA-1	54,765	40,000	134,000	6.6

A graphical comparison of the friction performance models is included in Figure 7. Additionally, the fitted models were contrasted against the observed friction in Appendix C. For the comparison, the average performance curve for the North Carolina’s dense-graded is included as well as the Non-Interchange investigatory threshold (0.57, see Table 6). As shown, both Microsurfacing surfaces start with an initial friction above the investigatory threshold, but Microsurfacing-Alt quickly reduces the available friction below that minimum friction. All the other surface types, except for the Dense-I/II and SMA-1, start with an initial friction closer to 0.57 and reach a friction value above the Non-Interchange investigatory threshold.

The models shown in Table 9 depend on the cumulative traffic. Therefore, to use the models to estimate the time (expressed in years) required for a given surface to reach the investigatory threshold proposed in the FHWA/NC 2022-5 project, it is required to know the AADT of the pavement beforehand. Because the friction model consists of two separate functions, an initial function that describes friction increase after construction and the second function that describes the deterioration once the maximum friction is reached. As mentioned earlier, the delineation of the two pieces of the friction deterioration curve occurs at T_{max} . Hence, except for the Microsurfacing and the UTBWC (that has an initial friction of 0.64, greater than the investigatory threshold of 0.57), there will be two points in time where the performance model will result in a friction number equal to the investigatory threshold, the first one when friction is increasing to reach the maximum friction and the second one when friction is decreasing.

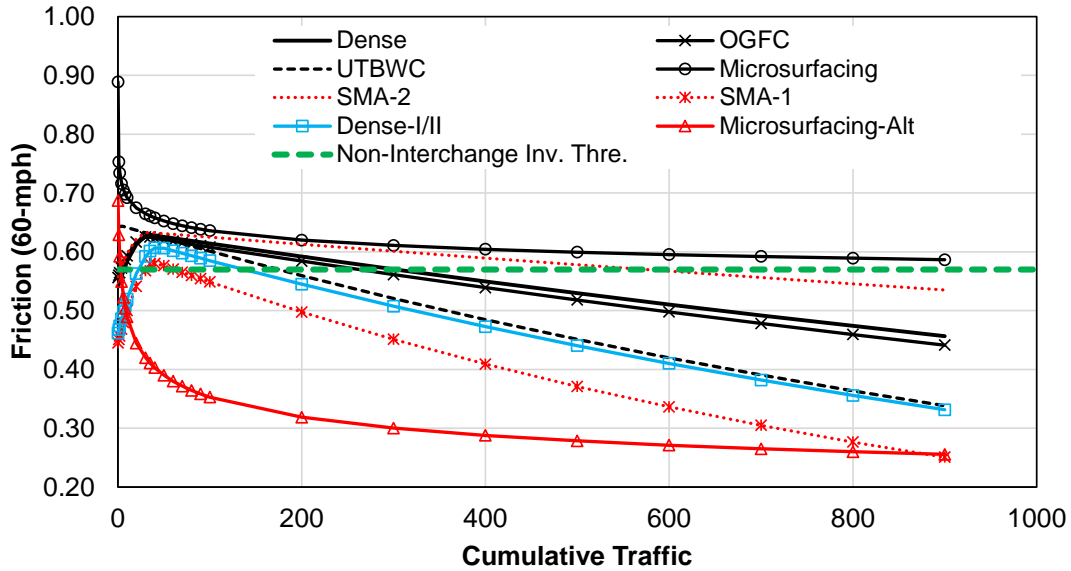


Figure 7. Graphical comparison of the friction performance models.

Using the performance models shown in Table 9, the first point in time when the performance model results in the Non-Interchange investigatory threshold was estimated and is summarized in Table 11 for different AADT values. Similarly, the second point in time when the performance model results in the Non-Interchange investigatory threshold, i.e., when friction is decreasing, is presented in Table 12.

For instance, using the OGFC friction performance model with an AADT of 30,000 vpd will result in two points in time at which friction is equal to the Non-Interchange investigatory level as shown in Figure 8. The first intersecting point will be at 0.3 years (see Table 11) and the second intersecting point will be at 23.8 years (see Table 12). This intersecting point varies depending on the value of the AADT. Because the OGFC, UTBWC, and the SMAs are used in road segments with high traffic volumes, based on the data collected a high traffic volume may be an AADT greater than 30,000 vpd, these surface treatments surpass the Non-Interchange investigatory threshold in less than half a year after construction and take more than 10 years on average to decrease the friction value below the Non-Interchange investigatory threshold. The calculations shown in Table 11 and Table 12 also indicate that the Dense-I/II surfaces take longer to reach the investigatory threshold and after reaching the maximum friction it gets below the investigatory threshold quicker than North Carolina’s dense-graded surfaces.

Table 11. Estimated number of years needed to reach the investigatory friction Non-Interchange investigatory threshold when friction is increasing.

Surface	AADT ²										
	1,000	2,000	5,000	10,000	20,000	30,000	40,000	50,000	80,000	100,000	150,000
Dense	17.8	8.9	3.6	1.8	0.9	0.6	0.4	0.4	0.2	0.2	0.1
OGFC	9.3	4.7	1.9	0.9	0.5	0.3	0.2	0.2	0.1	0.1	0.1
UTBWC						- ¹					
Microsurfacing						- ¹					
SMA-2	7.7	3.9	1.5	0.8	0.4	0.3	0.2	0.2	0.1	0.1	0.1
SMA-1	85.7	42.8	17.1	8.6	4.3	2.9	2.1	1.7	1.1	0.9	0.6
Dense-I/II	60.3	30.1	12.1	6.0	3.0	2.0	1.5	1.2	0.8	0.6	0.4
Microsurfacing-Alt						- ¹					

¹ Undefined, because the incremental portion of the performance model does not pass through the Non-Interchange investigatory threshold.

²Two-way AADT

Table 12. Estimated number of years needed to reach the investigatory friction Non-Interchange investigatory threshold when friction is decreasing.

Surface	AADT ¹										
	1,000	2,000	5,000	10,000	20,000	30,000	40,000	50,000	80,000	100,000	150,000
Dense	825.9	413.0	165.2	82.6	41.3	27.5	20.6	16.5	10.3	8.3	5.5
OGFC	715.2	357.6	143.0	71.5	35.8	23.8	17.9	14.3	8.9	7.2	4.8
UTBWC	476.7	238.3	95.3	47.7	23.8	15.9	11.9	9.5	6.0	4.8	3.2
Microsurfacing	20.8	10.4	4.2	2.1	1.0	0.7	0.5	0.4	0.3	0.2	0.1
SMA-2	1,569.8	784.9	314.0	157.0	78.5	52.3	39.2	31.4	19.6	15.7	10.5
SMA-1	167.8	83.9	33.6	16.8	8.4	5.6	4.2	3.4	2.1	1.7	1.1
Dense-I/II	374.0	187.0	74.8	37.4	18.7	12.5	9.4	7.5	4.7	3.7	2.5
Microsurfacing-Alt	3.7	1.9	0.7	0.4	0.2	0.1	0.1	0.1	0.0	0.0	0.0

¹Two-way AADT

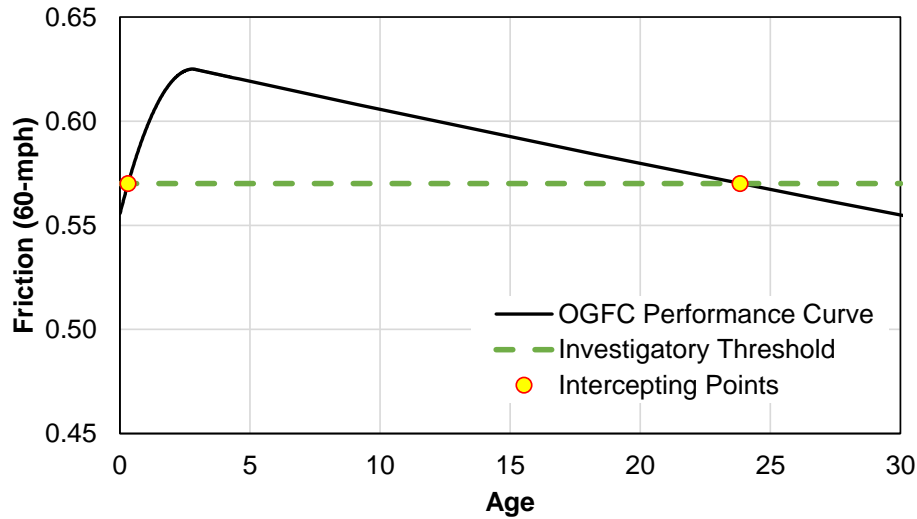


Figure 8. Points in time at which the OGFC reaches the Non-Interchange investigatory threshold.

3.3. Macrotexture

3.3.1. High-Speed Texture – RWP

The *MPD* observations collected with the AMES AccuTexture 100 laser in NC G1, G2, and G3 group of sites, as well as the measurements taken outside North Carolina, are graphically compared in Figure 9 for the measurements made in the RWP. The graphical comparison for the CL records is included in Appendix B. As indicated in Table 3, each surface type encompasses sites with different ages and traffic volumes, therefore, Figure 9 provides a general visualization of the *MPD* values one could expect over the entire performance curve for each surface type. For reference, the investigatory threshold proposed in FHWA/NC 2022-5 is included in Figure 9 to visually identify the surface types that have macrotexture values above the thresholds proposed in FHWA/NC 2022-5. These values are also summarized in Table 13. Additionally, Table 14, also shown below, includes a summary of the three statistics computed for the *MPD* values, i.e., the 25th and 75th *MPD* percentile of all the sites with a given surface type. For reference, the investigatory threshold is included in Figure 9 to visualize which surface types have *MPD* values above the thresholds. The dense-graded *MPD* values were included in Figure 9 as a reference of comparison.

As indicated in Figure 9, the dense-graded surfaces were the ones with the lowest *MPD* values, the IQR for this surface spanned from 0.38 to 0.61 mm, with an average value of 0.46 mm. As presented in Table 3, the average age of the dense-graded sites was 4.9 years. For the UTBWC sites, the research projects FHWA/NC 2020-11 and FHWA/NC 2022-5 focused on data collected from sites with an in-service period shorter than three years, although some sites with older ages were included. In contrast, the current project included more sites with ages greater than three years. Therefore, the distribution of UTBWC in the previous two projects had a lower mean than the data collected in this research (1.06 mm versus 1.16 mm). The opposite situation occurred for the OGFCs, where the previous two projects had a mean *MPD* of 1.28 mm compared against the latest project with a mean of 1.12 mm.

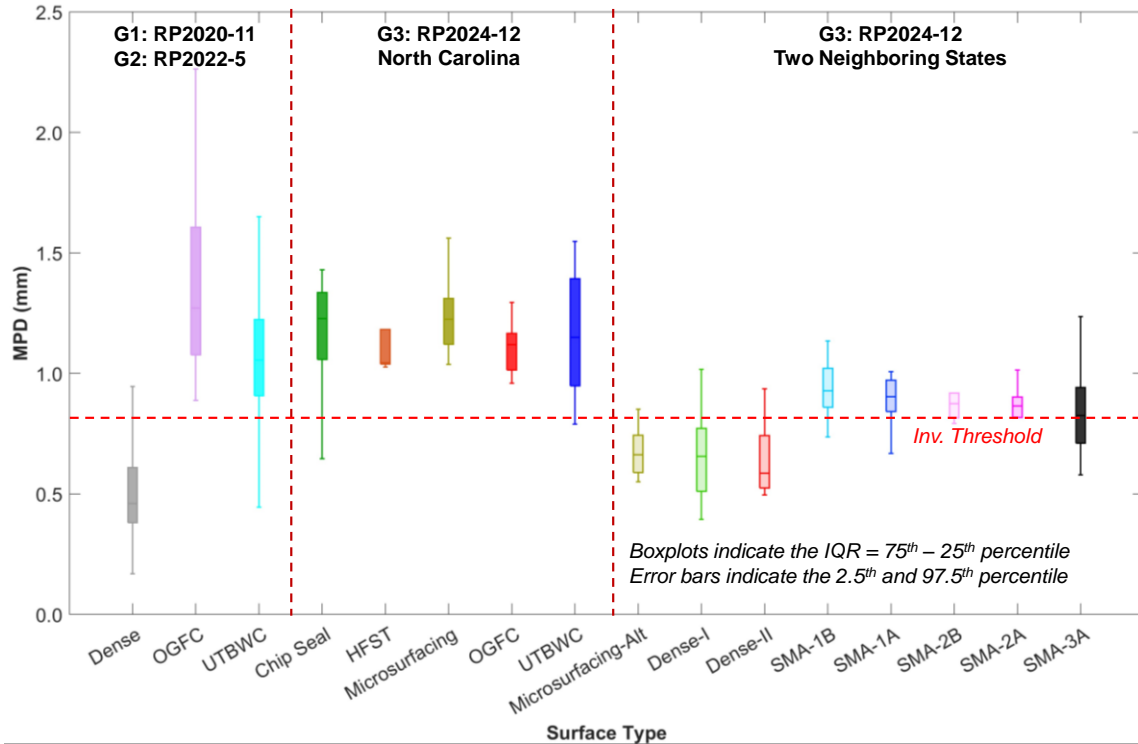


Figure 9. Distribution of the MPD measurements made in the RWP for each surface type.

Table 13. Recommended MPD investigatory and intervention thresholds.

Variable	Non-Interchanges	Interchanges
MPD_{INV}	0.80	0.80
MPD_{INT}	0.60	0.60

Table 14. Summary of MPD statistics computed for each surface type.

Data Set	Surface Type	MPD RWP (mm) ¹		
		P ₂₅	P ₇₅	Mean
NC G1 and G2	Dense	0.38	0.61	0.46
	OGFC	1.08	1.61	1.28
	UTBWC	0.90	1.22	1.06
NC G3	Chip Seal	1.06	1.34	1.23
	Microsurfacing	1.12	1.31	1.22
	OGFC	1.01	1.17	1.12
	UTBWC	0.95	1.40	1.16
	HFST	1.04	1.18	1.10
Two Neighboring States	Microsurfacing-Alt	0.59	0.74	0.67
	Dense-I	0.51	0.77	0.66
	Dense-II	0.53	0.74	0.58
	SMA-2A	0.82	0.90	0.87
	SMA-2B	0.82	0.92	0.87
	SMA-1A	0.84	0.97	0.90
	SMA-1B	0.86	1.02	0.93
	SMA-3A	0.71	0.94	0.82

¹ P₂₅ = 25th MPD percentile, P₇₅ = 75th MPD percentile, Mean = average MPD value

Also from Figure 9, the chip seals and the Microsurfacing sites are found to have similar *MPD* values, although the IQR of the chip seals is wider, reflecting the considerable variability observed in the chip seal surfaces. This outcome was expected considering different gradations may be used for the surface layer of chip seals, e.g., 78M versus #9 or 5/16th inch lightweight aggregate, which would yield different *MPDs*. The IQR of the HFST was close to that of the OGFCs tested in this project; however, only five sites with a HFST were tested. Although the Dense-I/II sites had higher texture values than the dense-graded sites tested in North Carolina, the difference was only 0.20 and 0.12 mm for the Dense-I and Dense-II, respectively. For the SMAs, the IQR of the SMA-1 and SMA-2 had similar values. On average, the sites with an SMA-1 and SMA-2 have an *MPD* above the investigatory threshold shown in Table 13. In contrast, the SMA-3A had the lowest *MPD* values recorded on this surface type (mean of 0.82 mm).

3.3.2. Static Measurements

The 3D surface scans collected with the AMES 9500 rlts were processed with the software that accompanies the laser and the *MPD*, *RMSD*, *Rsk*, and *Rku* were compared for the different surface types. The detailed analysis is included in Appendix D. The static laser measurements are intended to supplement the knowledge provided by the high-speed texture measurements. The *MPD* and *RMSD* obtained from the surface scans confirm the findings made with the high-speed texture records, i.e., both quantities increase with pavement age. The skewness of North Carolina's Microsurfacing increases with age and is similar to the values observed in the Microsurfacing-Alt. The surfaces with the highest *Rsk* are the OGFC, SMA-1, and SMA-2. The lowest *Rku* values were recorded in the Microsurfacing-Alt, followed by North Carolina's Microsurfacing. The *Rku* reduced with age, as a reflection of the traffic polishing that wear the peaks of the texture profile. The surface with the highest kurtosis is SMA-1.

3.4. Calibration of Texture Performance Models

Because previous performance models were derived using the RWP observations, the performance models for the alternative surfaces were also derived using the RWP records. Additionally, it must be noted that the *MPD* performance model calibrated in the research project FHWA/NC 2022-5 and shown in Equation (3) grouped the OGFC and UTBWC in a single category named 'high friction course' (HFC). This decision was made due to the limited sample size on these surface types in comparison to the dense-graded sites; however, due to the new observations from this research effort separate models were derived for OGFCs and UTBWCs. Additionally, for the OGFC, UTBWC, and for the other surface types only average values of the random effects could be obtained. For the observations made in the neighboring states, the data was categorized into the three climate regions, although these regions correspond to North Carolina boundaries, it is assumed that the same weather longitudinal variation prevails in both neighboring states, i.e., the vertical delineation of the polygons that delimits North Carolina's climate regions also applies for the neighboring states.

3.4.1. Texture Performance Models in FHWA/NC 2022-5

The functional form of the texture performance model is presented in Equation (3). As shown, the model incorporates random effects in the intercept and the rate of change. The former is specific for each site and the latter is a random term associated with the family the site belongs to. In total, six different families were defined based on the combination of surface type and climate region as indicated in Table 15. To get an average performance curve for each surface type, the average value of the intercept random effect is presented in Table 16.

$$MPD = (0.48 + \Delta a_{site}) \cdot T^{(0.13 + \Delta b_{family})} \quad (3)$$

where;

Δa_{site} = random effect of *MPD* intercept, one value per site,

T = cumulative traffic, and

Δb_{family} = random effect of *MPD* rate of change, one value per family.

Table 15. Random effect coefficients for the *MPD* rate of change.

Family	Parameter Δb_{family}	Surface Type	Climate Region
1	-0.070	Dense	Mountains
2	-0.055	Dense	Piedmont
3	-0.029	Dense	Coastal
4	-0.010	HFC	Mountains
5	0.070	HFC	Piedmont
6	0.095	HFC	Coastal

Table 16. The average value of the intercept random effect coefficient.

Surface Type	Δa_{site}
S9.5B	-0.15
S9.5C	-0.18
S9.5D	-0.12
OGFC	0.22
UTBWC	0.32

3.4.2. Updated Texture Performance Models for Alternative Surfaces

The texture performance models for each surface type, except for the chip seals, were updated by combining the records from the previous projects, datasets NC G1 and G2, with the new observations made in this research effort. A performance model was not calibrated for chip seals. This treatment type is used in low traffic roads, typical of a residential or rural setting with an undivided road geometry, which differs from the facilities evaluated in FHWA/NC 2022-5. Additionally, most of the observations were on surfaces that were less than one year old with just a few observations in older pavements. A detailed discussion of the procedure followed to update these coefficients is included in Appendix C and a summary of the results is provided in Table 17.

In Table 17, instead of providing the random effect of the intercept and the rate of change, the sum of the fixed effect and the random term is provided, i.e., $a + \Delta a_{site}$ and $b + \Delta b_{family}$, respectively. As shown in the table above, the only surface type that exhibited a texture deterioration was the Microsurfacing. A similar performance may be expected from chip seals, although a performance model for this surface was not derived. For the calibration, the rate of change estimated in the FHWA/NC 2022-5 for the three HFC families indicated in Table 15 were used whenever possible and the parameter that was updated was the intercept; however, based on the observations, in some instances both coefficients needed to be updated. Also, for some combinations of surface type and climate region, the data suggested different trends that needed separate performance curves, e.g., the OGFC in the coastal region in Table 17 has six performance curves. These individual trends were induced by differences in the traffic level or in the pavement age of the sites used for calibration. Lastly, for both the OGFCs and UTBWCs the original average performance curve (estimated based on the information of Table 15 and Table 16) is also included in Table 17. The calibrated performance curves were graphically compared against the observed *MPD* values for each surface type to verify the model fit. This comparison is presented in Appendix C.

Table 17. Texture model coefficients for alternative surfaces.

Surface Type	Family	Model	$a+\Delta a_{site}$	$b+\Delta b_{family}$	AADT			Avg Age
					Avg	Min	Max	
OGFC	Coastal	Average	0.70	0.225	22,968	5,900	47,000	5.4
		Model 1 ²	0.70	0.115	12,286	11,000	15,500	7.5
		Model 2 ²	0.63	0.390	57,500	47,500	65,000	4.4
	Piedmont	Average ¹	0.70	0.200	-	-	-	-
		Model 1 ²	0.94	0.055	55,944	14,500	115,000	4.9
	Mountains	Average	0.70	0.120	55,500	55,500	55,500	9.2
Model 1 ²		0.65	0.231	23,450	18,500	32,500	7.1	
UTBWC	Coastal	Average ¹	0.80	0.225	-	-	-	-
		Model 1 ²	1.11	0.083	31,285	8,900	40,000	2.6
	Piedmont	Average ¹	0.80	0.200	-	-	-	-
		Model 1 ²	0.81	0.087	58,284	11,000	148,000	6.4
	Mountains	Average ¹	0.80	0.120	39,083	18,500	65,500	4.0
		Model 1 ²	0.70	0.065	47,875	18,500	62,500	7.5
Microsurfacing	All Regions	Model 1 ²	0.90	-0.070	3,948	200	30,000	1.2
Microsurfacing-Alt	All Regions	Model 1 ²	0.73	-0.071	26,781	930	69,000	0.8
Dense-I/II	Coastal	Model 1 ²	0.48	0.225	70,500	42,000	119,000	2.2
		Model 2 ²	0.32	0.120	2,300	1,500	3,700	4.2
	Piedmont	Model 1 ²	0.36	0.200	19,036	2,300	40,000	4.7
SMA-1	Coastal	Model 1 ²	0.26	0.225	50,000	50,000	50,000	8.3
	Piedmont	Model 1 ²	0.38	0.200	47,500	40,000	56,000	6.5
	Mountains	Model 1 ²	0.58	0.120	44,600	42,000	47,000	5.2
SMA-2	Coastal	Model 1 ²	0.26	0.225	84,250	56,000	109,000	11.1
	Piedmont	Model 1 ²	0.33	0.200	41,429	40,000	42,000	11.0
	Mountains	Model 1 ²	-	-	-	-	-	-
SMA-3	-	Fit SMA-3A	0.48	0.200	58,000	35,500	102,600	0.36

¹ 'Average' means the average performance curve estimated in the FHWA/NC 2022-5 project.

² Model 1 and 2 are observed variations of the average performance curve.

A graphical comparison, like the one shown in Figure 10 for OGFCs, was made for each surface type. These graphs are included in Appendix C. The results indicate that the OGFC and UTBWC have an average texture value higher than 0.80 mm in all the performance curves, the latter surface tends to have higher initial texture on average, but the OGFC can reach higher texture values later on. The Microsurfacing used in North Carolina showed higher texture values; however, as indicated in Table 17, the sites with a Microsurfacing-Alt experienced higher traffic levels, on average the AADT on North Carolina's Microsurfacing was nearly 4,000 vpd, whereas the average AADT on the sites with Microsurfacing-Alt was around 27,000 vpd. The Dense-I/II surface has initial *MPD* values higher than the North Carolina dense-graded surfaces with a similar rate of change.

The models shown in Table 17 depend on the cumulative traffic. To use the models to estimate the time (in years) required for a given surface to reach the investigatory threshold proposed in FHWA/NC 2022-5, the AADT of the pavement should be known beforehand. For example, for the OGFCs six performance curves were proposed; three for the Coastal area, one for the Piedmont area, and two for the Mountains. These curves are plotted in Figure 10 and Figure 11. From these figures it can be seen that except for the Piedmont Model 1 (Pi-Model 1 in Figure 11), all the other

curves reach the investigatory threshold of 0.8 mm at approximately 1.1 years. If instead of 5,000 vpd, the AADT is equal to 50,000 vpd, then the threshold is reached in only 0.11 years. This process was repeated for different AADT values and the variation in the number of years needed to reach the investigatory threshold for the OGFC sites is shown in Figure 12.

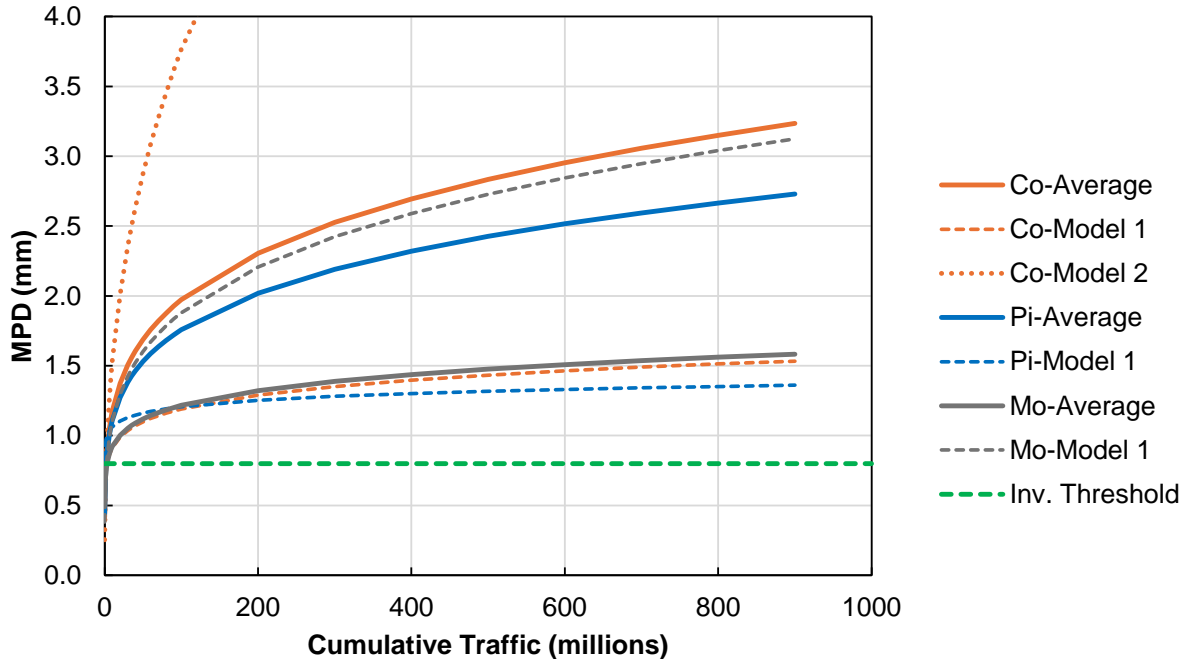


Figure 10. OGFCs proposed *MPD* performance curve (Co: Coastal, Pi: Piedmont, Mo: Mountains).

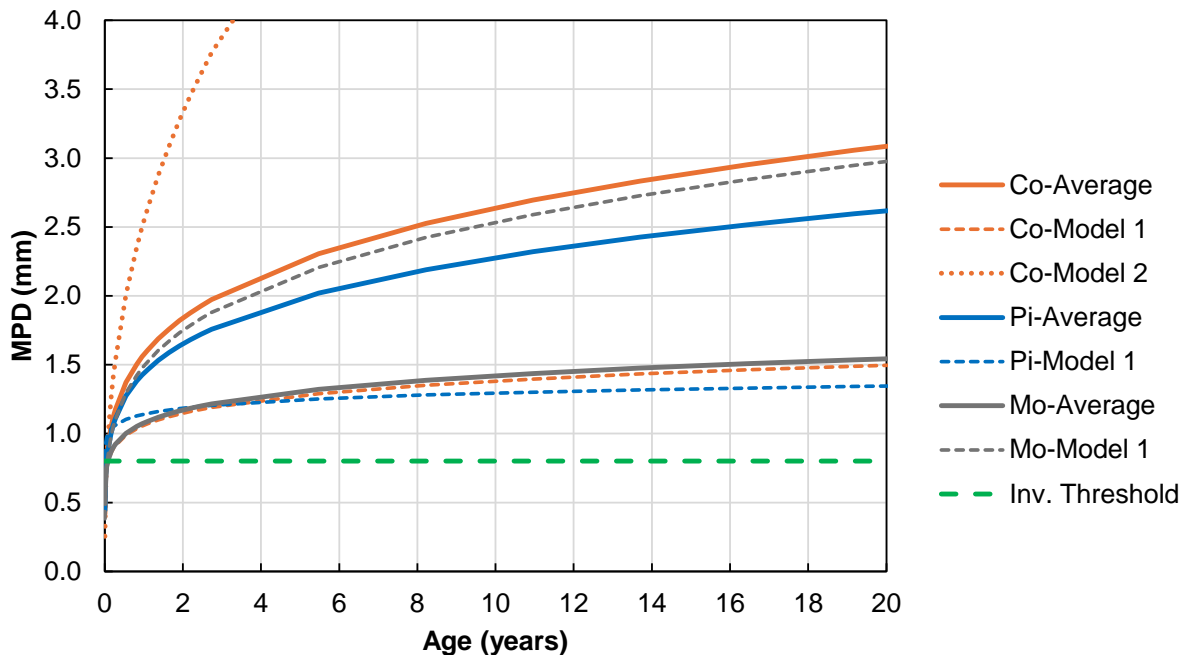


Figure 11. OGFCs proposed *MPD* performance curve when the AADT = 5,000 vpd (Co: Coastal, Pi: Piedmont, Mo: Mountains).

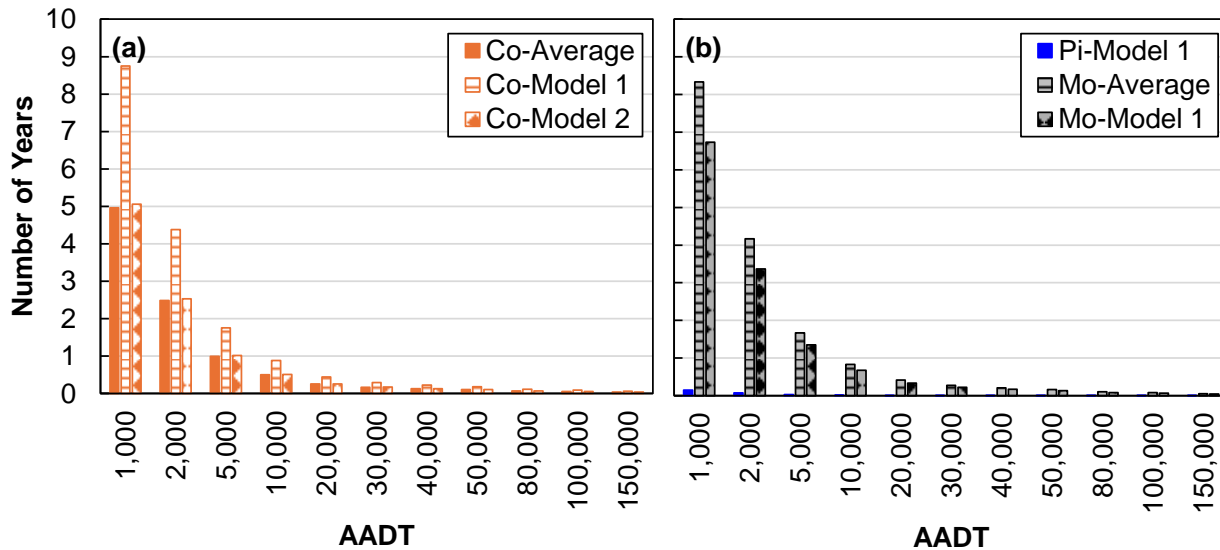


Figure 12. Number of years required to reach the texture investigatory threshold for: (a) sites in the coastal plain region and (b) sites in the piedmont and mountains.

A similar procedure was applied for all the performance models shown in Table 17. This process was made using the coefficients of the performance models and different AADT values. The estimated number of years needed to reach the investigatory texture threshold for each surface type is presented in Table 18.

Based on the average value of the coefficients for the dense-graded surfaces shown in Table 15 and Table 16 none of the dense-graded alternatives reach the investigatory threshold. As shown in Table 18, the OGFC and UTBWC are the surface treatments that reach the investigatory threshold quicker. For an AADT of 10,000 vpd, the time needed to reach the investigatory threshold is on average less than one year. For the same AADT, the North Carolina’s Microsurfacing drops to an *MPD* value less than 0.8 mm in approximately 1.5 years, whereas the Microsurfacing-Alt has *MPD* values lower than 0.8 mm in less than 2 months.

In the case of the Dense-I/II surface type, for an AADT of 10,000 vpd the time needed to reach the investigatory threshold varies from 2.7 to 14.8 years, with Model 2 never surpassing this value. This finding suggests that the Dense-I/II surface mix can be used in the Coastal region when traffic is high enough for texture to develop (higher than 50,000 vpd). Because the SMAs are typically used in high traffic locations, the texture in this pavement surface is expected to exceed the investigatory threshold in approximately half to four years if the AADT is higher than 100,000 vpd.

Table 18. Estimated number of years needed to reach the investigatory texture threshold.

Surface Type	Family	Model	AADT ³												
			1,000	2,000	5,000	10,000	20,000	30,000	40,000	50,000	80,000	100,000	150,000		
OGFC	Coastal	Original	5.0	2.5	1.0	0.5	0.2	0.2	0.1	0.1	0.1	0.0	0.0		
		Model 1	8.7	4.4	1.7	0.9	0.4	0.3	0.2	0.2	0.1	0.1	0.1		
		Model 2	5.1	2.5	1.0	0.5	0.3	0.2	0.1	0.1	0.1	0.1	0.0		
	Mountains	Original	8.3	4.2	1.7	0.8	0.4	0.3	0.2	0.2	0.1	0.1	0.1		
		Model 1	6.7	3.4	1.3	0.7	0.3	0.2	0.2	0.1	0.1	0.1	0.0		
		UTBWC	Model 1	0.1	0.0	0.0	0.0	0.0	0.0	0.0	0.0	0.0	0.0	0.0	
UTBWC	Piedmont	Model 1	2.4	1.2	0.5	0.2	0.1	0.1	0.1	0.1	0.0	0.0	0.0		
		Original	2.7	1.4	0.5	0.3	0.1	0.1	0.1	0.1	0.1	0.0	0.0		
	Mountains	Model 1	21.4	10.7	4.3	2.1	1.1	0.7	0.5	0.4	0.3	0.2	0.1		
		Microsurfacing ¹	All Regions	Model 1	14.7	7.4	2.9	1.5	0.7	0.5	0.4	0.3	0.2	0.1	
Microsurfacing-Alt ¹	All Regions	Model 1	0.8	0.4	0.2	0.1	0.0	0.0	0.0	0.0	0.0	0.0	0.0		
Dense-I/II	Coastal	Model 1	26.5	13.3	5.3	2.7	1.3	0.9	0.7	0.5	0.3	0.3	0.2		
		Model 2	- ²	- ²	- ²	- ²	- ²	- ²	- ²	- ²	- ²	70.9	56.7	37.8	
SMA-1	Piedmont	Model 1	- ²	74.2	29.7	14.8	7.4	4.9	3.7	3.0	1.9	1.5	1.0		
	Coastal	Model 1	- ²	- ²	80.9	40.5	20.2	13.5	10.1	8.1	5.1	4.0	2.7		
		Model 1	- ²	56.7	22.7	11.3	5.7	3.8	2.8	2.3	1.4	1.1	0.8		
SMA-2	Mountains	Model 1	40.0	20.0	8.0	4.0	2.0	1.3	1.0	0.8	0.5	0.4	0.3		
		Coastal	Model 1	- ²	- ²	80.9	40.5	20.2	13.5	10.1	8.1	5.1	4.0	2.7	
SMA-3	-	Fit SMA-3A	Piedmont	Model 1	- ²	- ²	45.9	22.9	11.5	7.6	5.7	4.6	2.9	2.3	1.5
			Model 1	35.2	17.6	7.0	3.5	1.8	1.2	0.9	0.7	0.4	0.4	0.2	

¹The Microsurfacing exhibited a decreasing MPD trend with respect to the cumulative traffic, therefore the time estimate shown here corresponds to the time when texture went down the investigatory threshold.

²Undefined.

³Two-way AADT

3.5. Future work

The friction and texture performance models presented here were derived by combining observations from pavements with different surface types, in different locations, and of different ages. Although estimates of the random effects, used to account for the heterogeneity in the friction/texture performance among pavements with the same surface type, were obtained by analyzing the data at this aggregate level, better estimates of the random variation could be obtained by recalibrating the random coefficients for each site as more observations become available, especially for pavements with SMA and Microsurfacing surfaces, as was done in FHWA/NC 2022-5.

Various research efforts have been made to evaluate the role of macrotexture in hydroplaning potential. Many of these studies were used to develop the Hydroplaning Assessment Tool (HAT) employed by the NCDOT to assess the hydroplaning potential of existing and new geometric designs. The models that are used to calculate water film thickness in the HAT tool use the pavement surface mean texture depth (*MTD*) as an input. However, these models do not account for the effect of rutting in hydroplaning speed predictions. A rutted pavement results in areas where water can pond, thereby increasing the hydroplaning risk for the same *MTD* value. More research is needed to account for the interaction effect between surface macrotexture and rutting in the prediction of the hydroplaning potential.

3.6. Conclusions

The observations collected in the current study supplemented the information and the analysis performed in the two previous studies. The friction and texture performance curves for the OGFC and UTBWC were updated to better reflect the variability of these surface types. The analysis presented here confirmed the hypothesis made in the FHWA/NC 2022-5 project, i.e., the variability in the friction and texture performance requires the use of site-specific models to properly describe the performance variation. This is achieved by using random effect terms, therefore the analysis presented here provided an initial estimate of the random effect terms for different combinations of surface type and climate regions.

The graphical comparison, and the results of the models, indicated that overall North Carolina Microsurfacing surfaces have high friction and macrotexture. Particularly, the friction of Microsurfacing surfaces is always above the Non-Interchange investigatory threshold but the macrotexture on this surface type showed a decreasing trend with time, meaning macrotexture will fall below the *MPD* investigatory threshold later in life. The Dense-I and Dense-II surfaces showed similar friction performance to North Carolina dense-graded surfaces, but the Dense-I/II have higher macrotexture and surpass the investigatory threshold quicker based on the analysis conducted. Lastly, all the SMAs, with the exception of SMA-3, have friction and texture higher than the Non-Investigatory threshold. The SMAs showed a faster *MPD* rate of change, while the friction rate of change varied between the SMAs evaluated. SMA-1 has a faster rate of change in contrast to North Carolina dense-graded surfaces, but SMA-2 has a lower rate of change than North Carolina dense-graded surfaces. Although a separate performance model was not derived for SMA-3, the data suggested a texture performance like SMA-2 with a faster friction rate of change than SMA-2.

This page is intentionally blank

4. PERFORMANCE COMPARISON OF ALTERNATIVE SURFACE TREATMENTS

4.1. Overview

This chapter presents the performance evaluation of SMA mixtures sampled from two adjacent states, States 1 and 2, in relation to typical dense-graded asphalt mixtures currently used in North Carolina. The evaluation consisted of linear viscoelastic (LVE) characterization using the dynamic modulus test (AASHTO TP 132), cracking characterization using the uniaxial cyclic fatigue test (AASHTO T 411) and IDT-CT test (ASTM D8225-19), and rutting characterization using the stress sweep rutting test (AASHTP TP 134).

The evaluation of the SMA mixtures was compared against dense-graded mixtures from the FHWA/NC 2019-20 research study, “*Calibration of Structural Layer Coefficients for North Carolina Asphalt Pavements.*” Seven surface mix designs from the FHWA/NC 2019-20 study served as benchmarks for comparing the SMAs sampled from States 1 and 2. These seven mixtures were sampled from the Mountain (MO), Piedmont (PI), and Coastal (CO) regions in North Carolina, allowing for performance comparisons of the SMAs based on climatic regions. The mix design information for the mixtures characterized in both the FHWA/NC 2019-20 study and this project is presented in Table 19. It should be noted that although the SMA-1A and SMA-3 mixes are identified in their corresponding JMFs as 12.5 mm and 9.5 mm mixtures, they are 19.0 mm and 12.5 mm mixtures, respectively, based on the NMAS definition.

4.2. Experimental test results

This section summarizes the relevant test results and statistical analysis, using the surface mixtures from the Piedmont region as a benchmark. Detailed testing procedures and results for the other regions are in Appendix F.

4.2.1. Dynamic Modulus Test Results

Figure 13 presents the dynamic modulus master curves in logarithmic and semi-logarithmic scales as well as the phase angle master curves for the SMAs and surface mixtures from the Piedmont region. All of these curves are shown at a reference temperature of 21.1°C. This figure also includes the 2S2P1D model fitting of the dynamic modulus and phase angle, obtained using FlexMAT Cracking v2.1.4.5.

Figure 13 shows that the SMA-3 mixture has moduli values like the RS9.5B-PI and RS9.5C-PI mixtures at the low reduced frequency range (corresponding to high temperatures), but slightly higher values at the high reduced frequency range (corresponding to low temperatures). Further, the linear viscoelastic characterization indicates that the SMA-1A has moduli values that are higher than the RS9.5B-PI and RS9.5C-PI mixtures across the entire frequency range. Yet, it is still softer than the RS9.5D-PI design. This aspect is notable because SMAs are typically used in pavements with high friction demand and high traffic volume. Therefore, the RS9.5D-PI mixture, designed for the highest traffic volume in North Carolina (more than 30 million ESALs), would be the most appropriate benchmark for comparing against the SMA mixtures. Substantial modulus differences are observed, which may impact the overall pavement response. The differences in the linear viscoelastic response can be traced back to differences in binder content between the dense-graded and SMA mixtures and other compositional factors. A detailed comparison of the SMAs results to surface mixtures from the Mountain and Coastal regions is presented in Appendix F.

Table 19. Mix design information of SMAs and surface mixtures evaluated in FHWA/NC 2019-20.

Properties	Mixture								
	RS9.5B			RS9.5C			RS9.5D	SMA	
	MO	PI	CO	MO	PI	CO	PI	SMA-3	SMA 1-A
JMF NMAS (mm)	9.5	9.5	9.5	9.5	9.5	9.5	9.5	9.5	12.5
Binder Grade (Mix Design)	64-22	58-28	64-22	64-22	58-28	64-22	76-22	_ ¹	_ ¹
Binder Grade (Pay Grade)	64-22	64-22	64-22	64-22	64-22	64-22	76-22	_ ¹	_ ¹
Binder Content (%)	6.5	6.3	5.8	5.5	5.8	7.0	5.6	6.0	6.3
RBR%	15%	33%	24%	25%	33%	14%	18%	10%	N.A
V _{be} (Mix Design)	14.4	13.4	13.2	11.9	12.6	14.6	12.4	N.A	N.A
RAP Content (%)	20	40	30	30	40	20	20	11	13
RAS Content (%)	0	0	0	0	0	0	0	0	0
N _{des}	50	50	50	65	65	65	100	_ ⁽³⁾	_ ⁽³⁾
VFA (Mix Design)	79	77.2	75.1	75	76.2	77.8	75.6	68	N.A. ²
VMA (Mix Design)	18.4	17.4	17.2	15.9	16.6	18.6	16.4	17.8	N.A. ²
G _{mm} (Mix Design)	2.475	2.458	2.449	2.46	2.439	2.328	2.496	2.428	2.639
G _{mm} (NCSU Measured)	2.495	2.422	2.408	2.473	2.452	2.367	2.499	2.432	2.647
Gradation (% Passing)									
19.0 mm	100	100	100	100	100	100	100	100	100
12.5 mm	100	100	100	100	99	100	100	97	85
9.5 mm	97	98	98	98	96	98	97	85	65
4.75 mm	87	80	73	74	75	83	72	46	26
2.36 mm	60	62	60	54	58	65	53	25	20
1.18 mm	44	48	51	41	45	53	41	-	-
0.600 mm	33	37	41	31	34	40	31	18	17
0.300 mm	22	24	27	21	22	27	22	-	-
0.150 mm	11	13	13	13	11	9	11	12	-
0.075 mm	6.2	7.2	7.1	7.0	6.5	5.2	6.0	8.1	10.0

¹ Binder grade not shown to ensure anonymity of the mixture source. However, both SMA mixtures contain polymer modified asphalt binder.

² Design gyrations omitted to ensure anonymity of the mixture source.

³ N.A: Not available

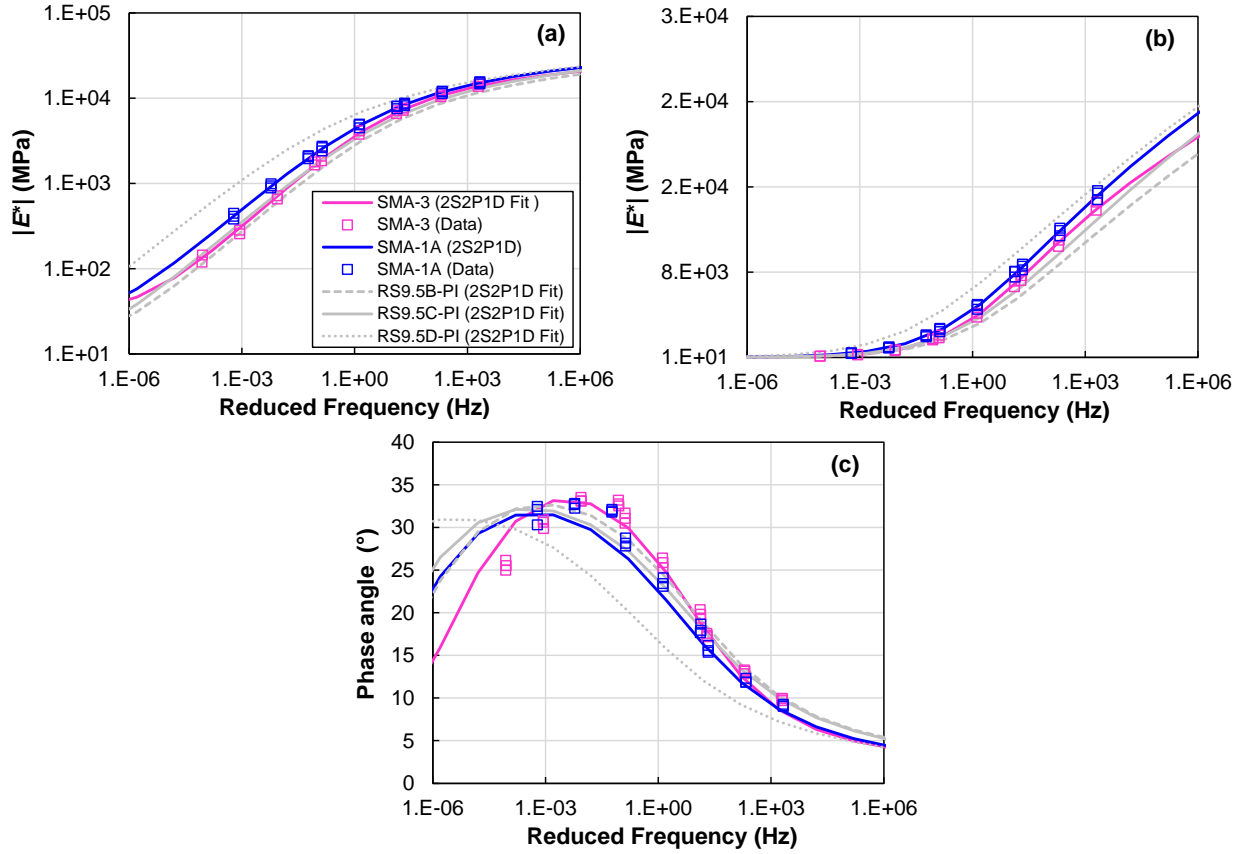


Figure 13. Dynamic modulus and phase angle results for SMAs and surface mixtures from the NC Piedmont region: (a) dynamic modulus master curve log-log plot, (b) dynamic modulus master curve semi-log plot, and (c) phase angle master curve.

4.2.2. Uniaxial Cyclic Fatigue Test Results

The results from the uniaxial cyclic fatigue test are presented in Figure 14 for the SMAs and surface mixtures from the Piedmont region. The results shown in Figure 14 (a) indicate that both SMA designs closely follow the same damage characteristic curve of the RS9.5C and RS9.5B designs from the Piedmont region. At the same time, the RS9.5D-PI mixture is situated in a higher position in the C versus S plot. This observation aligns with the expectation that damage characteristic curves of higher modulus mixtures tend to be positioned vertically higher than other mixtures.

Figure 14 (b) shows the relationship between the cumulative reduction in pseudo-stiffness ($1-C$) and the number of cycles, and the slope of such relationship, D^R . A higher D^R generally indicates a superior ability to absorb energy before failure. The results suggest that the SMAs mixtures have D^R values inferior to the RS9.5B-PI and RS9.5C-PI mixtures but superior to the RS9.5D-PI. In addition, it is seen that the SMA-1A has superior damage resistance compared to SMA-3. Figure 14 (c) presents the S_{app} parameter for the same set of mixtures. The S_{app} parameter is calculated using a location specific temperature, and for the analysis here the location chosen was Garner, NC. Additionally, the S_{app} of the SMAs has been calculated using the critical temperatures from Wilmington and Asheville, NC, and compared against the S_{app} of dense-graded mixtures sampled in Coastal and Mountainous region, respectively. This index parameter accounts for two main

factors that govern the fatigue cracking potential of asphalt mixtures: the mixtures' stiffness and damage resistance. As shown in Figure 14 (c), the SMA-1A has a S_{app} value comparable to the RS9.5D-PI mixture. The SMA-3 exhibits lower S_{app} values than RS9.5B-PI and RS9.5C-PI mixtures but higher S_{app} than the SMA-1A despite having a lower D^R value. This result suggests that other factors, such as material stiffness, among others, have a dominant role in the S_{app} of these mixtures. The comparison against the dense-graded mixtures from the Coastal and Mountainous regions suggests that the SMAs have equal or better fatigue damage performance in terms of S_{app} .

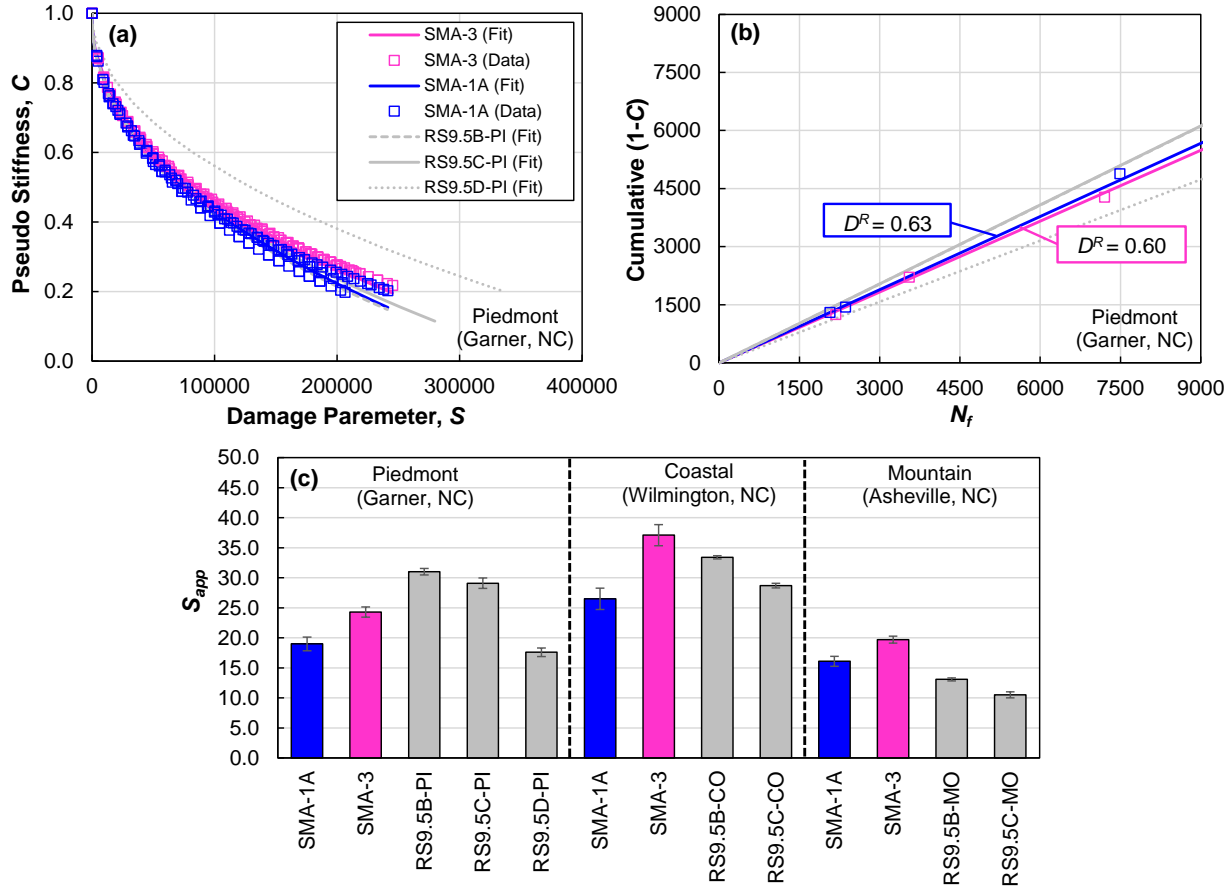


Figure 14. Cyclic fatigue test results for SMAs and surface mixtures: (a) damage characteristic curve, (b) failure criteria plot, and (c) S_{app} results.

4.2.3. IDT-CT Results

Figure 15 presents the CT_{Index} values for the SMA mixtures evaluated in this project, along with the dense-graded mixtures evaluated from the FHWA/NC 2019-20 and FHWA/NC 2023-3 projects. The IDT-CT characterization for the SMAs was performed using specimens compacted at $7.0 \pm 0.5\%$ air voids. In contrast, the FHWA/NC 2019-20 project mixtures were evaluated using specimens compacted at $5.0 \pm 0.5\%$ air voids. The CT_{Index} values from the FHWA/NC 2019-20 data set were adjusted with a correction factor developed by Montanez et al. (29) to normalize the results to a uniform air void level, equal to 7.0% in this study. Details of this method are presented in Appendix F. The FHWA/NC 2023-3 data is included to provide additional reference of North Carolina CT_{Index} values of dense-graded mixtures.

The results shown in Figure 15 suggest that the cracking performance of the SMAs mixtures from States 1 and 2 is substantially better than that of dense-graded mixtures for all climatic regions and traffic classifications in North Carolina. This result is unexpected, as the cyclic fatigue characterization suggested that the cracking performance of the SMAs is similar or inferior to that of dense-graded mixtures. However, previous studies have suggested that the CT_{Index} is more sensitive to compositional changes in the mixture than the S_{app} parameter. This sensitivity may explain the greater differentiation in performance observed between the SMAs and dense-graded mixtures, which have different aggregate structures and design characteristics. Despite this observation across mixture types, both tests show that the SMA-3 exhibits superior cracking performance than the SMA-1A design.

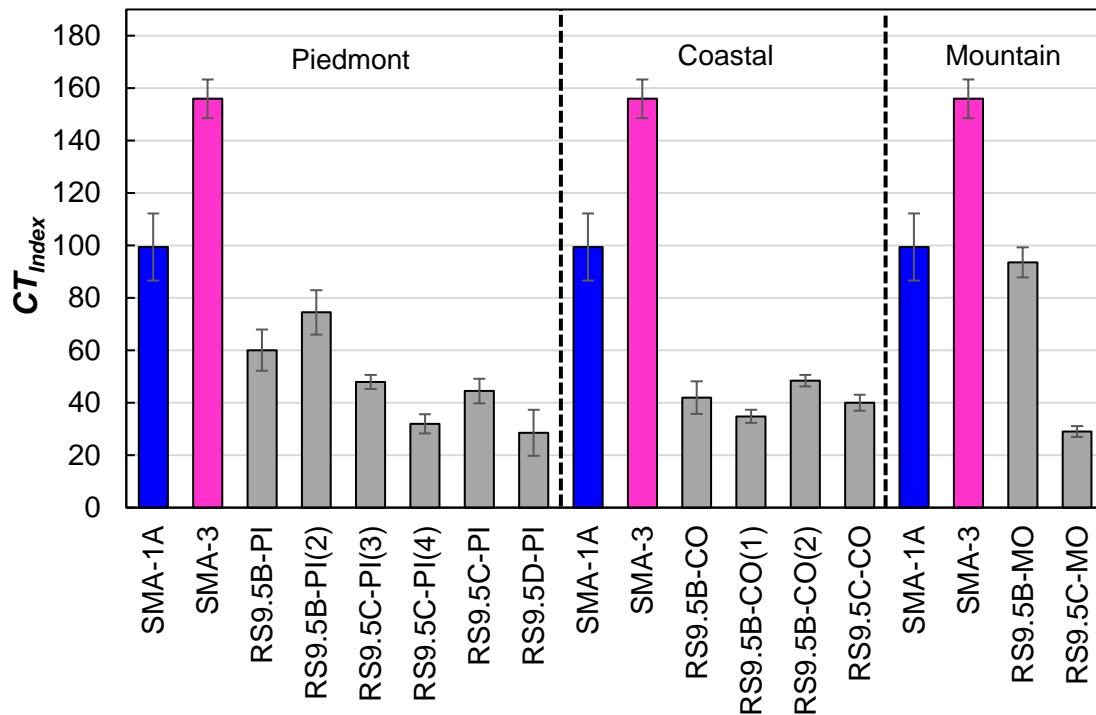


Figure 15. IDT-CT test results for SMAs and surface mixtures from the NC Piedmont region. The asterisk denotes the mixtures evaluated in the FHWA/NC 2023-3 project. The error bars indicate CT_{Index} variability plus/minus one standard deviation.

4.2.4. Stress Sweep Rutting Test Results

The results from the SSR test are presented in Figure 16 for the SMAs and surface mixtures from the Piedmont region. Figure 16 (a) and (b) illustrate the evolution of viscoplastic strain (ϵ_{vp}) with the number of cycles at temperatures of 29°C and 51°C, respectively. Lower permanent deformation resistance is observed with the RS9.5B-PI and RS9.5C-PI mixtures compared to the SMAs at both test temperatures. Additionally, the RS9.5D-PI mixture exhibits the highest resistance to permanent deformation. The trends observed in Figure 16 (a) and (b) with the dense-graded mixtures can be attributed to compositional factors such as binder content and grade. Interestingly, the SMA-1A accumulates less permanent deformation than SMA-3, despite having a slightly higher binder content. This difference may be explained by the variations in gradation and aggregate requirements in their specifications. The SMA-1A design allows for a coarse gradation than SMA-3, which increases the stone-on-stone contact and structural stability,

considerably impacting the viscoplastic response of the materials under compression. Additionally, the SMA-1A specification has stricter control over the maximum abrasion loss compared to the SMA-3 design, which may affect aggregate breakdown during compaction and ensure a more consistent final aggregate structure. These differences are also evident in Figure 23 (c) in terms of the rutting strain index (RSI), calculated using the climatic data from Garner, NC. The RSI represents the ratio of the permanent deformation in the asphalt layer to the thickness of that asphalt layer at the end of 30 million 18-kip single axle load repetition. A higher RSI indicates relatively less resistance to permanent deformation. The same trends observed in Figure 16 (a) and (b) are similarly reflected in the RSI parameter.

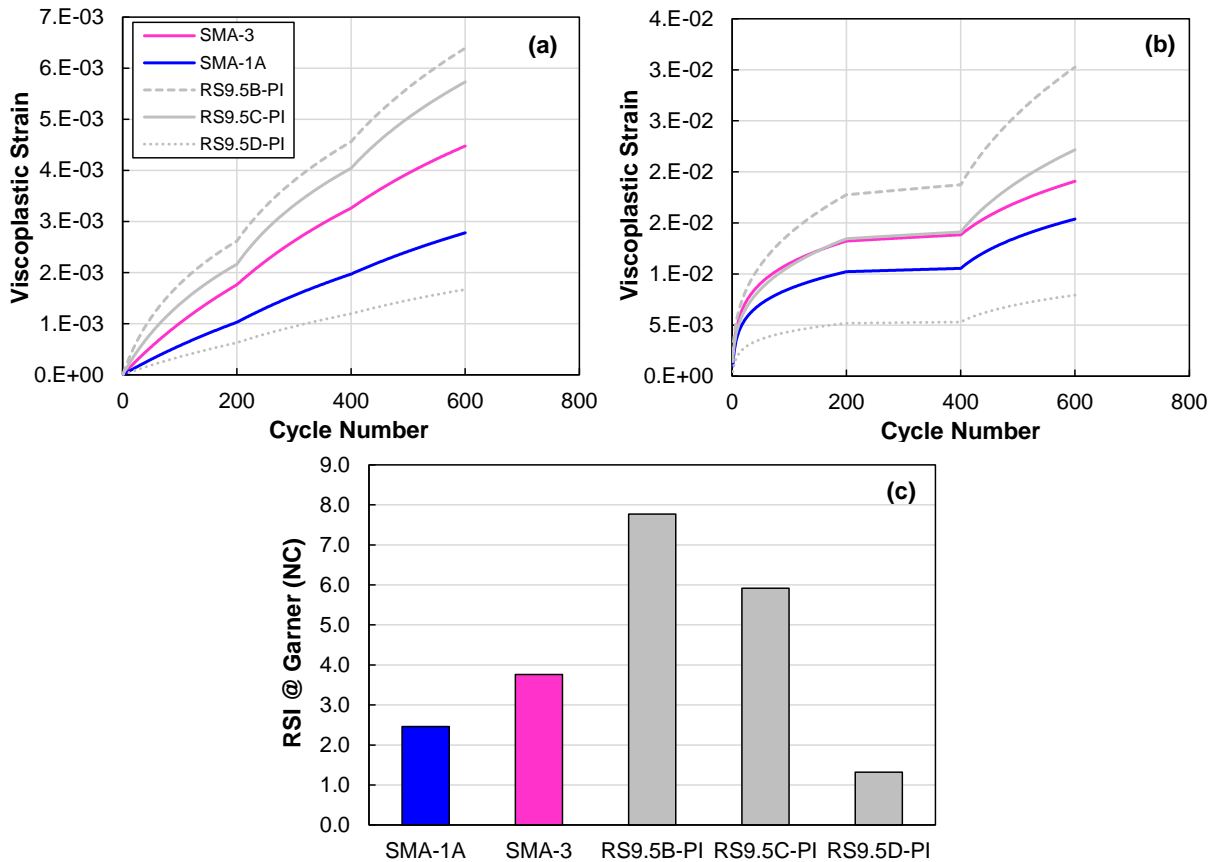


Figure 16. SSR test results for SMAs and surface mixtures from the NC Piedmont region: (a) ϵ_{vp} at 29°C, (b) ϵ_{vp} at 51°C, and (c) RSI results for Garner (NC).

4.3. Pavement Performance Simulations

Pavement simulations were conducted using FlexPAVE v.2.2 to evaluate the potential differences in performance when using SMA designs from States 1 and 2 as surface mixtures in pavement structures in North Carolina. Two sets of simulations were conducted: the first set used the SMAs as surface mixtures in conjunction with intermediate and base layers from NC. The properties of these additional layers were characterized as part of the FHWA/NC 2019-20 project. A second set of simulations were performed where the surface, intermediate, and base layers were all consistent with standard North Carolina mixtures. The second set of simulations served as the reference for comparison with the first set of simulations.

Table 20 and Table 21 summarize the parameters evaluated in the simulations and the levels of each factor. The different combinations of inputs described in these tables yielded 117 FlexPAVE simulations. An overview of the results for the Piedmont region and ABC-type structure is presented in this section. The results of the simulations for the other climatic regions and structures are presented in Appendix G.

Table 20. Matrix of performance simulation inputs.

Mix type	Pavement type ¹	Thickness type	Soil type	Climate zone
B-Mix	FDA	Thin	A-6	Piedmont (Garner)
C-Mix	ABC	Intermediate		Coastal (Wilmington)
D-Mix	DS	Thick		Mountains (Asheville)
SMA-mix				

¹ FDA: Full-depth asphalt pavement, ABC: pavement with aggregate base course, DS: pavement with asphalt base and aggregate base course.

Table 21. Pavement structures used in performance simulations.

Pavement Structure Type	Thickness Type ¹	Thickness (in.)				
		Surface AC	Intermediate AC	Base AC	ABC	Total
FDA	Thin	3	0	4	0	7
	Intermediate	3	4	4	0	11
	Thick	3	4	10	0	17
ABC	Thin	3	0	0	8	11
	Intermediate	3	4	0	8	15
	Thick	3	4	0	10	17
DS	Thin	3	2.5	3	8	16.5
	Intermediate	3	4	3	8	18
	Thick	3	4	5.5	10	22.5

¹ Daily ESALs were varied by thickness type: Thin = 2,000, Intermediate = 3,000, and Thick = 6,000

Figure 17 shows the total percent of damage and total pavement rutting for thin, intermediate, and thick ABC structures when using the Piedmont climatic data and a 20-year simulation period. The simulations suggest that the SMA-1A mixture in the Piedmont region exhibits a similar total percent damage as the RS9.5D-PI mixture across all thickness types at the end of the analysis period. Additionally, the results show that pavement structures with SMA-3 as the surface mix demonstrate comparable fatigue cracking performance to the RS9.5B and RS9.5C mixtures. Overall, the performance ranking in terms of total percent damage follows the same trends suggested by the S_{app} parameter shown in Figure 14.

Regarding the rutting performance, the pavement performance simulations show that the RS9.5D mixture experiences the least rutting at the end of the analysis period, followed by SMA-1A, SMA-3, RS9.5B-PI, and RS9.5C-PI across all thickness types. In the case of the rutting, the SMAs and RS9.5D mixtures seem to cluster together and be distinct from the other dense-graded mixtures. Overall, the trends observed in the simulation closely follow the ranking suggested by the RSI parameter. Additionally, as noted earlier, the SMA-3 mix exhibits similar cracking performance characteristics to the RS9.5B-PI and RS9.5C-PI mixtures but considerably less rutting than those mixtures.

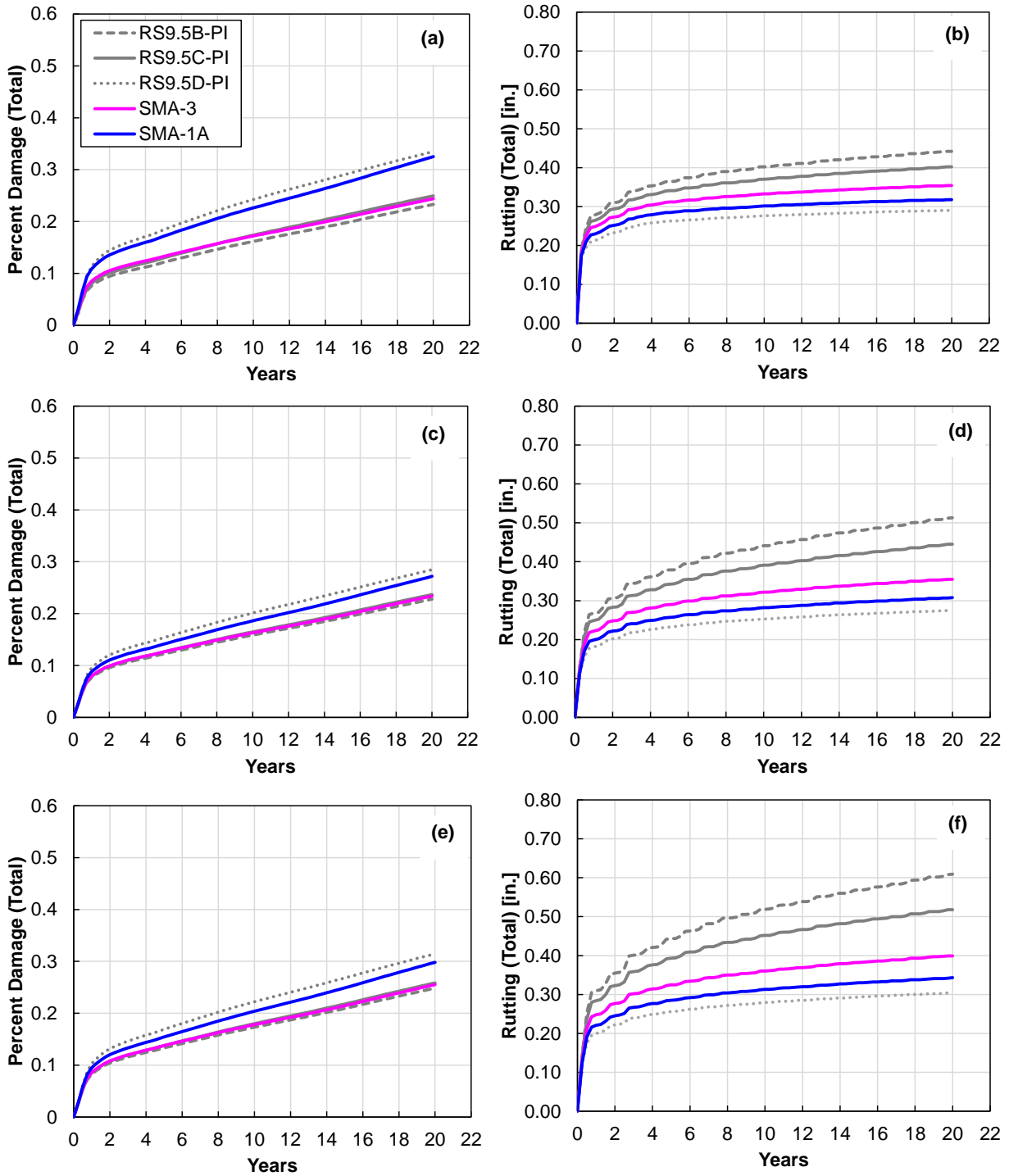


Figure 17. Pavement performance simulation results for NC Piedmont region and ABC structures: (a) total percent damage - thin structure, (b) total rutting - thin structure, (c) total percent damage - intermediate structure, (d) total rutting damage – intermediate structure, (e) total percent damage – thick structure, and (f) total rutting – thick structure.

The results of the pavement performance simulations were used to determine life ratio extensions achieved by using SMAs instead of dense-graded mixtures as surface layers in North Carolina

pavement structures. The methodology consisted of identifying the year when each SMA reached the same percent damage value as the RS9.5D-PI mixture at a point when major rehabilitation is needed. To determine the expected life extension of the SMAs over the RS9.5D-PI only the fatigue performance curve was used. This decision was made based on the observations made by Karanam et al. (30), that evaluated the yearly records of the automated distress survey since 2013 to 2023 and observed that the distress type that influenced the most the pavement condition rating (PCR) is the alligator cracking. Figure 18 illustrates this method, using a critical rehabilitation point of 12 years for the RS9.5D-PI mixture in an Intermediate-DS pavement structure. A 12-year rehabilitation period for the dense-graded surfaces was used based on the recommendations provided in the NCDOT pavement design guide. Additionally, based on the work of Karanam et al. (31), the expected uncertainty in the service life at a 95% confidence level for dense-graded pavements with an AADT greater than 40,000 vpd, is approximately four years. Therefore, in addition to the expected 12 years critical rehabilitation point, a lower and upper bound of eight and 16 years, respectively, were also analyzed.

The expected life extension for each of the structure configurations evaluated are summarized in Appendix F, Table F-8 for the SMA-1 and SMA-3. As shown, except for the SMA-1 when used with a thin structure, the SMA always have a higher expected life than the dense-graded surfaces. The average life extension of SMA-1 was 1.4 years with a range of -1.1 to 2.1 years. The average life extension of SMA-3 was 4.2 years with a range of 0.1 to 11.7 years.

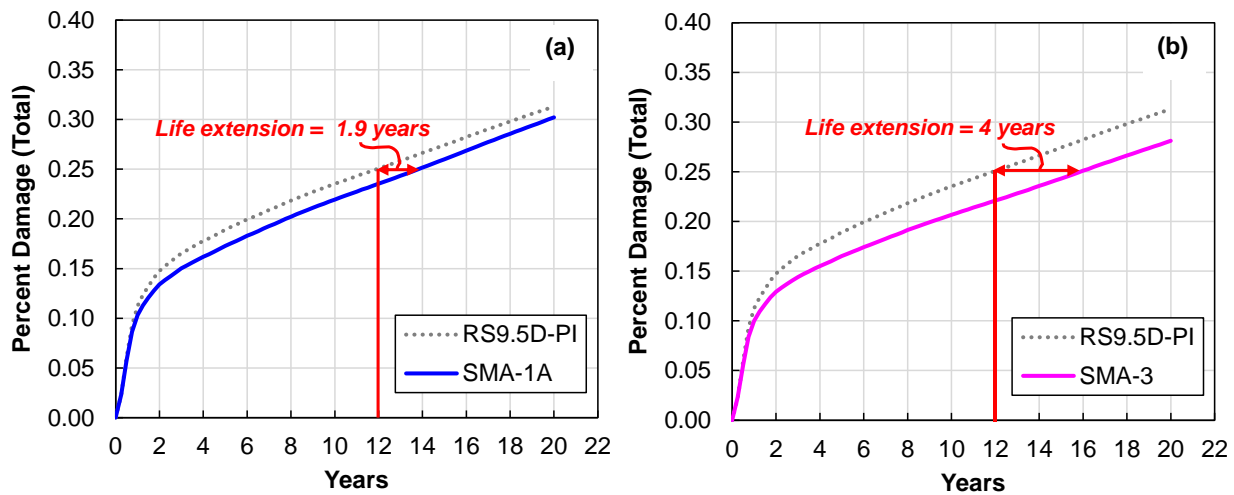


Figure 18. Example of life extension for Intermediate-DS structure using an SMA as a surface layer: (a) SMA-1A and (b) SMA-3.

4.4. Conclusions

In this chapter, a performance evaluation of SMAs sampled from two neighboring states, compared to typical dense-graded mixtures in North Carolina, was presented. The mixture-level assessment showed that both SMA mixtures have comparable LVE behaviors with the B and C mixes and that they are softer and more viscous (higher phase angle) than the D mixture. Mixed trends were observed regarding the fatigue cracking performance of the SMAs compared to the dense-graded mixtures. For instance, cyclic fatigue test results and statistical analyses suggested that the fatigue behavior of the SMA-1A is similar to that of the D design. However, the IDT-CT test ranks this SMA design substantially superior to the D mix. The rutting performance evaluation suggested

that the D design has more favorable characteristics to resist rutting than the SMAs. Nevertheless, the SMAs exhibited better resistance to permanent deformation than the B and C designs, despite having similar linear viscoelastic characteristics at high temperatures. This finding highlights the benefits of the SMA design and structure, which positively affect the material's response mechanisms to resist permanent deformation under repeated loading. Overall, the results of pavement structural simulations generally align with the findings from the experimental tests regarding.

5. EVALUATION OF THE EFFECT OF ALTERNATIVE ASPHALT SURFACES ON SAFETY

Although there are several factors that affect the occurrence of a crash event, it is accepted among practitioners that the pavement surface condition is a key safety predictor (32). Friction and texture are critical factors in ensuring road safety because they play a significant role in maintaining a vehicle's grip on the road surface. Adequate friction and texture on the road surface are necessary to ensure that vehicles can brake, accelerate, and steer effectively, particularly in wet or slippery conditions (33). Consequently, to meet the zero-death goal established by the FHWA and provide safer roads, state highway agencies are now proactively following federal recommendations and directives to develop a Pavement Friction Management Program (PFMP) (5).

Previous research studies have shown that crash rates, particularly wet crash rates, tend to increase after an asphalt overlay (1, 2). One of the factors that might cause this increment in the number of collisions is that friction and texture requires time, or a certain number of traffic repetitions, to reach its maximum value after construction. To assess the effect of a treatment on the safety of a roadway one must compare the number of crashes, or the crash rates, that were observed after the treatment to the estimated crash rate in the absence of that treatment. The difficulty of this process is the prediction of 'what would have been' if the treatment had not been applied. It is physically impossible to do this type of assessment with complete accuracy, but there are various ways to estimate the number of crashes that could have been expected.

According to Hauer (34), a before-after study can be accomplished using two tasks. The first task consists of predicting the expected number of target crashes for a specific entity (i.e., intersection, road segment, etc.) or series of entities in the 'after' period had the safety treatment not been implemented, π . The second task consists of estimating the number of target crashes for the specific entity (or group of entities) in the "after" period with the treatment in place, λ . In this study a simple (naïve) before-after study using aggregated crash statistics was conducted to evaluate the safety effect from different pavement surfaces. The pavements used in this analysis were selected because the same pavement surface type purportedly existed in both the 'before' and the 'after' period. As discussed elsewhere (34–37), such an analysis is appropriate given the lack of sufficient data to generate safety performance functions that could be used for crash reduction factor estimation.

The crash history for the sites evaluated in North Carolina and two neighboring states were used to conduct a before-after evaluation. Details of the data available for this analysis are provided in Chapter 2, Section 2.2. The target crashes in the analysis were the wet lane departure crashes. To keep consistency with the analysis developed in the FHWA/NC 2020-11 and 2022-5 projects, crashes were totaled by month, and it was assumed that the rehabilitation activity took place in June of the rehabilitation year, e.g., if a site was rehabilitated in year 2020, then the rehabilitation month was set as June of 2020. This assumption was made because for the sites available in the two neighboring states the only information available was about the rehabilitation year. Then, following the methodology of the two previous research projects, the rehabilitation period was set as six months prior and after the rehabilitation month, e.g., if the rehabilitation month for a given site is June 2019, then the rehabilitation period goes from December 2018 to January 2020 for a total of thirteen months. Once the rehabilitation period was defined for each site, the number of months and the sum of crashes before and after the overlay were computed and a set of constraints were defined prior to any calculation:

- The minimum length of a site to be included in the analysis is 0.5 miles, but not greater than 10 miles.
- The minimum and maximum ‘before’ period was defined as 13 and 48 months, respectively.
- The minimum and maximum ‘after’ period was defined as 13 and 48 months, respectively.
- Crashes were set as the total counts of wet lane departure crashes for both traffic directions.
- The sum of the ‘before’ and ‘after’ crashes for a given site must be different than zero.

5.1. Methodology

Three separate analyses were conducted: i) an aggregated crash analysis, ii) an individual crash analysis, and iii) a before-after crash rate comparison. Three separate analyses were completed because FHWA/NC 2022-5 evaluated the average trend of wet lane departure collisions and the analysis presented here refines the previous analysis and provides insights into the variation in crash frequency across sites with the same surface type. To this end, the aggregated analysis was performed first to compare the expected number of crashes per month per mile for the sites with a given surface type. The individual crash analysis was conducted next and focused on estimating the variability of the expected number of crashes among the sites with the same surface type. Finally, the ‘before’ and ‘after’ crash rate comparison was conducted to account for the traffic effect on the crash risk for the sites with a given surface type.

5.1.1. Analysis 1: Aggregated Crash Analysis

First, an aggregate evaluation was made by grouping the road segments by surface type and then totaling the crash frequencies, number of months, and number of miles in the ‘before’ and ‘after’ period. Afterwards, an average before-after comparison was carried out and the expected crash frequency per surface type in the ‘before’ and ‘after’ periods was computed using Equation (4) and (5), respectively. Then, the %change in the ‘after’ period crash frequency with respect to the values in the ‘before’ period were computed with Equation (6). This analysis provides a quantification of the average %change by computing the average number of crashes per month per mile for all the sites with a given surface type.

$$\pi_e = \frac{\sum_{i=1}^n Nb(i)}{\sum_{i=1}^n Mb(i) \times \sum_{i=1}^n L(i)} \quad (4)$$

$$\lambda_e = \frac{\sum_{i=1}^n Na(i)}{\sum_{i=1}^n Ma(i) \times \sum_{i=1}^n L(i)} \quad (5)$$

$$\% \text{ change} = \left(\frac{\lambda_e - \pi_e}{\pi_e} \right) \times 100 \quad (6)$$

where;

- π_e = expected number of crashes per month per mile in the ‘before’ period,
 λ_e = expected number of crashes per month per mile in the ‘after’ period,

$Mb(j)$ = number of months in the ‘before’ period for Site i ,
 $Ma(j)$ = number of months in the ‘after’ period for Site i ,
 $Nb(j)$ = number of crashes in the ‘before’ period for Site i ,
 $Na(j)$ = number of crashes in the ‘after’ period for Site i , and
 $L(i)$ = length of Site i , in miles.

5.1.2. Analysis 2: Individual Crash Analysis

The previous analysis aggregated the observations of all the sites with a given surface type to estimate the average %change of the crashes per month per mile in the ‘after’ period with respect to the values in the ‘before’ period. However, because of this aggregation, the resulting %change reflects the central tendency of the dataset and does not show the variability among the different sites. Consequently, Equation (4) to (6) were applied on an individual basis, i.e., without the summation operator, to quantify the variation in the %change among the different sites with a given surface type. The expected number of crashes per month per mile in the ‘before’ and ‘after’ period are defined as $\pi_e(i)$ and $\lambda_e(i)$, respectively. Where the subindex i indicates the site number within the group of sites with a given surface type.

5.1.3. Analysis 3: ‘Before’ and ‘After’ Crash Rate Comparison

Finally, Analysis 1 and 2 evaluated the %change using the estimated number of crashes per month per mile, but for these analyses the effect of different traffic exposure (understood as the number of vehicles miles traveled) was not accounted for. Hence, individual crash rates were computed in the ‘before’ and ‘after’ period using Equation (7) to evaluate the effect of different traffic exposure among sites, the traffic exposure is computed using the AADT of each site.

$$R(i) = \frac{N(i) \times 10^8}{30 \times M(i) \times L(i) \times AADT(i)} \quad (7)$$

where;

$R(i)$ = crash rate for Site i , in 100-million of vehicle-miles traveled (100-Mvmt),
 $M(i)$ = number of months in the period of analysis for Site i ,
 $N(i)$ = number of collisions observed during the number of months M ,
 $L(i)$ = length of Site i , in miles, and
 $AADT(i)$ = average annual daily traffic of Site i .

5.2. Results

5.2.1. Aggregated Crash Analysis

A summary of the aggregated crash analysis is shown in Table 22. It must be noted that for the observations in one of the two neighboring states, the analysis was not limited to only the sites where friction and texture were measured. For this state, the pavement management system was queried and all sites meeting the age and traffic limits in this project were identified. For the case of North Carolina, only the sites tested in FHWA/NC 2020-11 and 2022-5 and that met the above constraints were added to the analysis. For the second of the two neighboring states the sites tested were not added because they did not meet the third bullet point on the constraint list shown above.

The first and second column in Table 22 specify the number of months in the ‘before’ and ‘after’ periods, Mb and Ma , respectively. The third column shows the number of sites with the surface type shown in Column Four. The fifth and six columns include the number of crashes recorded in

all the sites with the surface type of Column Four during the number of month Mb and Ma . Column Seven shows the aggregated length of all sites with their respective surface. Columns Eight and Nine show the crashes/month/mile computed as indicated in Equation (4) and (5) for the before and after period respectively. Lastly, the percent change ($\%change$) was computed with Equation (6) and is shown in Column 10.

Table 22. Summary of the aggregated crash analysis.

#Months ¹		n ²	Surface	#Crashes ³		L (mi)	Crashes/month/mile		% change
Mb	Ma			Nb	Na		π_e	λ_e	
334	316	7	S9.5B	16	88	20.7	0.0023	0.0135	481
1,889	1,902	45	S9.5C	511	1,009	211.3	0.0013	0.0025	96
432	398	9	S9.5D	259	282	52.2	0.0115	0.0136	18
1,339	1,218	29	UTBWC	1,476	448	206.9	0.0053	0.0018	-67
1,434	1,260	32	OGFC	2,074	786	305.5	0.0047	0.0020	-57
96	36	2	Micro ⁵	43	3	19.2	0.0234	0.0044	-81
240	120	5	Chip seal	8	1	16.7	0.0020	0.0005	-75
2,117	1,930	53	SMA-1A	839	844	239.9	0.0017	0.0018	10
962	856	23	SMA-1B	284	311	160.7	0.0018	0.0023	23
166	152	4	SMA-2A	110	85	20.4	0.0325	0.0274	-16
0	0	0	SMA-2B ⁴	0	0	0	-	-	-
5,856	4,392	139	Dense-I	361	389	488.1	0.0001	0.0002	44
8,310	7,410	202	Dense-II	1,267	1,110	639.8	0.0002	0.0002	-2
1,536	320	32	Micro-Alt ⁵	234	22	154.6	0.0010	0.0004	-55

¹ Mb: Number of months in the ‘before’ period and Ma : Number of months in the ‘after’ period.

² n is the number of sites in corresponding surface type bracket that met the analysis constrains.

³ Nb: Number of crashes registered in the ‘before’ period of Mb months; and Na : number of crashes registered in the ‘after’ period of Ma months.

⁴ No crash records were obtained for this surface type.

⁵ Microsurfacing.

A positive $\%change$ indicates an increase in the number of crashes/month/mile in the ‘after’ period compared to the ‘before’ period; while a negative number indicates a reduction of crashes in the ‘after’ period compared to the ‘before’ period. As indicated in Table 22, the dense-graded sites showed the highest positive $\%change$ and within this category the surface types were ordered, from highest to lowest $\%change$, as follows S9.5B, S9.5C, and S9.5D with 481%, 96%, and 18%, respectively. Besides the dense-graded, three other surfaces had a positive $\%change$, the SMA-1A and -1B both had a $\%change$ of 10% and 23%, respectively, and the Dense-I had a $\%change$ of 44% and Dense-II had a $\%change$ of -2%. All the other surface types had a negative $\%change$, with the highest reduction resulting from Microsurfacing followed by the UTBWC and OGFCs.

A graphical comparison of the crashes/month/mile in the ‘before’ and ‘after’ period is included in Figure 19. It must be noted that North Carolina’s Microsurfacing and the SMA-2A included only two and four sites, respectively, and therefore the average value represented in Figure 19 may be biased towards a few sites with high crash counts. For the remaining surface types, it is shown that the highest difference between the ‘after’ and ‘before’ crashes/month/mile occurred in the dense-graded surfaces. The UTBWC and OGFC comes next and the crashes/month/mile in the ‘after’ period are almost a quarter of the dense-graded surfaces. The SMA-1 have similar results, and the Dense-I/II and Microsurfacing-Alt had the lowest crashes/month/mile in the ‘after’ period. As discussed in Section 3 of this report, during the friction and texture model update, the traffic levels on the sites evaluated varied considerably for some surface types. Therefore, the order shown in

Figure 19 may change if one includes the traffic volume at each site. This issue is discussed in Section 5.2.3.

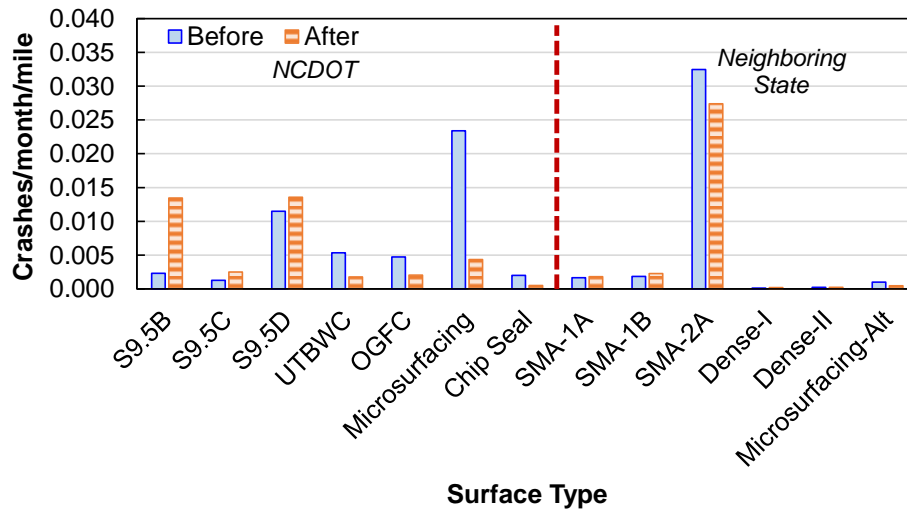


Figure 19. Graphic comparison of the ‘before’ and ‘after’ crashes/month/mile.

5.2.2. Individual Crash Analysis

To evaluate the variability of the %change among the different sites that are part of each surface type in Table 22, a graphical comparison was conducted as shown in Figure 20. In this figure, the results are summarized using a boxplot with the %change from individual sites plotted as dots on top of the boxplot. The red data series connects the mean value per surface type. To calculate the %change for individual sites, Equations (4) to (6) were applied in an individual basis by dropping the Σ sign. Sites that had zero crash counts in the ‘before’ period were removed from the analysis to avoid an algebraic error in Equation (6). The three dense-graded surfaces, S9.5B, S9.5C, and S9.5D, were grouped together in the Dense category, the same grouping process was done for the four SMAs and the Dense-I and Dense-II. Lastly, because of the limited sample size of North Carolina’s Microsurfacing and chip seals, these were not included in the graphical comparison.

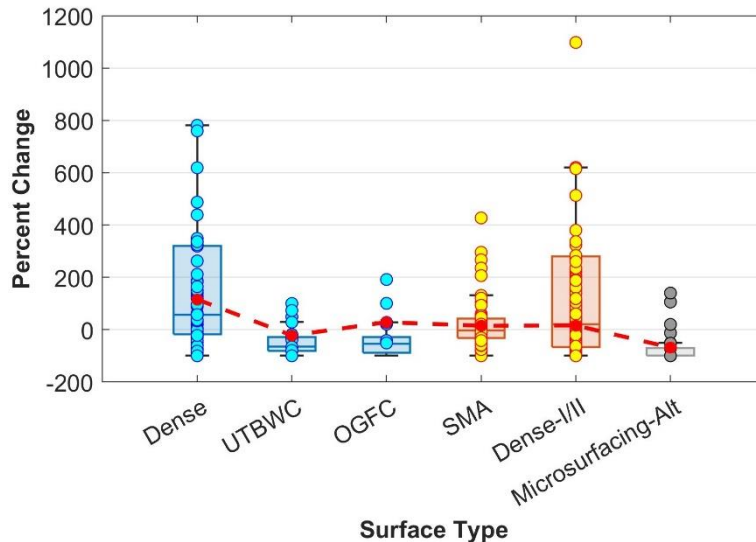


Figure 20. Summary of the %change computed for individual sites.

The results are congruent with those shown in Table 22, i.e., the dense-graded surfaces are the ones with the highest positive %change. Overall, the remaining surface types produce a %change that is on average closer to, or lower than zero. Also, from the boxplot distribution and the individual dots, it is observed that the SMA 75th percentile %change is closer to 75% and the sites with a %change higher than this value may be considered outliers. For the Dense-I/II, the 75th percentile %change is around 250%, but again just a few sites have a %change higher than 250%, which is evidenced by the fact the average is closer to zero.

The individual crash analysis highlights the fact that some sites deviate from the central tendency described in Table 22. This happens because in the first analysis, the aggregated crash analysis, the values are totaled by surface type and therefore the effect of extremes, i.e., sites with high crash counts in a short period of time and/or number of miles are smoothed out by most of the sites, i.e., those with low crash frequencies.

If one plots the distribution of values for the ‘before’ and ‘after’ period as presented in Figure 21, it is observed that the SMAs, Dense-I/II, and the Microsurfacing have overall lower number of crashes/month/mile than the dense-graded, UTBWC, and OGFC in both the ‘before’ and ‘after’ period. In fact, the UTBWC and OGFC had the highest %change because of the difference that exists in the distribution of values in the ‘before’ and ‘after’ period. This biggest difference in the distribution of values in the ‘before’ and ‘after’ period for the UTBWC and OGFC can be explained by two possible reasons. First, these surface treatments are placed on top of dense-graded surfaces, and sometimes the dense-graded surface may stay as the main surface course for a few years prior to receiving the top surface treatment. Second, the PMS database has some coding errors and even though the surface prior construction is named as OGFC or UTBWC, there is still a possibility that in fact the prior surface type is a dense-graded instead.

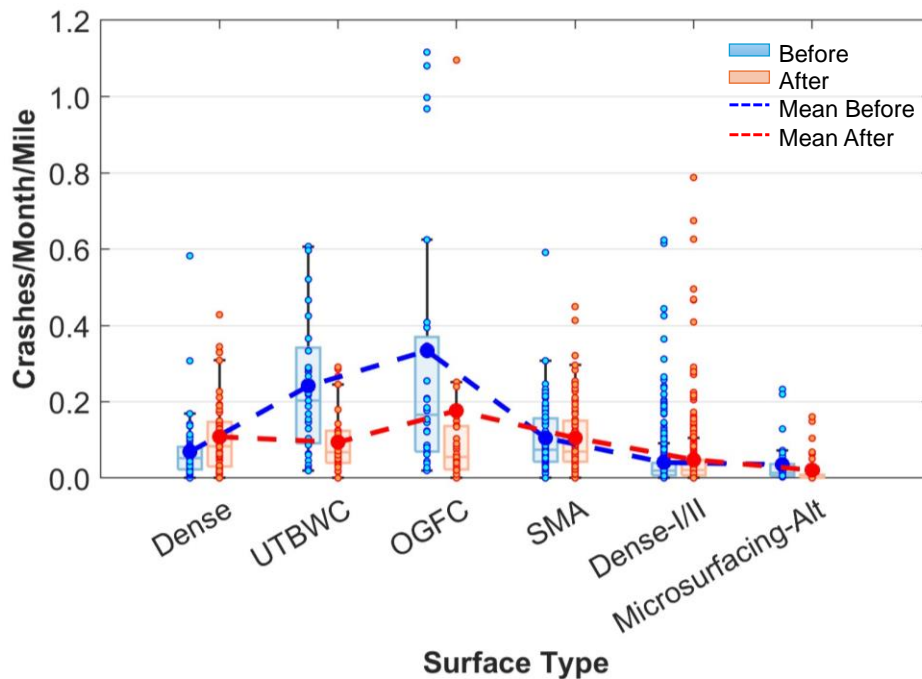


Figure 21. Summary of the number of crashes/month/mile in the ‘before’ and ‘after’ period.

Nevertheless, the distribution of crashes/month/mile shown in Figure 21 indicate that the Microsurfacing, the Dense-I/II, and the SMAs are surface types that overall have lower crash frequencies than the North Carolina’s dense grade surfaces. The UTBWC and OGFC have similar crashes/month/mile in the ‘after’ period than the SMAs. The Dense-I/II and Microsurfacing-Alt are the ones with the lowest crash frequencies in the ‘after’ period.

5.2.3. ‘Before’ and ‘After’ Crash Rate Comparison

One aspect that is missing in Figure 21 is the effect of traffic. To account for the effect of traffic volume in the number of collisions, the crash rate was computed using Equation (7). As shown in Figure 22, when accounting for traffic exposure, the Dense I/II surface mix had higher crash rates than the dense-graded surface, whereas the SMA surface ended up having the second lowest average crash rate in the ‘after’ period. Microsurfacing, on the other hand, is the surface type with the lowest crash rate in the ‘after’ period.

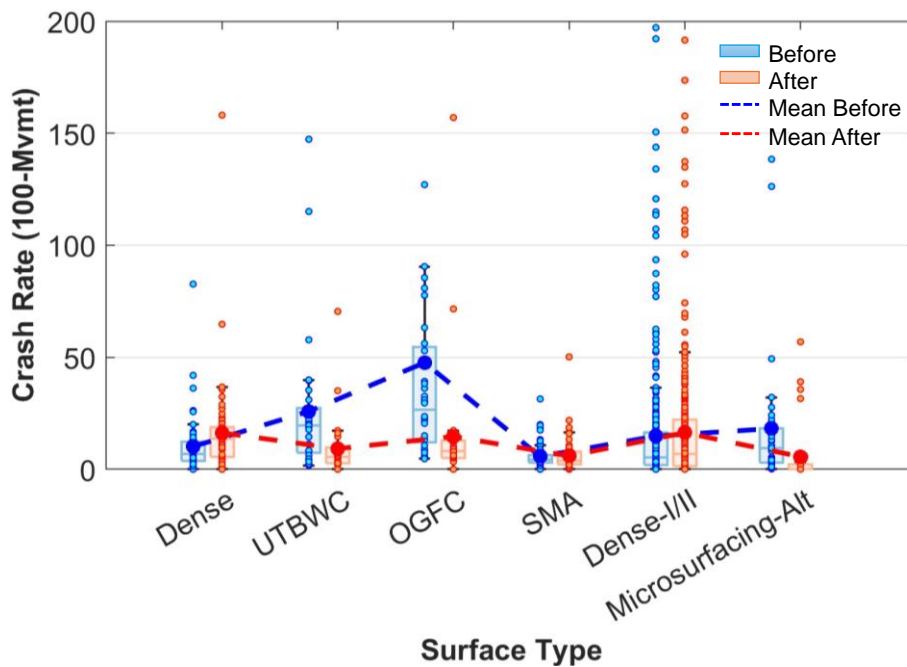


Figure 22. Summary of the crash rates in the ‘before’ and ‘after’ period.

5.3. Conclusions

The analysis presented above shows that among the surfaces tested, the dense-graded surface was the surface type with the highest crash frequencies. For the analysis conducted, sites with the same surface type in the ‘before and ‘after’ periods were selected. The aggregate crash analysis showed that the dense-graded surface had a %change of up to 400%, meaning the number of crashes/month/mile in the ‘after’ period was 400% higher than the number of crashed/month/mile in the ‘before’ period. By computing the %change for each site individually, it was observed that the Dense-I/II had similar %change variability, where the variability is understood as the IQR of the boxplot of the observations, in the ‘before’ and ‘after’ period. The alternative surface types had an average %change closer to zero than the dense-graded mixtures and in some cases were below zero, indicating a reduction in crashes. Finally, if one considers the traffic exposure, then the surface type with the lowest crash rates is the SMAs in both the ‘before’ and ‘after’ period; however, the Microsurfacing was the surface type with the lowest ‘after’ crash rate.

This page is intentionally blank

6. LIFE-CYCLE COST COMPARISON

The final step of the analysis consisted of a life-cycle cost analysis (LCCA) comparison of the construction and maintenance costs associated with different surface treatments used to improve friction and texture performance with respect to the performance provided by dense-graded surfaces. The precise details of all the analysis performed are provided in Appendix H. Here, an overview of the methodology, key findings, and qualified discussion of the limitations is given.

6.1. Methodology

The surface treatments evaluated were SMA, OGFC, UTBWC, and Microsurfacing. The LCCA of each surface treatment was evaluated for an analysis period of 45 years. The inputs required for the analysis are shown in Figure 23. First, the maintenance costs were estimated using the material costs and the expected performance. For the OGFC, UTBWC, and the Microsurfacing produced in North Carolina, the average unit cost was acquired from the historical bid price web page (38) as reported for 2023. Likewise, to obtain the average unit price for the SMA-1, SMA-3, and Microsurfacing-Alt, the respective state DOT web page was consulted (39). Afterward, the expected performance for each surface was determined based on the NCDOT Pavement Design Guide (40) and the expected service life uncertainty estimated by Karanam et al. (31). Three maintenance frequency scenarios were established: a high-frequency scenario with the lowest expected performance (Max Freq), an average scenario based on the NCDOT guide (Avg Freq), and a low-frequency scenario with the highest expected performance (Min Freq).

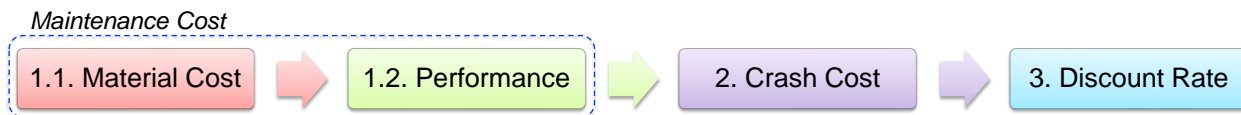


Figure 23. Life-cycle costs input.

Each scenario assumes a different baseline performance from pavements surfaced with dense-graded asphalt mixture. The Max Freq scenario assumes a lifespan of eight years, the Avg Freq scenario twelve years, and the Min Freq scenario sixteen years. Table 23 summarizes the maintenance schemes for these scenarios, which was established based on the sequence provided in the NCDOT Pavement Design Guide for LCCA. After the initial lifespan, the pavement is rehabilitated by milling and replacing the top 1.5 inches of the surface, as shown in the purple cells. A major rehabilitation occurs after two of these periodic minor rehabilitations, indicated by the green cells. The table also details the number of maintenance activities and the remaining service life at the end of the analysis period after the last major rehabilitation.

The maintenance schedule for the dense-graded surface was used as the baseline to define the maintenance scheme for the other surfaces. Of the four treatments analyzed, only the SMA contributes to structural performance. As indicated in Chapter 4, the structural performance of SMA and dense-graded mixtures was evaluated using FlexPAVE simulations. The performance of SMA as a surface course was compared with that of the dense-graded surface, and the difference in performance was used to estimate the life extension provided by SMA. Based on this life extension (see Table F-8 in Appendix F), the maintenance schedule shown in Table 23 was adjusted for SMA. For OGFC, UTBWC, and Microsurfacing, the maintenance schedule was adjusted according to recommendations from the NCDOT Material and Test Unit engineers. The resulting maintenance schedule for each surface treatment is included in Appendix H.

The maintenance schedule shown in Table 23 for the dense-graded surfaces and in Appendix H for the other surfaces, was also used to predict the expected friction and texture over the analysis period. To do so, the calibrated performance models presented in Chapter 3 were used. It must be noted that in some cases a single model was calibrated for a surface type, in other cases different models were proposed per climate region. For this latter case, the Piedmont models were used for the analysis. Because the friction and texture models were expressed in terms of the cumulative traffic, four AADT levels were evaluated; 30,000 vehicles per day (vpd), 60,000 vpd, 90,000 vpd, and 120,000 vpd. After predicting friction and texture for each year of the period of analysis, Equation (8) was used to estimate the expected crash rates, which then were converted to an expected number of collisions with Equation (9). The coefficients of the model were updated and adjusted as indicated in Appendix H.

$$R_{13} = a(X)^b = \frac{C_{13}}{VMT_{13}} \times 10^8 \quad (8)$$

$$C_{pred} = \frac{12}{13} \times \left(\frac{a \times VMT_{13}}{10^8} \right) \times (X)^b \quad (9)$$

where;

- R_{13} = crash rate in crashes per 100-million vehicle-miles traveled in a 13-month period,
- C_{13} = number of crashes registered in a 13-month period,
- VMT_{13} = number of vehicle-miles traveled in a 13-month period,
- X = predictor, i.e., friction or *MPD*, and
- a and b = model coefficients calibrated for each surface.

Once the expected number of collisions was obtained for each year of the analysis period, these numbers were used to estimate the associated costs. To this end, the average cost per lane departure crash, as reported by the NCDOT Traffic and Safety Unit in the standardized crash cost estimates for the year 2023, was \$233,000 per crash. This figure was used to calculate the cost associated with the number of collisions.

Lastly, the net present value (NPV) of the maintenance cost and the crash cost was computed. The maintenance cost included the initial construction cost, the cost of the maintenance activities, and the salvage value at the last major rehabilitation action at the end of the analysis period. For the NPV calculations, four discount rates were considered: 0.5%, 3%, 5%, and 7% to evaluate the uncertainty associated with this parameter. Then, taking the values registered with North Carolina's dense-graded surface as the base of comparison, Equation (10) was used to calculate the investment needed to build the surface treatment k to reduce the number of collisions. Consequently, Equation (11) was applied to compute the crash cost reduction achieved with surface treatment k .

$$Investment = NPV_{Surface\ k}^{Maintenance} - NPV_{Dense-NC}^{Maintenance} \quad (10)$$

$$Crash\ Cost\ Reduction = NPV_{Dense-NC}^{Crashes} - NPV_{Surface\ k}^{Crashes} \quad (11)$$

6.2. Conclusions

The detailed results are included in Appendix H. The main conclusions are as follows:

- The investments and crash reductions are of a different order of magnitude. Irrespective of the discount rate, the crash cost reductions are approximately ten times higher than the investments.
- A low discount rate, i.e., 0.5% is used for low-risk investments representing a low opportunity cost of capital. It is a conservative scenario and even with this assumption, the cash flow is positive, suggesting a net benefit from investing in the treatments instead of just using dense-graded surfaces.
- A high discount rate, i.e., 7.0%, is used for riskier investments reflecting a high degree of uncertainty. Under these conditions, the net present value of the investments and crash cost reductions for all the pavement structure configurations is nearly half of the values obtained with a 0.5% discount rate, and in all cases the benefits are higher than the investments.
- For all the pavement structures evaluated, the SMAs are the surface types with the lowest life-cycle investment requirements. In fact, for some combinations of discount rate and pavement structure, the investment ended up being negative, i.e., the cost of using a SMA over a dense-graded surface was lower in the long term, see for example the results for the ABC-Thin structure at a 0.5% discount rate.
- From the treatments that do not add structural capacity, Microsurfacing imposes the lowest life-cycle investment. The OGFC and UTBWC have similar investment values, which are almost twice that for Microsurfacing.
- The SMAs produce similar crash cost reductions compared to OGFC and UTBWC. Of the two SMAs, SMA-3 yielded the highest crash cost reductions. Of the two Microsurfacing, the one use in North Carolina offered the highest crash cost reductions.
- The results presented in this report cannot be compared directly to the analysis shown in FHWA/NC 2022-5 because:
 - The previous report conveyed a network-level assessment, whereas the current analysis centered on a hypothetical road segment, representative of a divided facility of one mile length and two lanes per direction.
 - Previously a single crash rate versus friction/texture relationship was used, whereas here separate expressions were derived for each surface type.
 - Lastly, in the previous report, the maintenance schedule only considered the surface course, while this analysis incorporated the cost associated with the entire pavement structure and the number and timing of the maintenance activities of each surface type was adjusted based on the results of pavement material mechanical characterization and performance simulations.

6.3. Limitations

Some of the limitations of the analysis presented here are:

- User costs were not evaluated. Some surfaces will result in lower user cost, e.g., the Microsurfacing is built quicker and therefore will produce lower delays and road closure times. The inclusion of the user costs may affect the ranking presented here.
- Another important component that was not included is the mobilization cost and the work zone delineation cost.
- The environmental implications were not accounted for. The overall carbon footprint of the surfaces evaluated will be very different given the number of maintenance activities, construction equipment needed, etc.

- There are secondary and tertiary economic implications that may affect how well the calculated cost and benefits would match real cost/benefits. Some of these are; i) the longer-term impact of shifting funding priorities on the maintenance, operations, and conditions of the entire transportation system in North Carolina to complete the activities resulting from the PFMP; ii) the availability and possible impacts on the supply and costs of component materials required for these treatments; and iii) the impacts on sustainability and the cost/benefits from downstream effects (if any) of the use of these treatments (e.g., changes in the balance of waste materials at material suppliers, an imbalance in the amount of RAP generated versus what is used, etc.
- Lastly, the analysis does not account for the implementation process of the SMAs. Some contractors are not familiar with the SMA design and construction, which may limit the number of contractors that can deliver this surface type, which may add extra costs for the adaptation of this material type by the NCDOT.

This page is intentionally blank

7. CONCLUSIONS AND RECOMMENDATIONS

7.1. Conclusions

The following conclusions have been reached on the basis of the research conducted in this study:

- The friction and texture observations collected in this study complemented the observations and analysis made in the previous research projects. The evaluation of friction and texture performance for the different surface types indicated that the variability in the friction and texture performance requires the use of site-specific models to properly describe the performance variation.
- The site-specific performance can be described by using random effect terms in the performance models; thereby, the analysis presented here provided an initial estimate of the random effect terms for different combinations of surface type and climate regions.
- The graphical comparison, and the calibrated performance models, indicated that overall North Carolina Microsurfacing surfaces have high friction and texture. Particularly, the friction of Microsurfacing surfaces is always above the Non-Interchange investigatory threshold recommended from FWHA/NC 2022-5, but the macrotexture on this surface type showed a decreasing trend with cumulative traffic. The Dense-I/II surfaces showed similar friction performance as North Carolina dense-graded surfaces, but the Dense-I/II have higher macrotexture and seems to surpass the investigatory threshold quicker. Lastly, all the SMAs, with the exception of SMA-3, have friction and texture higher than the Non-Investigatory threshold.
- The SMA mixtures have linear viscoelastic behavior similar to North Carolina's B and C mixes, but are softer and more viscous (higher phase angle) than the D mix. Fatigue cracking performance varied; SMA-1A's fatigue behavior resembles the D design, but IDT-CT tests indicate that it is substantially better than the D mix. The SMAs exhibited better resistance to permanent deformation than the B and C designs, despite having similar linear viscoelastic characteristics at high temperatures.
- A set of pavements with the same surface type in the 'before' and 'after' periods were selected. Of the surfaces evaluated, North Carolina's dense-graded surfaces had the highest crash frequencies. All other surface types had an average *%change* closer to or below zero. If one considers the traffic exposure, then the surface type with the lowest crash rates is the SMAs in both the 'before' and 'after' period; however, the Microsurfacing was the surface type with the lowest 'after' crash rate.
- A life-cycle cost assessment was conducted for a hypothetical road segment, set as a one mile long divided facility with two lanes per direction. The same structure configuration used in the material and performance characterization used for the SMA evaluation was used. The type and timing of maintenance activities were used to compute the investments and associated crash cost reductions. All surface treatments evaluated provide a positive return at the end of the analysis period.
- For all the pavement structures evaluated, the SMAs are the surface types imposing the lowest investment because of the life extension they provide with respect to North Carolina dense-graded surfaces. In fact, for some combinations of discount rate and pavement structure, the investment ended up being negative, i.e., the cost of using a SMA over a dense-graded surface was lower in the long term.

- Among the treatments that do not add structural capacity, Microsurfacing imposes the lowest investment. The OGFC and UTBWC have similar investment values, which are almost twice as much as that for Microsurfacing.
- The economic analysis presented has some limitations that may affect the final results; the user costs, the environmental footprint of each surface treatment, and the costs/time associated with the implementation of the SMAs at a network level were not accounted for. Other influential costs such as the mobilization costs for setting work zones, preparing detours and traffic control, and the cost of monitoring friction and texture during the period of analysis were not included.

7.2. Recommendations

Based on the aforementioned conclusions, the research team makes the following recommendations;

7.2.1. Pavement Friction Management Program Recommendations

- Evaluate the inclusion of Microsurfacing and SMA as candidate surface treatments in the Hydroplaning Assessment Tool v2.0.
- Define a calibration section that includes different surface types to verify the friction and texture device accuracy and repeatability.

7.2.2. Future Research Recommendations

- Evaluate possible coarse graded, dense-graded mixes using the materials currently available in North Carolina. A similar mixture and structural assessment should be made.
- Based on the crash analysis results, it is recommended to verify and adjust the investigatory/intervention thresholds proposed in FHWA/NC 2022-5, considering the variability in crash rates among sites with the same surface type.
- Categorize friction demand for existing pavement sections.
- Develop a decision framework that identifies the surface characteristics that satisfy the friction demand requirements. This framework must account for the structural performance, expressed in terms of rutting and cracking performance, and the functional performance expressed in terms of the IRI and skid resistance.
- Develop a protocol to evaluate the pavement surface friction and macrotexture at the time of construction.

8. IMPLEMENTATION AND TECHNOLOGY TRANSFER PLAN

The Traffic Safety Unit and Materials and Tests Unit of the NCDOT will be the primary users of this product. The products of this research will be used by the NCDOT to decide whether pavement mixture design specifications from neighboring states can be implemented to improve friction and texture performance. The SMA mixture design specifications were adapted to the NCDOT design practices and can be evaluated for implementation. The SMA can be included as a new mixture category instead of replacing existing mixtures. For follow-up activities, the research team believes that the NCDOT could consider the following activities:

- Allocate resources to define test sections to be constructed with a SMA as a final surface.
- Monitor the performance of this test section and adjust the specification draft if needed.
- Allocate resources to verify and update the investigatory and intervention thresholds proposed in FHWA/NC 2022-5 by considering the crash rate relationships for the different surface types.
- Allocate resources to refine and develop a quality assurance protocol for newly constructed pavements to ensure appropriate friction and texture are achieved at construction and flag pavements that might require early remediation.

This page is intentionally blank

9. REFERENCES

1. de Leon Izeppi, E., Flintsch, G., and McCarthy, R. *Evaluation of Methods for Pavement Surface Friction, Testing on Non-Tangent Roadways and Segments - NCDOT RP2017-2*. 2017.
2. Underwood, B. S., Castorena, C., Goenaga, B., and Rogers, P. *Evolution of Pavement Friction and Macrotexture After Asphalt Overlay - NCDOT RP2020-11*. 2022.
3. Underwood, B. S., Castorena, C., Goenaga, B., Munywoki, B., and Rogers, P. *Development of Friction and Texture Performance Models - NCDOT RP2022-5*. 2023.
4. Viner, A., Sinhal, E., and Parry, A. Linking Road Traffic Accidents with Skid Resistance – Recent UK Developments, TRL Paper Reference PA/INF4520/05. *Highways*. pp. 1–13. 2005.
5. Hall, J. W., Smith, K. L., Titus-Glover, L., Wambold, J. C., Yager, T. J., & Rado, Z. Guide for pavement friction. *Final Report for NCHRP Project, 1*, 43. 2009.
6. Rezaei, A., and Masad, E. Experimental-Based Model for Predicting the Skid Resistance of Asphalt Pavements. *International Journal of Pavement Engineering*, Vol. 14, No. 1, 2013.
7. Sullivan, B. W. *Development of a Fundamental Skid Resistance Asphalt Mix Design Procedure*. 2005.
8. Yang, G., K. Wang, J. Q. Li, Romero, M., and Liu, W. Laboratory and Field Performance Evaluation of Warm Mix Asphalt Incorporating RAP and RAS. *KSCE Journal of Civil Engineering*, Vol. 26, No. 1, pp. 107–119, 2022.
9. Underwood, B. S., Castorena, C., and Isied, M. *Evaluation of New Asphalt Concrete Job Mix Formula Specifications - NCDOT RP2020-12*. 2021.
10. FHWA. *Advances in the Design, Production, and Construction of Stone Matrix Asphalt (SMA)*. 2022.
11. Yin, F., and West. R. C. *NCAT Report 18-03: Performance and Life-Cycle Cost Benefits of Stone Matrix Asphalt*. 2018.
12. Wu, H., Yu, J., Song, W., Zou, J., Song, Q., and Zhou, L.. A Critical State-of-the-Art Review of Durability and Functionality of Open-Graded Friction Course Mixtures. *Construction and Building Materials*. Volume 237, 2020.
13. West, R., Timm, D., Powell, B., Tran, N., Yin, F., Bowers, B., Rodezno, C., Leiva, F., Vargas, A., Gu, F., Moraes, R., and Nakhaei, M. *Phase VII (2018-2021) NCAT Test Track Findings*. 2021.
14. Pranav, C., and Tsai, Y. C. J. High Friction Surface Treatment Deterioration Analysis and Characteristics Study. *Transportation Research Record: Journal of the Transportation Research Board*, pp. 370–384, 2021.
15. Woodward, D., Millar, P., Lantieri, C., Sangiorgi, C., and Vignali, V. The Wear of Stone Mastic Asphalt Due to Slow Speed High Stress Simulated Laboratory Trafficking. *Construction and Building Materials*, Vol. 110, pp. 270–277, 2016.
16. Kowalski, K. J., McDaniel, R. S. , Shah, A., and Olek, J. Long-Term Monitoring of Noise and Frictional Properties of Three Pavements: Dense-Graded Asphalt, Stone Matrix Asphalt, and Porous Friction Course. *Transportation Research Record: Journal of the Transportation Research Board*, No. 2127, pp. 12–19, 2009.
17. James, T., and Prowell, B. Evaluation of High Los Angeles Abrasion Loss Aggregate in Stone Matrix Asphalt. *Transportation Research Record: Journal of the Transportation Research Board*, Vol. 2676, No. 5, pp. 116–131, 2022.

18. FHWA. *Friction Management Program*.
https://safety.fhwa.dot.gov/roadway_dept/pavement_friction/friction_management/.
Accessed Jan. 4, 2024.
19. Chan, S., Lane, B., Kazmierowski, T., and Lee, W. Pavement Preservation: A Solution for Sustainability. *Transportation Research Record: Journal of the Transportation Research Board*, No. 2235, pp. 36–42, 2011.
20. Nikolaides, A., and Oikonomou, N. The Use of Fly Ash as a Substitute of Cement in Microsurfacing. *Waste Management Series*, pp. 234–240, 2000.
21. Hafezzadeh, R., and Kavussi, A. Application of Microsurfacing in Repairing Pavement Surface Rutting. *Road Materials and Pavement Design*, Vol. 22, No. 5, pp. 1219–1230, 2021.
22. Smith, R., and Beatty, K. Microsurfacing Usage Guidelines. *Transportation Research Record: Journal of the Transportation Research Board*, Vol. 1680, pp. 13–17, 1999.
23. Hicks, R. G., Moulthrop, J., and Daleiden, J. Selecting a Preventive Maintenance Treatment for Flexible Pavements. *Transportation Research Record: Journal of the Transportation Research Board*, Vol. 1680, pp. 1–12, 1999.
24. Labi, S., and Sinha, K. *The Effectiveness of Maintenance and Its Impact on Capital Expenditures - FHWA/IN/JTRP-2002/27*. 2003.
25. Adams, J. M., and Kim, Y. R. Mean Profile Depth Analysis of Field and Laboratory Traffic-Loaded Chip Seal Surface Treatments. *International Journal of Pavement Engineering*, Vol. 15, No. 7, pp. 645–656, 2014.
26. Oracheff, A. C. *Macrotexture Assessment of Florida Pavements*. University of North Florida, 2021.
27. Zuniga-Garcia, N., and Prozzi, J. A. High-Definition Field Texture Measurements for Predicting Pavement Friction. *Transportation Research Record: Journal of the Transportation Research Board*, Vol. 2673, No. 1, pp. 246–260, 2019.
28. Flintsch, G., de León Izeppi, E., Bongioanni, V., Katicha, S. W., Meager, K., Fernando, E., Perera, R., and McGhee, K. *Protocols for Network-Level Macrotexture Measurement*. Washington, D.C., 2021.
29. Montañez, J., Martin, A. E., and Arámbula-Mercado, E. Development and Verification of CTIndex Correction Methods to Normalize Air Void Content and Thickness of Field Cores. *Transportation Research Record: Journal of the Transportation Research Board*, Vol. 2677, No. 9, pp. 478–488, 2023.
30. Karanam, G. D., and Underwood, B. S. Mechanical Characterization and Performance Prediction of Fiber-Modified Asphalt Mixes. *International Journal of Pavement Research and Technology*, 2024.
31. Karanam, D., Goenaga, B., and Underwood, B. S. Quantifying Uncertainty with Pavement Performance Models: Comparing Bayesian and Non-Parametric Methods. *Transportation Research Record: Journal of the Transportation Research Board*, Vol. 2677, No. 7, pp. 661–679. 2023.
32. Kogbara, R. B., Masad, E. A., Kassem, E., Scarpas, A., and Anupam, K. A State-of-the-Art Review of Parameters Influencing Measurement and Modeling of Skid Resistance of Asphalt Pavements. *Construction and Building Materials*, Vol. 114, pp. 602–617, 2016.
33. Flintsch, G., McGhee, K., de Leon Izeppi, E., and Najafi, S. *The Little Book of Tire Pavement Friction*. 2012.

34. Hauer, E. Observational Before-After Studies in Road Safety. Estimating the Effect of Highway and Traffic Engineering Measures on Road Safety. 1997.
35. Hauer, E. Identification of Sites with Promise. *Transportation Research Record: Journal of the Transportation Research Board*, No. 1542, pp. 54–60, 1996.
36. Hauer, E., and Persaud, B. N. Problem of Identifying Hazardous Locations Using Accident Data. *Transportation Research Record: Journal of the Transportation Research Board*, pp. 531–540, 1994.
37. Ye, Z., and Lord, D. Estimating the Variance in Before-after Studies. *Journal of Safety Research*, Vol. 40, No. 4, pp. 257–263, 2009.
38. NCDOT. Bidding & Letting - Let Central. <https://connect.ncdot.gov/letting/LetCentral/Forms/AllItems.aspx>. Accessed Jul. 5, 2024.
39. VDOT. Technical Guidance and Support - Construction - Item Codes. <https://www.vdot.virginia.gov/doing-business/technical-guidance-and-support/construction/items-codes/>. Accessed Jul. 5, 2024.
40. North Carolina Department of Transportation (NCDOT). *Pavement Design Procedure AASHTO 1993 Method*. 2017.
41. AASHTO M323-22. Standard Specification for Superpave Volumetric Mix Design. *Standard Specification for Superpave Volumetric Mix Design*, 2022, pp. 1–15.
42. AASHTO R 35-22. *Standard Practice for Superpave Volumetric Design for Asphalt Mixtures*. 2022.
43. Fuller, W., and Thompson, S. American Society of Civil Engineers. *Science*, Vol. 1, No. 3, p. 84, 1985.
44. Hand, A. J., and Epps, A. L. Impact of Gradation Relative to Superpave Restricted Zone on Hot-Mix Asphalt Performance. *Transportation Research Record: Journal of the Transportation Research Board*, No. 1767, pp. 158–166, 2001.
45. Khasawneh, M. A., and Alsheyab, M. A. Effect of Nominal Maximum Aggregate Size and Gradation on Friction Properties of Hot Asphalt Mixture. *Construction and Building Materials*, Vol. 244, pp. 1–10, 2020.
46. Zhao, Y., Xu, T., Huang, X., and Li, Z. Gradation Design of the Aggregate Skeleton in Asphalt Mixture. *Journal Test Evaluation*, Vol. 40, No. 7, pp. 1071–1076, 2012.
47. Choudhary, R., Rajneesh K., Ankush K., Santanu P., and Abhinay K. Effect of Nominal Maximum Aggregate Size and Bitumen Content on Frictional Properties of Different Bituminous Surface Courses. In *International Conference on Transportation Infrastructure Projects: Conception to Execution*, pp. 295-310. Singapore: Springer Nature Singapore, 2022.
48. North Carolina Department of Transportation (NCDOT). *Standard Specifications for Roads and Structures*. 2012.
49. North Carolina Department of Transportation (NCDOT). *Asphalt Quality Management System*. 2016.
50. North Carolina Department of Transportation (NCDOT). *Asphalt Quality Management System*. 2018.
51. North Carolina Department of Transportation (NCDOT). *Asphalt Quality Management System*. 2023.
52. Kowalski, K. J., McDaniel, R. S., Shah, A., and Olek, J. Long-Term Monitoring of Noise and Frictional Properties of Three Pavements: Dense-Graded Asphalt, Stone Matrix

- Asphalt, and Porous Friction Course. *Transportation Research Record: Journal of the Transportation Research Board*, No. 2127, pp. 12–19, 2009.
53. Miao, Y., Li, J., Zheng, X., and Wang, L. Field Investigation of Skid Resistance Degradation of Asphalt Pavement during Early Service Skid Resistance Degradation of Asphalt Pavement. *International Journal of Pavement Research and Technology*, Vol. 9, No. 4, pp. 313–320, 2016.
 54. National Asphalt Pavement Association. *Designing and Constructing SMA Mixtures—State-of-the-Practice*. 2002.
 55. Hanson, D. Construction and Performance of an Ultrathin Bonded Hot-Mix Asphalt Wearing Course. *Transportation Research Record: Journal of the Transportation Research Board*, Vol. 1749, No. 1, pp. 53–59, 2001.
 56. Musa R., M., and Geib, J. *Performance of Ultra-Thin Bonded Wearing Course (UTBWC) Surface Treatment On US-169 Princeton, Minnesota*. Minnesota, 2007.
 57. Ji, Y., Nantung, T., and Tompkins, B. Evaluation for UTBWC on SR-11 as Pavement Preservation Treatment: A Case Study. *International Journal of Pavement Research and Technology*, Vol. 8, No. 4, pp. 267–275, 2015.
 58. Hajj, R., Filonzi, A., Smit, A., and Bhasin, A. Design and Performance of Mixes for Use as Ultrathin Overlay. *Journal of Transportation Engineering, Part B: Pavements*, Vol. 145, No. 3, 2019.
 59. Wegman, D., Sabouri, M., Holdhusen, B., Brand, C., Brazee, J., Falgren, J., Johnston, D., Kosobud, K., Meinen, D., Nienaber, C., and Nolan, P. *Ultra-Thin Bonded Wearing Course (UTBWC) Snow, Ice, and Wind Effects*. 2018.
 60. Game, D., Momen, M., and Hassan, M. *Performance Assessment of Ultra-Thin Asphalt Treatments in Louisiana*. 2021.
 61. Li, S., Noureldin, S., Jiang, Y., and Sun, Y. *Evaluation of Pavement Surface Friction Treatments*. 2012.
 62. Hanson, D. I. Construction and Performance of an Ultrathin Bonded Hot-Mix Asphalt Wearing Course. *Transportation Research Record: Journal of the Transportation Research Board*, Vol. 1749, No. 1, pp. 53–59, 2001.
 63. Wang, H., and Wang, Z. Evaluation of Pavement Surface Friction Subject to Various Pavement Preservation Treatments. *Construction and Building Materials*, Vol. 48, pp. 194–202, 2013.
 64. Wu, H., Yu, J., Song, W., Zou, J., Song, Q., and Zhou, L. A Critical State-of-the-Art Review of Durability and Functionality of Open-Graded Friction Course Mixtures. *Construction and Building Materials*. Vol. 237, 2020
 65. Xie, Z., Tran, N., Watson, D. E., and Blackburn, L. D. Five-Year Performance of Improved Open-Graded Friction Course on the NCAT Pavement Test Track. *Transportation Research Record: Journal of the Transportation Research Board*, Vol. 2673, No. 2, pp. 544–551, 2019.
 66. King, W. B., Kabir, S., Cooper, S. B., and Abadie, C. *Evaluation of Open Graded Friction Course (OGFC) Mixtures - FHWA/LA.13/513*. 2013.
 67. Huber, G. *Performance Survey on Open-Graded Friction Course Mixes - NCHRP Synthesis of Highway 284*, Transportation Research Board, National Research Council, Washington, D.C. 2000.

68. Jackson, N. C., Vargas, A., and Pucinelli, J. *Quieter Pavements Survey. Publication WA-RD 688.1. Washington State Transportation Commission, Department of Transportation, Olympia, WA. 2008.*
69. Abualia, A., Liu, J., Mohammad, L. N., Cooper III, S. B., and Cooper Jr, S. B. Effect of High Polymer, Crumb Rubber, and Epoxy-Modified Asphalt Binders on Laboratory Performance of Open-Graded Friction Course Mixtures. *Transportation Research Record: Journal of the Transportation Research Board, 2024.*
70. FHWA. Technical Advisory T 5040.31 Open Graded Friction Courses. *Pavements.* <https://www.fhwa.dot.gov/pavement/t504031.cfm#:~:text=Par.&text=PURPOSE..friction%20characteristics%20for%20pavement%20surfaces>. Accessed Oct. 15, 2023.
71. Watson, D., Qureshi, N. A., Xie, Z., and Tran, N. *Improvements Of Open Graded Friction Course In Alabama. 2020.*
72. Nekkanti, H., Putman, B. J., and Danish, B. Influence of Aggregate Gradation and Nominal Maximum Aggregate Size on the Performance Properties of OGFC Mixtures. *Transportation Research Record: Journal of the Transportation Research Board, Vol. 2673, No. 1, pp. 240–245, 2019.*
73. Albin, R. B., Brinkly, V., Cheung, J., Julian, F., Satterfield, C., Stein, W. J., Donnell, E. T., McGee, H. W., Holzem, A., Albee, M., Wood, J., and Hanscom, F. R. *Low-Cost Treatments for Horizontal Curve Safety. 2016.*
74. Heitzman, M., and Moore, J. *Evaluation of Laboratory Friction Performance of Aggregates for High Friction Surface Treatments. NCAT Report 17-01. 2017.*
75. Chen, X. W., Lanotte, M. A., Kutay, M. E., and Galehouse, L. Performance Evaluation of an Innovative High-Friction Surface Treatment. *Transportation Research Record: Journal of the Transportation Research Board, Vol. 2673, No. 3, pp. 485–493, 2019.*
76. Pranav, C., Do, M.-T., and Tsai, Y. Analysis of High-Friction Surface Texture with Respect to Friction and Wear. *Coatings, Vol. 11, No. 7, p. 758, 2021.*
77. Deef-Allah, E., K. Broaddus, and M. Abdelrahman. Life-cycle Cost Analysis of High Friction Surface Treatment Applications. *Transportation Research Record: Journal of the Transportation Research Board, Vol. 2676, No. 7, pp. 512–526, 2022.*
78. Merritt, D., Himes, S., and Porter, R. J. *High Friction Surface Treatment Site Selection and Installation Guide, FHWA. Washington, DC, 2021.*
79. Zhao, H., Wei, F., Wang, C., Li, S., and Shan, J. Determination of Friction Performance of High Friction Surface Treatment Based on Alternative Macrotecture Metric. *Materials (Basel, Switzerland), Vol. 14, No. 22, 2021.*
80. Li, S., Cong, P., Yu, D., Xiong, R., and Jiang, Y. Laboratory and Field Evaluation of Single Layer and Double Layer High Friction Surface Treatments. *Transportation Research Record: Journal of the Transportation Research Board, Vol. 2673, No. 2, pp. 552–561, 2019.*
81. Pittenger, D. M., Zaman, M., and Liam Cumberpatch, P. *Evaluate Densifier-Over-Shotblasting (DOS) Treatment Performance for Pavements and Bridge Decks. 2016.*
82. Chen, J. S., Huang, C. C., Chen, C. H., and Su, K. Y. Effect of Rubber Deposits on Runway Pavement Friction Characteristics. *Transportation Research Record: Journal of the Transportation Research Board, No. 2068, 2008.*
83. Tanvir Sarkar, A., Gu, F., Heitzman, M., and Powell, B. *Using Shotblasting Treatment to Improve Asphalt Pavement Friction at the NCAT Test Track. 2021.*

84. Gransberg, D. D. Life-Cycle Cost Analysis of Surface Retexturing with Shotblasting as an Asphalt Pavement Preservation Tool. *Transportation Research Record: Journal of the Transportation Research Board*, No. 2108, pp. 46–52, 2009.
85. Tran, N., Powell, B., Marks, H., West, R., and Kvasnak, A. Strategies for Design and Construction of High-Reflectance Asphalt Pavements. *Transportation Research Record: Journal of the Transportation Research Board*, No. 2098, pp. 124–130, 2009.
86. Zhan, Y., Luo, Z., Lin, X., Nie, Z., Deng, Q., Qiu, Y., and Wang, T. Pavement Preventive Maintenance Decision-Making for High Antiwear and Optimized Skid Resistance Performance. *Construction and Building Materials*, Vol. 400, 2023.
87. Bhargava, N., Siddagangaiah, A. K., and Ryntathieng, T. L. State of the Art Review on Design and Performance of Microsurfacing. *Road Materials and Pavement Design*, Vol. 21, No. 8, pp. 2091–2125, 2020.
88. Uzarowski, L., Maher, M., and Farrington, G. *Thin Surfacing-Effective Way of Improving Road Safety within Scarce Road Maintenance Budget*. 2005.
89. Hixon, C. D., and Ooten, D. A. *Maintenance of Roadway Pavement and Structures*. 1993.
90. Wang, A., Shen, S., Li, X., and Song, B. Micro-Surfacing Mixtures with Reclaimed Asphalt Pavement: Mix Design and Performance Evaluation. *Construction and Building Materials*, Vol. 201, pp. 303–313, 2019.
91. Zalnezhad, M., and Hesami, E. Effect of Steel Slag Aggregate and Bitumen Emulsion Types on the Performance of Microsurfacing Mixture. *Journal of Traffic and Transportation Engineering (English Edition)*, Vol. 7, No. 2, pp. 215–226, 2020.
92. Poursoltani, M., and Hesami, S. Performance Evaluation of Microsurfacing Mixture Containing Reclaimed Asphalt Pavement. *International Journal of Pavement Engineering*, Vol. 21, No. 12, pp. 1491–1504, 2020.
93. Ji, Y., Nantung, T., Tompkins, B., and Harris, D. Evaluation for Microsurfacing as Pavement Preservation Treatment. *Journal of Materials in Civil Engineering*, Vol. 25, No. 4, pp. 540–547, 2013.
94. Gransberg, D. *NCHRP Synthesis 411 - Microsurfacing*. 2010.
95. Praticò, F. G., Vaiana, R., and Iuele, T. Macrotecture Modeling and Experimental Validation for Pavement Surface Treatments. *Construction and Building Materials*, Vol. 95, pp. 658–666, 2015.
96. Sholar, G. A., and Kim, S. *Performance Report of Microsurfacing Experimental Project US-319/SR-369 in Leon County*. Florida, 2013.
97. Labi, S., and Sinha, K. *The Effectiveness of Maintenance and Its Impact on Capital Expenditures*. Indianapolis, 2003.
98. Plati, C. Sustainability factors in pavement materials, design, and preservation strategies: A literature review. *Construction and Building Materials*, 211, 539-555. 2019.
99. Peshkin, D., Smith, L., Wolters, A., Krstulovich, J., Moulthrop, J., and Alvarado, C. *Preservation Approaches for High-Traffic-Volume Roadways - SHRP2 Report S2-R26-RR-1*. 2011.
100. Guirguis, M., and Buss, A. Chip Sealing Macro Texture Performance Evaluation Using Split-Plot Repeated Measures. *Road Materials and Pavement Design*, Vol. 22, No. 1, pp. 185–199, 2021.
101. Estakhri, C. K., and Gonzalez, M. A. Estimating Voids in a Double Chip Seal. *Transportation Research Record: Journal of the Transportation Research Board*, 1990.

102. Shuler, S. Chip Seals for High Traffic Pavements. *Transportation Research Record: Journal of the Transportation Research Board*, Vol. 1259, pp. 24–34, 1990.
103. Lea, J. D., and Harvey, J. T. Using Spatial Statistics to Characterise Pavement Properties. *International Journal of Pavement Engineering*, Vol. 16, No. 3, 2015, pp. 239–255.
104. Najafi, S., Flintsch, G., and Khaleghian, S. Pavement Friction Management–Artificial Neural Network Approach. *International Journal of Pavement Engineering*, Vol. 20, No. 2, pp. 125–135, 2019.
105. McCarthy, R., de León Izeppi, E., Flintsch, G., and McGhee, K. *Comparison of Locked Wheel and Continuous Friction Measurement Equipment*. 2018.
106. de Leon Izeppi, E., Flintsch, G., Katicha, S., McGhee, K., McCarthy, R., and Smith, K. *PFM Program Utilizing CFME and State-of-the-Practice Safety Analysis Demonstration*. 2019.
107. Galvis, O., and Zhang, Z. Framework to Estimate the Benefit–Cost Ratio of Establishing Minimum Pavement Friction Levels for Roadway Networks. *International Journal of Pavement Engineering*, Vol. 23, No. 7, pp. 2135–2147, 2022.
108. Wu, Z., and King, B. *Development of Surface Friction Guidelines for LADOTD - Report No. FHWA/LA.11/485*. 2012.
109. Yu, W., Li, J.Q., Yang, G., Wang, K., and Attoh-Okine, N. Hilbert-Huang Transformation (HHT) Based Texture Profile Analysis for Continuous Friction Characterisation of Pavements. *International Journal of Pavement Engineering*, Vol. 23, No. 6, pp. 2074–2082, 2022.
110. Levine, N. Spatial Statistics and GIS: Software Tools to Quantify Spatial Patterns. *Journal of the American Planning Association*, Vol. 62, No. 3, pp. 381–391, 1996.
111. Bivand, R. S., Pebesma, E. J., Gómez-Rubio, V., and Pebesma, E. J. *Applied Spatial Data Analysis with R*. New York, 2008.

This page is intentionally blank.

APPENDIX A. DETAILED LITERATURE REVIEW

Introduction

This document presents a summary of the literature on the issues relevant to alternative surface types, including stone matrix asphalt (SMA) and different surface courses. This review includes aspects of the mixture design guidance, recommended application and use, and the expected performance. It also includes a section dedicated to the analysis tools that can be used to describe the spatial variability of friction and texture measurements. The document is organized as follows:

- First, a detailed description of the different surface treatments that are typically used in neighboring states to solve skid resistance problems. Eight different surface courses are included: Superpave mixtures, SMA, ultra-thin bonded wearing course (UTBWC), open-graded friction course (OGFC), high friction surface treatment (HFST), shotblasting, Microsurfacing, and chip seal. For each surface course, the typical friction and texture values reported by different researchers are identified and a summary of the main design methods is included. At the end of this section, a discussion of the main benefits and limitations associated with each surface type is presented.
- Next section provides a description of the concept of spatial analysis and the importance of characterizing spatial variability in friction and texture measurements. The variogram concept is introduced and discussed.
- Afterwards the main conclusions of the literature review are shown.
- Then, the last section summarizes the bibliographical references consulted to create this review.

Friction and Texture Performance of Surface Treatments

This section presents the generality of eight surface courses: 1) Superpave mixes, 2) SMA, 3) UTBWC, 4) OGFC, 5) HFST, 6) Shotblasting, 7) Microsurfacing, and 8) chip seals. At the end of the section a summary table is included with the pros and cons of each surface type.

Superpave Mixtures

The Superpave mixture design system is a comprehensive method for designing paving mixes tailored to the unique performance requirements dictated by the traffic, environment (climate), and structural section at a particular pavement site (41, 42). It facilitates selecting and combining asphalt binder, aggregate, and any necessary modifier to achieve the required level of pavement performance. According to Fuller and Thompson (43), aggregates can be packed with a maximum density if the aggregate particles are well graded, specifically if they follow the N-method grading curve, Equation (12). In the 1960's the Federal Highway Administration (FHWA) adopted this method to represent the maximum density aggregate gradation more easily in a graphical form.

$$p = 100 \cdot \left(\frac{d}{D} \right)^n \quad (12)$$

where;

p = percent passing of particle size ' d ',

d = aggregate particle size,

D = maximum size of aggregate particle, and

n = 0.5 in Fuller and Thompson's work, but 0.45 for the FHWA method.

According to the Superpave mix design specification (42), the Nominal Maximum Aggregate Size (NMAS) is one size larger than the first sieve that retains more than 10 percent of the aggregates, and the Maximum Aggregate Size (MAS) is one size larger than the NMAS. This concept is illustrated in Figure A-1 where the maximum density lines for mixtures with MAS values of 37.5, 25, 19, 12.5, 9.5, and 4.75 mm are presented. Figure A-1 shows that the slope of the maximum density line increases when the MAS reduces.

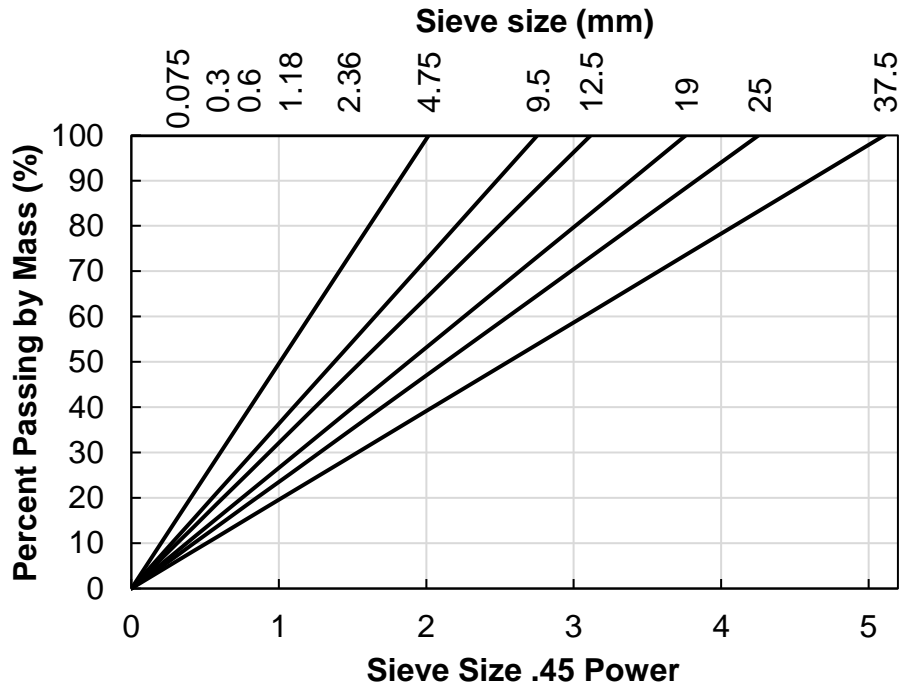


Figure A-1. Maximum density lines on FHWA 0.45 power gradation curves.

The Superpave mix design procedure consist of the following steps (41):

- Select asphalt binder,
- Select aggregate stockpiles that meet property requirements,
- Select a design aggregate structure, and
- Optimize the asphalt content for the selected aggregate structure.

The binder selection consists of analyzing the rheological properties of the binder that satisfy the temperature and traffic requirements. The individual aggregate properties must satisfy the consensus properties such as abrasion, angularity, and elongated particles, etc. The aggregate blend is characterized based on the NMAS, gradation control points, and gradation classification. According to the specification (41) the combined gradation must pass between the control points presented in Table A-1. These control points are used to guarantee a proper aggregate size distribution. The zone allowed for the gradation to pass for each NMAS is depicted in Figure A-2.

The gradation classification is made based on the primary control sieve (PCS), which varies depending on the NMAS. The PCS for each NMAS is presented in Table A-2. Mixes where the percent passing value of the PCS is below the value presented in Table A-2 are classified as coarse, while those with a percent passing greater than the values shown in Table A-2 are classified as fine

mixes. In the past, the gradation specifications within the Superpave mix design procedure incorporated recommendations that gradations avoid passing through a restricted zone and that coarse- rather than fine- graded mixtures be employed for heavily trafficked facilities (44). There was controversy when the restricted zone was implemented and the recommendation of using coarse mixes over fine mixes because several agencies had evidence that many fine mixes have performed equally to coarse mixes and, in some cases, fine mixes perform better than coarse mixes.

Table A-1. Aggregate gradation control points.

Sieve Size	Nominal Maximum Aggregate Size - Control Points (%Passing)											
	37.5 mm		25 mm		19 mm		12.5 mm		9.5 mm		4.75 mm	
	Min	Max	Min	Max	Min	Max	Min	Max	Min	Max	Min	Max
2" (50 mm)	100	-	-	-	-	-	-	-	-	-	-	-
1.5" (37.5 mm)	90	100	100	-	-	-	-	-	-	-	-	-
1" (25 mm)	-	90	90	100	100	-	-	-	-	-	-	-
3/4" (19.5 mm)	-	-	-	90	90	100	100	-	-	-	-	-
1/2" (12.5 mm)	-	-	-	-	-	90	90	100	100	-	100	-
3/8" (9.5 mm)	-	-	-	-	-	-	-	90	90	100	95	100
#4 (4.75 mm)	-	-	-	-	-	-	-	-	-	90	90	100
#8 (2.36 mm)	15	41	19	45	23	49	28	58	32	67	-	-
#16 (1.18 mm)	-	-	-	-	-	-	-	-	-	-	30	55
#200 (0.075 mm)	0	6	1	7	2	8	2	10	2	10	6	13

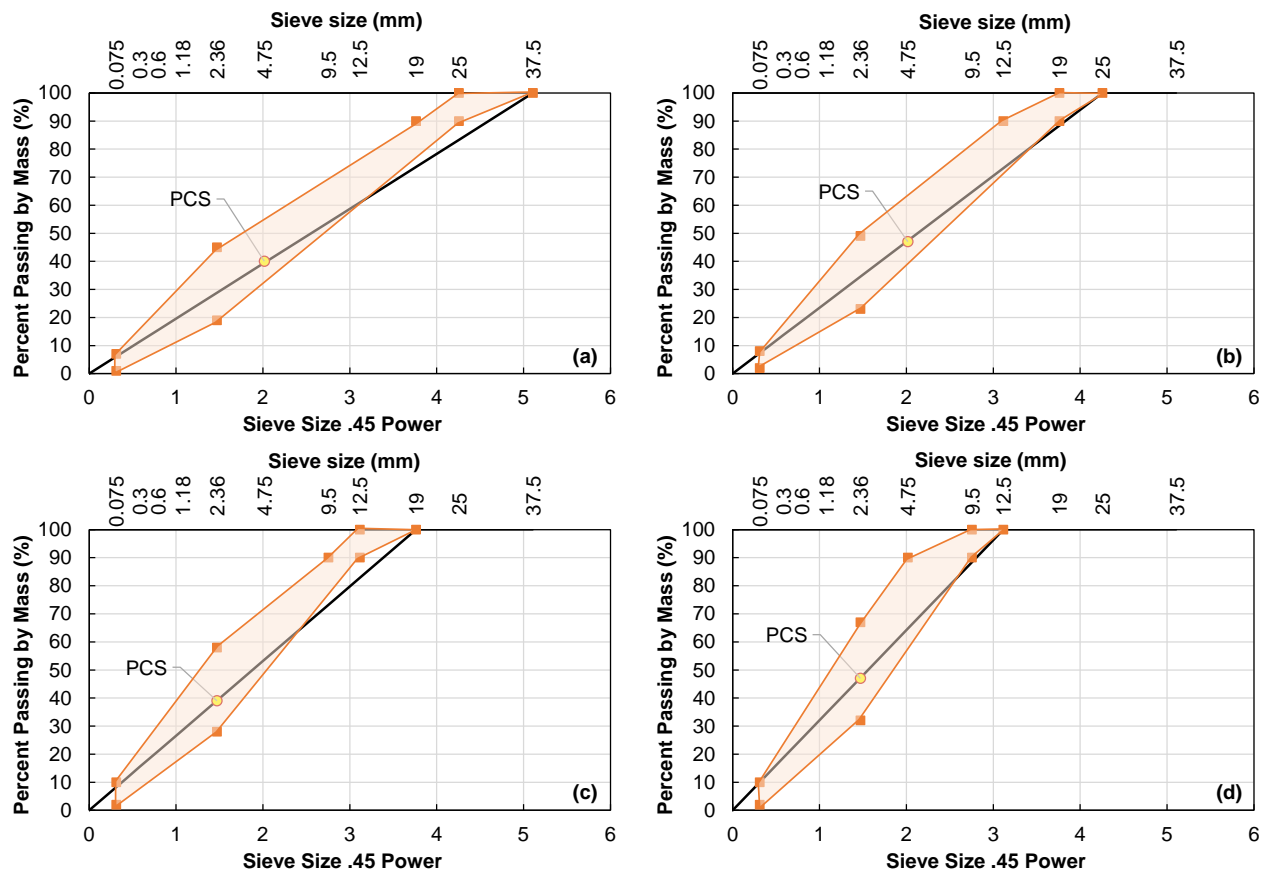


Figure A-2. Gradation Control Zone of different NMAS: (a) NMAS = 25.0 mm, (b) NMAS = 19.0 mm, (c) NMAS = 12.5 mm, and (d) NMAS = 9.5 mm.

Table A-2. Gradation classification.

PCS Control Point for Mixture Nominal Maximum Aggregate Size (%Passing)					
Nominal Maximum Aggregate Size	37.5 mm	25 mm	19 mm	12.5 mm	9.5 mm
Primary Control Sieve	9.5 mm	4.75 mm	4.75 mm	2.36 mm	2.36 mm
PCS Control Point, %Passing	47	40	47	39	47

Role of Gradation Type

According to NCHRP Report 108 (5), dense, coarse-graded mixtures have mean profile depths (*MPDs*) that range between 0.6 to 1.2 mm (0.025 to 0.05 in.) whereas the *MPD* of dense, fine-graded mixtures range between 0.4 to 0.6 mm (0.015 to 0.025 in.). In terms of friction, the same report also indicates that the coarse aggregate fractions contribute the most to friction hysteresis, and the quality of the aggregates (hardness and polishing/abrasion resistance) contributes to the microtexture friction component (5). In this sense, the percentage of material passing the 9.5 mm (3/8 in.) sieve through the 2.36 mm (#8), sieve size affects the asphalt mixture macrotexture. Evidence suggests that increasing the amount of material passing these sieve sizes reduces the asphalt mixture macrotexture.

Generally, the amount of aggregate passing the 9.5 mm (3/8 in.) sieve through the 2.36 mm (#8) sieve depends on the asphalt mixture type (i.e., dense-graded, open-graded, and so on). Hence, coarse-graded mixtures are expected to have higher friction hysteresis potential than fine-graded mixtures. However, some authors like Khasawneh and Alsheyab (45) have found the microtexture friction component, tends to reduce when the gradation moves from fine to coarse.

Role of NMAS

Zhao et al. (46) conducted a laboratory test using five gradations with different design curves and different NMAS to understand the role of gradation on skid resistance. The results showed that the mass content of the coarse aggregate, larger than 4.75 mm (#4 sieve), and the maximum aggregate size had significant influences on the skid resistance of a pavement. Likewise, Choudhary et al. (47) evaluated the role of the NMAS on the friction and texture performance of asphalt mixes. The authors used dense-graded mixes with two different NMAS, 13.2 and 19 mm (0.52 and 3/4 in.). They measured friction with a British Pendulum Tester (BPT) in dry and wet conditions and measured texture with a Sand Patch Test (SPT). The authors observed that both the wet and dry British Pendulum Numbers (*BPNs*) and the mean texture depth (*MTD*) values increase with the NMAS.

A 12.5 mm Superpave mixture is an asphalt mixture with a NMAS of 12.5 mm. This mixture type was previously included in asphalt mixture specifications in North Carolina but was removed in February 2018 with the introduction of a special provision that modified the 2018 NCDOT Quality Manual Specification (QMS). Based on a discussion held with personnel from the NCDOT Materials and Tests unit, it is known that the decision to eliminate surface mixes with a 12.5 mm NMAS was associated with common complaints with the mixture included challenging workability, ‘poor’ performance, challenges in obtaining and maintaining the stockpiles necessary to produce the mixture, and permeability issues. Despite these challenges, when used in the past, this mixture was generally reserved for higher volume roadways. While the NCDOT no longer maintains a specification for 12.5 mm mixtures, other states like Kentucky, Alabama, and South Carolina continue to allow this type of mixture.

Evaluation of Mixture Specifications

North Carolina DOT Specification

Table A-3 through Table A-8 show the NCDOT asphalt mixture design tables and aggregate gradation requirements for years 2012-2016, 2016-2017, and 2018-2023. As indicated in Table A-3, the 2012 version of the specifications included two NMAS's for surface courses, 9.5 mm and 12.5 mm. The 9.5 mm included four traffic levels were considered (A to D) and the 12.5 mm NMAS included two traffic categories (C and D). Also in 2012, the S4.75 mixture was not an option. This mixture type was included in later versions of the manual as indicated in Table A-5. Then, in 2017, the SF9.5A and all the 12.5 NMAS mixtures were removed from the specification as indicated in Table A-6. Other modifications made in 2017 are changes in the compaction levels, minimum VMA, the VFA range for S9.5B, and the use of PG 64-22 instead of PG 70-22 for S9.5C.

Table A-3. Summary of the NCDOT mixture designs and volumetric factors in 2012 (48).

Mix Type	20-Year ESALs, millions	Binder PG Grade	Compaction		Volumetric Properties				
			G_{mm} @ N_{ini}	N_{des}	VMA % Min.	VTM %	VFA Min.-Max.	% G_{mm} @ N_{ini}	Max. Rut Depth (mm)
SF9.5A	< 0.3	64-22	6	50	16.0	3.0-5.0	70-80	≤ 91.5	11.5
S9.5B	0.3 - 3	64-22	7	65	15.5	3.0-5.0	65-80	≤ 90.5	9.5
S9.5C	3 - 30	70-22	7	75	15.5	3.0-5.0	65-78	≤ 90.5	6.5
S9.5D	> 30	76-22	8	100	15.5	3.0-5.0	65-78	≤ 90.0	4.5
S12.5C	3 - 30	70-22	7	75	14.5	3.0-5.0	65-78	≤ 90.5	6.5
S12.5D	> 30	76-22	8	100	14.5	3.0-5.0	65-78	≤ 90.0	4.5
All Mix Types	Dust to Binder Ratio (P0.075/P _{be})				0.6 - 1.4				
	Tensile Strength Ratio (TSR)				85% Min.				

Table A-4. NCDOT aggregate gradation criteria in 2012 Specifications (48).

Sieve Size	9.5 mm		12.5 mm	
	Min	Max	Min	Max
3/4" (19.5 mm)	-	-	100	-
1/2" (12.5 mm)	100	-	90	100
3/8" (9.5 mm)	90	100	-	90
#4 (4.75 mm)	-	90	-	-
#8 (2.36 mm)	32	67	28	58
#200 (0.075 mm)	4	8	4	8

Table A-5. Summary of the NCDOT mixture designs and volumetric factors in 2016 (49).

Mix Type	20-Year ESALs, millions	Binder PG Grade	Compaction		Volumetric Properties				
			G_{mm} @ N_{ini}	N_{des}	VMA % Min.	VTM %	VFA Min.-Max.	% G_{mm} @ N_{ini}	Max. Rut Depth (mm)
S4.75A	<1	64-22	6	50	16	4.0-6.0	65-80	≤ 91.5	11.5
SF9.5A	< 0.3	64-22	6	50	16.0	3.0-5.0	70-80	≤ 91.5	11.5
S9.5B	0.3 - 3	64-22	7	65	15.5	3.0-5.0	65-80	≤ 90.5	9.5
S9.5C	3 - 30	70-22	7	75	15.5	3.0-5.0	65-78	≤ 90.5	6.5
S9.5D	> 30	76-22	8	100	15.5	3.0-5.0	65-78	≤ 90.0	4.5
S12.5C	3 - 30	70-22	7	75	14.5	3.0-5.0	65-78	≤ 90.5	6.5
S12.5D	> 30	76-22	8	100	14.5	3.0-5.0	65-78	≤ 90.0	4.5
All Mix Types	Dust to Binder Ratio (P0.075/P _{be})				0.6 - 1.4				
	Tensile Strength Ratio (TSR)				85% Min.				

Table A-6. NCDOT aggregate gradation criteria in 2016 specifications (49).

Sieve Size	4.75 mm		9.5 mm		12.5 mm	
	Min	Max	Min	Max	Min	Max
3/4" (19.5 mm)	-	-	-	-	100	-
1/2" (12.5 mm)	100	-	100	-	90	100
3/8" (9.5 mm)	95	100	90	100	-	90
#4 (4.75 mm)	90	100	-	90	-	-
#8 (2.36 mm)	-	-	32	67	28	58
#16 (1.18 mm)	30	60	-	-	-	-
#200 (0.075 mm)	6	12	4	8	4	8

Table A-7. Summary of NCDOT mixture designs and volumetric factors for 2018-2023 (50, 51).

Mix Type	20-Year ESALs, millions	Binder PG Grade	Compaction		Volumetric Properties				
			G _{mm} @		VMA	VTM	VFA	%G _{mm}	Max. Rut Depth (mm)
			N _{ini}	N _{des}	% Min.	%	Min.-Max.	@ N _{ini}	
S4.75A	< 1	64-22	6	50	16.0	4.0-6.0	65-80	≤ 91.5	11.5
S9.5B	0 - 3	64-22	6	50	16.0	3.0-5.0	70-80	≤ 91.5	9.5
S9.5C	3 - 30	64-22	7	65	15.5	3.0-5.0	65-78	≤ 90.5	6.5
S9.5D	> 30	76-22	8	100	15.5	3.0-5.0	65-78	≤ 90.0	4.5
All Mix Types	Dust to Binder Ratio (P0.075/P _{be})				0.6 - 1.4				
	Tensile Strength Ratio (TSR)				85% Min.				

Table A-8. NCDOT aggregate gradation criteria for 2018-2023 specifications (50, 51).

Sieve Size	4.75 mm		9.5 mm	
	Min	Max	Min	Max
3/4" (19.5 mm)	-	-	-	-
1/2" (12.5 mm)	100	-	100	-
3/8" (9.5 mm)	95	100	90	100
#4 (4.75 mm)	90	100	-	90
#8 (2.36 mm)	-	-	32	67
#16 (1.18 mm)	30	60	-	-
#200 (0.075 mm)	6	12	4	8

Virginia DOT Specification

For the Virginia DOT (VDOT), dense-graded mixtures are designated as either A, D, or E.

- The ‘A’ designation mixes use a Performance Graded (PG) asphalt binder of PG 64S-22 (formerly PG 64-22). This designation should perform well in low to medium traffic loading situations.
- The ‘D’ designation mixes use a PG 64H-22 (formerly PG 70-22). This designation should perform well in medium to high traffic loading situations.
- The ‘E’ designation uses PG 64E-22 (formerly PG 76-22). Mixes with this binder designation should perform well in high to extremely high traffic loading situations.

Generally, mix stiffness increases from ‘A’ to ‘E’, with ‘A’ being the softest. Hence, the mix type and the binder selection are made based on annual average daily truck traffic (AADTT) and selected as indicated in Table A-9. As shown in the table, the 12.5 mm mix can be used when truck traffic is less than 2,500 trucks per day (i.e., A-D categories). Using typical NCDOT truck factors and assuming 1% multi-unit trucks, 2% single unit trucks, and a 2% growth rate, 2,500 AADTT

equates to between approximately 9.7 and 13 million ESALs over 20 years. Also, Table A-10 indicates where the 12.5 mm mix type can be used depending on the geometry requirements. Gradation and volumetric requirements for the 9.5 mm and 12.5 mm surface mix are presented in Table A-11 and Table A-12 respectively. The VDOT mix designs use N_d of 65 gyrations in all their mixes and the asphalt content is specified at 4% air void target, with a minimum VMA of 14 and 15% for the 12.5 mm and 9.5 mm NMAS, respectively. All mixtures are designed with a dust to binder ratio in the range of 0.6 to 1.2.

Table A-9. Mix designation for flexible pavements in Virginia.

AADTT	Mix Designation
0-299	SM-4.75A, SM-9.0A, SM-9.5A or SM-12.5A
300-999	SM-9.5D or SM-12.5D
1,000-2,499	SM-9.5E, SM-12.5E , SMA-9.5(64H-22) or SMA-12.5(64H-22)
>2,500	SMA-9.5(64E-22) or SMA-12.5(64E-22)

Table A-10. Specialized pavement locations.

Location	Mix Designation
Truck climbing lane and roads with excessive grades (>6%)	SM-9.5 E, SM-12.5E , SM-19.0D, SMA-9.5 (64E-22), SMA-12.5 (64E-22)
Industrial route, quarry	SM-9.5D, SM-9.5E, SM-12.5D , SM-12.5E
Truck parking area	SM-9.5E, SM-12.5E
Intersections and railroads crossings with moderate to heavy truck percentage	SM-9.5E, SM-12.5E
Heavy urban traffic with buses	SM-9.5E, SM-12.5E

Table A-11. Percentage by weight passing sieve sizes.

Mix Type	2"	1 1/2"	1"	3/4"	1/2"	3/8"	#4	#8	#30	#50	#200
SM-9.5 A, D, E	-	-	-	-	100	90-10	80 max	38-67	-	-	2-10
SM-12.5 A, D, E	-	-	-	100	95-100	90 max	-	34-50	-	-	2-10

Table A-12. VDOT VMA and VFA requirements for Superpave mixtures.

Mix Type	VFA (%)	VMA⁽¹⁾ (%)
SM-9.5 A, D, E	73-79	15
SM-12.5 A, D, E	70-78	14

⁽¹⁾ Minimum value

Georgia DOT Specification

The Georgia DOT (GDOT) uses the 12.5 mm Superpave mix for state routes and shoulders of Interstates, whereas the 9.5 mm Superpave mix is used in State and off-system routes. The GDOT uses a 12.5 mm Superpave mix with polymer modified asphalt for state routes with high traffic, Interstates routes when recommended by the office of materials and testing (OMAT), and Interstates ramps and roundabouts. When used as a surface course, the thickness is usually 1.5 inches with a maximum of 2.5 inches. The gradation requirements for this mix type as specified by GDOT are included in Table A-13. The number of gyrations is not explicitly specified for the 12.5 mm Superpave mix, but Level A (the lowest traffic category) has a N_d of 50 gyrations, while Level D (highest traffic category) has a N_d of 125 gyrations. Finally, the criteria for VMA and VFA at N_d is summarized in Table A-14 and Table A-15, respectively. GDOT uses a dust to binder ratio of 0.6-1.2 to 9.5 mm (A) NMAS mixes, whereas for the other mix types use a ratio of 0.8-

1.6. The optimum asphalt content (OAC) is set at a 4% air void target. Then, the concepts of credited and non-credited asphalt content (CAC and NCAC, respectively) are utilized to adjust the OAC to the final design asphalt content, also known as the corrected optimum asphalt content (COAC). The CAC and NCAC are calculated using an applied factor as follows: the CAC uses a factor of 0.60 while the NCAC factor is 0.40.

Table A-13. GDOT gradation limits (%passing) for Superpave mixes.

Mixture Control Tolerance	Sieve Size	12.5 mm	9.5 mm (Level B, C, D)	9.5 mm (A)
	1" (25 mm)	-	-	-
± 8.0	3/4" (19.5 mm)	100 ⁽¹⁾	-	-
± 8.0	1/2" (12.5 mm)	90-100	100*	100*
± 6.0	3/8" (9.5 mm)	70-85	90-100	90-100
± 5.6	#4 (4.75 mm)	-	55-75	65-85
± 4.6	#8 (2.36 mm)	34-39	42-47	53-58
± 2.0	#200 (0.075 mm)	3.5-7.0	4.0-7.0	4.0-7.0

⁽¹⁾ Mixture control tolerance not applicable to this sieve for this mix

Table A-14. GDOT VMA criteria for Superpave mixes.

Nominal Maximum Aggregate Size (NMAS)	Minimum %VMA ¹
1" (25 mm)	12
3/4" (19.5 mm)	13
1/2" (12.5 mm)	14
3/8" (9.5 mm)	15

¹ VMA at Nd is to be determined based on effective specific gravity of the aggregate (Gse)

Table A-15. GDOT VFA criteria for Superpave mixes.

Mix Design Level	Range %VFA at N _d	
	Minimum	Maximum
A	67	80
B	65	78
C	65	76
D	65	75

South Carolina DOT Specification

The South Carolina DOT (SCDOT) has five different surface mix types. The Type A mix is used on Interstates and is mostly used as a base for OGFCs and SMAs. The mix Type B is used in high volume primary roads. Both mixes have the same gradation and can be catalogued as a 12.5 mm mix, the only difference is that the Type A mix uses a PG 76-22 binder, whereas the Type B mix uses a PG 64-22. The gradation and design criteria are presented in Table A-16. While these band specifications technically permit 12.5 mm mixtures on Type A-C mixes, informal conversations with SCDOT personnel suggest that such mixtures are rarely if ever used in today's market.

Table A-16. SCDOT gradation and design requirements for Superpave mixes.

Sieve Size	Type A Interstates and Intersections	Type B High Volume Primary	Type C High Volume Secondary	Type D Low Volume Secondary
1" (25 mm)	-	-	-	-
3/4" (19.5 mm)	100	100	100	100
1/2" (12.5 mm)	95-100	95-100	97-100	97-100
3/8" (9.5 mm)	76-100	76-100	83-100	90-100
#4 (4.75 mm)	52-75	52-75	58-80	70-95
#8 (2.36 mm)	36-56	36-56	42-62	50-82
#30 (0.60 mm)	16-36	16-36	20-40	20-50
#100 (0.15 mm)	5-18	5-18	5-20	6-20
#200 (0.075 mm)	2-8	2-8	2-9	2-10
Required Design Criteria				
Gyrations	75	75	50	50
Binder (%)	4.8-6.0 ¹	4.8-6.0 ¹	5.0-6.8 ¹	5.0-6.8 ¹
Binder Grade	PG 76-22	PG 64-22	PG 64-22	PG 64-22
Air Voids	3-4	3-4	3.5-4.5	4-9
Min VMA (%)*	-	-	-	-
VFA (%)	70-80	70-80	70-77	60-70

¹ VMA requirements are not explicitly indicated by SCDOT

Tennessee DOT Specification

Although Tennessee DOT (TDOT) uses the Marshall mix design method, it is included here due to its proximity to North Carolina. The TDOT gradation requirements for surface mixes, Grading D, E, TL, TLD/TLE, and OGFC are shown in Table A-17. In this table, Grading D and E are 12.5 mm NMAS mixes. Specific provisions for asphalt cement, mineral aggregate is required when using each type of surface mix as shown in Table A-18. It must be noted that these criteria were set based on the Marshall mix design method. Modifications are allowed when using Grading D and E for non-traffic lane construction or shoulder surfacing. The TDOT indicates a total of 75 blows as per the Marshall guidelines. All the mixtures are designed to a minimum VMA of 14% and a dust to binder ratio of 0.6-1.2.

Table A-17. TDOT gradation criteria for Superpave mixes.

Sieve Size	Grading D	Grading E	Grading TL	Grading TLD/TLE	Grading OGFC
3/4" (19 mm)	-	-	-	-	100
5/8" (16 mm)	100	100	-	-	-
1/2" (12.5 mm)	95-100	95-100	100	100	85-100
3/8" (9.5 mm)	80-93	80-93	100	90-100	55-75
#4 (4.75 mm)	54-76	54-76	89-94	54-76	10-25
#8 (2.36 mm)	35-57	35-57	53-77	35-57	5-10
#30 (0.60 mm)	17-29	17-29	23-42	17-33	-
#50 (0.30 mm)	10-18	10-18	-	10-18	-
#100 (0.150 mm)	3-10	3-11	9-18	3-10	-
#200 (0.075 mm)	0-6.5	0-8	6-14	3-7	2-4

Table A-18. TDOT criteria for mineral aggregate and asphalt cement proportions.

Surface Course	Effective Combined Mineral Aggregate %	Asphalt %
Grading D	93.0-94.3	5.7-7.0
Grading E	93.0-94.3	5.7-7.0
Grading D (shoulders)	92.0-94.7	6.0-6.5
Grading TL	92.5-94.3	5.7-7.5
Grading TLD	93.0-94.3	5.7-7.0
Grading TLE	93.0-94.3	5.7-7.0
Grading OGFC	92.0-94.3	6.0-8.0

Kentucky DOT Specification

The Kentucky DOT (KTDOT) requires that the asphalt mixtures satisfy with the AASHTO M 323 gradation control points (see Table A-1). In addition, the volumetric mix design is performed according to the AASHTO R 35 and AASHTO M 323. For surface mixtures, the KTDOT requires a dust-to-binder ratio range of 0.6 to 1.4 and a relative density at $N_{max} \leq 98.5\%$. Pavements are designed using annual average daily truck traffic (AADTT) categorization according to the AASHTO guidelines and the same number of gyrations N_d is used for all the truck traffic categories as indicated in Table A-19. The asphalt content is set at a target air void of 3.5%.

Table A-19. KTDOT traffic categorization for pavement design.

Class	AADTT	Number of Gyration		
		N_{ini}	N_d	N_{max}
2	<600	7	65	105
3	600 to 2,999	7	65	105
4	$\geq 3,000$	7	65	105

Based on a dataset shared by members of the KTDOT for average gradations between 2017 and 2019, it is observed that the dense asphalt surfaces in Kentucky are designed as coarse-graded mixtures. The results of this analysis are shown in Figure A-3, which shows that the 9.5 mm NMAS mixtures are all below the PCS limit of 47% (see Table A-2)

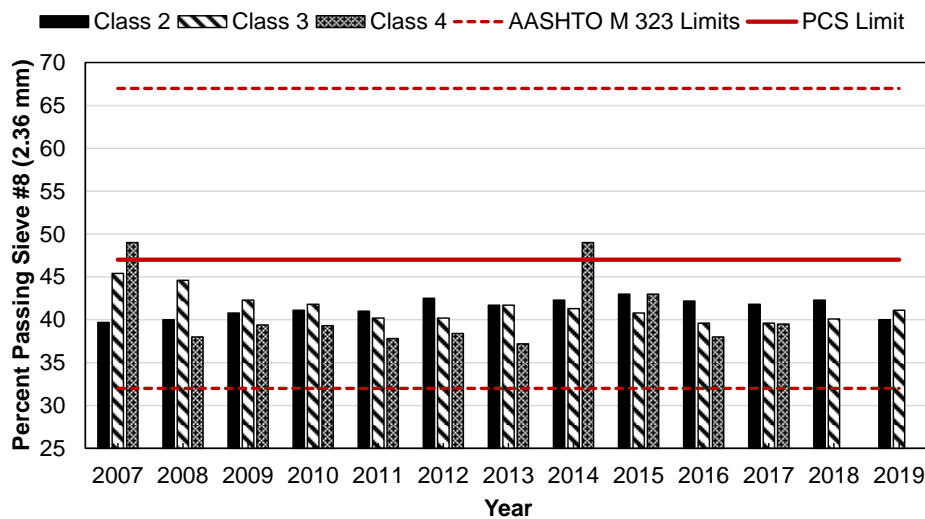


Figure A-3. Variation of the percent passing Sieve #8 (2.36 mm) in 9.5 mm mixes used by KTDOT.

Alabama DOT Specification

In Alabama, the coarse and fine aggregates, mineral filler, and recycled materials are blended to a mix that falls within the gradation limits determined by the maximum and minimum control points as shown in Table A-20. Note that the ALDOT follows a convention using maximum aggregate size and not NMAS. In general, the NMAS is one size lower than the maximum aggregate size. Thus, what is shown in Table A-20 as a 12.5 mm mixture would most closely align with the NCDOT 9.5 mm NMAS mixtures. The design air void content for all traffic levels is 3.5% for mixes containing RAS and 4.0% for other mixes. The mixes are designed at the minimum VMA values given in Table A-21 and to the asphalt binder content shown in Table A-22. The design number of gyrations, N_d , is 60 for mixes with and without RAS.

Table A-20. ALDOT criteria for gradations for Superpave mixes.

Sieve Size (mm)	Maximum Aggregate Size Mix - Control Points (% Passing)										
	37.5 mm		25.0 mm		19.0 mm		12.5 mm		9.5 mm		
	Min	Max	Min	Max	Min	Max	Min	Max	Min	Max	
1 1/2" (37.5 mm)	100	-	-	-	-	-	-	-	-	-	-
1" (25 mm)	90	100	100	-	-	-	-	-	-	-	-
3/4" (19 mm)	19	90	90	100	100	-	-	-	-	-	-
1/2" (12.5 mm)	-	-	23	90	90	100	100	-	-	-	-
3/8" (9.5 mm)	-	-	-	-	28	90	90	100	95	100	-
#4 (4.75 mm)	-	-	-	-	-	-	32	90	75	100	-
#8 (2.36 mm)	19	45	23	49	28	58	32	67	-	-	-
#16 (1.18 mm)	-	-	-	-	-	-	-	-	30	60	-
#30 (0.60 mm)	-	-	-	-	-	-	-	-	-	-	-
#50 (0.30 mm)	-	-	-	-	-	-	-	-	-	-	-
#200 (0.075 mm)	1	7	2	8	2	10	2	10	6	12	-

Table A-21. ALDOT criteria voids in mineral aggregate (VMA) specifications.

MAS (mm)	NMAS (mm)	Minimum VMA (%)
9.5	4.75	16.5
12.5	9.5	15.5
19.0	12.5	14.5
25.0	19.0	13.5
37.5	25.0	12.5

Table A-22. ALDOT criteria for asphalt binder content (AC%).

MAS (mm)	NMAS (mm)	Minimum AC%	Minimum AC% for mixes with RAP
9.5	4.75	5.9	6.1
12.5	9.5	5.5	5.7
19.0	12.5	5.1	5.3
25.0	19.0	4.4	4.6
37.5	25.0	4.2	4.4

Comparison of State Gradation Specifications

Figure A-4 is introduced to compare the different requirements presented in the previous sections. This figure presents the various state DOTs requirements for the percent passing of Sieve #8 (2.36 mm). This sieve was selected because it delineates the difference between a fine- and coarse-graded mixture. For the 9.5 mm and 12.5 mm NMAS, the percent passing in this sieve (i.e., PCS)

is 47% and 39%, respectively, as represented by the dotted blue lines in Figure A-4. The NCDOT, KTDOT, and ALDOT use the percent passing range indicated in the AASHTO M 323 specification. On the other hand, the highest variation is observed in the requirements of GDOT and SCDOT. In particular, the SCDOT Type D (used for secondary roads) allows a percent passing above the AASHTO M323 upper limit. Although not shown in the figure, the actual percent passing used in KTDOT mixtures is closer to the lower limit, with an average of 41% (see Figure A-3). In contrast, the average percent passing for NCDOT mixes (using the JMFs reported after year 2018) is 60%.

In the case of the 12.5 mm NMAS mixtures, the GDOT mixes are completely in the coarse-graded region, the TDOT (D and E) gradation bands cover coarse and fine but have a larger range in the fine side than the coarse side, and the VDOT (Level A, D, and E) bands provide a narrower range in the fine side of the gradation. The NCDOT 12.5 mm NMAS mixtures that were included in the pre-2018 classification have an allowable range that allows both dense- and coarse-graded surfaces. After inspecting the JMFs reported in the period of 2011-2017 with a 12.5 mm NMAS the average percent passing by Sieve #8 (2.36 mm) was 49.2%, resulting in fine-graded, dense structures.

Finally, a comparison of the number of gyrations, VMA, and VFA specified by each agency is presented in Figure A-5 to Figure A-7. As shown, the requirement is similar between DOTs, except for GDOT that has a number of gyrations of 125 for Level D surfaces (highest traffic category). In terms of VFA, the VDOT has the narrowest range followed by SCDOT. Lastly, the ALDOT specifies the highest VMA values for both 9.5 mm and 12.5 mm NMAS mixtures. Except for GDOT, which uses 0.8 for all their mixture and ALDOT that uses 0.9 for the 9.5 mm NMAS mix, all the states use the lower limit of 0.6 indicated in AASHTO M 323 for the dust to binder ratio. The upper limit for the dust to binder ratio is 1.2 for most states except GDOT, which uses 1.6, and KTDOT and ALDOT that specify a maximum value of 1.6 and 1.4 respectively.

Table A-23. Gradation specifications for Superpave mixtures.

Sieve Size	VDOT		GDOT			SCDOT			
	SM-12.5 (A, D, E)	SM-9.5 (A, D, E)	12.5 mm	9.5 mm (B, C, D)	9.5 mm (A)	Type A (Interstates and Intersections)	Type B (High Volume Primary)	Type C (High Volume Secondary)	Type D (Low Volume Secondary)
3/4" (19.5 mm)	100	-	100*	-	-	100	100	100	100
5/8" (16 mm)	-	-	-	-	-	-	-	-	-
1/2" (12.5 mm)	95-100	100	90-100	100*	100*	95-100	95-100	97-100	97-100
3/8" (9.5 mm)	90 max	90-10	70-85	90-100	90-100	76-100	76-100	83-100	90-100
#4 (4.75 mm)	-	80 max	-	55-75	65-85	52-75	52-75	58-80	70-95
#8 (2.36 mm)	34-50	38-67	34-39	42-47	53-58	36-56	36-56	42-62	50-82
#16 (1.18 mm)	-	-	-	-	-	-	-	-	-
#30 (0.60 mm)	-	-	-	-	-	16-36	16-36	20-40	20-50
#50 (0.30 mm)	-	-	-	-	-	-	-	-	-
#100 (0.15 mm)	-	-	-	-	-	5-18	5-18	5-20	6-20
#200 (0.075 mm)	2-10	2-10	3.5-7.0	4.0-7.0	4.0-7.0	2-8	2-8	2-9	2-10
Gyrations	65	65	100	B: 75, C: 100, D: 125	50	75	75	50	50
%Range for Asphalt	Selected at 4% Air void		Selected at 4% Air void			4.8-6	4.8-6	5-6.8	5-6.8
Air Voids (%)	2-5	2-5	-	-	-	3-4	3-4	3.5-4.5	4-9
VFA	70-78	73-79	65-78	65-78	67-80	70-80	70-80	70-77	60-70
Min VMA (%)	14	15	14	15	15	-	-	-	-
Dust/Binder Ratio	0.6-1.2	0.6-1.2	0.8-1.6	0.8-1.6	0.6-1.2	0.6-1.2	0.6-1.2	0.6-1.2	0.6-1.2

Table A-23. Gradation specifications for Superpave mixtures. (Continued).

Sieve Size	TDOT				KTDOT		ALDOT ⁽¹⁾	
	Grading D	Grading E	Grading TL	Grading TLD/TLE	12.5 mm Class 2, 3, 4	9.5 mm Class 2, 3, 4	12.5 mm	9.5 mm
3/4" (19.5 mm)	-	-	-	-	-	-	-	-
5/8" (16 mm)	100	100	-	-	100	-	-	-
1/2" (12.5 mm)	95-100	95-100	100	100	90-100	100	100	-
3/8" (9.5 mm)	80-93	80-93	100	90-100	90 max	90-100	90-100	95-100
#4 (4.75 mm)	54-76	54-76	89-94	54-76	-	90	32-90	75-100
#8 (2.36 mm)	35-57	35-57	53-77	35-57	28-58	32-67	32-67	-
#16 (1.18 mm)	-	-	-	-	-	-	-	30-60
#30 (0.60 mm)	17-29	17-29	23-42	17-33	-	-	-	-
#50 (0.30 mm)	10-18	10-18	-	10-18	-	-	-	-
#100 (0.15 mm)	3-10	3-11	9-18	3-10	-	-	-	-
#200 (0.075 mm)	0-6.5	0-8	6-14	3-7	2-10	2-10	2-10	6-12
Gyrations	Marshall: 75 blows SGC: 65				65	65	60	60
%Range for Asphalt	5.7-7	5.7-7	5.7-7.5	5.7-7	5.3 min	5.6 min	5.5 min	5.9 min
Air Voids (%)	-	-	-	-	-	-	-	-
VFA	-	-	-	-	-	-	-	-
Min VMA (%)	14	14	14	14	-	-	15.5	16.5
Dust/Binder Ratio	0.6-1.2	0.6-1.2	0.6-1.2	0.6-1.2	0.6-1.6	0.6-1.6	0.6-1.4	0.9-2

⁽¹⁾ ALDOT sets mix design designations according to the maximum aggregate size. So, 12.5 mm from ALDOT is most similar to what other state's would refer to as a 9.5 mm mixture.

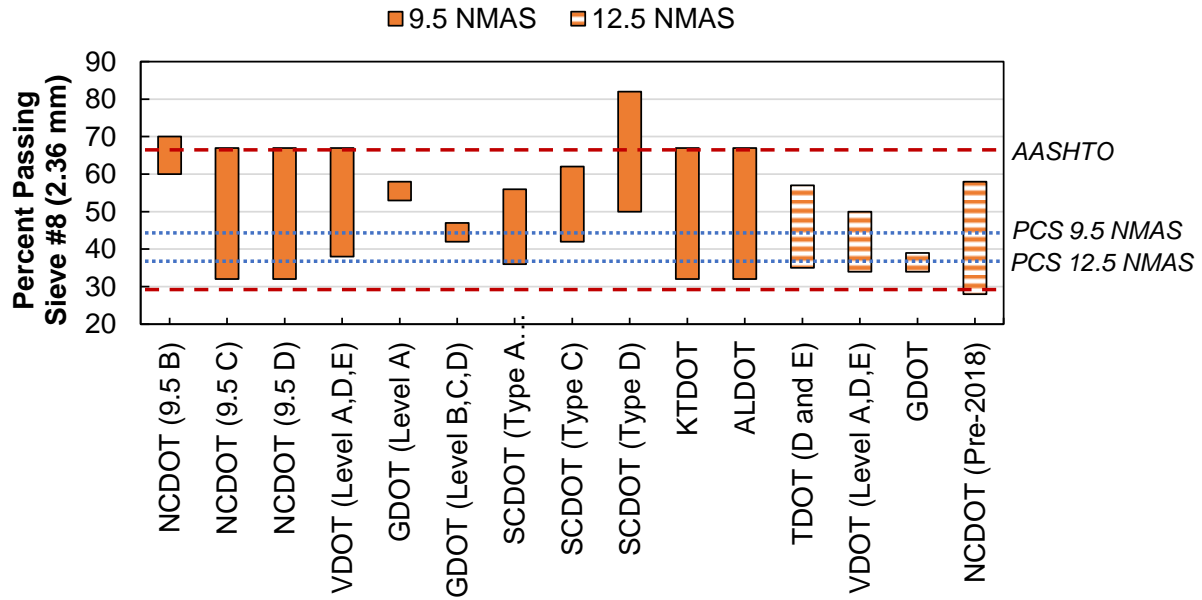


Figure A-4. Comparison of the different state requirements on the percent passing Sieve #8 (2.36 mm).

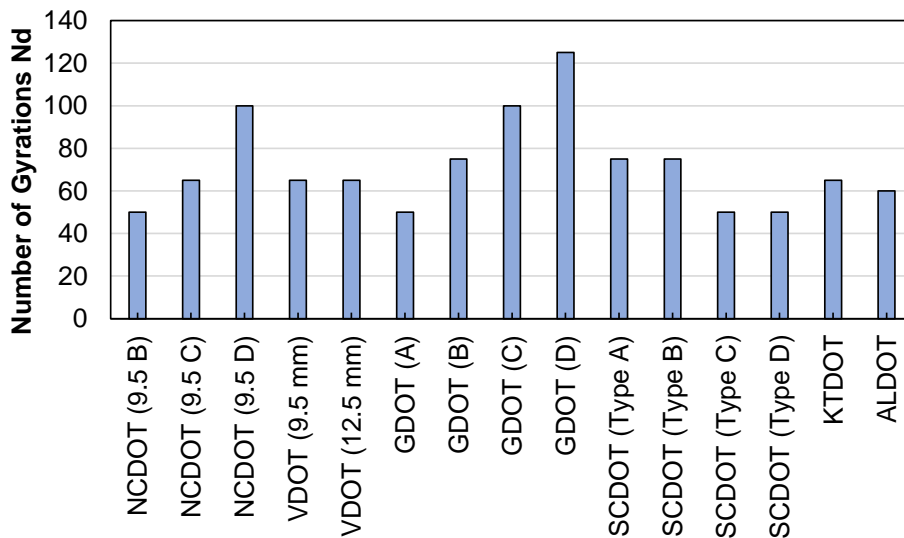


Figure A-5. Comparison of the number of gyrations (Nd).

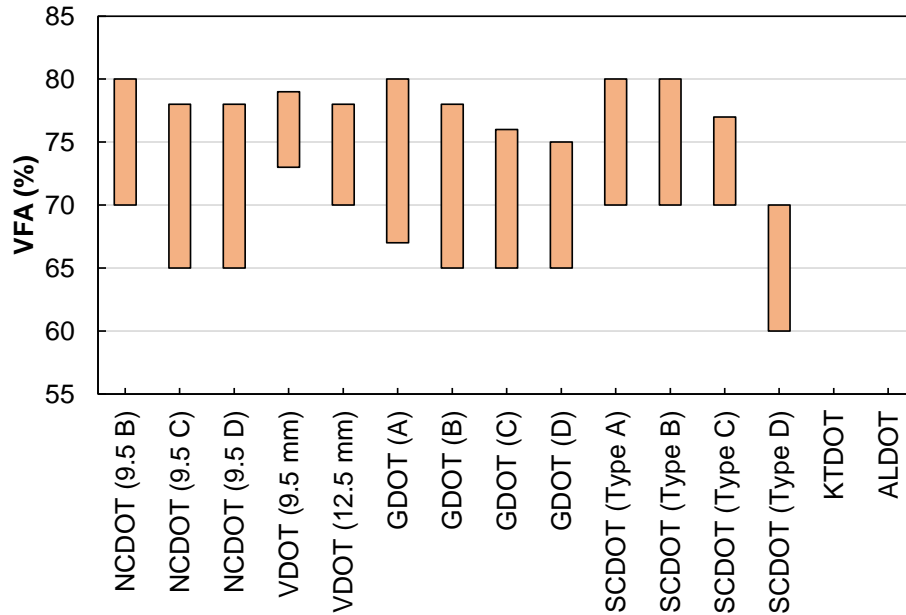


Figure A-6. Comparison of the VFA.

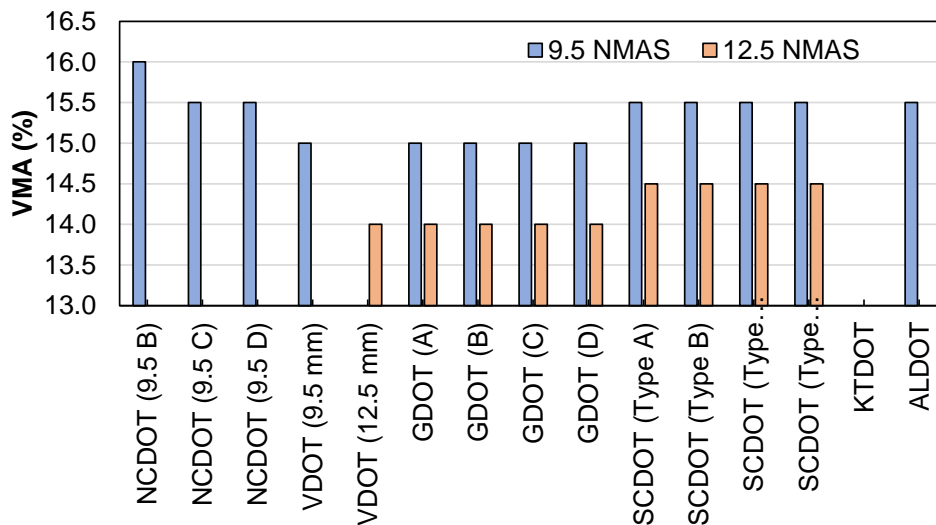


Figure A-7. Comparison of the VMA.

SMA

SMA mixes are based on a coarse aggregate gradation that is filled with asphalt binder to form a load bearing matrix (5). Its asphalt content is usually higher than conventional dense-graded mixes and it is typical that SMA includes stabilizing fiber, polymer modified asphalt, or both. Since its adoption in the U.S., SMA mixes have proved to be a hardwearing, and durable mix (17). The gap graded structure provides for greater in-service functional performance over dense-graded mixes. According to a survey conducted by state asphalt pavement associations, SMA is widely used by 18 states, and applied on routes with high traffic volumes, typically interstates (11). Yin and West (11), conducted an online questionnaire in 2016 and created the map depicted in Figure A-8, which shows states where SMA have been implemented. SMA is also typically used on pavement

sections where frequent maintenance is costly, high-stress pavement areas such as toll booths, bus stops and intersections, thin overlays, racetracks, and airfields (10).

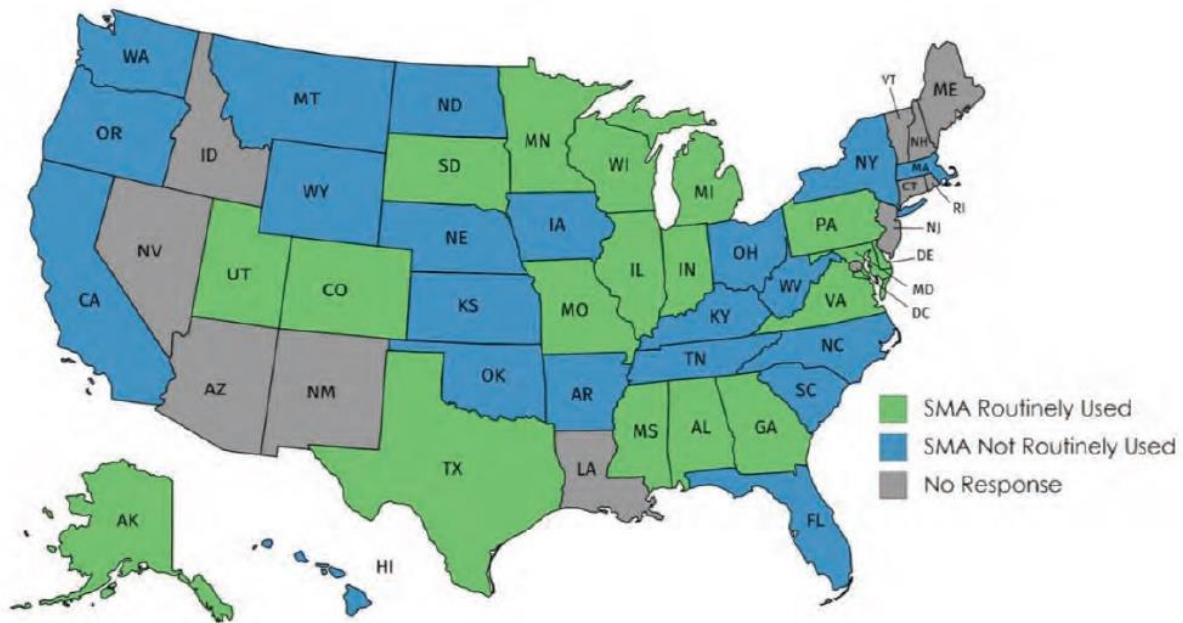


Figure A-8. SMA usage in the United States (11).

Friction

A study on two test sections, one with SMA mix and another one with the dense-graded mix at the NCAT test track was conducted by Yin and West (11). Surface friction was measured using a full-scale locked-wheel skid trailer and using the ASTM E274-11 standard test method. The trailer used a ribbed test tire and travelled at a speed of 40 mph. The results showed that the SMA section had higher Skid Number (*SN*) values than the dense-graded sections. The average *SN* numbers for the SMA and dense-graded sections were 35.3 and 30.4, respectively. Similarly, Kowalski et.al (52) monitored the friction on a dense-graded, SMA and porous friction course (PFC) to study the friction characteristic over 4 years. SMA and PFC exhibited similar friction characteristics in terms of *SN* measured following ASTM E524 at a speed of 40 mph. The study reported higher *SN* values for SMA than the dense-graded section. Miao et al. (53) measured friction using a dynamic friction tester (DFT) at different speeds and showed that SMA mixtures also exhibits an exponential decay in friction with traffic repetitions, but the asymptote value tends to be higher than the one observed in dense-graded surfaces. The asymptotic values also tend to be lower than those observed in UTBWC or OGFCs.

Texture

SMA is usually used as a wet weather safety countermeasure since its macrotexture does help regarding hydroplaning and sliding friction by offering a place for water to escape under the tire. The higher surface texture of SMA mixes could provide safety benefits through increased visibility of pavement markings, reduced glare from light reflections, and reduced splash and spray (5). A study by James and Prowell (17) on SMA mixes showed *MPD* values between 0.82 mm and 1.95

mm (0.03 and 0.08 in.). These values were collected from specimens with 7.0% air voids using the AMES Engineering Laser Texture Scanner Model 9400 HD.

The same Yin and West (11) study mentioned earlier also evaluated surface texture differences between dense-graded and SMA mixtures. Surface texture was measured weekly in the right wheel path of the pavement section using an ARAN inertial profiler. In their observation of *MTD*, the SMA section showed a reduction in *MTD* from 1.3 mm to 0.9 mm (0.05 to 0.035 in.) between September 2000 and January 2004 but exhibited a steady increase with time thereafter. A statistical comparison of the SMA section with the dense-graded section showed that the SMA section had consistently and statistically higher *MTD* than the dense-graded section and that the average difference between the two sections was approximately 0.24 mm (0.009 in.) (11). Likewise, Miao et al. (53) reported a reduction in *MTD*, measured with a sand path test, due to the traffic repetitions.

Design Methods

AASHTO developed a design standard for SMA mixes, AASHTO R 46-08 “*Standard Practice for Designing Stone Matrix Asphalt.*” and AASHTO M 325-08 “*Standard Specification for Stone Matrix Asphalt.*”. The design concept aimed at providing a rut resistant and durable mix relies on a stone-stone structure. As such aggregate hardness and shape are of key concern with maximum Los Angeles (LA) Abrasion value of 30 recommended to achieve the desired hardness. Other coarse aggregate quality requirements are shown in Table A-24. Because of the aggregate structure, SMA mixes usually require higher binder content (in the range of 5-7%) compared with typical Superpave mixes binder requirements (54). Figure A-9 shows the difference in structure between the SMA mixes and the traditional HMA mixes. Resistance to cracking and durability is also aided with the use of stabilizing agents such as fibers and polymers. The use of a higher binder content makes SMA admixes to be susceptible to draindown and as a preventive measure, mineral or cellulose fibers are added to the mixtures.

Table A-24. AASHTO M325-18 SMA Coarse Aggregate quality Requirements.

Test	Method	Min	Max
LA Abrasion percent loss	AASHTO T 96	-	30 ¹
Flat and Elongated percent ²			
	3 to 1	ASTM D 4791	-
	5 to 1	ASTM D 4791	20
Absorption, percent	AASHTO T 85	-	5
Soundness (5 Cycles), percent ³			
	Sodium Sulfate	AASHTO T 104	-
	Magnesium Sulfate	AASHTO T 104	15
Crushed Content, percent			
	One face	ASTM D 5821	100
	Two faces	ASTM D 5821	90

¹ Aggregates with higher L.A. Abrasion values have been used successfully to produce SMA mixes. However, when the L. A. Abrasion exceeds 30, excessive breakdown may occur in the laboratory compaction process or during in-place compaction.

² Flat and elongated criteria apply to the design aggregate blend.

³ Sodium sulfate or magnesium sulfate may be used. It is not a requirement to perform both methods.

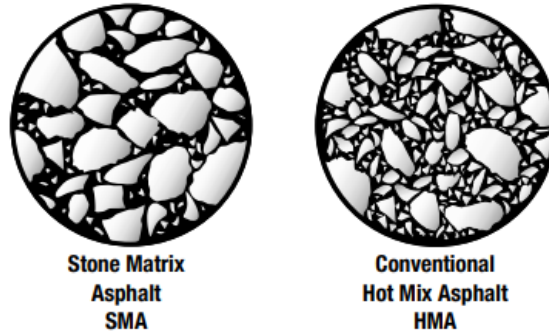


Figure A-9. The structure of SMA versus conventional HMA (54).

For SMA design across the USA, state highway agencies have either adopted the AASHTO guidelines or modified the guidelines to fit their local conditions. The results of a survey done by Yin and West to identify the most highly preferred design methods is shown in Table A-25 (11). As shown in the table, as of 2018, eight state agencies designed SMA mixes following AASHTO R 46-08, six agencies had their own specifications, while the other four agencies followed the AASHTO R 35-22 or M 325-08 requirements. A summary of the gradation and mixture volumetric requirements for some state DOTs is shown in Table A-26.

Table A-25. SMA Mixture Design Procedures for state DOTs (10, 11).

Highway Agency	Design Method
Alabama DOT	ALDOT Procedure 395
Colorado DOT	AASHTO R 46-08, with 50-blow Marshall design
Georgia DOT	GTD 123
Illinois DOT	AASHTO R 46-08 with modifications
Indiana DOT	Illinois Tollway SMA special provision
Kansas DOT	KDOT special provision
Maryland SHA	AASHTO R 35-22
Michigan DOT	AASHTO R 46-08
Minnesota DOT	AASHTO R 46-08
Missouri DOT	AASHTO R 46-08
Pennsylvania DOT	AASHTO R 46-08 with modifications
South Dakota DOT	AASHTO R 46-08
Texas DOT	Tex-204-F
Utah DOT	AASHTO R 46-08
Virginia DOT	Virginia Test Method 99
Wisconsin DOT	AASHTO R 35-22 and AASHTO M 323-17
Louisiana DOT	AASHTO M 325-08

Also, a graphical comparison of the gradation requirements is included in Figure A-10 and Figure A-11, where the percent passing ranges on the 4.75 and 2.36 mm (#4 and #8 sieves) are plotted. As shown, for the SMA 9.5 mm (Part a of both figures), the GDOT and Maryland State Highway Agency (MDSHA) follow closely the AASHTO M 325-08 limits for both sieve sizes. The ALDOT and the Mississippi DOT (MDOT) allow a wider range in Sieve #4 than the one specified by AASHTO but comply with the range for Sieve #8. It must be noted that ALDOT uses MAS to classify mixes according to the gradation, hence, a 12.5 mm MAS mix is equivalent to the 9.5 mm NMAS. The gradation ranges for Minnesota DOT (MnDOT) and VDOT specify the coarser structures from all the states agencies compared. For the SMA 12.5 mm (part b of both figures),

for Sieve #4 except for MDSHA all the states follow the AASHTO limits. For Sieve #8, MDSHA uses a narrower band. Again, given the fact that ALDOT uses MAS to classify its mixtures, a 19.0 mm MAS mix is analogous to a 12.5 mm NMAAS.

Experience has indicated that SMA mixes tend to be highly sensitive to construction quality and the properties of the selected materials. This mixture type also has low tolerance to small deviations from the mix design parameters (5). The success of SMA mixes therefore requires better precision in the mix design, material proportion during production, good control of the placement temperature and proper compaction.

Table A-26. Gradation specification for SMA design for state DOTs.

Sieve Size	AASHTO M 325-08			Georgia			Maryland			Minnesota ¹
	19.0 mm	12.5 mm	9.5 mm	19.0 mm	12.5 mm	9.5 mm	19.0 mm	12.5 mm	9.5 mm	
1" (25 mm)	100	-	-	100	-	-	100	-	-	-
3/4" (19.5 mm)	90-100	100	-	90-100	100	-	100	100	-	100
1/2" (12.5 mm)	50-88	90-100	100	44-70	85-100	100	82-88	90-99	100	86-96
3/8" (9.5 mm)	25-60	50-80	70-95	25-60	50-75	70-100	60 max	70-85	70-90	60-85
#4 (4.75 mm)	20-28	20-35	30-50	20-28	20-28	28-50	20-28	30-42	30-50	23-35
#8 (2.36 mm)	16-24	16-24	20-30	15-22	16-24	15-30	14-20	20-23	20-30	15-25
#16 (1.18 mm)	-	-	21 max	-	-	-	-	-	-	-
#30 (0.60 mm)	-	-	18 max	-	-	-	-	-	-	-
#50 (0.30 mm)	-	-	15 max	10-20	10-20	10-17	-	-	-	-
#200 (0.075 mm)	8-11	8-11	8-12	8-12	8-12	8-13	9-11	8-11	8-13	10-12
%Range for Asphalt	6.0 min	6.0 min	6.0 min	5.5-7.5	5.8-7.5	6.0-7.5	6.5 min	6.5 min	6.5 min	5.5-6.8
Air Voids (%)	4	4	4	3.5±0.5	3.5±0.5	3.5±0.5	3.5	3.5	3.5	4
VFA	-	-	-	70-90	70-90	70-90	-	-	-	70-80
Draindown (%)	<0.3	<0.3	<0.3	<0.3	<0.3	<0.3	<0.3	<0.3	<0.3	≤0.3
Sieve Size	Mississippi			Virginia			Alabama ²			
	19.0 mm	12.5 mm	9.5 mm	19.0 mm	12.5 mm	9.5 mm	19.0 mm	12.5 mm	9.5 mm	
1" (25 mm)	100	-	-	100	-	-	-	-	-	-
3/4" (19.5 mm)	90-100	100	-	85-95	100	100	100	-	-	-
1/2" (12.5 mm)	50-74	90-100	100	50-60	85-95	90-100	90-100	100	-	-
3/8" (9.5 mm)	25-60	26-78	90-100	30-45	80 max	70-85	26-78	90-100	100	-
#4 (4.75 mm)	20-28	20-28	26-60	-	22-30	25-40	20-28	26-60	90-100	-
#8 (2.36 mm)	16-24	16-24	20-28	16-24	16-24	15-25	16-24	20-28	28-65	-
#16 (1.18 mm)	13-21	13-21	13-21	-	-	-	13-21	13-21	22-36	-
#30 (0.60 mm)	12-18	12-18	12-18	12-16	15-20	-	12-18	12-18	18-28	-
#50 (0.30 mm)	12-15	12-15	12-15	-	-	-	12-15	12-15	15-22	-
#200 (0.075 mm)	8-10	8-10	8-10	8-10	10-12	10-12	8-10	8-10	12-15	-
%Range for Asphalt	5.3-6.6	5.3-6.6	5.3-6.6	5.5 min	6.3 min	6.3 min	-	-	-	-
Air Voids (%)	-	-	-	-	-	-	-	-	-	-
VFA	4	4	4	-	-	-	-	-	-	-
Draindown (%)	-	-	-	-	-	-	-	-	-	-

¹ Minnesota only has a single aggregate size gradation. ²ALDOT uses Maximum Aggregate Size (MAS) to categorize their mixes, hence the 12.5 mm MAS is equivalent to 9.5 mm NMA. - indicates that no limits are specified

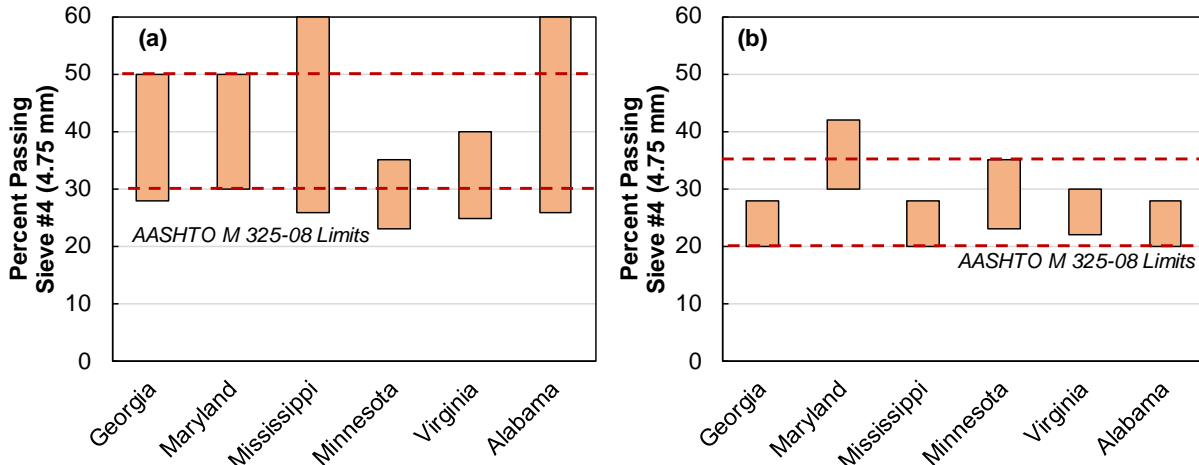


Figure A-10. Percent passing limits in Sieve #4 (4.75 mm) for SMA mixtures: (a) 9.5 mm and (b) 12.5 mm NMA.

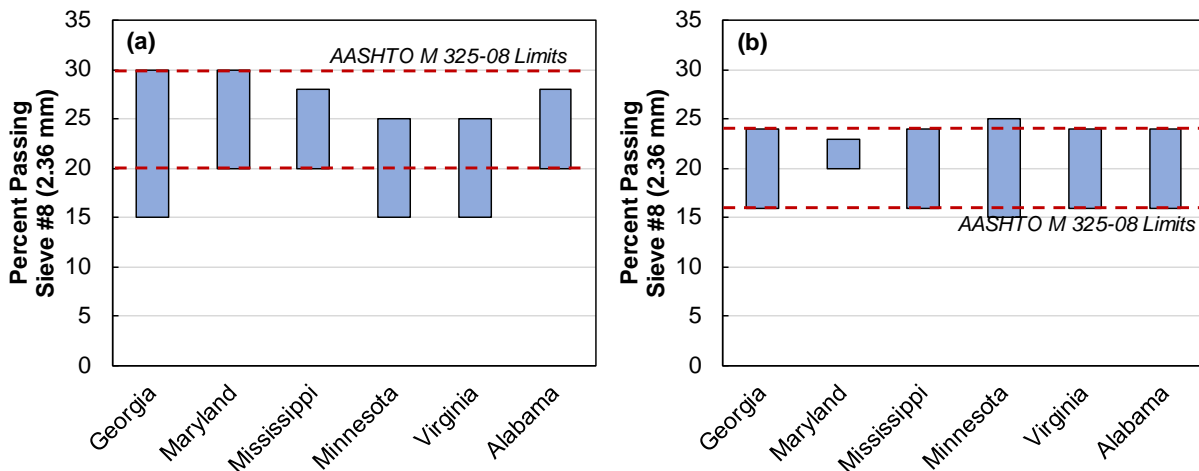


Figure A-11. Percent passing limits in Sieve #8 (2.36 mm) for SMA mixtures: (a) 9.5 mm and (b) 12.5 mm NMA.

UTBWC

Ultra-Thin Bonded Wearing Course (UTBWC) surface treatments were introduced to United States in the early 1990s. Early sections of UTBWC were placed by Mississippi, Alabama, and Texas. The idea was to enhance pavement durability by applying a gap graded asphalt mix over a polymer modified asphalt emulsion. The thickness of the UTBWC surface ranges from 9.5 mm (0.37 in.) to 19 mm (0.75 in.) (55). The polymer modified emulsion membrane seals the existing pavement surface and provides high binder content at the interface of the existing pavement and the gap graded HMA. The open surface structure provides friction benefits under wet conditions, reduces noise, allows water to easily flow, hence reducing splash and spray (56). A schematic of UTBWC is illustrated in Figure A-12.

The performance of UTBWC has been studied across different states. Studies have concluded some of the benefits of UTBWC surfaces such as: reducing the rate of deterioration caused by traffic, weathering, raveling, oxidation, sealing small cracks, tire noise reduction, high skid

resistance, reducing splash, back spray, and reducing the hydroplaning potential (55, 56). A case study done by Ji et al. (57), indicated that the performance life of a UTBWC treatment, based on the Pavement Condition Rating (*PCR*), is 3 to 4 years compared to a 6 to 8 years that can be achieved from an overlay. Although reported not to be economically feasible in all situations, UTBWC overlays can provide a better alternative to seal coating with improved ride quality and noise characteristics (58). The cost analysis in the study by Ji et.al. (57), showed that UTBWC can be cost-effective if it can provide more than 3.6 years of service life.

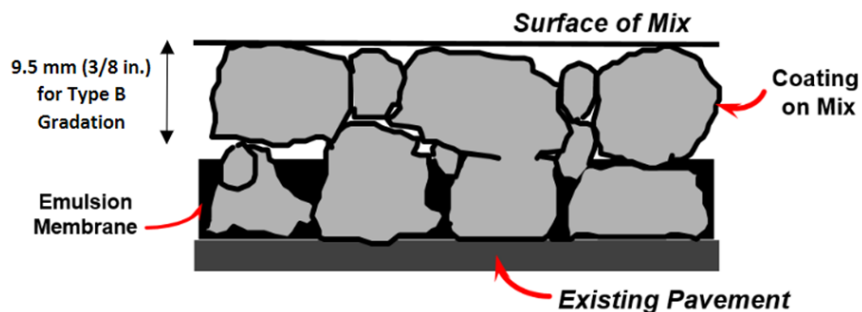


Figure A-12. A schematic of UTBWC (59).

A study in Louisiana showed that UTBWC treatment extended the life of a pavement by an average of 8.8 years with an expected variability of ± 3.5 years (60). However, the benefits of UTBWC are also dependent on the condition of the pavement prior to treatment. Game et al. (60) found out that the benefits from UTBWC treatment were obtained when the pavement was subjected to a lower truck volume in the range of 0-500 trucks per day and pre-treatment Pavement Condition Index (*PCI*) of 70 to 60. Furthermore, the open texture of UTBWC poses a challenge in cold regions where a substantial amount of deicing material is required to achieve a clear and dry pavement surface during winter maintenance (59). The open structure of UTBWC surfaces requires more deicing material compared to dense-graded surfaces, thus allowing the snow to melt at the surface and form a bond with the existing pavement.

Friction

In terms of skid resistance, UTBWC mixes have comparable, and in most cases better, friction performance (58) than a dense-graded asphalt mix. In a literature review of some of the early UTBWC projects, Hanson (55) noted a substantial increase in friction, measured with a Locked-Wheel Skid Tester (LWST) in pavement sections after the placement of UTBWC surfaces. In one instance, in US-280 in Alabama, the *SN* of a UTBWC section after 3.75 years was 49 compared to 41 for a control section paved with a dense-graded surface.

In 2012, Li et.al. (61) evaluated four UBTWC sections in Indiana, with traffic volume from low (1,900 vehicles per day) to high (105,000 vehicles per day) and the ages spanning between 12 and 48 months. The results of the study indicated that UTBWC can provide sufficient and consistent skid resistance to allow quick opening to traffic. The *SN* on the fresh UTBWC pavements, measured with a Locked-Wheel Tester (LWST), varied between 48 and 59 in the test sections. The friction numbers also tended to peak after 6 months of service or less, which is about 6 months earlier compared to conventional dense-graded mixes (61). It was concluded that the UTBWC has the potential to provide durable friction performance as the friction number in one test section decreased by only 8.3% after 48 months in service. However, a significant friction decrease over time may also be observed, as evidenced in one test section where friction decreased by more than

34% after 33 months in service. The main cause for the friction reduction was associated with the polishing process occurring to limestone aggregate.

Texture

UTBWC is reported to provide good surface macrotexture and excellent aggregate retention (57). The texture performance of UTBWC has been observed across different projects. For example, the Pennsylvania DOT (PennDOT) constructed three projects in September 1993 and one in May 1996 (62). The four projects were monitored at regular intervals over a five-year period. Macrotexture was quantified using a sand path test, and the researchers compared *MTD* values of HMA control sections against those of the newly constructed UTBWC. In one of the project sites evaluated, the *MTD* of the UTBWC sites ranged from 1.07 mm (0.042 in.) to 1.98 mm (0.078 in.), whereas the *MTD* of the control sections ranged between 0.56 mm (0.022 in.) and 0.69 mm (0.027 in.). Similarly, in another of the four projects the *MTD* of the UTBWC section ranged from a low of 0.97 mm (0.038 in.) to a high of 1.98 mm (0.078 in.), and the *MTD* of the control section constructed using a cold-laid asphalt emulsion pavement ranged between 0.48 mm (0.019 in) and 0.99 mm (0.039 in) (55). Overall, the *MTD* of the UTBWC was more than twice as high as the control sections.

Another published report from Indiana DOT (61) indicated that UTBWC can provide a coarse pavement surface. The measured *MPD* using a circular texture meter (CTM) was between 0.95 mm (0.037 in.) and 0.99 mm (0.039 in.), which is higher than normal dense-graded mixes. These studies indicate that UTBWC surfaces have higher texture than normal dense-graded mixes. However, Miao et al. (53) reported a texture reduction caused by traffic repetitions, changing from an initial value of 1.1 mm (0.04 in.) to 0.8 mm (0.03 in.) over a period of 2.5 years and after more than 7 million traffic repetitions.

Design Methods

The performance of UTBWC depends on the quality of the materials and construction methods which are dependent on the mix design. Like any other asphalt mix, the design of UTBWC incorporates several variables, including aggregate size and gradation, binder grade, and binder content. As earlier mentioned, UTBWC mixes are characterized by the heavy polymer modified asphalt emulsion membrane that is used. AASHTO has developed guidelines for UTBWC mix design, AASHTO PP 100-20 “*Standard Practice for Ultrathin Bonded Wearing Course Design*”. Several DOTs have adopted these guidelines but with modifications to fit within the agency requirements. The gradation criteria as specified by the AASHTO PP 100-20, and the adaptations made by the NCDOT, PennDOT, and INDOT are shown in Table A-27. Similarly, for other properties of the UTBWC mix design criteria, such as draindown, and moisture sensitivity, state highway agencies conduct the corresponding tests following the applicable AASHTO test methods.

The NCDOT adjusted the AASHTO PP 100-20 guidelines as shown in Table A-27. Aggregate-type material such as crystalline limestone, crystalline-dolomitic limestone or marble are not allowed for use in the mix design. The specifications also do not allow the use of Recycle Asphalt Pavement (RAP); however Recycled Asphalt Shingles (RAS) may be used. Similarly, the Pennsylvania DOT (PennDOT) and the Indiana DOT (INDOT) developed their own specifications for UTBWC design. The gradation specifications established by PennDOT and INDOT are included in Table A-27. A graphical comparison of the gradation bands is presented in Figure A-13 and Figure A-14, for the percent passing sieves #4 and #8 (4.75 and 2.36 mm), respectively. As

shown, there is no difference in the percent passing Sieve #4 and #8 for the two NMAS of 9.5 and 12.5 mm. The NCDOT allows a higher percent passing Sieve #4 than the AASHTO limit and permits a wider range for Sieve #8. The other two DOTs permit a gradation band closer to the AASHTO limits. Finally, the NCDOT allows the largest percent passing Sieve #200 (0.075 mm), even higher than the AASHTO recommendation.

Table A-27. UTBWC mix design specification for state DOTs.

Sieve Size	AASHTO PP 100-20			NCDOT ¹	PennDOT			INDOT		
	12.5 mm	9.5 mm	4.75 mm		12.5 mm	9.5 mm	6.3 mm	12.5 mm	9.5 mm	4.75 mm
1" (25 mm)	-	-	-	-	-	-	-	-	-	-
3/4" (19.5 mm)	100	-	-	-	100	100	100	100	-	-
1/2" (12.5 mm)	85-100	100	-	100	85-100	100	100	85-100	100	-
3/8" (9.5 mm)	55-80	85-100	100	85-100	65-85	75-100	100	55-80	85-100	100
#4 (4.75 mm)	22-38	22-38	40-55	28-44	23-37	23-37	40-60	22-38	22-38	40-55
#8 (2.36 mm)	19-32	19-32	20-32	17-34	21-31	21-31	15-30	19-32	19-32	20-32
#16 (1.18 mm)	15-24	15-24	15-24	13-23	15-23	15-23	12-20	15-24	15-24	15-24
#30 (0.60 mm)	11-18	11-18	11-18	8-18	10-18	10-18	8-15	11-18	11-18	11-18
#50 (0.30 mm)	8-14	8-14	8-14	6-13	8-14	8-14	6-12	8-14	8-14	8-14
#100 (0.15 mm)	5-10	5-10	5-10	4-10	6-10	5-10	5-10	5-10	5-10	5-10
#200 (0.075 mm)	4-5.5	4-5.5	4-5.5	3-7	4-6.5	4.0-6.5	4-6.5	4-5.5	4-5.5	4-5.5
%Range for asphalt content	4.6-6.1	4.8-6.1	5.0-6.3	4.6-5.8	4.5-5.7	4.5-5.7	4.5-5.8	4.6-6.1	4.8-6.1	5-6.3
Recommended placement rate (lb./yd ²)	90	75	65	70	- ²	- ²	- ²	90	75	65
Draindown (%)	- ²	- ²	- ²	<0.1	<0.1	<0.1	<0.1	-	-	-

¹ North Carolina only has a single aggregate size gradation.

² Indicates that no limits are specified

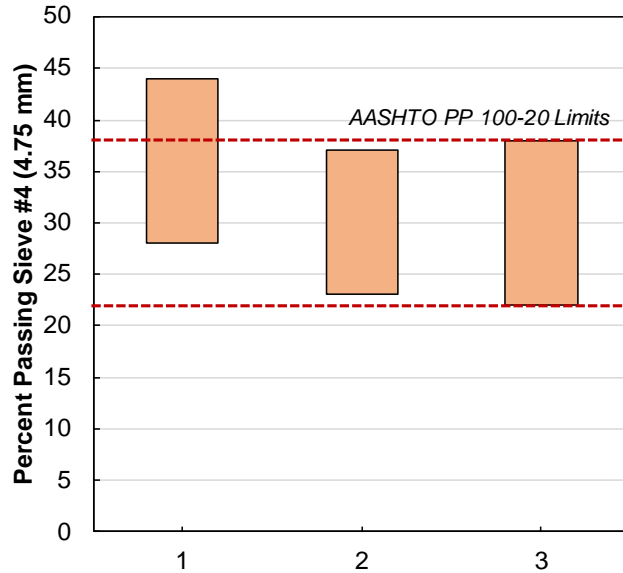


Figure A-13. Comparison of the percent passing Sieve #4 (4.75 mm) for UTBWC mixes: (a) 9.5 mm and (b) 12.5 mm.

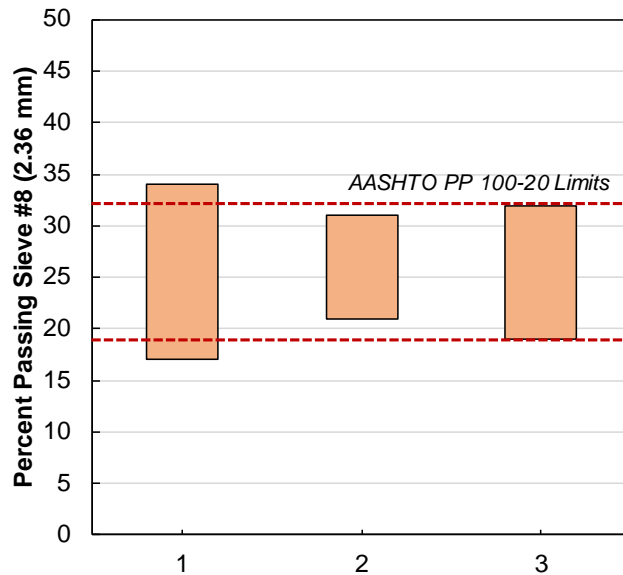


Figure A-14. Comparison of the percent passing Sieve #8 (2.36 mm) for UTBWC mixes: (a) 9.5 mm and (b) 12.5 mm.

OGFC

Open-graded friction course (OGFC) has been widely used in the United States and other parts of the world to improve friction resistance on asphalt pavements. The open structure of OGFC surfaces allow water to drain through, hence improving friction on wet weather conditions. A high void content usually results in the open structure with enhanced surface drainage (5). OGFC mixtures have several benefits such as reducing the risk of hydroplaning, improving wet surface friction, reduced splash and spray which increases visibility behind vehicles, and reduced crashes associated with wet pavement conditions (63). OGFC mixtures also reduce pavement tire-noise.

Different names have been used for OGFC mixtures; these include porous friction course, permeable friction course, open-graded surface course, porous asphalt, etc.

Despite the benefits of OGFC, durability has been a main problem facing this mixture type since its introduction (64, 65). Raveling and stripping due to the loss of the bond between the binder and aggregate are common distresses in OGFC leading to shorter lifespan and increased maintenance costs. The interconnected voids in the OGFC mixes help surface water to drain quickly, but also accelerate the aging process of the mixes as air can pass through the pavement structure easily (66). In cold climates, OGFC surfaces pose a challenge in maintenance. Huber (67) noted that OGFC surfaces tend to be among the first sections to freeze yet the last to thaw. Sand and salt application during snow removal has the potential to cause clogging of the pores. Clogging may reduce the effectiveness of OGFC surfaces to drain surface water from the pavement and noise reduction.

Friction

One of the main functional benefits of OGFC mixes is improving pavement friction. Researchers have concluded that OGFC surfaces provide better friction than regular dense-graded surfaces (65–67). The friction performance of OGFC surfaces results from a complex interaction of both microtexture and macrotexture of the surface, and therefore Jackson et al. (68) recommended utilizing both *MPD* and *SN* to better characterize friction performance. Surfaces with higher texture provide better drainage, reduce hydroplaning potential, and hence provide greater resistance to skidding. A study made by King et.al. (66), conducted across the state of Louisiana, showed that OGFC sections overall had higher *SN* values than non OGFC sections, even after 5 years under similar traffic loads. The *SN* for OGFC surfaces collected using a LWST at 50 mph, ranged between 41.5 to 49.8 compared to non OGFC surfaces with 36.5 to 38.4 (66).

Texture

On a five-year performance study of an OGFC section on the NCAT test track, Xie et al. (65) evaluated *MPD* values collected using a high frequency laser. The values collected, shown in Figure A-15, were in the range of 1.0 mm (0.039 in.) to 1.7 mm (0.067 in.). The *MPD* values decreased to the range of 1.0 mm (0.039 in.) to 1.4 mm (0.055 in.) as the ESALS were increased and remained relatively constant between 13 million ESALS and 20 million ESALS. The study noted that there was no significant difference in *MTD* between a 9.5 mm OGFC mix and a 12.5 mm OGFC mix with synthetic fiber; but lower *MTD* values were observed for a 12.5 mm ground-tire-rubber (GTR) modified OGFC mix. In the figure, E9A, E9B and E10 were the three test sections. Each test section was paved with a different OGFC mix. For E9A the OGFC mixture was designed with a 9.5 mm NMAS gradation while the E9B used a 12.5 mm NMAS gradation. Additionally, the E9A mix used cellulose fiber while E9B used synthetic fiber. The mix for test section E10 was a 12.5mm NMAS mix, like E9B, but used a GTR modified asphalt (69).

According to the NCHRP Report 108 (5), the *MPD* for a new OGFC overlay should range between 1.5 mm (0.059 in.) to 3.0 mm (0.118 in.). In this sense, a field performance evaluation study across three road sections in Louisiana, I-20, US-61, and US-171, indicated that the *MPD* values were on average 1.3 mm, 1.5 mm, and 2.5 mm, respectively.

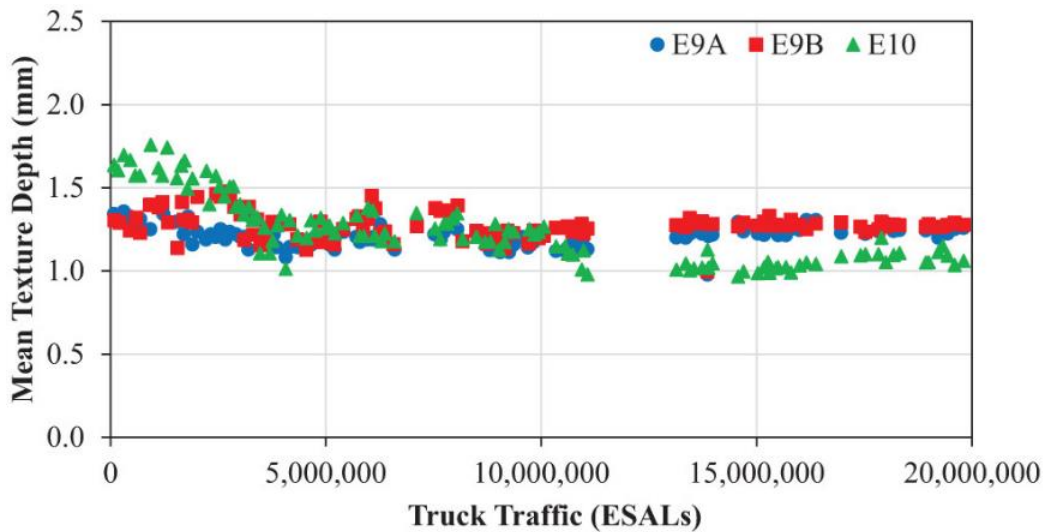


Figure A-15. OGFC mean texture depth comparison; where, E9A: 9.5 mm OGFC; E9B: 12.5 mm OGFC with synthetic fiber; E10: 12.5 mm GTR modified OGFC mix (65).

Design Methods

The FHWA developed a mix design method for OGFC based on the Marshall Mix Design and published it in the technical advisory T5040.31 (70). The basic steps included in the FHWA design procedure include determining the optimum asphalt content, mixing temperature, air voids, and moisture damage susceptibility. The recommended grade of asphalt binder is AC-20. The recommended gradation for OGFC according to FHWA design method is shown in Table A-28. The optimum mixing temperature is established by conducting a Pyrex glass plate test and checking for any excessive draindown. Moisture susceptibility is conducted following the Immersion-Compression Test (AASHTO T165 and T167) on the designed mixture.

NCAT also developed OGFC design procedure that includes material selection, gradation specification, determination of optimum asphalt content, and evaluation of moisture susceptibility (71). ASTM has also developed a standard design procedure for OGFC mixes, ASTM D7064/D7064M “Standard Practice for Open-Graded Friction Course (OGFC) Mix Design.” Different SHAs have adopted different specifications and design methods for OGFC mixtures based upon the FHWA, NCAT, ASTM, and AASHTO guidelines and informed by their experience with working with these mixture types.

Table A-28. FHWA gradation specifications for OGFC mixes (70).

Sieve Size	Percent Passing (by weight)
1/2" (12.5 mm)	100
3/8" (9.5 mm)	95-100
#4 (4.75 mm)	30-50
#8 (2.36 mm)	5-15
#200 (0.075 mm)	2-5

Aggregate gradation is one of the main controlling factors in the functional and structural performance of OGFC mixes (5). The coarse aggregate portion controls the porosity while the finer proportion is kept low to enable contact between the larger aggregates and prevent their separation (72). Gradation specifications for OGFC vary between states, with some states using

only one gradation, while others permit selecting between two or more possible gradations. In the 2012 material specifications, the NCDOT used three different gradation specifications, as shown in Table A-29. These gradations were complemented with the set of design parameters indicated in Table A-30. However, after 2018 the NCDOT specifications only allow OGFC Type FC-1 Modified with binder grade PG 76-22. A summary of the OGFC mix design specifications as established by different state agencies is presented in Table A-31.

The comparison of the gradation bands specified by each agency is presented in Figure A-16. In this figure the blue box indicates the NCDOT OGFC values, and the red horizontal lines show the FHWA guidelines. As presented, most of the gradations bands lies between the FHWA requirements, with a special case of Alabama, Florida, New Mexico, Oregon, and the NCDOT FC-2 Mod type. In these cases, the gradation falls below the minimum value suggested by the FHWA for the 4.75 mm sieve (see Part (a) of Figure A-16). gradation. These gradations provide coarser surfaces than the ones that the FHWA guidelines would produce. Data for the 2.36 mm sieve size is also shown in Figure A-16 (b). As indicated here, except for California, Arizona, and Wisconsin the gradations follow the FHWA guidelines. It important to note that New Mexico, Oregon, and Oklahoma do not limit this sieve.

Table A-29. NCDOT OGFC gradation criteria (NCDOT 2012 specifications, Table 650-1).

Sieve Size	Total Percent Passing		
	Type FC-1	Type FC-1 Modified ¹	Type FC-2 Modified
3/4" (19.0 mm)	-	-	100
1/2" (12.5 mm)	100	100	85-100
3/8" (9.5 mm)	75-100	75-100	55-75
#4 (4.75 mm)	25-45	25-45	15-25
#8 (2.36 mm)	5-15	5-15	5-10
#200 (0.075 mm)	1-3	1-3	2-4

¹ Currently, this is the only OGFC mix type used by the NCDOT as indicated in the 2024 specifications

Table A-30. NCDOT OGFC mix design criteria (NCDOT 2012 specifications, Table 650-2).

Property	Design Parameters		
Asphalt Binder Grade	PG 64-22	PG 76-22 ¹	PG 76-22
Asphalt Binder, % Range	5.0-8.0	5.0-8.0	5.0-8.0
Mixing Temperature Range Established by Engineer	200-275°F	300-350°F	300-350°F
Draindown, % AASHTO T 305	0.3 max	0.3 max	0.3 max

¹ The 2024 specification only allows FC-1 Modified OGFC with a PG76-22 binder.

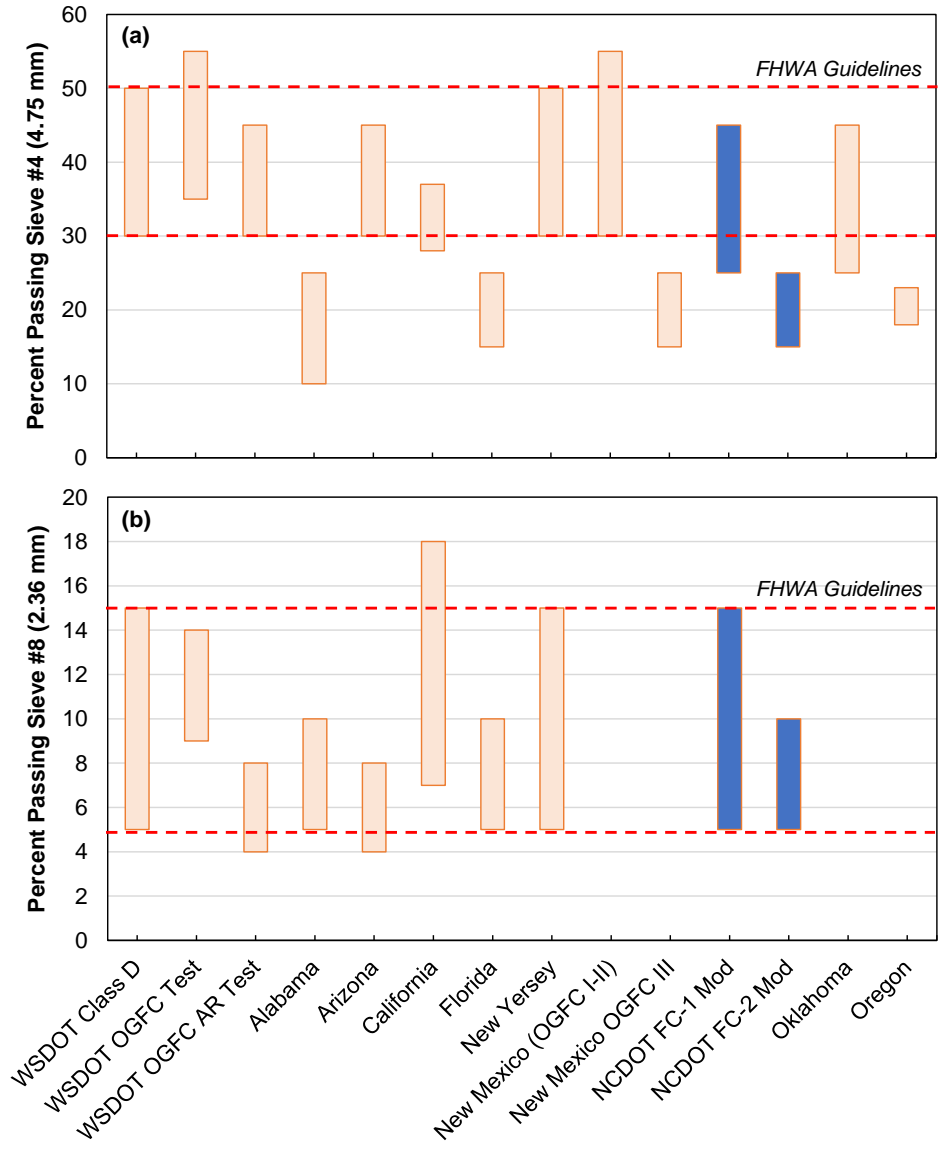


Figure A-16. Comparison of the percent passing by sieves: (a) 4.75 mm and (b) 2.36 mm.

Table A-31. OGFC mix design specifications for state DOTs (68).

Sieve Size and Mix Parameters	WSDOT Class D	WSDOT OGFC Test	WSDOT OGFC - AR Test	Alabama OGFC	Arizona ARFC	California O-G RAC	Florida FC-5
3/4" (19.0 mm)	-	-	-	100	-	100	100
1/2" (12.5mm)	100	-	-	85-100	-	95-100	85-100
3/8" (9.5 mm)	97-100	100	100	55-65	100	78-89	55-75
#4 (4.75 mm)	30-50	35-55	30-45	10-25	30-45	28-37	15-25
#8 (2.36 mm)	5-15	9-14	4-8	5-10	4-8	7-18	5-10
#16 (1.18 mm)	-	-	-	-	-	0-10	-
#200 (0.075 mm)	2-5	0-2.5	0-2.5	2-4	0-3	0-3	2-4
% Asphalt	4-6	9	9	5.6-9	-	-	ARB12
Binder Grade	PG 58-22	PG 70-22	A-R	PG 76-22	A-R	A-R	PG 76-22
Min Air Temp.	55°F	55°F	55°F	40°F	70°F*	70°F	65°F
Sieve Size and mix parameters	New Jersey OGFC	New Mexico OGFC I & II	New Mexico OGFC III	North Carolina OGFC FC-1 Mod	North Carolina OGFC FC-2 Mod	Oklahoma OGFC	Oregon OGM 1/2"
3/4" (19.0 mm)	-	100	100	-	100	-	99-100
1/2" (12.5 mm)	100	100	70-90	100	85-100	100	90-98
3/8" (9.5 mm)	80-100	90-100	40-65	75-100	55-75	90-100	-
#4 (4.75 mm)	30-50	30-55	15-25	25-45	15-25	25-45	18-23
#8 (2.36 mm)	5-15	-	-	5-15	5-10	-	3-15
#10 (2.0 mm)	-	0-20	6-12	-	-	0-10	-
#40 (0.425 mm)	-	0-12	0-8	-	-	-	-
#200 (0.075 mm)	2-5	0-6	0-5	1-3	2-4	0-5	1-5
% Asphalt	-	-	-	5-8	5 - 8	-	-
Binder Grade	-	-	-	PG 76-22	PG 76-22	-	-
Min Air Temp	60° F	70° F	70° F	-	-	60° F	-

Table A-31. OGFC mix design specifications for state DOTs (68). (Continued).

Sieve Size and mix parameters	Georgia OGFC 12.5	Idaho PMS-OG	Indiana OGFC OG19.0	Nevada OGFC
3/4" (19.0 mm)	100	-	70-98	-
1/2" (12.5 mm)	85-100	100	40-68	100
3/8" (9.5 mm)	55-75	95-100	20-52	90-100
#4 (4.75 mm)	15-25	30-50	10-30	35-55
#8 (2.36 mm)	5-10	5-15	7-23	-
#16 (1.18 mm)	-	-	-	5-18
#200 (0.075 mm)	2-4	2-5	0-8	0-4
% Asphalt	5.75-7.25	-	-	-
Binder Grade	PG 76-22	-	-	-
Min Air Temperature	55°F	60°F	60°F	-
Sieve Size and mix parameters	Oregon OGM 3/4" Open	South Carolina OGFC	Texas PGFC	Texas A-R
3/4" (19.0 mm)	85-96	100	100	100
1/2" (12.5 mm)	55-71	85-100	80-100	95-100
3/8" (9.5 mm)	-	55-75	35-60	50-80
#4 (4.75 mm)	10-24	15-25	1-20	0-8
#8 (2.36 mm)	6-16	5-10	1-10	0-4
#10 (2.0 mm)	-	-	-	-
#40 (0.425 mm)	-	-	-	-
#200 (0.075 mm)	1-6	0-4	1-4	0-4
% Asphalt	-	5 - 7	5.5-7.0	8-10
Binder Grade	-	PG 76-22	PG 76-22	A-R
Min Air Temperature	60°F	60°F	70°F	70°F

High Friction Surface Treatment

High friction surface treatment (HFST) has been used as a safety countermeasure to address insufficient friction on high friction demand locations (14). For HFST, a thin layer of high quality, polish-resistant aggregate, is applied to the surface bonded using a polymer resin binder. A common aggregate type used in HFST is calcined bauxite which has a high polish resistance and good friction performance (73). Other types of aggregates available which have been studied include, basalt, flint rock, copper slag, armor stone, and corundum sand (74, 75).

Friction

Properly constructed HFST on a pavement in good condition typically maintains a high friction value throughout its expected life, usually 7–12 years (14). A long-term study done by Tsai and Pranav in 2020 using an HFST section at the NCAT Test track and some curves where HFST had been applied in Georgia showed that friction dropped significantly after 9 years of the pavement life (76). In a laboratory study, Chen et.al. (75), observed that the *BPN* on untreated asphalt samples was 58 and 61 and after treatment with calcium bauxite the *BPN* numbers increased to 78 and 80 respectively. Different aggregates used in HFST systems exhibit different friction characteristics, calcined bauxite shows the highest friction characteristics in all studies conducted (77). A summary from a study conducted by Deef-Allah et.al (77) is shown Table A-32.

Table A-32. Friction for different aggregate types used in HFST (77).

Test Results	Aggregate Type	Calcined Bauxite	Meramec River Aggregate	Earthworks	Rhyolite	Flint	Steel Slag
Dynamic Friction Tester (DFT)	<i>DFT</i> ₄₀ at 0 cycles (initial)	0.95	0.66	0.82	0.81	0.85	0.75
	<i>DFT</i> ₄₀ at 70k cycles	0.82	0.6	0.62	0.65	0.69	0.67
	<i>DFT</i> ₄₀ at 140k cycles (terminal)	0.78	0.56	0.55	0.55	0.64	0.63
British Pendulum Tester (BPT)	<i>BPN</i> before polishing	82.9	80.5	77.5	78.3	78.5	77.5
	<i>BPN</i> after polishing	78.9	79	77	73	71.5	76.8

A potential explanation for the loss of friction in HFST surfaces is the nature of aggregate used in the mix. In their study, Tsai, and Pranav (14) found out that friction value decreased almost in a linear manner with the loss of calcite bauxite aggregate. For a HFST section with calcite bauxite aggregate, friction is controlled by the calcite bauxite aggregate loss which is related to the macrotexture of the surface. However, for granitic aggregates, there is no direct relationship between the observed friction loss and loss in granitic aggregate surface and therefore the friction loss may not be entirely controlled by the aggregate like in the case of calcium bauxite.

Texture

Macrotexture of HFST is a function of the system itself and not the aggregate. However, it is affected by the aggregate type and loss of the aggregate surface over time (14). According to the FHWA, HFST surfaces should have an *MPD* or *MTD* of at least 1.0 mm (0.039 in.) and maintain that value over the life of the treatment (78). Effort has been made to broaden the characterization of HFST surface texture. A study by Zhao and others on 21 HFST projects used *MPD* to evaluate HFST's texture variation with time (79). The study showed that *MPD* values for a new HFST surface averaged 1.9 mm (0.075 in.). However, this value decreases to 1.4 mm (0.055 in.) after

only 1 month of service and to 1.2 mm (0.047 in.) after 2 months. With time, the *MPD* reduced to 1.1 mm (0.043 in.). Additionally, texture in a HFST varies depending on the type of aggregate used. Laboratory testing at NCAT on different aggregate types showed a variation in texture (74), where the macrotexture measured using the CTM ranged between 1.2 to 1.8 mm (0.05 to 0.07 in.) after polishing following the NCAT three-wheel-polishing-device (TWPD) procedure.

Design Methods

HFST is usually installed by first spreading a thin layer of polymeric resin binder over the pavement surface to be treated, then placing a layer of abrasion and polish-resistant aggregate of 1 to 3 mm in size (0.04 to 0.12 in.) onto the resin layer (78). The resin bonds the aggregate to the pavement surface, leaving a thin, pavement surface treatment that can be applied during a short closure of the roadway. Key physical properties for the resin binder which affect the installation and performance of the treatment include viscosity, gel time, cure rate, adhesion, and thermal compatibility. Gel time is the time taken after the resin is applied to the pavement to thicken and no longer flow. The important aggregate properties for HFST surface include gradation and size, abrasion and polish resistance, aluminum oxide content, texture, and cleanliness. Typical requirements for resin and aggregate are shown in Table A-33 and Table A-34.

The AASHTO specification for HFST is AASHTO MP 41-19 “*Standard Specification for High Friction Surface Treatment for Asphalt and Concrete Pavements Using Calcined Bauxite.*” The specifications have been used by different agencies without any modifications, while some agencies have developed their own specifications with specific requirements for materials and installation methods, although the main process still bases on the AASHTO guidelines. Usually, before opening to traffic, a subjective assessment of the surface is required to check that all the resin binder has been cured, and all loose aggregate removed. Also testing is conducted to characterize friction properties.

Table A-33. Physical property requirements for HFST resin binder materials (78).

Resin Binder Property	AASHTO/ASTM Test Method	AASHTO Specification Requirements
Viscosity	ASTM D2556 (spindle and speed selection based on ASTM D2556-11)	1000 cP min (epoxy and polyester) 1,500-2,500 cP min. (MMA)
Flash Point	ASTM D3278 (Note 3 of D3278)	See safety Data Sheet (DDS)
Cure Rate (at 75°F)	ASTM D1640	Typical: 3 hours max (Not included in AASHTO)
Adhesive strength (at 24 hours)	ASTM C1583	Typical: 250 psi min. or 100% substrate failure (Not included in AASHTO)
Thermal compatibility	ASTM C884	PASS
Adsorption	ASTM D570	1% max

The AASHTO specification requires *SN40R* = 65 for acceptance (the *R* stands for ribbed tire), while agency-specific values range from *SN40R* of 65-75 and *SN40S* of 55-70 (the *S* stands for smooth tire). Several state highway agencies (Delaware, Illinois, Indiana, Louisiana, Montana, South Carolina, Tennessee, and Virginia) require macrotexture testing in addition to friction testing (78). The minimum requirement for macrotexture whether *MTD* or *MPD* is 1.0 mm. Table A-35 shows the frictional metrics and requirements currently used by different state DOTs for QA or performance inspection of HFST.

Table A-34. Physical property requirements for HFST aggregate materials (78).

Aggregate Property	AASHTO/ASTM Test Method	AASHTO Specification Requirements
Los Angeles Abrasion (LAA)	AASHTO T 96 (Grading D)	20% max
MDA	ASTM D 7428	5% max
British Wheel	ASTM D3319/AAHTO T 279	Typical: 38 min. (<i>Not Included in AASHTO</i>)
Aluminum Oxide	ASTM E1621	87±2%
Gradation	AASHTO T 27	#4 sieve: 100% passing #6 sieve: 95-100% passing #16 sieve: 0-5% passing #30 sieve: 0-0.2% passing
Soundness	AASHTO T104	Typical 12-15% max (<i>Not Included in AASHTO</i>)
Moisture Content	AASHTO T255	0.2% max

Table A-35. Friction metrics used by State DOTs for quality assurance of HFST (80).

State DOT	Friction Number ¹ AASHTO T 242	DFT Friction ASTM E1911	MPD (mm) ASTM E2157/E965
Alabama	65	-	-
Alaska	-	0.75	-
California	-	0.75	-
Florida	65 (90 days)	-	-
Georgia	65 (90 days)	-	-
Illinois	72 (60 days)	0.90 (20 km/h)	1.0 (60 days)
Iowa	60 (90 days)	-	-
Pennsylvania	65 (90 days)	-	-
South Carolina	70 (90 days)	-	-
South Dakota	72	0.90	1.0
Tennessee	70	-	1.0
Texas	65	-	-
Virginia	55 (90 days)	-	-

¹All friction numbers, except for that by Virginia DOT, are measured with a standard ribbed tire. The friction number for Virginia DOT is measured with a standard smooth tire.

Shot Blasting

Shot blasting is a preservation technique for asphalt pavements that is usually applied to restore texture and friction. The blasting process consists of the action of abrasive material (small steel balls or pellets) over an existing coating surface to remove any contaminants, such as excess bitumen while adding texture and recovering skid resistance, microtexture, and macrotexture. The improvement in friction and texture characteristics achieved with blasting is directly associated with the surface mix and the type of aggregate. In addition, the method had no detrimental effects on roughness, rutting, and cracking (81–84).

Sarkar et al. (83) identified increases in friction coefficient, measured with a DFT at 20 km/h (12.5 mph), between 0.2 to 0.4 (60% to 200%) and *SN* values, measured with a LWST, from 10 to 20 (30% to 50 %) higher than pre-treatment with shotblasting, respectively. However, a significant decrease was observed after 6 months, especially for higher contents of polishable dolomite. The abrasion process caused by shotblasting equipment might lead to more angular faces, being rapidly polished by subsequent traffic. The method was also effective in improving the surface texture,

with *MPD* values between 0.5 and 1 mm (30% to 60%) higher after the shotblasting treatment, maintaining most of the macrotexture gain after six months of application (63).

The main components of a typical shotblasting system are the shot propelling system, vacuum system, magnetic separator, residue container, and follow-on magnetic brush and loom to pick up any debris. The procedure is considered environmentally clean due to the self-contained operation of the blaster, while loose materials and blasting agents are magnet and vacuumed into the machine. In addition, the method is cost-effective because it does not require the application of bituminous materials and aggregates, so the procedure does not depend on fluctuating asphalt prices or a shortage of high-quality aggregates. As the equipment blows the abrasive particles at high speed and at a specific angle, the exposed sand grains will improve macrotexture and friction. For these reasons, this method is also effectively applied as rubber removal to recover friction parameters on airport pavements (82, 85).

Microsurfacing

This treatment consists of spreading and applying a mixture of dense-graded aggregate, polymer-modified asphalt emulsion, water, and mineral fillers in a layer that is usually 10 to 12 mm thick (0.4 to 0.5 in.) over an existing pavement surface as preventive maintenance. The pavement life extension expected from this treatment, when applied as preventive maintenance before the onset of structural damage, generally ranges from 7 to 9 years (19, 20). Microsurfacing emulsions are formulated to break due to chemical interactions with aggregate shortly after placement. Consequently, Microsurfacing can be placed at night and cure rapidly, allowing traffic to typically open as soon as one hour after application (19–21). The main benefits observed in the field when implementing Microsurfacing are as follows (19, 22):

- Reducing rut depth.
- Less traffic delays during construction even with a higher application rate due to a faster cure process.
- Road crash rate reduction with improved riding characteristics such as skid resistance.
- Decreasing air and water infiltration into the existing asphalt concrete, achieving uniformity, and surface visibility.
- Increasing the *PCR* and lowering the international roughness index (*IRI*) in cases where the treatment is placed on conditions where the overall condition and roughness of the pavement are relatively good.

Microsurfacing treatments do not contribute to the structural capacity of a pavement and are ideally applied only to pavements in good structural condition. The Ohio Department of Transportation (ODOT), for example, uses Microsurfacing when a pavement's condition rating value is greater than 70 (86). In addition, Microsurfacing should be avoided if cracks are the predominant source of pavement distress or if they are larger than a hairline. Finally, it is also essential to note that this technique is not suitable for correcting problems with extreme roughness (22, 87).

It has been observed that the application of Microsurfacing can improve the friction characteristics of a pavement and maintain a good condition for up to 9 years (88, 89). Zhan et al. (86) observed an improvement of around 60% in *BPN* where the Microsurfacing increased the *BPN* from 48 before the treatment to 77 after the treatment. Generally, *BPN* values are between 54 and 72 for surfaces treated with Microsurfacing (5).

The International Slurry Seal Association (ISSA) protocol is the most widely used mixture design method for Microsurfacing. This approach utilizes aggregate loss from a 1-hour wet track abrasion test (WTAT) and sand adhesion from a loaded wheel test (LWT) to calculate the values of lower and upper potential asphalt content PAC_1 and PAC_2 , respectively, and then uses an empirical formula to calculate the median asphalt content (OAC) (87, 90). Figure A-17 illustrates the graphical method prosed by ISSA to determine OAC for Microsurfacing.

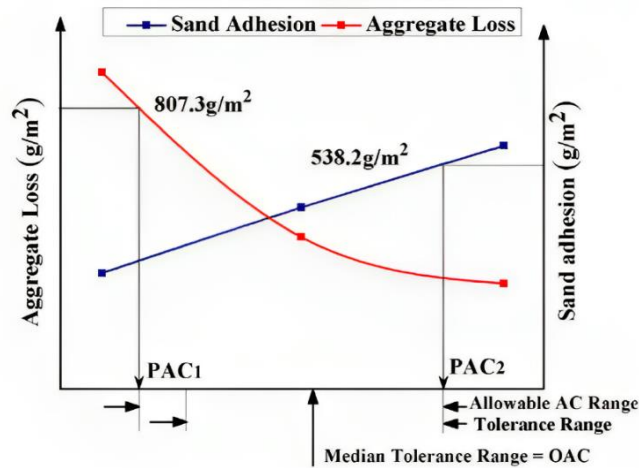


Figure A-17. Method for obtaining OAC for Microsurfacing mixtures.

The aggregate must be 100% crushed and densely graded to a Type II or III gradation (the ISSA includes two gradation types, where number II is the finer and number III is the coarser). In general, stones such as granite, slag, limestone, and chert are used. Type III aggregates (with a coarser gradation) are often applied to achieve the highest level of skid resistance, Type II aggregates are usually used to fill surface voids and improve the durability of the coating surface. Type II aggregates are also more suitable for urban areas with moderate traffic volumes, especially when excessive traffic noise needs to be avoided (87, 91). Some US specifications for aggregate gradations are presented in Table A-36 and Table A-37 and recommendations on the asphalt content to be used are shown in Table A-38.

One failure mode reported in the literature for Microsurfacing is the stripping of the applied treatment from the existing pavement surface (92). To address this potential failure mechanism, it is recommended that mix designers perform a wet stripping test. This test identifies the ability of a cured slurry surfacing mixture to remain coated under wet conditions. This test is used to indicate the potential for stripping, which may lead to premature raveling. According to the ISSA wet stripping test guidelines, if the retained coating after the wet stripping test is greater than 90%, the result is satisfactory, between 75% and 90% it is marginal, and for less than 75% it is unsatisfactory (92, 93).

Another failure mechanism is Microsurfacing delamination, which occurs when the Microsurfacing debonds and separates from the underlying pavement. According to NCHRP Research Synthesis 411, delamination can occur because of a failure to remove contaminants from the pavement. In this sense, road markings must also be removed or abraded to produce a rough surface before placing Microsurfacing (94). Additionally, Ji et al. (93) reported that some of the Microsurfacing they analyzed has separated from the underlying pavement. Widespread

documentation of delamination in Microsurfacing has not been noted from the literature review, but as the sources above suggest, such a distress is possible.

Table A-36. Microsurfacing aggregate gradations requirements (25, 95–97).

Sieve Size and mix parameters	ISSA		Texas	Georgia	
	Type II	Type III		Type II	Type III
3/8" (9.5 mm)	100	100	100	100	100
#4 (4.75 mm)	90-100	70-90	86-94	90-100	60-95
#8 (2.36 mm)	65-90	45-70	45-65	65-90	45-75
#16 (1.18 mm)	45-70	28-50	25-46		
#30 (0.60 mm)	30-50	19-34	15-35		
#50 (0.30 mm)	18-30	12-25	10-25	20-45	15-35
#100 (0.15 mm)	10-21	17-18	7-18		
#200 (0.075 mm)	5-15	5-15	5-15	5-15	5-15

Sieve Size and mix parameters	Oklahoma			Florida
	Type I	Type II	Type III	
3/8" (9.5 mm)	100	99 -100	98 -100	100
#4 (4.75 mm)	98-100	80-94	70-90	90-100
#8 (2.36 mm)	71-88	45-65	45-70	65-90
#16 (1.18 mm)	44-63	25-45	28-50	45-70
#30 (0.60 mm)	27-46	15-34	19-34	30-50
#50 (0.30 mm)	15-33	9-25	12-25	18-30
#100 (0.15 mm)	8-23	7-19	7-18	10-21
#200 (0.075 mm)	5-15	5-15	5-15	5-15

Table A-37. Tolerance limits for aggregate gradation (25, 95–97).

Source	Sieve Size						
	#4 (4.75 mm)	#8 (2.36 mm)	#16 (1.18 mm)	#30 (0.60 mm)	#50 (0.30 mm)	#100 (0.15 mm)	#200 (0.075 mm)
ISSA	± 5	± 5	± 5	± 5	± 4	± 3	± 2
Texas	± 5	± 5	± 5	± 3	± 3	± 3	± 3
Georgia	± 6	± 5			± 4		± 3

Table A-38. Tolerance limits for residual asphalt content.

Source	Residual Asphalt Content (by weight of dry aggregate)	Residual asphalt content from job mix formula
ISSA	5.5–10.5%	±1.5%
Florida	5.5–10.5%	±0.5%
Oklahoma	6.0–9.0%	±0.5%
Minnesota	6.0–9.0%	-
Georgia	7.0–10.5%	±0.5%

Chip Seal

Chip seals are used for the preservation of asphalt pavements. This treatment type has been reported to be useful for treating surfaces that exhibit raveling and low severity/extent shoving (98, 99). With respect to shoving, objective evidence demonstrating the treatment’s ability to address the distress is not provided in these sources. Converse to the cited references, guidance published by the FHWA suggests that no pavement with a shoving distress is a viable candidate for preservation treatments (23). In addition, this technique is often used to improve skid resistance,

prevent oxidation, seal small cracks, improve friction, and correct surface defects. Although it is most typically applied to roads with low total traffic volumes and low truck volumes, the treatment may also be employed to prevent further deterioration on roads with high traffic volumes (23–25).

If successfully executed on pavements in good structural condition, chip seal treatments can provide satisfactory friction for around five years, with *SN* values generally ranging from 40 to 60. However, the occurrence of excessive chip loss and bleeding can negatively impact the performance of the surface in the first 12 months, leading to premature failure (23, 25). Guirguis and Buss (100) observed the efficiency of chip seal in regaining texture for pavements with low texture. In their study, the *MTD* of roads increased by around 2 mm after the implementation of this technique. Moreover, Zhan et al. (86) recorded a change in *BPN* from a value of approximately 45 before a chip seal treatment to approximately 68 after the chip seal treatment.

The process of applying chip seals can be carried out in one or several layers. In single layer implementation, cold asphalt emulsion or hot bitumen is sprayed over the existing pavement, filling in small cracks in the surface of the coating. Subsequently, a single layer of uniformly graded aggregate or crushed stone is applied and partially embedded in the binder by a roller. A double chip seal is a bituminous surface that results from two successive alternating applications of bituminous binder and cover aggregate to an existing paved surface. In the design of double chip seals, an important factor to be computed is the amount of bituminous material required to fill the voids between the aggregate to an optimum depth (101). Generally, a smaller aggregate size is used in the surface layer to create a surface appearing more similar to asphalt concrete.

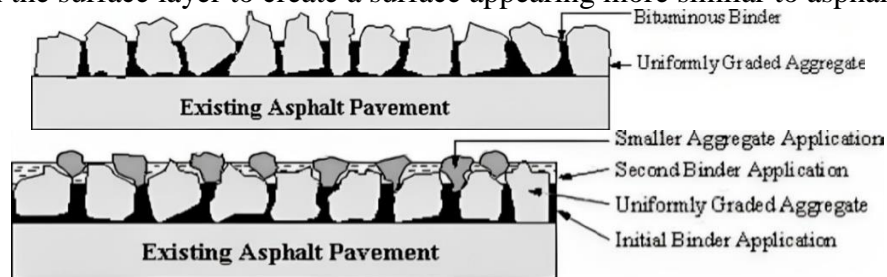


Figure A-18. (a) Single layer and (b) double layer chip seal application scheme (5).

To achieve more effective preservation performance, it is essential to control several factors during chip seal construction to minimize aggregate loss, including but not limited to traffic control while the emulsion is curing and sweeping to remove excess aggregate (25). The size of the aggregates is also an important characteristic to control, as the thickness of the chip seal layer is limited to the maximum size of the stone chips. Additionally, gradation, shape, and abrasion resistance must be considered too. Generally, smaller stone chips are used on residential streets or those with lower traffic volumes (1,000-4,000 vehicles per day), as they are associated with less noise, while larger chips have been used successfully on roads with heavy traffic (more than 7,500 vehicles per day) (25, 102). The aggregate and emulsion application rates and binder-aggregate compatibility also strongly influence performance of chip seals.

Summary

Overall Comparison of Surface Treatments

A summary of the findings discussed above is presented in Table A-39. The table organizes the pros and cons in terms of construction/traffic opening times, friction and texture performance, and cost.

Table A-39. Summary of the pros and cons of alternative surface treatments.

Treatment	Pros	Cons
12.5 mm Superpave	<ul style="list-style-type: none"> • It may offer better durability due to the larger aggregate size in comparison to a traditional 9.5-mm mix. • Greater load-bearing capability. • May be more rutting resistance. • Better drainage. • Higher macrotexture. 	<ul style="list-style-type: none"> • Higher noise than a 9.5-mm mix. • May be harder to compact, especially when used in a thin overlay. • More susceptible to temperature fluctuations and climate effects. • Lower microtexture component than a 9.5-mm mix.
SMA	<ul style="list-style-type: none"> • Contribute to the pavement structural capacity. • High macrotexture. • Reduced noise. • Can be used to reduce splash and spray. • High rutting resistance. • High cracking resistance. 	<ul style="list-style-type: none"> • High initial cost. • Delayed traffic opening caused by cooling waiting times. • Initial skid resistance may be low until the thick binder film is worn off the surface by traffic. • Construction challenges have been noted especially when SMA designs are first implemented.
UTBWC	<ul style="list-style-type: none"> • Resists raveling and delamination. • High skid resistance. • Quick traffic opening. • Small cracks sealing. • Can be used to reduce splash, back spray, and hydroplaning. 	<ul style="list-style-type: none"> • More expensive than other treatments such as micro surfacing, slurry seals and chip seals. • Reflective cracks may need periodic sealing. • Initial skid resistance may be low until the thick binder film is worn off the surface by traffic.
OGFC	<ul style="list-style-type: none"> • High texture. • High friction. • Can be used to reduce splash, back spray, and hydroplaning. • Can be used for noise reduction. 	<ul style="list-style-type: none"> • High material cost. • Difficult to maintain in winter seasons resulting in higher life-cycle costs. • High potential for raveling – shorter life spans. • Initial skid resistance may be low until the thick binder film is worn off the surface by traffic.
HFST	<ul style="list-style-type: none"> • High friction and texture. • Minimal traffic disruption. • Durable and long lasting. • It is a spot treatment that can be used to reduce braking distance, hydroplaning, splash, and spray potential. 	<ul style="list-style-type: none"> • Aggregate loss is common and can lead to abrupt friction reductions. • Prone to delamination and cracking. • High cost associated to materials. • The effectiveness of the treatment depends on the aggregates polishing resistance.

Table A-39. Summary of the pros and cons of alternative surface treatments. (Continued).

Treatment	Pros	Cons
Shotblasting	<ul style="list-style-type: none"> • Fast application. • Environmentally friendly. • Low cost associated. 	<ul style="list-style-type: none"> • Evidence has shown the effects reduced over time, with some pavements returning to their previous values after one year of treatment. • Can accelerate pavement oxidation and aging.
Microsurfacing	<ul style="list-style-type: none"> • Can be used to solve rutting problems. • Can be open to traffic within an hour of application. • Can be used to increase friction. 	<ul style="list-style-type: none"> • Not suitable if cracking is a major problem. Existing cracks must be sealed first. • Does not add any structural capacity, therefore the pavement must be in good condition before treatment. • Bleeding, while not a consistently reported issue, has been noted to occur in some instances.
Chip seal	<ul style="list-style-type: none"> • Low-cost treatment. • Provides high macrotexture and, depending on the aggregate quality, provides high friction. • High spatial variability in friction/texture. • Quick traffic opening times. • Protects the pavement against oxidation. • Seals small cracks. 	<ul style="list-style-type: none"> • Prone to bleeding problems. • Prone to aggregate loss that can constitute a safety hazard. • Not recommended for high-speed facilities.

Alternative Surface Type Usage in North Carolina

The HiCAMS database has been queried to pull the asphalt mix gradations that have been approved by the NCDOT since 2019. A total of 1,915 gradations have been identified, as shown in Figure A-19. With the exception of the OGFC and UTBWC, all gradations can be categorized as dense-graded. Figure A-20 shows maps of surface type production by county. As seen, dense-graded mixtures are produced across most counties in North Carolina. For some counties, either no plants exist or none of the plants that exist produced a dense-graded mixture in the period evaluated.

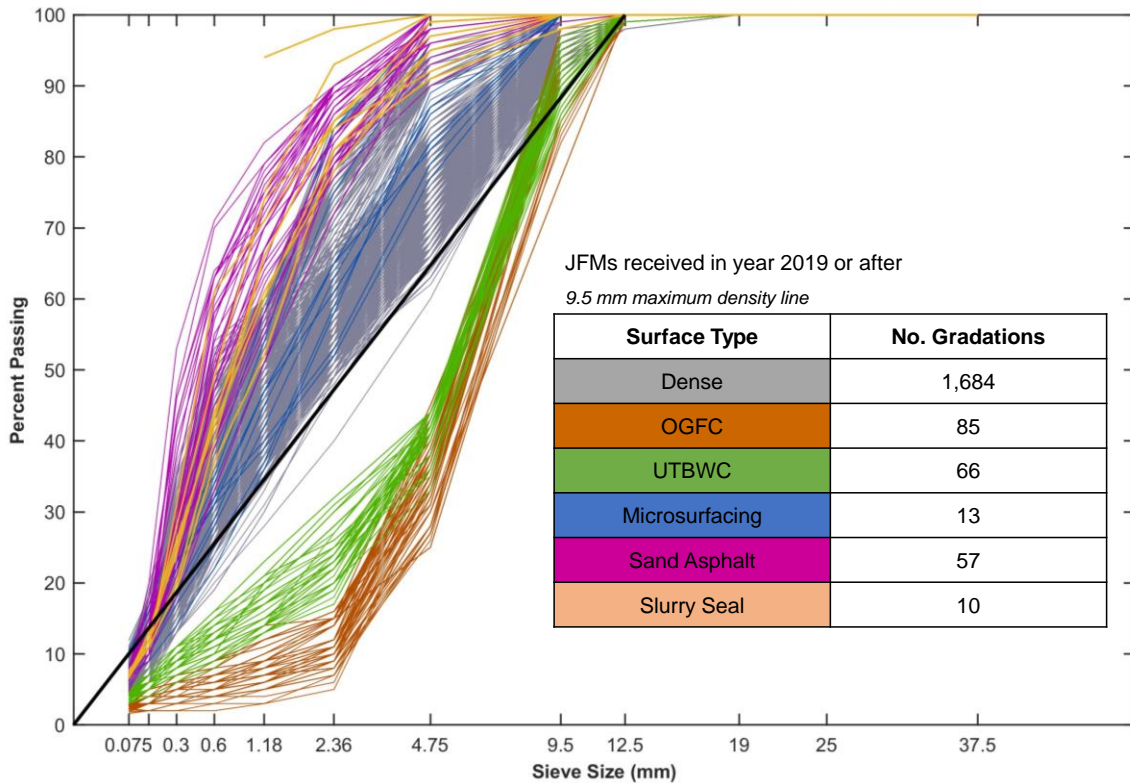


Figure A-19. North Carolina’s surface mix gradations.

The OGFC mixes are produced mostly in the eastern side of the states, but some countries in the piedmont and in the mountains also produce OGFCs. In contrast, the UTBWC are predominantly produced in the western counties, with some plants located in the central divisions. Interestingly, the eastern divisions use a surface treatment coded as sand asphalt, and the slurry seals are produced in a single county. Finally, all the Microsurfacing treatments are produced in Virginia. Finally, the distribution of 12.5 mm Superpave mixes approved by the NCDOT during the period of 2011 to 2017 is depicted in Figure A-21. As shown, the majority of the JMFs existed in two counties: Wilson and Mecklenburg.

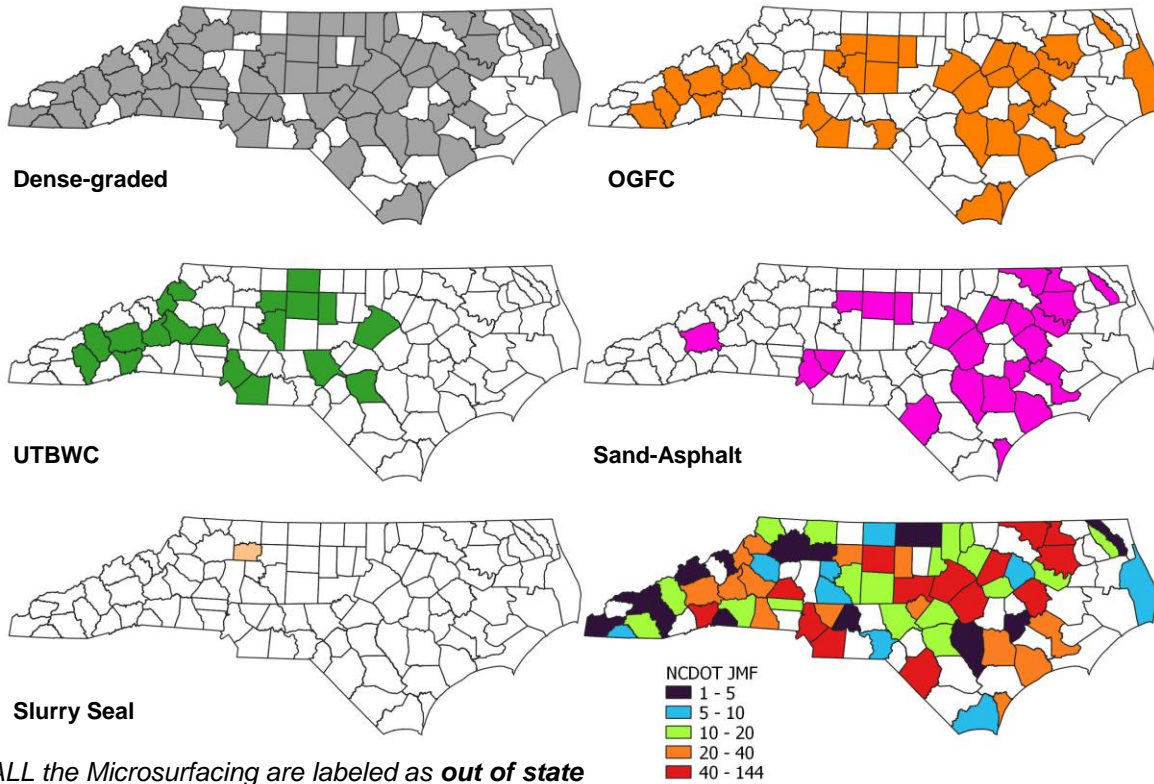


Figure A-20. Distribution of the counties where the mix is produced.

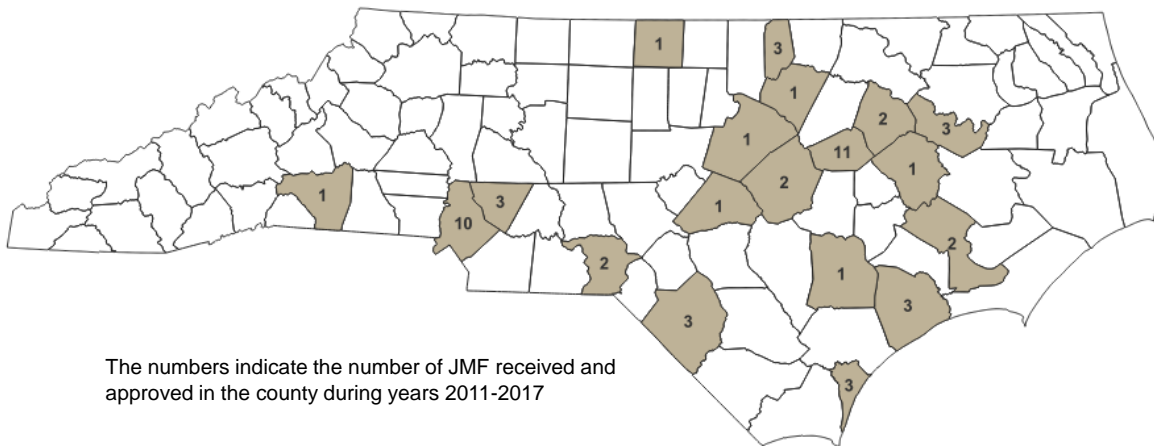


Figure A-21. Distribution of 12.5 mm Superpave mix that were received and approved by the NCDOT during years 2011-2017.

Spatial Analysis

Spatial statistics, or more generally spatio-temporal statistics, is a branch of statistics that deals with data collected at physical locations and specific points in time, where the location and time have some explanatory power for the observed value. The data collected on a pavement are likely to be linked to a specific location and time (103). In this sense, as shown in projects RP2020-11 and RP2022-05, friction and texture measurements can vary with time after construction. In the case of friction, there is an initial increase until a peak value is reached, afterwards the peak value

is followed by a decrease. In contrast, surface texture is expected to increase continuously for dense-graded asphalt mixes and OGFC/UTBWC surfaces.

Hence, previous projects have described the temporal component of friction/texture performance. Even though these previous models categorized the pavements according to their friction demand category (which was a function of road geometry), the models did not account for possible spatial patterns within a pavement section that could indicate differences in the friction/texture values along the pavement length. Additionally, in both RP2020-11 and RP2022-05 projects, the representative friction/texture values of a pavement section were first summarized into 0.1-mile segments. For friction, the 2.5th percentile of the continuous friction measurement was used as the representative value, whereas for texture, the 50th percentile was the statistic used as the representative value of the section. Then, the average of the statistics reported in the 0.1-mile segments was taken as the representative value of a section. This process is intended to account for the spatial variation along the pavement length, and although the 0.1-mile evaluation unit matches the current NCDOT practice for the PMS, this evaluation unit may not be the best aggregation distance for a PFMP.

Other researchers have also used 0.1-mile segments to summarize friction and texture values at a network level (104–108), however none of these works have presented a detailed analysis that justify the selection of that spatial window.

Within statistics, there are three closely related fields of study: time series analysis, stochastic (or random) processes and random fields, all of which have some relevance to spatial variability (103). Autocorrelation is when the data in a data set are correlated because of the order in which they were collected. This implies some kind of underlying stochastic process in the data, which is generating data that are random, but not totally so (109, 110). Civil engineers are familiar with time series, which are typically used to describe climate, earthquake occurrence, temperature variations, among others. Random fields are a general case of a random process, where the process that generates the random field can be described as a random variable.

If Z represents a random field, e.g., pavement elevation, pavement temperature, in-place density, etc., measured in certain locations s , then the values of the field at the measured locations are represented by $Z(s)$. The goal is then, based on the observed values, to predict the value of the field Z in a different set of locations, or to determine the average value of Z in spatial window w .

Geostatistical analysis involves estimation and modelling of spatial correlation (covariance or semivariance) and evaluates whether simplifying assumptions, such as stationarity, can be justified or need refinement (111). In geostatistics, the spatial correlation is modelled by the variogram, where the variogram plots semivariance as a function of distance. Then, the variogram is a function that describes the degree of spatial dependence of a spatial random field and is represented as indicated in Equation (13).

$$2\gamma(h) = \frac{1}{N(h)} \sum_{N(h)} [Z(s) - Z(s+h)]^2 \quad (13)$$

where;

$\gamma(h)$ = is the semivariogram,

s = position or coordinate,

h = is the lag distance, and

$N(h)$ = number of pair datapoints that are separated by a distance h .

To estimate the variogram an empirical process is followed, where the data is binned by the distance h , the semivariance is averaged in each bin, and a model is fitted to all the bins. As the correlation function is nonlinear, it needs to be represented by some type of nonlinear regression. In addition, because of the binning of the data in determining the correlation coefficients, it is common to use a weighted regression, based on the number of points used to determine the correlation coefficient for each bin (103). The variogram is $2\gamma(h)$, so the ‘semi’ here denotes half, not partial. The reason for this formulation is that in spatial statistics one includes both $Cov[s_i, s_j]$ and $Cov[s_j, s_i]$ in the analysis, as it is more difficult to keep track of which points have been included in various bins and which have not. It is an empirical process because the modeler must choose the model, or model combinations to use that better describe the semi-variance variation.

In this sense, all the variogram models follow Equation (14), and the difference between models is the way the term $\rho(h)$ is described (103, 110).

$$\gamma(h) = \sigma^2 (1 - \rho(h)) \quad (14)$$

where;

$\rho(h)$ = correlation coefficient, and

$\sigma^2(h)$ = standard deviation between two points infinitively apart (also known as sill value).

Only after the variogram is defined by Equation (14), is it possible to start making inferences about the random field, i.e., making predictions on locations of interest or determining the average value of the field in a predefined region (or spatial window).

Conclusions and Knowledge Gaps

Based on the literature reviewed in previous sections, the following statements can be made:

- Surface treatments in asphalt pavements are applied to enhance the durability, safety, and performance of the road. The choice of the appropriate surface type depends on various factors, including the condition of the existing pavement, the intended use of the road, climate, budget constraints, and other local considerations.
- Most of the neighboring states follow AASHTO recommendations for gradation bands and asphalt content, with some adjustments to meet local requirements. The review indicated that 12.5 mm NMA mixtures are used by other states on their primary road networks, these mixtures are mostly designed with a fine gradation configuration.
- Based on the review, SMA surfaces are an attractive treatment that can be used instead of OGFC/UTBWC, because they provide similar friction and texture values with the benefit that add to the structural capacity of the pavement, by providing a sound and long-lasting material layer. In contrast, SMAs are more expensive, require longer construction times, and depending on the material source that is used it may demand more natural resources.
- The variogram concept can be used to determine if friction/texture measurements exhibit spatial correlation. The spatial variability of friction and texture measurements has not been fully described in the literature.
- Past studies have collected friction measurements using LWSTs. Therefore, research is needed to compare the friction and texture performance of dense-graded mixtures with alternative surface treatments using continuous friction measurement equipment (CFME) and high-speed texture profilers (HSTP). This comparison must account for the structural and functional performance expected from each surface type.

APPENDIX B. FRICTION AND TEXTURE MEASUREMENTS – COMPLEMENTARY ANALYSIS

Friction

The number of observations per surface type for each of the group of sites tested in North Carolina, G1 to G3 and the sites tested outside North Carolina are presented in Table 4. The data was filtered out and those measurements collected before construction were removed and only the records collected in the center of the lane (CL) at 60-mph were processed. The discussion for the values collected at 40-mph and 60-mph in the right wheel path (RWP) are shown in Section 3.1.

The distribution of the friction values in the CL at 60-mph are presented in Figure B-1. The interquartile range (IQR) for the dense-graded surfaces shows that the 75th percentile of the sites have a friction slightly higher than the interchange investigatory thresholds of 0.65 and the 25th percentile was 0.53. The OGFC surface was evaluated in the FHWA/NC 2020-11 and 2022-5 projects but only two records remained for the analysis and both sites have a friction value closer to the non-interchange investigatory threshold. In contrast, the boxplot of the OGFC made with the records collected in the current research project, G3 in Figure B-1, indicates that the IQR is 0.60 to 0.72. As mentioned in Section 3.1, in this research project newer OGFC sites were tested which matches the higher friction observed in the red boxplot data series. In contrast, the UTBWC sites had a higher friction in the G1 and G2 group of sites, with an IQR of 0.68 to 0.77, versus the values in the G3 group of sites with an IQR of 0.63 to 0.67. As mentioned in Section 3.1, the UTBWC tested in the current project are slightly older than those tested earlier.

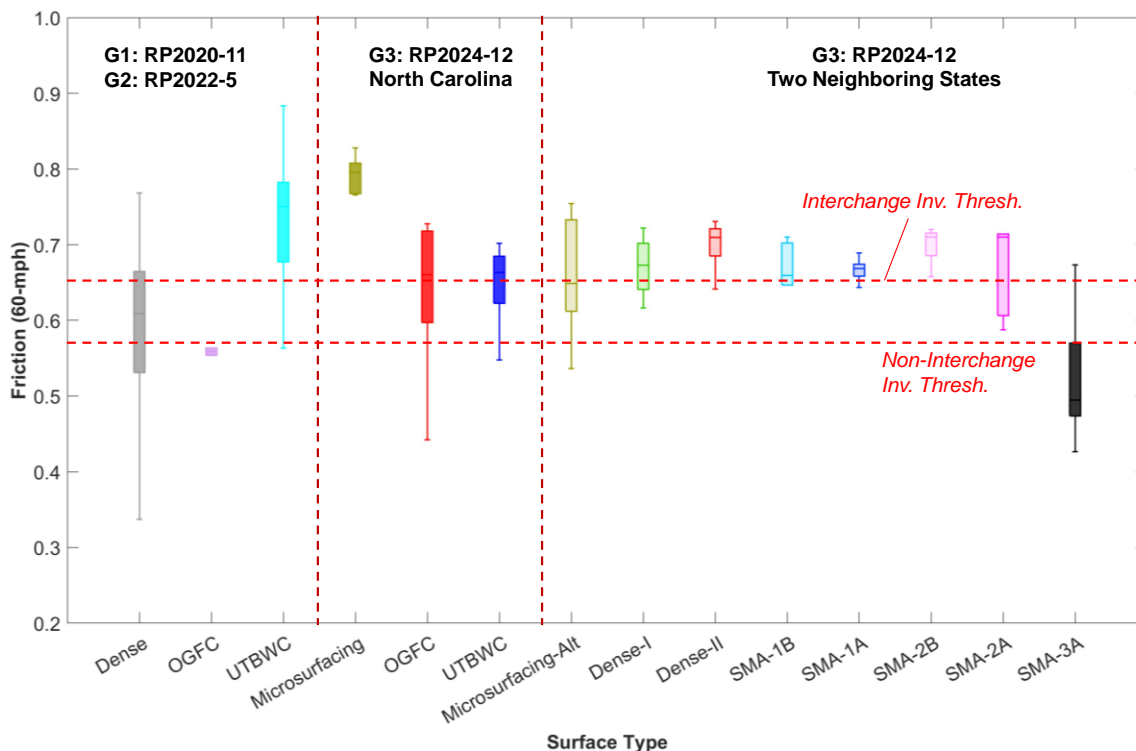


Figure B-1. Distribution of the friction measurements made in the CL at 60-mph for each surface type.

As with the RWP records, the North Carolina Microsurfacing has higher friction values in the CL than Microsurfacing-Alt, on average the friction of the North Carolina Microsurfacing is 0.79, whereas the Microsurfacing-Alt friction average value is 0.65. Both Dense-I and Dense-II on average have a friction value above the interchange investigatory threshold; however, the 25th value of the sites tested with a Dense-I surface have a friction value slightly lower than 0.65. Except for the SMA-3A, all the SMAs have average friction values above 0.65.

Macrotexture

The number of macrotexture observations per surface type for each of the group of sites tested in North Carolina, G1 to G3 and the sites tested outside North Carolina are presented in Table 4. The data was filtered out and those measurements collected before construction were removed and only the records collected in the CL were processed. The discussion for the values collected in the RWP are shown in Section 3.3.

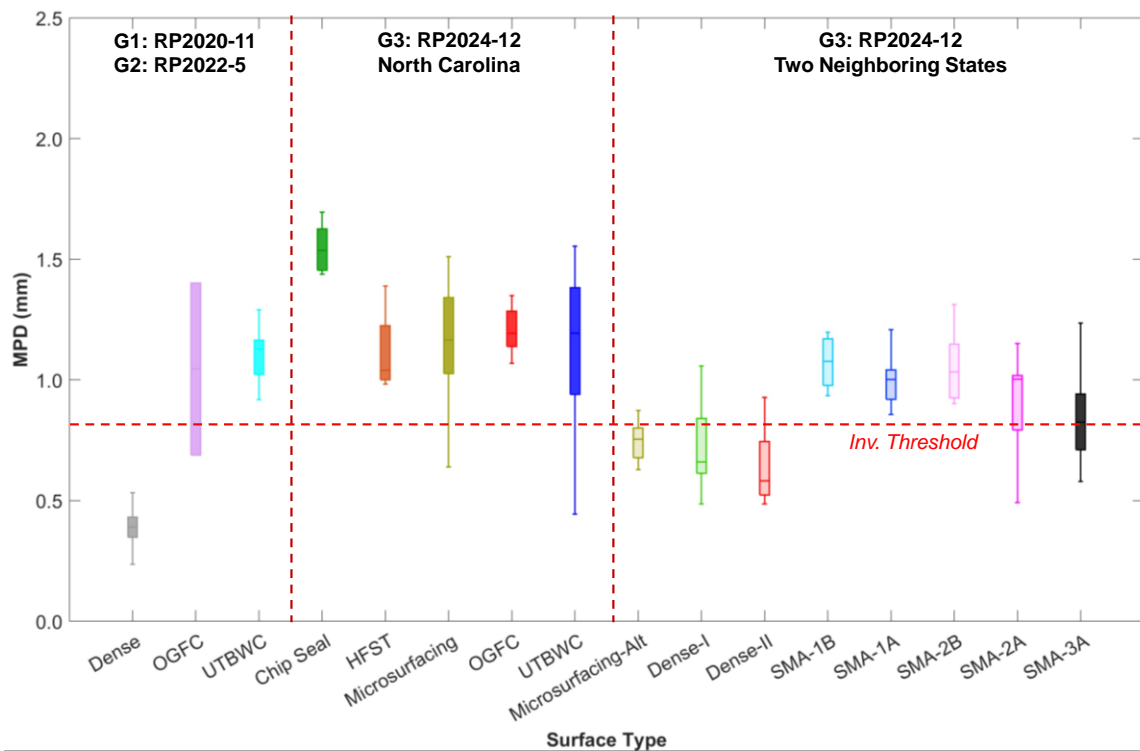


Figure B-2. Distribution of the MPD measurements made in the CL for each surface type.

The dense-graded surfaces have an average *MPD* of 0.40 mm. with the IQR between 0.35 to 0.45 mm. After the filtering process, the OGFCs in North Carolina G1 and G2 ended up having only two records, both belonging to the same site, with an average of 1.05 mm. In the G3 sites, the average is 1.20 mm with an IQR of 1.15 to 1.35 mm. For the UTBWC, the North Carolina G1 and G2 sites have an *MPD* IQR of 1.05 to 1.25 mm, whereas G3 sites have an IQR of 0.95 to 1.40 mm. The High Friction Surface Treatment (HFST) has an average *MPD* of 1.05 mm with an IQR of 1.00 to 1.30 mm. The chip seals have the highest *MPD* values. North Carolina Microsurfacing has higher *MPD* values than Microsurfacing-Alt, in the latter case the IQR is below the investigatory threshold of 0.80 mm. Both Dense-I and Dense-II have *MPD* IQR values below 0.80 mm and all the SMAs, except for the SMA-3A, have *MPD* IQR values above the investigatory threshold.

APPENDIX C. PERFORMANCE MODELS CALIBRATION DETAILS

Friction

The functional form of the friction performance model is presented in Equation (2), the model incorporates random effects in the intercept and in the friction rate of change. The average value of these random terms was estimated for the following surface types; OGFC, UTBWC, Microsurfacing, Dense-I/II, and SMAs. For the observations made outside North Carolina, the data was categorized into the three climate regions, although these regions correspond to North Carolina boundaries, it is assumed that the same weather longitudinal variation prevails in the neighboring states, i.e., the vertical delineation of the polygons that delimits these regions in North Carolina also applies in its surroundings.

OGFC

The NC G1, G2, and G3 sites with an OGFC surface type were combined to create a single dataset. After that, the sites were grouped per climate region – coastal, mountains, or piedmont - and two set of plots were generated as shown in Figure C-1. Part (a) of Figure C-1 shows the friction variation with respect the surface age, expressed in years, while Part (b) presents the friction variation with respect the cumulative traffic. As shown in Figure C-1 (a), the data does not exhibit a trend when analyzed with respect the age; when the friction data are evaluated with respect to the cumulative traffic, Figure C-1 (b), the data distribute more clearly and show some trend but still with a scattered distribution. This distribution is like that observed in the previous project and was the main reason that a random model structure was adopted, because site specific parameters are needed to accurately explain the deterioration process.

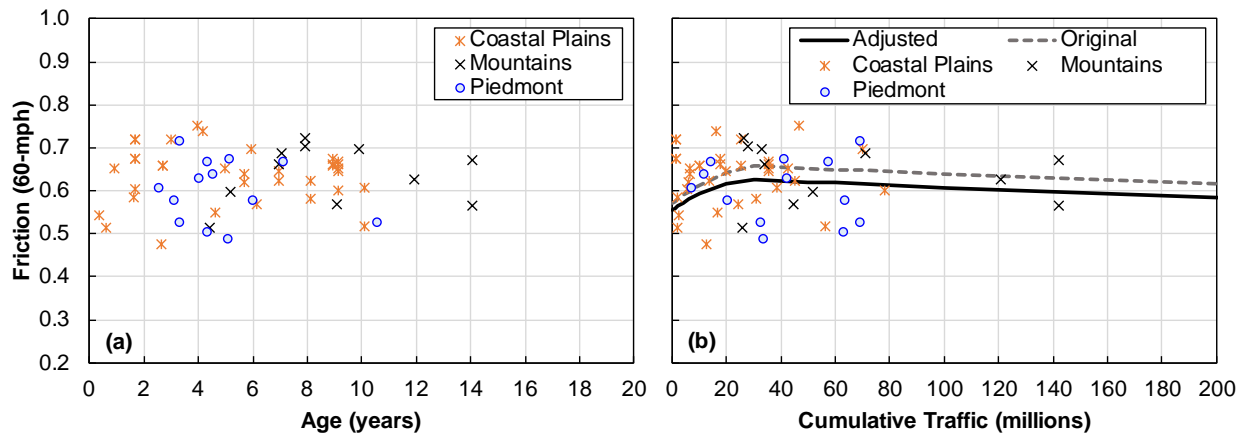


Figure C-1. Variation of OGFC friction values at 60-mph with respect to: (a) age and (b) cumulative traffic.

However, because these random terms (Δa_{site} , Δb_{site} , ΔA_{site}) cannot be estimated for each site the term was estimated using all sites at once and in this way the average value of these coefficients was estimated for the OGFC surface, i.e., Δa_{OGFC} , Δb_{OGFC} , ΔA_{OGFC} . A first estimation of Δa_{OGFC} , Δb_{OGFC} , and ΔA_{OGFC} was made previously as indicated in Table 8, these values were used as a seed to recalibrate the models. This process was made using Solver in Excel by minimizing the sum of square errors between the measured and predicted friction values. The fitted model of Equation (2) with the value of the coefficients originally estimated for the OGFC is shown in Figure C-1 (b)

as the gray dashed line, whereas the adjusted curve with the new observations is represented by the black continuous line. The original and updated model coefficients are shown in Table C-1, as shown the traffic to reach the maximum friction reduced from 34.93 to 30.86 million repetitions and the curve was shifted downwards.

Table C-1. Updated friction model coefficients for the OGFCs.

Parameter	Original	Adjusted
$a + \Delta a_{OGFC}$	0.57	0.56
$b + \Delta b_{OGFC}$	0.0051	0.0045
c	-0.000073	-0.000073
T_{max}	34.93	30.86
$A + \Delta A_{OGFC}$	0.66	0.63
B	-0.00037	-0.0004
SSE	0.24	0.19

UTBWC

Following the same procedure described for the OGFCs, the NC G1, G2, and G3 sites were combined into a single dataset. The friction variation with respect to age and cumulative traffic is depicted in Figure C-2 (a) and (b), respectively. As shown, the sites in the mountain region tend to have the highest friction but also exhibit the lowest values. The values of the coefficients for the UTBWC shown in Table 8 were fitted in Equation (2) to create the ‘Original’ performance curve shown in Figure C-2 (b) with the gray dashed line. Then using Solver in Excel to minimize the sum of square errors the average value of the random terms, Δa_{UTBWC} , Δb_{UTBWC} , and ΔA_{UTBWC} , was estimated and the ‘Adjusted’ curve is represented by the black continuous line. The updated set of coefficients is shown in Table C-2.

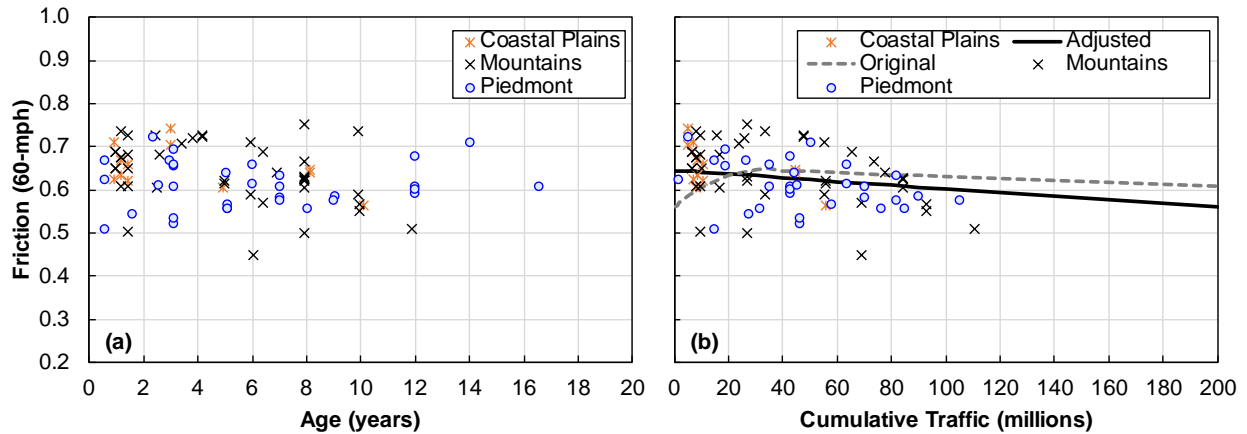


Figure C-2. Variation of UTBWC friction values at 60-mph with respect to: (a) age and (b) cumulative traffic.

As shown in Table C-2, the biggest change reflected in the value of T_{max} , it went from 34.93 to 5.0 million repetitions, suggesting that the initial friction increment described by the second order polynomial in Equation (2) describes only a small portion of the variation and the main process observed in the data is a friction reduction with traffic. The other significant change was the increase in the rate of deterioration B , it went from 3.7×10^{-4} to -7.2×10^{-4} friction units per million traffic repetitions which is almost twice as the original value. Lastly, the initial friction increased from 0.56 to 0.64.

Table C-2. Updated friction model coefficients for the UTBWCs.

Parameter	Original	Adjusted
$a + \Delta a_{UTBWC}$	0.56	0.64
$b + \Delta b_{UTBWC}$	0.0051	0.0007
c	-0.000073	-0.000073
T_{max}	34.93	5.00
$A + \Delta A_{UTBWC}$	0.65	0.65
B	-0.00037	-0.00072
SSE	0.50	0.27

Microsurfacing

The Microsurfacing surface type was not evaluated in the FHWA/NC 2022-5 project, therefore there are no previous values of the performance curve coefficients. The friction variation with respect to age and cumulative traffic is depicted for the North Carolina sites in Figure C-3 (a) and (b), respectively, and for the sites with the Microsurfacing-Alt in Figure C-4 (a) and (b), respectively. As shown in both panels of Figure C-3 and Figure C-4, the friction values exhibit a decreasing trend with respect to age and traffic, there is no evidence of an initial friction increase as the one observed in the dense-graded surfaces, OGFC, and UTBWC. Therefore, for this surface type, the performance model was described using only the exponential decay portion of Equation (2) and the only parameters to be calibrated were $A + \Delta A_{Microsurfacing}$ and B .

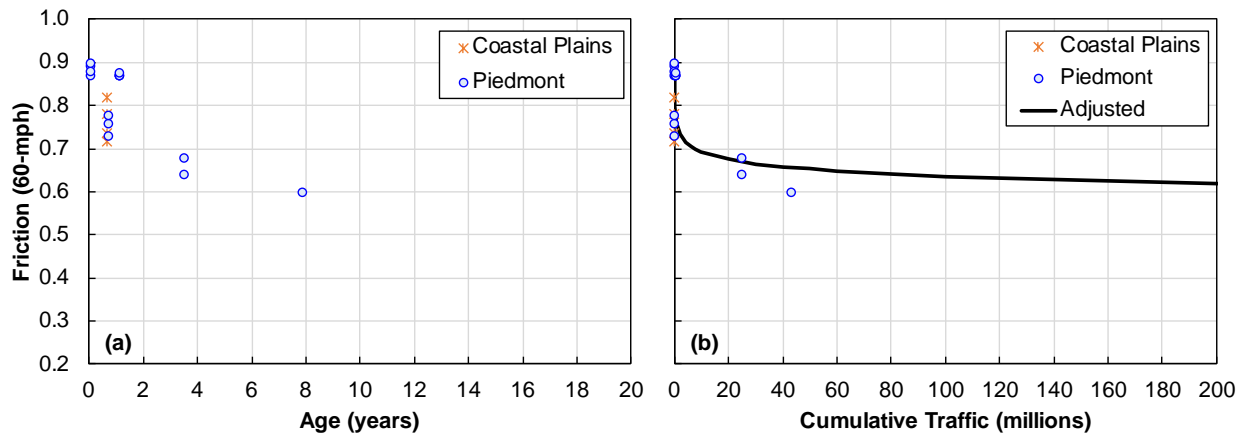


Figure C-3. Variation of North Carolina’s Microsurfacing friction values at 60-mph with respect to: (a) age and (b) cumulative traffic.

Additionally, as shown in Figure C-3 and Figure C-4 North Carolina’s Microsurfacing have higher initial friction and lower deterioration rates than the Microsurfacing-Alt. The estimates of the model coefficients are shown in Table C-3. As shown in the table, the deterioration rate obtained with the Microsurfacing-Alt dataset is almost four times higher than the value obtained for North Carolina. However, it should be noted that the traffic type, timespan, and surface finishing characteristics between the two surfaces differ. Under the exact same conditions, it is not clear whether the same observations regarding deterioration rates would be replicated.

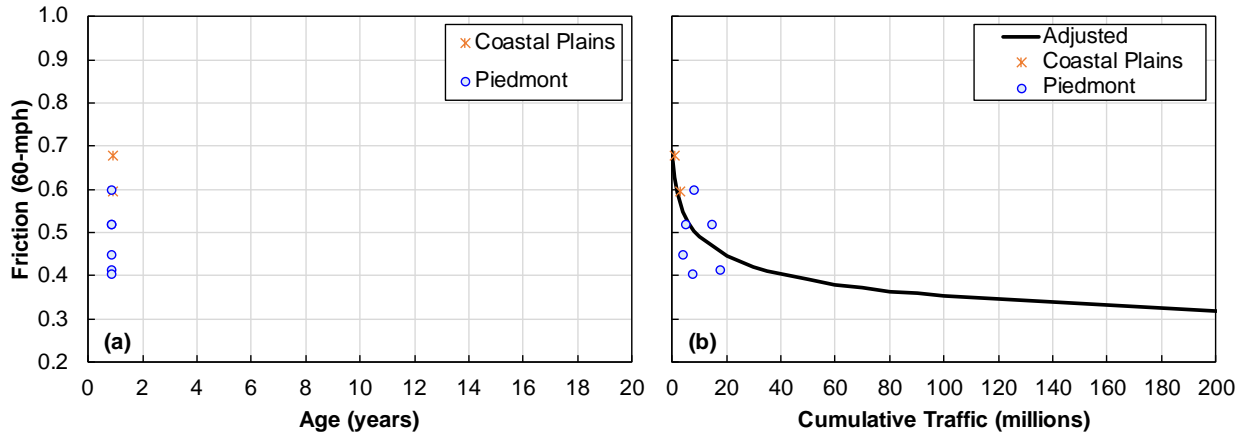


Figure C-4. Variation of Microsurfaging-Alt friction values at 60-mph with respect to: (a) age and (b) cumulative traffic.

Table C-3. Microsurfacing friction model coefficients.

Parameter	North Carolina	Microsurfacing-Alt
$A + \Delta A_{Microsurfacing}$	0.753	0.697
B	-0.037	-0.147
SSE	0.06	0.04

Dense-I/II

The model of Equation (2) was calibrated for the data collected on sites with a Dense-I and Dense-II surface type. To do so, the data of the two surface types were combined and a single model was calibrated. As before, the data was categorized into the three climate regions, although these regions correspond to North Carolina boundaries, it is assumed that the same weather longitudinal variation prevails in the neighboring states, i.e., the vertical delineation of the polygons that delimits these regions also applies for the two states where data was collected. The friction variation with respect to the age and cumulative traffic is depicted in Figure C-5 (a) and (b), respectively. As shown in Figure C-5 (b), except for the two datapoints circled in red, the data follows the pattern described by Equation (2), i.e., friction increases following a second order polynomial up to a maximum value and then decreases following an exponential decay.

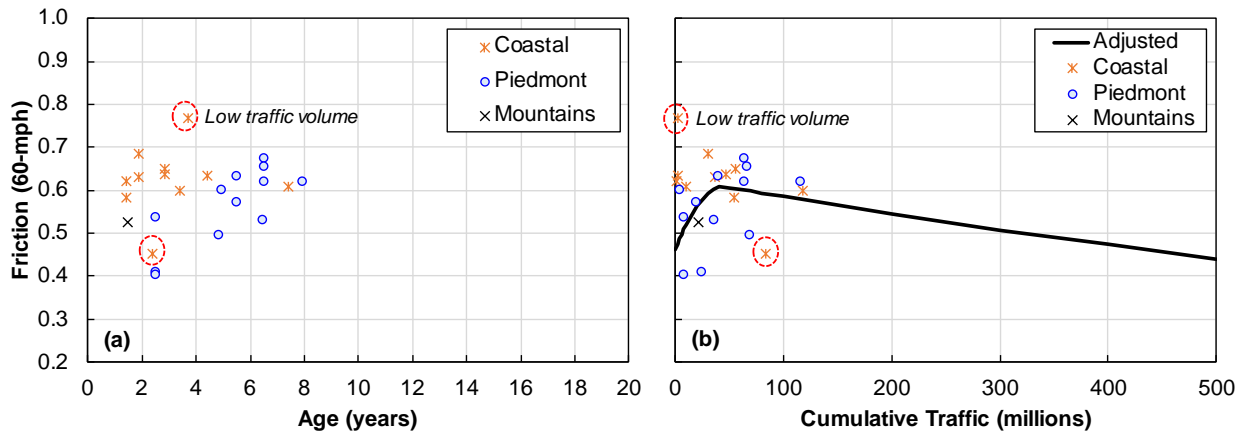


Figure C-5. Variation of the Dense-I/II friction values at 60-mph with respect to: (a) age and (b) cumulative traffic.

The solver tool in Excel was used to minimize the sum of square errors and estimate the value of the average random terms $\Delta a_{Dense-I/II}$, $\Delta b_{Dense-I/II}$, and $\Delta A_{Dense-I/II}$. The value of the resulting coefficients is shown in Table C-4. The results indicate that on average the number of traffic repetitions that are required for the surface to reach the maximum friction is 44.9 million repetitions. The rate of friction deterioration with respect to the cumulative traffic, Parameter B , is -7.1×10^{-4} which is quite close to the value obtained for UTBWCs (-7.2×10^{-4}). The initial expected friction is 0.46.

Table C-4. Updated friction model coefficients for the Dense-I/II.

Parameter	Value
$a + \Delta a_{Dense-I/II}$	0.46
$b + \Delta b_{Dense-I/II}$	0.0066
c	-0.000073
T_{max}	44.91
$A + \Delta A_{Dense-I/II}$	0.63
B	-0.00071
SSE	0.15

SMA-1

Again, the model of Equation (2) was calibrated for the data collected on sites with a SMA-1 mix. The data from the two binder types (SMA-1A and -1B, see Table 2) were combined and a single model was derived. The variation of friction with respect to the age and cumulative traffic is depicted in Figure C-6 (a) and (b), respectively.

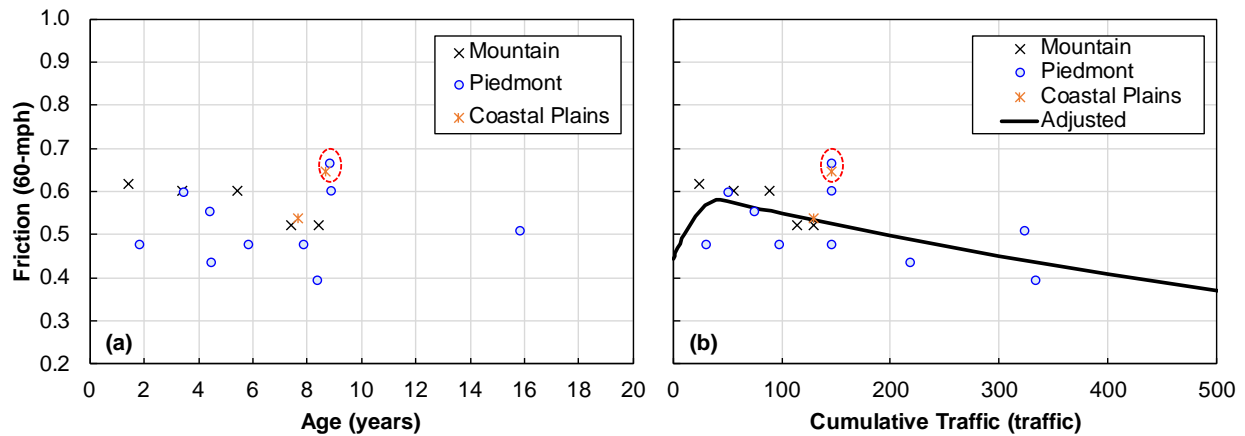


Figure C-6. Variation of the SMA-1 friction values at 60-mph with respect to: (a) age and (b) cumulative traffic.

The sites with a SMA-1 mix, follows the trend shown in Equation (2), i.e., friction increase until a maximum value is reached at T_{max} , the cumulative traffic needed for the maximum friction to occur, after which friction decreases with an exponential decay. The two data records enclosed by the red circle in Figure C-6 (b) are possible outliers from two different sites, in each of these sites a measurement was taken per traffic direction, but the average representative friction differs in more than 0.1 friction units, which is higher than the difference observed in previous studies for the measurements taken in the two traffic directions of a given site. This result may suggest that the highest values may be associated to a different age (i.e., the highest friction may be the result of a rehabilitation not reported in the PMS database used to establish the age of the surface). In

consequence, these two observations were not used during the calibration of model coefficients, Δa_{SMA-1} , Δb_{SMA-1} , and ΔA_{SMA-1} . The sum of square errors between measured and predicted friction was minimized using the solver tool in Excel and the resulting coefficients are shown in Table C-5. As shown, the initial expected friction is 0.44, the cumulative traffic needed to reach the maximum friction is 43.1 million repetitions, and the rate of deterioration is -9.8×10^{-4} friction units per million traffic repetitions, which is almost three times higher than the values recorded in Table 8 for dense-graded surfaces. When compared with the SMA-2 results, it is observed that the SMA-2 has a higher initial friction coefficient (0.56) and the SMA-1 has a higher deterioration rate. Therefore, higher friction values are expected with the SMA-2.

Table C-5. Updated friction model coefficients for the SMA-1.

Parameter	Value
$a + \Delta a_{SMA-1}$	0.44
$b + \Delta b_{SMA-1}$	0.0063
c	-0.000073
T_{max}	43.1
$A + \Delta A_{SMA-1}$	0.61
B	-0.00098
SSE	0.04

SMA-2

Similarly, the model of Equation (2) was calibrated for the data collected on sites with a SMA-2. The data from the two binder types (SMA-2A and -2B, see Table 2) were combined and a single model was derived. The variation of friction with respect the age and cumulative traffic is depicted in Figure C-7 (a) and (b), respectively.

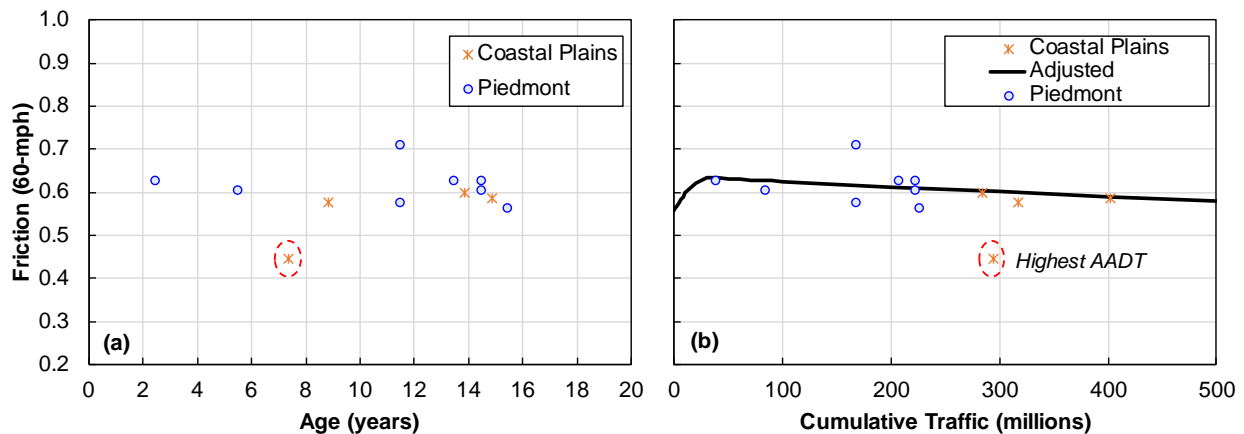


Figure C-7. Variation of the SMA-2 friction values at 60-mph with respect to: (a) age and (b) cumulative traffic.

The sites with a SMA-2 mix have an AADT between 40,000 and 56,000 vpd, except for the site enclosed in the red circle that has an AADT of 109,000 vpd. Therefore, this site was not used for the calibration of the average random effects in Equation (2), i.e., Δa_{SMA-2} , Δb_{SMA-2} , and ΔA_{SMA-2} . The sum of square errors was minimized using the solver tool in Excel and the resulting coefficients are shown in Table C-6. As shown, the initial expected friction is 0.56, the cumulative traffic needed to reach the maximum friction is 32.2 million repetitions, and the rate of

deterioration is -1.9×10^{-4} friction units per million traffic repetitions, which is almost half of the values recorded in Table 8 for dense-graded surfaces.

Table C-6. Updated friction model coefficients for the SMA-2.

Parameter	Value
$a + \Delta a_{SMA-2}$	0.56
$b + \Delta b_{SMA-2}$	0.0047
c	-0.000073
T_{max}	32.2
$A + \Delta A_{SMA-2}$	0.64
B	-0.00019
SSE	0.01

SMA-3A

There is not sufficient data to calibrate the friction performance model for the SMA-3A because all the observations are less than one and a half year old with only three records having a cumulative traffic greater than ten million repetitions. The data available is shown in Figure C-8. In the figure, the model developed for the SMA-2 is also shown. Besides the record corresponding to the 24.9 million traffic repetitions, the data point in Figure C-8 (b), seems to indicate a decreasing trend and the SMA-2 model provides a poor coefficient of determination. As such it is believed that the limited number of observations are essentially random effects around some central tendency represented by the SMA-2 model. More observations are needed to calibrate a model for SMA-3A.

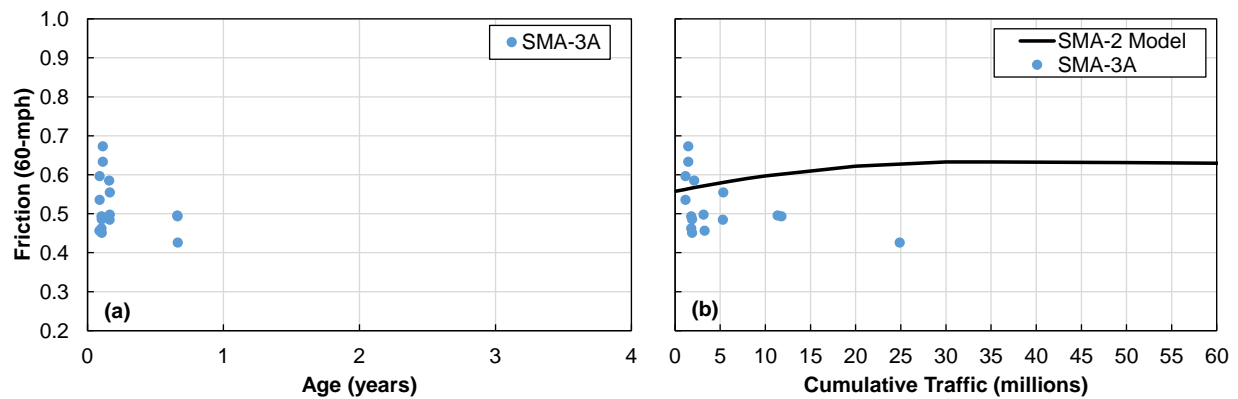


Figure C-8. Variation of the SMA-3A friction values at 60-mph with respect to: (a) age and (b) cumulative traffic.

Texture

The functional form of the texture performance model is presented in Equation (3), the model incorporates random effects in the intercept and in the texture rate of change. The former is specific for each site and the latter is a random term associated with the family the site belongs to. The average value of these random terms was estimated for the following surface types; OGFC, UTBWC, Microsurfacing, Dense-I/II, and SMAs.

OGFC

The variation of the OGFC *MPD* values with respect to the surface age and traffic are depicted in Figure C-9 (a) and (b), respectively. In this figure, the observations are grouped by the three climate regions defined in Table 15. Based on the data in this graph, it was observed that the sites that belong to the coastal plain region exhibited three distinct trends with respect to the cumulative traffic as shown in Figure C-10. In this figure, the filled dots represent the observations collected in the previous two research projects, NC_G1 and NC_G2, whereas the empty diamonds indicate the records collected in the current effort, NC_G3. As shown, some of the observations in NC_G1 and NC_G2 are sequential measurements collected in the same site, as noted by the dotted lines joined by line segments. The original model corresponding to the average value of the coefficients shown in Table 15 and Table 16 was plotted in Figure C-10 and was represented by the blue-thick dashed line. This model describes the central portion of the NC_G1 and NC_G2 and most of the NC_G3 observations. Model 2 describes the variation for three sites that were adjacent, i.e., they were in the same route with similar traffic but with different age. Hence, these observations were spatially related and therefore a model was proposed for those. Model 1 was fitted using the observations of two sites that were relatively old (with an age greater than six years) and relatively close to each other (they were in the same division).

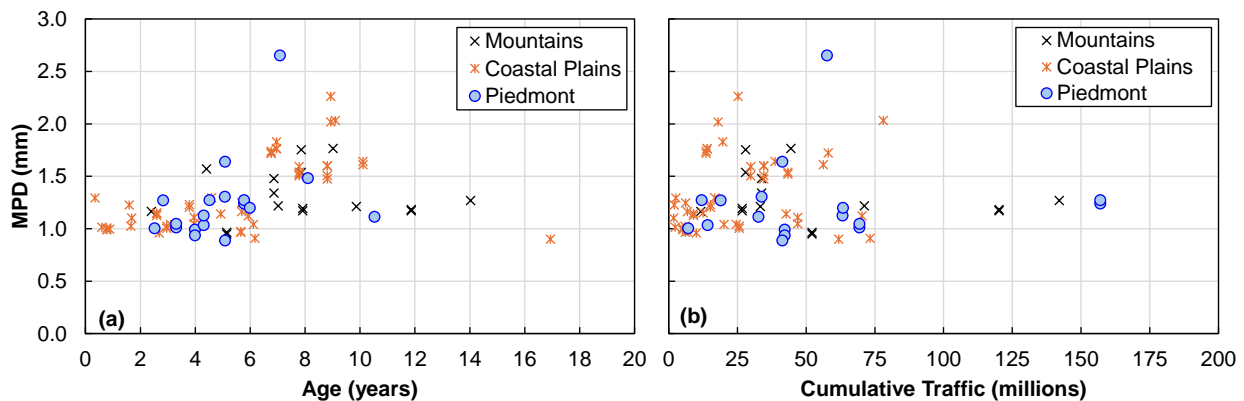


Figure C-9. Variation of OGFC *MPD* values in the RWP with respect to: (a) age and (b) cumulative traffic.

The model coefficients of the three curves shown in Figure C-10 are presented in Table C-7. In the table, the average, minimum, and maximum AADT of the sites used for the model calibration are presented. As shown, Model 1 was fitted using sites with the lowest AADT, on average 12,286 vpd, whereas Model 2 was fitted using sites with the highest AADT, on average 57,500 vpd. Consequently, the original model represents the average rate of change whereas the other two models depict the amount of variation in the texture performance expected in the sites located in the Coastal region.

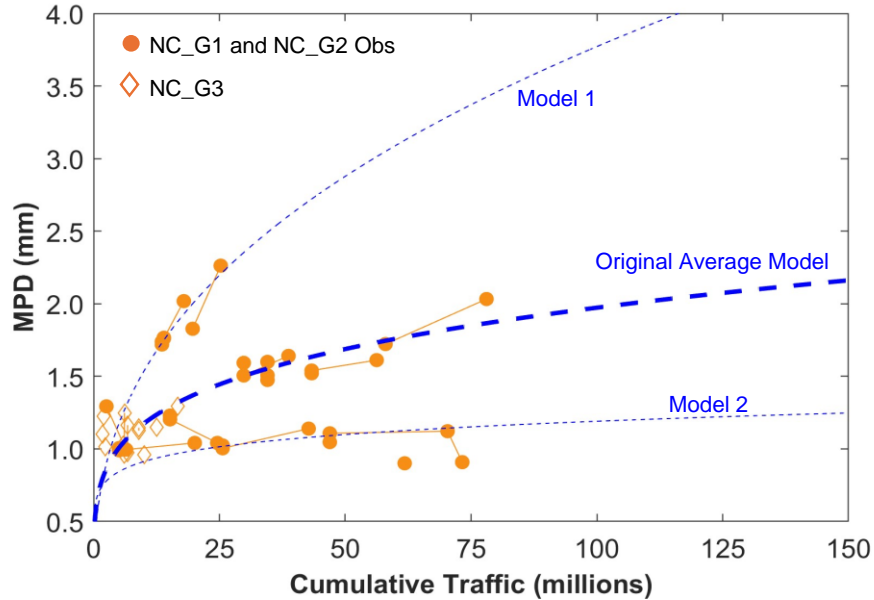


Figure C-10. Calibration of texture performance model for the OGFCs in the Coastal climate region.

Table C-7. Texture model coefficients for OGFC surfaces.

Family	Model	$a + \Delta a_{site}$	$b + \Delta b_{family}$	AADT			Avg Age
				Avg	Min	Max	
Coastal	Original	0.70	0.225	22,968	5,900	47,000	5.4
	Model 1	0.70	0.115	12,286	11,000	15,500	7.5
	Model 2	0.63	0.390	57,500	47,500	65,000	4.4
Piedmont	Original	0.70	0.200	-	-	-	-
	Model 1	0.94	0.055	55,944	14,500	115,000	4.9
Mountains	Original	0.70	0.120	55,500	55,500	55,500	9.2
	Model 1	0.65	0.231	23,450	18,500	32,500	7.1

Similarly, the MPD variation observed in the Piedmont region is included in Figure C-11. Like before, the filled dots indicate the observations of NC_G1 and NC_G2, and the empty diamonds indicate the records collected in NC_G3. The original model corresponding to the average value of the coefficients shown in Table 15 and Table 16 was plotted in Figure C-11 and was represented by the thick blue dashed line. Combining the observations from all three groups, the model coefficients were updated as indicated in Table C-7. These updated coefficients produce the new performance curve labeled as Model 1 in Figure C-11. In this case, the original model does not fit the data for the OGFC in the Piedmont region, which happens because previously the UTBWC and the OGFC were combined in a single category (HFC) and the average performance curve represents the performance of both surface types. In this sense, the Model 1 updated here should be used to describe the average texture performance of the OGFC in the Piedmont region.

Lastly, the data collected on sites with an OGFC in the Mountain region is depicted in Figure C-12. The original model is represented by the thick blue dashed line whereas the updated model is represented by the thin blue dashed line. Except for two sites that follow closely the original performance curve, the remaining observations were used to estimate the coefficients of Model 1. The original and updated model coefficients are shown in Table C-7.

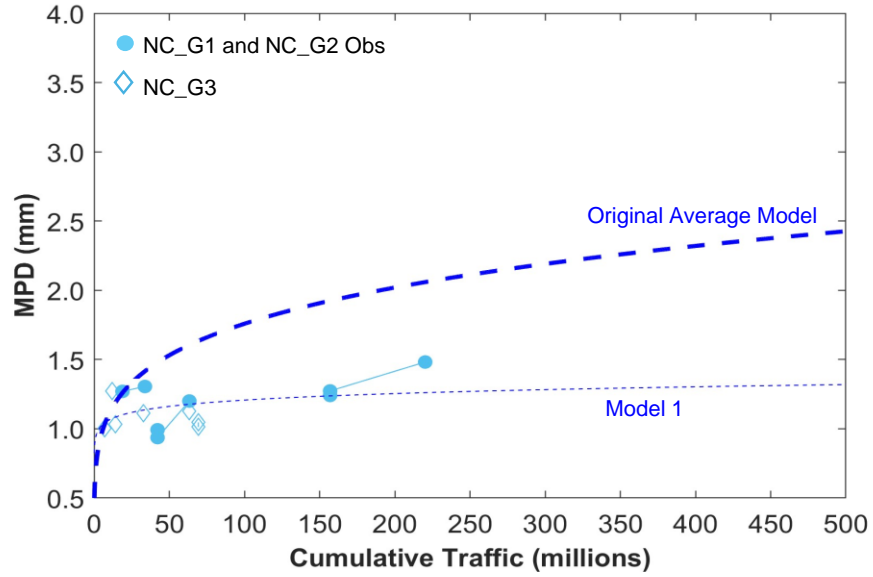


Figure C-11. Calibration of texture performance model for the OGFCs in the Piedmont climate region.

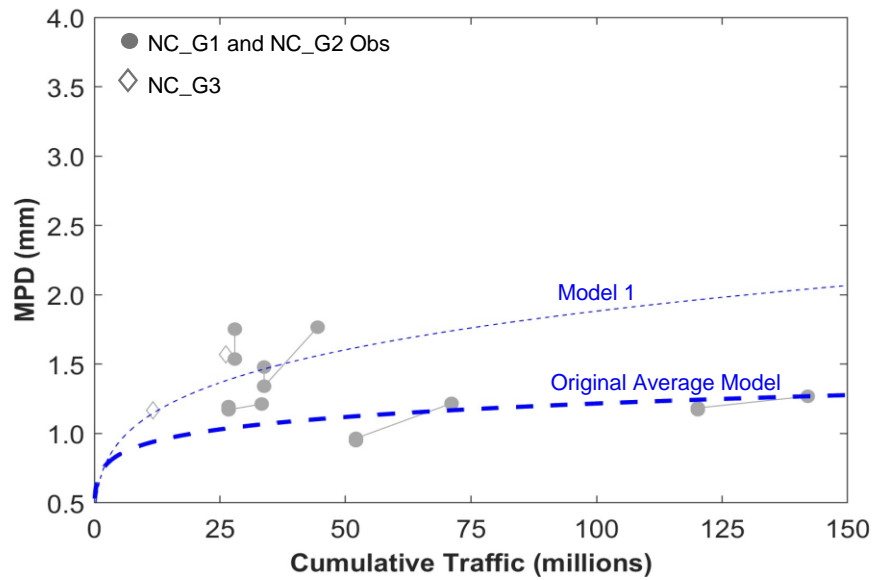


Figure C-12. Calibration of texture performance model for the OGFCs in the Mountains climate region.

A graphical comparison of all the OGFC models derived is shown in Figure C-13.

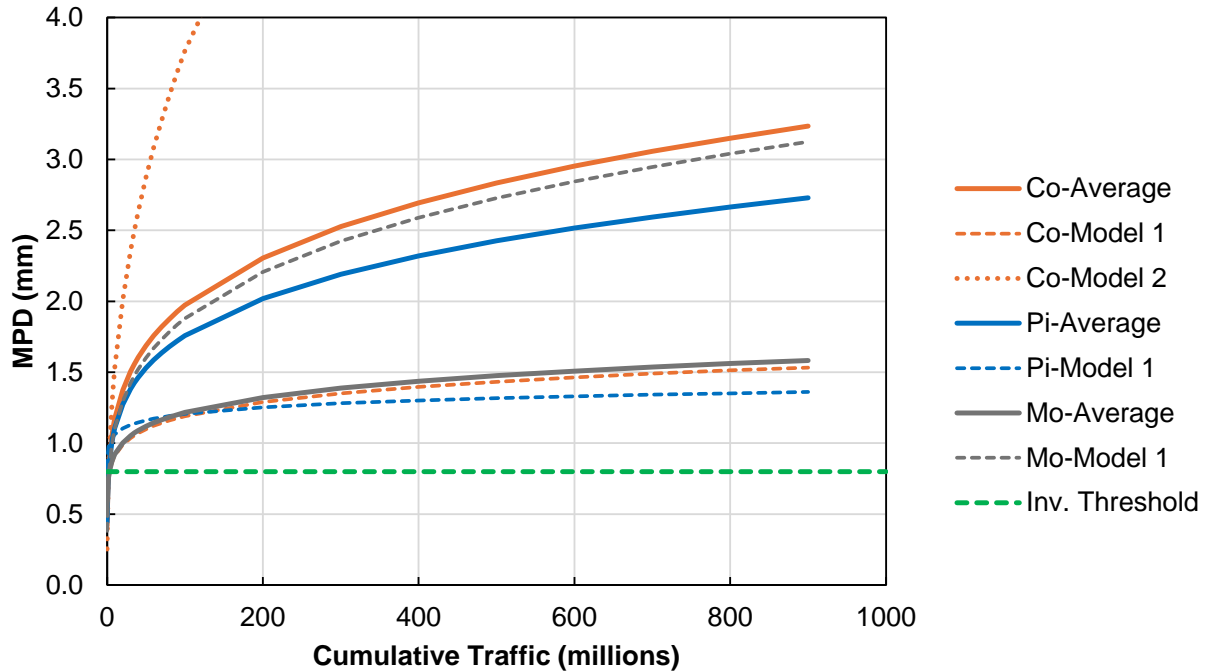


Figure C-13. OGFC performance models graphical comparison.

UTBWC

The variation of *MPD* values with respect to age and traffic for the UTBWC sites is shown in Figure C-14 (a) and (b), respectively. Like with the OGFCs, the performance curves were evaluated by climate region. For the sites in the coastal plain region, the model of Equation (3) was updated and the new coefficients are shown in Table C-8. The sites in the coastal plain region are in administrative Division 1 and 4. For the sites in the piedmont region, most of the sites are in Division 7 and 9. The sites in the mountain region were located mostly in Division 13.

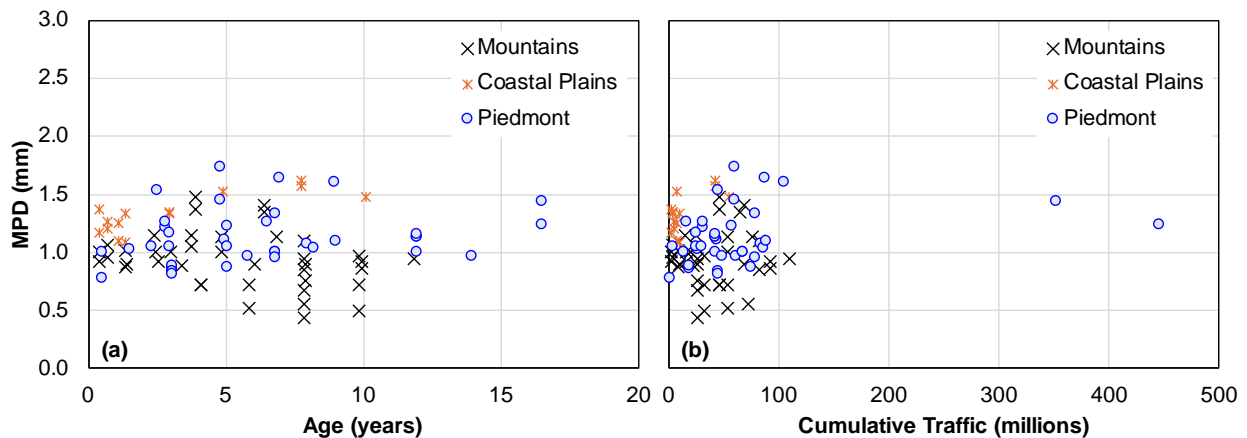


Figure C-14. Variation of UTBWC *MPD* values in the RWP with respect to: (a) age and (b) cumulative traffic.

Table C-8. Texture model coefficients for UTBWC surfaces.

Family	Model	$a + \Delta a_{site}$	$b + \Delta b_{family}$	AADT			Avg Age
				Avg	Min	Max	
Coastal	Original	0.80	0.225	-	-	-	-
	Model 1	1.11	0.083	31,285	8,900	40,000	2.6
Piedmont	Original	0.80	0.200	-	-	-	-
	Model 1	0.81	0.087	58,284	11,000	148,000	6.4
Mountains	Original	0.80	0.120	39,083	18,500	65,500	4.0
	Model 1	0.70	0.065	42,600	18,500	65,500	5.4

The *MPD* variation with respect the cumulative traffic for the sites located in the Coastal Plain region is depicted in Figure C-15, the average performance curve calibrated in the FHWA/NC 2022-5 project is represented by the thick blue dashed line, whereas the updated model is represented by the thin blue dashed line. This updated model was named Model 1. As shown, the updated curve has a lower rate of change and a higher intercept than the original model.

Likewise, for the sites located in the Piedmont region, the performance curve was updated to the one named as Model 1 in Figure C-16. As illustrated, the *MPD* values vary considerably across sites, a few observations are closer to the original model than to Model 1, but Model 1 is proposed as the performance curve for this pavement family because it added two records with a high age (16 years). However, it is important to note that some observations do not follow the trend and are closer to the original model. The original average model from FHWA/NC 2022-5 was the result of fitting that combined OGFC and UTBWC into a single series, which may explain why some sites tend to follow this trend. The two curves presented here show the expected performance variability that could be expected from UTBWC surfaces in the Piedmont region.

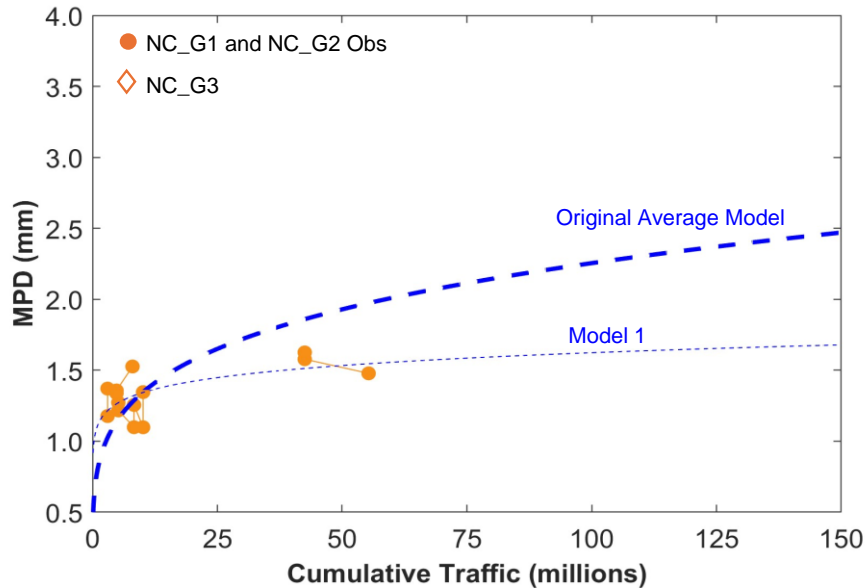


Figure C-15. Calibration of texture performance model for the UTBWCs in the Coastal climate region.

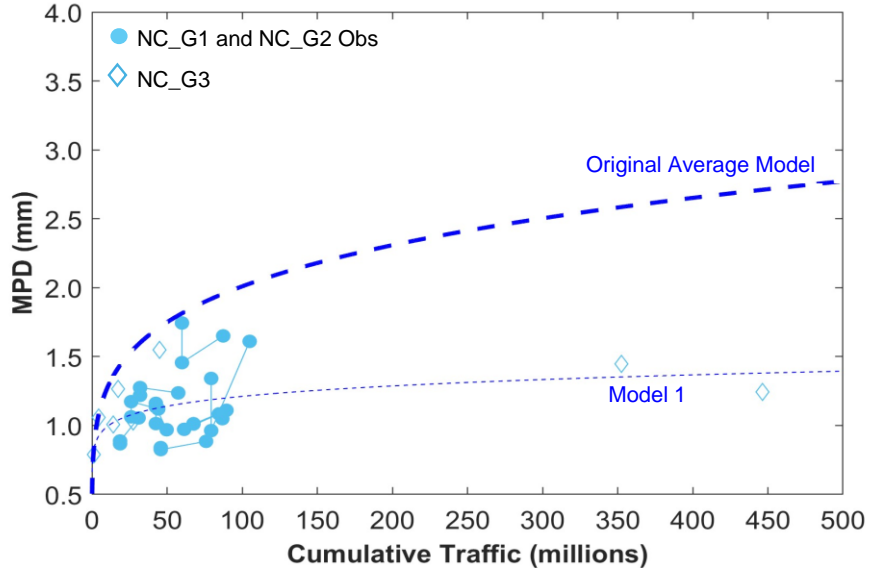


Figure C-16. Calibration of texture performance model for the UTBWCs in the Piedmont climate region.

Lastly, as depicted in Figure C-17, the sites in the Mountains exhibited two trends, one group follow closely the original average performance curve from the FHWA/NC 2022-5 project whereas the second group follow the curve of Model 1. The rate of change of Model 1 is almost half of the rate of change of the original average curve, as shown in Figure C-17 these sites have similar AADT and age, therefore the difference in the two curves may reflect normal random variation between pavements. The two curves bring a first estimate of the expected performance variability among the pavements in the Mountains region.

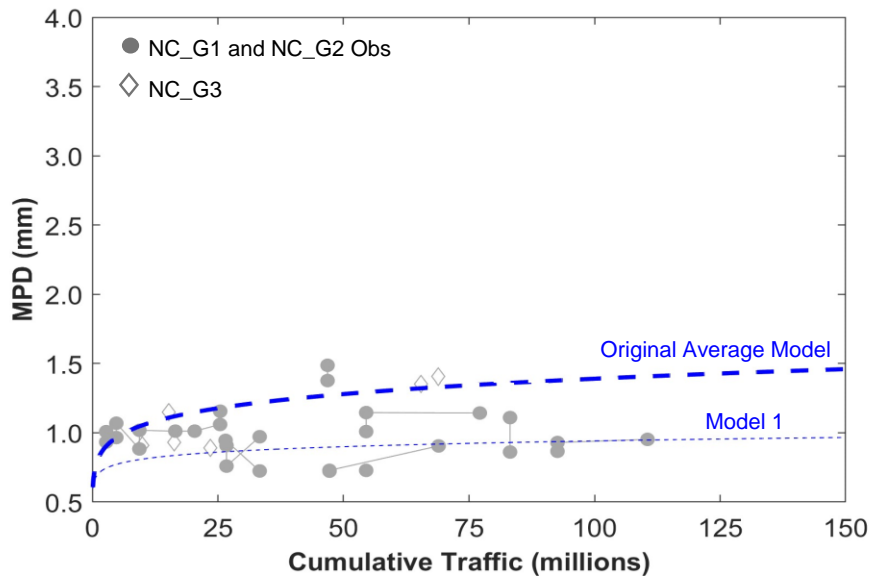


Figure C-17. Calibration of texture performance model for the UTBWCs in the Mountains climate region.

A graphical comparison of all the UTBWC performance models observed is presented in Figure C-18.

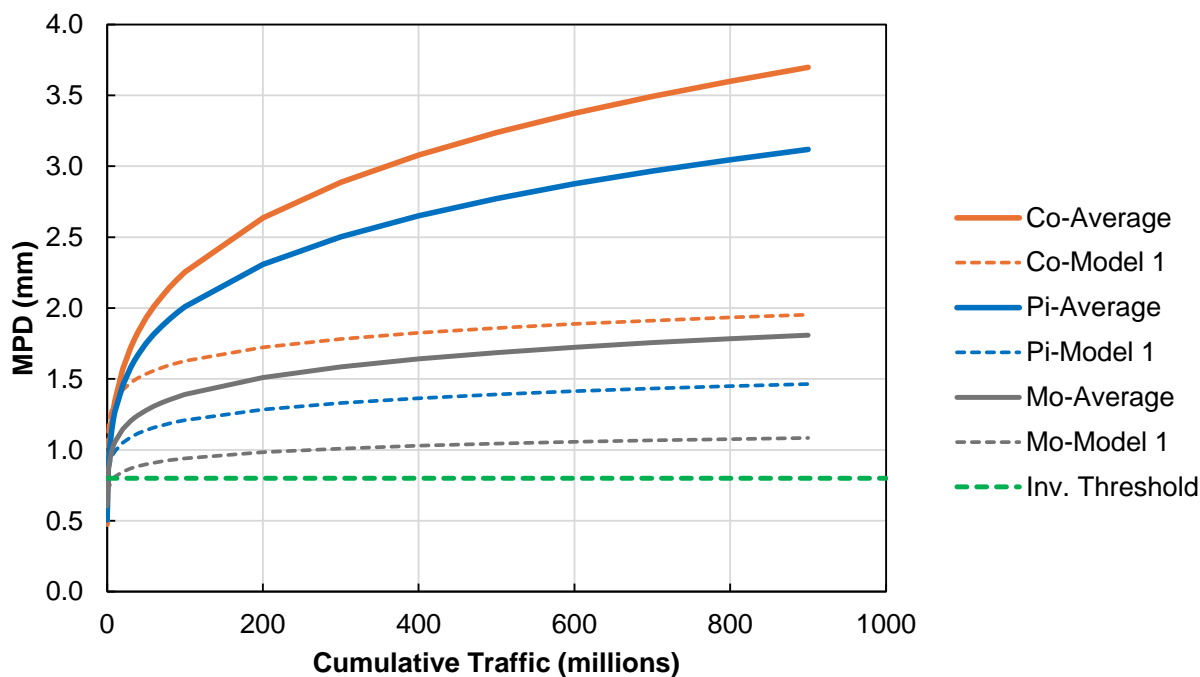


Figure C-18. UTBWC performance models graphical comparison.

Microsurfacing

The Microsurfacing surface type was not evaluated in the FHWA/NC 2022-5 project, therefore there are no previous values of the performance curve coefficients. The *MPD* variation with respect to age and cumulative traffic is depicted for North Carolina in Figure C-19 (a) and (b), respectively, and for the Microsurfacing-Alt in Figure C-20 (a) and (b), respectively. As shown in both panels of Figure C-19 and Figure C-20, the *MPD* values exhibited a decreasing trend with respect to age and traffic. The updated model coefficients are shown in Table C-9. As shown in Figure C-19 and Figure C-20 the North Carolina's Microsurfacing have higher initial *MPD* but has the same rate of change as the Microsurfacing-Alt.

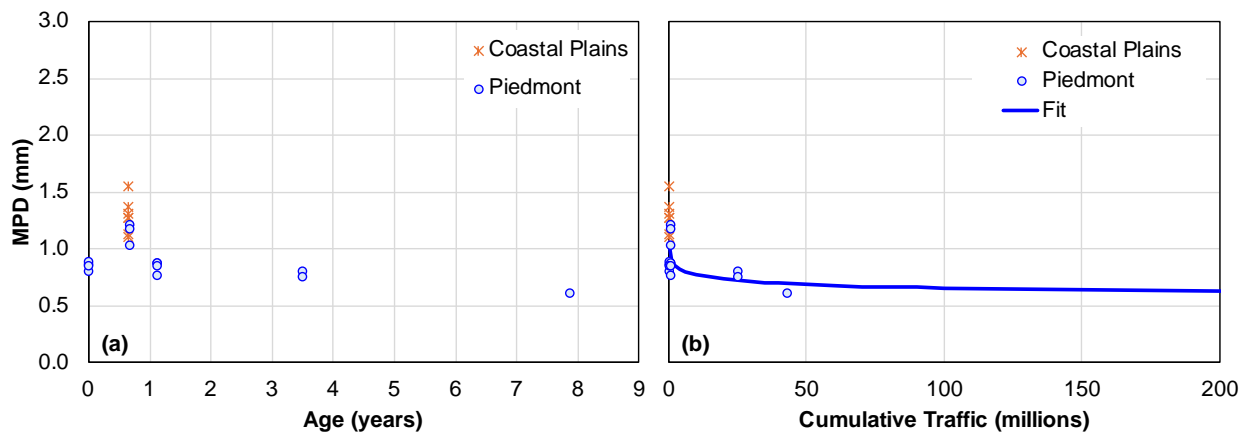


Figure C-19. Variation of North Carolina's Microsurfacing *MPD* values with respect to: (a) age and (b) cumulative traffic.

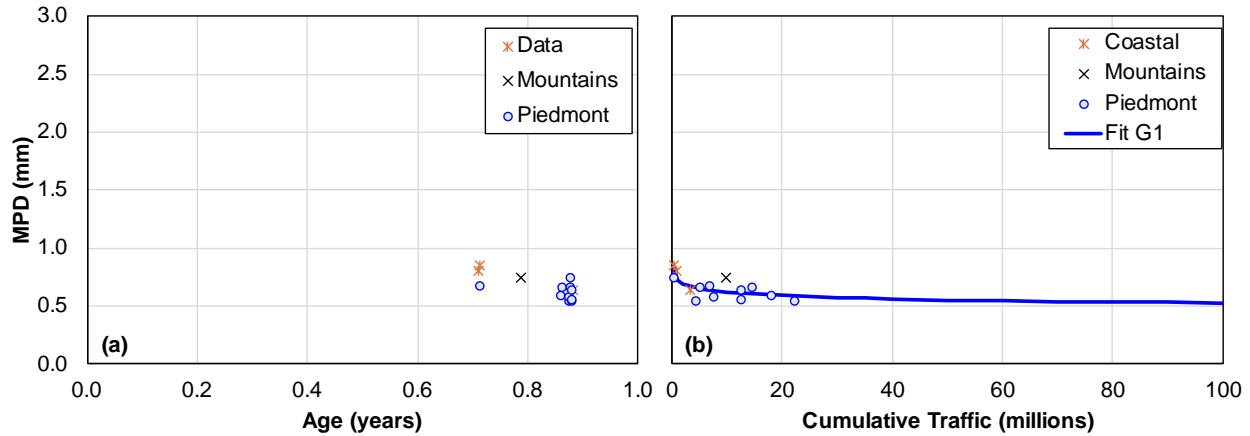


Figure C-20. Variation of Microsurfacing-Alt MPD values with respect to: (a) age and (b) cumulative traffic.

Table C-9. Texture model coefficients for Microsurfacing.

Surface Type	Family	$a + \Delta a_{site}$	$b + \Delta b_{family}$	AADT			Avg Age
				Avg	Min	Max	
Microsurfacing	All Regions	0.90	-0.070	3,948	200	30,000	1.2
Microsurfacing-Alt	All Regions	0.73	-0.071	26,781	930	69,000	0.9

A graphical comparison of the performance models derived for the Microsurfacing is included in Figure C-22.

Dense-I/II

The MPD variation with respect to age and cumulative traffic for the sites with a Dense-I/II surface is presented in Figure C-21 (a) and (b), respectively. In Figure C-21 (b) the observations the performance curves obtained after calibrating the value of the coefficients of Equation (3) are plotted. The performance curves were calibrated for the Coastal and Piedmont region, a curve for the Mountains was not derived because there is only one record available.

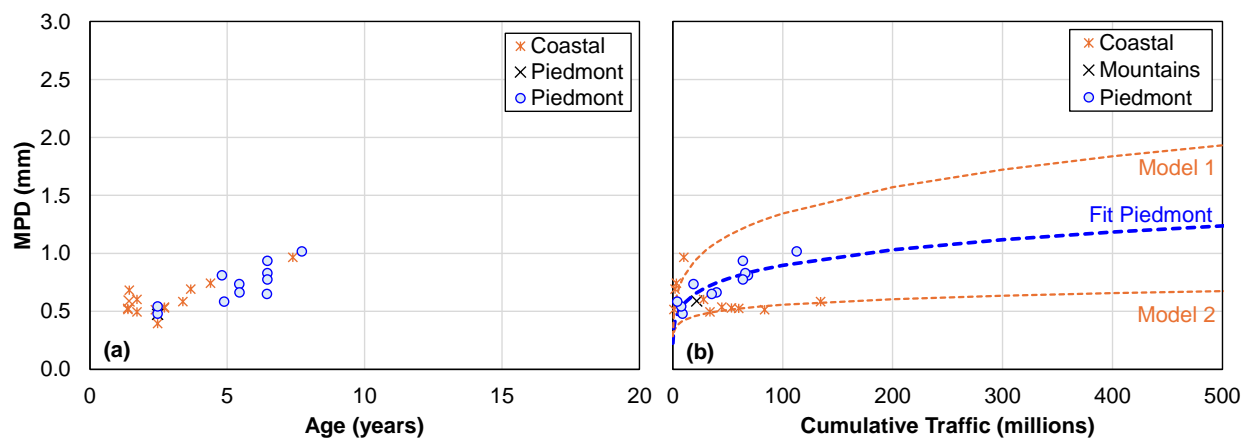


Figure C-21. Variation of Dense-I/II MPD values with respect to: (a) age and (b) cumulative traffic.

The two trends observed in the Coastal regions is caused by the two different traffic levels observed. These differences are reflected in the value of the rate of change for each group as shown

in Table C-10. Hence, the two curves reflect the expected variation in the performance curve for the Dense-I/II surface type. The two performance curves for the Coastal region are shown by the thin orange dashed lines, whereas the curve for the Piedmont region is represented by the thick blue dashed line.

Table C-10. Texture model coefficients for Dense-I/II.

Family	Model	$a+\Delta a_{site}$	$b+\Delta b_{family}$	AADT			Avg Age
				Avg	Min	Max	
Coastal	Model 1	0.48	0.225	70,500	42,000	119,000	2.2
	Model 2	0.32	0.120	2,300	1,500	3,700	4.2
Piedmont	Model 1	0.36	0.200	19,036	2,300	40,000	4.7

A graphical comparison of the performance models derived for the Microsurfacing and Dense I/II is presented in Figure C-22.

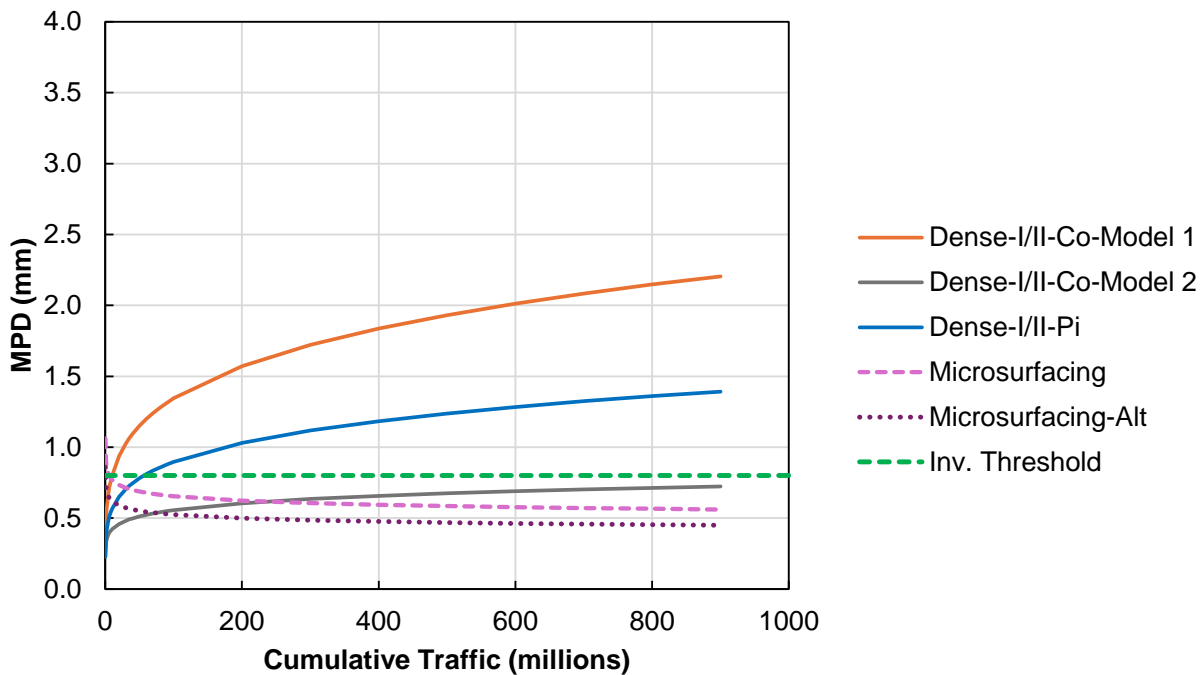


Figure C-22. Dense I/II and Microsurfacing performance models graphical comparison.

SMA-1

The MPD variation with respect to age and cumulative traffic for the SMA-1 is presented in Figure C-23 (a) and (b), respectively. A performance curve was obtained for each climate region, to do so the rate of change estimated in the FHWA/NC 2022-5 for the high friction course (HFC) in each climate region was used (see Table 15) and the intercept was estimated. The sites were grouped by climate region as before, and the three different regions were evaluated. The values of the updated coefficients are shown in Table C-11.

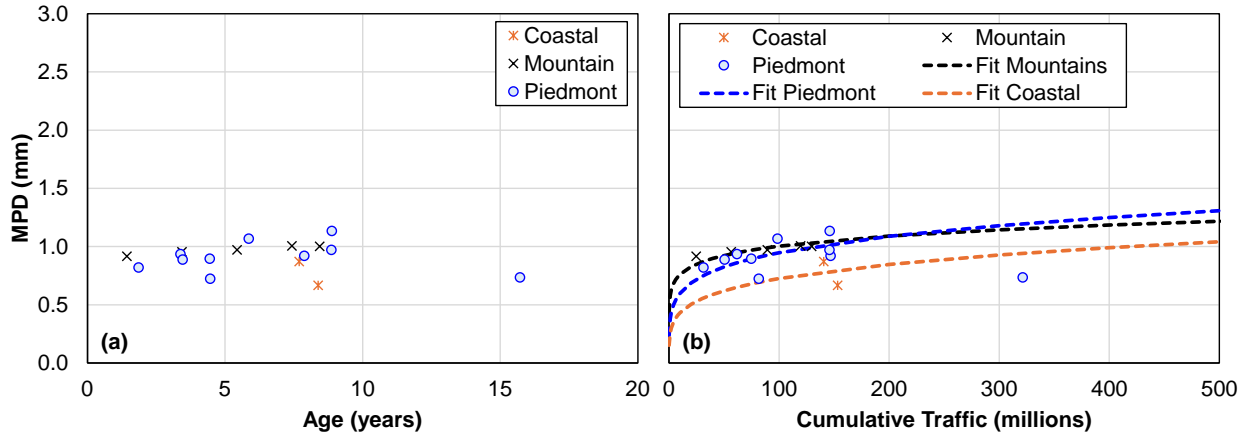


Figure C-23. Variation of SMA-1 MPD values with respect to: (a) age and (b) cumulative traffic.

Table C-11. Texture model coefficients for SMA-1.

Family	Model	$a + \Delta a_{site}$	$b + \Delta b_{family}$	AADT			Avg Age
				Avg	Min	Max	
Coastal	Model 1	0.26	0.225	50,000	50,000	50,000	8.3
Piedmont	Model 1	0.38	0.200	47,500	40,000	56,000	6.5
Mountains	Model 1	0.58	0.120	44,600	42,000	47,000	5.2

SMA-2

The MPD variation with respect to age and cumulative traffic for the SMA-2 is presented in Figure C-24 (a) and (b), respectively. Two performance curves were estimated, one for the Coastal and other for the Piedmont region. No observations were collected in the Mountains. The performance curves obtained for each region are included in the graph and represented by the dashed lines. To estimate these curves, the rate of change for each region as estimated in the FHWA/NC 2022-5 project were used and the intercept was estimated using Solver in Excel. The updated coefficients are included in Table C-12. Because no records were collected in the Mountains, it is recommended to use the Piedmont performance curve to describe the expected texture performance in the sites with SMA-2 in the Mountains.

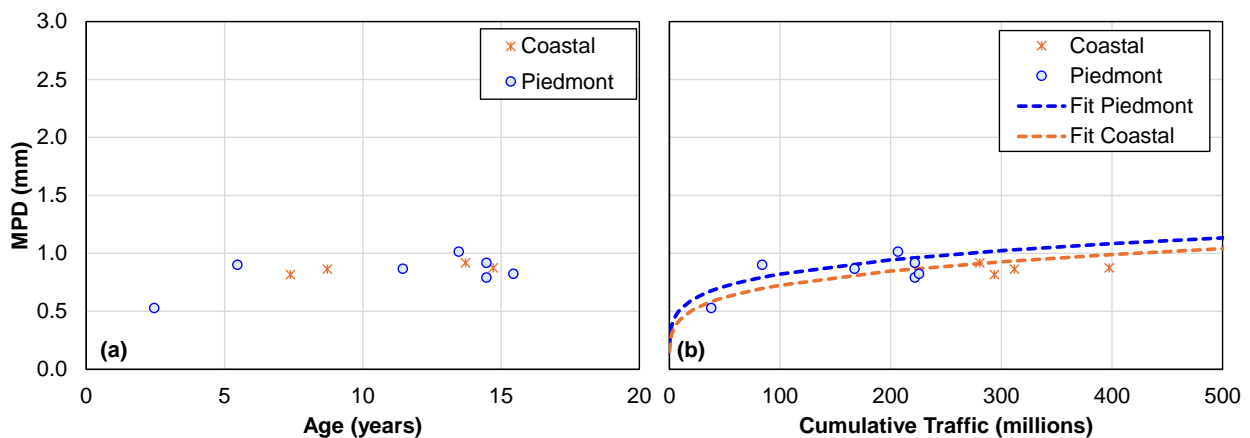


Figure C-24. Variation of SMA-2 MPD values with respect to: (a) age and (b) cumulative traffic.

Table C-12. Texture model coefficients for SMA-2.

Family	Model	$a+\Delta a_{site}$	$b+\Delta b_{family}$	AADT			Avg Age
				Avg	Min	Max	
Coastal	Model 1	0.26	0.225	84,250	56,000	109,000	11.1
Piedmont	Model 1	0.33	0.200	41,429	40,000	42,000	11.0
Mountains	Model 1	-	-	-	-	-	-

SMA-3A

There is not sufficient data to calibrate the macrotexture performance model for the SMA-3A because all the observations are less than one and a half year old with only three records with a cumulative traffic greater than ten million repetitions. The data available is shown in Figure C-25, in the figure the models developed for the SMA-2 in the Piedmont and Coastal regions are also shown. The SMA-3A data are higher than both models and the variability in the values with a cumulative traffic lower than 11 million repetitions appears to behave like random variation in the initial macrotexture. Therefore, the Piedmont model (the closest to the SMA-3A records) was vertically shifted to obtain the performance curve named as Fit SMA-3A in Figure C-25 (b) and with parameters shown in Table C-13.

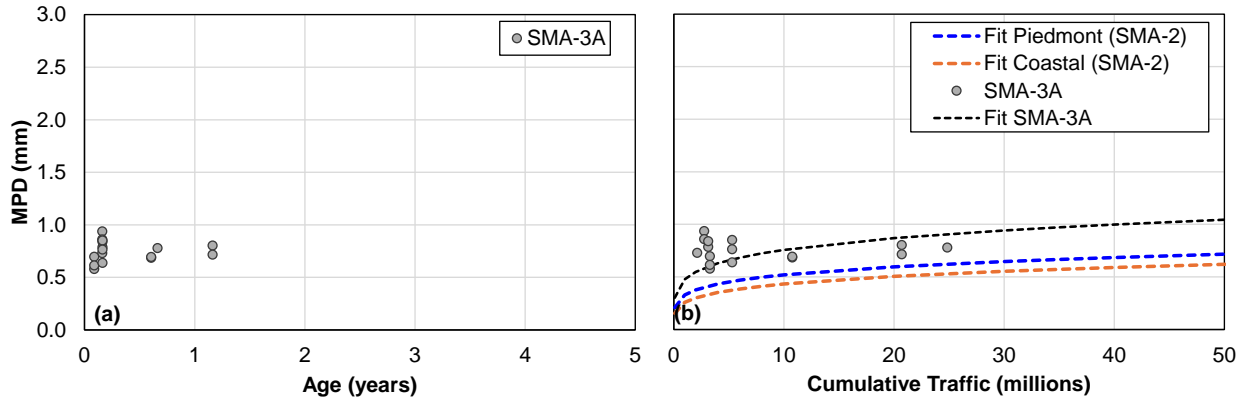


Figure C-25. Variation of the SMA-3A MPD values with respect to: (a) age and (b) cumulative traffic.

Table C-13. Texture model coefficients for SMA-3A.

Family	Model	$a+\Delta a_{site}$	$b+\Delta b_{family}$	AADT			Avg Age
				Avg	Min	Max	
SMA-3A	Fit SMA-3A	0.48	0.20	58,000	35,500	102,600	0.36

A graphical comparison of the SMA performance models is included in Figure C-26.

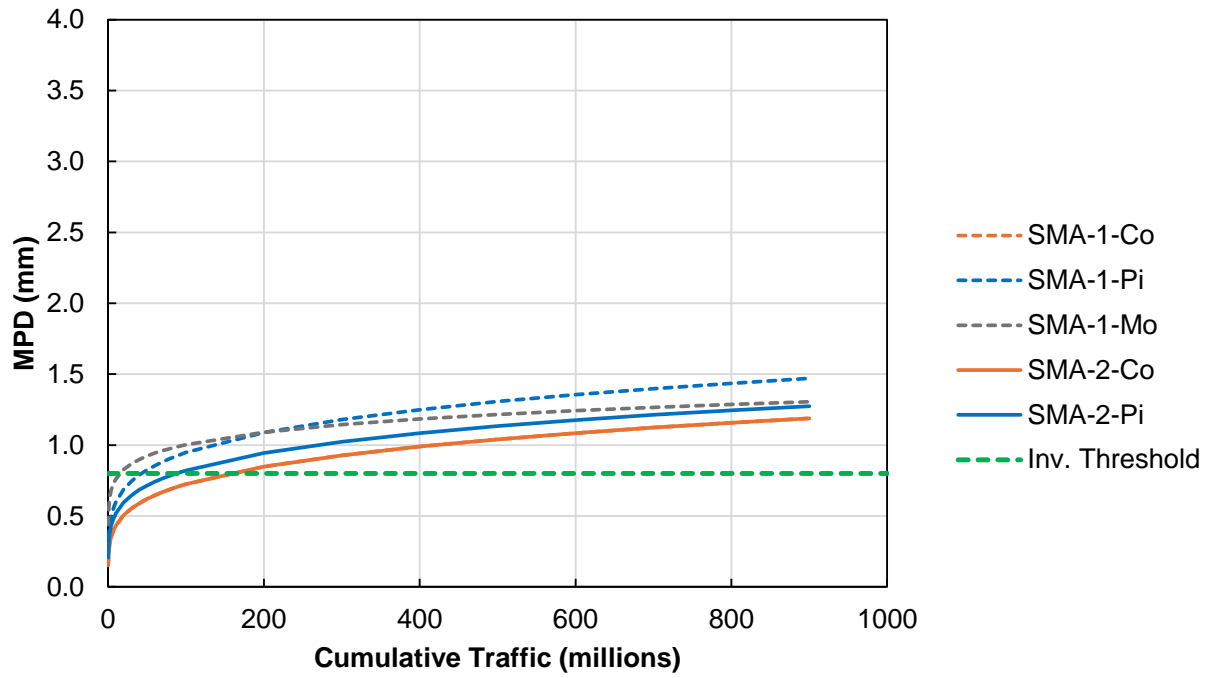


Figure C-26. SMA performance models graphical comparison.

APPENDIX D. STATIC TEXTURE MEASUREMENTS

A total of 79 surface scans were conducted using the AMES 9500 rapid laser texture scanner (rlts). These observations were made either in the center of the lane or in the right wheel path of the outermost lane on each site. The number of surface scans made on each surface type is presented in Table 5. The rlts collects more than 4,000,000 data points and the software that controls the laser processes the information in lines each with 2,400 data points. Each profile line is processed using the ISO 13473-1 standard and the mean profile depth (*MPD*) and the root mean square depth (*RMSD*) are reported. Additionally, the software also provides two more indices, the skewness (*Rsk*) and kurtosis (*Rku*), computed on unprocessed profiles.

Mean Profile Depth (*MPD*) Results

The average *MPD* values of the surface scans are depicted in Figure D-1 to Figure D-5. The distribution of values matches the findings discussed in Section 3.3 and in the Appendix C, i.e., the *MPD* increases with the surface age. The ranking of the surfaces, from low to high *MPD* also aligns with the discussion presented in Section 3.3.

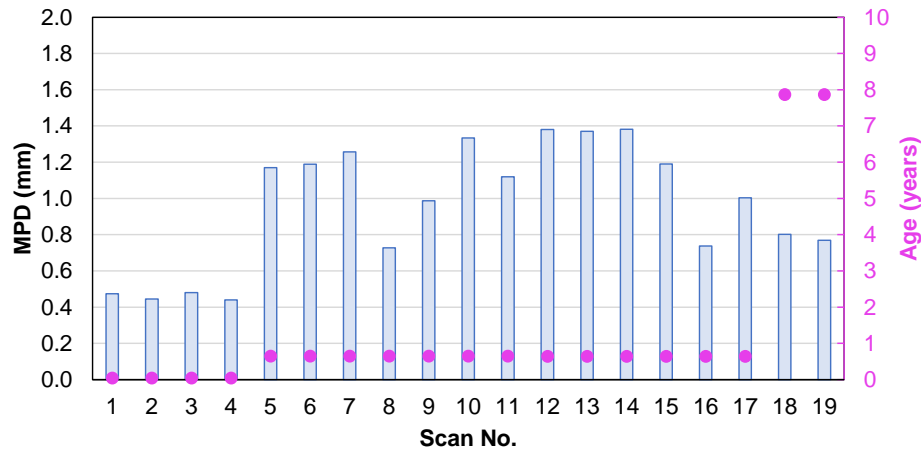


Figure D-1. Average *MPD* of the surface scans for North Carolina's Microsurfacing.

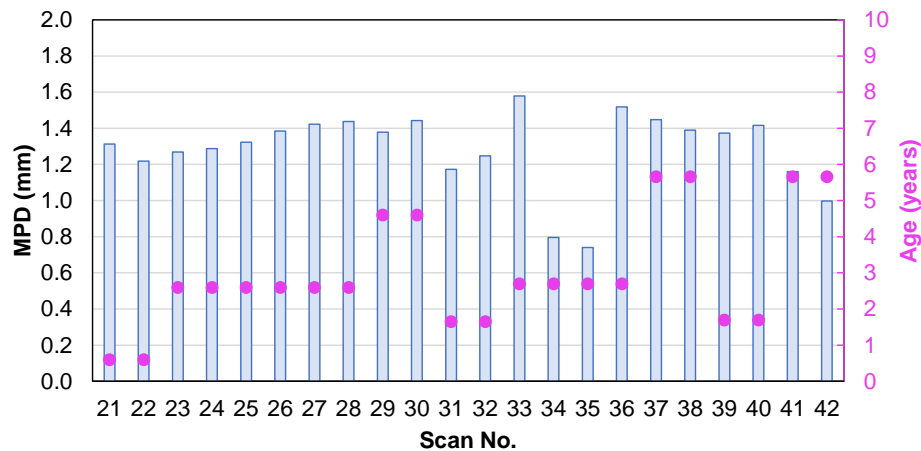


Figure D-2. Average *MPD* of the surface scans for North Carolina's OGFC.

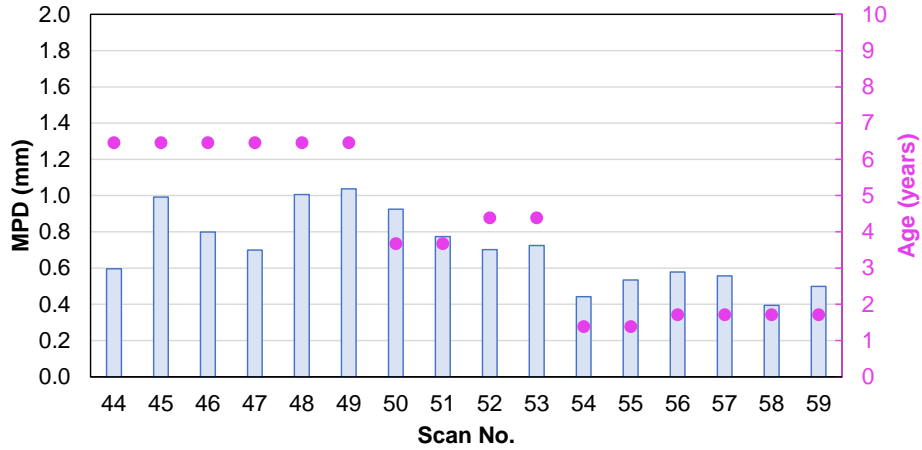


Figure D-3. Average *MPD* of the surface scans for Dense-II.

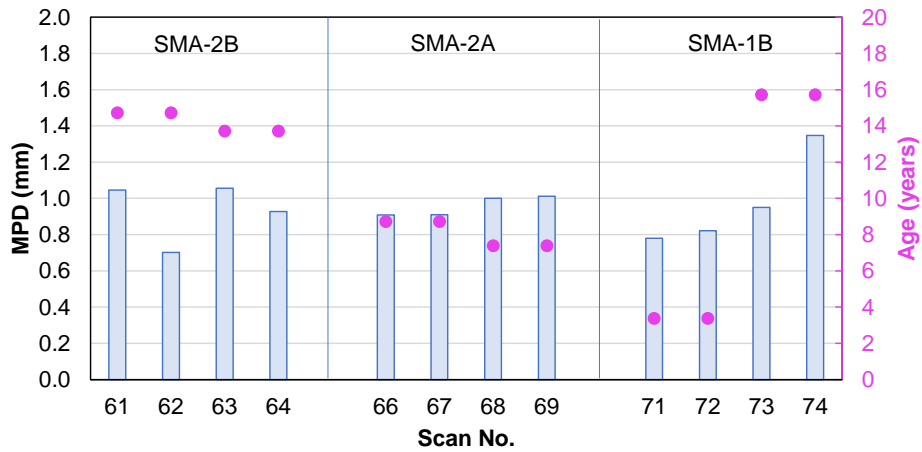


Figure D-4. Average *MPD* of the surface scans for SMA-2 and SMA-1.

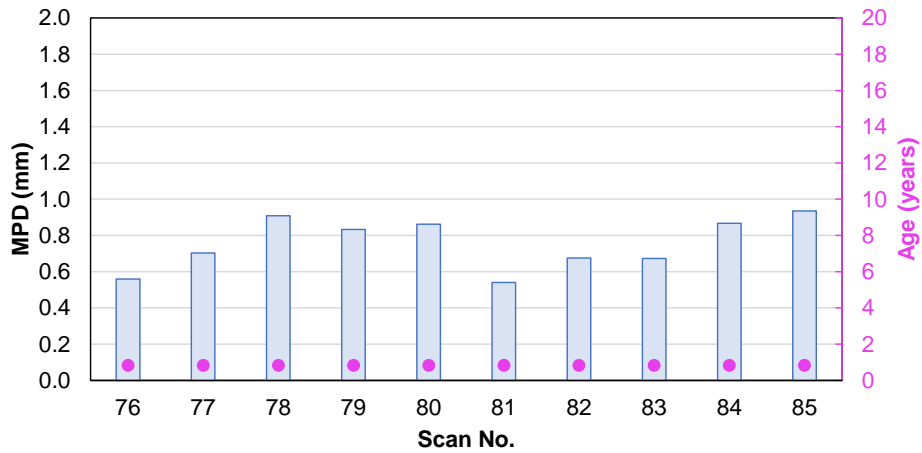


Figure D-5. Average *MPD* of the surface scans for the Microsurfacing-Alt.

Root Mean Square Depth (*RMSD*) Results

The average *RMSD* values of the surface scans are depicted in Figure D-6 to Figure D-10. The distribution of values follows the same trend of *MPD*, i.e., the *RMSD* increases with pavement age. This finding was expected because the *RMSD* is a representation of the standard deviation of the texture profile, so when the pavement aged the surface deterioration such as raveling, cracking, etc. contributes to increase the voids in the surface and therefore increase the texture variability.

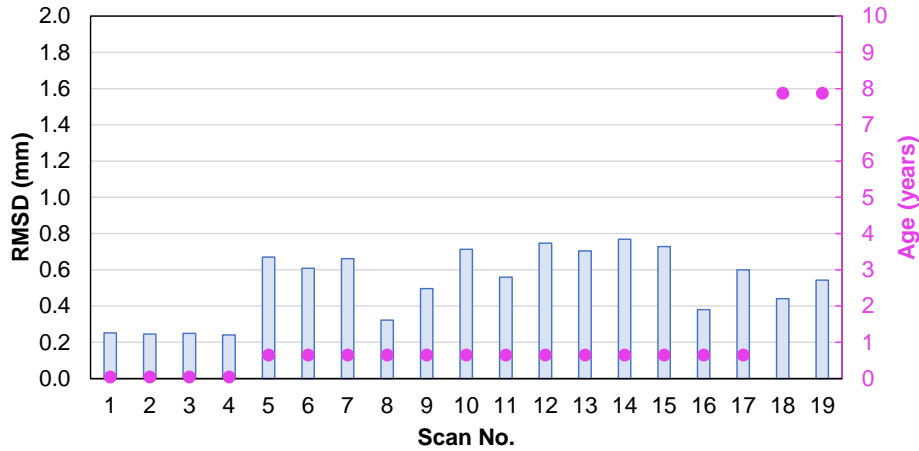


Figure D-6. Average *RMSD* of the surface scans for North Carolina's Microsurfacing.

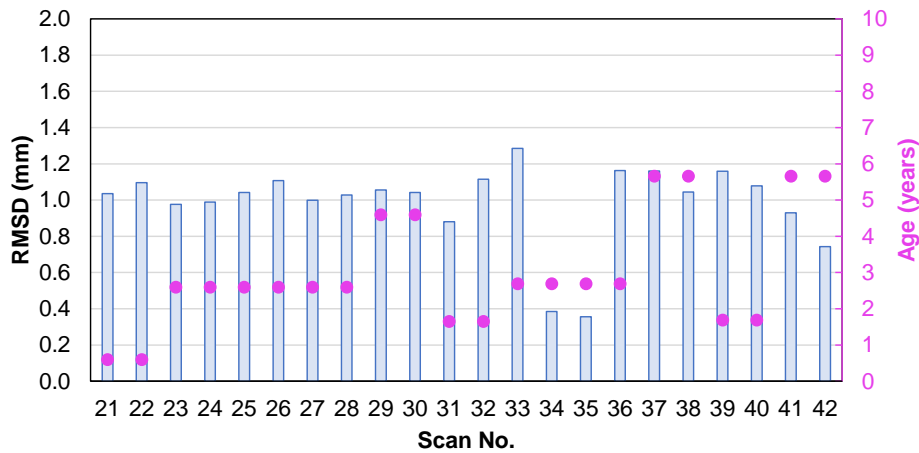


Figure D-7. Average *RMSD* of the surface scans for North Carolina's OGFC.

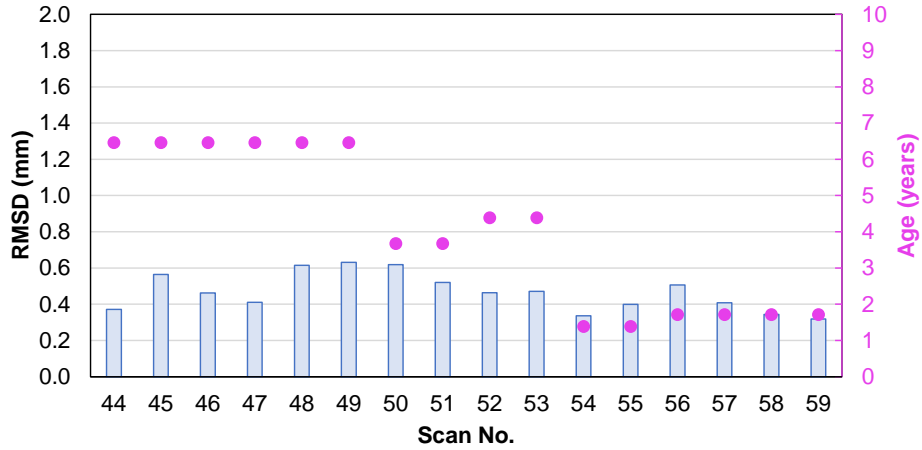


Figure D-8. Average *RMSD* of the surface scans for Dense-II.

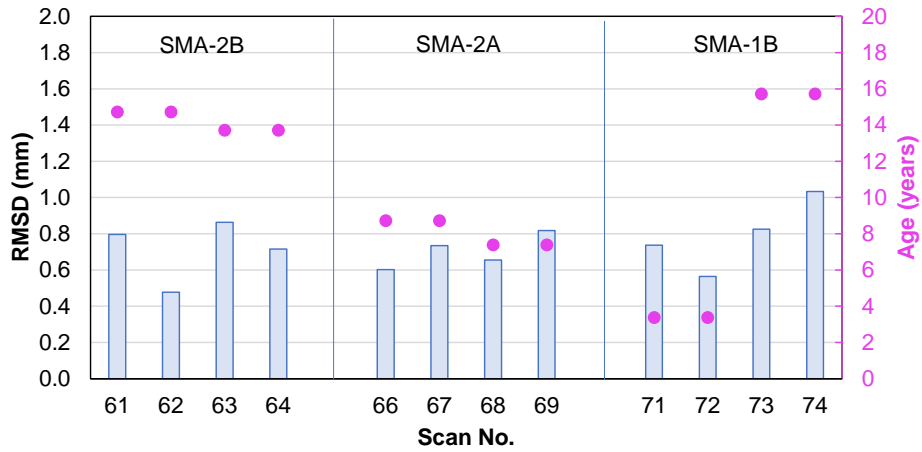


Figure D-9. Average *RMSD* of the surface scans for SMA-2 and SMA-1.

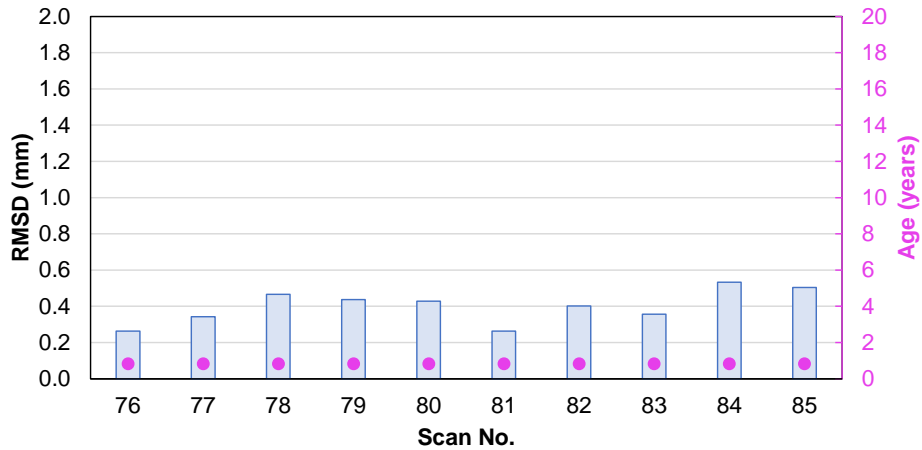


Figure D-10. Average *RMSD* of the surface scans for the Microsurfacing-Alt.

Skewness (*Rsk*) Results

The average *Rsk* value for each surface scan collected in the different sites is depicted in Figure D-11 to Figure D-15. As presented, the skewness of North Carolina's Microsurfacing increases with age and is like the values observed in the Microsurfacing-Alt. The surface with the highest *Rsk* is the OGFC and SMA-1B and SMA-2.

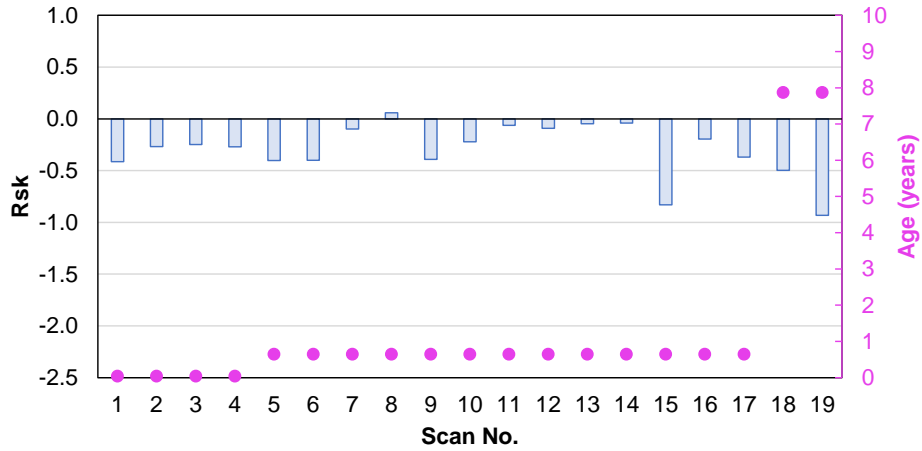


Figure D-11. Average *Rsk* of the surface scans for North Carolina's Microsurfacing.

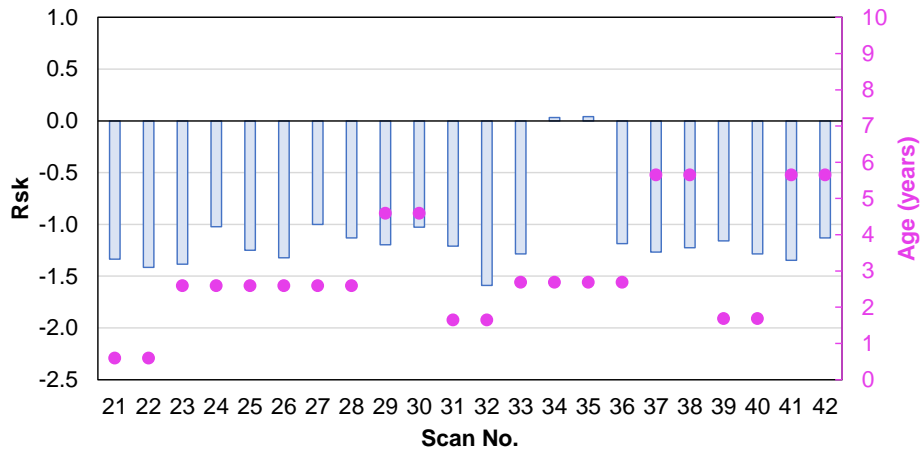


Figure D-12. Average *Rsk* of the surface scans for North Carolina's OGFC.

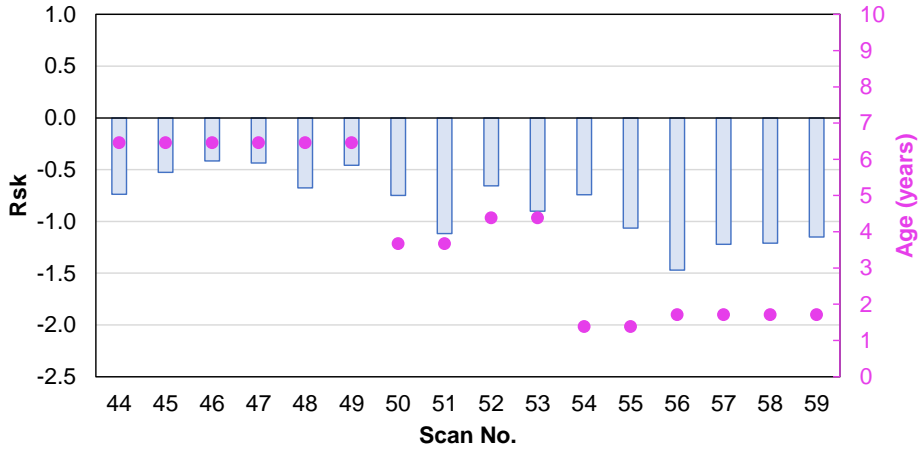


Figure D-13. Average *Rsk* of the surface scans for Dense-II.

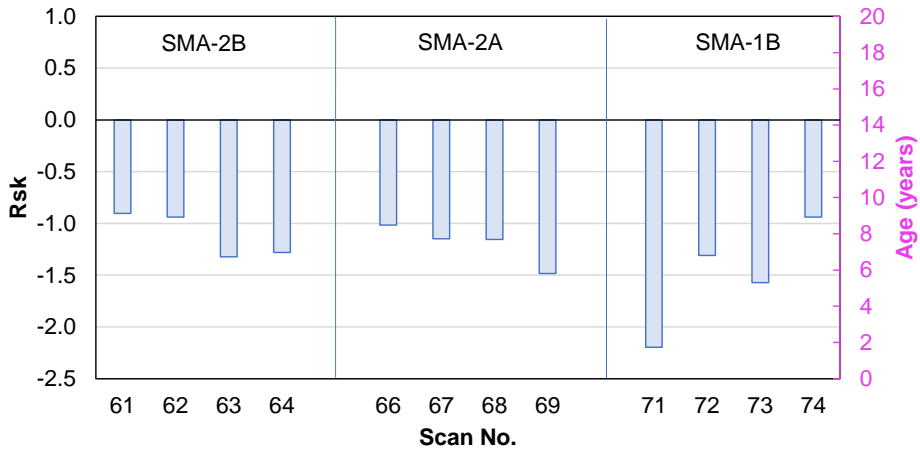


Figure D-14. Average *Rsk* of the surface scans for SMA-2 and SMA-1.

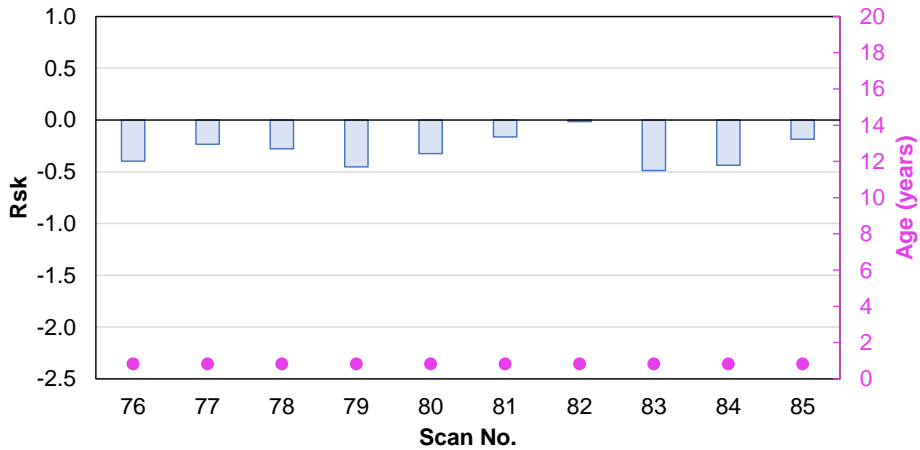


Figure D-15. Average *Rsk* of the surface scans for the Microsurfacing-Alt.

Kurtosis (*Rku*) Results

The average *Rku* for each surface scan is presented in Figure D-16 to Figure D-20. The lowest *Rku* values were recorded in the Microsurfacing-Alt, followed by North Carolina's Microsurfacing.

The Rku reduced with age, as a reflection of the traffic polishing that wear the peaks of the texture profile. The surface with the highest kurtosis is SMA-1.

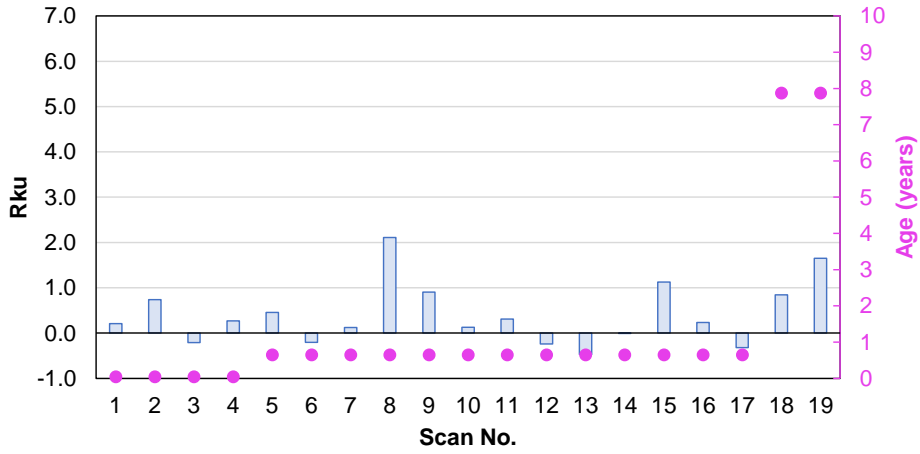


Figure D-16. Average Rku of the surface scans for North Carolina's Microsurfacing.

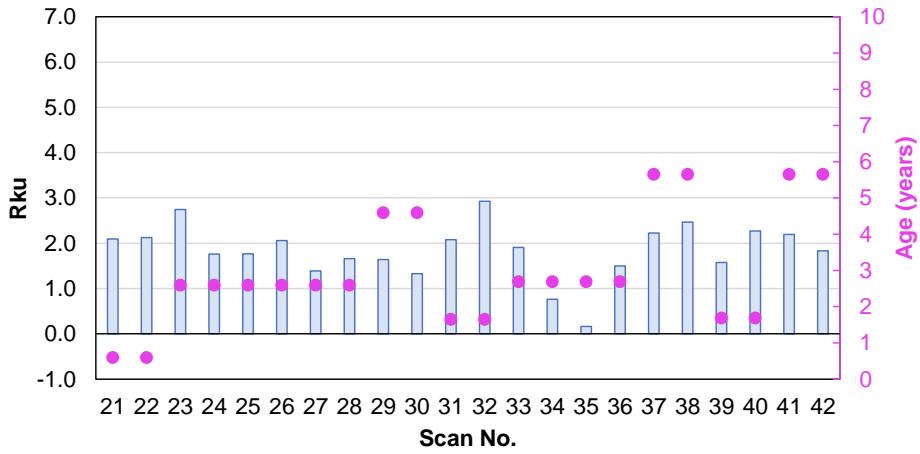


Figure D-17. Average Rku of the surface scans for North Carolina's OGFC.

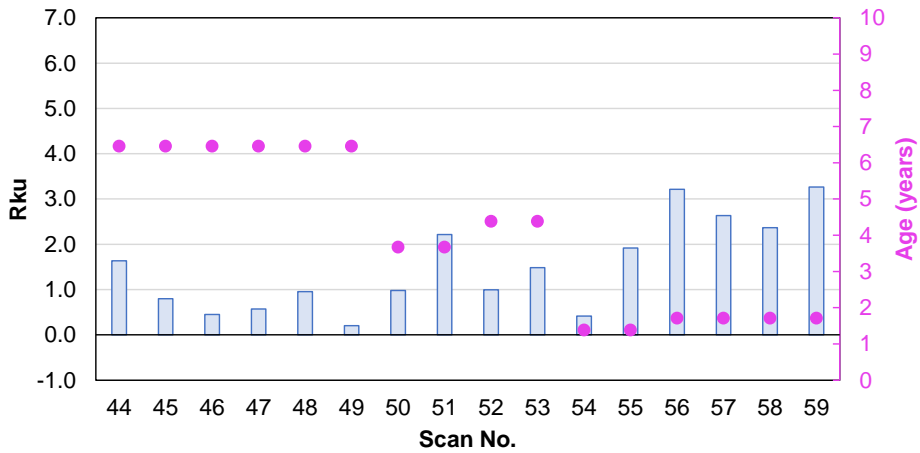


Figure D-18. Average Rku of the surface scans for Dense-II.

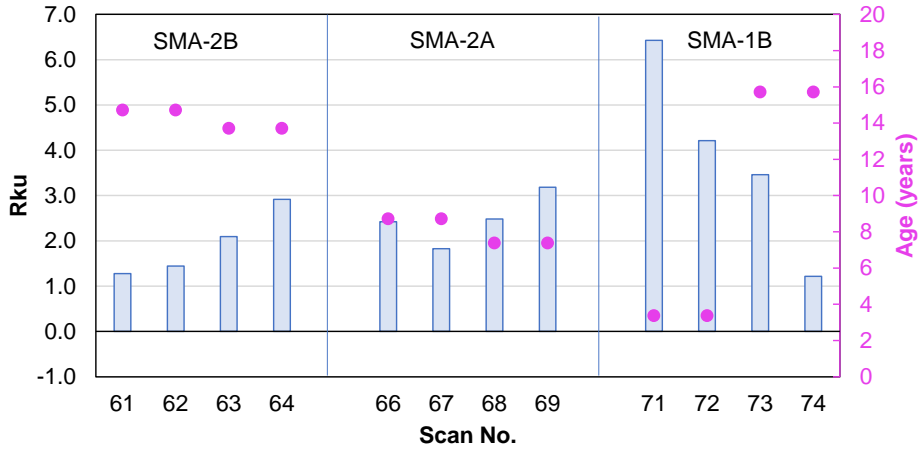


Figure D-19. Average Rku of the surface scans for SMA-2 and SMA-1.

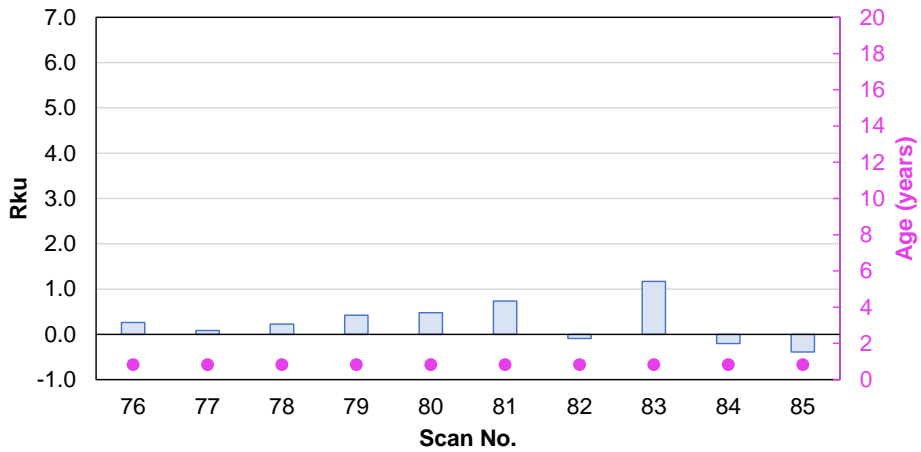


Figure D-20. Average Rku of the surface scans for the Microsurfacing-Alt.

Surface Scans
Microsurfacing

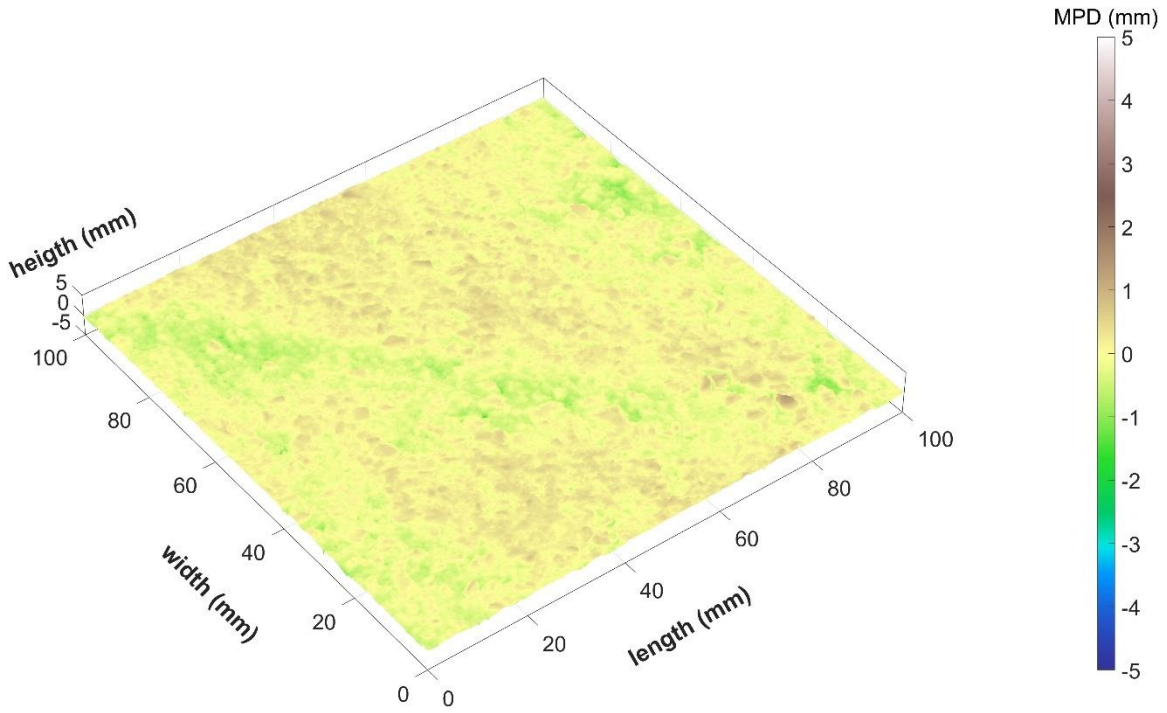


Figure D-21. Microsurfacing surface scan 1.

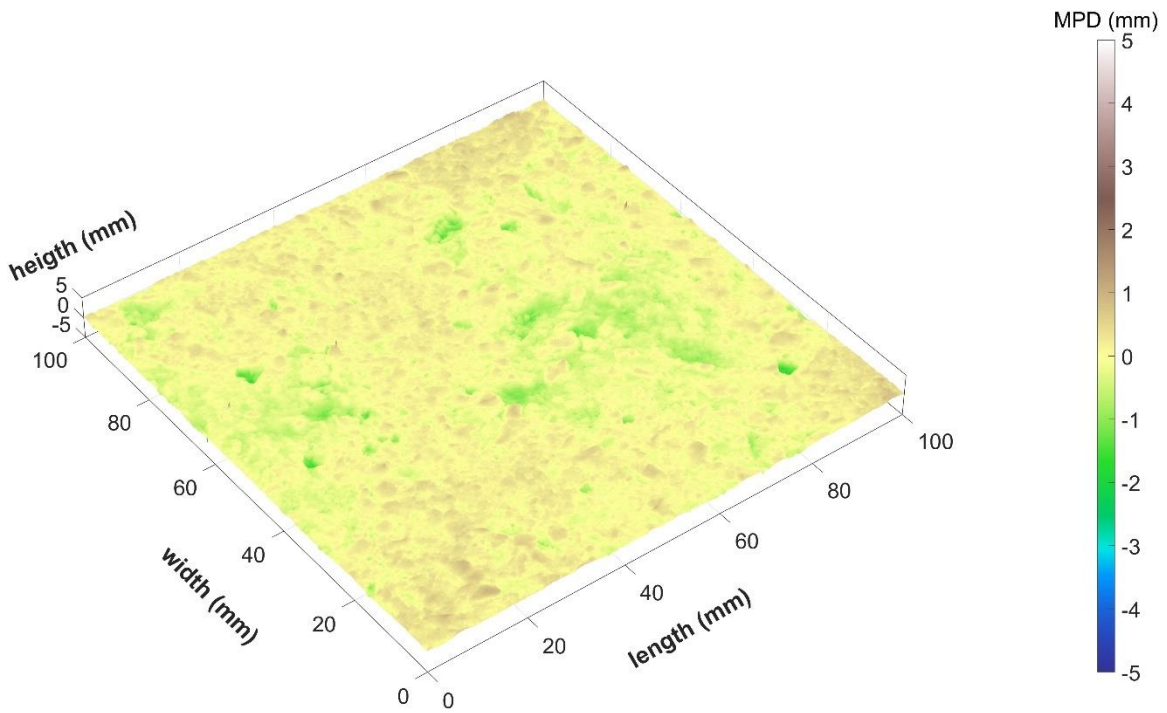


Figure D-22. Microsurfacing surface scan 2.

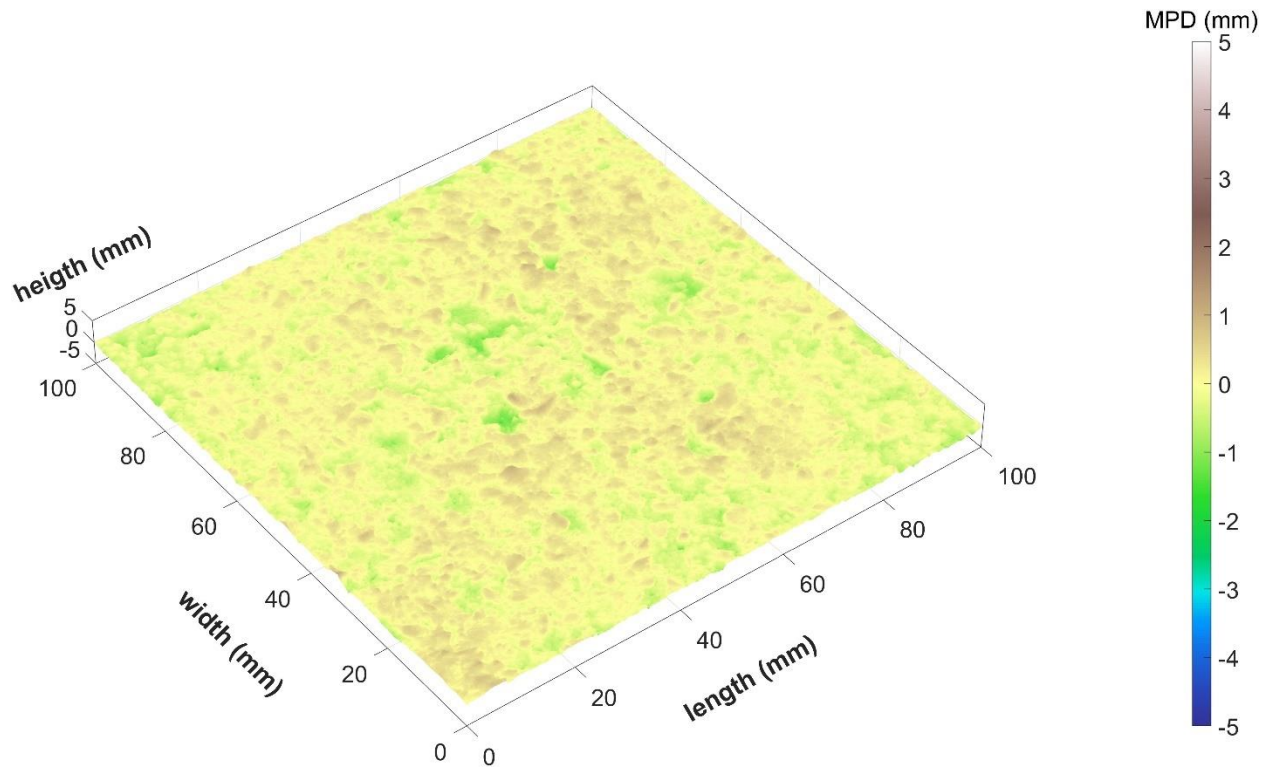


Figure D-23. Microsurfacing surface scan 3.

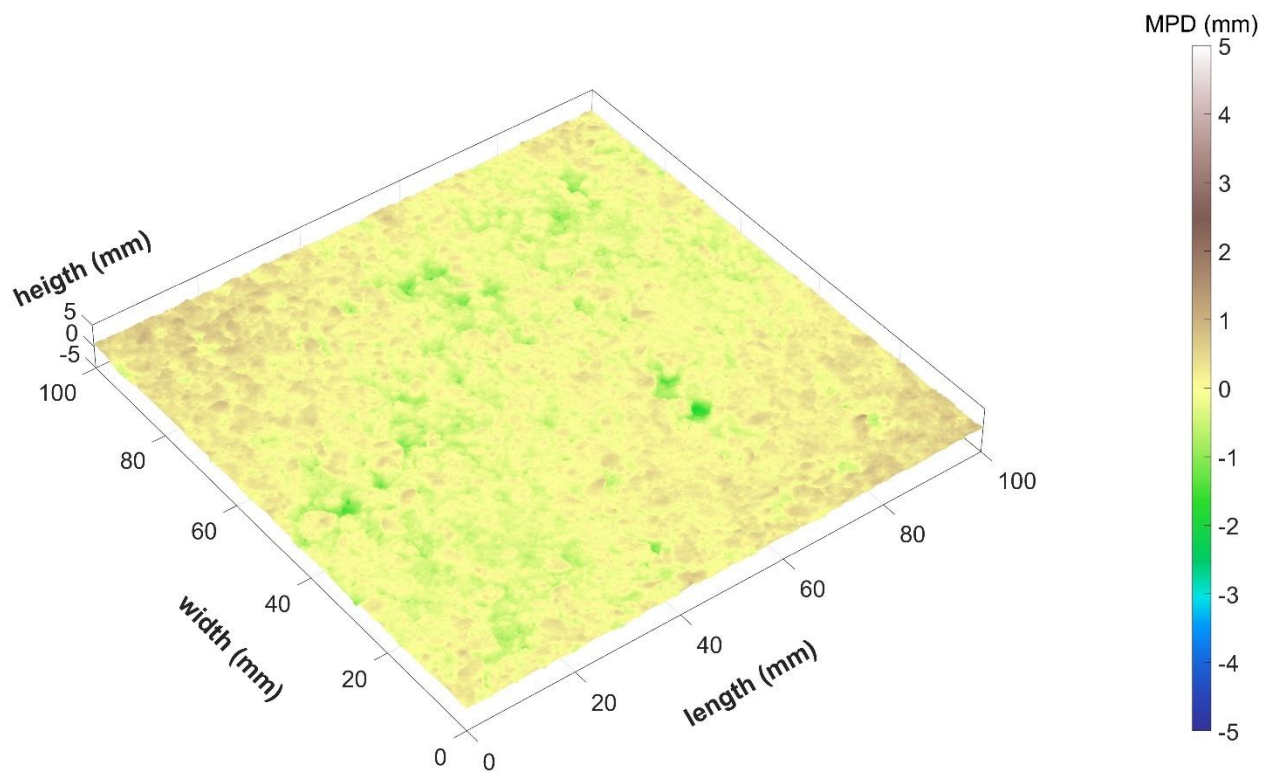


Figure D-24. Microsurfacing surface scan 4.

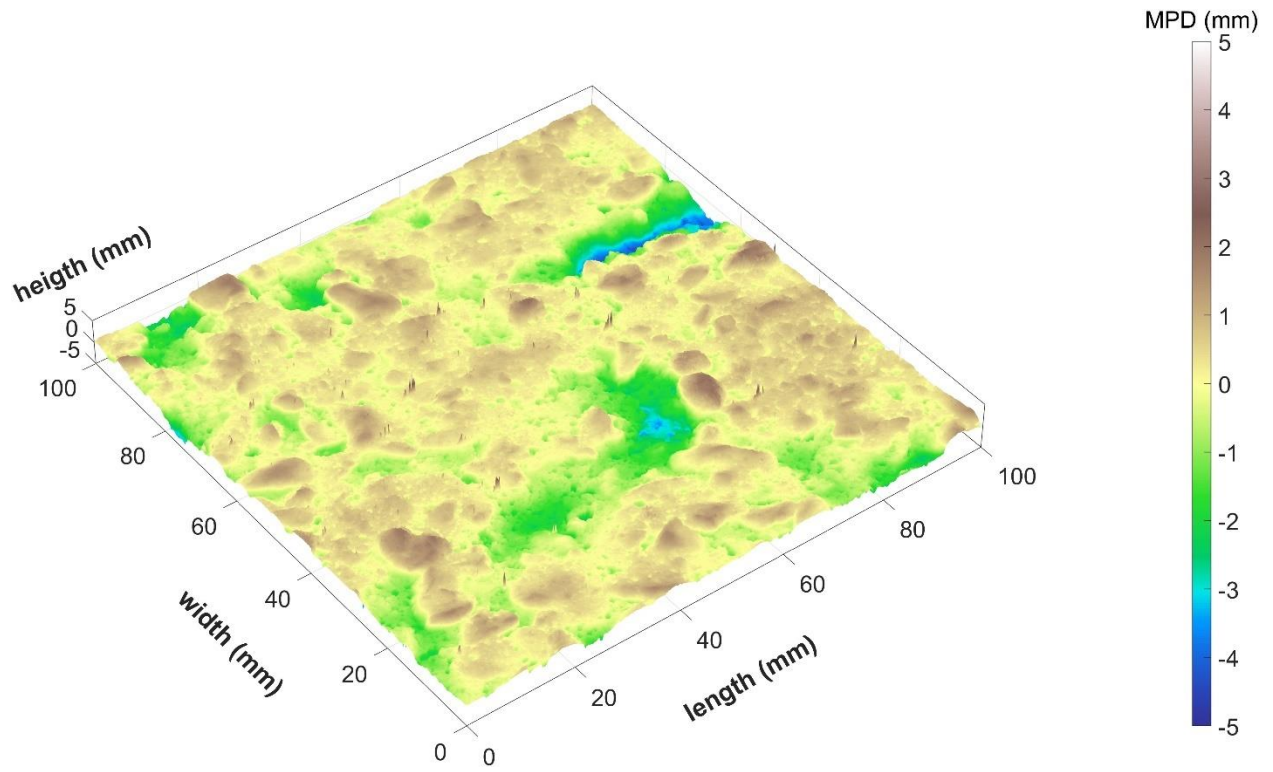


Figure D-25. Microsurfacing surface scan 5.

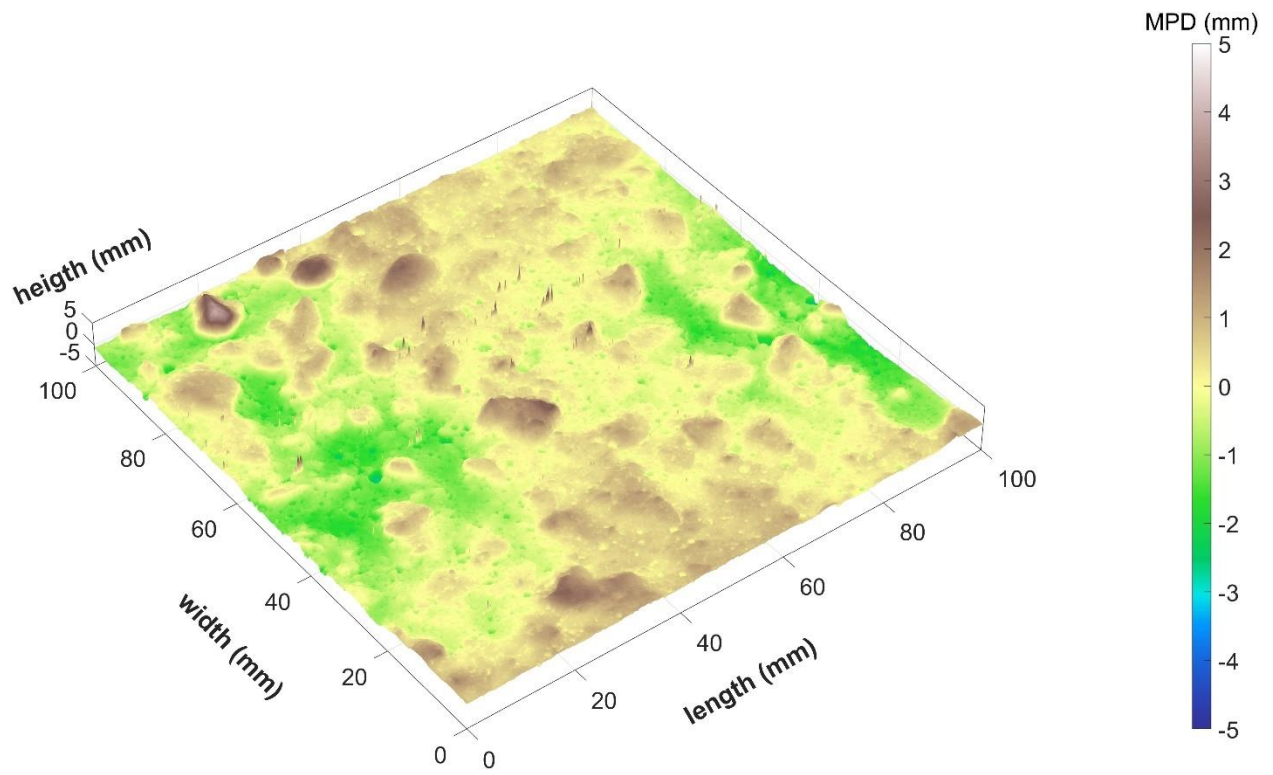


Figure D-26. Microsurfacing surface scan 6.

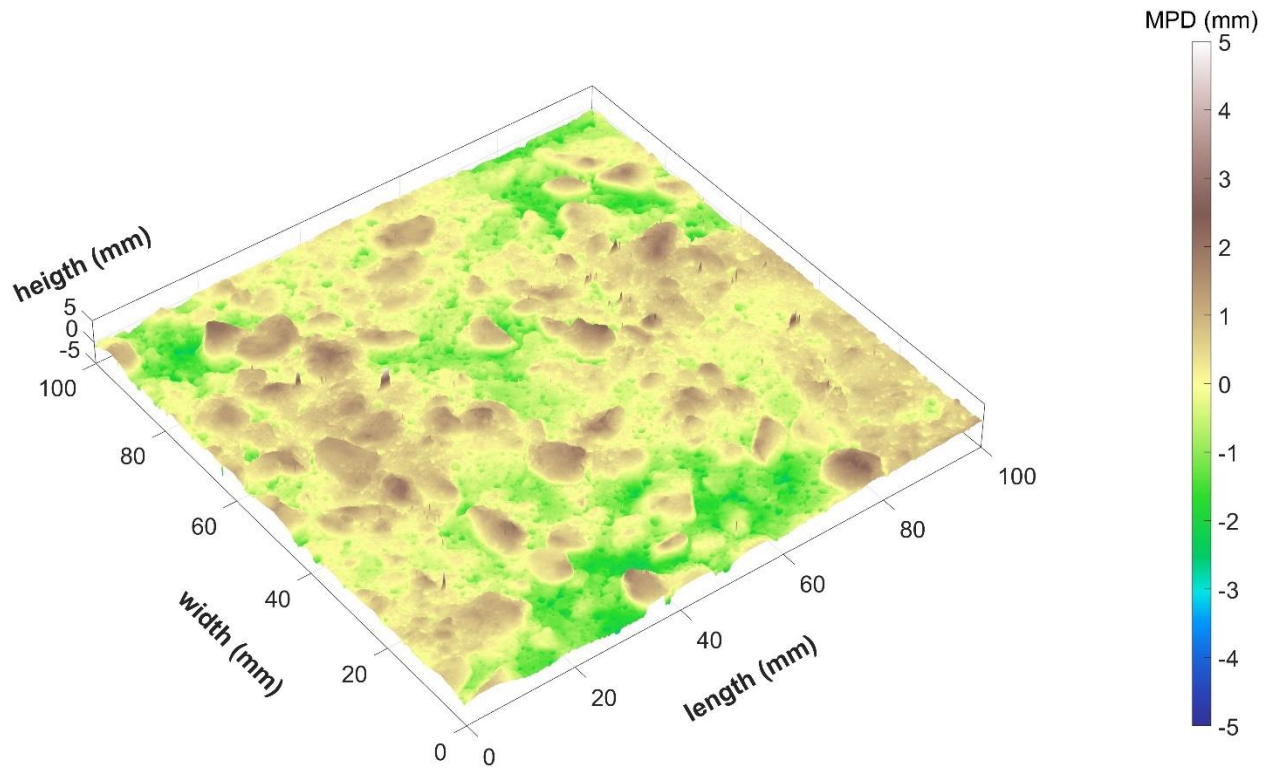


Figure D-27. Microsurfacing surface scan 7.

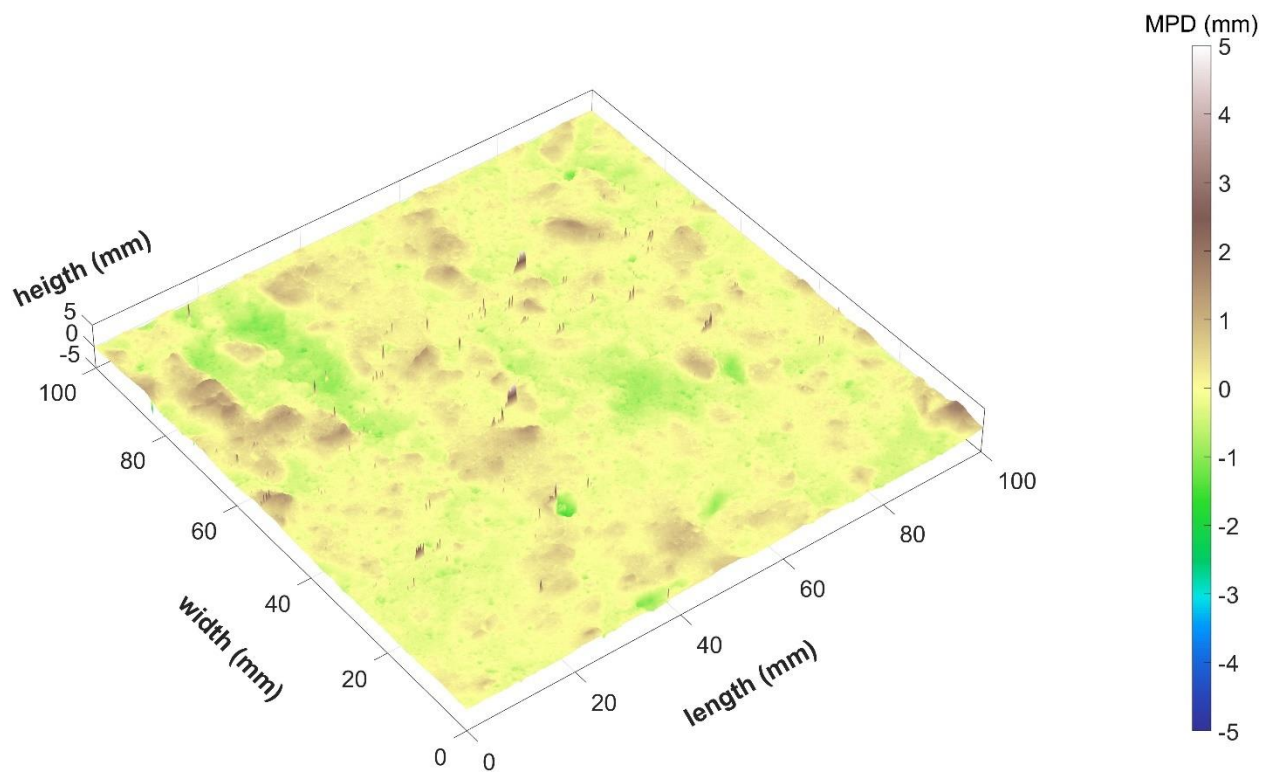


Figure D-28. Microsurfacing surface scan 8.

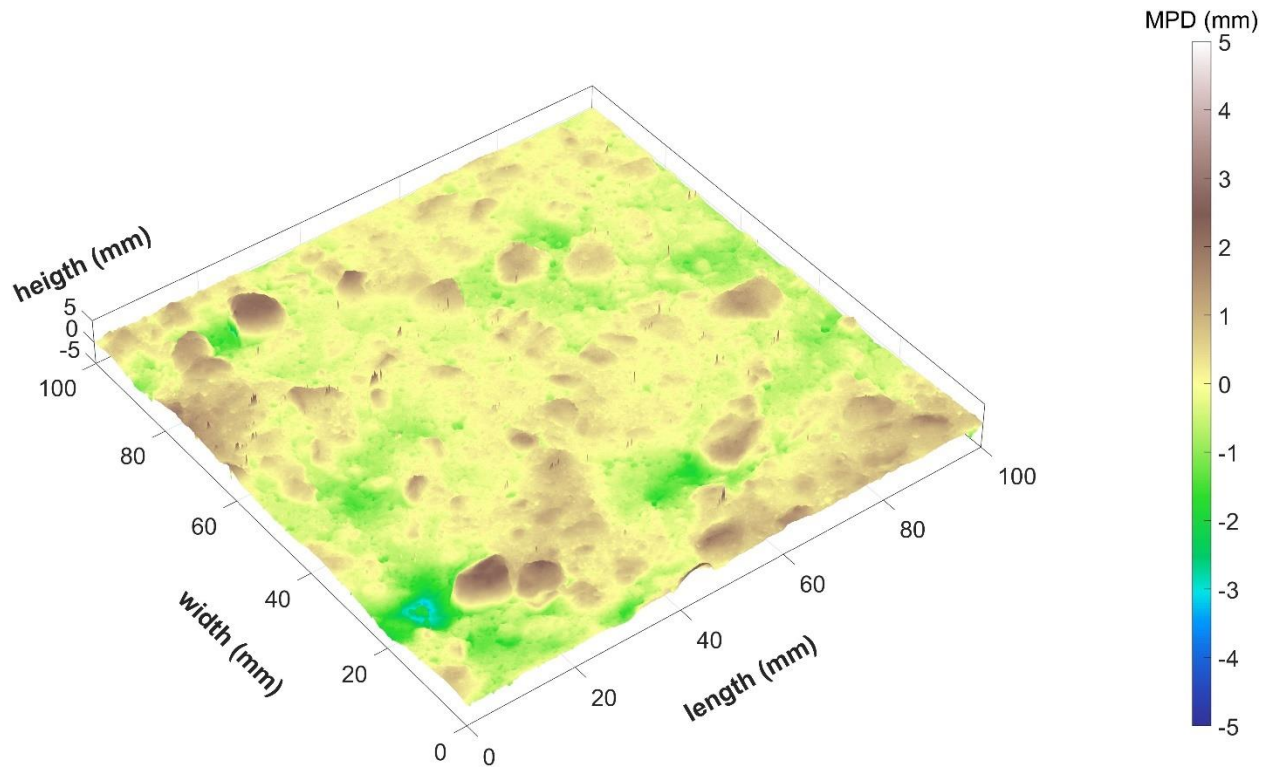


Figure D-29. Microsurfacing surface scan 9.

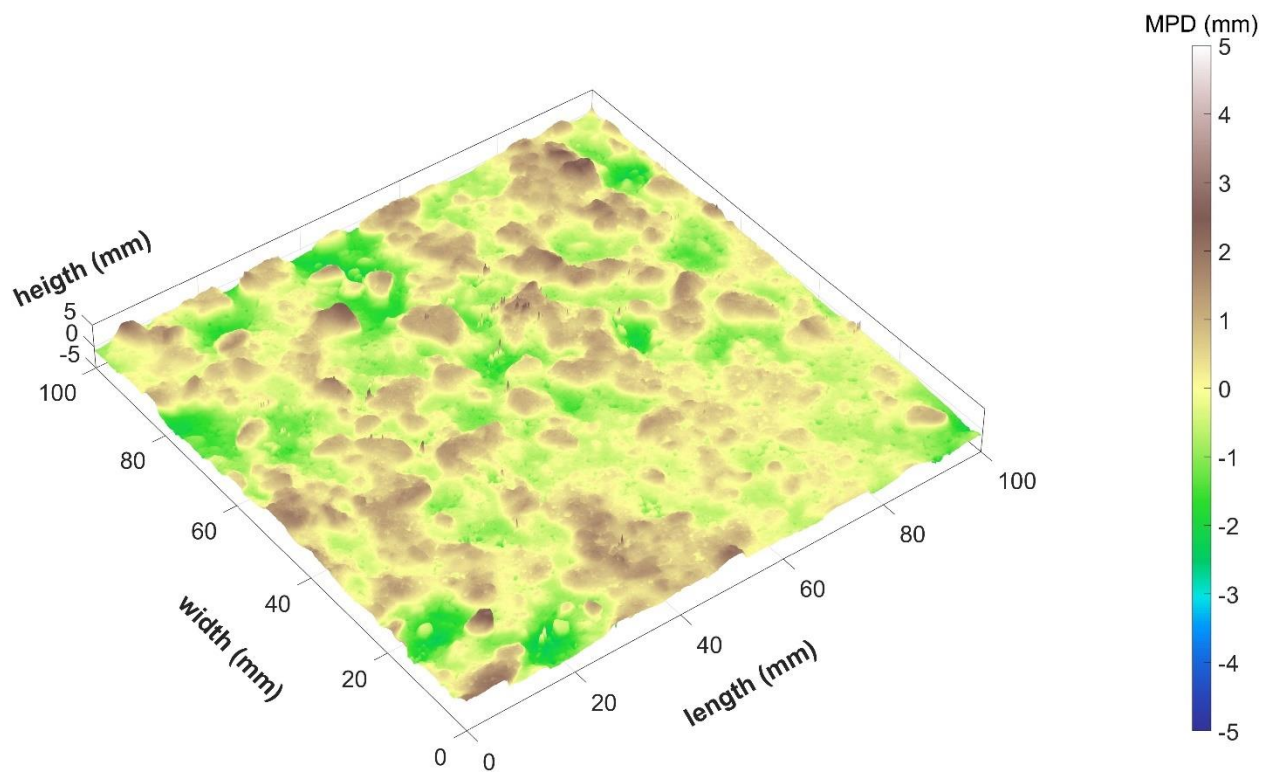


Figure D-30. Microsurfacing surface scan 10.

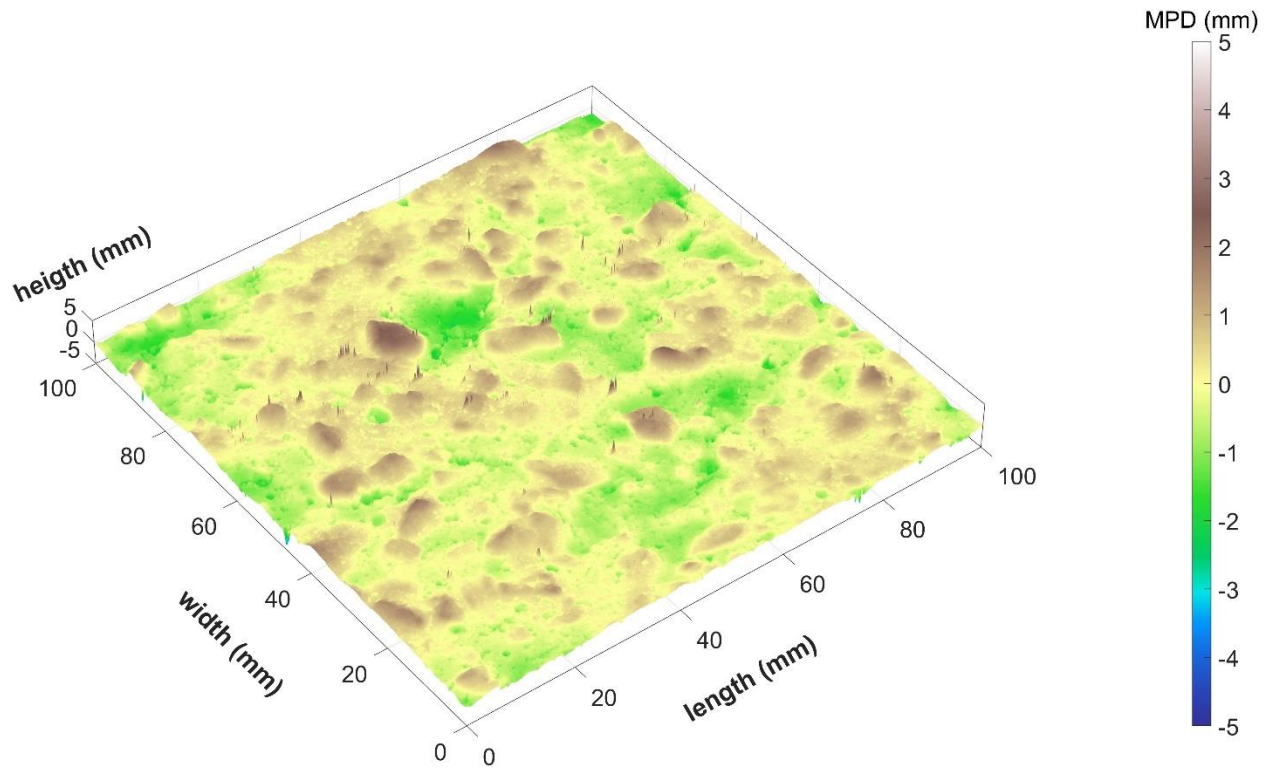


Figure D-31. Microsurfacing surface scan 11.

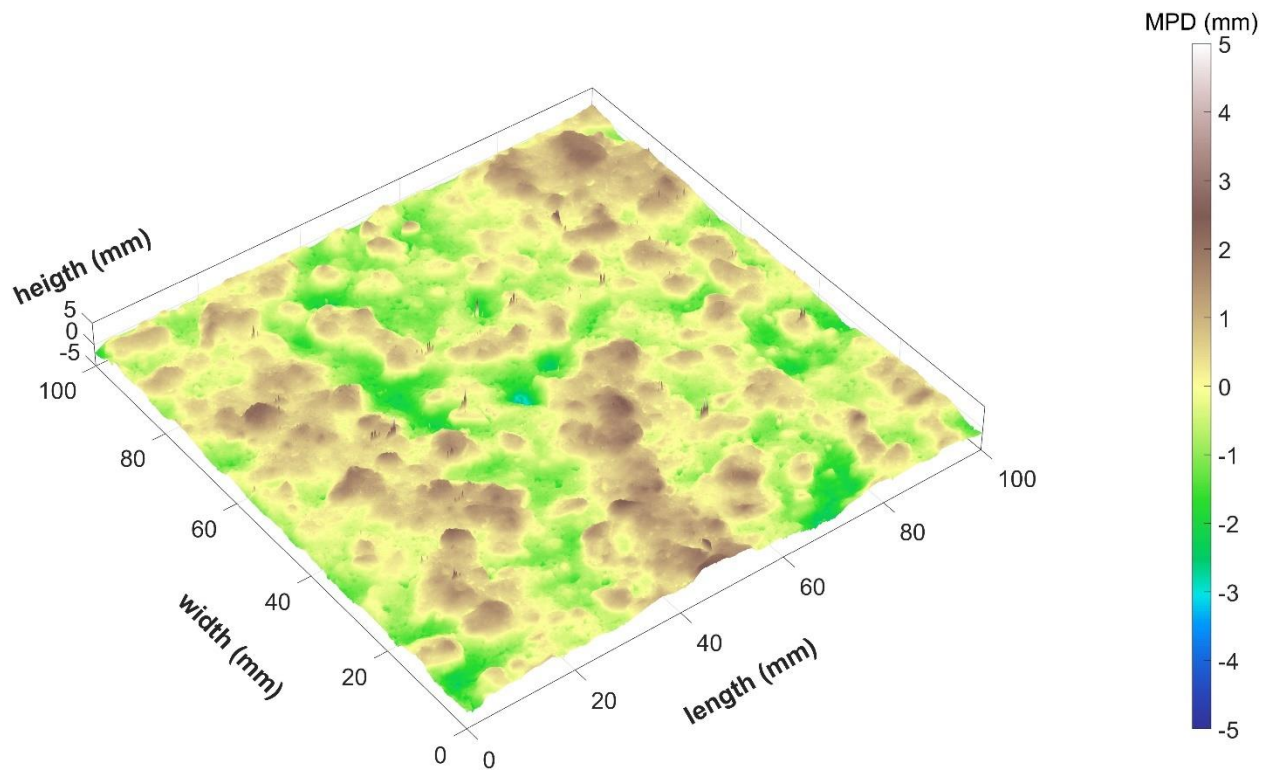


Figure D-32. Microsurfacing surface scan 12.

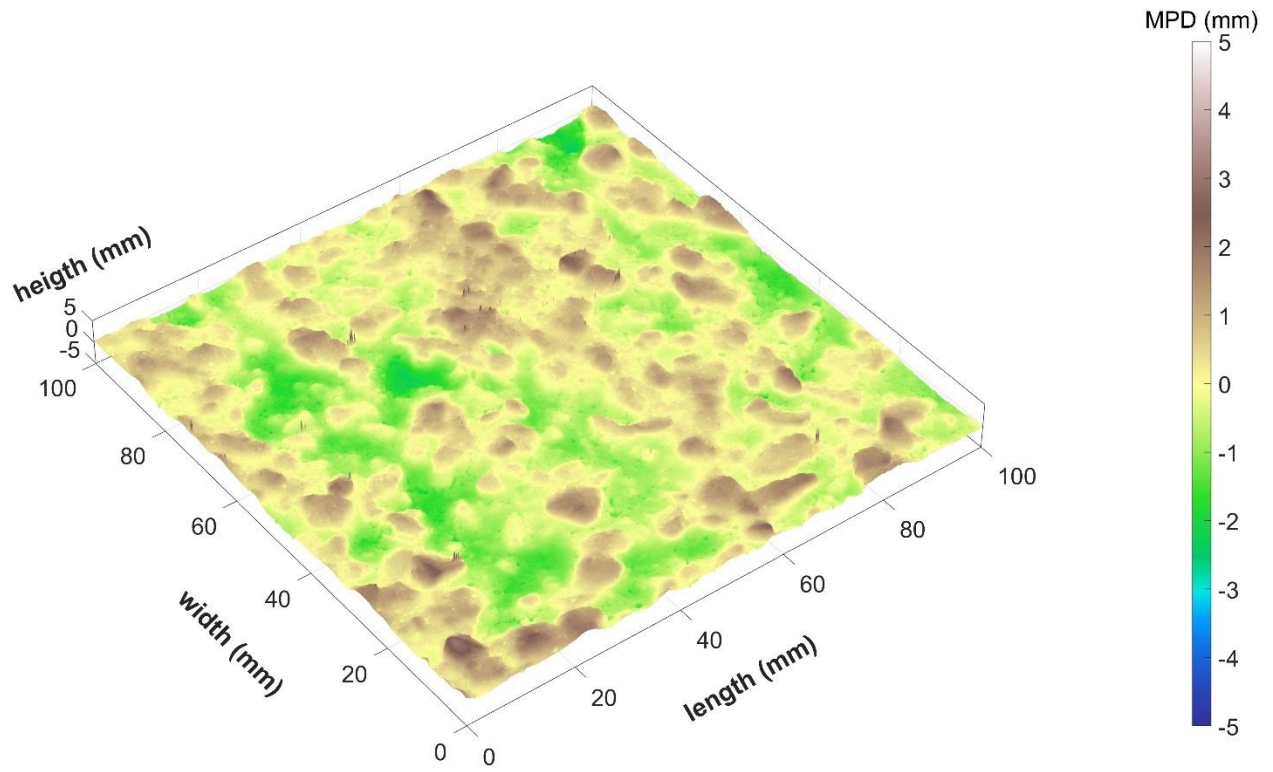


Figure D-33. Microsurfacing surface scan 13.

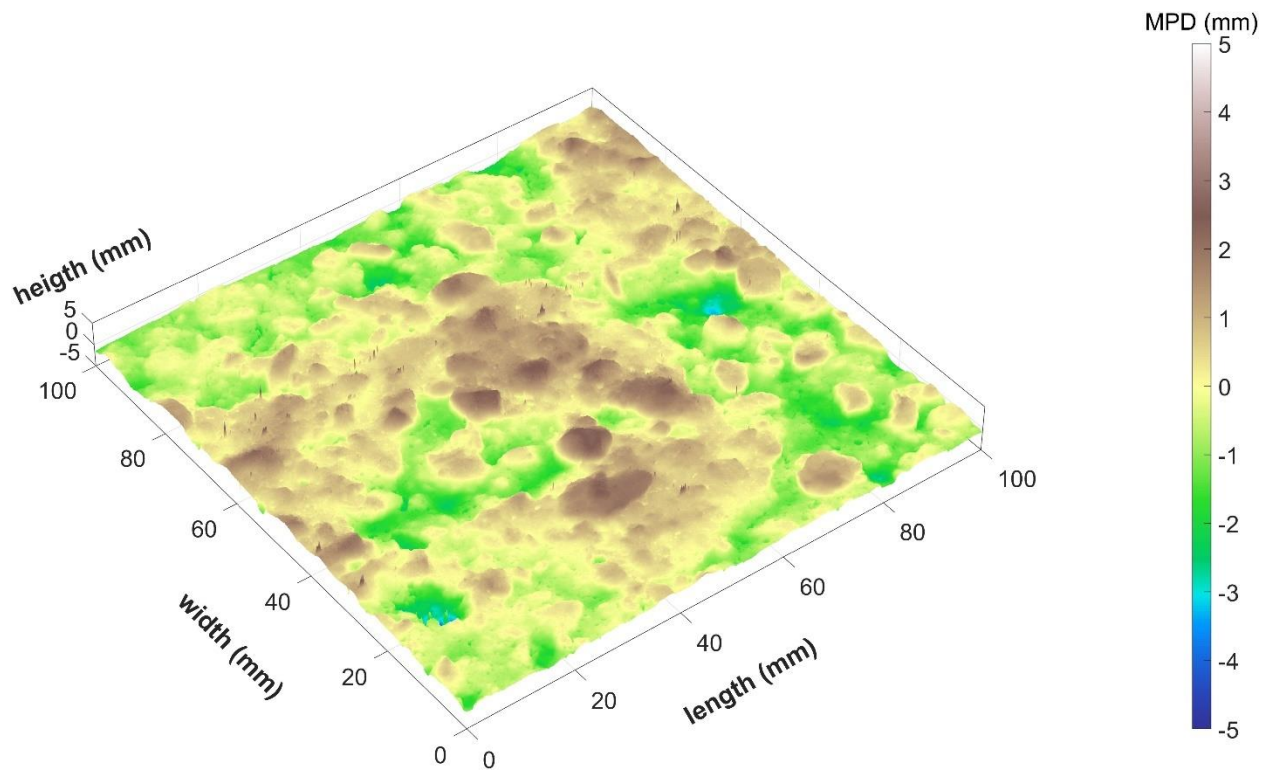


Figure D-34. Microsurfacing surface scan 14.

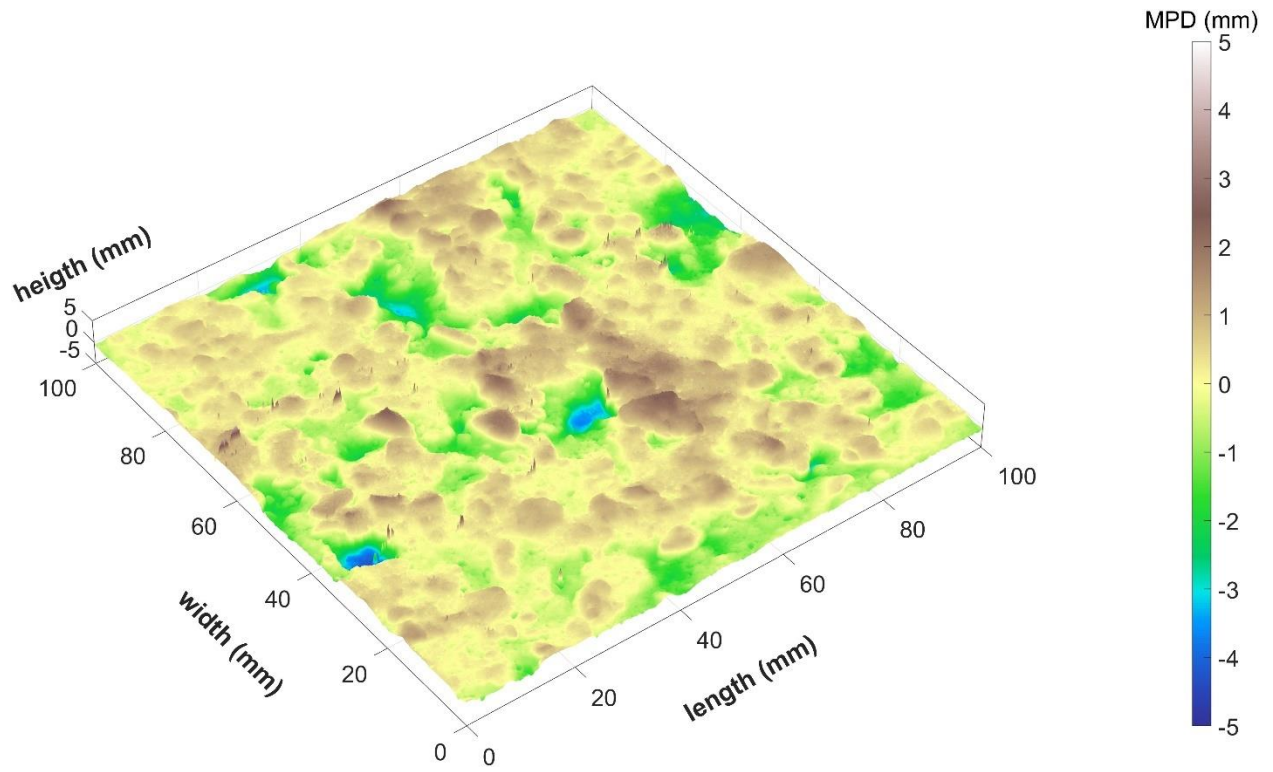


Figure D-35. Microsurfacing surface scan 15.

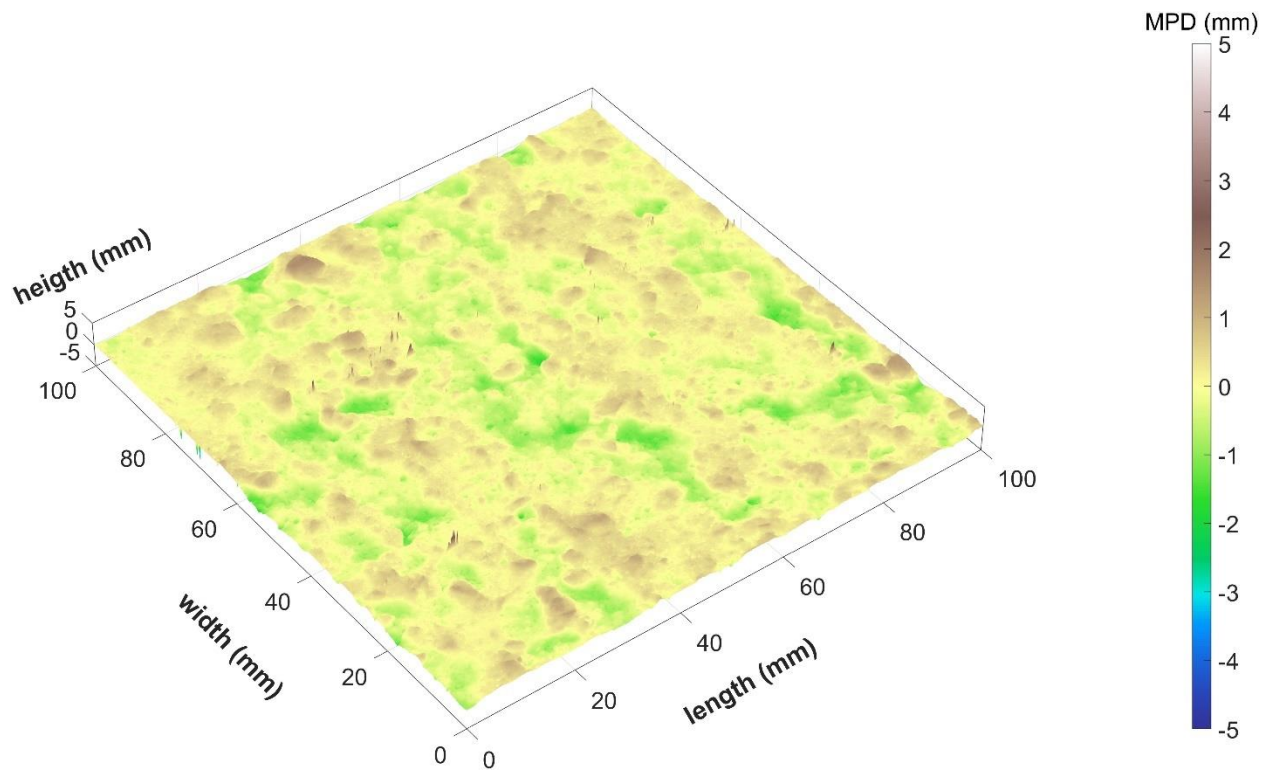


Figure D-36. Microsurfacing surface scan 16.

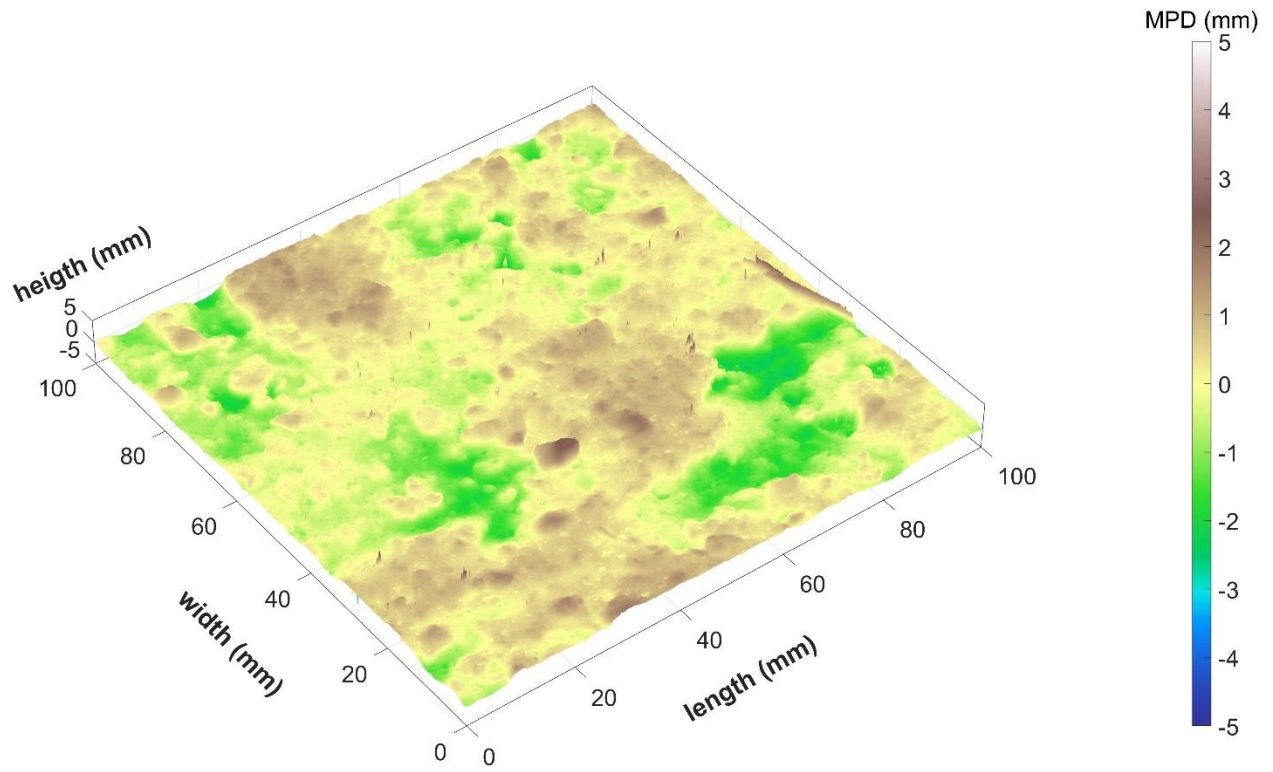


Figure D-37. Microsurfacing surface scan 17.

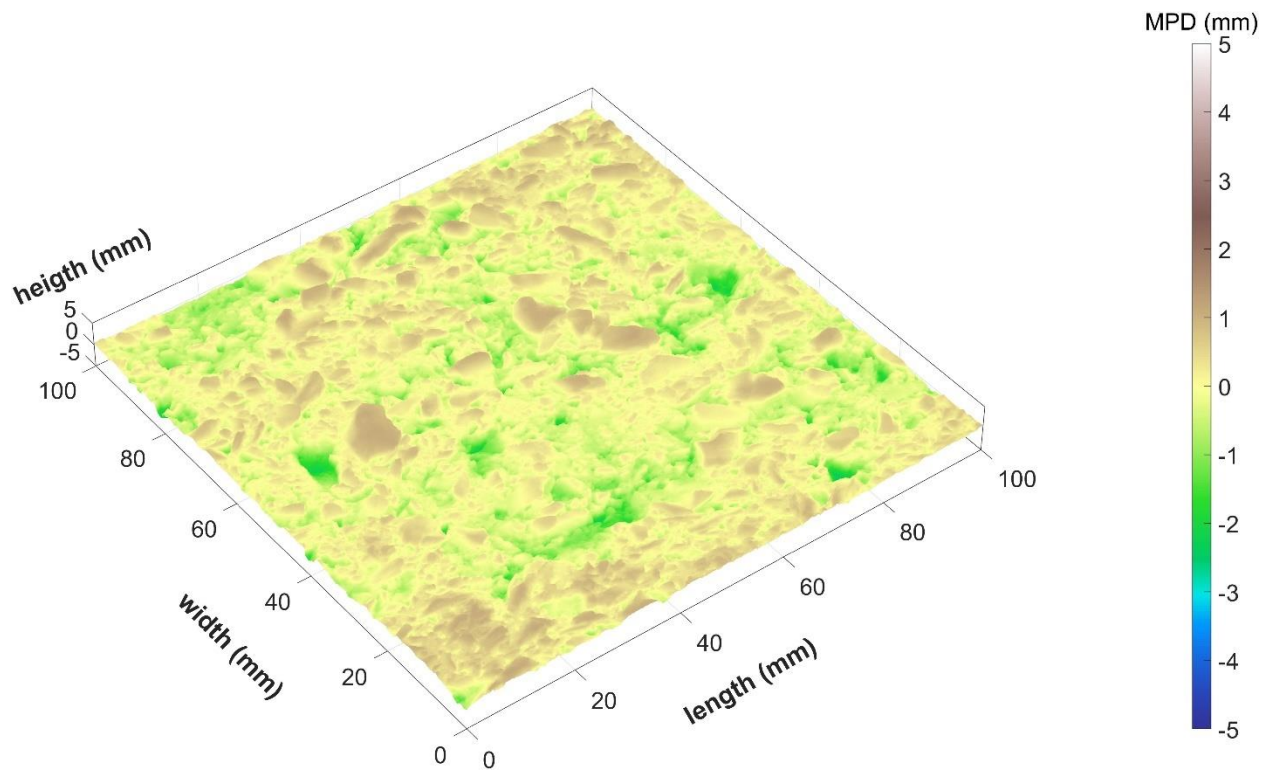


Figure D-38. Microsurfacing surface scan 18.

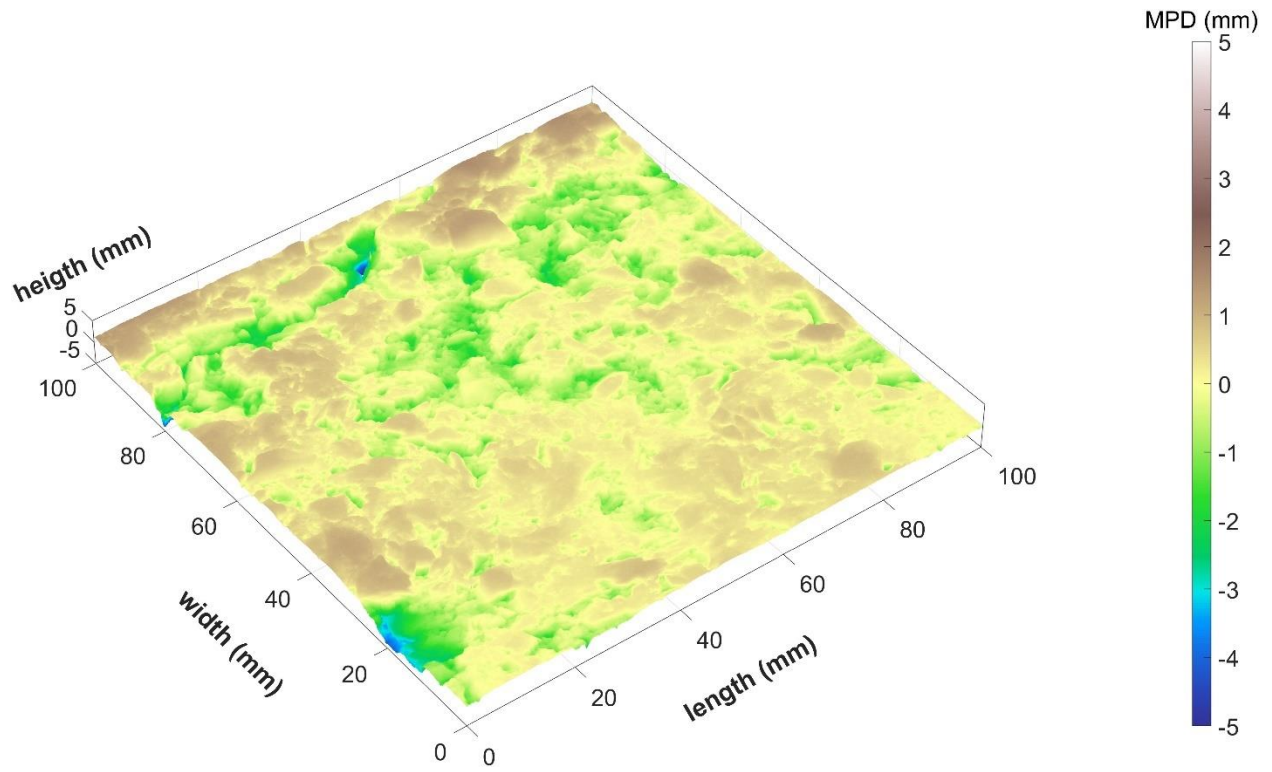


Figure D-39. Microsurfacing surface scan 19.

OGFC

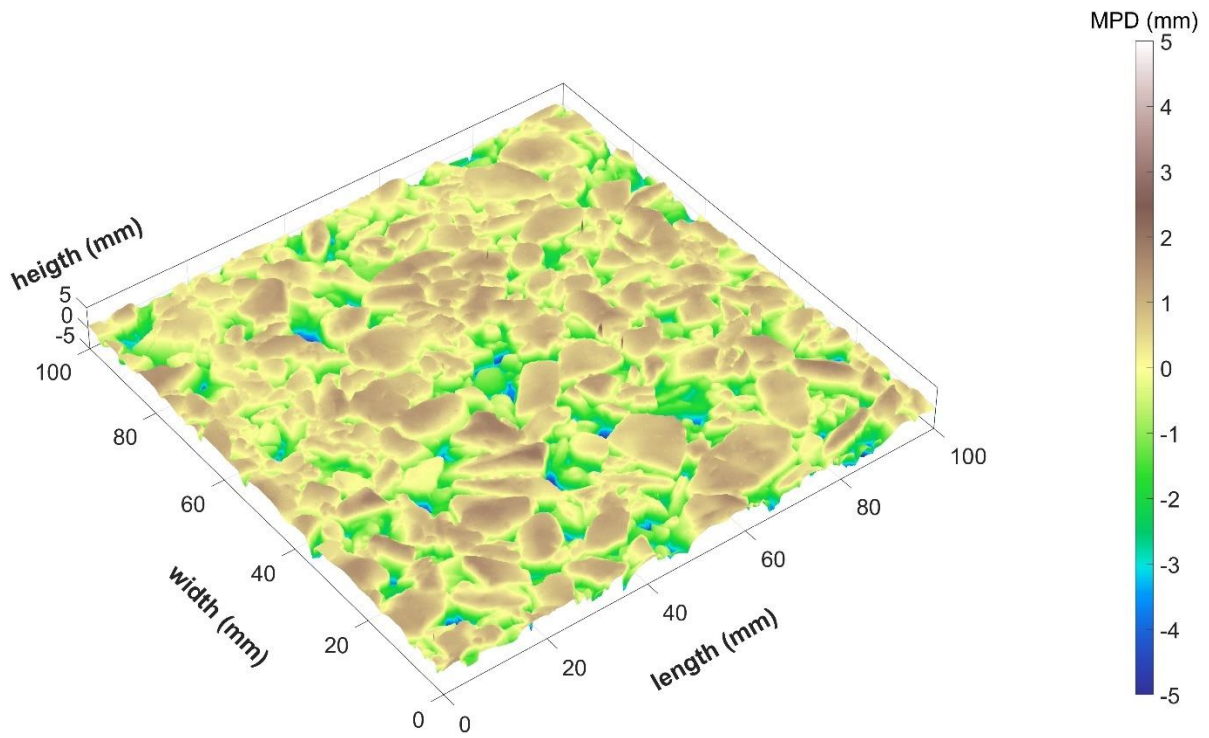


Figure D-40. OGFC surface scan 21.

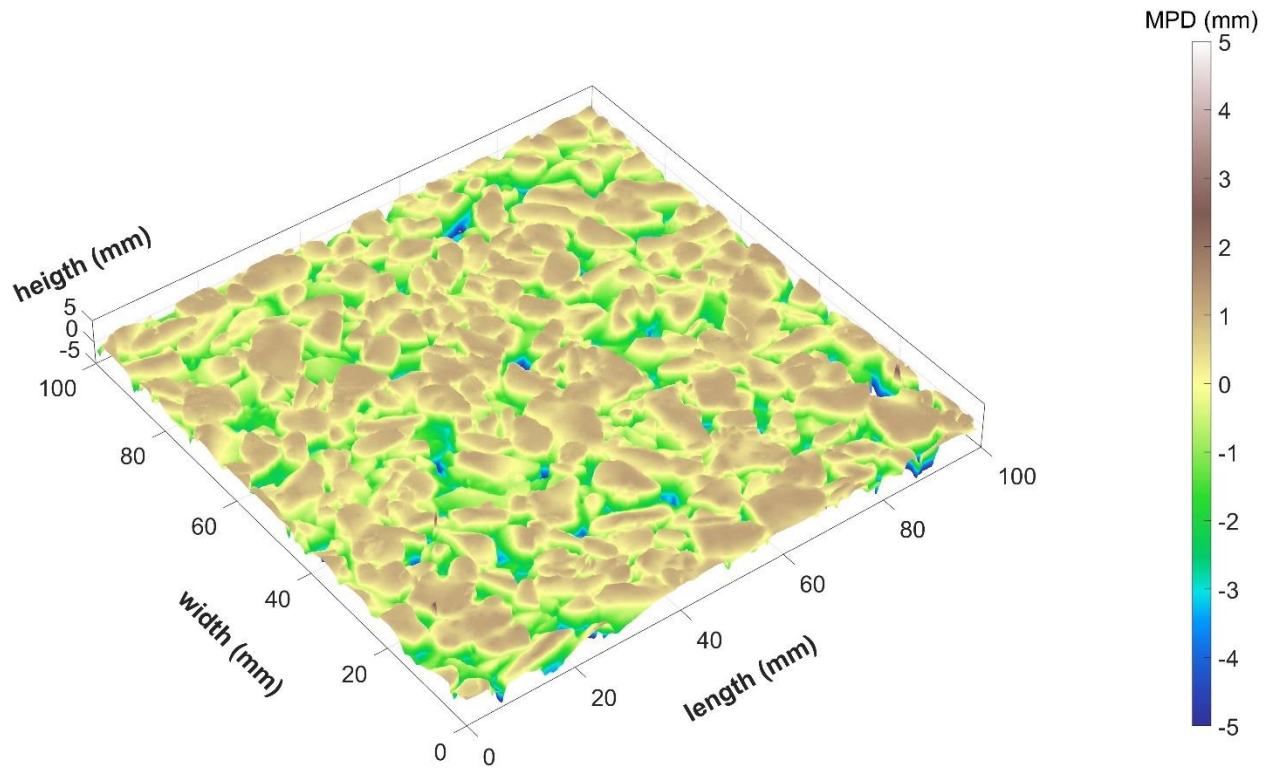


Figure D-41. OGFC surface scan 22.

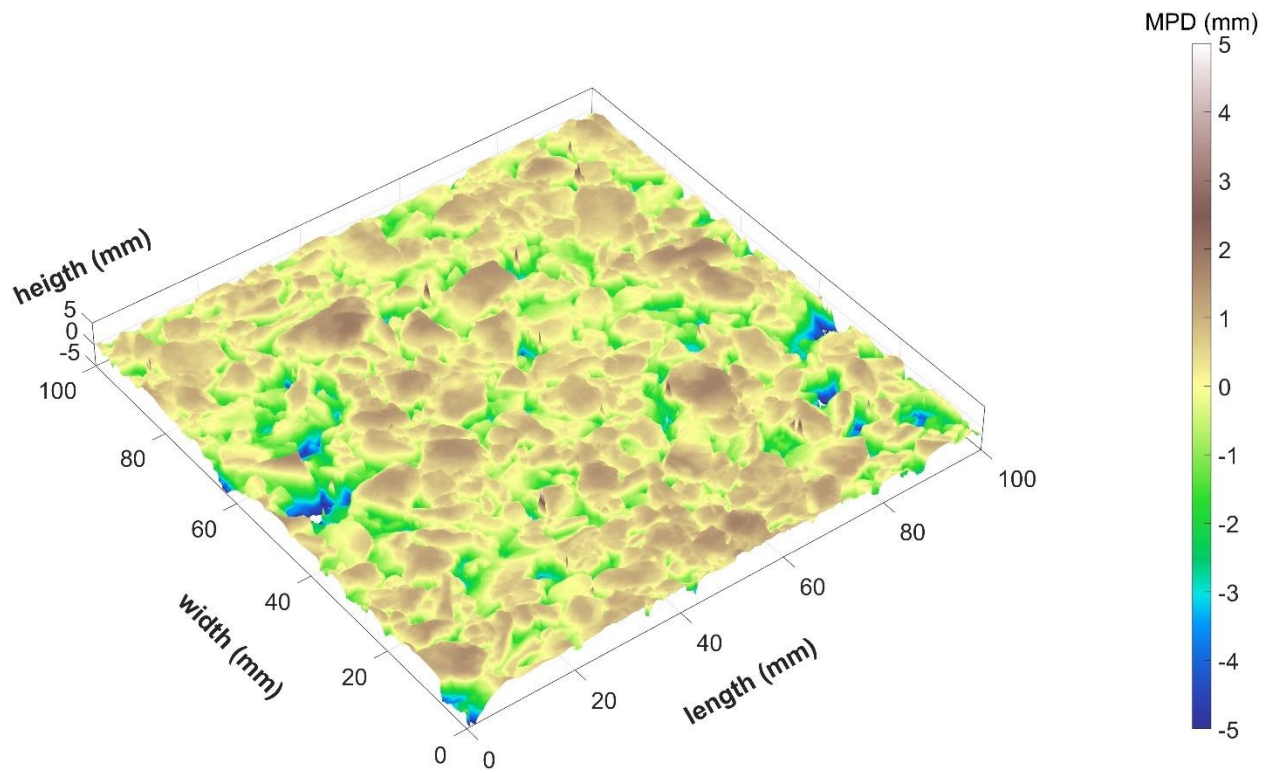


Figure D-42. OGFC surface scan 23.

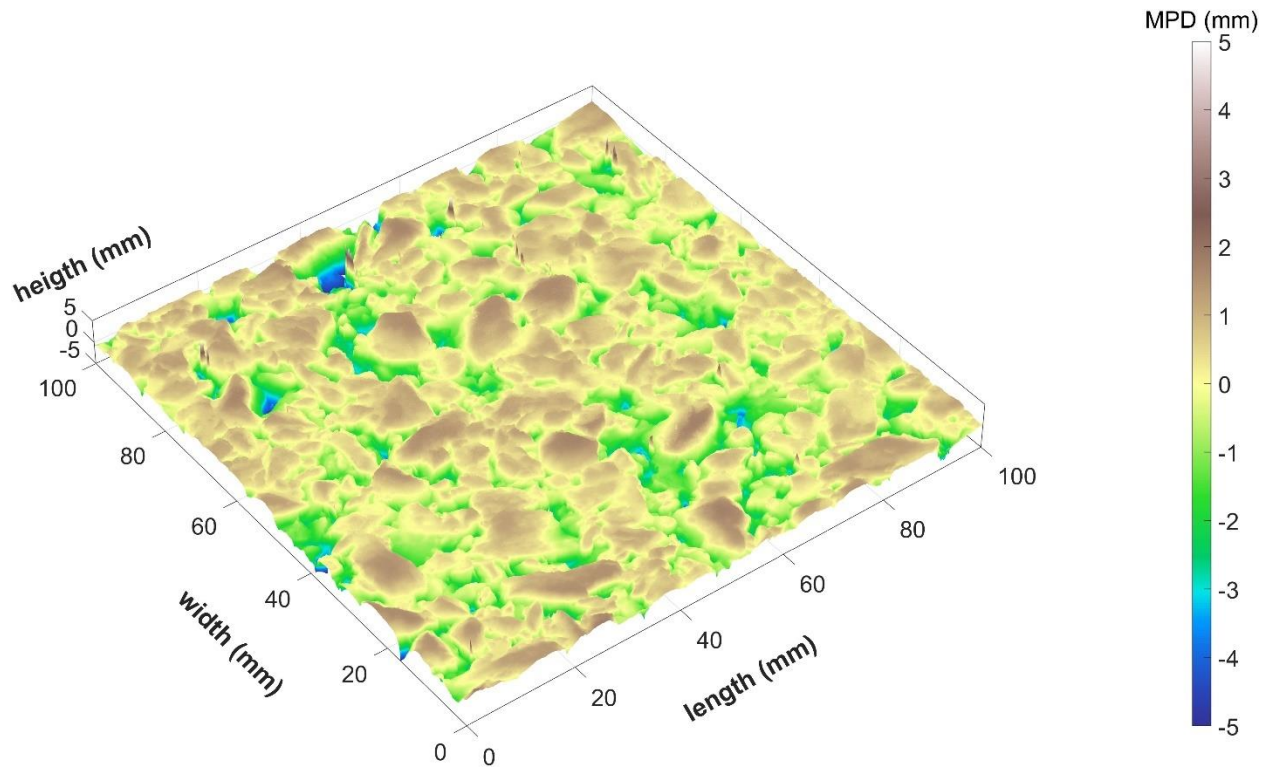


Figure D-43. OGFC surface scan 24.

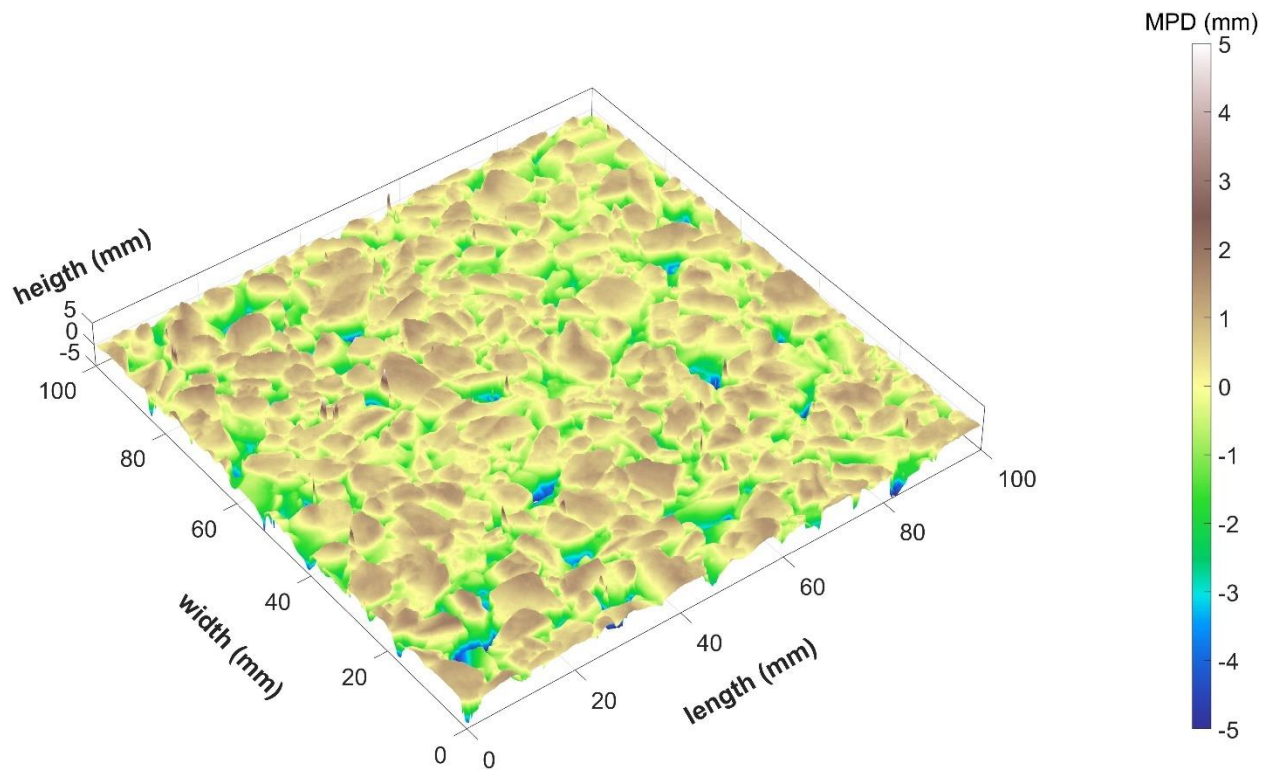


Figure D-44. OGFC surface scan 25.

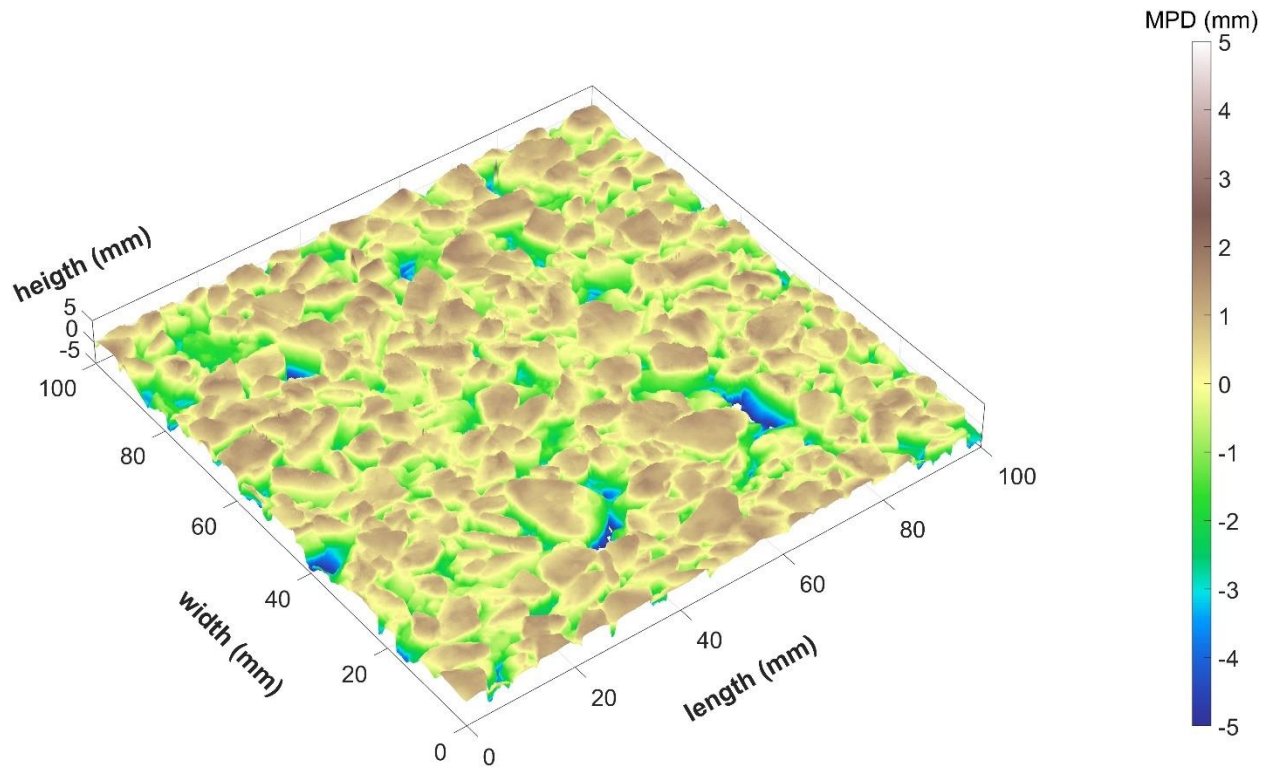


Figure D-45. OGFC surface scan 26.

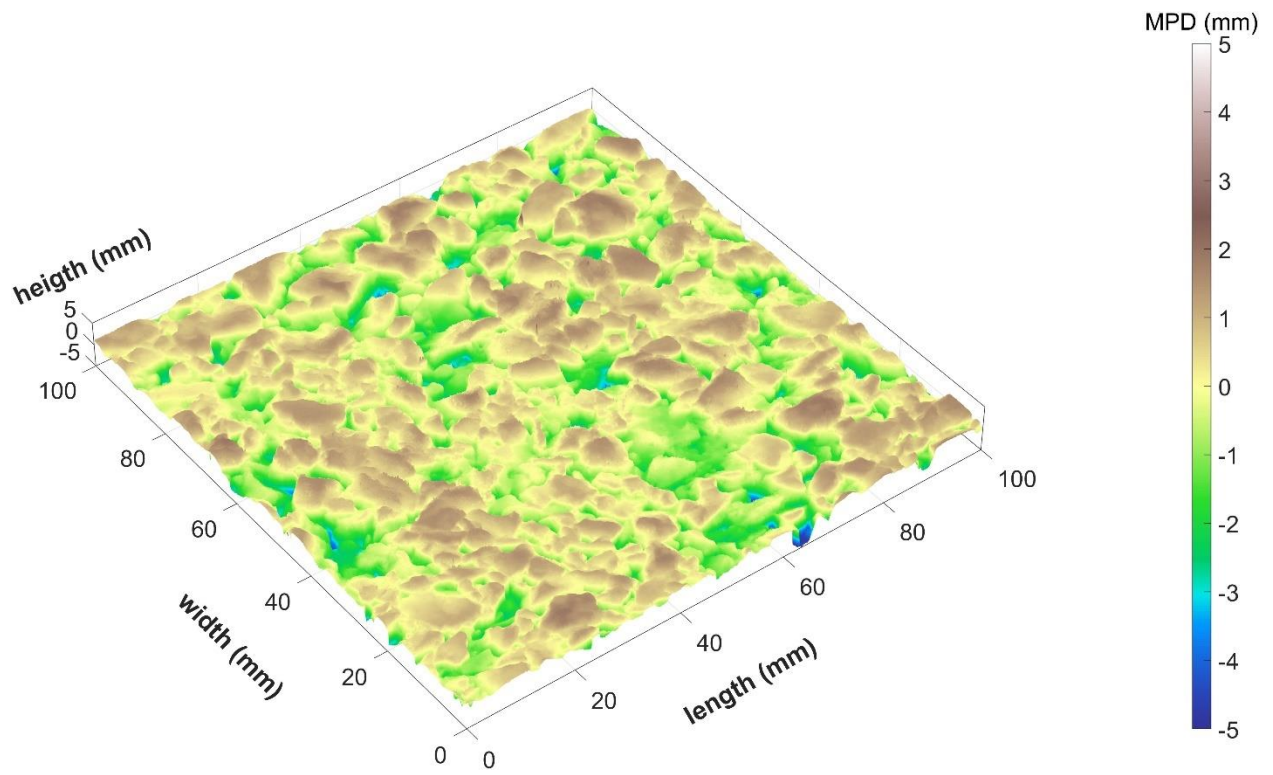


Figure D-46. OGFC surface scan 27.

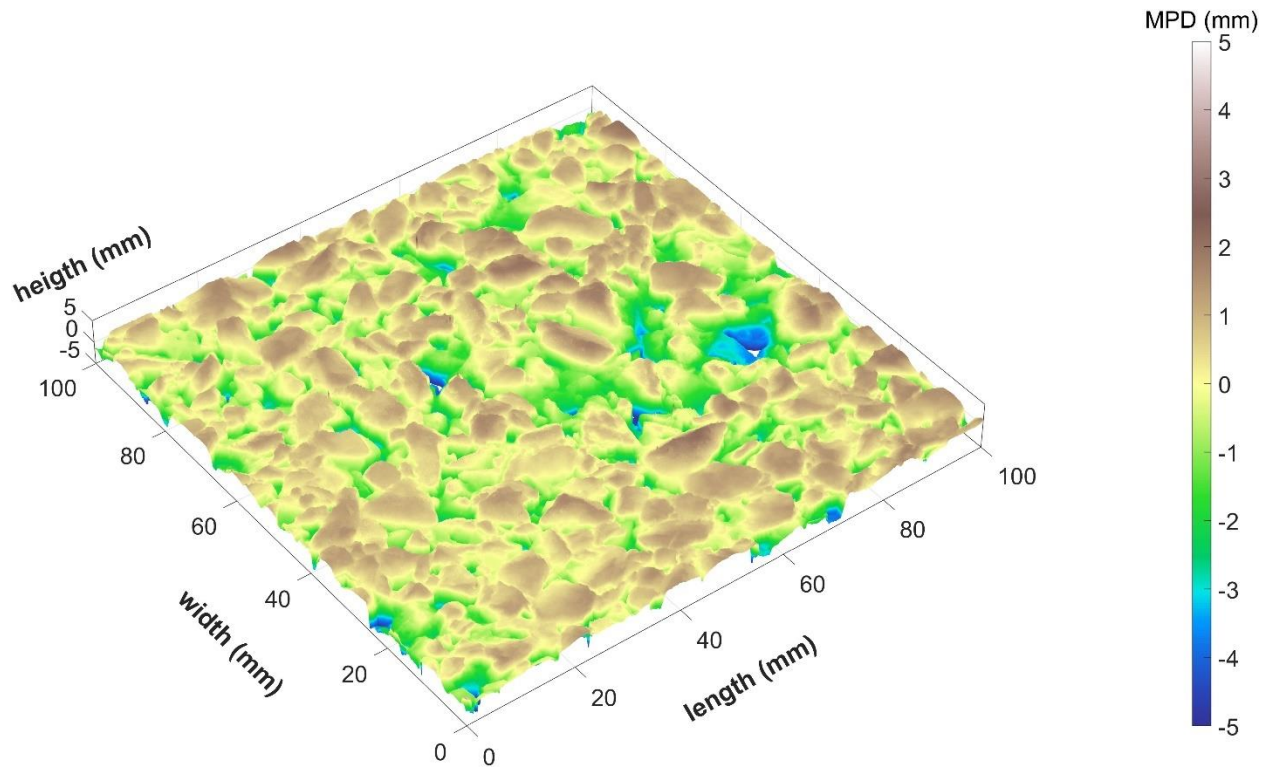


Figure D-47. OGFC surface scan 28.

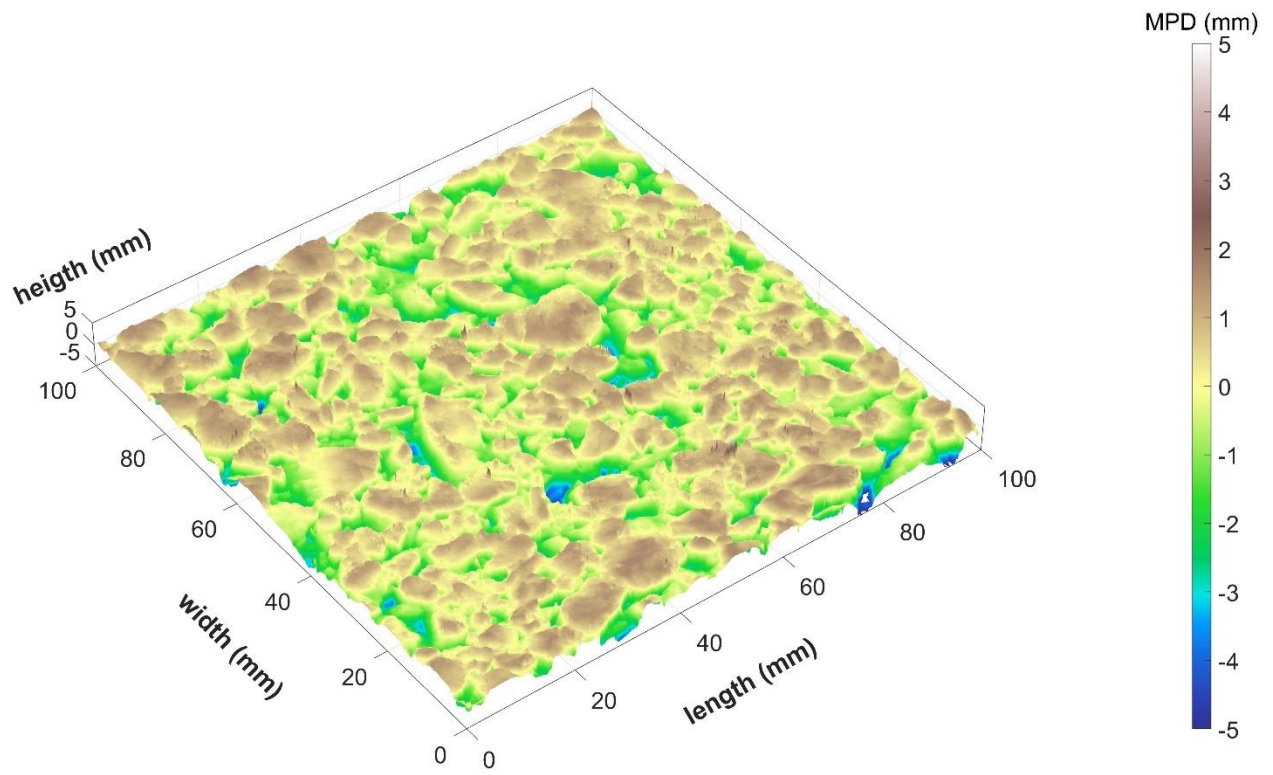


Figure D-48. OGFC surface scan 29.

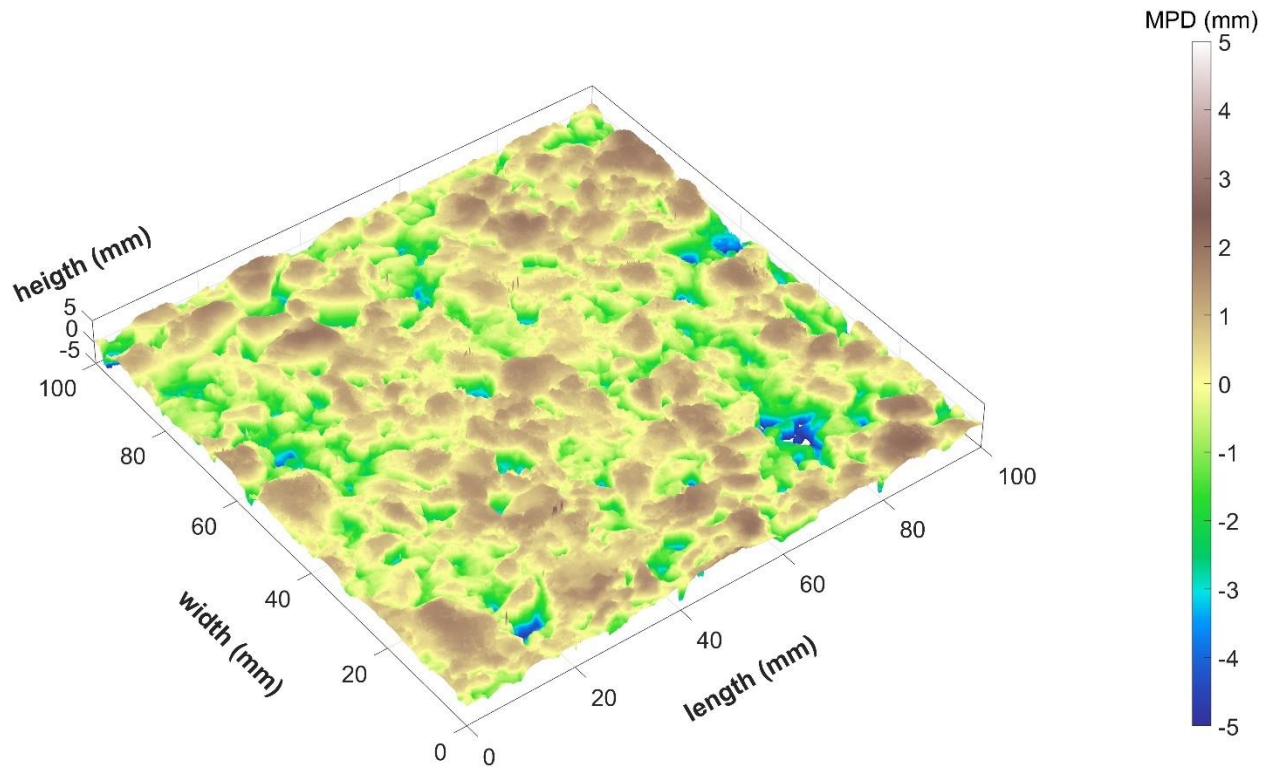


Figure D-49. OGFC surface scan 30.

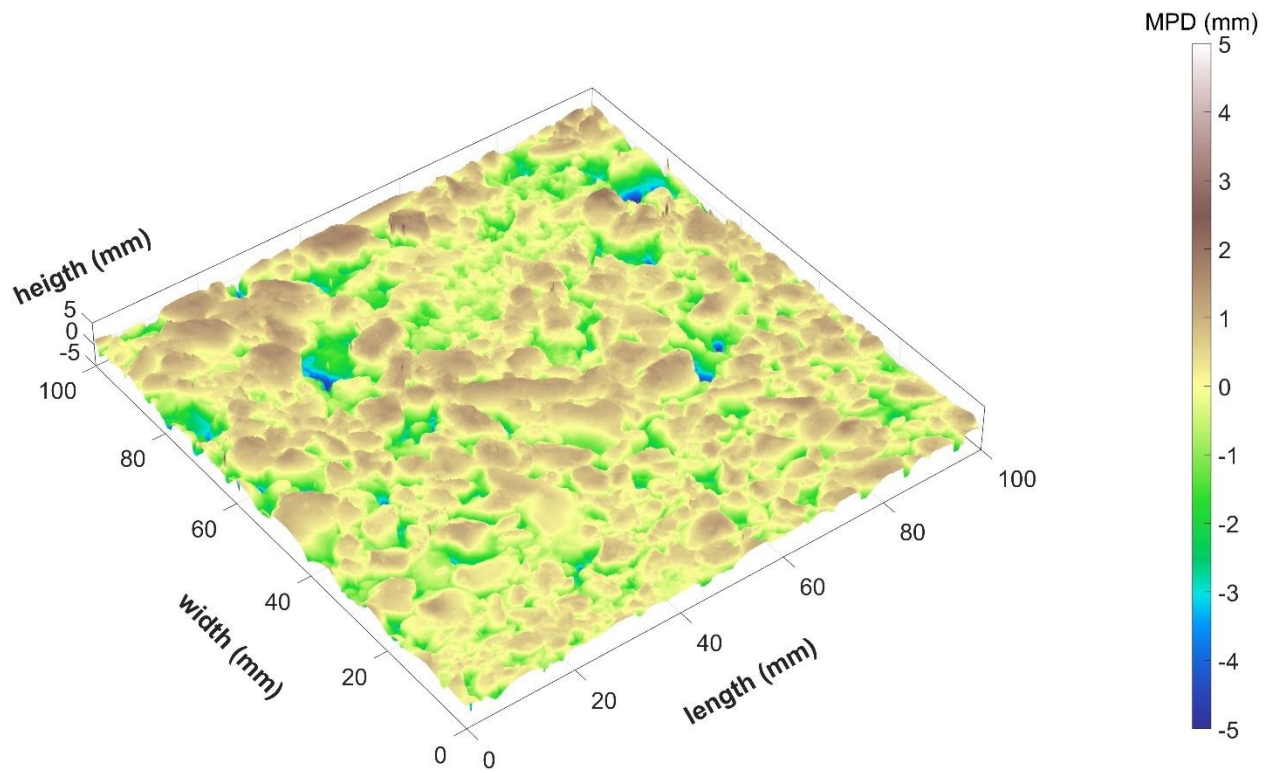


Figure D-50. OGFC surface scan 31.

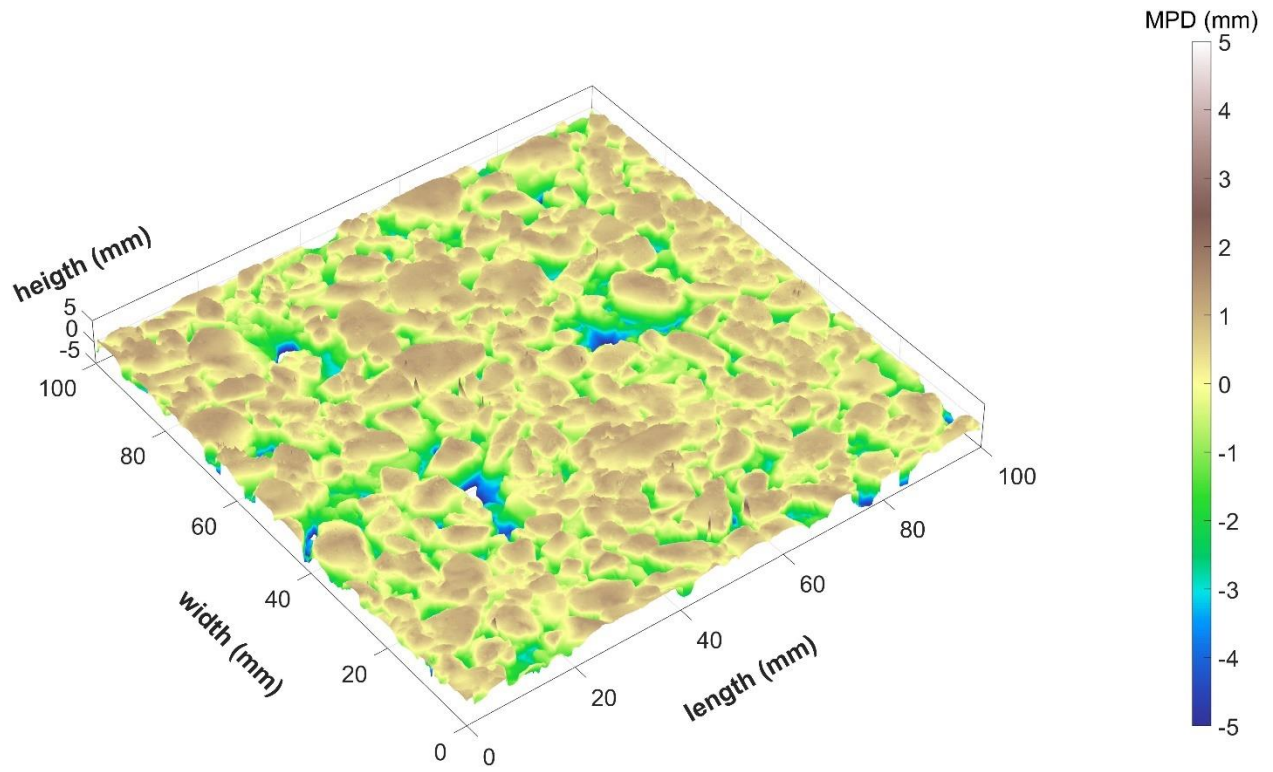


Figure D-51. OGFC surface scan 32.

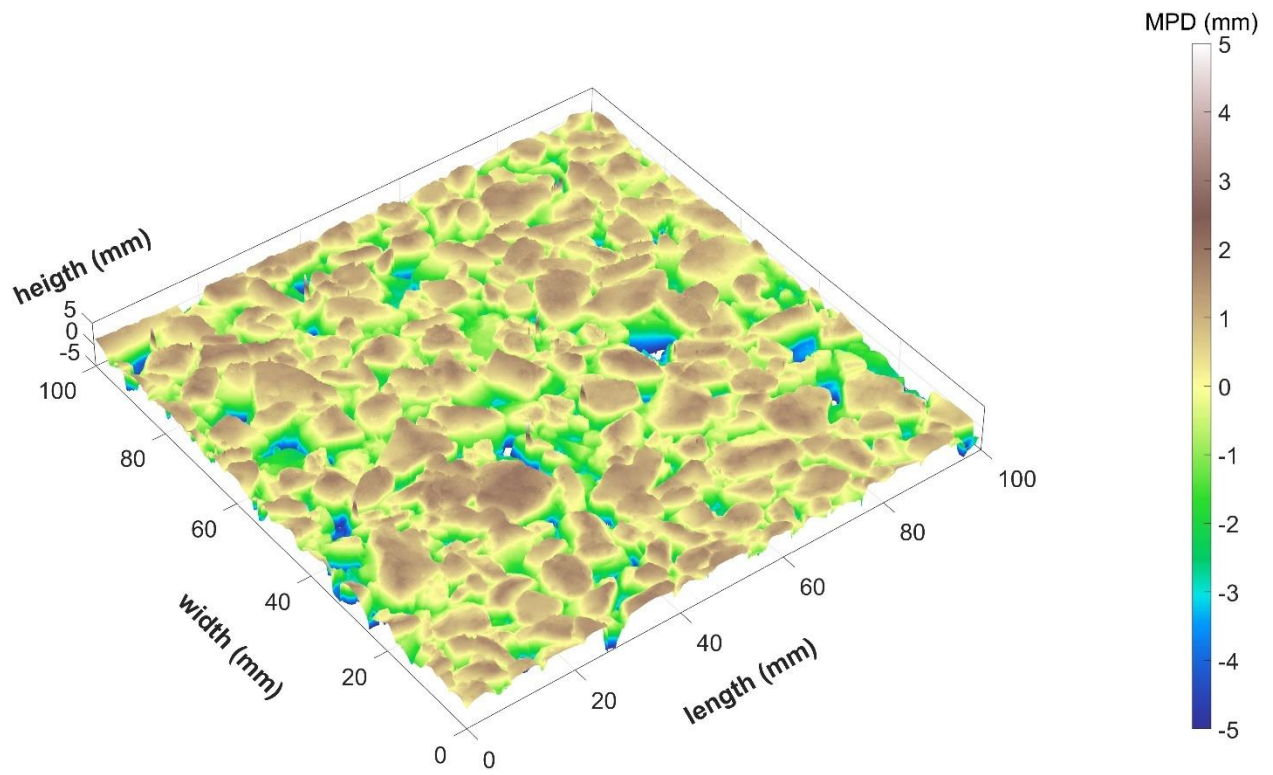


Figure D-52. OGFC surface scan 33.

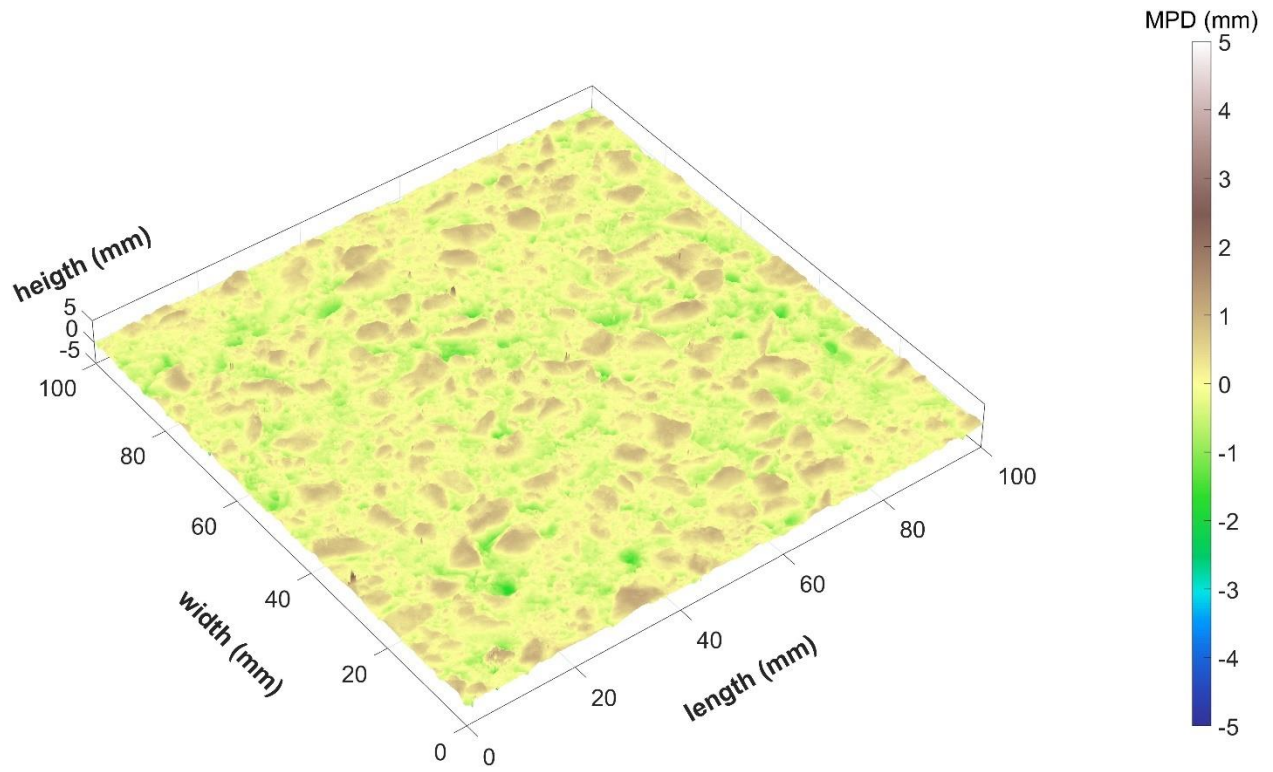


Figure D-53. OGFC surface scan 34.

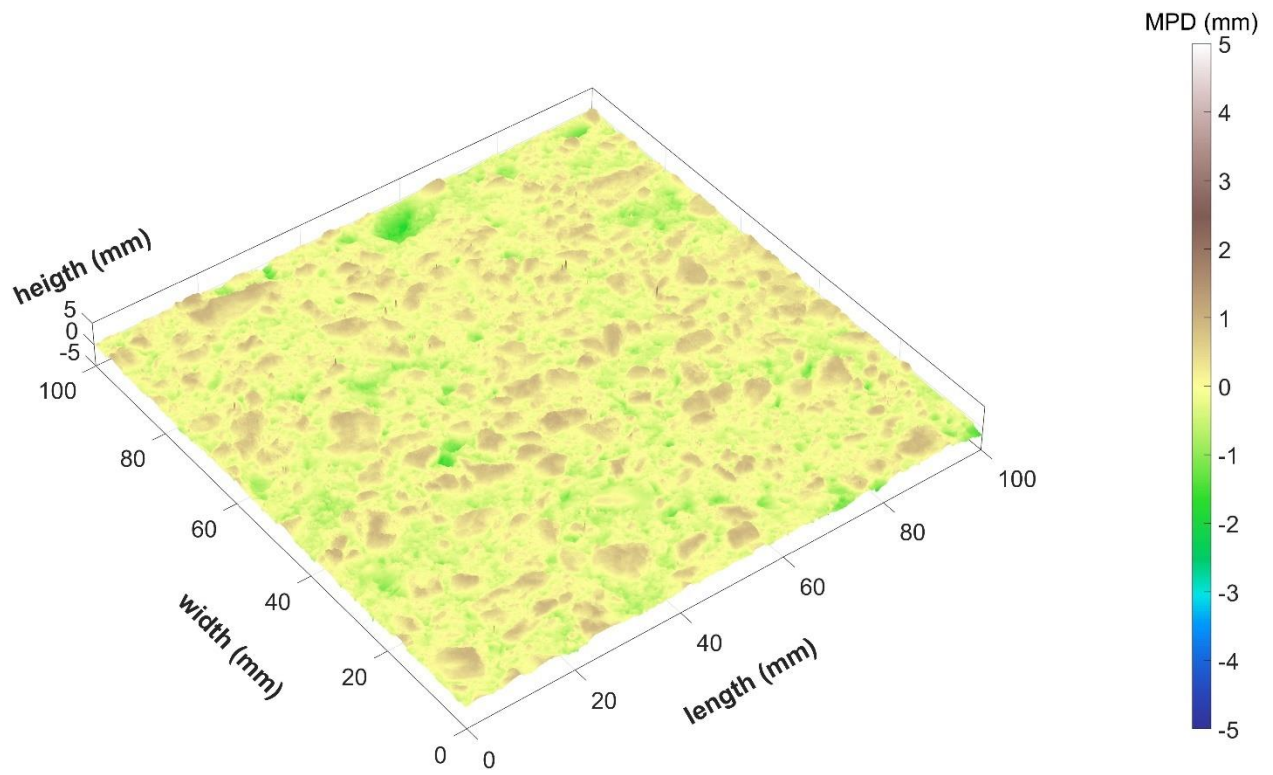


Figure D-54. OGFC surface scan 35.

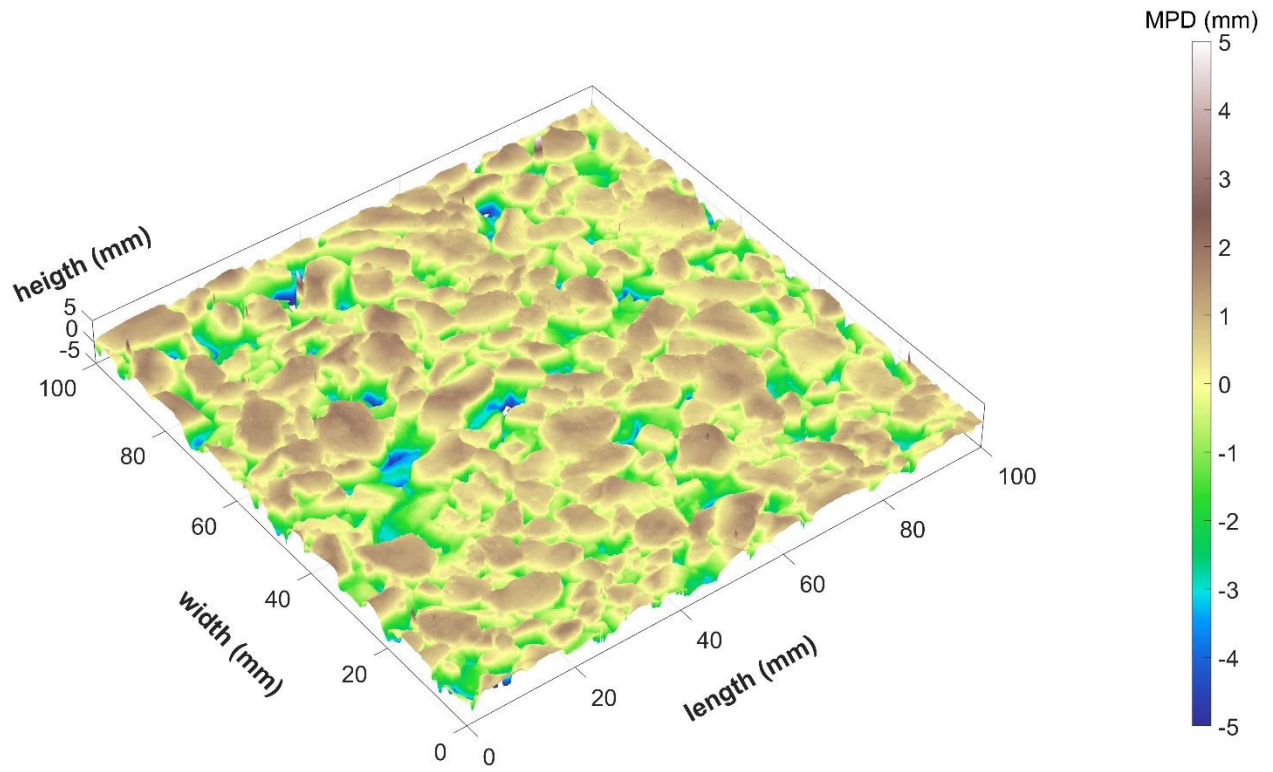


Figure D-55. OGFC surface scan 36.

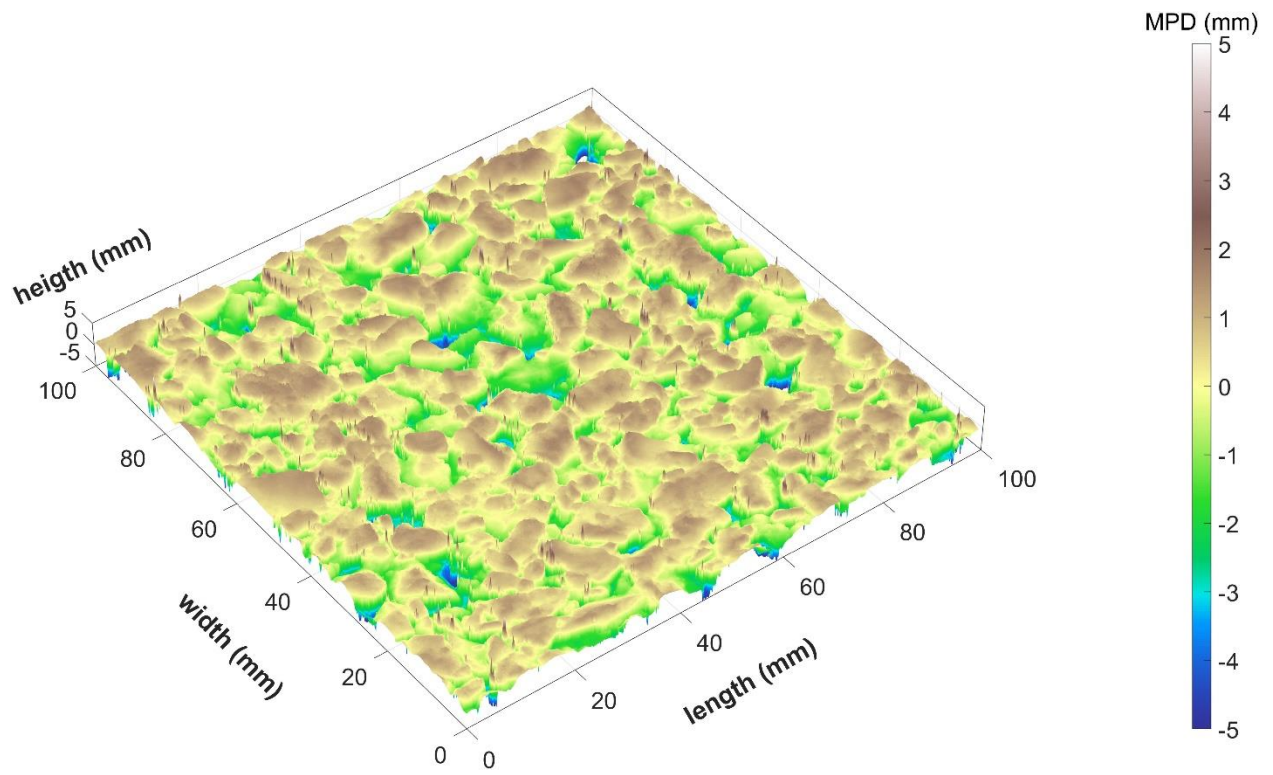


Figure D-56. OGFC surface scan 37.

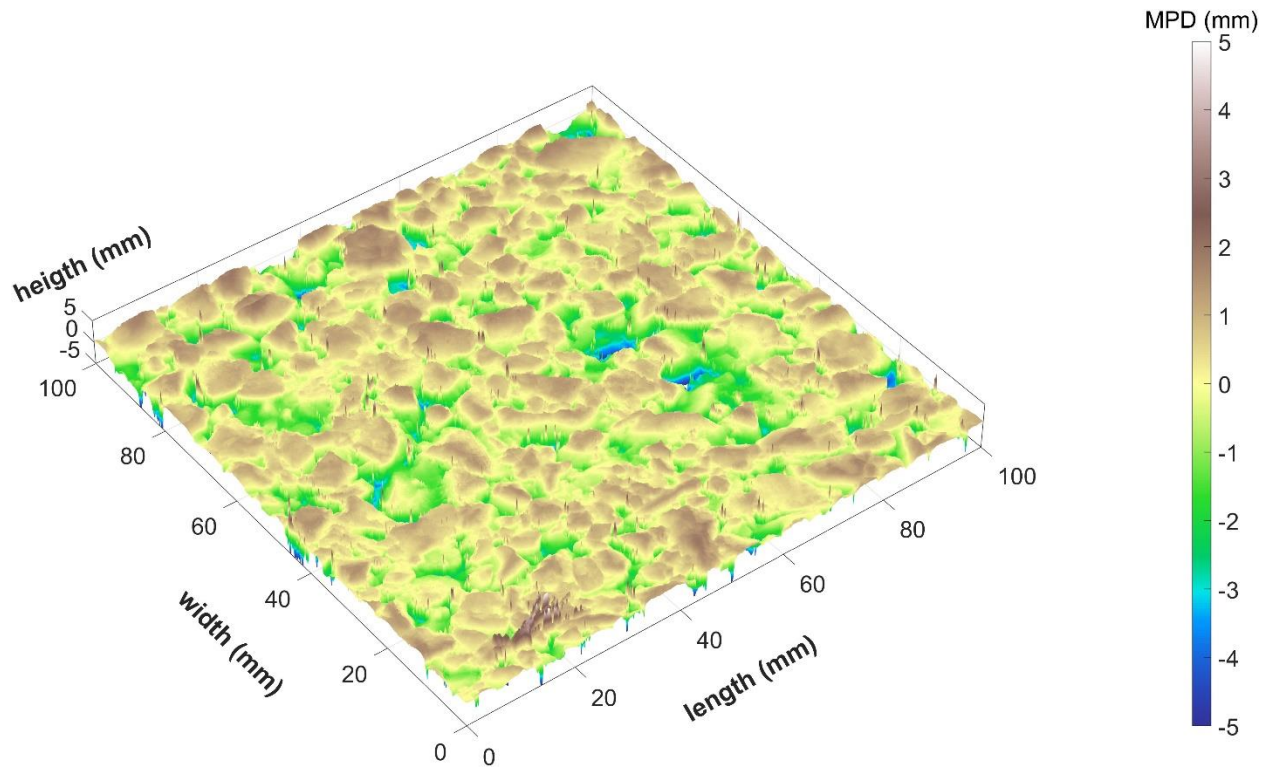


Figure D-57. OGFC surface scan 38.

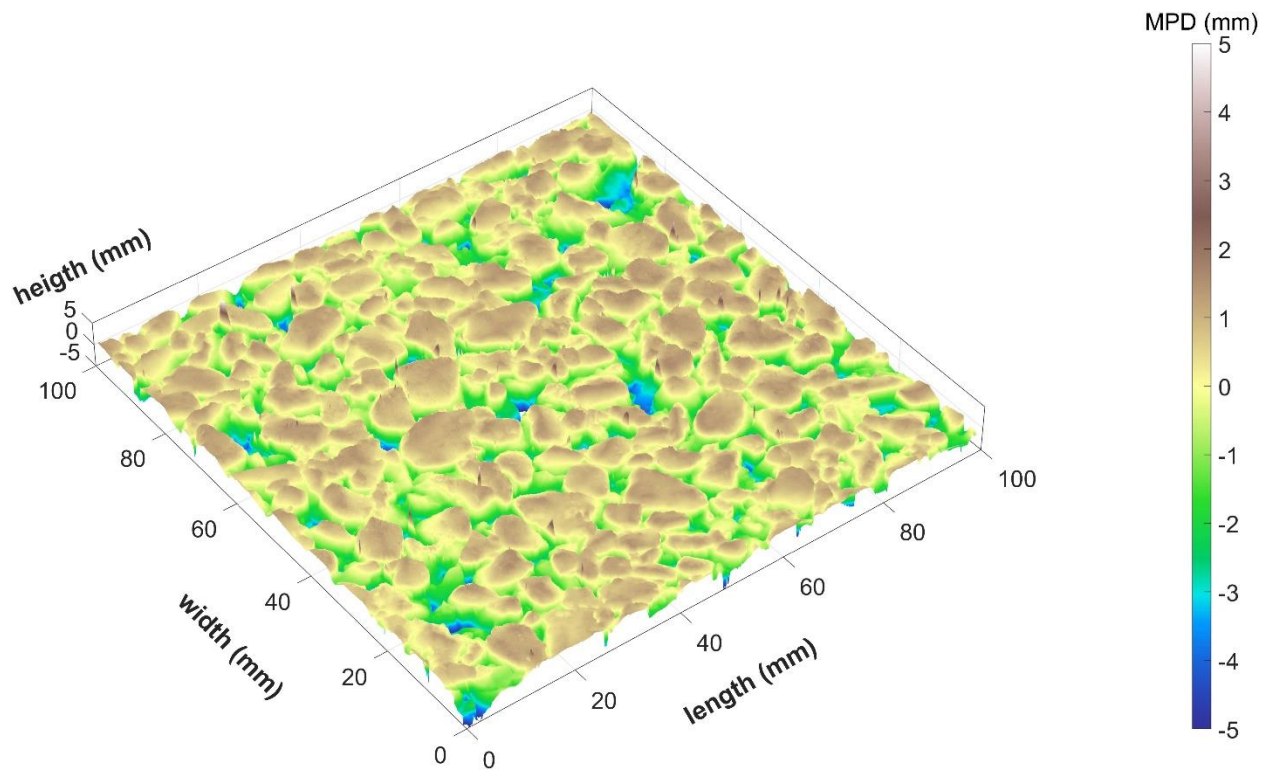


Figure D-58. OGFC surface scan 39.

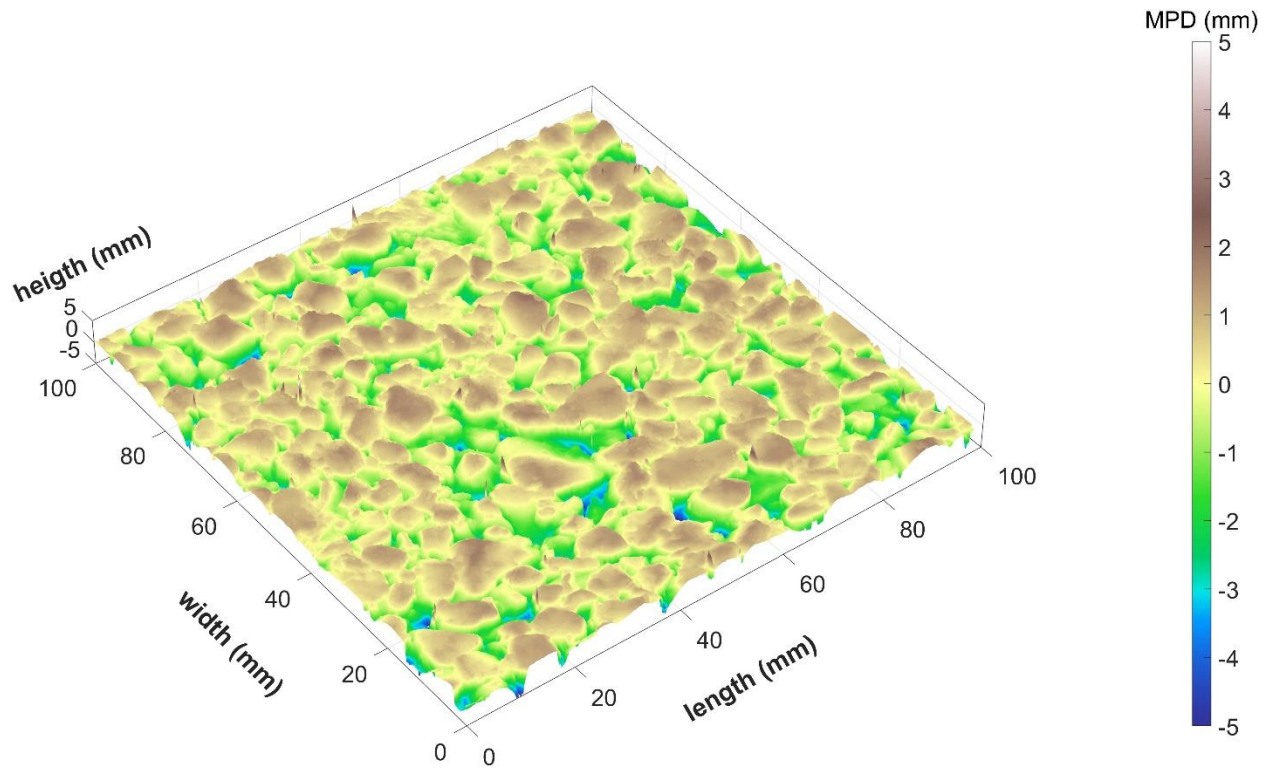


Figure D-59. OGFC surface scan 40.

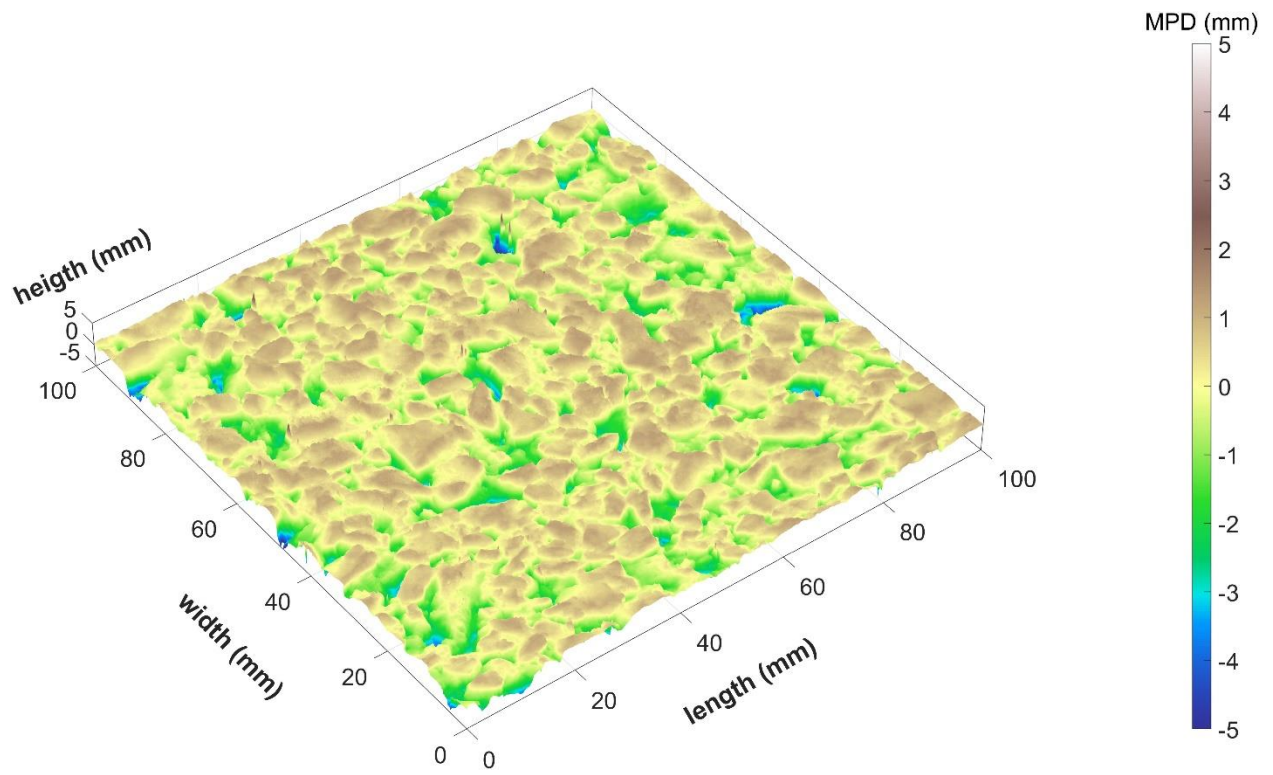


Figure D-60. OGFC surface scan 41.

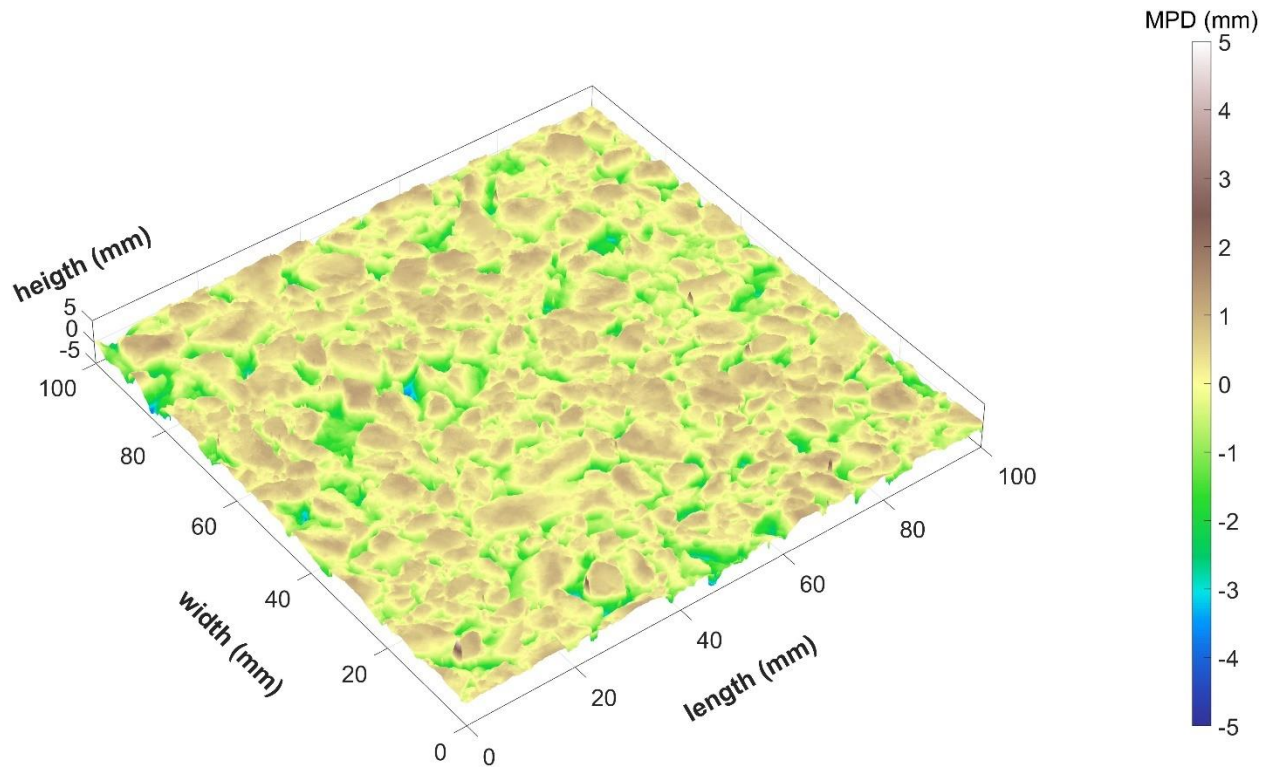


Figure D-61. OGFC surface scan 42.

Dense-II

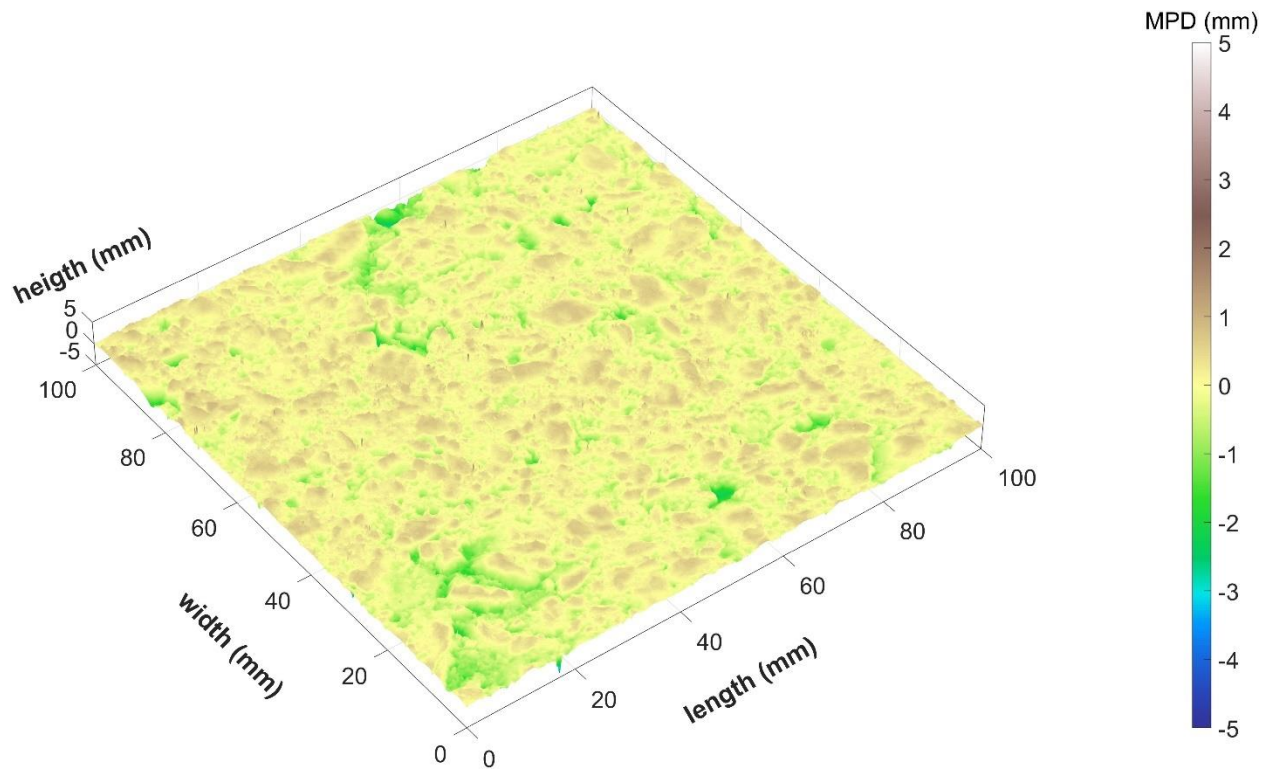


Figure D-62. Dense-II surface scan 44.

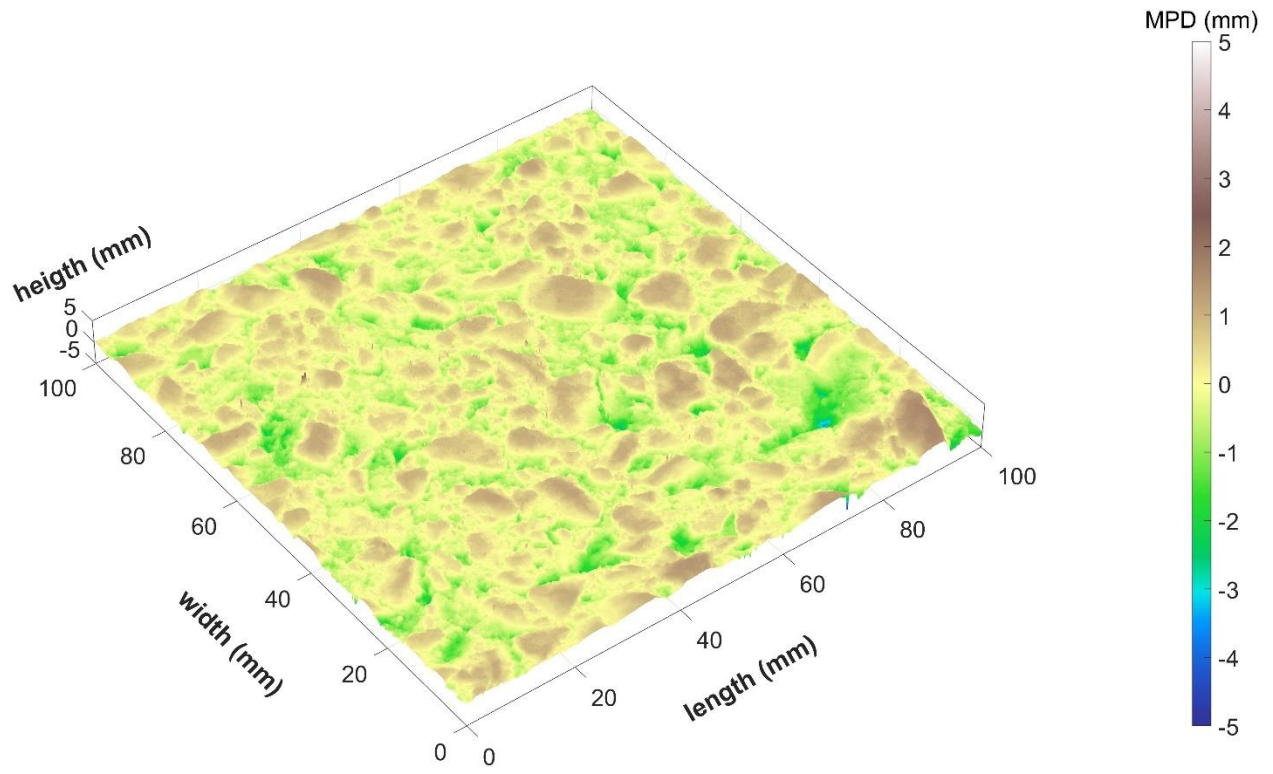


Figure D-63. Dense-II surface scan 45.

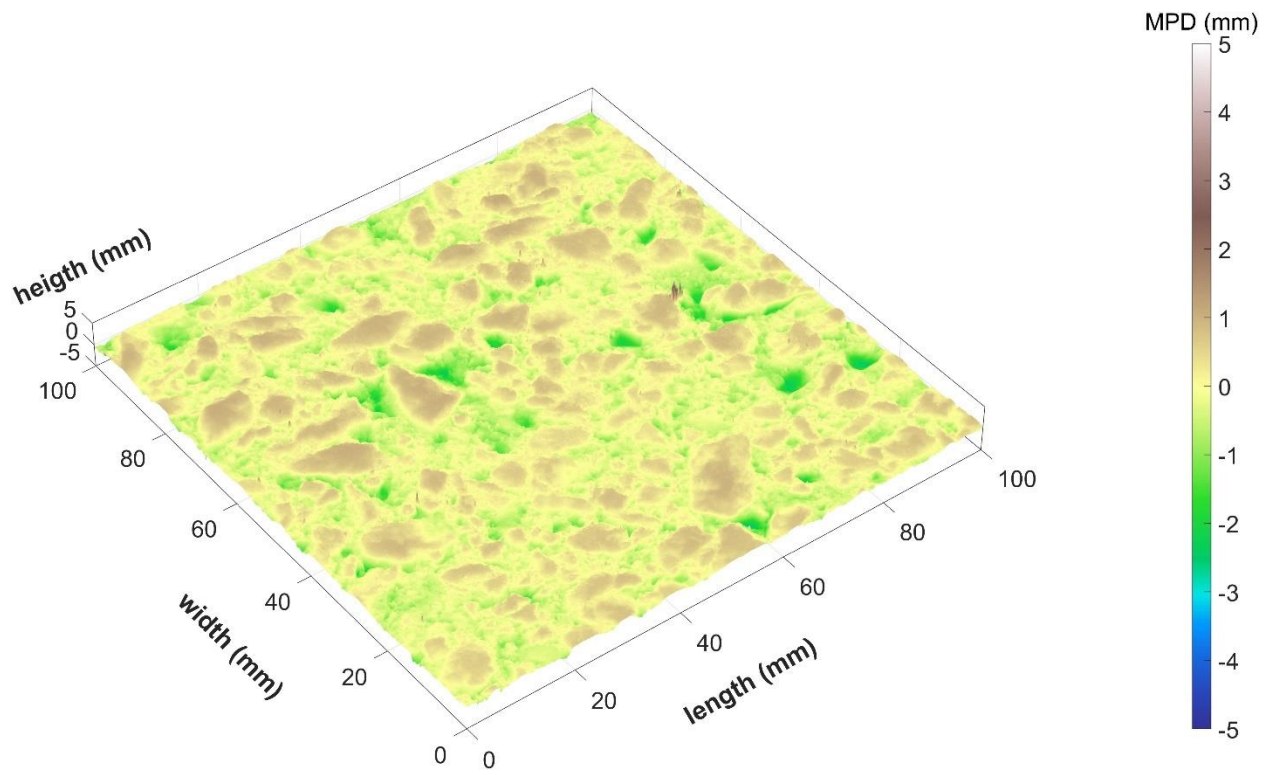


Figure D-64. Dense-II surface scan 46.

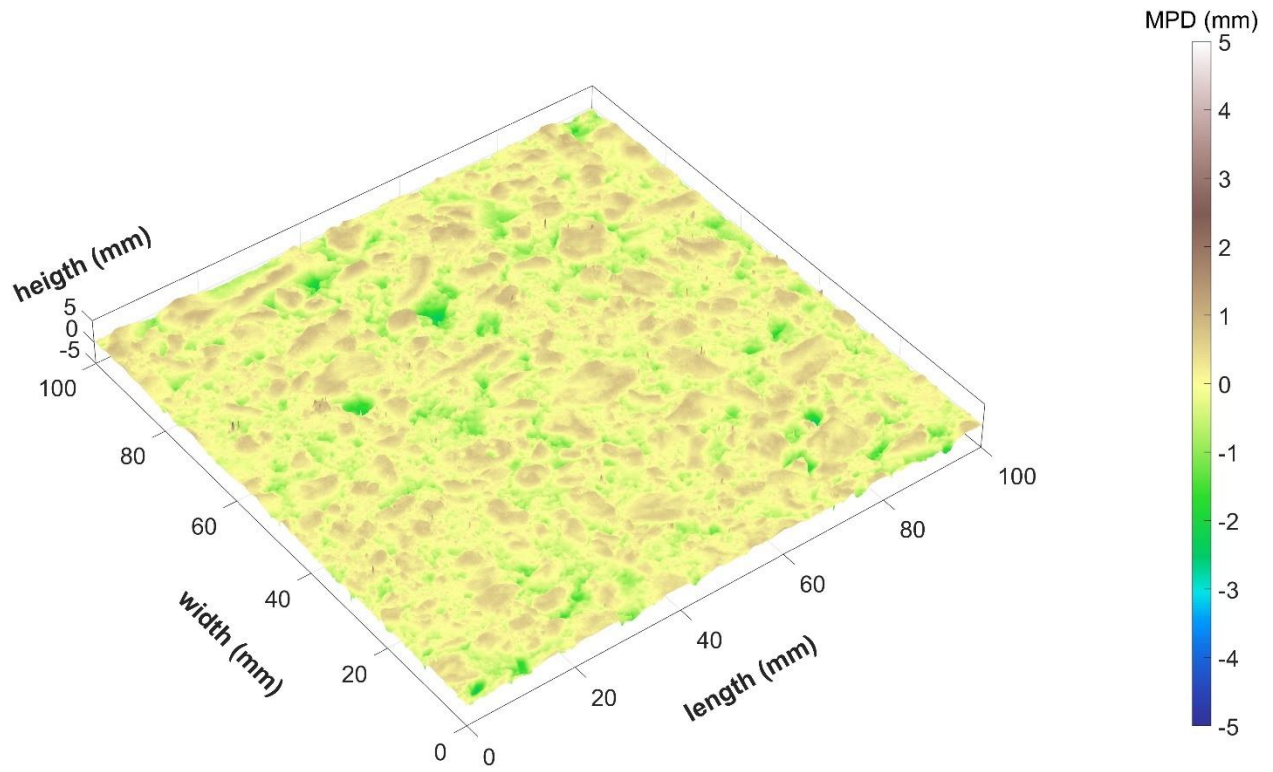


Figure D-65. Dense-II surface scan 47.

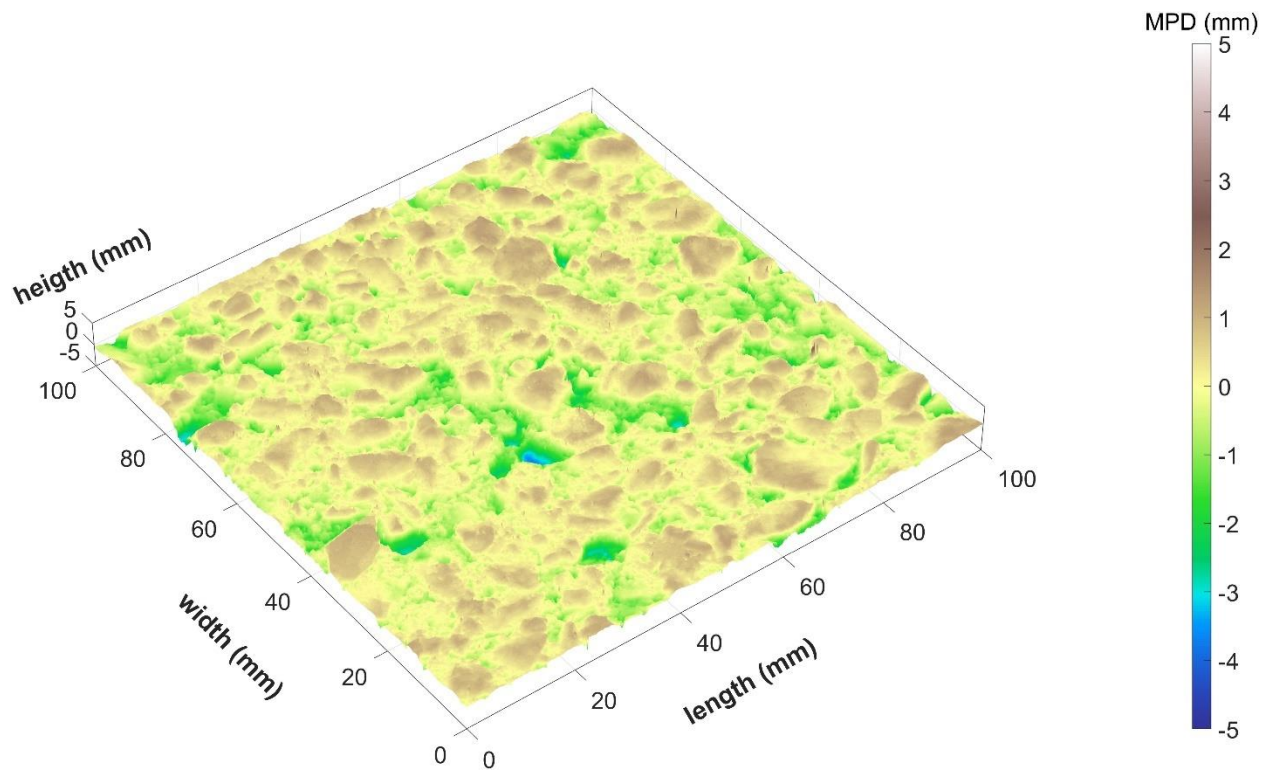


Figure D-66. Dense-II surface scan 48.

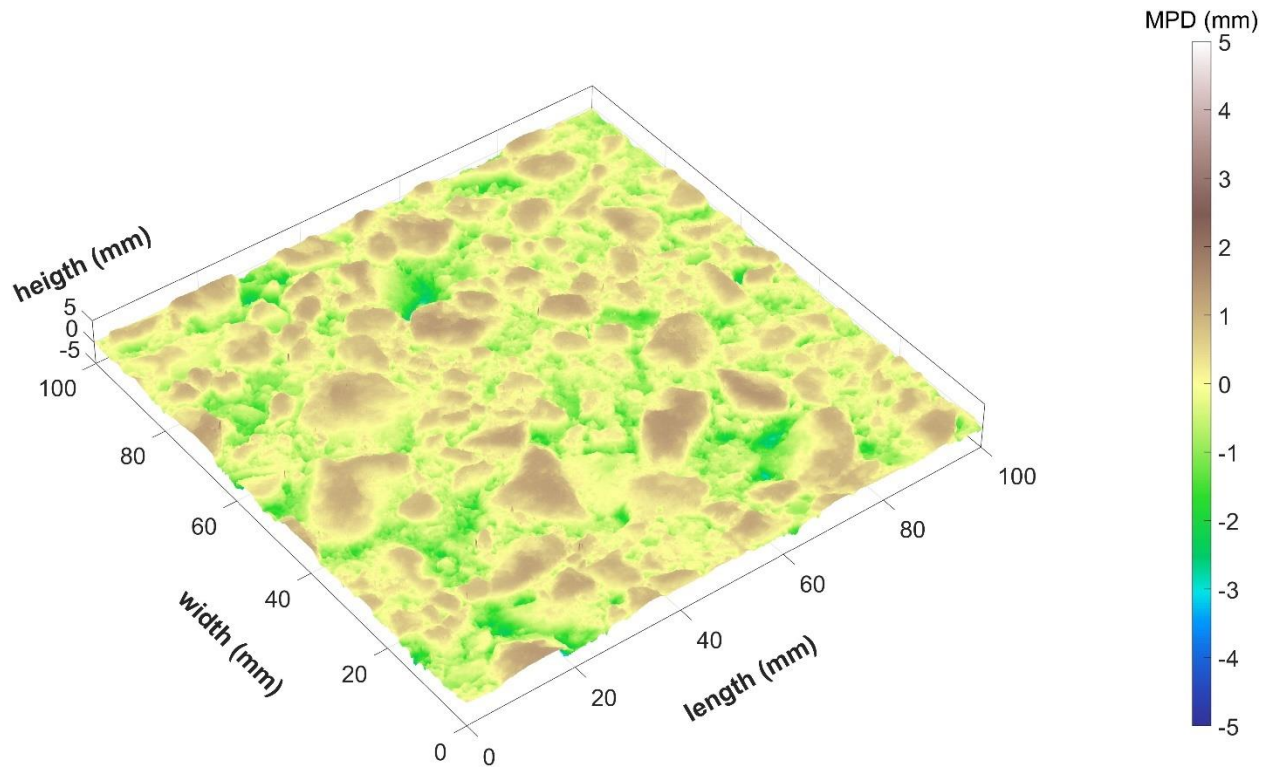


Figure D-67. Dense-II surface scan 49.

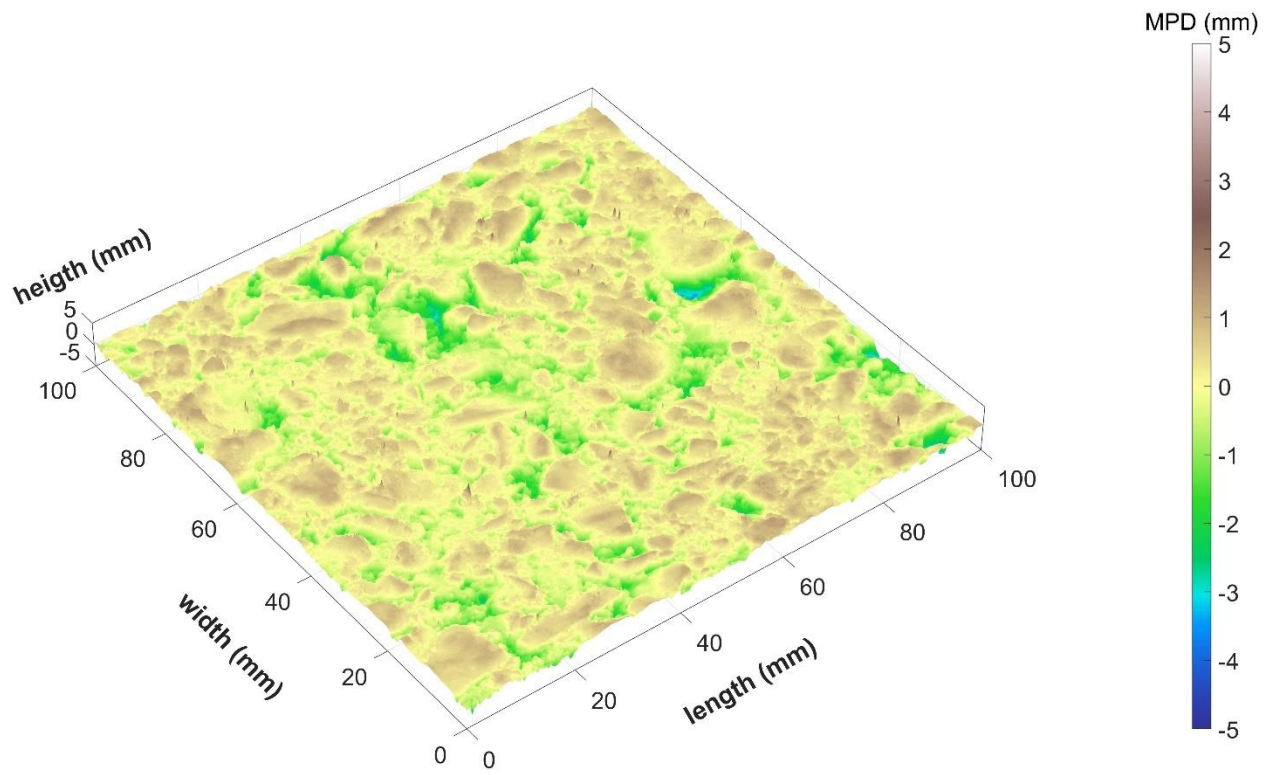


Figure D-68. Dense-II surface scan 50.

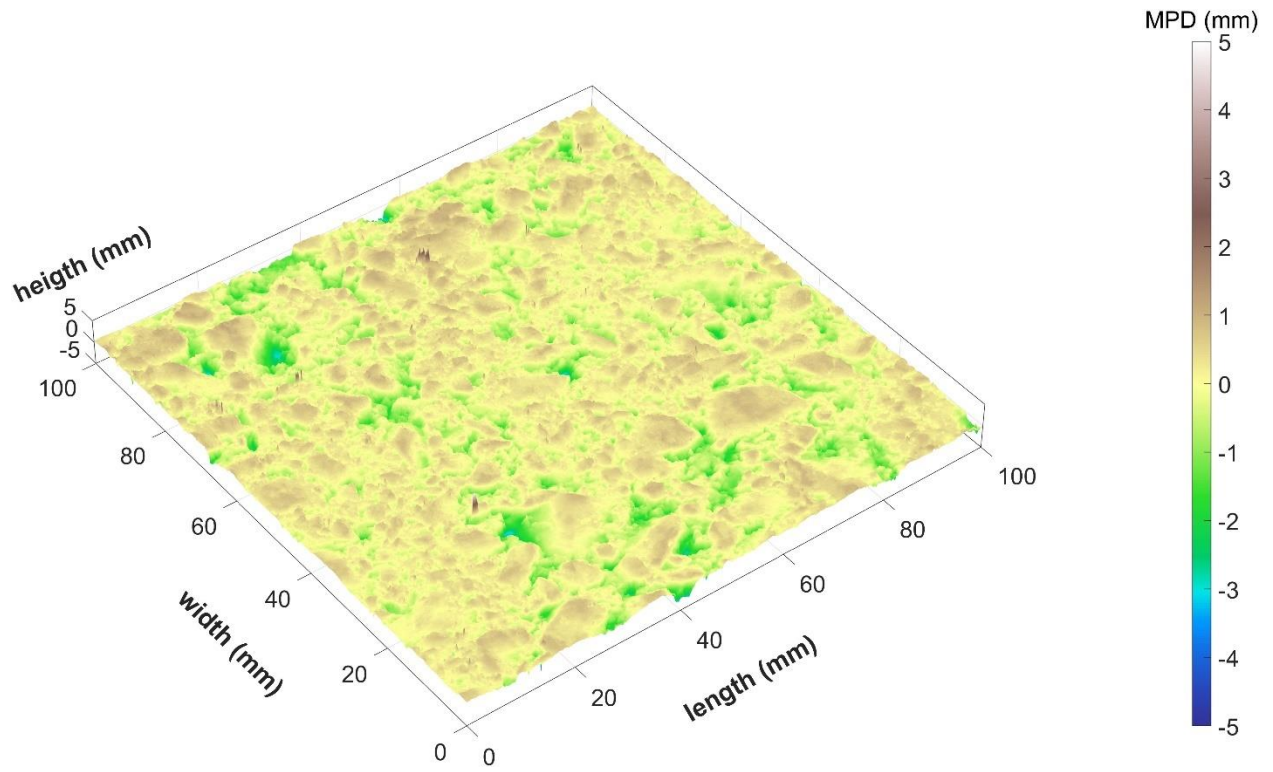


Figure D-69. Dense-II surface scan 51.

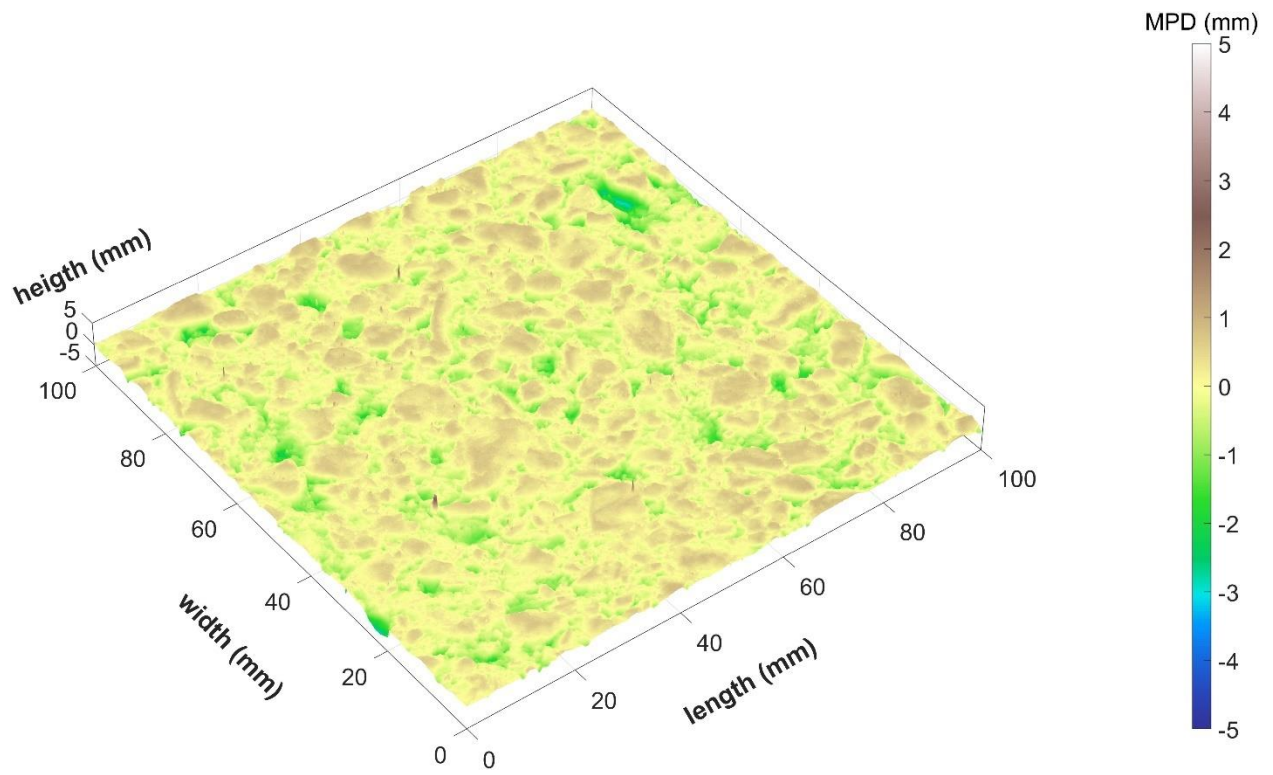


Figure D-70. Dense-II surface scan 52.

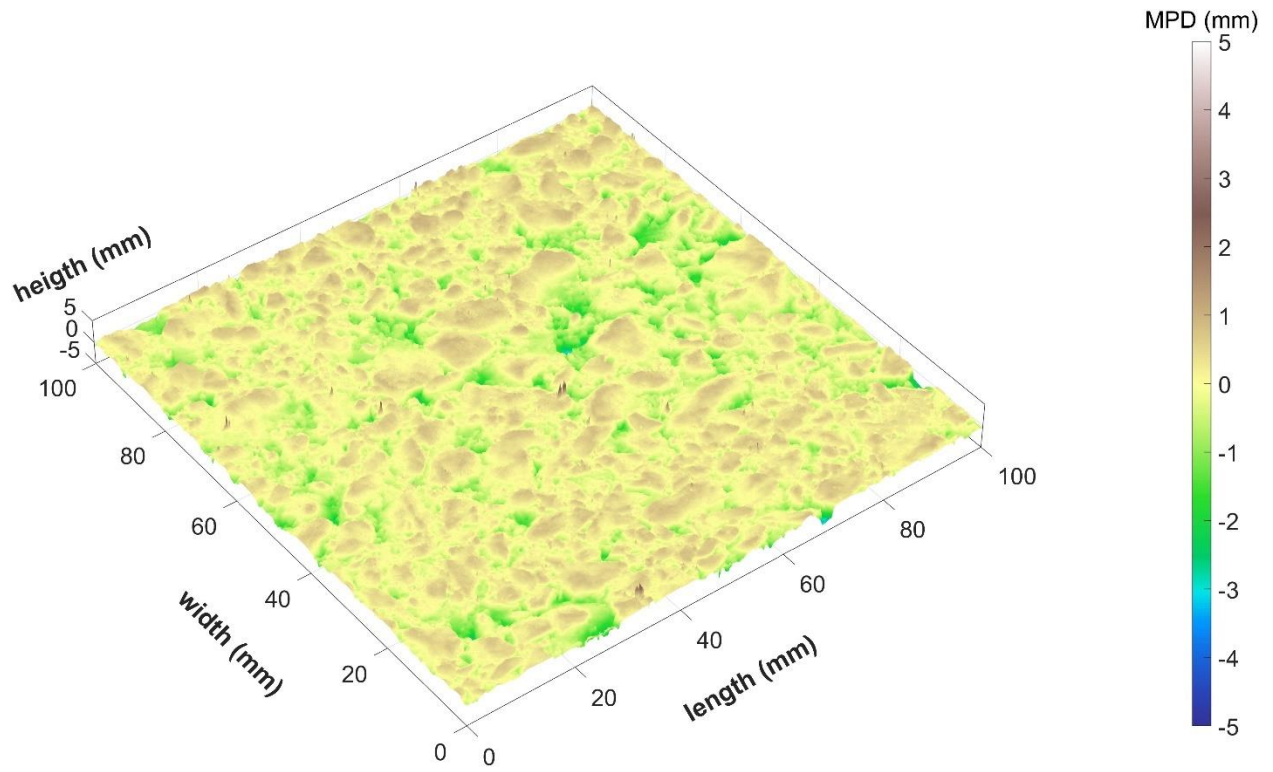


Figure D-71. Dense-II surface scan 53.

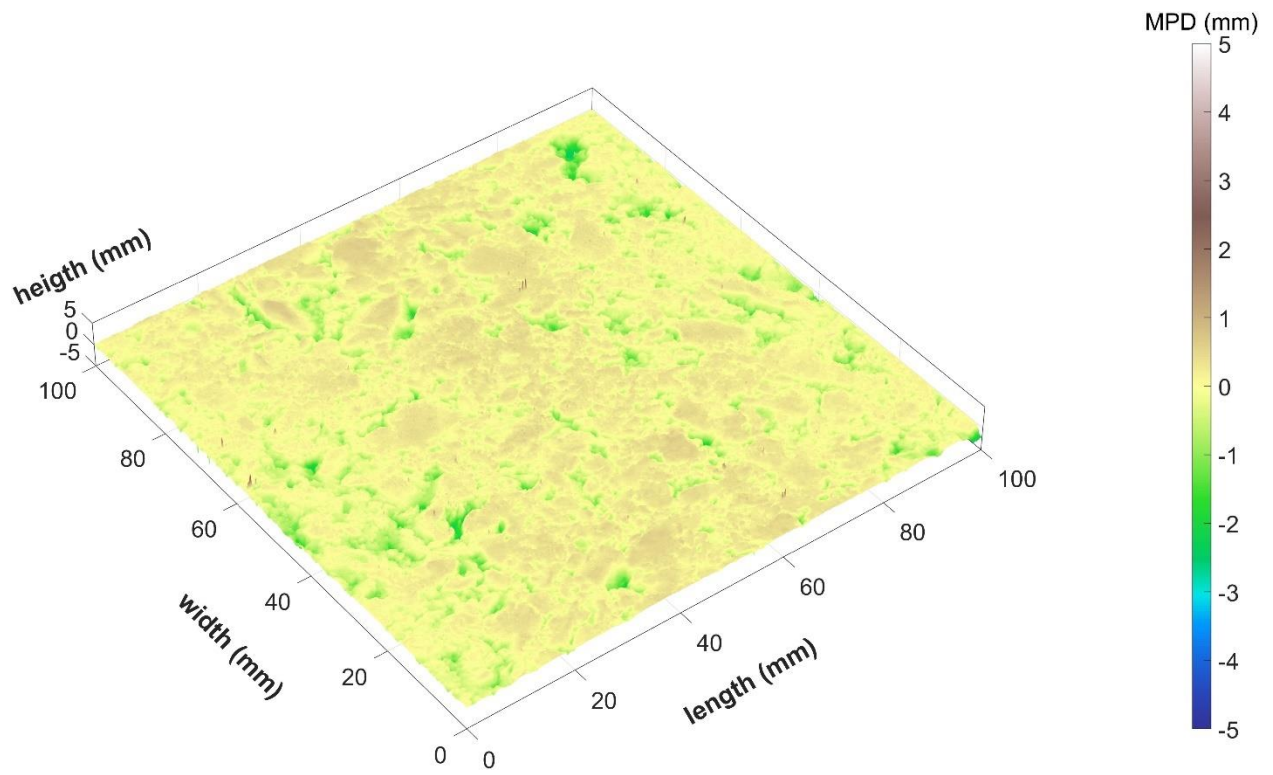


Figure D-72. Dense-II surface scan 54.

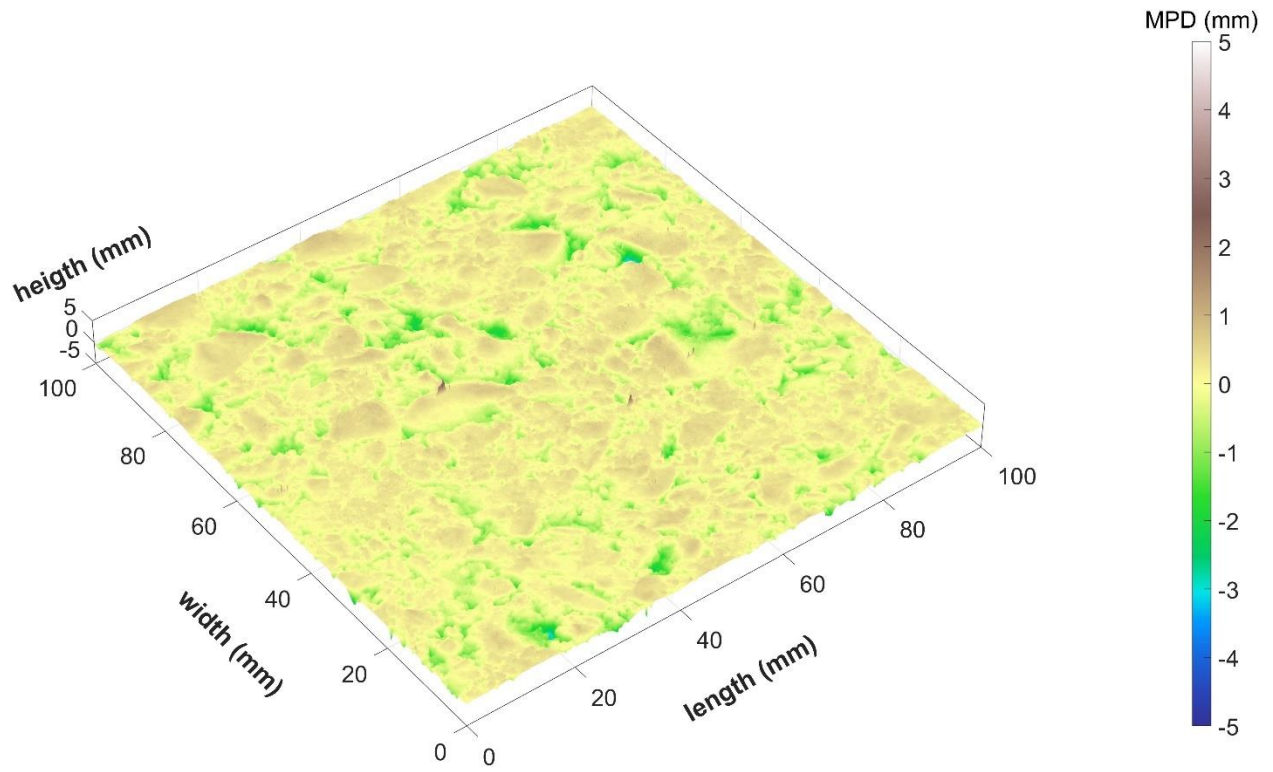


Figure D-73. Dense-II surface scan 55.

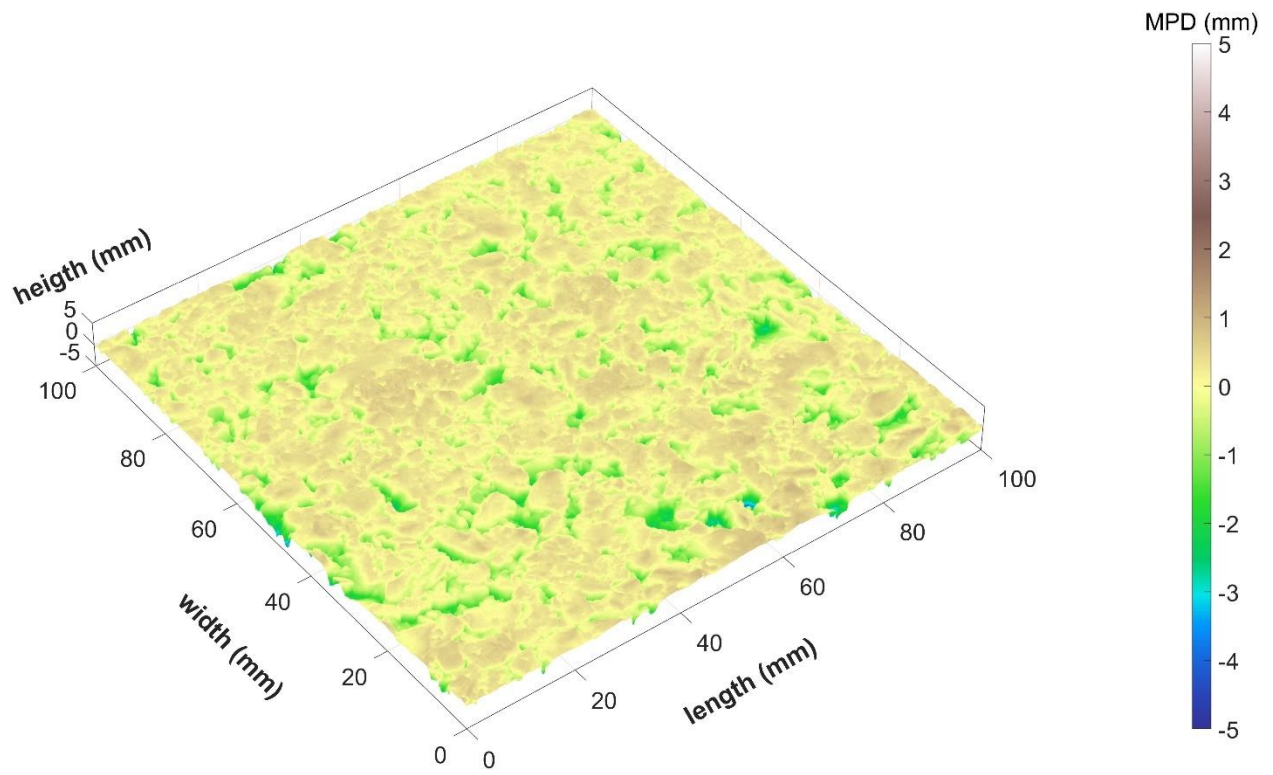


Figure D-74. Dense-II surface scan 56.

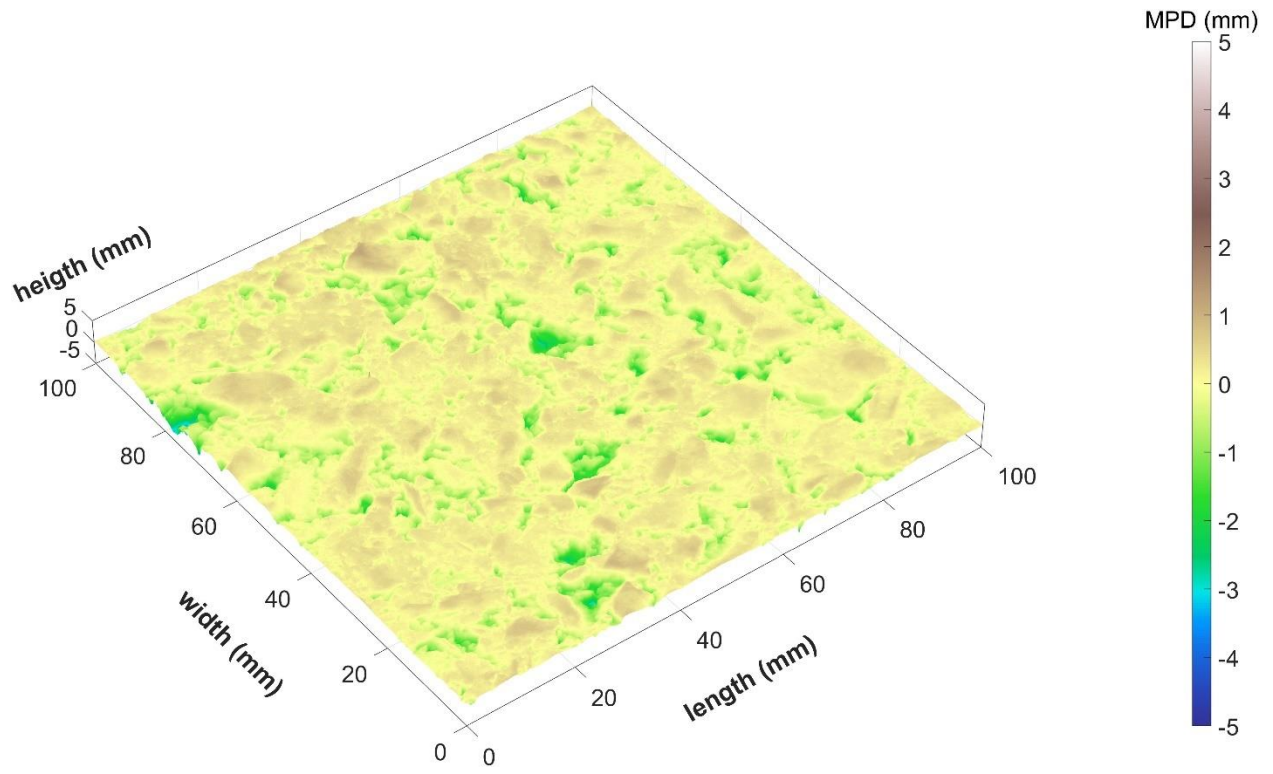


Figure D-75. Dense-II surface scan 57.

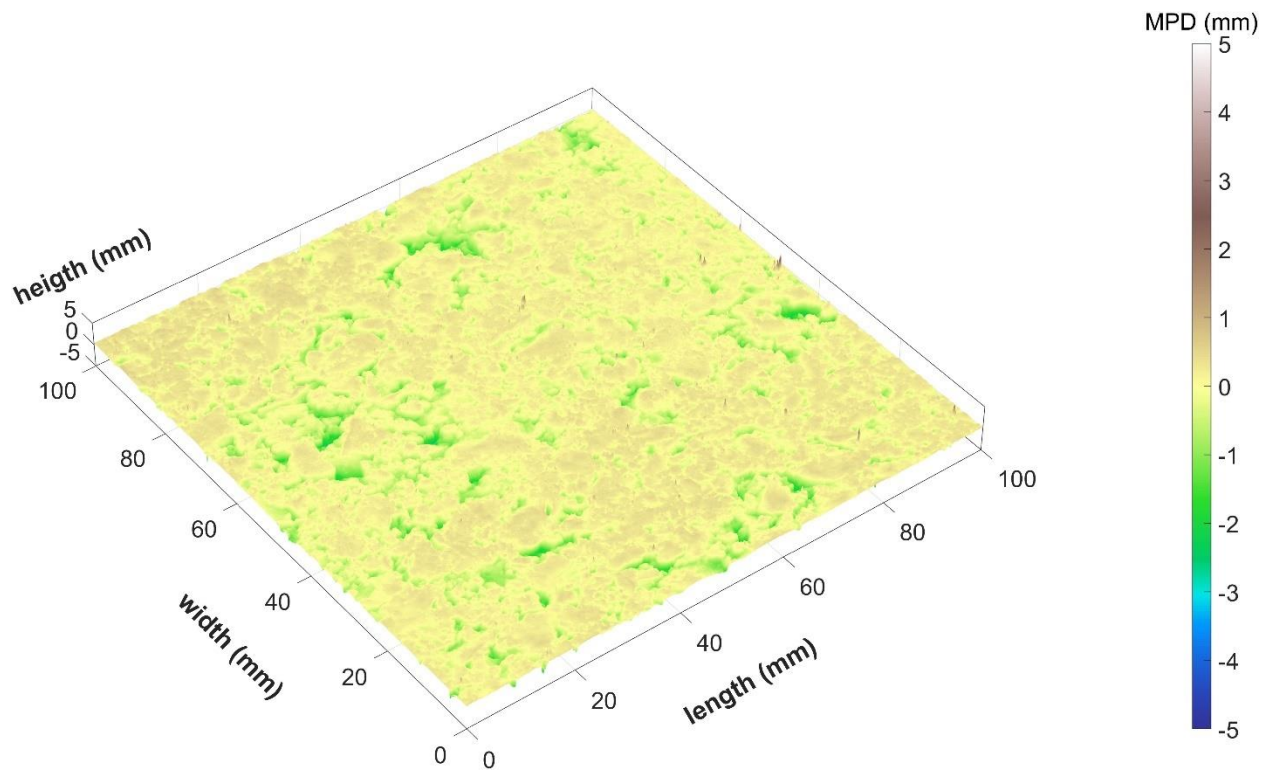


Figure D-76. Dense-II surface scan 58.

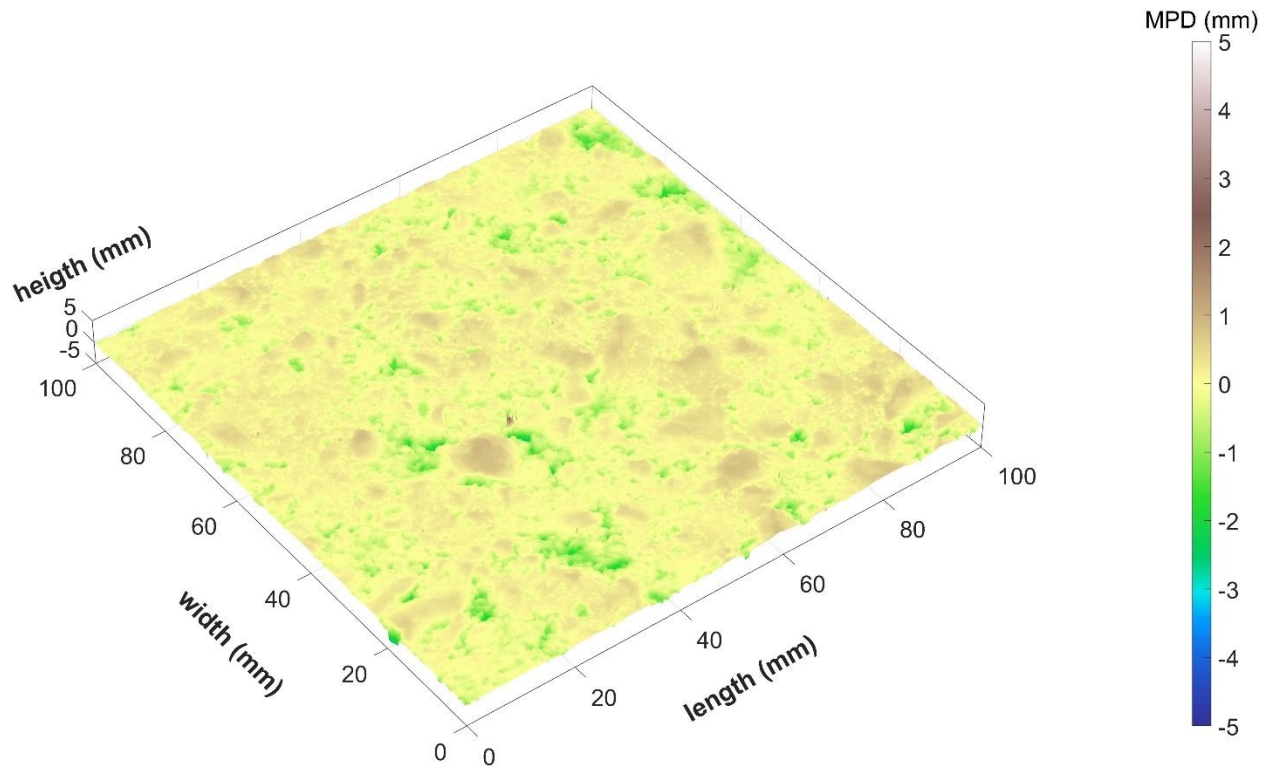


Figure D-77. Dense-II surface scan 59.

SMA-2B

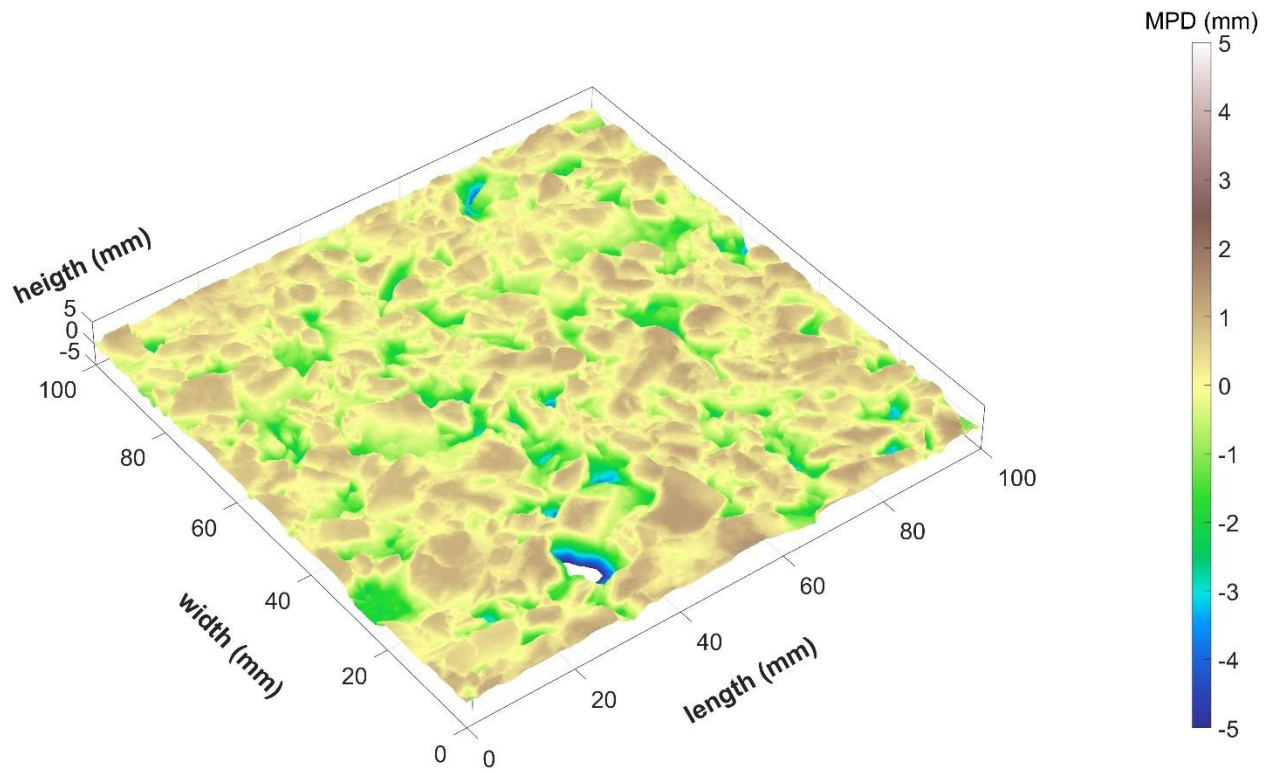


Figure D-78. SMA-2B surface scan 61.

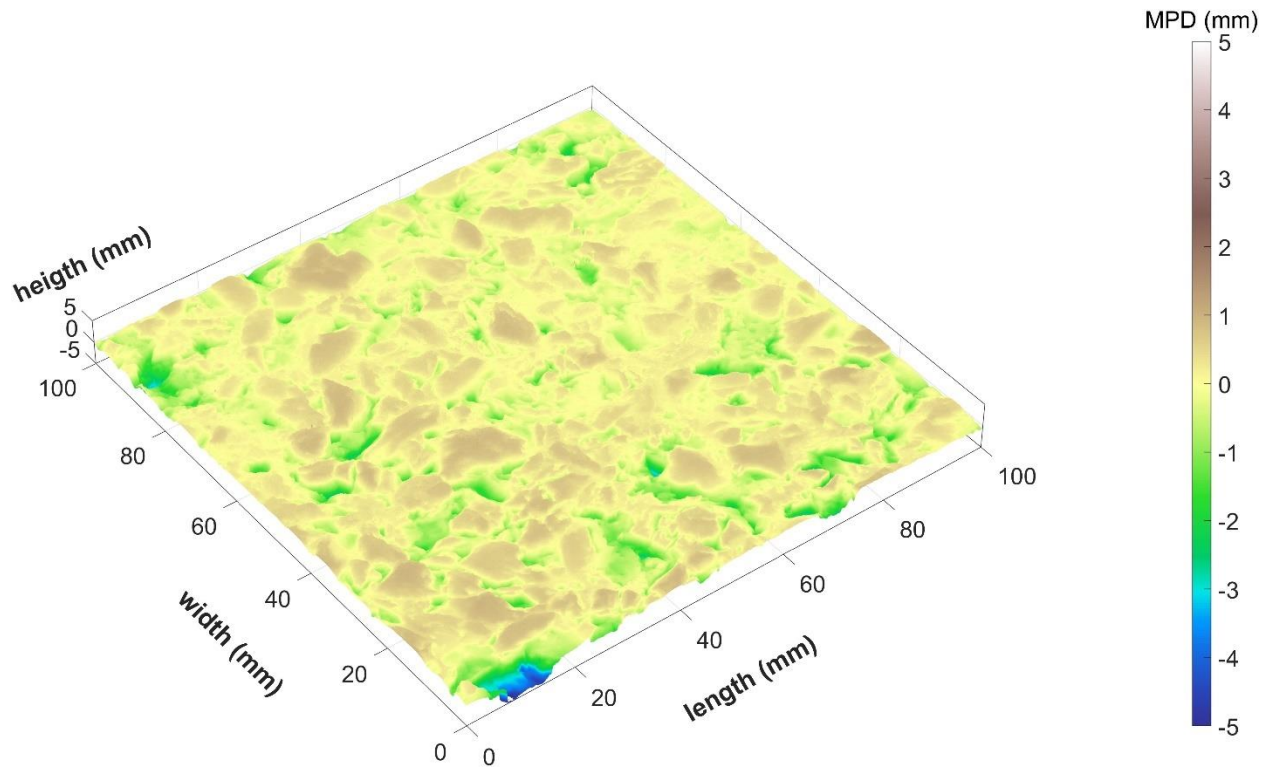


Figure D-79. SMA-2B surface scan 62.

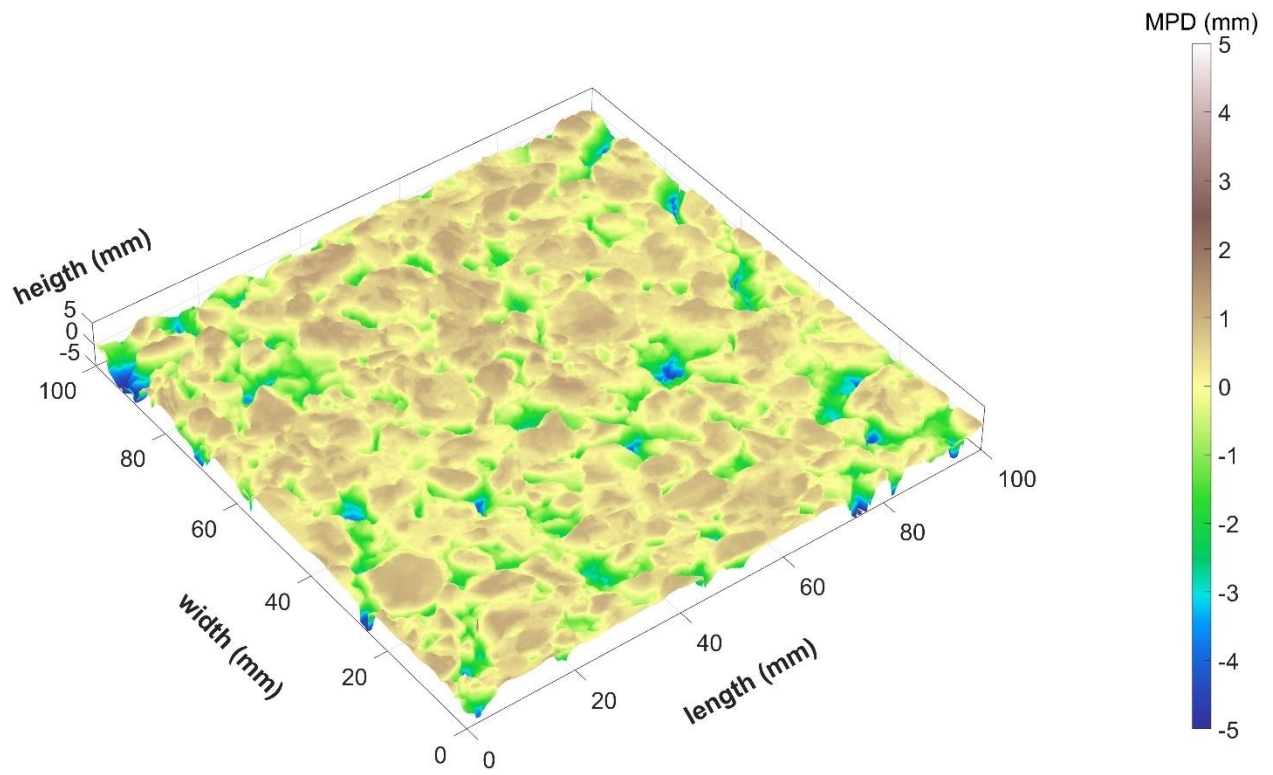


Figure D-80. SMA-2B surface scan 63.

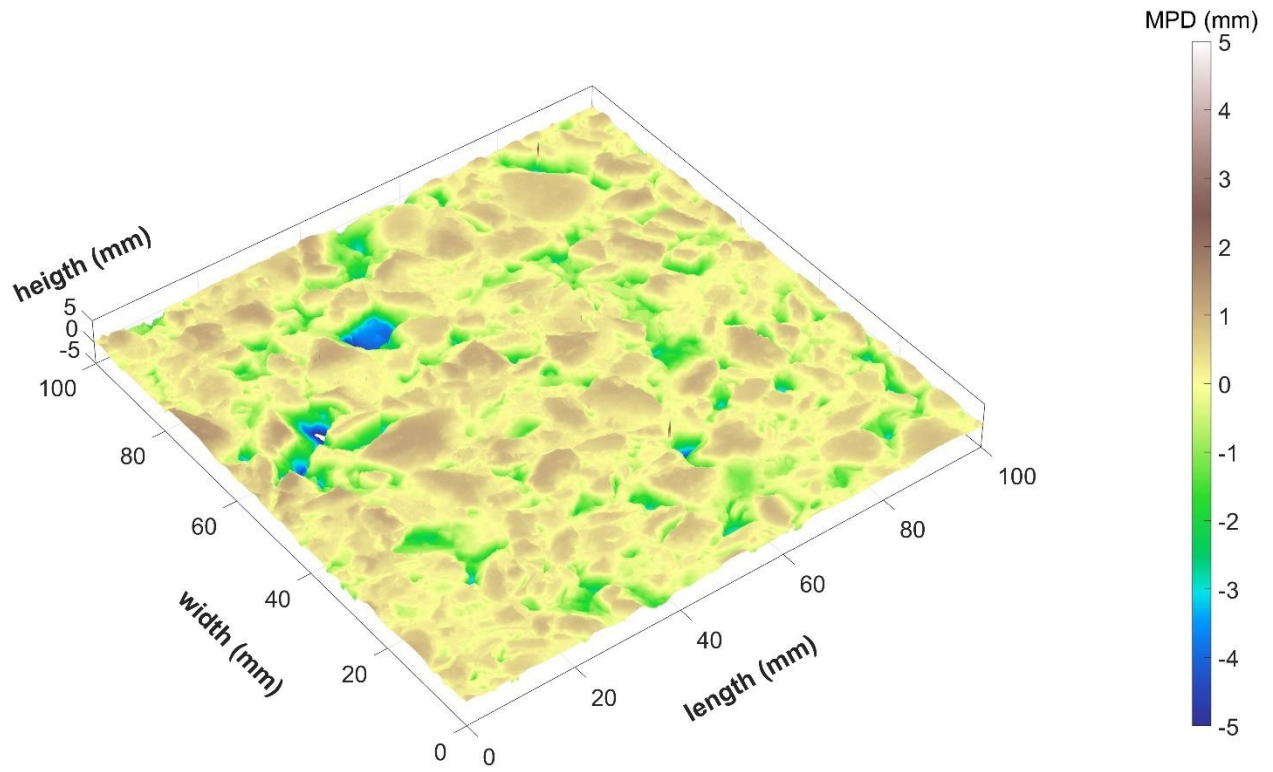


Figure D-81. SMA-2B surface scan 64.

SMA-2A

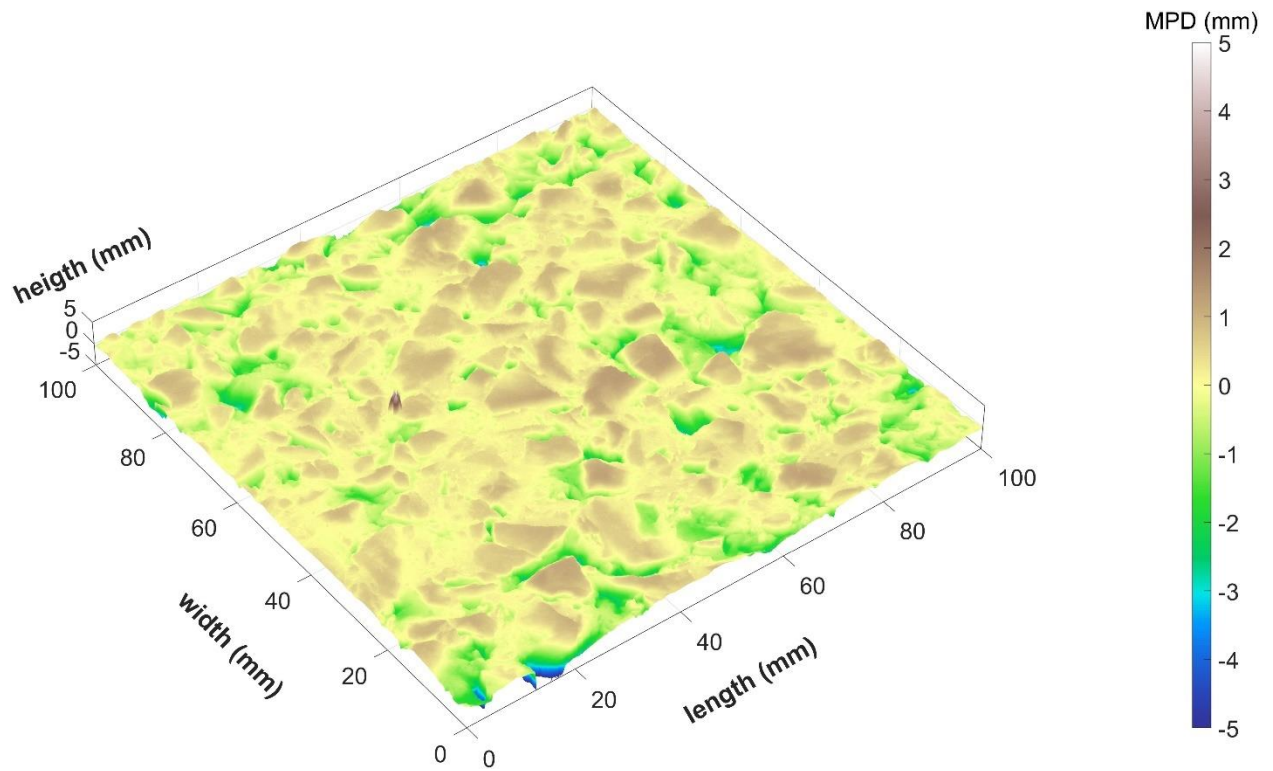


Figure D-82. SMA-2A surface scan 66.

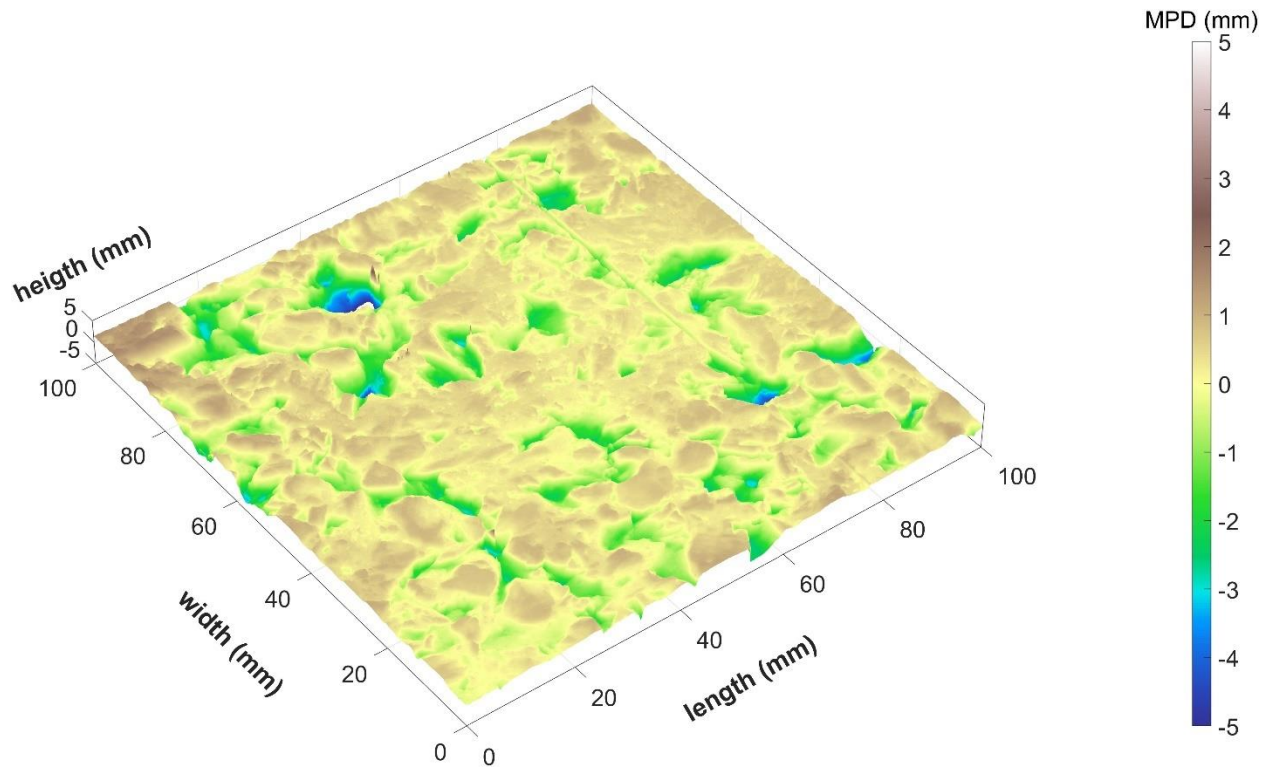


Figure D-83. SMA-2A surface scan 67.

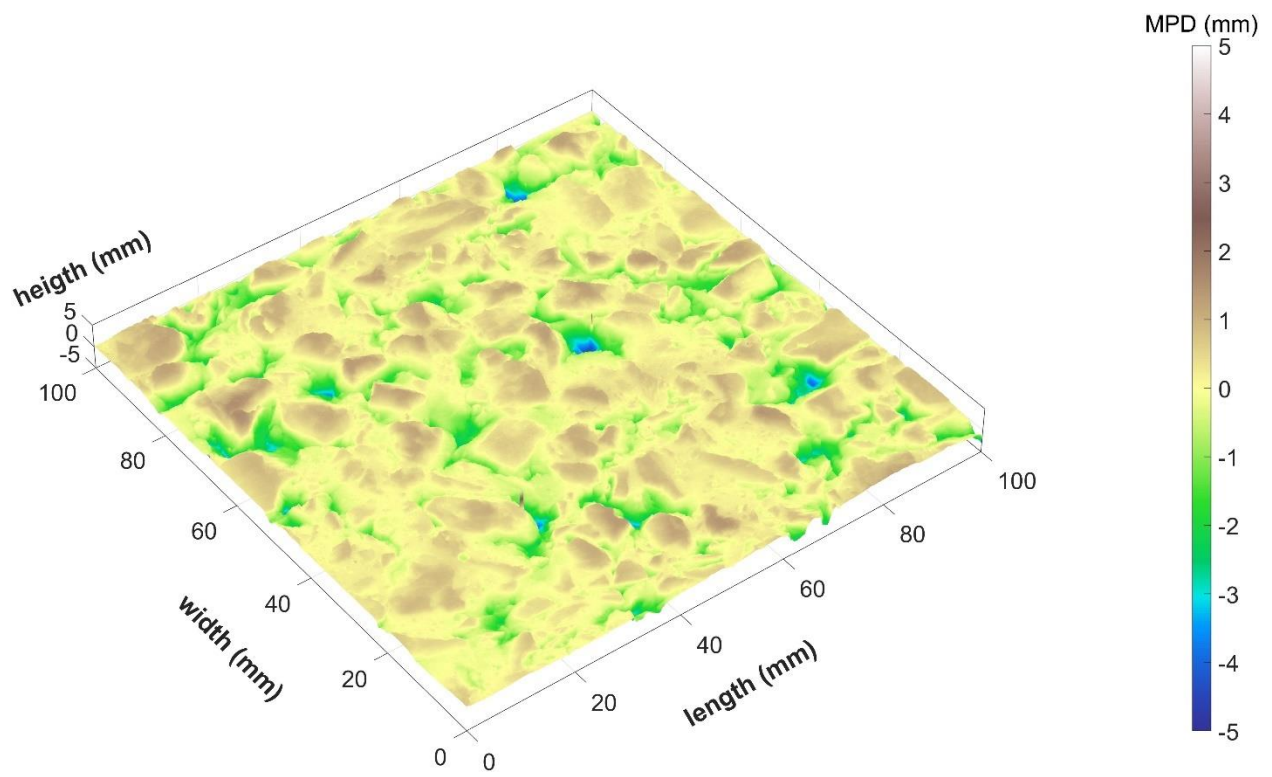


Figure D-84. SMA-2A surface scan 68.

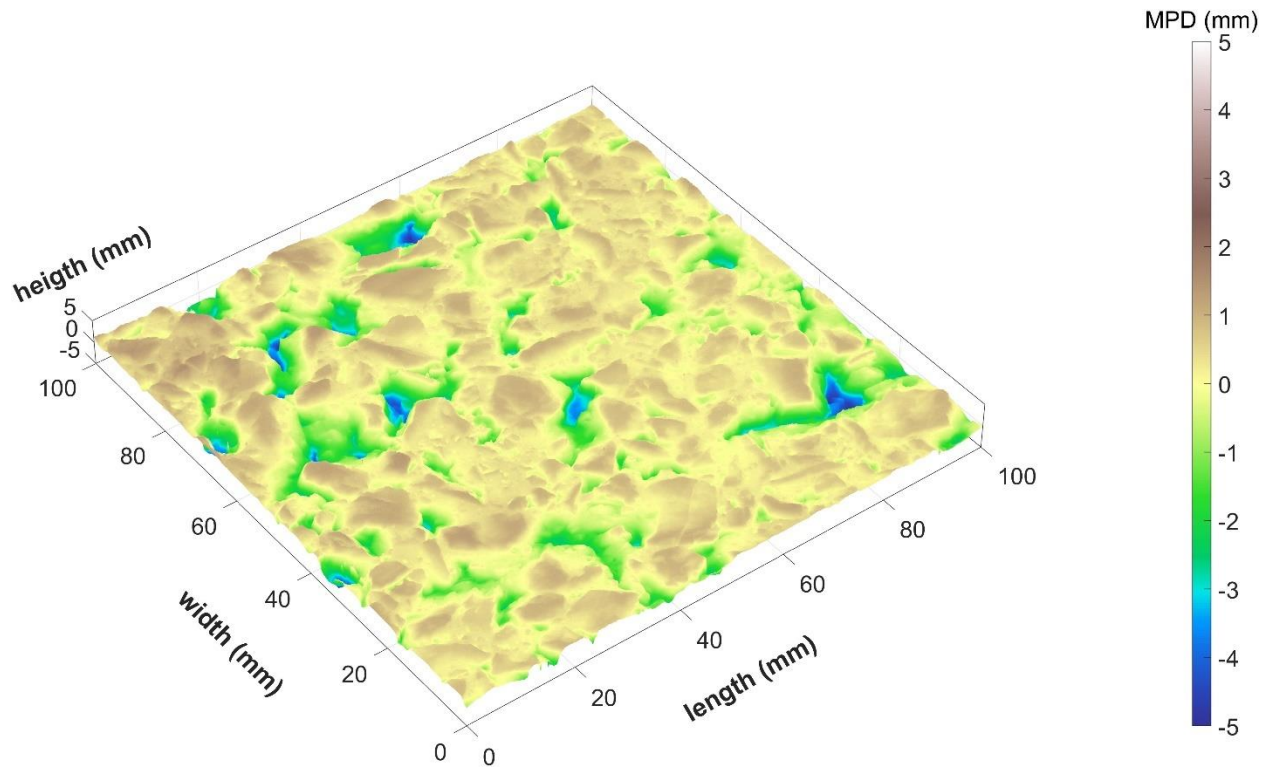


Figure D-85. SMA-2A surface scan 69.

SMA-1B

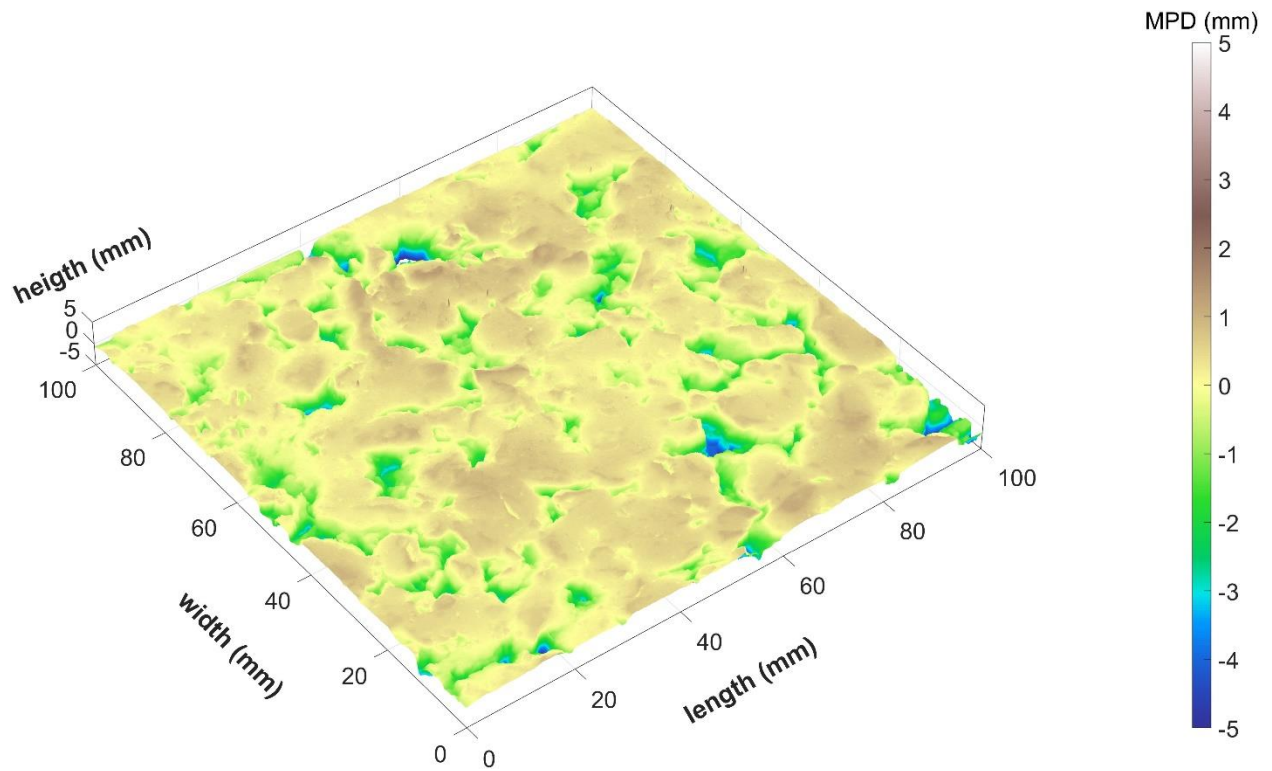


Figure D-86. SMA-1B surface scan 71.

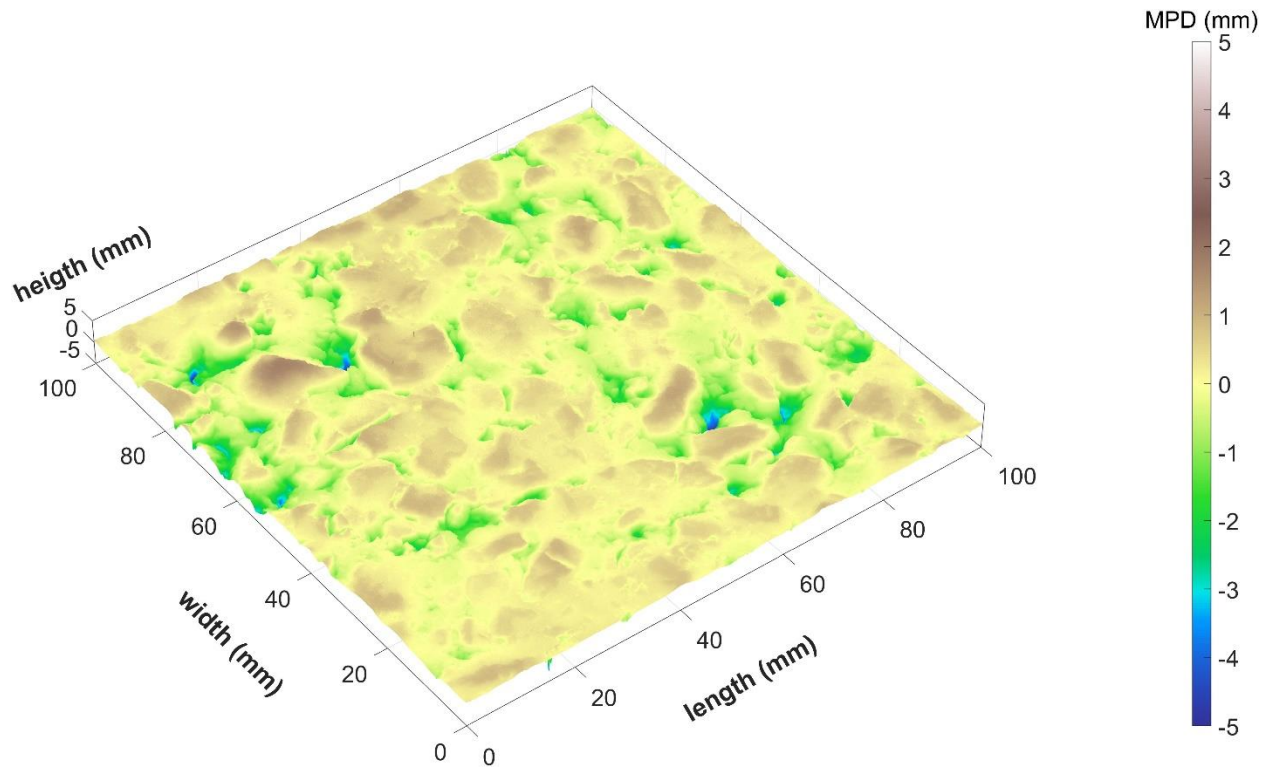


Figure D-87. SMA-1B surface scan 72.

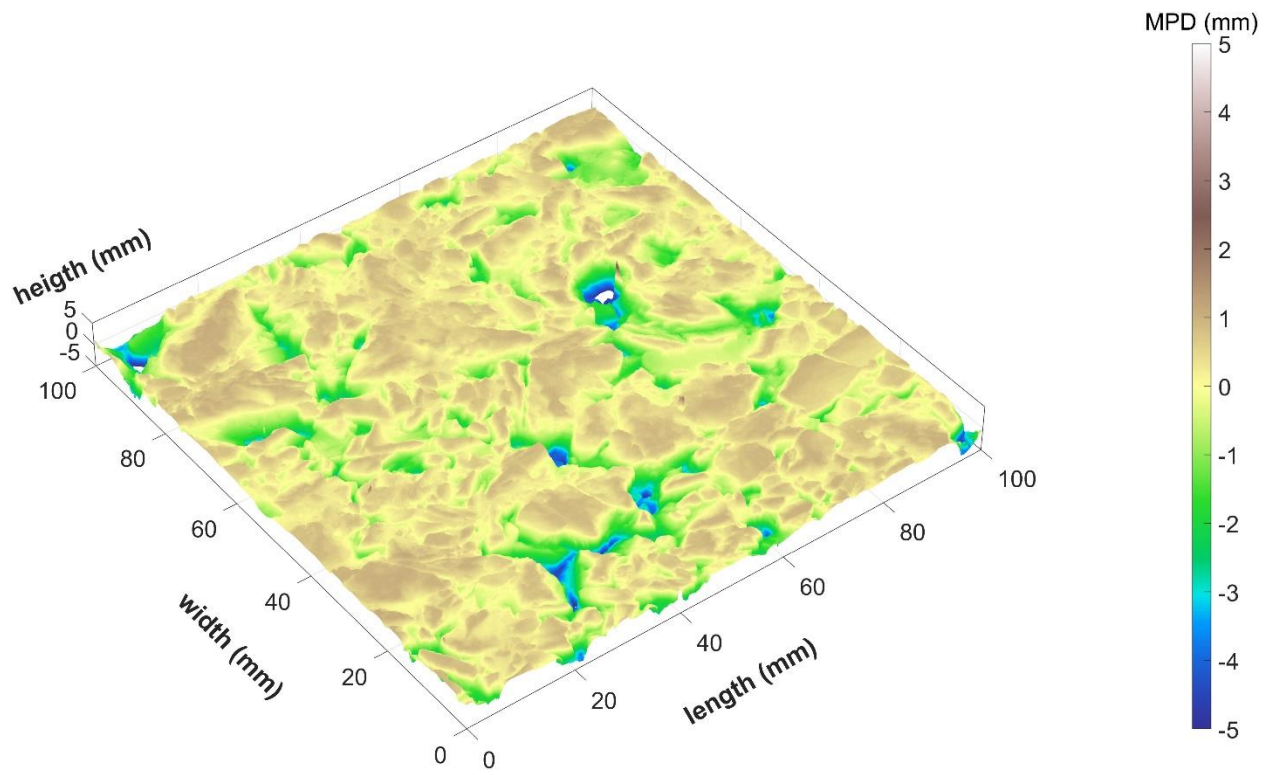


Figure D-88. SMA-1B surface scan 73.

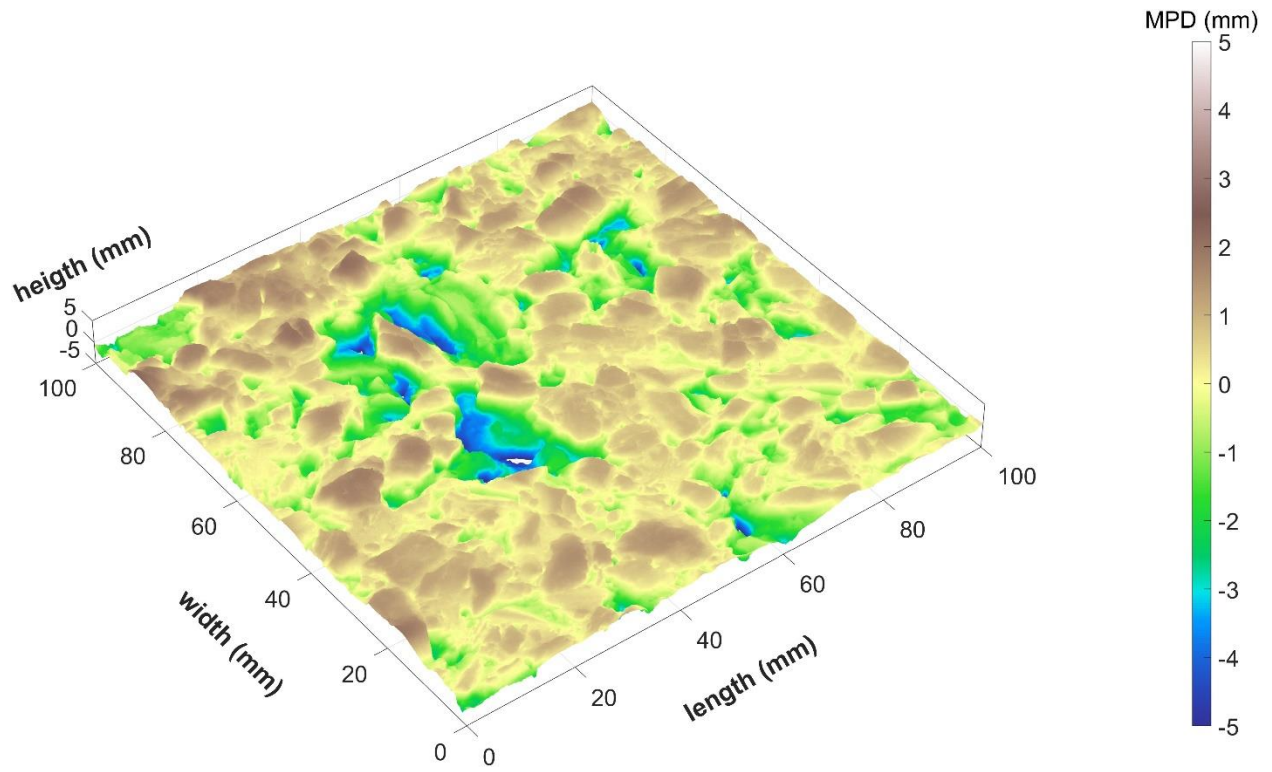


Figure D-89. SMA-1B surface scan 74.

Microsurfacing-Alt

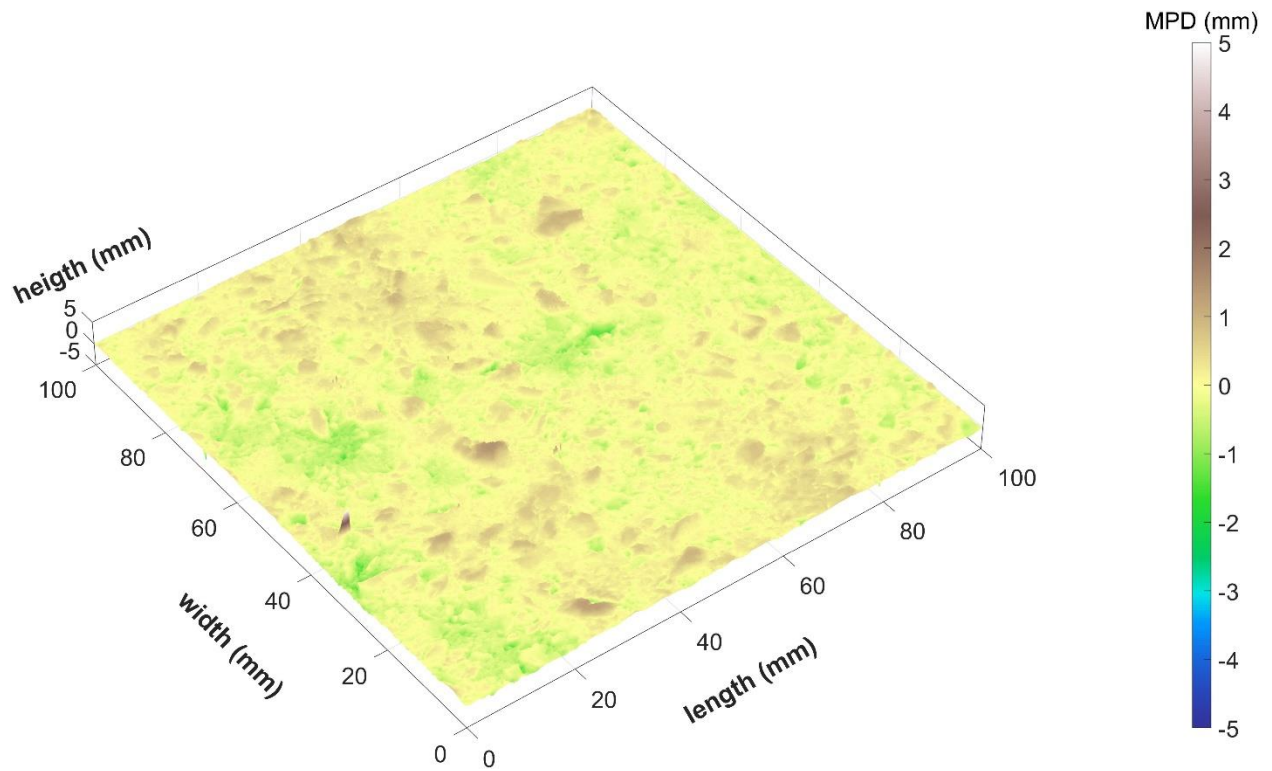


Figure D-90. Microsurfacing-Alt surface scan 76.

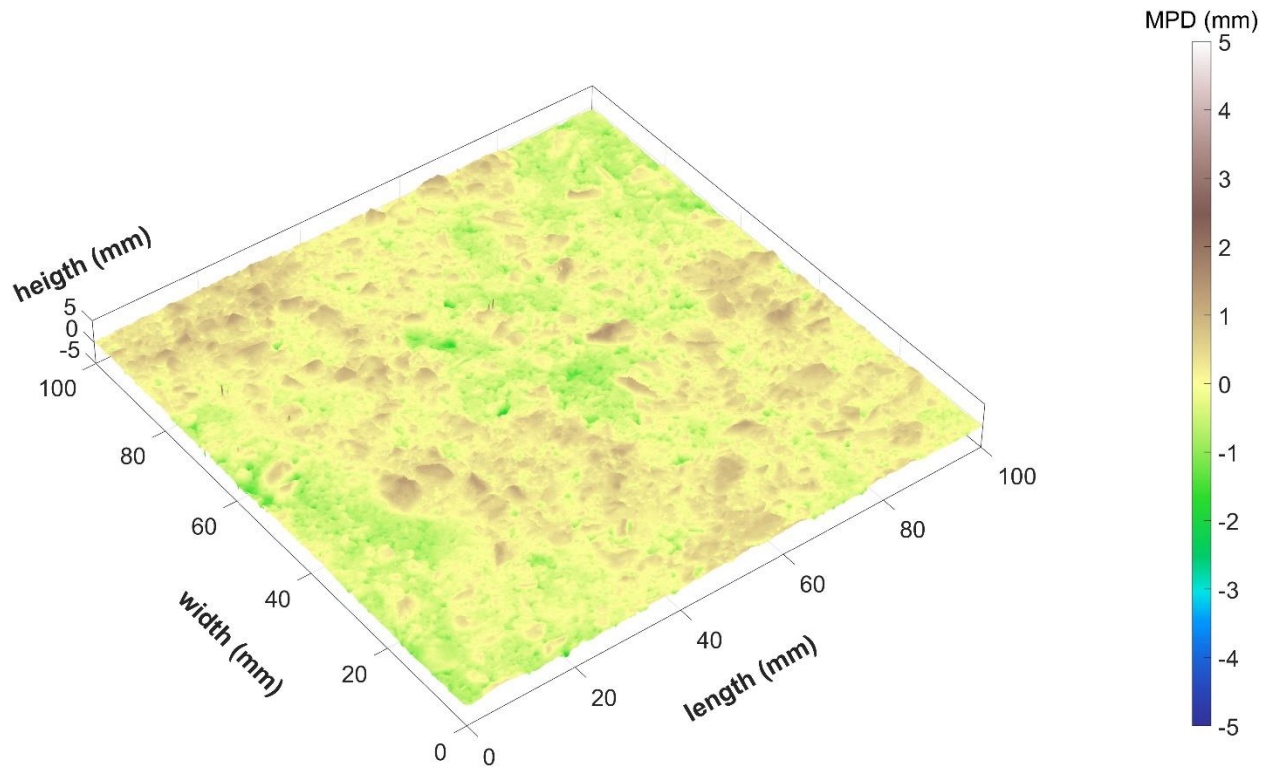


Figure D-91. Microsurfacing-Alt surface scan 77.

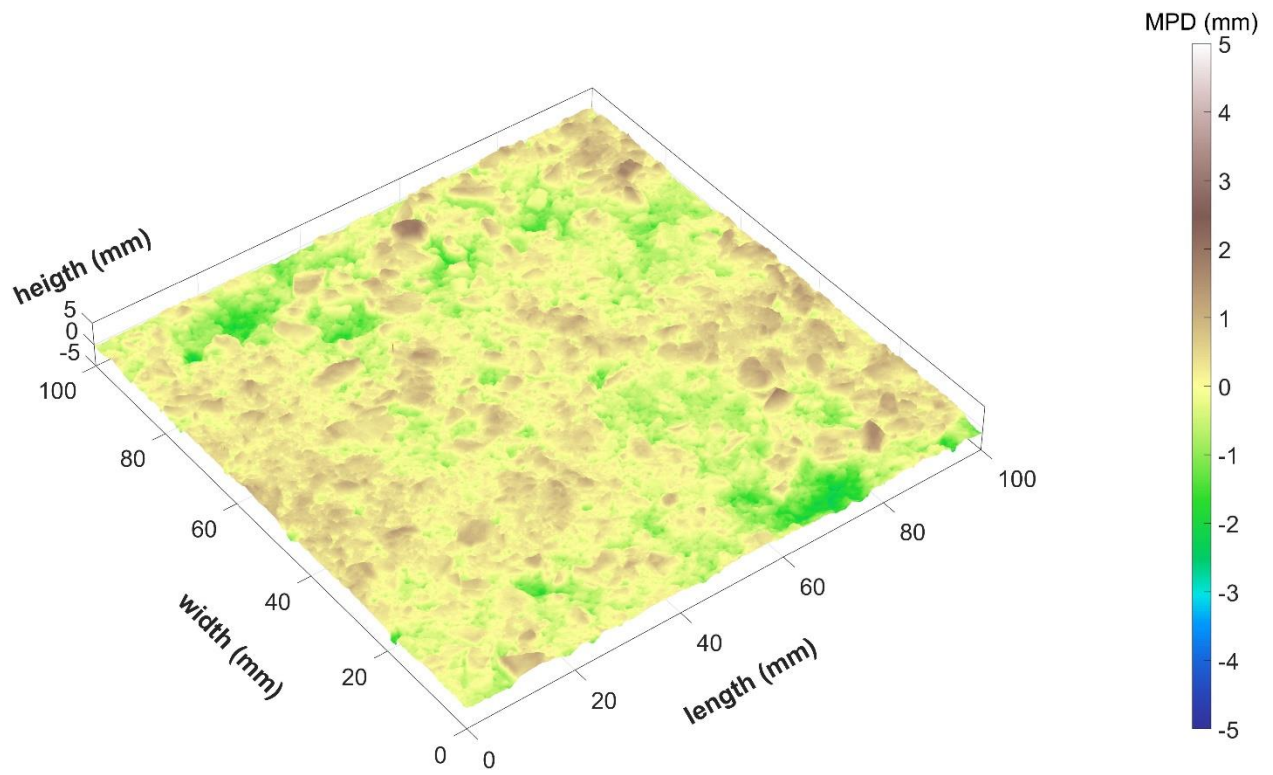


Figure D-92. Microsurfacing-Alt surface scan 78.

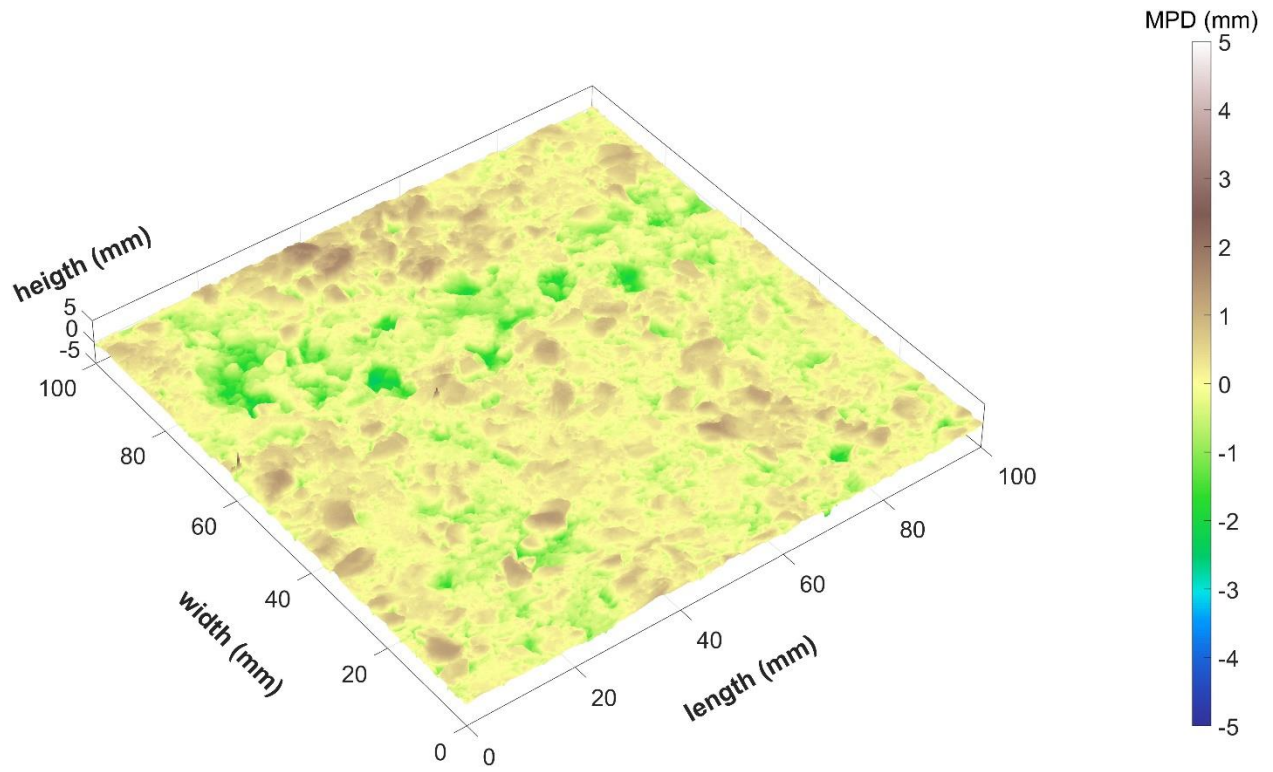


Figure D-93. Microsurfacing-Alt surface scan 79.

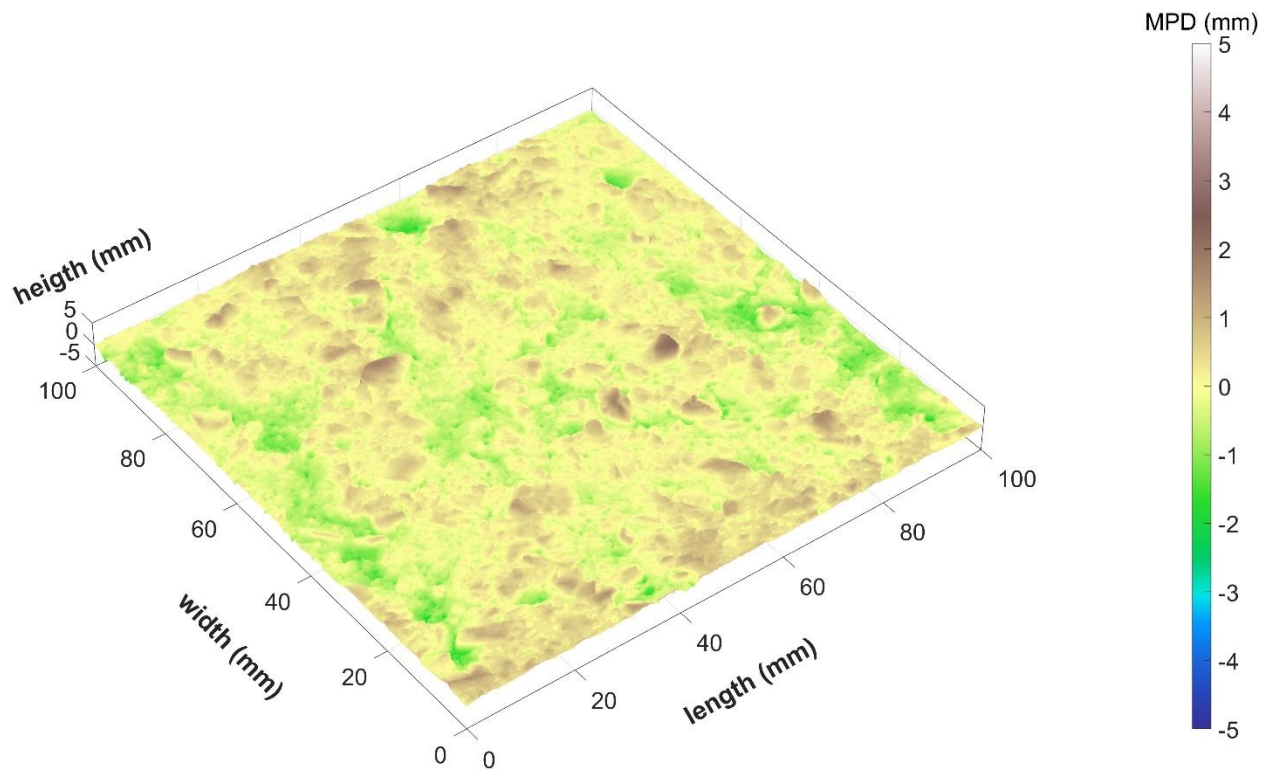


Figure D-94. Microsurfacing-Alt surface scan 80.

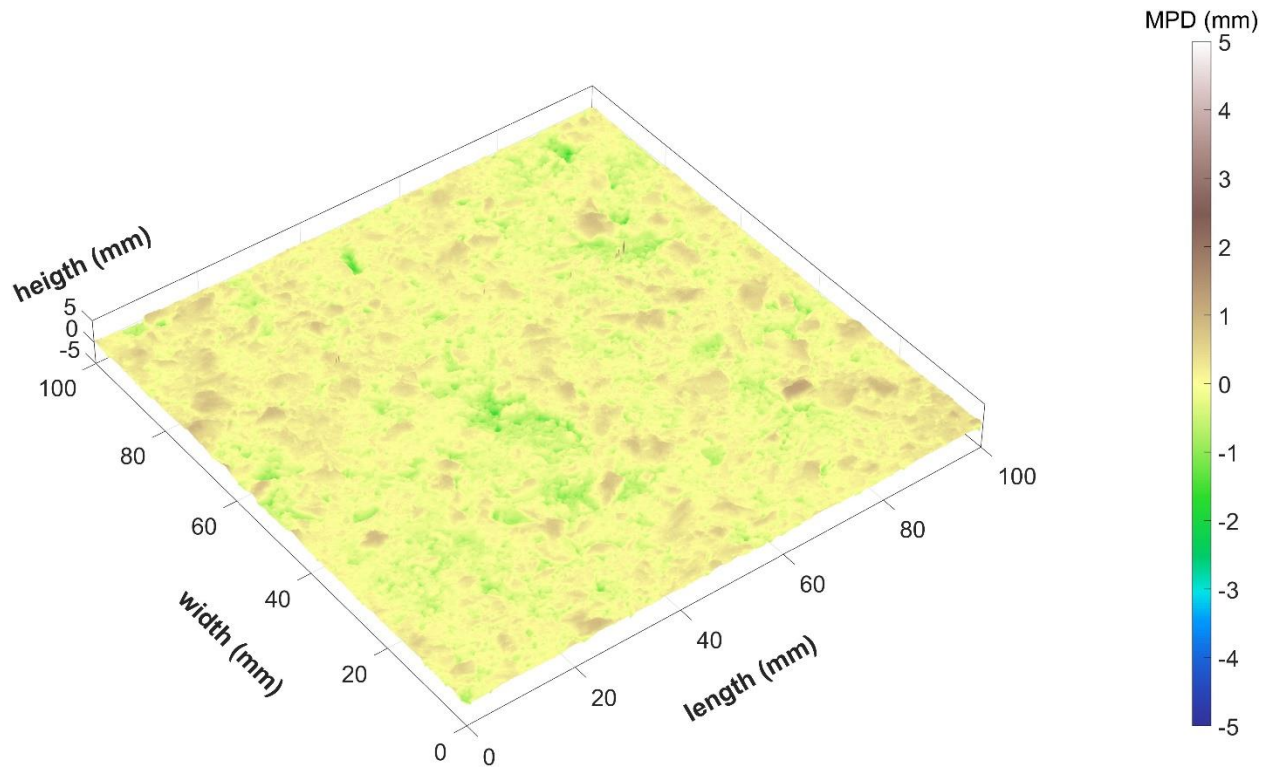


Figure D-95. Microsurfacing-Alt surface scan 81.

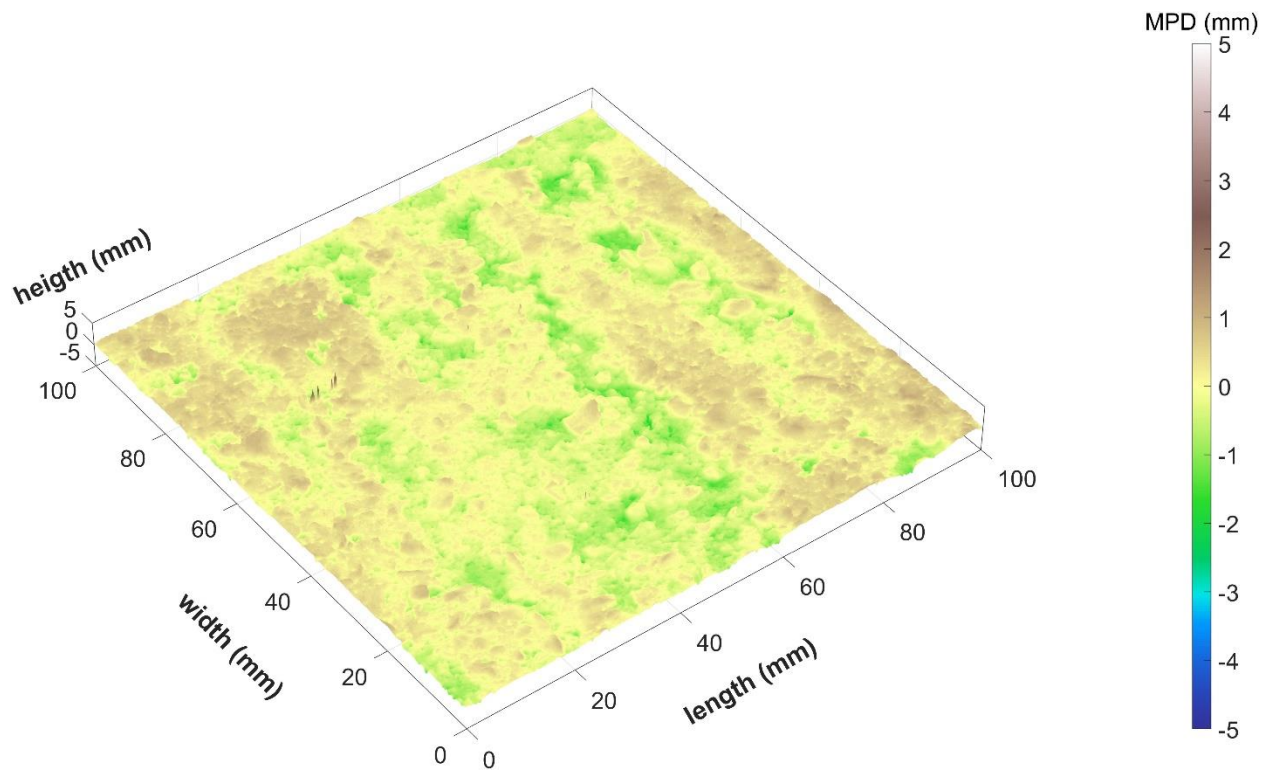


Figure D-96. Microsurfacing-Alt surface scan 82.

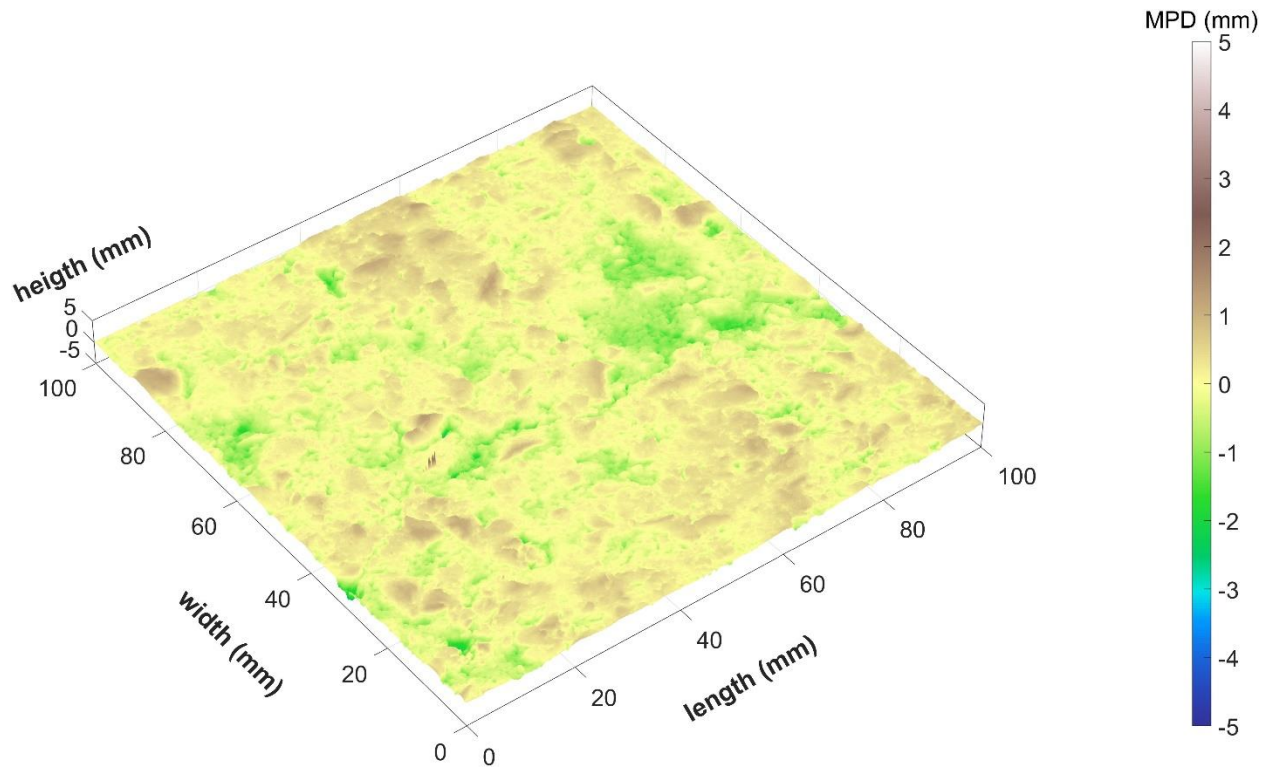


Figure D-97. Microsurfacing-Alt surface scan 83.

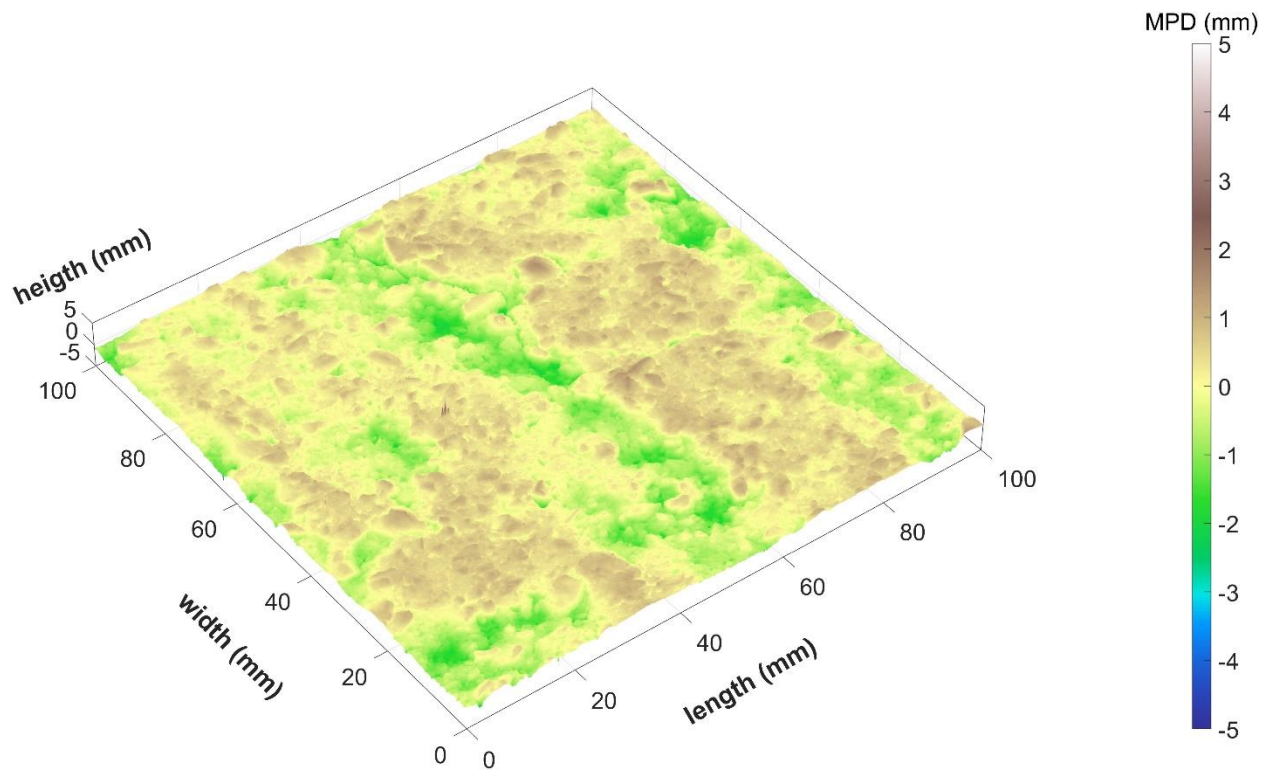


Figure D-98. Microsurfacing-Alt surface scan 84.

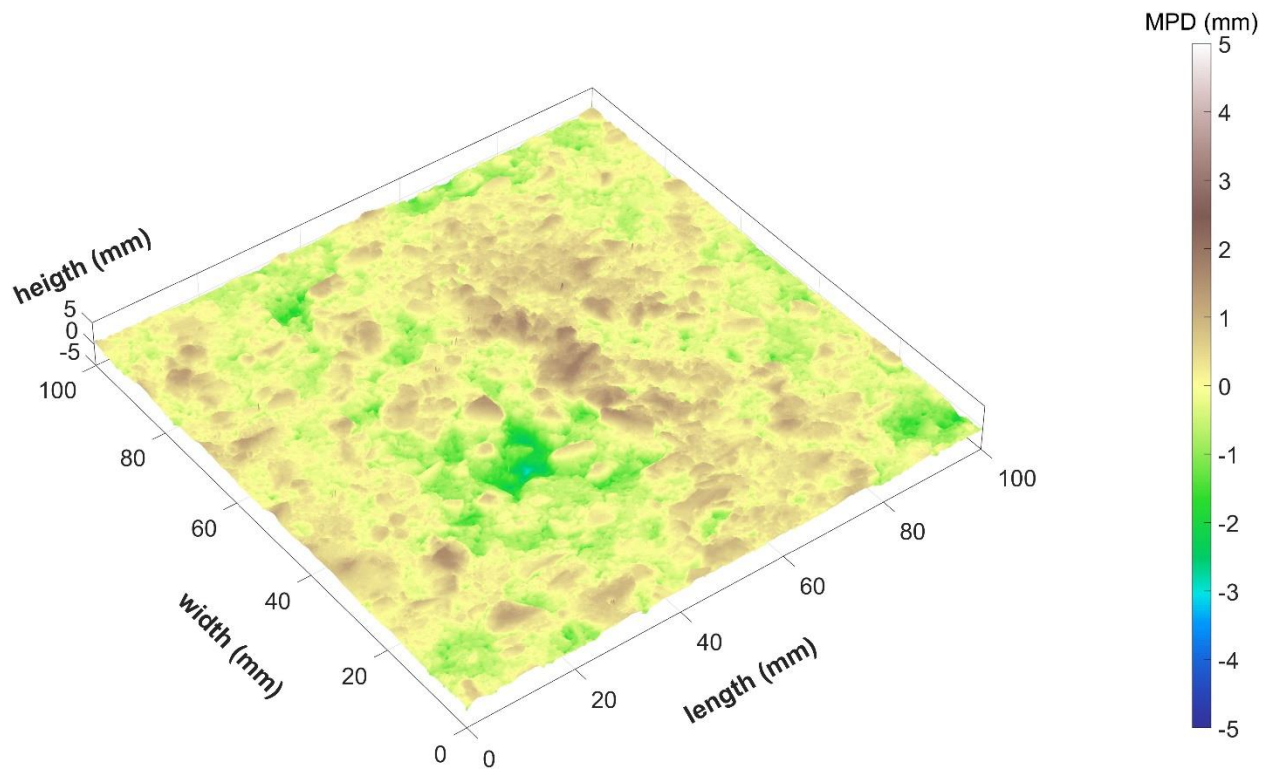


Figure D-99. Microsurfacing-Alt surface scan 85.

APPENDIX E. SPECIFICATION DRAFT FOR THE IMPLEMENTATION OF SMA SURFACE MIX IN NORTH CAROLINA

INTRODUCTION TO THE APPENDIX

This section contains a draft specification for implementing SMA surface mixes in North Carolina. The language, format, and content used in this section closely follow other sections from Division 6 – ASPHALT PAVEMENTS from the 2024 NCDOT Standard Specifications for Road and Structures. The draft specification includes details gathered from the review of SMA specifications in adjacent states. Additionally, this section includes comments by the authors of this report on several aspects of the specification that may require attention or input from the NCDOT Material and Tests unit. In this draft specification, suggested edits to some existing tables in the standard specification are made. In these cases, the existing table number is shown. However, in other cases, new tables are developed and, in these cases, a preceding ‘XXX’ is listed because the exact section number where a potential SMA specification would be inserted is unknown.

DESCRIPTION

Perform the work covered by this section including, but not limited to, the construction of a plant mixed, stone matrix asphalt course (SMA) properly laid upon a prepared surface in accordance with these specifications and in conformity with the lines, grades, thickness, and typical sections shown on the plans; producing, weighing, transporting, placing and rolling the plant mix as specified in Section 610; furnishing the asphalt binder, anti-strip additive, fiber additive, and all other materials for the plant mix; furnishing and applying tack coat as specified; providing QC as specified in Section 609 as modified for SMA; surface testing of the completed pavement; furnishing scales; making any repairs or corrections to the SMA that may become necessary and maintaining the SMA until final acceptance of the project.

MATERIALS

Refer to Division 10.

Item	Section
Anti-Strip Additives	1020-8
Asphalt Binder, Performance Grade	1020-2
Coarse Aggregate	1012-1 (B)
Fine Aggregate	1012-1 (C)
Fiber Additive	1020-10
Hydrated Lime	1020-8
Mineral Filler	1012-1 (D)
Reclaimed Asphalt Pavement (RAP)	1012-1 (F)

Comments

- Section 1012-1 (B) should include a maximum percentage loss of coarse aggregate by Los Angeles abrasion test (AASHTO T 96) of 40%. This recommendation is based on VDOT’s specifications.

- Section 1012-1 (B) should include a maximum absorption value (AASHTO T 85) of 2.0% for SMA mixtures. This recommendation is based on VDOT’s specification.
- Section 1012-1 (C) should specify that the fine aggregates used for SMAs should consist of a blend of 100 percent crushed aggregates. This recommendation is based on VDOT and SCDOT’s specifications.
- Section 1012-1 (D) should specify that the mineral filler or mineral filler blend used in SMAs should have a minimum of 55 percent passing the No. 200 sieve, 95 percent passing the No. 50 sieve, and 100 percent passing the No. 30 sieve. It should also specify that it should be ensured that the mineral filler is sufficiently dry to flow freely and be free from lumps or agglomerations. These recommendations are based on VDOT and SCDOT’s specifications.
- Section 1012-10 should specify that cellulose fiber in either loose or pelletized form must be used for SMAs at a minimum dosage of 0.3 percent by weight of the total mixture. When using pelletized fiber, the dosage rate shall be adjusted to comply with the specified minimum dosage rates for cellulose fiber. The dosage may be increased during production if visual inspection or drain-down testing on plant-produced material indicates that drain-down in excess of 0.30 percent by weight of mixture is occurring. This recommendation is based on VDOT’s specification
- Table 1012-1 should be modified by adding a row specifying the aggregate consensus properties requirements for SMAs. A draft of this modified table appears below. In this table, the requirement on coarse aggregate angularity (ASTM D5821) is based on VDOT’s and SCDOT’s specifications. The requirement on fine aggregate angularity (AASHT T 304) is based on VDOT’s and SCDOT’s specifications. There is no sand equivalent (AASHTO T 176) requirement for SMAs in SCDOT’s and VDOT’s specifications, but a value consistent with S9.5D mixtures is suggested in order to ensure high angularity. The requirement on flat and elongated particles (ASTM D4791) is based on VDOT’s specification.

TABLE 1012-1 AGGREGATE CONSENSUS PROPERTIES				
Mix Type	Coarse Aggregate Angularity	Fine Aggregate Angularity %Minimum	Sand Equivalent % Minimum	Flat and Elongated 5:1 Ratio %Maximum
<i>Test Method</i>	<i>ASTM D5821</i>	<i>AASHTO T 304</i>	<i>AASHTO T 176</i>	<i>ASTM D4791</i>
S4.75A; S9.5B	75/-	40	40	-
S9.5C; I19.0C; B25.0C	95/90	45	45	10
S9.5D	100/100	45	50	10
OGFC	100/100	45	45	10
UBWC	100/85	45	45	10
SMA	100/90	45	50	5

COMPOSITION OF SMA MIXTURE (MIX DESIGN)

(A) General

Design the stone matrix asphalt using a mixture of coarse aggregate, fine aggregate, mineral filler, fiber additives, and liquid asphalt binder mechanically mixed to produce a mix meeting Table XXX-1 and Table XXX-2.

At least 20 days before the start of asphalt mix production, submit the mix design and proposed JMF targets for each required mix type and combination of aggregates to the Engineer for review and approval. The mix design shall be prepared by a mix design technician approved by the Department in an approved mix design laboratory.

The mix design and JMF target values will be established within the mix design criteria specified in Table XXX-2 for the particular type of mixture to be produced.

Comments:

- The content of this section was based on Section 650-3 of NCDOT's Standard Specifications for Road and Structures.

(B) Mix design

Design the stone matrix asphalt (SMA) mixtures conforming to the gradation requirements in Table XXX-1 and the mix design criteria specified in Table XXX-2. An anti-strip additive shall be used in all SMAs. It may be hydrated lime, a chemical additive or a combination of both as needed to meet the retained strength requirements specified in Table XXX-2. When a chemical additive is used, add at a rate of not less than 0.5% by weight of binder in the mix, or as approved by the Engineer. When hydrated lime is used, add a rate of not less than 1.0% by weight of the total dry aggregate. Add the anti-strip additive in accordance with Article 620-3.

Use a fiber additive to prevent asphalt draindown in accordance with Section 1020-10. Add the fiber additive at a dosage rate by weight of total mixture approved by the Engineer.

Use the asphalt binder grade shown in Table XXX-3 depending on the recycled binder ratio. RAS is not permitted in SMA designs.

The recommended plant mix temperature for PG 76-22 binder should be 300 – 325°F. For the PG 70-22, the plant mixing temperatures should be 275 – 305°F. The JMF mix temperature shall be within the ranges shown unless otherwise approved by the Engineer.

In addition to the required mix design submittal, the Contractor shall prepare and deliver gyratory compactor specimens to the Department's Central Asphalt Laboratory for Cantabro Durability testing. The Contractor shall prepare these specimens using lab-produced mix in accordance with NCDOT procedures. Provide the samples at least 20 days before anticipated beginning placement of SMA mixture.

TABLE XXX-1 SMA DESIGN GRADATION		
Graduation Requirements	Total Percent Passing	
Sieve Size (mm)	SMA9.5	SMA12.5
19.0	100	100
12.5	90-100	83-93
9.50	65-75	<80
4.75	25-32	22-28
2.36	15-25	16-24
0.60	-	15-20
0.075	9-11	9-11

TABLE XXX-2 MIX DESIGN CRITERIA SMA9.5 and SMA12.5									
Mix Type	Design ESALs millions ^A	N _{des}	Max. Rut Depth (mm)	Volumetrics ^B			AC %Min	Draindown %Max	TSR ^D %
				VMA %Min	VTM %	VCA ^C (%)			
SMA	>30	75	4.5	18.0	2.0-4.0	<VCA _{DRC}	6.3	0.3	85

- A. Based on 20-year design traffic
- B. Volumetric properties based on specimen compacted at N_{des}
- C. The voids in coarse aggregate (VCA) of the dry rodded condition (DRC) shall be determined by AASHTO T 19.
- D. NCDOT-T-283
- E. Dust-to-binder ratio shall be 1.2-2.0

TABLE XXX-3 SPECIFIED PERFORMANCE GRADE AND MAXIMUM RBR	
Asphalt binder grade	Maximum RBR%
PG 76-22	12

Comments

- The guidelines regarding the type of anti-strip additive specified in NCDOT's Section 610 Asphalt Concrete Plant Mix Pavements are also applied to SMAs. VDOT's SMA specification requires 1.0% hydrated lime as an anti-strip additive, though an alternative additive may be used with the Engineer's approval. Similarly, SCDOT's special provision for SMAs specifies the use of hydrated lime at a rate of 1.0% by weight of dry aggregates. The dosage level for the chemical additive is based on the requirements from Section 650 Open-Graded Friction Courses, which is higher than what is typically used for regular dense-graded mixtures. Additional research is needed to determine a suitable anti-strip dosage level for SMAs.
- The use of fiber additives is specified based on VDOT's and SCDOT's specifications to prevent asphalt binder draindown.
- The SMA design gradation and criteria were mainly based on VDOT's specification, considering that the SMAs produced with this specification exhibited superior friction and texture characteristics compared to the SMA from SCDOT. In general, VDOT's 12.5 mm

gradation band is similar to SCDOT's 12.5 mm band but slightly coarser and narrower. More notable differences lie in the 9.5 mm gradation bands between Virginia and South Carolina, with the latter being finer and wider.

- The number of gyrations specified for the SMA mix design is based on VDOT's specification. This value aligns with NAPA's recommendation for the mix design of SMAs containing aggregates with LA abrasion between 30 and 45.
- A maximum draindown of 0.3% is consistent with SCDOT's and VDOT's SMA specifications.
- A maximum rut depth of 4.5 mm is specified for SMAs. This value is the same as that required for "D" mixes in North Carolina and was selected considering that SCDOT's specification for SMAs requires the same rut depth as their highest-traffic mix design. No rut depth requirement is specified in VDOT's SMA specification.
- A minimum TSR of 80 percent is consistent with NCDOT's requirements for dense-graded mixtures and VDOT's specification for SMAs.
- A dust-to-binder ratio is specified based on VDOT's specifications, which is similar to the values on NCDOT's specification for dense-graded mixtures. SCDOT does not specify a requirement on this property.
- Table XXX-3 was constructed based on VDOT's requirements of asphalt binder grade for different RAP content. The RAP content was converted to RBR, assuming a RAP binder content of 5.0 percent.
- The plant mix temperatures were specified based on the 2018 NCDOT QMS Manual Table 610-1.

PLANT EQUIPMENT

Plants used for preparation of the SMA mixtures shall conform to Article 610-5 and the requirements herein.

Adequate dry storage shall be provided for the fiber additive. Use a separate feed system capable of accurately proportioning the required quantity into the mixture and in such a manner that uniform distribution will be obtained. Interlock the proportioning device with the aggregate feed or weight system so as to maintain the correct proportions for all rates of production and batch sizes. Accurately control the proportioning of the fibers to within $\pm 10\%$ of the amount required. Provide flow indicators or sensing devices for the fiber system that are interlocked with plant controls such as that mixture production will be interruption if introduction of the fiber tails.

When a batch type plant is used, add the fiber to the aggregate in the weight hopper or as approved by the Engineer. Increase the batch dry and wet mixing time by 8 to 12 seconds, or as directed by the Engineer, to assure the fibers are uniformly distributed before the injection of asphalt binder into the mixer. When a continuous mix or dryer-rum type plant is used, add the fiber to the aggregate and uniformly disperse at the point of injection of asphalt binder. Add the fiber in such a manner that it will not become entrained in the exhaust system of the drier or plant.

Comments

- The description provided in this section is mainly adopted from Section 650 Open-Graded Asphalt Friction Course, in which the use and handling of fibers is specified.

Adequate dry storage shall be provided for the mineral filler that will, at minimum, consist of a waterproof cover that shall completely cover the stockpile at all times. Provisions shall be made for metering of the filler into the mixture uniformly and in the desired quantities. In a batch plant, mineral filler shall be added directly into the weight hopper. In a drum plant, mineral filler shall be added directly into the cold feed belt. The equipment shall be capable of accurately and uniformly metering the large amounts of mineral filler up to 25 percent of the total mix.

If the SMA is not to be hauled immediately to the project and placed, the contractor shall provide suitable bins for storage of the hot mixture. Such bins shall be either surge bins to balance the production capacity with hauling and placing capacity or storage bins that are heated and insulated and that have a controlled atmosphere around the mixture. The Engineer will impose limitations on the holding times based on laboratory test results of the stored mixture. In no case shall the SMA be kept in storage for more than 4 hours.

Comments

- The description provided here regarding the handling of the mineral filler and mix storage is based on VDOT's and SCDOT's SMA specifications.
- The storage limit is the stricter of the VDOT (8 hours) and SCDOT (4 hours) specification.
- The handling and storage requirements for mineral filler in VDOT and SCDOT's SMA specifications are more detailed than those for dense-graded mixtures. VDOT's SMA specification, for instance, provides more details regarding the storage and proportioning of the mineral filler, due to the large amounts of mineral filler required for producing SMAs. Additionally, stricter storage time limits are imposed for SMAs compared to dense-graded mixtures. SCDOT allows dense-graded mixtures to be stored for up to 18 hours, whereas VDOT permits a maximum storage time based on the ability of the bins to maintain quality of the mix, with a 10-day limit. For bins without a VDOT-approved heating system, material can be stored for no more than 24 hours.

CONSTRUCTION METHODS

Produce, transport to the site and place the SMA in accordance with Section 610, except as otherwise provided below.

Do not place the SMA between October 31 and April 1 of the next year, unless otherwise approved by the Engineer. The minimum air and road surface temperature for placing SMAs will be 60°F.

Clean the existing surface in an acceptable manner before placement of any asphalt material. For all surfaces to be overlaid, apply tack coat in accordance with Section 605 and the following:

- (A) Use Asphalt Binder PG 58-28, Grade PG 64-22 tack coat material or an approved non-tracking hot applied (NTHA) asphalt tack coat material.
- (B) Uniformly apply the asphalt binder tack coat material at an applied rate of 0.08 gallons per square yard or as deemed necessary by the Engineer.

Comments

- The description given above is based on the construction methods specified in Section 650-5 of NCDOT specification, which shares similarities with some of the construction requirements for SMAs in SCDOT specification. For example, both require the use of a non-tracking material for bonding the layer between the existing riding surface and the SMA, and an application rate of 0.08 gallons per square yard. No details regarding this aspect are provided in VDOT's SMA specification.

Place the SMA course in a manner to prevent segregation and spread and finish as specified in Article 610-8. Roll the SMA as specified in Article 610-9 except that compaction shall be accomplished with steel wheel roller(s) with a minimum weight of 10 tons. A minimum of three rollers shall be available at all times for compaction and/or finishing.

The placed SMA should follow the density requirements specified in Article 610-10. It shall be the Contractor's responsibility to adjust the rolling procedures to provide the specified pavement density.

Comments

- The compaction method is based on Section 650-5 of NCDOT specification considering VDOT's recommendation for the number of rollers used for SMA rolling.
- Table 610-7 of Article 610-10 should be modified to show the target minimum %G_{mm} to be achieved for SMAs. A 94 percent of the maximum theoretical density is recommended by NAPA. A payment schedule is specified in VDOT's specification in which a 100% of payment is given for density levels between 94.0 and 98.0%.

Mix type	Minimum %G_{mm} (Maximum Specific Gravity)
S4.75A	85.0
S9.5B	90.0
S9.5C, S9.5D, I19.0C, B25.0C	92.0
SMA	94.0

Perform this work in accordance with and using equipment meeting Section 9.5 of the *Asphalt QMS Manual*.

Use a Material Transfer Vehicle (MTV) when placing all types of SMAs. Use a MTV meeting Section 9.5.1 of the *Asphalt QMS Manual*.

Remove and replace any part of the finished SMA course that shows non-uniform distribution of asphalt binder, aggregate, or fiber at no additional cost to the Department.

Coordinate plant production, transportation and paving operations such that the uniform continuity of operation is maintained.

Comments

- The description provided in this section is mainly adopted from Section 650 Open-Graded Asphalt Friction Course.

QUALITY MANAGEMENT SYSTEM

Produce the SMA mixture in accordance with Section 609 with the following exceptions. Sample and test the completed mixture from each mix design per plant per year at the following minimum frequency during production:

<u>Accumulative Production Increment</u>	<u>Number of Samples Per Increment</u>
750 tons	1

Record the following data on the standardized control charts and in accordance with the requirements of Section 7.4 of the *Asphalt QMS Manual*:

- (a) Aggregate Gradation Test Results:
 - (i) 2.36 mm
 - (ii) 0.075 mm sieves
- (b) Binder Content, %, P_b
- (c) Voids in Total Mix, %, VTM
- (d) Voids in Mineral Aggregate, %, VMA
- (e) Dust-to-Binder Ratio, $(P_{0.075}/P_{be})$
- (f) Tensile Strength Ratio, %, TSR

Comments

- The accumulative production increment specified is adopted from NCDOT's Section 609 Quality Management System for Asphalt Pavements. This increment is consistent with SCDOT's approach of applying the acceptance criteria used for dense-graded mixtures to SMAs.
- The properties used for mix production control are mainly adopted from NCDOT's Section 609 Quality Management System for Asphalt Pavements. VDOT's SMA specification has additional requirements in the acceptance process. These requirements include checking and reporting the voids in coarse aggregate (VCA) of the mix during production for each gyratory sample, as well as the percentage of flat and elongated particles in the coarse aggregates.

Measurement and Payment

Stone Matrix Asphalt, 9.5 NMAS, and *Stone Matrix Asphalt, 12.5 NMAS* will be measured and paid as the actual number of tons of SMA incorporated into the completed and accepted work. The SMAs will be measured by being weighed in trucks on certified platform scales or other certified weighing devices.

Furnishing asphalt binder for the mix will be paid as provided in Article 620-4 for *Asphalt Binder for Plant Mix*. Adjustments in contract unit price due to asphalt binder price fluctuation will be made in accordance with Section 620.

No direct payment will be made for providing and using the materials transfer vehicle or any associated equipment, as the cost of providing same shall be included in the contract unit bid price per ton for the mixture type to be placed.

Payment will be made under:

Pay Item	Pay Unit
Stone Matrix Asphalt, 9.5 NMAS	Ton
Stone Matrix Asphalt, 12.5 NMAS	Ton

Comments

- The description provided in this section is mainly adopted from Section 650 Open-Graded Asphalt Friction Course and Section 661 Ultra-thin Bonded Wearing Course.

APPENDIX F. SUPPLEMENTARY INFORMATION ON ASPHALT CONCRETE EXPERIMENTS AND ANALYSES

Testing Methods

Dynamic Modulus Test

The dynamic modulus test was conducted according to AASHTO TP 132. The test was conducted on 38-mm-diameter by 110-mm-height specimens at temperatures of 4°C, 20°C, and 40°C. The test was conducted at 10 Hz, 1 Hz, and 0.1 Hz at each test temperature. An on-specimen strain between 50 and 75 macrostrains was maintained for all temperature-frequency combinations to ensure the measurement of only the linear viscoelastic response of the material. All test specimens were compacted to an air void of 5% ± 0.5%. At least three replicates were tested for each mixture.

The time-temperature shift factors used to construct dynamic modulus, $|E^*|$, and phase angle, δ , master curves were obtained based on simultaneous optimization of the storage modulus, E' , to a sigmoidal function as described in AASHTO T 400. Then, the E' master curve was fitted to the two springs, two parabolic elements, and one dashpot (2S2P1D) model. Master curves were constructed at a reference temperature of 21.1°C. Equations (15) to (19) show the mathematical form of the 2S2P1D model, including the storage, loss modulus, and dynamic modulus. FlexMAT™ Cracking v.2.1.4.5 was used as a processing and analysis tool for dynamic modulus test data.

$$E'_{2S2P1D} = E_{00} + \frac{E'_1}{\left(\left(\frac{E'_1}{E_0 - E_{00}} \right)^2 + \left(\frac{E'_2}{E_0 - E_{00}} \right)^2 \right)} \quad (15)$$

$$E''_{2S2P1D} = \frac{E'_2}{\left(\frac{E'_1}{E_0 - E_{00}} \right)^2 + \left(\frac{E'_2}{E_0 - E_{00}} \right)^2} \quad (16)$$

$$E'_1 = (E_0 - E_{00}) \times \left[1 + \delta \times (\omega_R \times \tau_E)^{-\kappa} \times \cos\left(\frac{\kappa\pi}{2}\right) + (\omega_R \times \tau_E)^{-h} \times \cos\left(\frac{h\pi}{2}\right) \right] \quad (17)$$

$$E'_2 = (E_0 - E_{00}) \times \left[\delta \times (\omega_R \times \tau_E)^{-\kappa} \times \sin\left(\frac{\kappa\pi}{2}\right) + (\omega_R \times \tau_E)^{-h} \times \sin\left(\frac{h\pi}{2}\right) + (\omega_R \times \tau_E \times \beta)^{-1} \right] \quad (18)$$

$$|E^*|_{2S2P1D} = \sqrt{(E'_{2S2P1D})^2 + (E''_{2S2P1D})^2} \quad (19)$$

Where E_0 is the maximum storage modulus, E_{00} is the minimum storage modulus, ω_R is the reduced frequency, κ , δ , γ , h , β , and τ_E are fitting coefficients, and E'_{2S2P1D} , E''_{2S2P1D} and $|E^*|_{2S2P1D}$ are the storage, loss, and dynamic modulus from the 2S2P1 D model respectively.

Uniaxial Cyclic Fatigue

The uniaxial cyclic fatigue (CF) was conducted using the AMPT on cylindrical specimens according to AASHTO T 411. The test was conducted on a 38-mm diameter by 110-mm tall specimen at a temperature of 18°C. Each test specimen was conditioned in the AMPT chamber for

40 minutes total. The test used a tension-only actuator controlled sinusoidal displacement at 10 Hz. The strain level for each test was determined in accordance with values recommended in the standard. All the test specimens were compacted to an air void of $5.0 \pm 0.5\%$. The CF test data were analyzed using the Simplified Viscoelastic Continuum Damage (S-VECD) theory using FlexMAT™ Cracking v.2.1.4.5. All the temperatures and strain input values for testing are shown in Table F-1.

Table F-1. Cyclic fatigue test temperatures and input strain for tested mixtures.

Mixture	Specimen ID	Test Temperature (°C)	Input Strain Level
SMA-1A	5-1-1	18	400
	5-1-4	18	380
	5-2-3	18	380
SMA-3	1	18	490
	2	18	540
	3	18	540
	4	18	480

Three key test outcomes were obtained from the CF tests. First, the damage characteristic curve, also referred to as the material integrity (C) versus damage (S) curve, is represented by the power model in Equation (20). Second, the pseudo-energy-based failure criterion, D^R , Equation (21). Third, the apparent damage capacity, S_{app} , Equation (22). This last parameter measures the amount of fatigue damage the material can tolerate considering the effect of the material's toughness and modulus. A higher S_{app} indicates higher fatigue cracking resistance.

$$C = 1 - C_{11}S^{C_{12}} \quad (20)$$

$$D^R = \frac{Sum(1-C)}{N_f} \quad (21)$$

$$S_{app} = 1000^{\frac{\alpha-1}{2}} \frac{a_{T(S_{app})}^{\frac{1}{\alpha+1}} \left(\frac{D^R}{C_{11}} \right)^{\frac{1}{C_{12}}}}{\left| E_{LVE, S_{app}}^* \right|^{\frac{\alpha}{4}}} \quad (22)$$

Where C_{11} and C_{12} are fitting coefficients of the power model, $Sum(1-C)$ is the integral area below the curve of $(1-C)$ versus cycle number until the failure cycle, N_f is the number of cycles to failure, α is the damage growth rate, a_T is the time-temperature shift factor at a given temperature and E_{LVE}^* is the average representative dynamic modulus in kPa. In Equation (22), $\alpha = 1/m + 1$, where m is the maximum log-log slope of the storage modulus master curve.

Indirect Tensile Cracking Test

The indirect tensile cracking test (IDT-CT) was conducted at 25°C following ASTM D8225-19. The test was conducted at a rate of 50 ± 2 mm/mm on 150-mm in diameter and 62-mm height specimens compacted in the Superpave gyratory compactor. Specimens with air void content of $7.0 \pm 0.5\%$ were tested, and the load-displacement curve of the mixture was obtained to calculate the CT_{Index} parameter as expressed in Equation (23).

$$CT_{Index} = \frac{t}{62} \times \frac{l_{75}}{D} \times \frac{G_f}{|m_{75}|} \times 10^6 \quad (23)$$

Where t is the specimen thickness, D is the specimen diameter, l_{75} is the displacement at 75% of the peak load after the peak, G_f is the failure energy, and m_{75} is the slope at 75% peak load after the peak.

Stress Sweep Rutting Test

The stress sweep rutting (SSR) test was used to characterize the resistance to permanent deformation of asphalt mixtures in accordance with AASHTO TP 134-19. The test was conducted on 100-mm diameter and 150-mm height specimens cored and cut from a 150-mm diameter and 180-mm height Superpave gyratory compacted specimens. The low and high temperatures (T_L and T_H) were determined using the long-term pavement performance bind (LTPPBind) online web-based tool. The low and high temperatures in this study were 29°C and 51°C, respectively. Three deviatoric stress levels, with 200 cycles each, were applied at each temperature in the following pattern: 483 kPa, 689 kPa, and 895 kPa at 29°C, and 689 kPa, 483 kPa, and 895 kPa at 51°C. The loading pulses had a duration of 0.4 s and were followed by a rest time of 3.6 s at 51°C and 1.6 s at 29°C. The test specimens were subjected to a confining pressure of 69 kPa.

Experimental Results and Discussions

Introduction

This section presents the experimental results obtained during this study and results from the data analysis using FlexMAT. This section compares the SMAs with respect to the dense-graded mixtures from the Coastal and Mountain regions, as the comparison with Piedmont region mixes is covered in Chapter 4. It should be noted that while this comparison is necessary for a comprehensive understanding of how the SMA designs perform relative to dense-graded mixtures, the NCDOT RP 2019-20 dataset lacks “D” mixtures from the Coastal and Mountain regions, which would serve as the most appropriate benchmark for the SMAs.

Dynamic Modulus Test Results

Figure F-1 and Figure F-2 present the dynamic modulus master curves in logarithmic and semi-logarithmic scales and the phase angle master curves for the SMAs and surface mixtures from the Coastal and Mountain regions, respectively, at a reference temperature of 21.1°C. It also includes the 2S2P1D model fitting of the dynamic modulus and phase angle, obtained using FlexMAT Cracking v2.1.4.5. The detailed dynamic modulus values of the surface mixtures from the Coastal and Mountain regions are presented in Table F-2 and Table F-3, respectively. Figure F-1 shows that the SMA-1A has moduli values like the RS9.5B-CO and RS9.5C-CO mixtures across the entire frequency range, while the SMA-3 mixture exhibits a slightly softer behavior (higher phase angle), especially at the high-temperature frequency range. Figure F-2 shows that SMA-1 mixture exhibits similar linear viscoelastic properties to the RS9.5B-MO while the SMA-3 behaves similarly to the RS9.5C-MO.

The collective analysis of the linear viscoelastic properties of the SMAs relative to dense-graded mixtures indicates that the two SMA designs evaluated behave similarly to mixes with “B” and “C” categories from North Carolina, independently of the climatic region of interest. This finding would suggest that SMAs could be potentially used in settings where “B” and “C” mixtures are

typically used. However, “B” and “C” mixtures are often placed in locations where the friction demand may not justify using an SMA, as it can lead to higher costs without significant performance benefits.

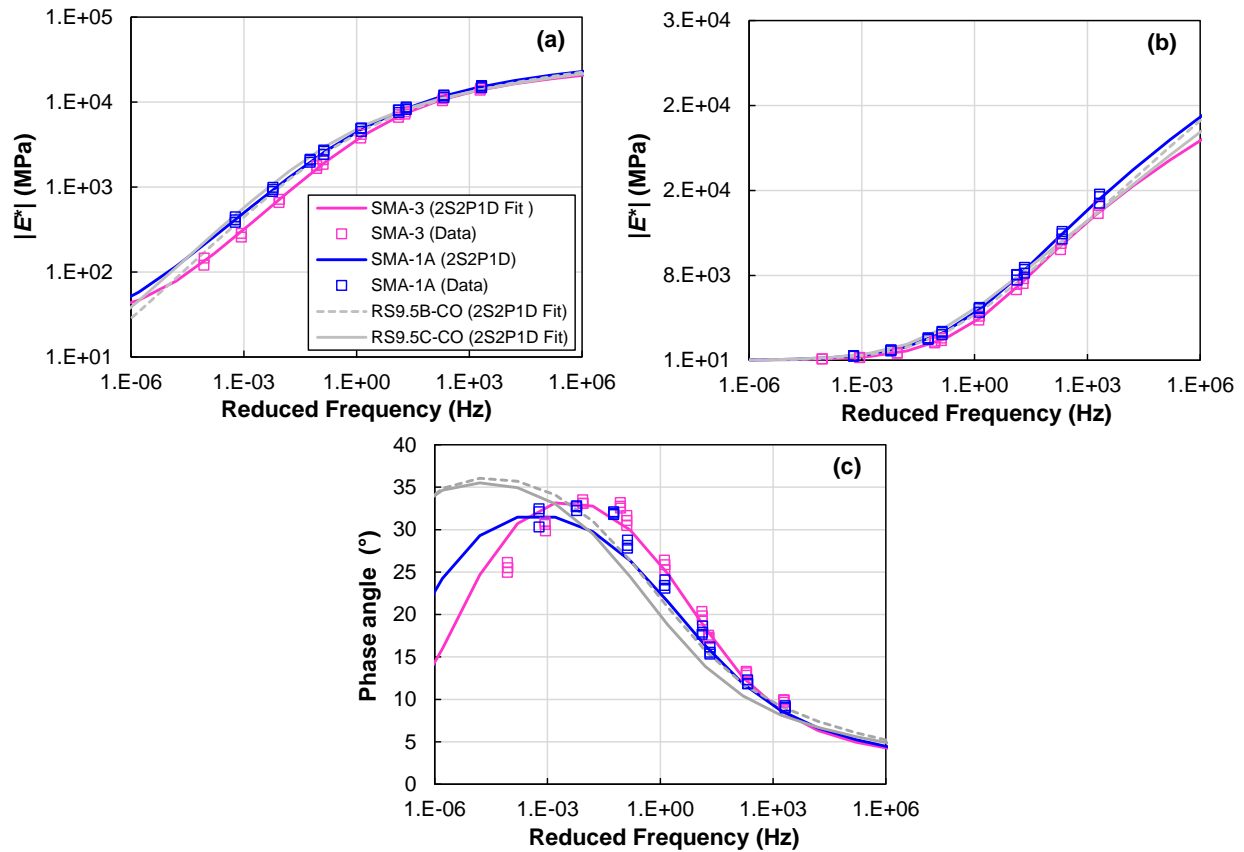


Figure F-1. Dynamic modulus and phase angle results for SMAs and surface mixtures from the Coastal region: (a) dynamic modulus master curve log-log plot, (b) dynamic modulus master curve semi-log plot, and (c) phase angle master curve.

Table F-2. Dynamic modulus results.

Mixture	4°C- 10Hz	4°C- 1Hz	4°C- 0.1Hz	20°C -10Hz	20°C- 1Hz	20°C- 0.1Hz	40°C- 10Hz	40°C -1Hz	40°C -0.1Hz
CO_RS9.5B	14668	11448	8459	7398	4582	2506	1878	836.4	328.5
	15519	12209	9076	7770	4858	2706	1982	879.9	353.8
	14666	11452	8484	7355	4540	2491	1862	822.6	329.9
CO_RS9.5C	15110	12315	9577	8423	5612	3317	2429	1132	474.2
	14528	11749	9037	7583	4917	2810	2129	958.9	398.7
	14959	12068	9313	8011	5236	3035	2218	993.9	400.9
SMA-1A	14810	11427	8224	8093	4984	2739	2132	995	448
	15660	12144	8760	8045	4882	2643	2072	941	413
	15412	11923	8569	7561	4528	2424	1960	890	384
SMA-3	13830	11019	7693	7157	4167	2102	718	285	146
	14008	10424	7238	6647	3784	1856	658	258	120
	14589	10673	7462	6639	3825	1899	691	281	144

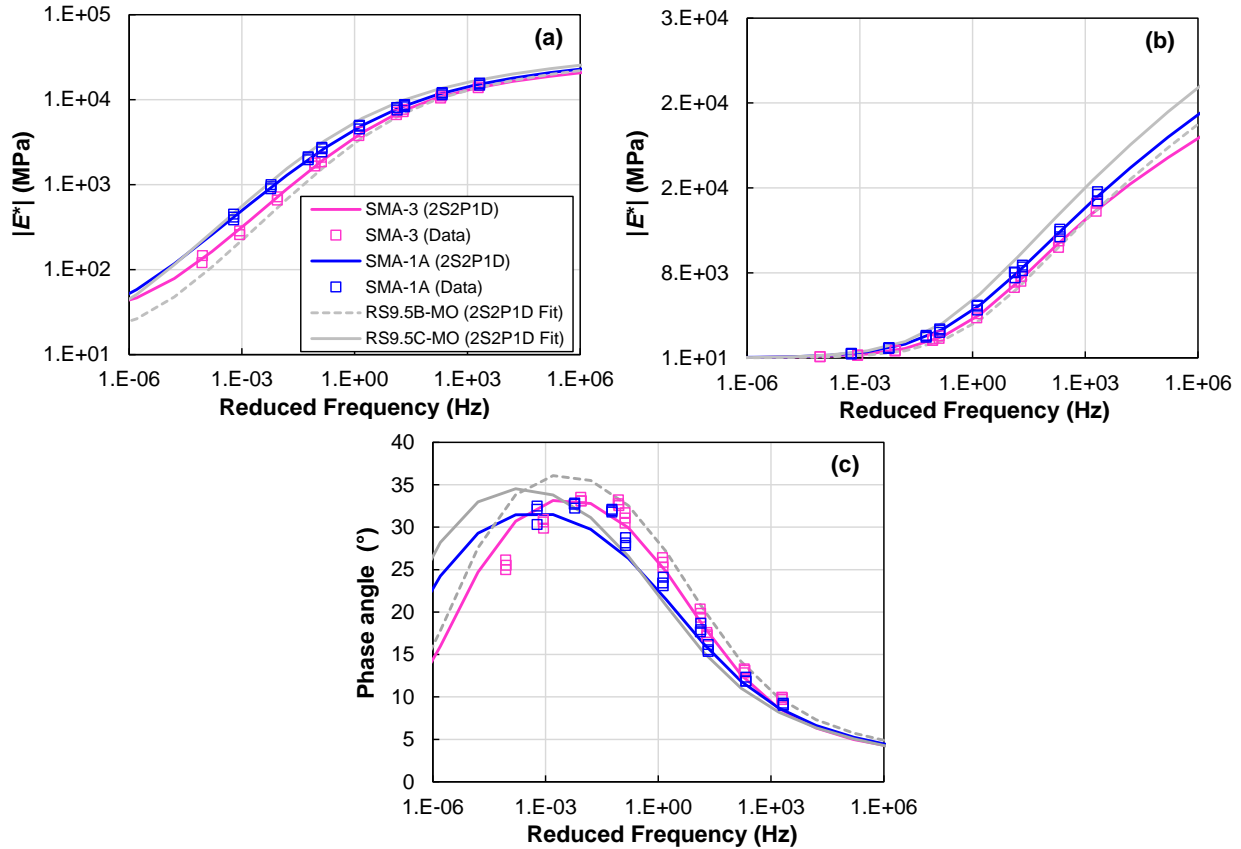


Figure F-2. Dynamic modulus and phase angle results for SMAs and surface mixtures from the Mountain region: (a) dynamic modulus master curve log-log plot, (b) dynamic modulus master curve semi-log plot, and (c) phase angle master curve.

Table F-3. Dynamic modulus results.

Mixture	4°C - 10 Hz	4°C - 1 Hz	4°C - 0.1 Hz	20°C - 10 Hz	20°C - 1 Hz	20°C - 0.1 Hz	40°C - 10 Hz	40°C - 1 Hz	40°C - 0.1 Hz
MO_RS9.5B	14114	10406	7029	6200	3373	1550	1201	450.7	181.6
	14537	10832	7359	6407	3489	1612	1203	443.7	162.6
	14637	10926	7480	6506	3561	1652	1268	481.1	201.3
MO_RS9.5C	17472	13830	10251	9303	5855	3222	2515	1096	473.4
	17905	14240	10639	9393	5949	3312	2507	1091	450.7
	17698	14135	10600	9208	5766	3171	2400	1032	427.4
SMA-1A	14810	11427	8224	8093	4984	2739	2132	995	448
	15660	12144	8760	8045	4882	2643	2072	941	413
	15412	11923	8569	7561	4528	2424	1960	890	384
SMA-3	13830	11019	7693	7157	4167	2102	718	285	146
	14008	10424	7238	6647	3784	1856	658	258	120
	14589	10673	7462	6639	3825	1899	691	281	144

Uniaxial Cyclic Fatigue Test Results

The results from the uniaxial cyclic fatigue test are presented in Figure F-3 for the SMAs and surface mixtures from the Coastal and Mountain regions. The results shown in Figure F-3 (a) and (c) demonstrate that both SMA designs closely follow the same damage characteristic curve of the

dense-graded mixtures from these regions. This observation is anticipated since the positioning in the C versus S plot is related to the moduli of the mixtures, shown in Figure F-1 and Figure F-2.

Figure F-3 (b) and (d) shows the relationship between the cumulative reduction in pseudo-stiffness ($1-C$) and the number of cycles, and the slope of such relationship, D^R . A higher D^R generally indicates a superior ability to absorb energy before failure. The results suggest that the SMAs mixtures have D^R similar or superior to the ‘B’ and ‘C’ mixtures from the Coastal and Mountain regions. Although both SMAs exhibit similar damage characteristic curves to the dense-graded mixtures, they have D^R significantly higher values than the RS9.5B and RS9.5C mixes from the Mountain region. This result indicates that the SMA mixtures possess superior damage tolerance, likely due to features such as their interlocking aggregate structure, use of polymer-modified binders, and others.

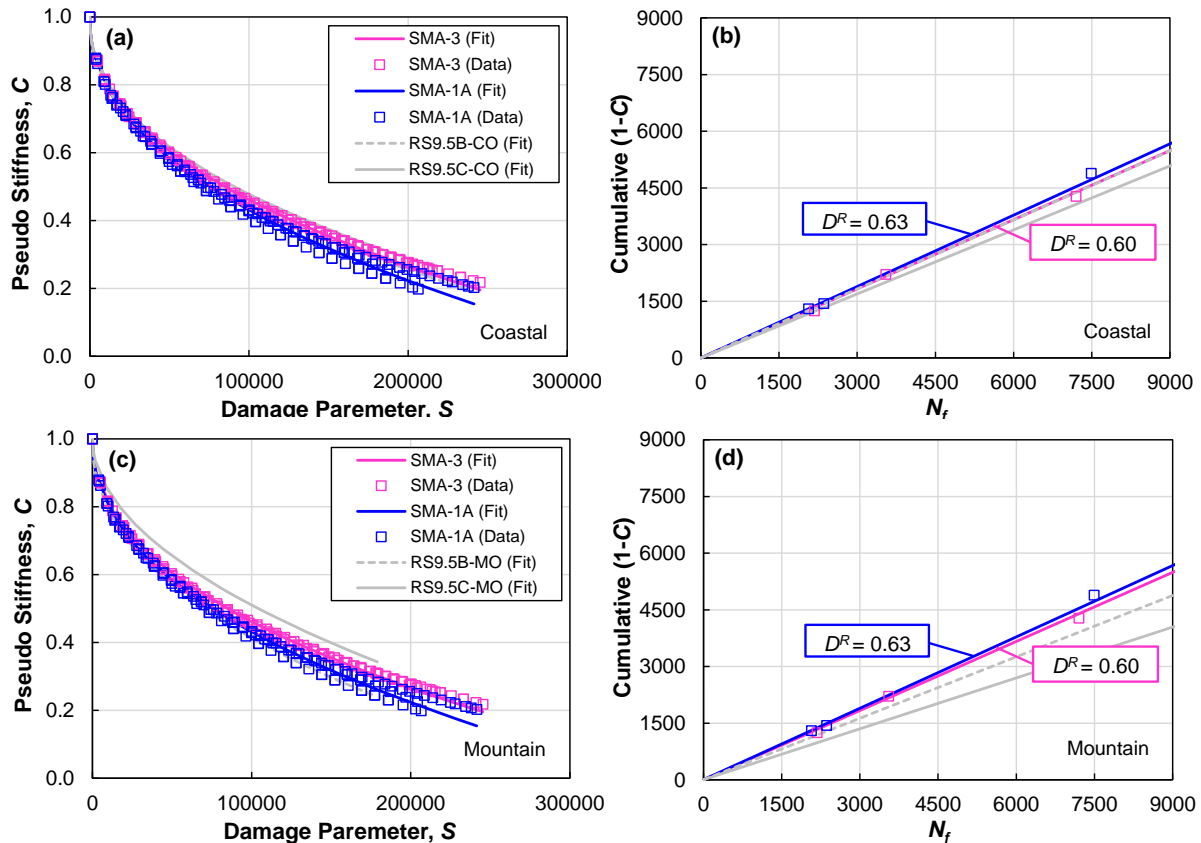


Figure F-3. Cyclic fatigue test results for SMAs and surface mixtures: (a) damage characteristic curve for Coastal region, (b) failure criteria plot for Coastal region, (c) damage characteristic curve for Mountain region, and (d) failure criteria plot for Mountain region.

Table F-4. Linear viscoelastic and FlexPAVE™ S-VECD fatigue properties.

Properties	RS9.5B-CO	RS9.5C-CO	RS9.5B-MO	RS9.5C-MO	SMA-1A	SMA-3
α	3.47	3.51	3.44	3.57	3.80	3.65
C_{11}	0.0034	0.0030	0.0036	0.0015	0.0031	0.0031
C_{12}	0.44	0.45	0.44	0.51	0.45	0.44
a_1	0.0008	0.0008	0.0007	0.0006	0.0004	0.0007
a_2	-0.14	-0.14	-0.13	-0.13	-0.12	-0.12

Indirect Tensile Cracking Test

The discussion of the IDT-CT results is presented in Section 4.2.3. The detailed parameters obtained from the IDT-CT test are presented in Table F-5.

Table F-5. Detailed IDT-CT results.

Mixture	Target air void (%)	G_f (kN mm)	l_{75}	m_{75}	CT_{Index}
SMA-1A	7.0	93.6	4.3	3.0	98
SMA-3	7.0	93.5	5.7	2.5	155
RS9.5B-CO	5.0	76.4	3.4	8.2	23
RS9.5C-CO	5.0	75.2	3.4	8.7	22
RS9.5B-PI	5.0	73.3	3.7	6.0	32
RS9.5C-PI	5.0	63.6	3.4	6.4	24
RS9.5D-PI	5.0	62.9	2.9	9.1	15
RS9.5B-MO	5.0	89.3	4.2	5.3	51
RS9.5C-MO	5.0	79.5	3.0	11.1	15

G_f : Work of fracture

l_{75} : displacement at 75% of the peak load after the peak

m_{75} : slope at 75% peak load after the peak.

As mentioned earlier and shown in Table F-5, the IDT-CT test conducted as part of the NCDOT RP 2019-12 project used specimens compacted at 5.0% air voids, while the SMAs were tested at a target air void content of 7.0%. Montanez *et al.* (2023) developed and verified correction methods to normalize CT_{Index} results of specimens tested at different air void contents and thicknesses (not relevant in this study). The method to obtain equivalent CT_{Index} values at a reference air void of 7.0% consists of dividing $CT_{Index, Measured}$ value by a factor called $CF_{AV,E}$, given by Equation (24).

$$CF_{AV,E} = 0.151e^{0.255AV} \quad (24)$$

Where AV corresponds to the air void level used in the test (5.0% in this case). In this study, $CF_{AV,E}$ is equal to 0.54. Then, the values of the dense-graded mixes shown in Table F-5 are divided by 0.54 to obtain an equivalent CT_{Index} value at 7.0% air voids, which are shown in Section 4.2.3. The tabulated results are presented in Table F-6.

Table F-6. Corrected CT_{Index} values.

Mixture	Air void (%)	$CF_{7,E}$	$CT_{Index, Measured}$	$CT_{Index, 7\%}$
RS9.5B-CO	5.0	0.54	23	42
RS9.5C-CO	5.0	0.54	22	40
RS9.5B-PI	5.0	0.54	32	60
RS9.5C-PI	5.0	0.54	24	45
RS9.5D-PI	5.0	0.54	15	29
RS9.5B-MO	5.0	0.54	51	94
RS9.5C-MO	5.0	0.54	15	29

Stress Sweep Rutting Test

The results of the stress sweep rutting test are presented in Figure F-4 for the three climatic regions evaluated. This section only presents the RSI, excluding the evolution of the viscoplastic strain, because the test temperatures of the dense-graded mixtures from the Coastal and Mountain regions differ from those used for the SMAs. Overall, the comparison between the RSI of the SMAs to the

dense-graded mixtures from the Coastal and Mountain supports the earlier findings that SMAs exhibit similar or better rutting performance than “B” and “C” mixtures from North Carolina.

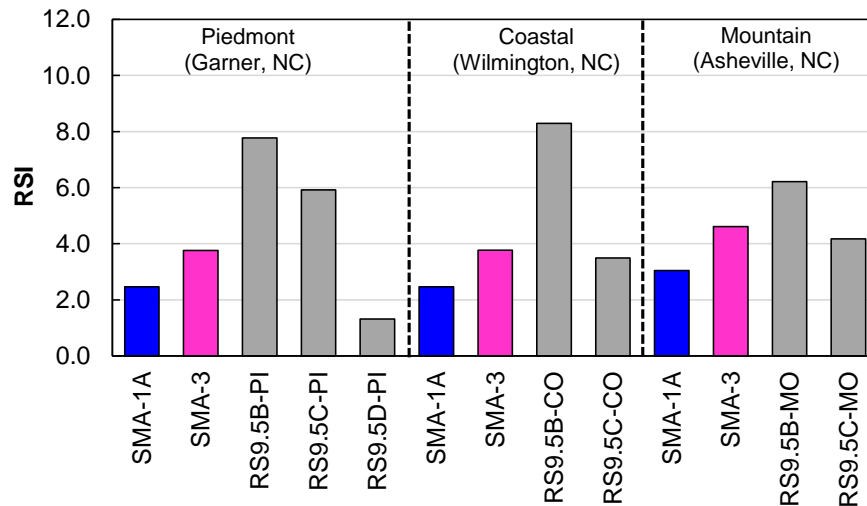


Figure F-4. RSI results for SMA and dense-graded mixtures.

Statistical Comparison

Statistical analyses were conducted to determine if the performance differences between the SMAs and dense-graded mixtures in North Carolina are significant. This analysis compared dynamic modulus values ($|E^*|$) at 18°C and 10 Hz, D^R , S_{app} , and CT_{Index} . Dunnett’s test was used for a one-to-many statistical comparison, with dense dense-graded mixtures as the benchmark against each SMA design. Dunnett’s test was chosen over Tukey’s test to focus on the comparison with SMAs rather than among dense-graded mixtures. A 95% confidence level ($\alpha = 0.05$) was set for statistical significance for all parameters. Bartlett’s test was performed to assess homoscedasticity before Dunnett’s test was conducted. The results indicated that all datasets evaluated follow a similar distribution.

Table F-7 shows the p -values from Dunnett’s test results for each parameter. A p -value less than 0.05 indicates that the difference in the materials’ properties is statistically significant. For instance, the D^R of SMA-3 is significantly different from the D^R value of the RS9.5B-MO mix at a confidence level of 95%, with a p -value of 0.0124 (less than 0.05).

The statistical results suggest that the SMAs are significantly different in all the properties tested except in terms of D^R , highlighting the impact of the different design considerations in the specifications that control the two designs evaluated. Additionally, both SMAs have significantly different cracking performances compared to the RS9.5B mixtures, based on the cracking performance indices CT_{Index} and S_{app} . The results also show some mixed trends in terms of $|E^*|$ and D^R compared to the “B” mixture, which aligns with findings from the FHWA/NC 2020-12 project that North Carolina mixtures of the same classification exhibit differences in performance measures.

Furthermore, the SMAs seem to behave more distinctly compared to the “C” mixes than to the “B” mixes, especially the SMA-3 design, which is statistically different from all the “C” mixtures except for the RS9.5C-CO in terms of D^R . Finally, the statistical results confirm that both SMAs

are significantly different from the RS9.5D-PI in terms of cracking performance, as indicated by both S_{app} and CT_{Index} , although no difference is observed in terms of D^R .

Table F-7. p-values obtained from Dunnett’s test.

Property	Control Group	RS9.5B			RS9.5C			RS9.5D	SMA 3	SMA 1A
		MO	PI	CO	MO	PI	CO	PI		
$ E^* $ @18°C, 10 Hz	SMA-3	0.5269	<.0001	0.0640	<.0001	0.0467	0.0021	<.0001	-	<.0001
	SMA-1A	<.0001	<.0001	0.0513	0.0012	<.0001	0.5808	0.9445	<.0001	-
D^R	SMA-3	0.0124	0.0065	1.0000	<.0001	0.0057	0.1616	0.46008	-	0.9001
	SMA-1A	0.0023	0.0693	0.8722	<.0001	0.0870	0.0311	0.0979	0.8766	-
CT_{Index}	SMA-3	<.0001	<.0001	<.0001	<.0001	<.0001	<.0001	<.0001	-	<.0001
	SMA-1A	0.8752	<.0001	<.0001	<.0001	<.0001	<.0001	<.0001	<.0001	-
S_{app} Mountain	SMA-3	<.0001	-	-	<.0001	-	-	-	-	<.0001
	SMA-1A	0.0003	-	-	<.0001	-	-	-	<.0001	-
S_{app} Piedmont	SMA-3	-	<.0001	-	-	<.0001	-	<.0001	-	<.0001
	SMA-1A	-	<.0001	-	-	<.0001	-	0.1749	<.0001	-
S_{app} Coastal	SMA-3	-	-	0.0143	-	-	<.0001	-	-	<.0001
	SMA-1A	-	-	0.0004	-	-	0.1757	-	<.0001	-

Expected Life Extension

As indicated in Chapter 4, the results of the pavement performance simulations were used to determine life ratio extensions achieved by using SMAs instead of dense-graded mixtures as surface layers in North Carolina pavement structures. The methodology consisted of identifying the year when each SMA reached the same percent damage value as the RS9.5D-PI mixture at a point when major rehabilitation is needed. The expected life extension for each of the structure configurations evaluated are summarized in Table F-8 for the SMA-1 and SMA-3. As shown, except for the SMA-1 when used with a thin structure the SMA always have a higher expected life than the dense-graded surfaces.

Table F-8. Life extension of the SMA-1 versus RS9.5D.

Structure type	Thickness type	SMA-1 vs. RS9.5D			SMA-3 vs. RS9.5D		
		Critical year			Critical year		
		8	12	16	8	12	16
FDA	Thin	-1.0	-1.1	-1.1	0.1	0.9	1.3
	Intermediate	1.6	1.7	1.5	3.1	3.6	3.8
	Thick	1.1	1.0	0.7	2.2	2.5	2.4
ABC	Thin	1.5	1.8	1.5	8.9	10.5	11.7
	Intermediate	1.7	1.9	1.7	5.1	5.8	6.4
	Thick	1.8	2.1	1.9	5.4	6.2	6.8
DS	Thin	0.3	0.1	-0.3	1.6	1.8	1.8
	Intermediate	1.9	1.9	1.6	3.6	4.0	4.2
	Thick	1.5	1.5	1.2	3.1	3.4	3.5

APPENDIX G. SUPPLEMENTARY INFORMATION ON PAVEMENT SIMULATIONS

The performance of reference and current materials was evaluated through 117 pavement simulations using FlexPAVE v2.2. The results of the simulations over a 20-year analysis period are presented in Figure G-1 to Figure G-8 for the Piedmont, Coastal, and Mountain regions in North Carolina.

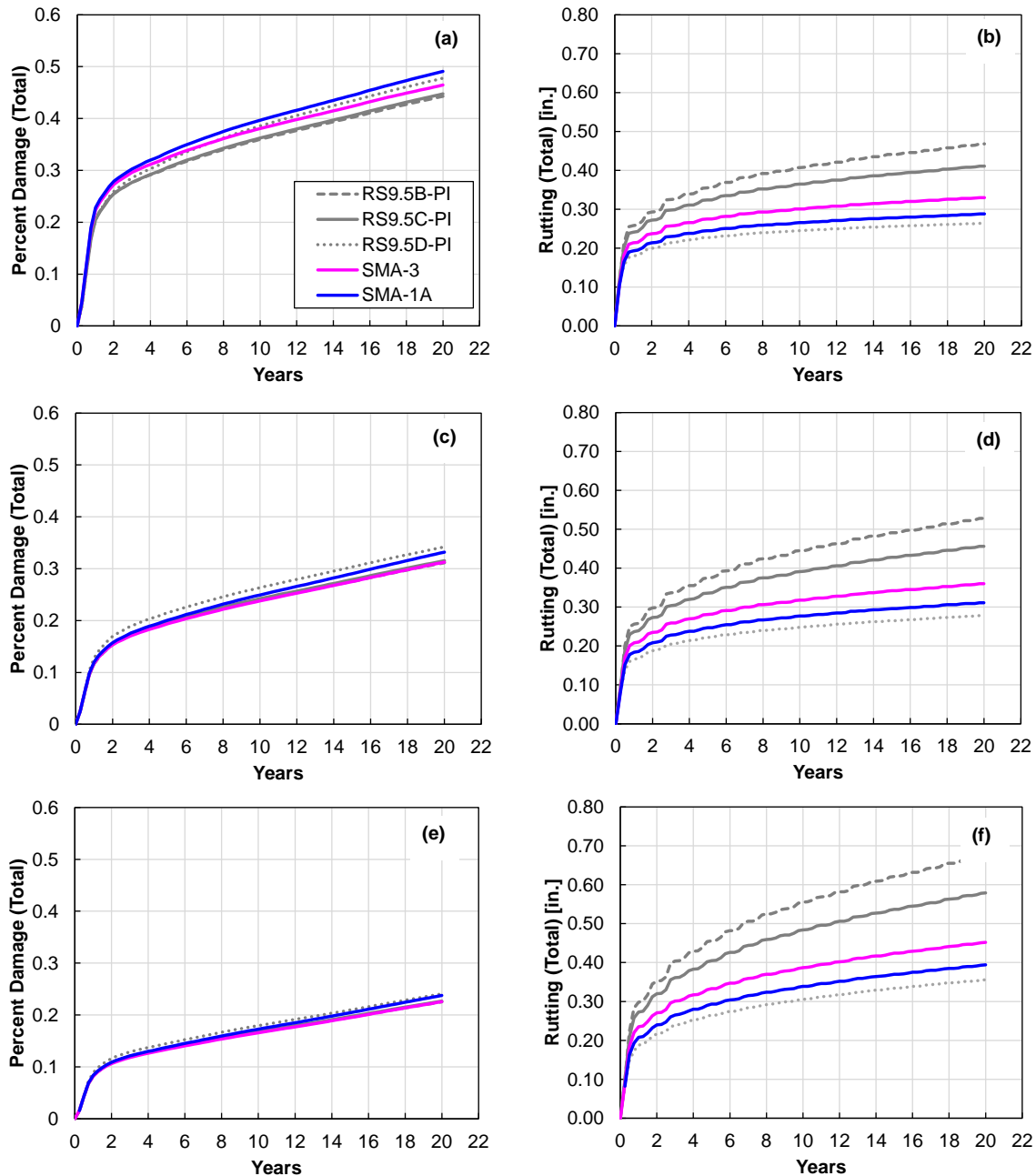


Figure G-1. Pavement performance simulation results for NC Piedmont region and FDA structures: (a) total percent damage - thin structure, (b) total rutting - thin structure, (c) total percent damage - intermediate structure, (d) total rutting damage – intermediate structure, (e) total percent damage – thick structure, and (f) total rutting – thick structure.

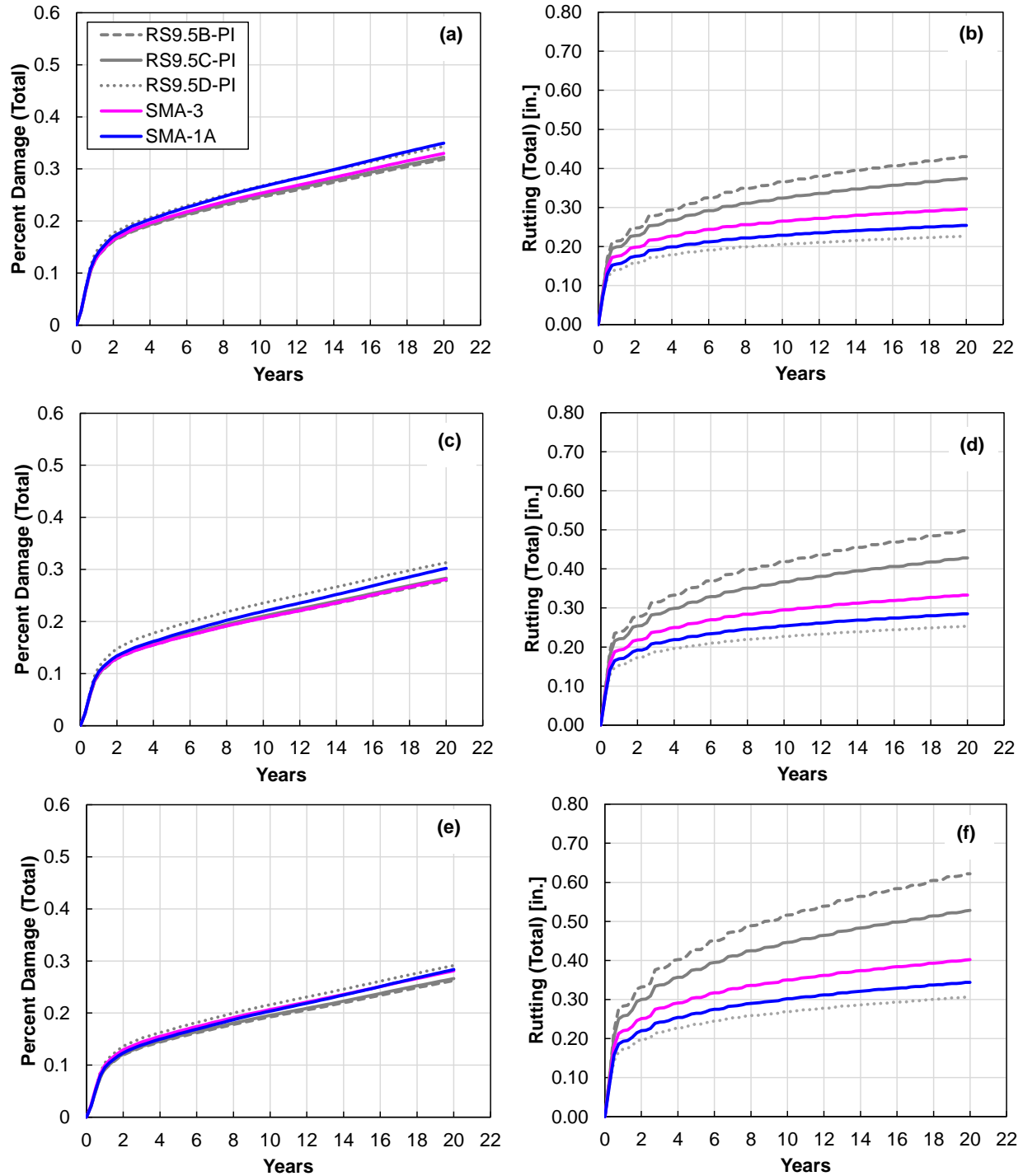


Figure G-2. Pavement performance simulation results for NC Piedmont region and DS structures: (a) total percent damage - thin structure, (b) total rutting - thin structure, (c) total percent damage - intermediate structure, (d) total rutting damage – intermediate structure, (e) total percent damage – thick structure, and (f) total rutting – thick structure.

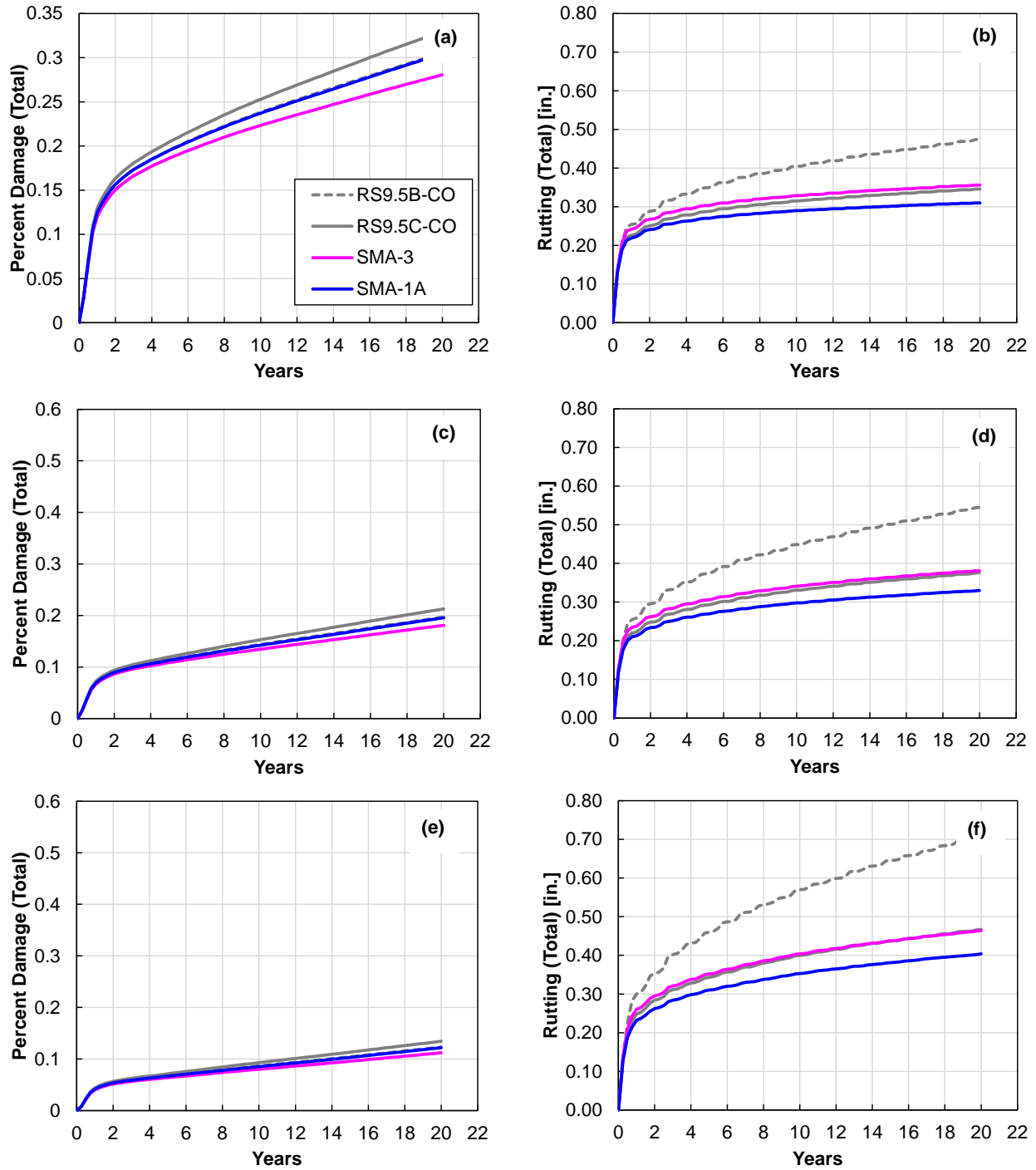


Figure G-3. Pavement performance simulation results for NC Coastal region and FDA structures: (a) total percent damage - thin structure, (b) total rutting - thin structure, (c) total percent damage - intermediate structure, (d) total rutting damage – intermediate structure, (e) total percent damage – thick structure, and (f) total rutting – thick structure.

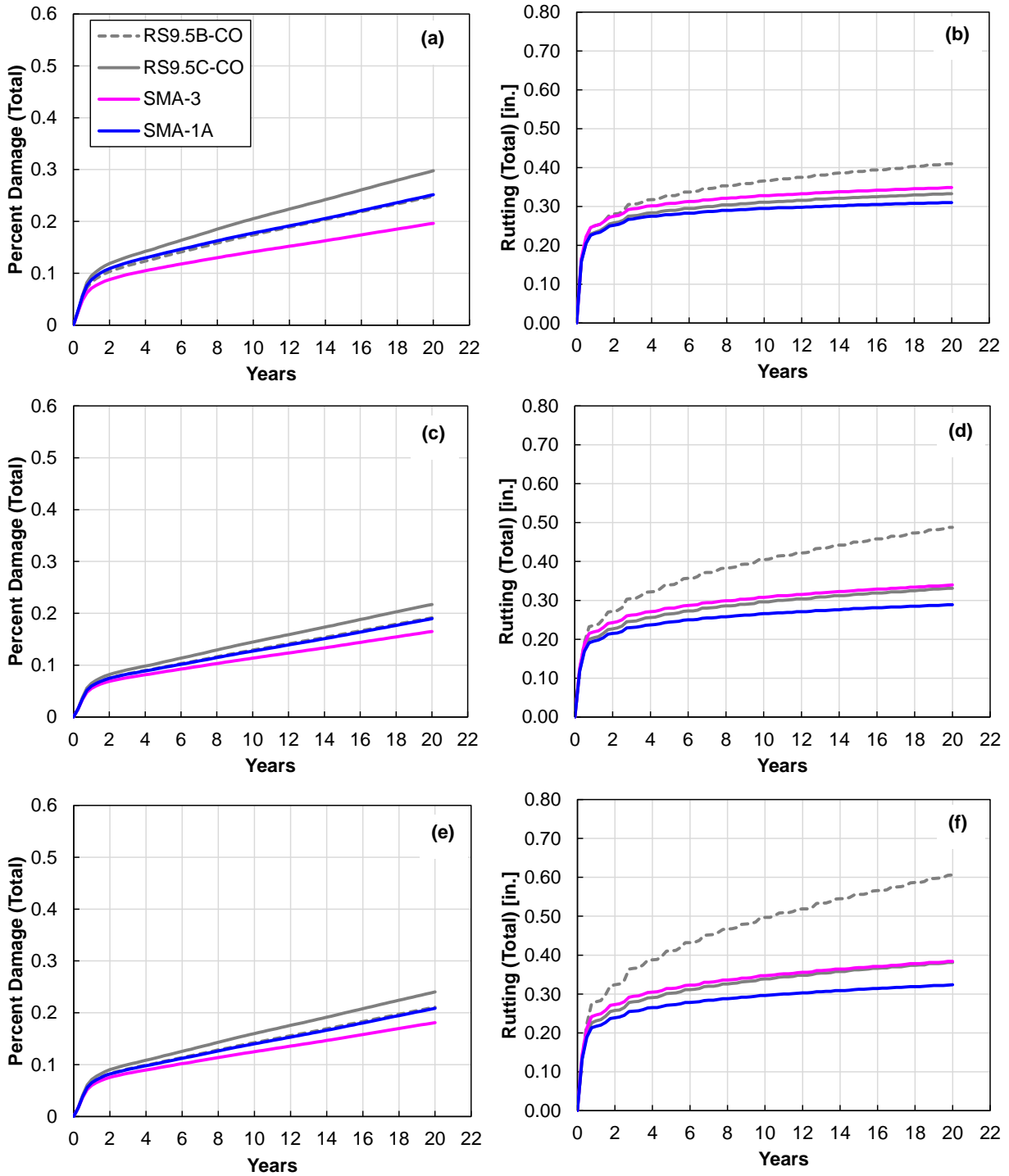


Figure G-4. Pavement performance simulation results for NC Coastal region and ABC structures: (a) total percent damage - thin structure, (b) total rutting - thin structure, (c) total percent damage - intermediate structure, (d) total rutting damage – intermediate structure, (e) total percent damage – thick structure, and (f) total rutting – thick structure.

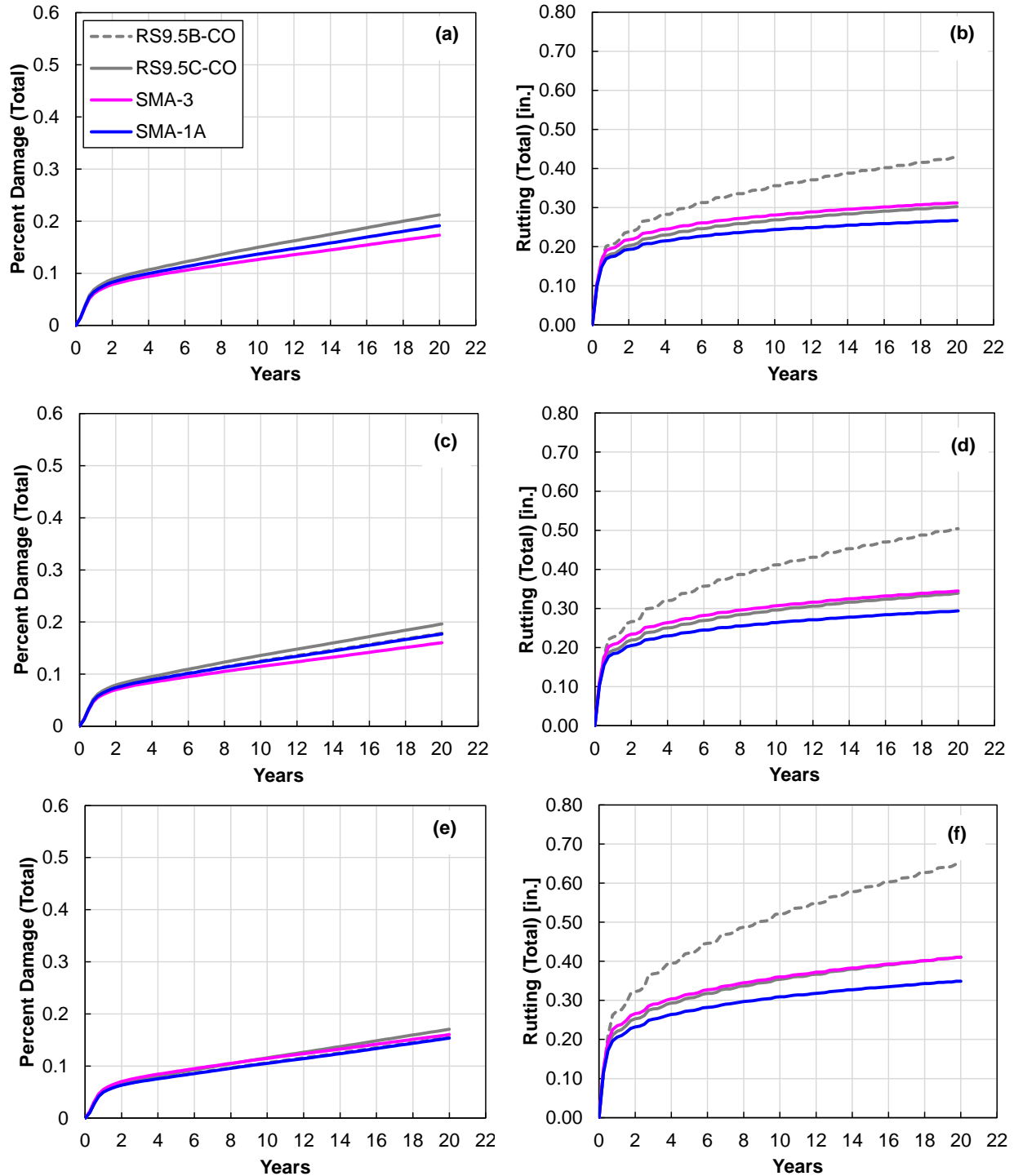


Figure G-5. Pavement performance simulation results for NC Coastal region and DS structures: (a) total percent damage - thin structure, (b) total rutting - thin structure, (c) total percent damage - intermediate structure, (d) total rutting damage – intermediate structure, (e) total percent damage – thick structure, and (f) total rutting – thick structure.

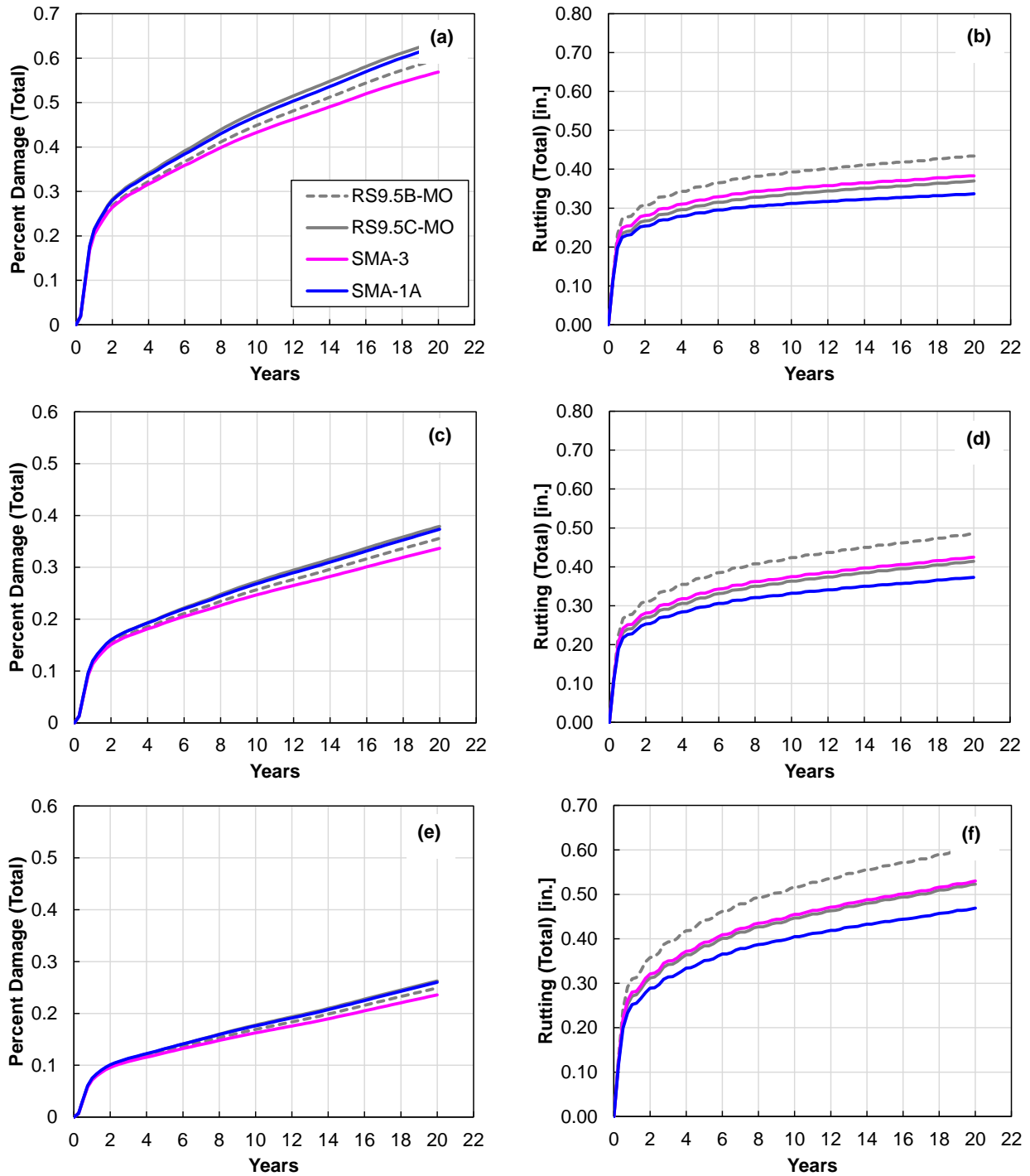


Figure G-6. Pavement performance simulation results for NC Mountain region and FDA structures: (a) total percent damage - thin structure, (b) total rutting - thin structure, (c) total percent damage - intermediate structure, (d) total rutting damage – intermediate structure, (e) total percent damage – thick structure, and (f) total rutting – thick structure.

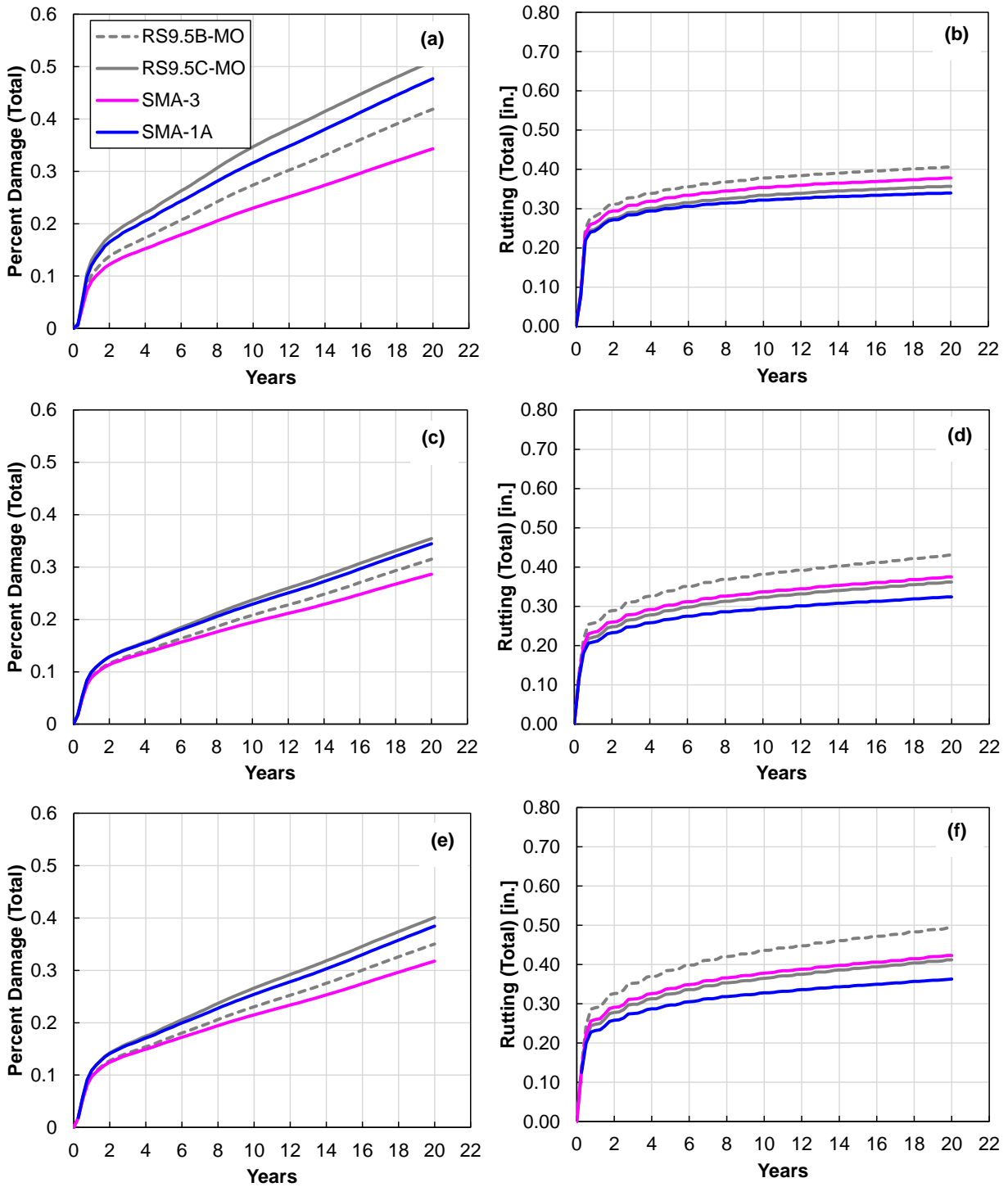


Figure G-7. Pavement performance simulation results for NC Mountain region and ABC structures: (a) total percent damage - thin structure, (b) total rutting - thin structure, (c) total percent damage - intermediate structure, (d) total rutting damage – intermediate structure, (e) total percent damage – thick structure, and (f) total rutting – thick structure.

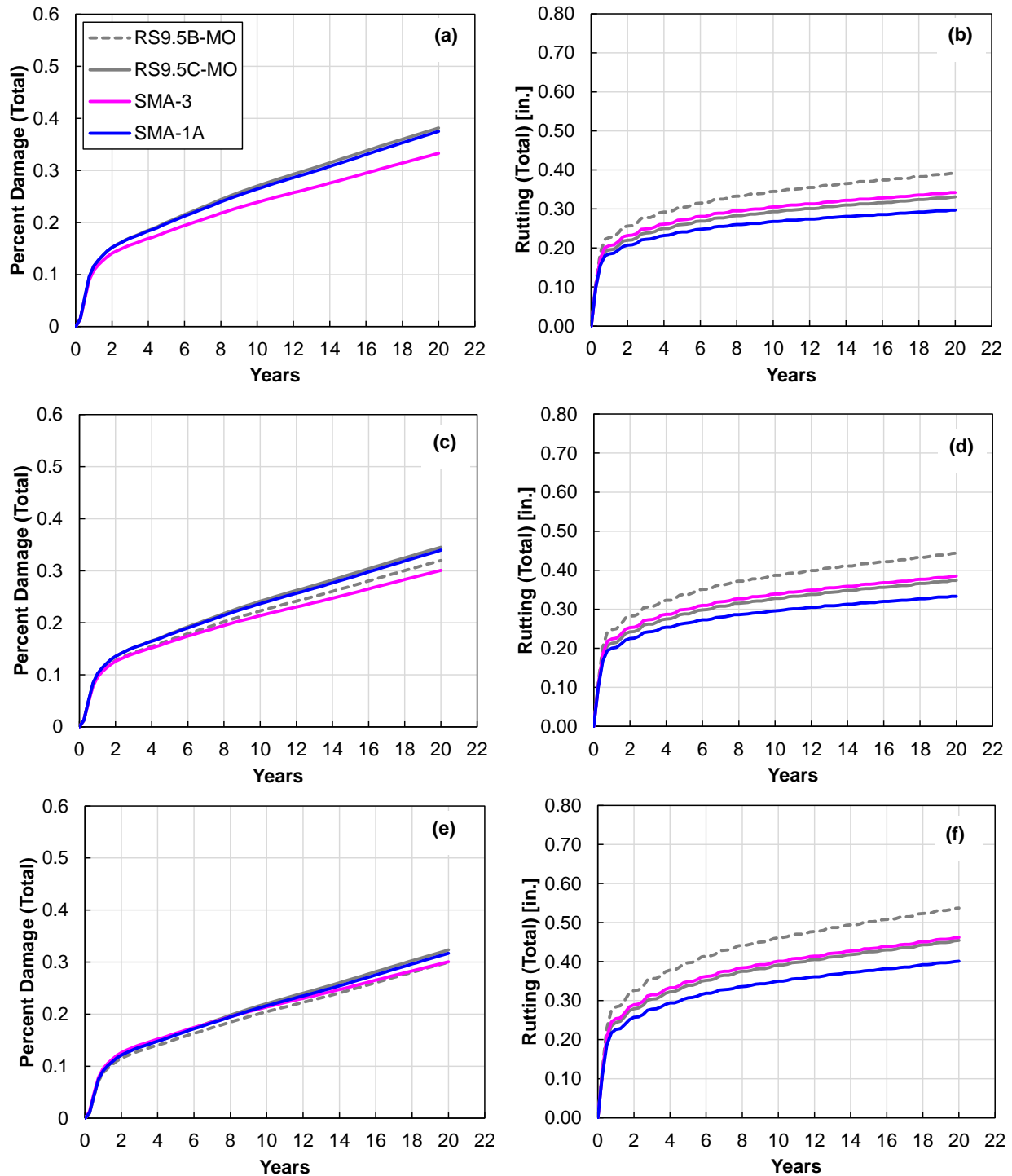


Figure G-8. Pavement performance simulation results for NC Mountain region and DS structures: (a) total percent damage - thin structure, (b) total rutting - thin structure, (c) total percent damage - intermediate structure, (d) total rutting damage – intermediate structure, (e) total percent damage – thick structure, and (f) total rutting – thick structure.

APPENDIX H. SUPPLEMENTARY INFORMATION ON LIFE-CYCLE COST ANALYSIS

This appendix contains the documentation of information that supplements the results presented in Chapter 6. The analysis conducted focused on a hypothetical road segment that is a divided facility, one mile long, and with two lanes per direction. The appendix is organized as follows:

- First, the maintenance schedules defined for each surface type are included in Table H-1 to Table H-6, these schedules are presented in a tabular form where year zero corresponds to the construction date and it is assumed that the structure is built completely at year zero. As shown, the period of analysis was set as 45 years based on the NCDOT pavement design guide. The maintenance schedule for the dense-graded surfaces was included in Chapter 6, see Table 23. As mentioned in Chapter 6, the number and timing of the maintenance activities for the dense grade surface was set based on the NCDOT pavement design guide; for the SMAs, this schedule was established based on the dense-graded maintenance scheme modified with the expected performance gains for each structure combination (See Appendix F).
- Next, for each structure configuration the associated cost of the number and type of maintenance activities was converted to cash flow with the unit cost of the different materials and thicknesses. The cost per lane/mile of the different surface materials evaluated are reported in Table H-9. These costs were estimated using the material densities reported in Table H-7 and for the SMAs and Microsurfacing from the two neighboring states, the values reported by these state DOTs and shown in Table H-8 were converted to values equivalent to North Carolina's practice using Equation (25).

$$\text{Cost-NC}_{\text{Surface } k} = \text{Cost}_{S9.5D-NC} \times \frac{\text{Cost}_{\text{Surface } k}}{\text{Cost}_{S9.5D-Neighboring}} \quad (25)$$

where;

- $\text{Cost-NC}_{\text{Surface } k}$ = equivalent North Carolina cost per lane/mile of Surface k ,
 $\text{Cost}_{S9.5D-NC}$ = cost per lane/mile of the S9.5D in North Carolina,
 $\text{Cost}_{S9.5D-Neighboring}$ = cost per lane/mile of the S9.5D in the neighboring states, and
 $\text{Cost}_{\text{Surface } k}$ = cost per lane/mile of Surface k as reported by neighboring states.

These costs were later converted to net present values using Equation (26). The results are presented in tabular form in Table H-10 to Table H-13 for the seven surfaces evaluated for the four discount rates; 0.5%, 3%, 5%, and 7%. These tables refer to these costs collectively as 'Maintenance Costs' for convenience.

$$NPV = \frac{C_j}{(1+r)^j} \quad (26)$$

where;

- NPV = net present value,
 C_j = net cash flow at year j , and
 r = discount rate.

- Afterward, using the maintenance schedule of each surface, the performance models presented in Chapter 2 were used to predict the friction and texture for each year j of the period of analysis. Then, for the sites where friction and texture observations were collected and that met the constraints established for the before-after comparison in the crash analysis presented in Chapter 5, the crash rates were plotted as a function of friction/texture and the crash rate relationship with friction and texture, shown in Equation (8), were updated. The observed crash rates values and the updated models are presented in Figure H-1 and Figure H-2, and Table H-14 and Table H-15.
- Next, because the friction and texture performance models are a function of the cumulative traffic, four AADT values were evaluated; 30,000, 60,000, 90,000, and 120,000 vehicles per day (vpd). Then, using Equation (9) the crash rates were converted to an expected number of collisions. This process was performed separately for friction and texture. Then the average of the predicted collisions was used to compute the cost associated with the collisions and with Equation (26) the annual costs were translated to a *NPV*. The summary of the crash cost *NPV* is included by surface type in Table H-16 to Table H-22.
- Lastly, the investments and the associated crash cost reductions were computed using Equation (27) and (28), which are the same as Equation (10) and (11), respectively, included in the main body of the document.

$$Investment = NPV_{Surface\ k}^{Maintenance} - NPV_{Dense-NC}^{Maintenance} \quad (27)$$

$$Crash\ Cost\ Reduction = NPV_{Dense-NC}^{Crashes} - NPV_{Surface\ k}^{Crashes} \quad (28)$$

These values were organized by structure type and are included in Figure H-3 to Figure H-5 for a 0.5% discount rate, Figure H-6 to Figure H-8 for a 3.0% discount rate, Figure H-9 to Figure H-11 for 5% discount rate, and Figure H-12 to Figure H-14 for a 7.0% discount rate. The following conclusions are derived from these figures:

- The investments and crash reductions are in a different order of magnitude. Irrespective of the discount rate, the crash cost reductions are approximately ten times higher than the investments. This means that all the surface treatments evaluated provide a positive return.
- A low discount rate, i.e., 0.5% is used for low-risk investments representing a low opportunity cost of capital. It is a conservative scenario and even then, the cash flow is positive suggesting a net benefit from the investment (using one of the treatments instead of the dense-graded surfaces).
- A high discount rate, i.e., 7.0% in our analysis, is used for riskier investments reflecting a high degree of uncertainty. Under these conditions, the net present value of the investments and crash cost reductions for all the pavement structure configurations is nearly half of the values obtained with a 0.5% discount rate, and in all cases the benefits are higher than the investments.
- For all the pavement structures evaluated, the SMAs are the surface types with the lowest investments. In fact, for some combinations of discount rate and pavement structure the investment ended up being negative, i.e., the cost of using a SMA over a dense-graded surface was lower in the long term, see for example the results for the ABC-Thin structure at a 0.5% discount rate.

- From the treatments that do not add structural capacity, Microsurfacing has the lowest investment values. The Microsurfacing that has been used in North Carolina has the lowest investment value of the two Microsurfacing studied. The OGFC and UTBWC have similar investment values, which are almost twice as the one reported with Microsurfacing.
- The SMAs produce similar crash cost reductions than the OGFC and UTBWC. Of the two SMAs, SMA-3 is the one with the highest crash cost reductions. Of the two Microsurfacing, the one used in North Carolina is the one with the highest crash cost reductions.
- The analysis presented has some limitations:
 - User costs were not evaluated. Some surfaces will result in lower user cost, e.g., the Microsurfacing is built quicker and therefore will produce lower delays and road closure times. The inclusion of the user costs may affect the ranking presented here.
 - Another important component that was not included is the mobilization cost and the work zone delineation cost.
 - The environmental implications were not accounted for. The overall carbon footprint of the surfaces evaluated will be very different given the number of maintenance activities, construction equipment needed, etc.
 - There are secondary and tertiary economic implications that may affect how well the calculated cost and benefits would match real cost/benefits. Some of these are; i) the longer-term impact of shifting funding priorities on the maintenance, operations, and conditions of the entire transportation system in North Carolina to complete the activities resulting from the PFMP; ii) the availability and possible impacts on the supply and costs of component materials required for these treatments; and iii) the impacts to sustainability and the cost/benefits from downstream effects (if any) of the use of these treatments (e.g., changes in the balance of waste materials at material suppliers, an imbalance in the amount of RAP generated versus what is used, etc.
 - Lastly, the analysis does not account for the implementation process of the SMAs. Some contractors are not familiar with the SMA design and construction, which may limit the number of contractors that are capable of delivering this surface type and may add extra costs for the adaptation of this material type by the NCDOT.

Maintenance Costs Net Present Value

Table H-7. Material density used for unit cost calculation.

Material	Density (pcf)
Asphalt Concrete (AC)	149.3
Intermediate	152.0
OGFC	120.0
UTBWC	145.0
Microsurfacing	130.0
ABC	150.0
Base AC	152.0

Table H-8. Unit cost as reported by the two neighboring states websites.

Surface	USD/Ton	USD/Lane/mile ⁽¹⁾
SM-9.5D	134.0	160.8
Dense-I/II	159.6	191.6
SMA-1	168.7	210.0
SMA-2	176.6	204.0
SMA-3	176.6	204.0

⁽¹⁾cost per lane/mile computed for a segment one mile long, with two lanes of 12-ft each.

Table H-9. Material cost used for the life-cycle cost analysis.

Surface	USD/Ton	USD/Lane/mile ⁽⁴⁾
S9.5D (1.5") ⁽¹⁾	70.1	41,448
S9.5D (3") ⁽¹⁾	70.1	82,897
Intermediate (4") ⁽¹⁾	89.0	142,856
Intermediate (2.5") ⁽¹⁾	89.0	89,285
Base AC (3") ⁽¹⁾	94.1	113,317
Base AC (4") ⁽¹⁾	94.1	151,090
Base AC (5.5") ⁽¹⁾	94.1	207,749
Base AC (10") ⁽¹⁾	94.1	377,725
ABC (8") ⁽¹⁾	50.8	160,934
ABC (10") ⁽¹⁾	50.8	201,168
OGFC (0.75") ⁽¹⁾	180.0	42,768
UTBWC (0.625") ⁽¹⁾	220.0	52,635
Microsurfacing Type III (0.5") ³	-	31,680
Dense-I/II (3") ²	83.5	98,752
SMA-1 (3") ²	88.2	104,332
SMA-2 (3") ²	92.4	109,226
SMA-3 (3") ²	92.4	109,226
Microsurfacing -Alt (0.5") ²	310.0	53,203

⁽¹⁾Cost per ton reported in the NCDOT connect website.

²Cost per ton adjusted with Equation (25) for the neighboring state materials.

³Cost per lane/mile provided by the NCDOT material and test unit personnel.

⁽⁴⁾cost per lane/mile computed for a segment one mile long, with two lanes of 12-ft each.

Table H-10. Summary of the maintenance cost NPV in 100,000 USD for a discount rate of 0.5%.

Surface	Frequency	Dense-NC	SMA-1	SMA-3	OGFC	UTBWC	Micro-NC	Micro-Alt
(FDA-Thin)	Max	13.1	17.3	15.1	21.7	22.7	20.2	22.6
	Avg	8.9	11.7	9.5	19.9	21.2	14.2	17.0
	Min	6.8	8.0	7.7	14.5	15.4	11.9	14.2
(FDA-Interm)	Max	16.0	15.3	14.9	24.6	25.6	23.1	25.5
	Avg	12.7	11.5	12.4	22.7	24.1	17.0	19.9
	Min	9.6	10.4	10.5	17.3	18.2	14.7	17.1
(FDA-Thick)	Max	20.5	21.6	20.1	29.1	30.1	27.6	30.0
	Avg	17.2	16.7	16.2	27.3	28.6	21.6	24.4
	Min	14.1	14.9	15.1	21.9	22.8	19.3	21.6
(ABC-Thin)	Max	13.3	14.4	7.9	21.9	22.9	20.4	22.8
	Avg	10.0	8.8	7.8	20.1	21.4	14.4	17.2
	Min	7.0	7.7	6.6	14.7	15.6	12.1	14.4
(ABC-Interm)	Max	16.2	15.4	12.6	24.8	25.7	23.3	25.7
	Avg	12.9	11.7	10.8	22.9	24.3	17.2	20.1
	Min	9.8	10.6	10.7	17.5	18.4	14.9	17.3
(ABC-Thick)	Max	17.0	16.3	13.4	25.6	26.6	24.1	26.5
	Avg	13.7	12.5	11.6	23.7	25.1	18.0	20.9
	Min	10.6	11.4	11.5	18.3	19.2	15.7	18.1
(DS-Thin)	Max	17.4	19.0	16.9	26.0	26.9	24.5	26.9
	Avg	14.1	15.3	13.1	24.1	25.4	18.4	21.3
	Min	11.0	11.8	12.0	18.7	19.6	16.1	18.4
(DS-Interm)	Max	18.4	17.7	16.6	27.1	28.0	25.5	27.9
	Avg	15.2	14.0	13.1	25.2	26.5	19.5	22.4
	Min	12.1	12.9	13.0	19.8	20.7	17.2	19.5
(DS-Thick)	Max	21.1	20.4	20.0	29.8	30.7	28.2	30.6
	Avg	17.9	16.7	16.2	27.9	29.2	22.2	25.0
	Min	14.8	15.6	15.7	22.5	23.4	19.9	22.2

Table H-11. Summary of the maintenance cost NPV in 100,000 USD for a discount rate of 3.0%.

Surface	Frequency	Dense-NC	SMA-1	SMA-3	OGFC	UTBWC	Micro-NC	Micro-Alt
(FDA-Thin)	Max	9.7	12.3	11.1	15.3	15.9	14.3	15.9
	Avg	7.2	8.8	7.7	13.6	14.5	10.6	12.5
	Min	5.9	6.8	6.6	11.0	11.6	9.0	10.5
(FDA-Interm)	Max	12.5	12.1	11.8	18.1	18.8	17.1	18.7
	Avg	10.3	10.0	10.5	16.5	17.3	13.5	15.4
	Min	8.7	9.3	9.3	13.8	14.4	11.9	13.4
(FDA-Thick)	Max	17.1	17.6	16.9	22.7	23.3	21.6	23.3
	Avg	14.9	14.9	14.7	21.0	21.9	18.0	19.9
	Min	13.3	13.9	13.9	18.3	19.0	16.4	17.9
(ABC-Thin)	Max	9.9	10.4	6.8	15.5	16.1	14.4	16.1
	Avg	7.7	7.4	6.6	13.8	14.7	10.8	12.7
	Min	6.1	6.7	6.0	11.1	11.8	9.2	10.7
(ABC-Interm)	Max	12.7	12.3	10.8	18.3	19.0	17.3	18.9
	Avg	10.5	10.2	9.6	16.7	17.5	13.7	15.6
	Min	8.9	9.5	9.4	14.0	14.6	12.1	13.6
(ABC-Thick)	Max	13.5	13.1	11.6	19.1	19.8	18.1	19.7
	Avg	11.3	11.0	10.4	17.5	18.3	14.5	16.4
	Min	9.7	10.3	10.2	14.8	15.4	12.9	14.4
(DS-Thin)	Max	13.9	15.1	13.7	19.5	20.2	18.5	20.1
	Avg	11.7	12.6	11.6	17.9	18.7	14.9	16.8
	Min	10.1	10.8	10.8	15.2	15.8	13.2	14.8
(DS-Interm)	Max	15.0	14.6	13.8	20.6	21.2	19.6	21.2
	Avg	12.8	12.5	12.0	19.0	19.8	16.0	17.9
	Min	11.2	11.7	11.8	16.3	16.9	14.3	15.8
(DS-Thick)	Max	17.7	17.3	17.0	23.3	23.9	22.3	23.9
	Avg	15.5	15.2	15.0	21.6	22.5	18.7	20.5
	Min	13.9	14.5	14.5	19.0	19.6	17.0	18.5

Table H-12. Summary of the maintenance cost NPV in 100,000 USD for a discount rate of 5.0%.

Surface	Frequency	Dense-NC	SMA-1	SMA-3	OGFC	UTBWC	Micro-NC	Micro-Alt
(FDA-Thin)	Max	7.4	10.1	8.5	11.5	12.0	10.7	11.9
	Avg	6.2	7.6	6.7	11.0	11.6	8.8	10.2
	Min	5.5	6.1	6.1	9.2	9.7	7.7	8.9
(FDA-Interm)	Max	10.3	10.8	10.6	14.3	14.8	13.6	14.8
	Avg	9.4	9.1	9.6	13.8	14.5	11.6	13.0
	Min	8.3	8.8	8.8	12.1	12.6	10.6	11.8
(FDA-Thick)	Max	14.8	15.9	15.5	18.9	19.4	18.1	19.3
	Avg	14.0	13.9	13.8	18.4	19.0	16.2	17.5
	Min	12.9	13.4	13.4	16.6	17.1	15.1	16.3
(ABC-Thin)	Max	7.6	8.7	6.3	11.7	12.2	10.9	12.1
	Avg	6.8	6.5	6.1	11.2	11.8	9.0	10.4
	Min	5.7	6.2	5.8	9.4	9.9	7.9	9.1
(ABC-Interm)	Max	10.5	11.0	9.7	14.5	15.0	13.8	15.0
	Avg	9.6	9.3	9.1	14.0	14.7	11.8	13.2
	Min	8.5	9.0	8.9	12.3	12.8	10.8	12.0
(ABC-Thick)	Max	11.3	11.8	10.5	15.3	15.8	14.6	15.8
	Avg	10.4	10.1	9.9	14.8	15.5	12.6	14.0
	Min	9.3	9.8	9.7	13.1	13.6	11.6	12.8
(DS-Thin)	Max	11.7	12.5	12.3	15.7	16.2	15.0	16.2
	Avg	10.8	11.5	10.7	15.2	15.9	13.0	14.4
	Min	9.7	10.3	10.3	13.5	14.0	12.0	13.2
(DS-Interm)	Max	12.8	13.2	12.8	16.8	17.3	16.1	17.3
	Avg	11.9	11.6	11.5	16.3	16.9	14.1	15.5
	Min	10.8	11.3	11.3	14.5	15.1	13.1	14.2
(DS-Thick)	Max	15.5	15.9	15.7	19.5	20.0	18.8	20.0
	Avg	14.6	14.3	14.2	19.0	19.6	16.8	18.2
	Min	13.5	14.0	14.0	17.2	17.8	15.8	16.9

Table H-13. Summary of the maintenance cost NPV in 100,000 USD for a discount rate of 7.0%.

Surface	Frequency	Dense-NC	SMA-1	SMA-3	OGFC	UTBWC	Micro-NC	Micro-Alt
(FDA-Thin)	Max	6.8	8.6	7.7	10.0	10.5	9.4	10.4
	Avg	5.7	6.7	6.2	9.4	9.9	7.8	9.0
	Min	5.2	5.8	5.8	8.2	8.6	7.0	7.9
(FDA-Interm)	Max	9.7	9.9	9.7	12.9	13.3	12.3	13.3
	Avg	8.7	8.8	9.1	12.2	12.7	10.7	11.8
	Min	8.1	8.6	8.5	11.0	11.5	9.8	10.8
(FDA-Thick)	Max	14.2	14.8	14.5	17.4	17.8	16.8	17.8
	Avg	13.3	13.5	13.5	16.8	17.3	15.2	16.4
	Min	12.6	13.1	13.2	15.6	16.0	14.4	15.3
(ABC-Thin)	Max	7.0	7.6	6.0	10.2	10.6	9.6	10.6
	Avg	6.1	6.1	5.8	9.6	10.1	8.0	9.2
	Min	5.4	5.9	5.6	8.4	8.8	7.2	8.1
(ABC-Interm)	Max	9.9	10.1	9.3	13.1	13.5	12.5	13.5
	Avg	8.9	9.0	8.8	12.4	12.9	10.9	12.0
	Min	8.3	8.7	8.7	11.2	11.7	10.0	11.0
(ABC-Thick)	Max	10.7	10.9	10.1	13.9	14.3	13.3	14.3
	Avg	9.8	9.8	9.6	13.2	13.7	11.7	12.8
	Min	9.1	9.5	9.4	12.0	12.5	10.8	11.8
(DS-Thin)	Max	11.0	11.8	11.4	14.3	14.7	13.7	14.7
	Avg	10.1	10.8	10.3	13.6	14.1	12.1	13.2
	Min	9.5	10.0	10.0	12.4	12.9	11.2	12.2
(DS-Interm)	Max	12.1	12.3	12.0	15.4	15.8	14.7	15.8
	Avg	11.2	11.3	11.2	14.7	15.2	13.1	14.3
	Min	10.5	11.0	11.0	13.5	13.9	12.3	13.3
(DS-Thick)	Max	14.8	15.0	14.9	18.0	18.5	17.4	18.4
	Avg	13.9	14.0	13.9	17.4	17.9	15.8	17.0
	Min	13.2	13.7	13.7	16.2	16.6	15.0	15.9

Crash Cost Net Present Value

Updated Crash Rate – Friction Relationship

The crash rate – friction relationship was updated for the following surface types; North Carolina’s dense-graded (Dense NC), Dense-I/II, SMAs (the data available was the SMA-1), UTBWC, and OGFC. The parameters of the updated functions are shown in Table H-14 and the resulting curves are plotted in Figure H-1. Note that in this figure, in addition to the new curves, the Non-Interchange crash rate-friction curve derived in FHWA/NC 2022-5 project was included for comparison. In the authors’ opinions there are three main reasons for which the Non-Interchange curve resulted in higher crash rates values than the updated curves; 1) the relationship was established using the aggregated values of a histogram, therefore some of the low crash rates may have been shadowed by a few high crash rates in a given bracket, whereas in the current curve the crashes were evaluated individually; 2) the previous curve combined dense-graded, UTBWC, and OGFC; and 3) the analysis period in the Non-Interchange curve was always 13-months, whereas the data points shown in Figure H-1 included observations that varied from 13 to 48 months.

The surfaces ranked in terms of crash risk as a function on the available friction, from high to low risk, are: i) Dense NC, ii) Dense I/II, iii) OGFC/UTBWC, iv) SMA. Although a data series named Microsurfacing was included in the figure, a crash rate-friction relationship was not derived for this surface type because there were only two records available for calibration because most of the Microsurfacing sites did not meet the before-after crash analysis constrains presented in Chapter 5.

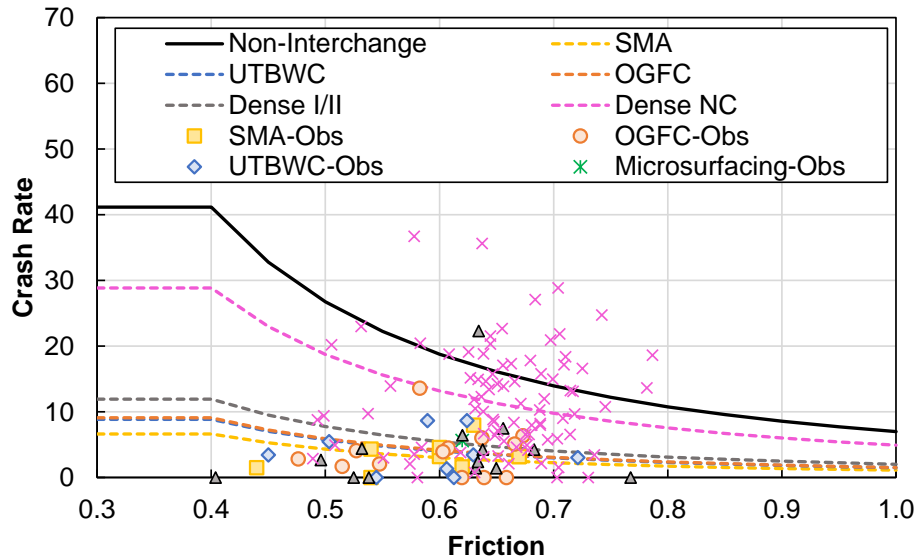


Figure H-1. Crash risk – friction relationship.

Table H-14. Parameters of the crash risk – friction relationship.

Surface Type	a	b
Non-Interchange	7.00	-1.933
SMA	1.13	-1.933
OGFC	1.55	-1.933
UTBWC	1.51	-1.933
Microsurfacing	2.23	-1.933
Dense I/II	2.03	-1.933
Dense NC	4.91	-1.933

Updated Crash Rate – MPD Relationship

The crash rate – MPD relationship was updated for the same surface types evaluated for the crash rate – friction case. The same assumptions were made, and the updated model coefficients are summarized in Table H-15 and the updated curves are plotted in Figure H-2. The resulting surfaces ranked in terms of crash risk as a function on the available MPD, from high to low risk, are: i) Dense NC, ii) OGFC/UTBWC, iii) Dense-I/II, iv) SMA. Like before, although a data series named Microsurfacing was included in the figure, a crash rate-friction relationship was not derived for this surface type because there were only two records available for calibration due to the fact that most of the Microsurfacing sites did not meet the before-after crash analysis constrains presented in Chapter 5.

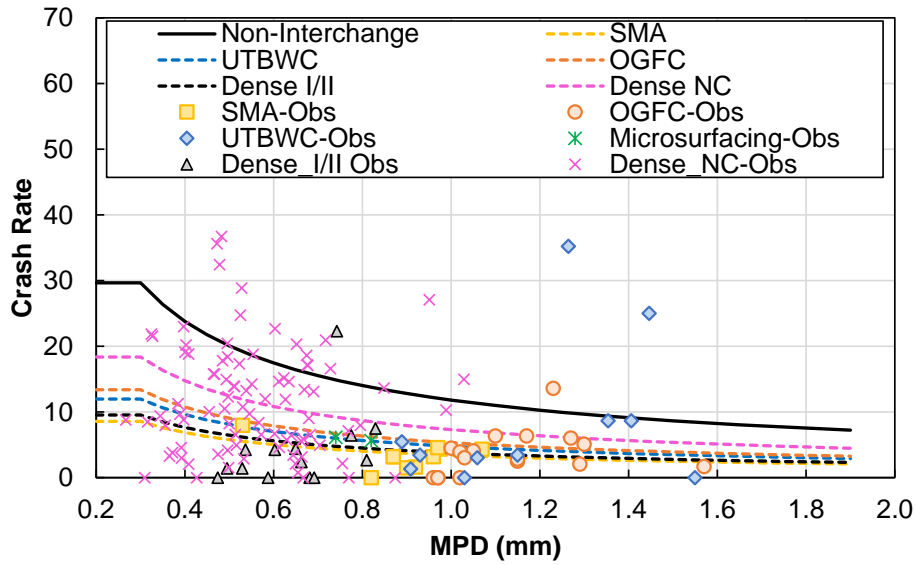


Figure H-2. Crash risk – MPD relationship.

Table H-15. Parameters of the crash risk – MPD relationship.

Surface Type	<i>a</i>	<i>b</i>
Non-Interchange	11.82	-0.764
SMA	3.41	-0.764
OGFC	5.34	-0.764
UTBWC	4.77	-0.764
Microsurfacing	7.43	-0.764
Dense I/II	3.80	-0.764
Dense NC	7.33	-0.764

Crash Cost Net Present Value

Table H-16. Summary of the Crash Cost NPV in 100,000 USD for North Carolina dense graded surface (Dense-NC).

Surface	Frequency	0.5% Discount Rate				3% Discount Rate				5% Discount Rate				7% Discount Rate			
		AADT (thousands)				AADT (thousands)				AADT (thousands)				AADT (thousands)			
		30	60	90	120	30	60	90	120	30	60	90	120	30	60	90	120
(FDA-Thin)	Max	147.2	290.0	434.7	582.7	91.5	180.1	269.8	361.6	67.5	132.8	198.9	266.5	52.6	103.6	155.1	207.8
	Avg	144.4	287.1	434.0	586.7	89.8	178.4	269.4	363.8	66.3	131.6	198.5	267.9	51.8	102.6	154.7	208.7
	Min	143.1	287.1	437.9	597.4	89.1	178.3	271.4	369.6	65.8	131.5	199.8	271.7	51.4	102.5	155.6	211.2
(FDA-Interm)	Max	147.2	290.0	434.7	582.7	91.5	180.1	269.8	361.6	67.5	132.8	198.9	266.5	52.6	103.6	155.1	207.8
	Avg	144.4	287.1	434.0	586.7	89.8	178.4	269.4	363.8	66.3	131.6	198.5	267.9	51.8	102.6	154.7	208.7
	Min	143.1	287.1	437.9	597.4	89.1	178.3	271.4	369.6	65.8	131.5	199.8	271.7	51.4	102.5	155.6	211.2
(FDA-Thick)	Max	147.2	290.0	434.7	582.7	91.5	180.1	269.8	361.6	67.5	132.8	198.9	266.5	52.6	103.6	155.1	207.8
	Avg	144.4	287.1	434.0	586.7	89.8	178.4	269.4	363.8	66.3	131.6	198.5	267.9	51.8	102.6	154.7	208.7
	Min	143.1	287.1	437.9	597.4	89.1	178.3	271.4	369.6	65.8	131.5	199.8	271.7	51.4	102.5	155.6	211.2
(ABC-Thin)	Max	147.2	290.0	434.7	582.7	91.5	180.1	269.8	361.6	67.5	132.8	198.9	266.5	52.6	103.6	155.1	207.8
	Avg	144.4	287.1	434.0	586.7	89.8	178.4	269.4	363.8	66.3	131.6	198.5	267.9	51.8	102.6	154.7	208.7
	Min	143.1	287.1	437.9	597.4	89.1	178.3	271.4	369.6	65.8	131.5	199.8	271.7	51.4	102.5	155.6	211.2
(ABC-Interm)	Max	147.2	290.0	434.7	582.7	91.5	180.1	269.8	361.6	67.5	132.8	198.9	266.5	52.6	103.6	155.1	207.8
	Avg	144.4	287.1	434.0	586.7	89.8	178.4	269.4	363.8	66.3	131.6	198.5	267.9	51.8	102.6	154.7	208.7
	Min	143.1	287.1	437.9	597.4	89.1	178.3	271.4	369.6	65.8	131.5	199.8	271.7	51.4	102.5	155.6	211.2
(ABC-Thick)	Max	147.2	290.0	434.7	582.7	91.5	180.1	269.8	361.6	67.5	132.8	198.9	266.5	52.6	103.6	155.1	207.8
	Avg	144.4	287.1	434.0	586.7	89.8	178.4	269.4	363.8	66.3	131.6	198.5	267.9	51.8	102.6	154.7	208.7
	Min	143.1	287.1	437.9	597.4	89.1	178.3	271.4	369.6	65.8	131.5	199.8	271.7	51.4	102.5	155.6	211.2
(DS-Thin)	Max	147.2	290.0	434.7	582.7	91.5	180.1	269.8	361.6	67.5	132.8	198.9	266.5	52.6	103.6	155.1	207.8
	Avg	144.4	287.1	434.0	586.7	89.8	178.4	269.4	363.8	66.3	131.6	198.5	267.9	51.8	102.6	154.7	208.7
	Min	143.1	287.1	437.9	597.4	89.1	178.3	271.4	369.6	65.8	131.5	199.8	271.7	51.4	102.5	155.6	211.2
(DS-Interm)	Max	147.2	290.0	434.7	582.7	91.5	180.1	269.8	361.6	67.5	132.8	198.9	266.5	52.6	103.6	155.1	207.8
	Avg	144.4	287.1	434.0	586.7	89.8	178.4	269.4	363.8	66.3	131.6	198.5	267.9	51.8	102.6	154.7	208.7
	Min	143.1	287.1	437.9	597.4	89.1	178.3	271.4	369.6	65.8	131.5	199.8	271.7	51.4	102.5	155.6	211.2
(DS-Thick)	Max	147.2	290.0	434.7	582.7	91.5	180.1	269.8	361.6	67.5	132.8	198.9	266.5	52.6	103.6	155.1	207.8
	Avg	144.4	287.1	434.0	586.7	89.8	178.4	269.4	363.8	66.3	131.6	198.5	267.9	51.8	102.6	154.7	208.7
	Min	143.1	287.1	437.9	597.4	89.1	178.3	271.4	369.6	65.8	131.5	199.8	271.7	51.4	102.5	155.6	211.2

Table H-17. Summary of the Crash Cost NPV in 100,000 USD for SMA-1.

Surface	Frequency	0.5% Discount Rate				3% Discount Rate				5% Discount Rate				7% Discount Rate			
		AADT (thousands)				AADT (thousands)				AADT (thousands)				AADT (thousands)			
		30	60	90	120	30	60	90	120	30	60	90	120	30	60	90	120
(FDA-Thin)	Max	44.0	84.2	125.8	169.6	27.4	52.4	78.3	105.4	20.2	38.7	57.8	77.8	15.8	30.3	45.2	60.8
	Avg	41.9	82.4	126.7	175.8	26.0	51.2	78.4	108.6	19.3	37.8	57.8	79.8	15.1	29.5	45.1	62.1
	Min	40.8	82.9	131.4	181.4	25.4	51.3	80.9	111.5	18.8	37.8	59.3	81.7	14.8	29.5	46.1	63.4
(FDA-Interm)	Max	42.0	82.1	125.1	172.3	26.2	51.1	77.8	107.0	19.4	37.8	57.5	78.9	15.2	29.6	44.9	61.5
	Avg	41.1	82.4	129.4	178.7	25.6	51.1	80.0	110.5	18.9	37.7	58.8	81.2	14.8	29.5	45.8	63.1
	Min	40.3	82.5	130.8	180.2	25.2	51.3	81.0	111.4	18.7	37.9	59.6	81.8	14.7	29.6	46.3	63.6
(FDA-Thick)	Max	42.6	82.9	125.8	172.4	26.5	51.5	78.0	106.6	19.6	38.0	57.5	78.5	15.4	29.7	44.9	61.2
	Avg	41.1	81.8	127.4	176.6	25.6	50.9	79.1	109.5	19.0	37.6	58.3	80.6	14.9	29.4	45.5	62.7
	Min	40.3	82.5	130.8	180.2	25.2	51.3	81.0	111.4	18.7	37.9	59.6	81.8	14.7	29.6	46.3	63.6
(ABC-Thin)	Max	42.6	82.9	125.8	172.4	26.5	51.5	78.0	106.6	19.6	38.0	57.5	78.5	15.4	29.7	44.9	61.2
	Avg	41.1	82.4	129.4	178.7	25.6	51.1	80.0	110.5	18.9	37.7	58.8	81.2	14.8	29.5	45.8	63.1
	Min	40.3	82.5	130.8	180.2	25.2	51.3	81.0	111.4	18.7	37.9	59.6	81.8	14.7	29.6	46.3	63.6
(ABC-Interm)	Max	42.0	82.1	125.1	172.3	26.2	51.1	77.8	107.0	19.4	37.8	57.5	78.9	15.2	29.6	44.9	61.5
	Avg	41.1	82.4	129.4	178.7	25.6	51.1	80.0	110.5	18.9	37.7	58.8	81.2	14.8	29.5	45.8	63.1
	Min	40.4	83.1	131.2	180.1	25.2	51.6	81.3	111.5	18.7	38.1	59.8	81.9	14.7	29.7	46.5	63.7
(ABC-Thick)	Max	42.0	82.1	125.1	172.3	26.2	51.1	77.8	107.0	19.4	37.8	57.5	78.9	15.2	29.6	44.9	61.5
	Avg	41.1	82.4	129.4	178.7	25.6	51.1	80.0	110.5	18.9	37.7	58.8	81.2	14.8	29.5	45.8	63.1
	Min	40.4	83.1	131.2	180.1	25.2	51.6	81.3	111.5	18.7	38.1	59.8	81.9	14.7	29.7	46.5	63.7
(DS-Thin)	Max	43.0	83.0	124.8	169.5	26.8	51.7	77.7	105.4	19.9	38.3	57.5	77.9	15.6	29.9	44.9	60.8
	Avg	41.1	81.5	126.2	175.7	25.7	50.8	78.5	108.9	19.1	37.6	57.9	80.2	15.0	29.4	45.2	62.4
	Min	40.3	82.2	130.6	180.2	25.2	51.2	80.8	111.3	18.7	37.8	59.4	81.7	14.7	29.5	46.2	63.4
(DS-Interm)	Max	42.0	82.1	125.1	172.3	26.2	51.1	77.8	107.0	19.4	37.8	57.5	78.9	15.2	29.6	44.9	61.5
	Avg	41.1	82.4	129.4	178.7	25.6	51.1	80.0	110.5	18.9	37.7	58.8	81.2	14.8	29.5	45.8	63.1
	Min	40.4	83.1	131.2	180.1	25.2	51.6	81.3	111.5	18.7	38.1	59.8	81.9	14.7	29.7	46.5	63.7
(DS-Thick)	Max	42.0	82.1	125.1	172.3	26.2	51.1	77.8	107.0	19.4	37.8	57.5	78.9	15.2	29.6	44.9	61.5
	Avg	41.1	82.4	129.4	178.7	25.6	51.1	80.0	110.5	18.9	37.7	58.8	81.2	14.8	29.5	45.8	63.1
	Min	40.3	82.5	130.8	180.2	25.2	51.3	81.0	111.4	18.7	37.9	59.6	81.8	14.7	29.7	46.5	63.7

Table H-18. Summary of the Crash Cost NPV in 100,000 USD for SMA-3.

Surface	Frequency	0.5% Discount Rate				3% Discount Rate				5% Discount Rate				7% Discount Rate			
		AADT (thousands)				AADT (thousands)				AADT (thousands)				AADT (thousands)			
		30	60	90	120	30	60	90	120	30	60	90	120	30	60	90	120
(FDA-Thin)	Max	35.4	67.5	99.2	130.9	22.0	42.1	61.9	81.6	16.3	31.2	45.8	60.5	12.8	24.4	35.9	47.4
	Avg	33.5	64.3	94.8	125.6	20.9	40.1	59.2	78.4	15.5	29.7	43.8	58.0	12.2	23.3	34.4	45.5
	Min	32.5	62.6	92.8	123.5	20.4	39.2	58.0	77.2	15.1	29.1	43.1	57.2	11.9	22.9	33.8	44.9
(FDA-Interm)	Max	34.2	65.6	96.7	127.8	21.3	40.8	60.1	79.5	15.8	30.2	44.5	58.8	12.4	23.7	34.8	46.1
	Avg	32.5	62.7	92.8	123.4	20.4	39.3	58.1	77.2	15.2	29.2	43.2	57.3	11.9	22.9	33.9	45.0
	Min	32.3	62.5	92.9	124.0	20.2	39.0	57.9	77.2	15.0	28.9	42.9	57.1	11.8	22.7	33.7	44.8
(FDA-Thick)	Max	34.5	65.9	97.0	128.2	21.5	41.1	60.5	79.9	15.9	30.4	44.8	59.2	12.5	23.9	35.1	46.4
	Avg	33.4	64.1	94.7	125.6	20.8	39.9	59.0	78.2	15.4	29.6	43.7	57.9	12.1	23.2	34.2	45.4
	Min	32.5	62.6	92.8	123.6	20.3	39.1	58.0	77.1	15.1	29.0	43.0	57.2	11.9	22.8	33.8	44.9
(ABC-Thin)	Max	32.5	62.6	92.8	123.5	20.4	39.2	58.0	77.2	19.6	38.0	57.5	78.5	11.9	22.9	33.8	44.9
	Avg	32.0	62.2	92.8	124.4	20.0	38.8	57.7	77.2	18.9	37.7	58.8	81.2	11.7	22.6	33.6	44.8
	Min	31.3	61.0	91.4	123.1	19.7	38.2	57.2	76.8	18.7	37.9	59.6	81.8	11.6	22.4	33.4	44.7
(ABC-Interm)	Max	33.5	64.3	94.8	125.6	20.9	40.1	59.2	78.4	15.5	29.7	43.8	58.0	12.2	23.3	34.4	45.5
	Avg	32.5	62.6	92.8	123.6	20.3	39.1	58.0	77.1	15.1	29.0	43.0	57.2	11.9	22.8	33.8	44.9
	Min	32.0	62.2	92.8	124.4	20.0	38.8	57.7	77.2	14.9	28.8	42.8	57.1	11.7	22.6	33.6	44.8
(ABC-Thick)	Max	33.5	64.3	94.8	125.6	20.9	40.1	59.2	78.4	15.5	29.7	43.8	58.0	12.2	23.3	34.4	45.5
	Avg	32.5	62.6	92.8	123.6	20.3	39.1	58.0	77.1	15.1	29.0	43.0	57.2	11.9	22.8	33.8	44.9
	Min	31.4	61.0	91.2	122.5	19.8	38.3	57.2	76.6	14.8	28.6	42.5	56.8	11.7	22.5	33.5	44.6
(DS-Thin)	Max	34.5	65.9	97.0	128.2	21.5	41.1	60.5	79.9	15.9	30.4	44.8	59.2	12.5	23.9	35.1	46.4
	Avg	33.4	64.1	94.7	125.6	20.8	39.9	59.0	78.2	15.4	29.6	43.7	57.9	12.1	23.2	34.2	45.4
	Min	32.5	62.6	92.8	123.6	20.3	39.1	58.0	77.1	15.1	29.0	43.0	57.2	11.9	22.8	33.8	44.9
(DS-Interm)	Max	33.6	64.4	94.9	125.6	21.0	40.3	59.3	78.5	15.6	29.9	44.0	58.3	12.2	23.4	34.6	45.7
	Avg	32.5	62.7	92.8	123.4	20.4	39.3	58.1	77.2	15.2	29.2	43.2	57.3	11.9	22.9	33.9	45.0
	Min	32.3	62.5	92.9	124.0	20.2	39.0	57.9	77.2	15.0	28.9	42.9	57.1	11.8	22.7	33.7	44.8
(DS-Thick)	Max	34.2	65.6	96.7	127.8	21.3	40.8	60.1	79.5	15.8	30.2	44.5	58.8	12.2	23.3	34.4	45.5
	Avg	33.0	63.7	94.3	125.3	20.6	39.7	58.7	77.9	15.3	29.4	43.5	57.7	11.9	22.8	33.8	44.9
	Min	32.4	62.5	92.9	123.8	20.2	39.0	57.9	77.2	15.0	29.0	42.9	57.2	11.7	22.5	33.5	44.6

Table H-19. Summary of the Crash Cost NPV in 100,000 USD for OGFC.

Surface	Frequency	0.5% Discount Rate				3% Discount Rate				5% Discount Rate				7% Discount Rate			
		AADT (thousands)				AADT (thousands)				AADT (thousands)				AADT (thousands)			
		30	60	90	120	30	60	90	120	30	60	90	120	30	60	90	120
(FDA-Thin)	Max	47.4	94.0	141.3	189.7	29.4	58.3	87.6	117.6	21.7	42.9	64.5	86.6	16.9	33.5	50.3	67.5
	Avg	48.1	95.0	142.4	190.6	29.8	58.8	88.2	118.1	21.9	43.3	65.0	86.9	17.1	33.8	50.6	67.7
	Min	47.1	93.7	141.3	190.3	29.3	58.2	87.7	118.0	21.6	42.9	64.6	86.9	16.9	33.5	50.4	67.7
(FDA-Interm)	Max	47.4	94.0	141.3	189.7	29.4	58.3	87.6	117.6	21.7	42.9	64.5	86.6	16.9	33.5	50.3	67.5
	Avg	48.1	95.0	142.4	190.6	29.8	58.8	88.2	118.1	21.9	43.3	65.0	86.9	17.1	33.8	50.6	67.7
	Min	47.1	93.7	141.3	190.3	29.3	58.2	87.7	118.0	21.6	42.9	64.6	86.9	16.9	33.5	50.4	67.7
(FDA-Thick)	Max	47.4	94.0	141.3	189.7	29.4	58.3	87.6	117.6	21.7	42.9	64.5	86.6	16.9	33.5	50.3	67.5
	Avg	48.1	95.0	142.4	190.6	29.8	58.8	88.2	118.1	21.9	43.3	65.0	86.9	17.1	33.8	50.6	67.7
	Min	47.1	93.7	141.3	190.3	29.3	58.2	87.7	118.0	21.6	42.9	64.6	86.9	16.9	33.5	50.4	67.7
(ABC-Thin)	Max	47.4	94.0	141.3	189.7	29.4	58.3	87.6	117.6	21.7	42.9	64.5	86.6	16.9	33.5	50.3	67.5
	Avg	48.1	95.0	142.4	190.6	29.8	58.8	88.2	118.1	21.9	43.3	65.0	86.9	17.1	33.8	50.6	67.7
	Min	47.1	93.7	141.3	190.3	29.3	58.2	87.7	118.0	21.6	42.9	64.6	86.9	16.9	33.5	50.4	67.7
(ABC-Interm)	Max	47.4	94.0	141.3	189.7	29.4	58.3	87.6	117.6	21.7	42.9	64.5	86.6	16.9	33.5	50.3	67.5
	Avg	48.1	95.0	142.4	190.6	29.8	58.8	88.2	118.1	21.9	43.3	65.0	86.9	17.1	33.8	50.6	67.7
	Min	47.1	93.7	141.3	190.3	29.3	58.2	87.7	118.0	21.6	42.9	64.6	86.9	16.9	33.5	50.4	67.7
(ABC-Thick)	Max	47.4	94.0	141.3	189.7	29.4	58.3	87.6	117.6	21.7	42.9	64.5	86.6	16.9	33.5	50.3	67.5
	Avg	48.1	95.0	142.4	190.6	29.8	58.8	88.2	118.1	21.9	43.3	65.0	86.9	17.1	33.8	50.6	67.7
	Min	47.1	93.7	141.3	190.3	29.3	58.2	87.7	118.0	21.6	42.9	64.6	86.9	16.9	33.5	50.4	67.7
(DS-Thin)	Max	47.4	94.0	141.3	189.7	29.4	58.3	87.6	117.6	21.7	42.9	64.5	86.6	16.9	33.5	50.3	67.5
	Avg	48.1	95.0	142.4	190.6	29.8	58.8	88.2	118.1	21.9	43.3	65.0	86.9	17.1	33.8	50.6	67.7
	Min	47.1	93.7	141.3	190.3	29.3	58.2	87.7	118.0	21.6	42.9	64.6	86.9	16.9	33.5	50.4	67.7
(DS-Interm)	Max	47.4	94.0	141.3	189.7	29.4	58.3	87.6	117.6	21.7	42.9	64.5	86.6	16.9	33.5	50.3	67.5
	Avg	48.1	95.0	142.4	190.6	29.8	58.8	88.2	118.1	21.9	43.3	65.0	86.9	17.1	33.8	50.6	67.7
	Min	47.1	93.7	141.3	190.3	29.3	58.2	87.7	118.0	21.6	42.9	64.6	86.9	16.9	33.5	50.4	67.7
(DS-Thick)	Max	47.4	94.0	141.3	189.7	29.4	58.3	87.6	117.6	21.7	42.9	64.5	86.6	16.9	33.5	50.3	67.5
	Avg	48.1	95.0	142.4	190.6	29.8	58.8	88.2	118.1	21.9	43.3	65.0	86.9	17.1	33.8	50.6	67.7
	Min	47.1	93.7	141.3	190.3	29.3	58.2	87.7	118.0	21.6	42.9	64.6	86.9	16.9	33.5	50.4	67.7

Table H-20. Summary of the Crash Cost NPV in 100,000 USD for UTBWC.

Surface	Frequency	0.5% Discount Rate				3% Discount Rate				5% Discount Rate				7% Discount Rate			
		AADT (thousands)				AADT (thousands)				AADT (thousands)				AADT (thousands)			
		30	60	90	120	30	60	90	120	30	60	90	120	30	60	90	120
(FDA-Thin)	Max	43.8	87.7	132.9	180.0	27.2	54.3	82.4	111.6	20.0	40.0	60.7	82.2	15.6	31.2	47.3	64.0
	Avg	44.3	88.3	133.1	179.2	27.4	54.7	82.5	111.0	20.2	40.3	60.7	81.7	15.7	31.4	47.3	63.6
	Min	43.6	87.7	133.8	182.6	27.1	54.4	82.9	112.8	20.0	40.1	61.0	82.9	15.6	31.3	47.5	64.4
(FDA-Interm)	Max	43.8	87.7	132.9	180.0	27.2	54.3	82.4	111.6	20.0	40.0	60.7	82.2	15.6	31.2	47.3	64.0
	Avg	44.3	88.3	133.1	179.2	27.4	54.7	82.5	111.0	20.2	40.3	60.7	81.7	15.7	31.4	47.3	63.6
	Min	43.6	87.7	133.8	182.6	27.1	54.4	82.9	112.8	20.0	40.1	61.0	82.9	15.6	31.3	47.5	64.4
(FDA-Thick)	Max	43.8	87.7	132.9	180.0	27.2	54.3	82.4	111.6	20.0	40.0	60.7	82.2	15.6	31.2	47.3	64.0
	Avg	44.3	88.3	133.1	179.2	27.4	54.7	82.5	111.0	20.2	40.3	60.7	81.7	15.7	31.4	47.3	63.6
	Min	43.6	87.7	133.8	182.6	27.1	54.4	82.9	112.8	20.0	40.1	61.0	82.9	15.6	31.3	47.5	64.4
(ABC-Thin)	Max	43.8	87.7	132.9	180.0	27.2	54.3	82.4	111.6	20.0	40.0	60.7	82.2	15.6	31.2	47.3	64.0
	Avg	44.3	88.3	133.1	179.2	27.4	54.7	82.5	111.0	20.2	40.3	60.7	81.7	15.7	31.4	47.3	63.6
	Min	43.6	87.7	133.8	182.6	27.1	54.4	82.9	112.8	20.0	40.1	61.0	82.9	15.6	31.3	47.5	64.4
(ABC-Interm)	Max	43.8	87.7	132.9	180.0	27.2	54.3	82.4	111.6	20.0	40.0	60.7	82.2	15.6	31.2	47.3	64.0
	Avg	44.3	88.3	133.1	179.2	27.4	54.7	82.5	111.0	20.2	40.3	60.7	81.7	15.7	31.4	47.3	63.6
	Min	43.6	87.7	133.8	182.6	27.1	54.4	82.9	112.8	20.0	40.1	61.0	82.9	15.6	31.3	47.5	64.4
(ABC-Thick)	Max	43.8	87.7	132.9	180.0	27.2	54.3	82.4	111.6	20.0	40.0	60.7	82.2	15.6	31.2	47.3	64.0
	Avg	44.3	88.3	133.1	179.2	27.4	54.7	82.5	111.0	20.2	40.3	60.7	81.7	15.7	31.4	47.3	63.6
	Min	43.6	87.7	133.8	182.6	27.1	54.4	82.9	112.8	20.0	40.1	61.0	82.9	15.6	31.3	47.5	64.4
(DS-Thin)	Max	43.8	87.7	132.9	180.0	27.2	54.3	82.4	111.6	20.0	40.0	60.7	82.2	15.6	31.2	47.3	64.0
	Avg	44.3	88.3	133.1	179.2	27.4	54.7	82.5	111.0	20.2	40.3	60.7	81.7	15.7	31.4	47.3	63.6
	Min	43.6	87.7	133.8	182.6	27.1	54.4	82.9	112.8	20.0	40.1	61.0	82.9	15.6	31.3	47.5	64.4
(DS-Interm)	Max	43.8	87.7	132.9	180.0	27.2	54.3	82.4	111.6	20.0	40.0	60.7	82.2	15.6	31.2	47.3	64.0
	Avg	44.3	88.3	133.1	179.2	27.4	54.7	82.5	111.0	20.2	40.3	60.7	81.7	15.7	31.4	47.3	63.6
	Min	43.6	87.7	133.8	182.6	27.1	54.4	82.9	112.8	20.0	40.1	61.0	82.9	15.6	31.3	47.5	64.4
(DS-Thick)	Max	43.8	87.7	132.9	180.0	27.2	54.3	82.4	111.6	20.0	40.0	60.7	82.2	15.6	31.2	47.3	64.0
	Avg	44.3	88.3	133.1	179.2	27.4	54.7	82.5	111.0	20.2	40.3	60.7	81.7	15.7	31.4	47.3	63.6
	Min	43.6	87.7	133.8	182.6	27.1	54.4	82.9	112.8	20.0	40.1	61.0	82.9	15.6	31.3	47.5	64.4

Table H-21. Summary of the Crash Cost NPV in 100,000 USD for Microsurfacing-NC.

Surface	Frequency	0.5% Discount Rate				3% Discount Rate				5% Discount Rate				7% Discount Rate			
		AADT (thousands)				AADT (thousands)				AADT (thousands)				AADT (thousands)			
		30	60	90	120	30	60	90	120	30	60	90	120	30	60	90	120
(FDA-Thin)	Max	82.5	167.9	254.3	341.3	51.0	103.7	157.1	210.8	37.4	76.2	115.3	154.8	29.1	59.1	89.5	120.2
	Avg	82.6	168.2	254.7	341.9	51.1	104.1	157.6	211.6	37.6	76.5	115.8	155.5	29.2	59.4	89.9	120.7
	Min	83.4	169.7	257.0	345.1	51.4	104.7	158.6	212.9	37.7	76.8	116.3	156.2	29.3	59.6	90.2	121.1
(FDA-Interm)	Max	82.5	167.9	254.3	341.3	51.0	103.7	157.1	210.8	37.4	76.2	115.3	154.8	29.1	59.1	89.5	120.2
	Avg	82.6	168.2	254.7	341.9	51.1	104.1	157.6	211.6	37.6	76.5	115.8	155.5	29.2	59.4	89.9	120.7
	Min	83.4	169.7	257.0	345.1	51.4	104.7	158.6	212.9	37.7	76.8	116.3	156.2	29.3	59.6	90.2	121.1
(FDA-Thick)	Max	82.5	167.9	254.3	341.3	51.0	103.7	157.1	210.8	37.4	76.2	115.3	154.8	29.1	59.1	89.5	120.2
	Avg	82.6	168.2	254.7	341.9	51.1	104.1	157.6	211.6	37.6	76.5	115.8	155.5	29.2	59.4	89.9	120.7
	Min	83.4	169.7	257.0	345.1	51.4	104.7	158.6	212.9	37.7	76.8	116.3	156.2	29.3	59.6	90.2	121.1
(ABC-Thin)	Max	82.5	167.9	254.3	341.3	51.0	103.7	157.1	210.8	37.4	76.2	115.3	154.8	29.1	59.1	89.5	120.2
	Avg	82.6	168.2	254.7	341.9	51.1	104.1	157.6	211.6	37.6	76.5	115.8	155.5	29.2	59.4	89.9	120.7
	Min	83.4	169.7	257.0	345.1	51.4	104.7	158.6	212.9	37.7	76.8	116.3	156.2	29.3	59.6	90.2	121.1
(ABC-Interm)	Max	82.5	167.9	254.3	341.3	51.0	103.7	157.1	210.8	37.4	76.2	115.3	154.8	29.1	59.1	89.5	120.2
	Avg	82.6	168.2	254.7	341.9	51.1	104.1	157.6	211.6	37.6	76.5	115.8	155.5	29.2	59.4	89.9	120.7
	Min	83.4	169.7	257.0	345.1	51.4	104.7	158.6	212.9	37.7	76.8	116.3	156.2	29.3	59.6	90.2	121.1
(ABC-Thick)	Max	82.5	167.9	254.3	341.3	51.0	103.7	157.1	210.8	37.4	76.2	115.3	154.8	29.1	59.1	89.5	120.2
	Avg	82.6	168.2	254.7	341.9	51.1	104.1	157.6	211.6	37.6	76.5	115.8	155.5	29.2	59.4	89.9	120.7
	Min	83.4	169.7	257.0	345.1	51.4	104.7	158.6	212.9	37.7	76.8	116.3	156.2	29.3	59.6	90.2	121.1
(DS-Thin)	Max	82.5	167.9	254.3	341.3	51.0	103.7	157.1	210.8	37.4	76.2	115.3	154.8	29.1	59.1	89.5	120.2
	Avg	82.6	168.2	254.7	341.9	51.1	104.1	157.6	211.6	37.6	76.5	115.8	155.5	29.2	59.4	89.9	120.7
	Min	83.4	169.7	257.0	345.1	51.4	104.7	158.6	212.9	37.7	76.8	116.3	156.2	29.3	59.6	90.2	121.1
(DS-Interm)	Max	82.5	167.9	254.3	341.3	51.0	103.7	157.1	210.8	37.4	76.2	115.3	154.8	29.1	59.1	89.5	120.2
	Avg	82.6	168.2	254.7	341.9	51.1	104.1	157.6	211.6	37.6	76.5	115.8	155.5	29.2	59.4	89.9	120.7
	Min	83.4	169.7	257.0	345.1	51.4	104.7	158.6	212.9	37.7	76.8	116.3	156.2	29.3	59.6	90.2	121.1
(DS-Thick)	Max	82.5	167.9	254.3	341.3	51.0	103.7	157.1	210.8	37.4	76.2	115.3	154.8	29.1	59.1	89.5	120.2
	Avg	82.6	168.2	254.7	341.9	51.1	104.1	157.6	211.6	37.6	76.5	115.8	155.5	29.2	59.4	89.9	120.7
	Min	83.4	169.7	257.0	345.1	51.4	104.7	158.6	212.9	37.7	76.8	116.3	156.2	29.3	59.6	90.2	121.1

Table H-22. Summary of the Crash Cost NPV in 100,000 USD for Microsurfacing-Alt.

Surface	Frequency	0.5% Discount Rate				3% Discount Rate				5% Discount Rate				7% Discount Rate			
		AADT (thousands)				AADT (thousands)				AADT (thousands)				AADT (thousands)			
		30	60	90	120	30	60	90	120	30	60	90	120	30	60	90	120
(FDA-Thin)	Max	100.7	204.0	308.3	413.4	62.1	125.9	190.3	255.2	45.6	92.4	139.7	187.2	35.4	71.7	108.4	145.3
	Avg	100.8	204.3	308.8	414.0	62.4	126.4	191.1	256.2	45.8	92.9	140.4	188.2	35.6	72.1	109.0	146.1
	Min	102.0	206.6	312.4	418.9	62.8	127.4	192.5	258.1	46.1	93.4	141.1	189.2	35.7	72.4	109.4	146.7
(FDA-Interm)	Max	100.7	204.0	308.3	413.4	62.1	125.9	190.3	255.2	45.6	92.4	139.7	187.2	35.4	71.7	108.4	145.3
	Avg	100.8	204.3	308.8	414.0	62.4	126.4	191.1	256.2	45.8	92.9	140.4	188.2	35.6	72.1	109.0	146.1
	Min	102.0	206.6	312.4	418.9	62.8	127.4	192.5	258.1	46.1	93.4	141.1	189.2	35.7	72.4	109.4	146.7
(FDA-Thick)	Max	100.7	204.0	308.3	413.4	62.1	125.9	190.3	255.2	45.6	92.4	139.7	187.2	35.4	71.7	108.4	145.3
	Avg	100.8	204.3	308.8	414.0	62.4	126.4	191.1	256.2	45.8	92.9	140.4	188.2	35.6	72.1	109.0	146.1
	Min	102.0	206.6	312.4	418.9	62.8	127.4	192.5	258.1	46.1	93.4	141.1	189.2	35.7	72.4	109.4	146.7
(ABC-Thin)	Max	100.7	204.0	308.3	413.4	62.1	125.9	190.3	255.2	45.6	92.4	139.7	187.2	35.4	71.7	108.4	145.3
	Avg	100.8	204.3	308.8	414.0	62.4	126.4	191.1	256.2	45.8	92.9	140.4	188.2	35.6	72.1	109.0	146.1
	Min	102.0	206.6	312.4	418.9	62.8	127.4	192.5	258.1	46.1	93.4	141.1	189.2	35.7	72.4	109.4	146.7
(ABC-Interm)	Max	100.7	204.0	308.3	413.4	62.1	125.9	190.3	255.2	45.6	92.4	139.7	187.2	35.4	71.7	108.4	145.3
	Avg	100.8	204.3	308.8	414.0	62.4	126.4	191.1	256.2	45.8	92.9	140.4	188.2	35.6	72.1	109.0	146.1
	Min	102.0	206.6	312.4	418.9	62.8	127.4	192.5	258.1	46.1	93.4	141.1	189.2	35.7	72.4	109.4	146.7
(ABC-Thick)	Max	100.7	204.0	308.3	413.4	62.1	125.9	190.3	255.2	45.6	92.4	139.7	187.2	35.4	71.7	108.4	145.3
	Avg	100.8	204.3	308.8	414.0	62.4	126.4	191.1	256.2	45.8	92.9	140.4	188.2	35.6	72.1	109.0	146.1
	Min	102.0	206.6	312.4	418.9	62.8	127.4	192.5	258.1	46.1	93.4	141.1	189.2	35.7	72.4	109.4	146.7
(DS-Thin)	Max	100.7	204.0	308.3	413.4	62.1	125.9	190.3	255.2	45.6	92.4	139.7	187.2	35.4	71.7	108.4	145.3
	Avg	100.8	204.3	308.8	414.0	62.4	126.4	191.1	256.2	45.8	92.9	140.4	188.2	35.6	72.1	109.0	146.1
	Min	102.0	206.6	312.4	418.9	62.8	127.4	192.5	258.1	46.1	93.4	141.1	189.2	35.7	72.4	109.4	146.7
(DS-Interm)	Max	100.7	204.0	308.3	413.4	62.1	125.9	190.3	255.2	45.6	92.4	139.7	187.2	35.4	71.7	108.4	145.3
	Avg	100.8	204.3	308.8	414.0	62.4	126.4	191.1	256.2	45.8	92.9	140.4	188.2	35.6	72.1	109.0	146.1
	Min	102.0	206.6	312.4	418.9	62.8	127.4	192.5	258.1	46.1	93.4	141.1	189.2	35.7	72.4	109.4	146.7
(DS-Thick)	Max	100.7	204.0	308.3	413.4	62.1	125.9	190.3	255.2	45.6	92.4	139.7	187.2	35.4	71.7	108.4	145.3
	Avg	100.8	204.3	308.8	414.0	62.4	126.4	191.1	256.2	45.8	92.9	140.4	188.2	35.6	72.1	109.0	146.1
	Min	102.0	206.6	312.4	418.9	62.8	127.4	192.5	258.1	46.1	93.4	141.1	189.2	35.7	72.4	109.4	146.7

Investment and Crash Cost Reduction (0.5% Interest Rate)

Thin Structures

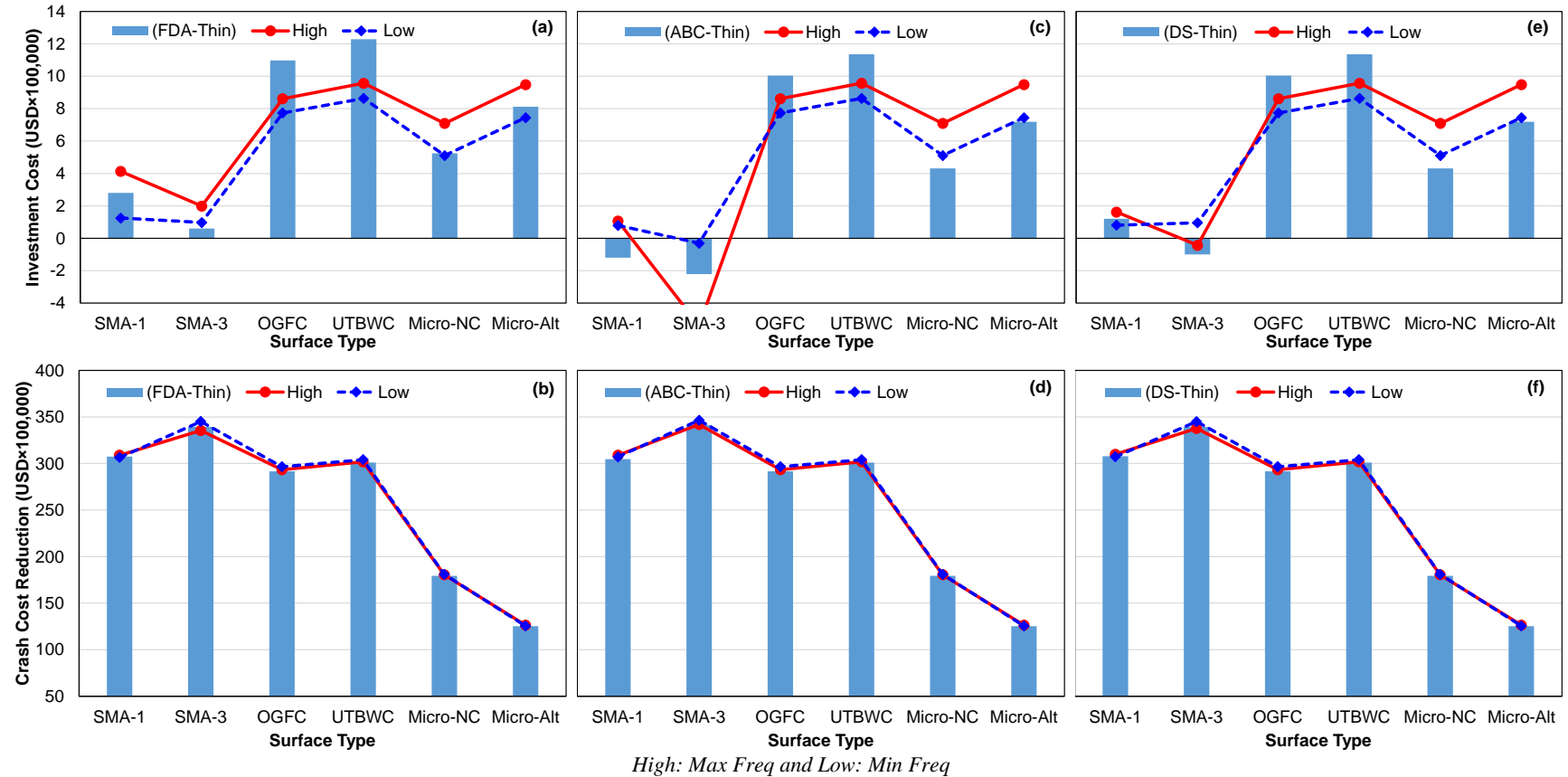


Figure H-3. FDA Thin: (a) investment and (b) crash cost reduction. ABC Thin: (c) investment and (d) crash cost reduction. DS Thin: (e) investment and (f) crash cost reduction.

Intermediate Structures

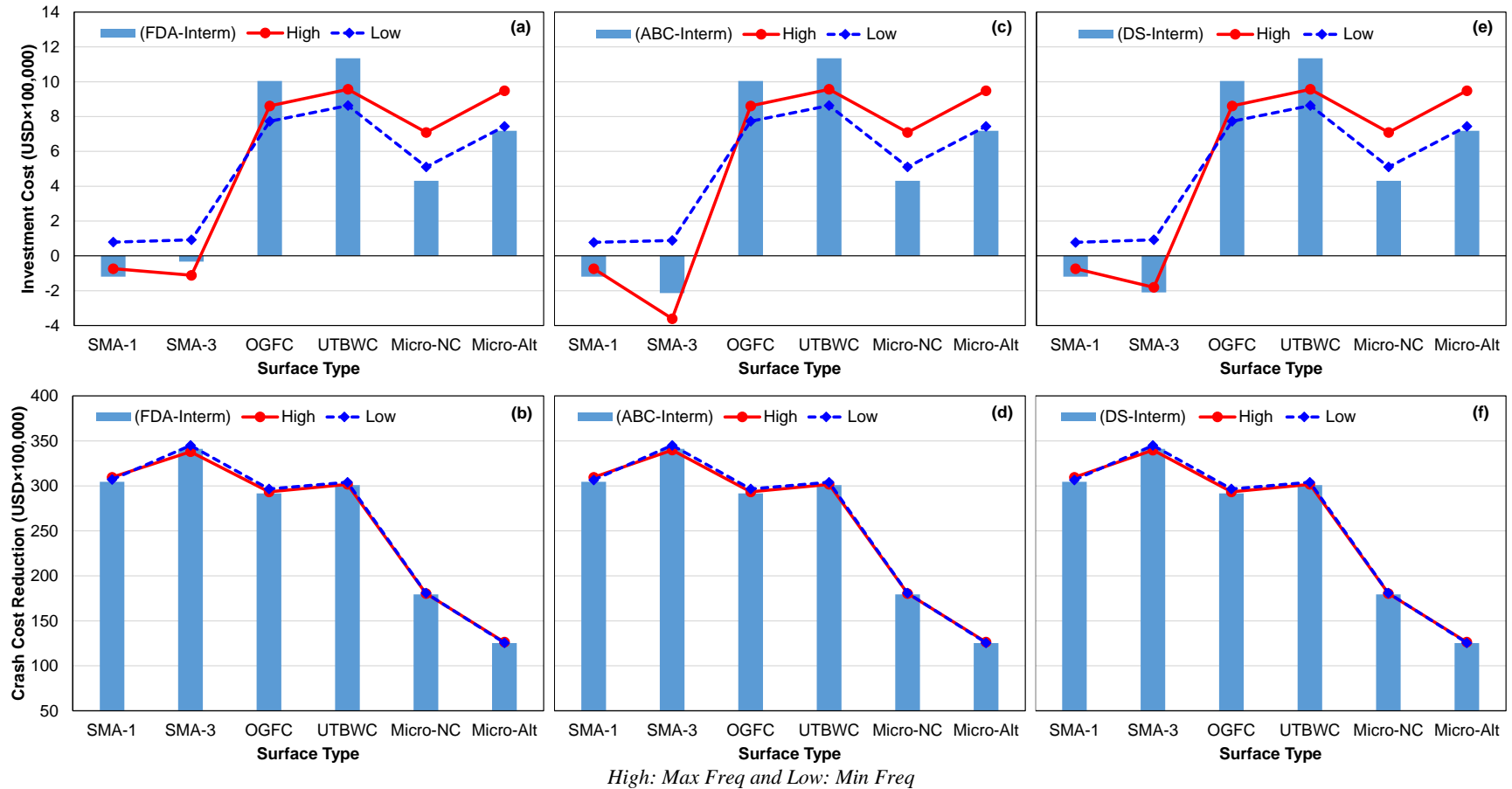
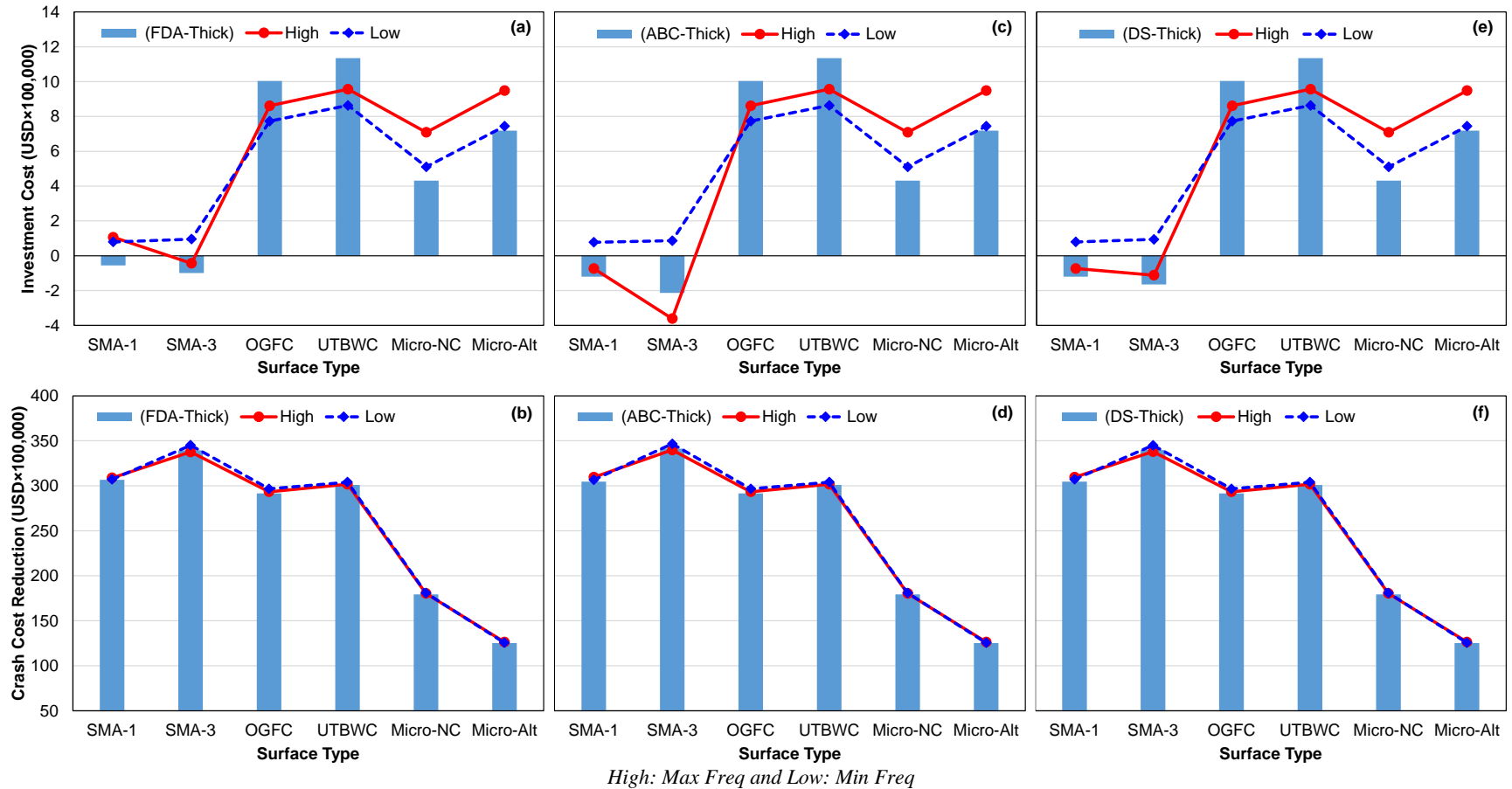


Figure H-4. FDA Intermediate: (a) investment and (b) crash cost reduction. ABC Intermediate: (c) investment and (d) crash cost reduction. DS Intermediate: (e) investment and (f) crash cost reduction.

Thick Structures



High: Max Freq and Low: Min Freq

Figure H-5. FDA Thick: (a) investment and (b) crash cost reduction. ABC Thick: (c) investment and (d) crash cost reduction. DS Thick: (e) investment and (f) crash cost reduction.

Investment and Crash Cost Reduction (3% Interest Rate)

Thin Structures

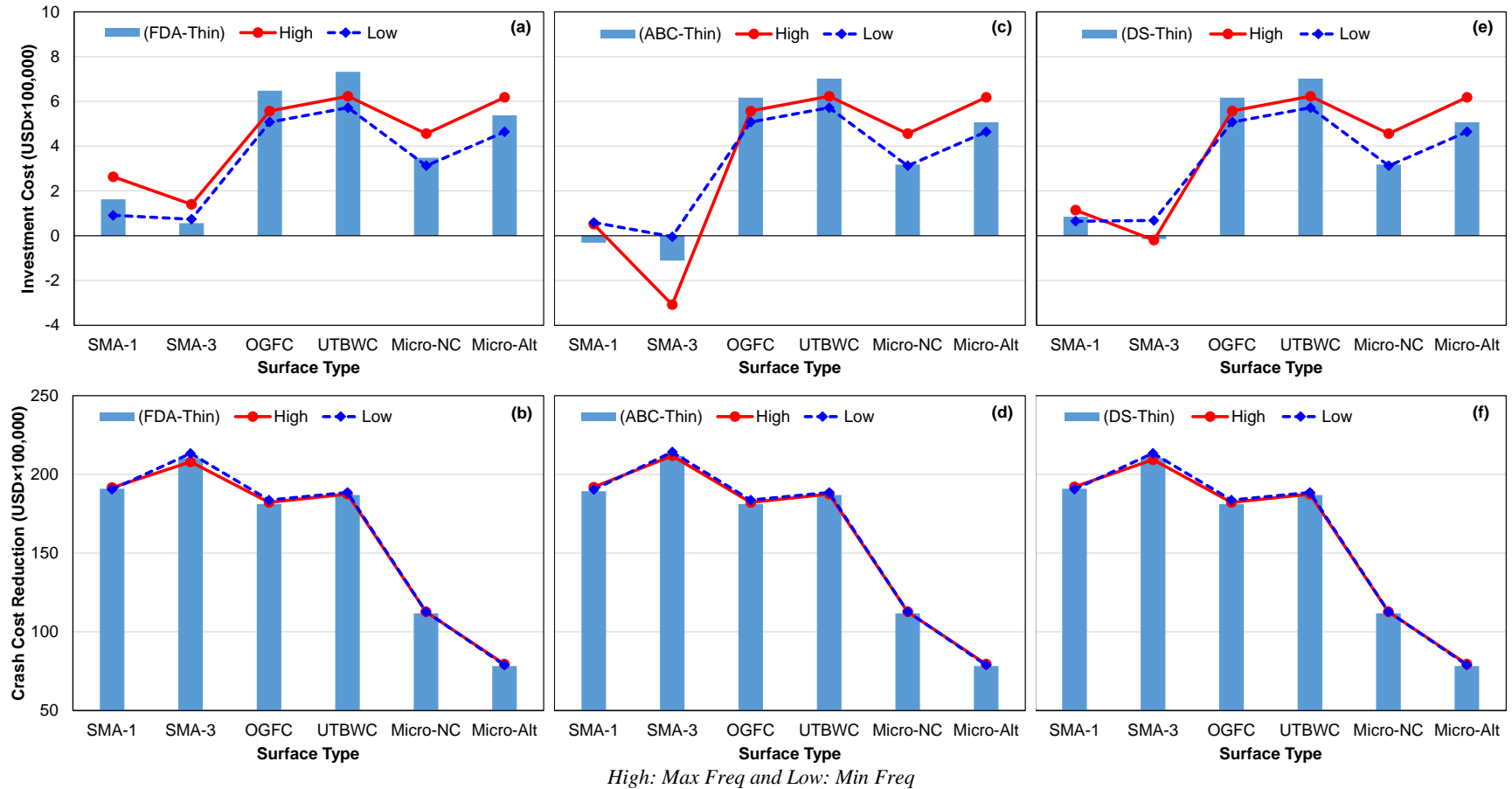


Figure H-6. FDA Thin: (a) investment and (b) crash cost reduction. ABC Thin: (c) investment and (d) crash cost reduction. DS Thin: (e) investment and (f) crash cost reduction.

Intermediate Structures

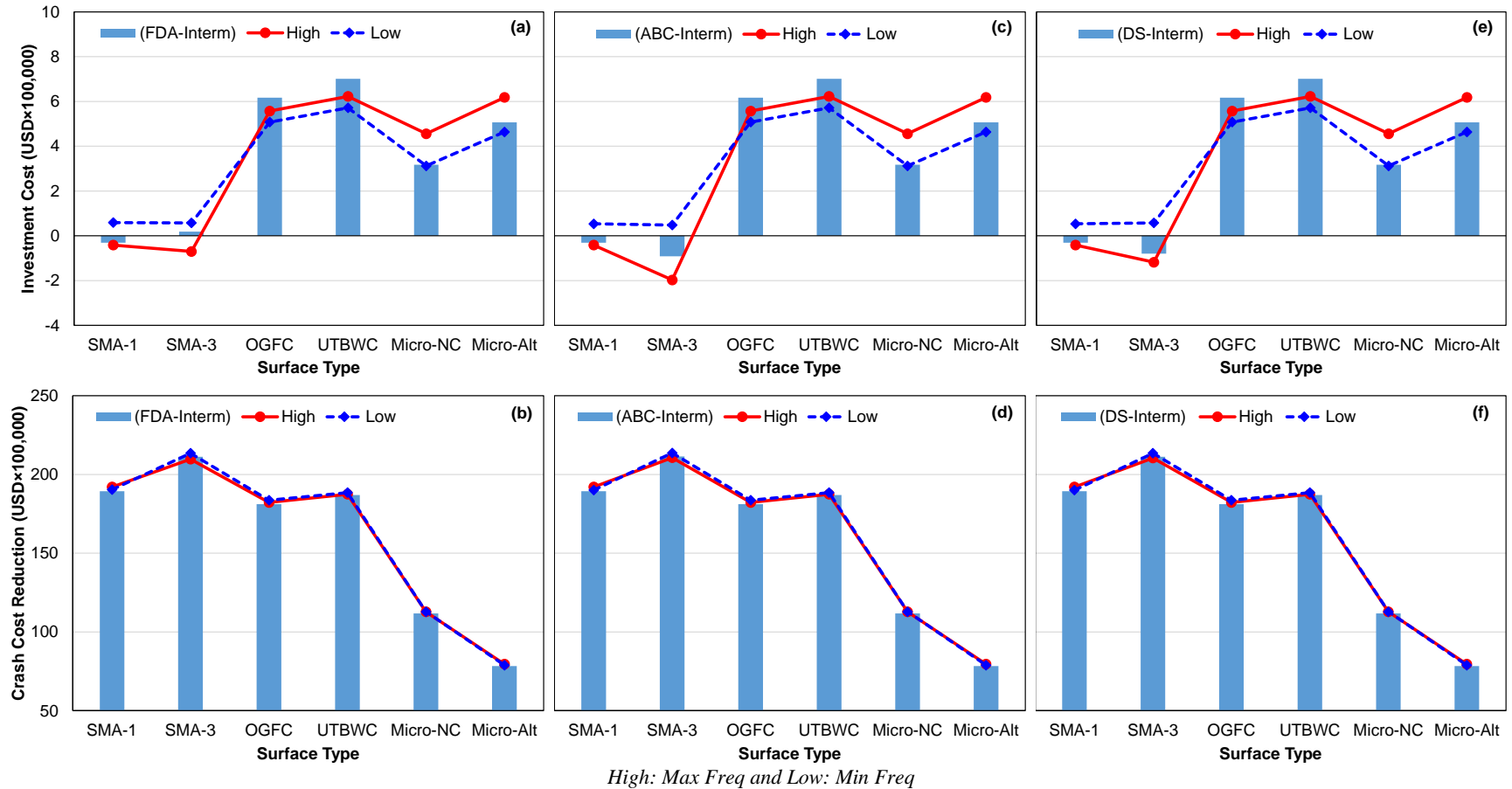


Figure H-7. FDA Intermediate: (a) investment and (b) crash cost reduction. ABC Intermediate: (c) investment and (d) crash cost reduction. DS Intermediate: (e) investment and (f) crash cost reduction.

Thick Structures

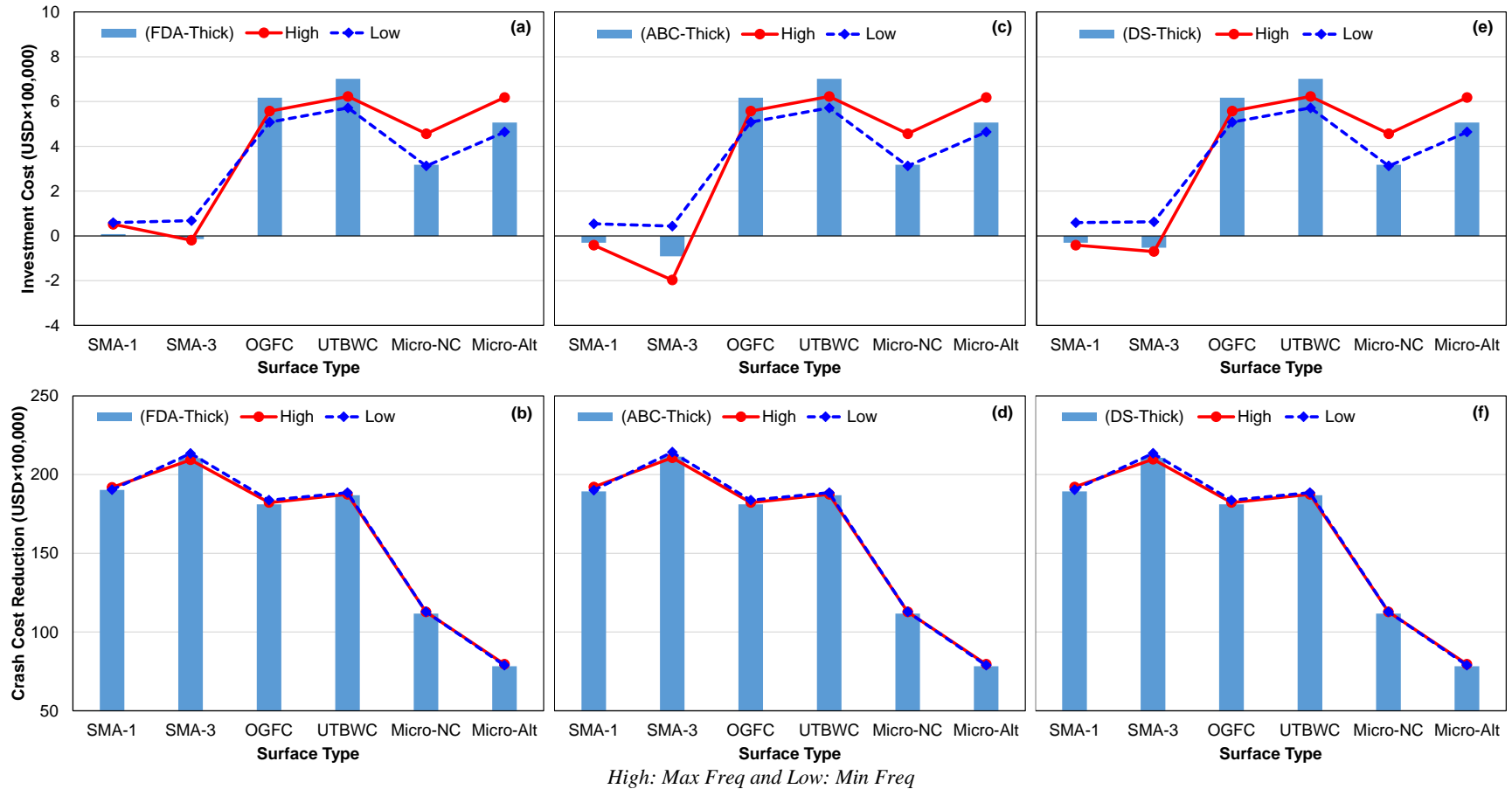


Figure H-8. FDA Thick: (a) investment and (b) crash cost reduction. ABC Thick: (c) investment and (d) crash cost reduction. DS Thick: (e) investment and (f) crash cost reduction.

Investment and Crash Cost Reduction (5% Interest Rate)

Thin Structures

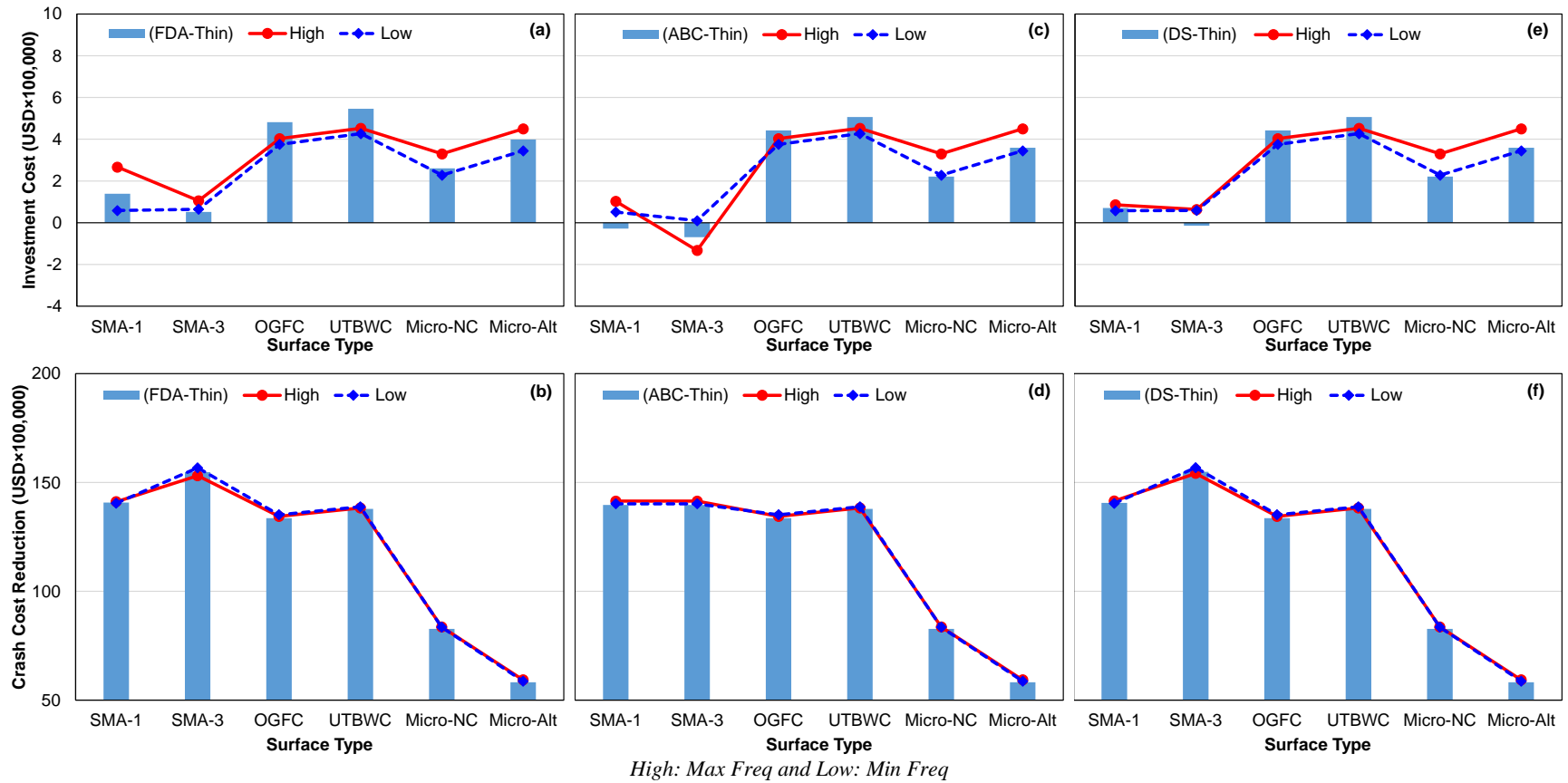
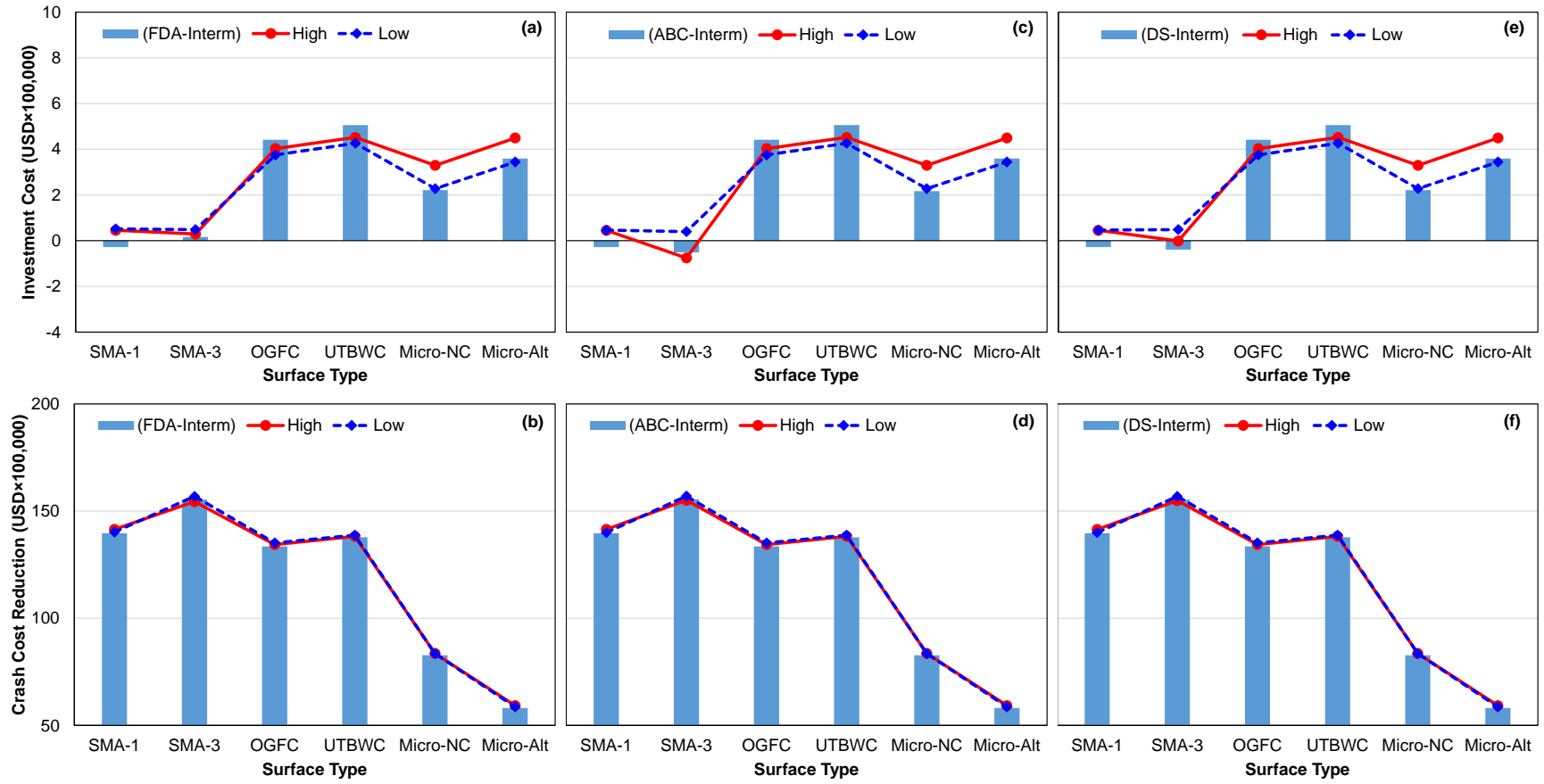


Figure H-9. FDA Thin: (a) investment and (b) crash cost reduction. ABC Thin: (c) investment and (d) crash cost reduction. DS Thin: (e) investment and (f) crash cost reduction.

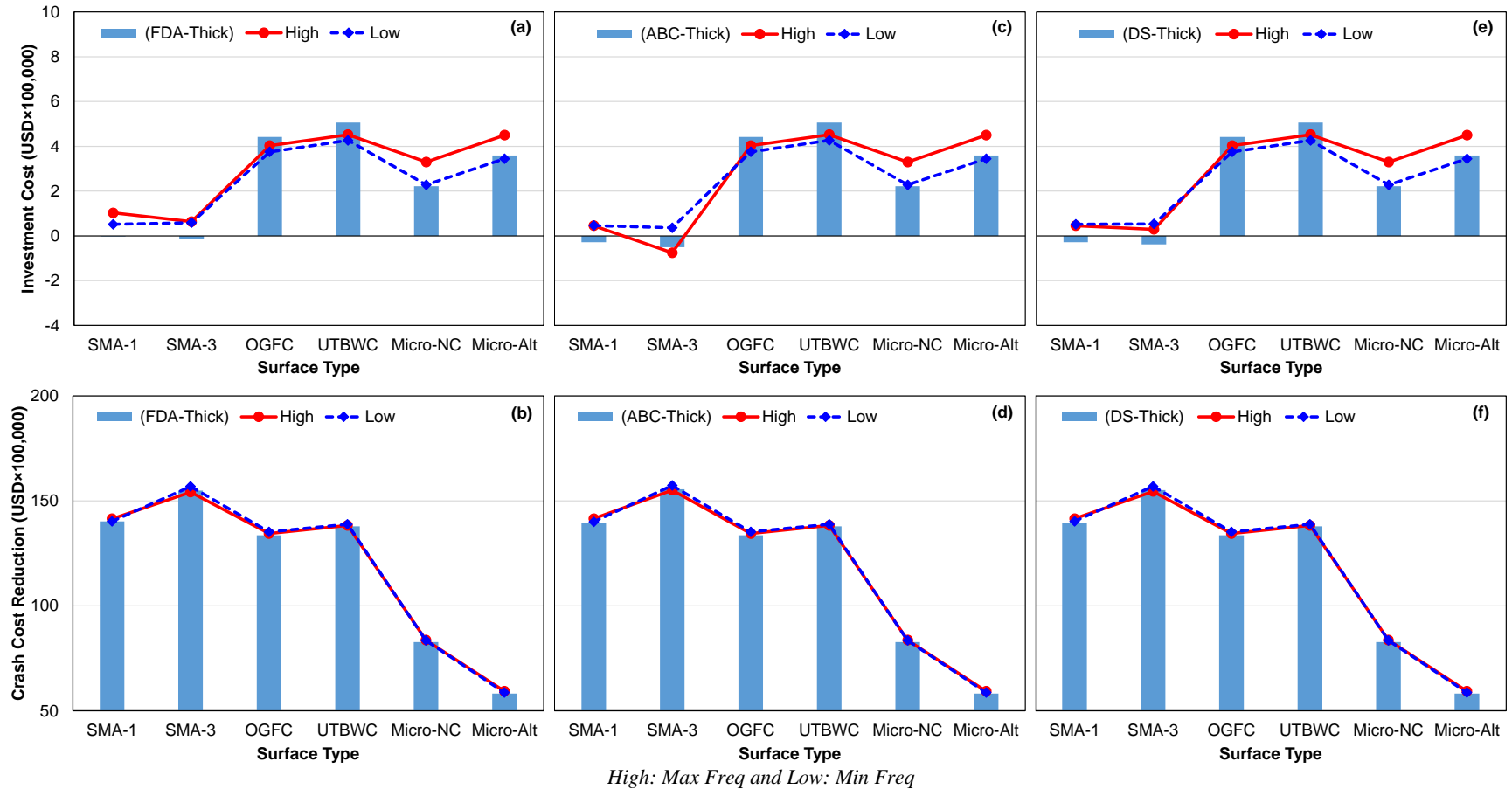
Intermediate Structures



High: Max Freq and Low: Min Freq

Figure H-10. FDA Intermediate: (a) investment and (b) crash cost reduction. ABC Intermediate: (c) investment and (d) crash cost reduction. DS Intermediate: (e) investment and (f) crash cost reduction.

Thick Structures



High: Max Freq and Low: Min Freq

Figure H-11. FDA Thick: (a) investment and (b) crash cost reduction. ABC Thick: (c) investment and (d) crash cost reduction. DS Thick: (e) investment and (f) crash cost reduction.

Investment and Crash Cost Reduction (7% Interest Rate)

Thin Structures

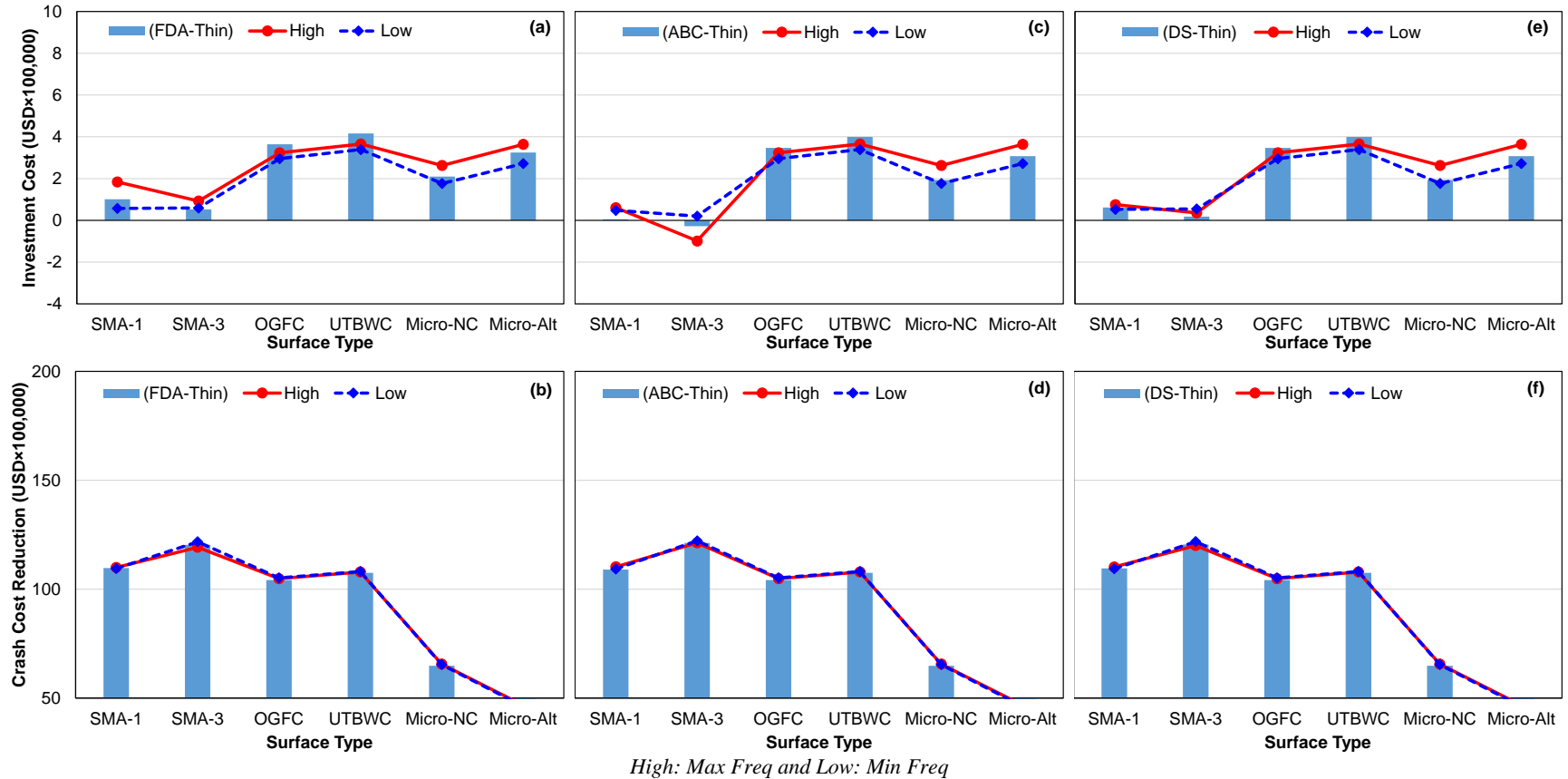


Figure H-12. FDA Thin: (a) investment and (b) crash cost reduction. ABC Thin: (c) investment and (d) crash cost reduction. DS Thin: (e) investment and (f) crash cost reduction.

Intermediate Structures

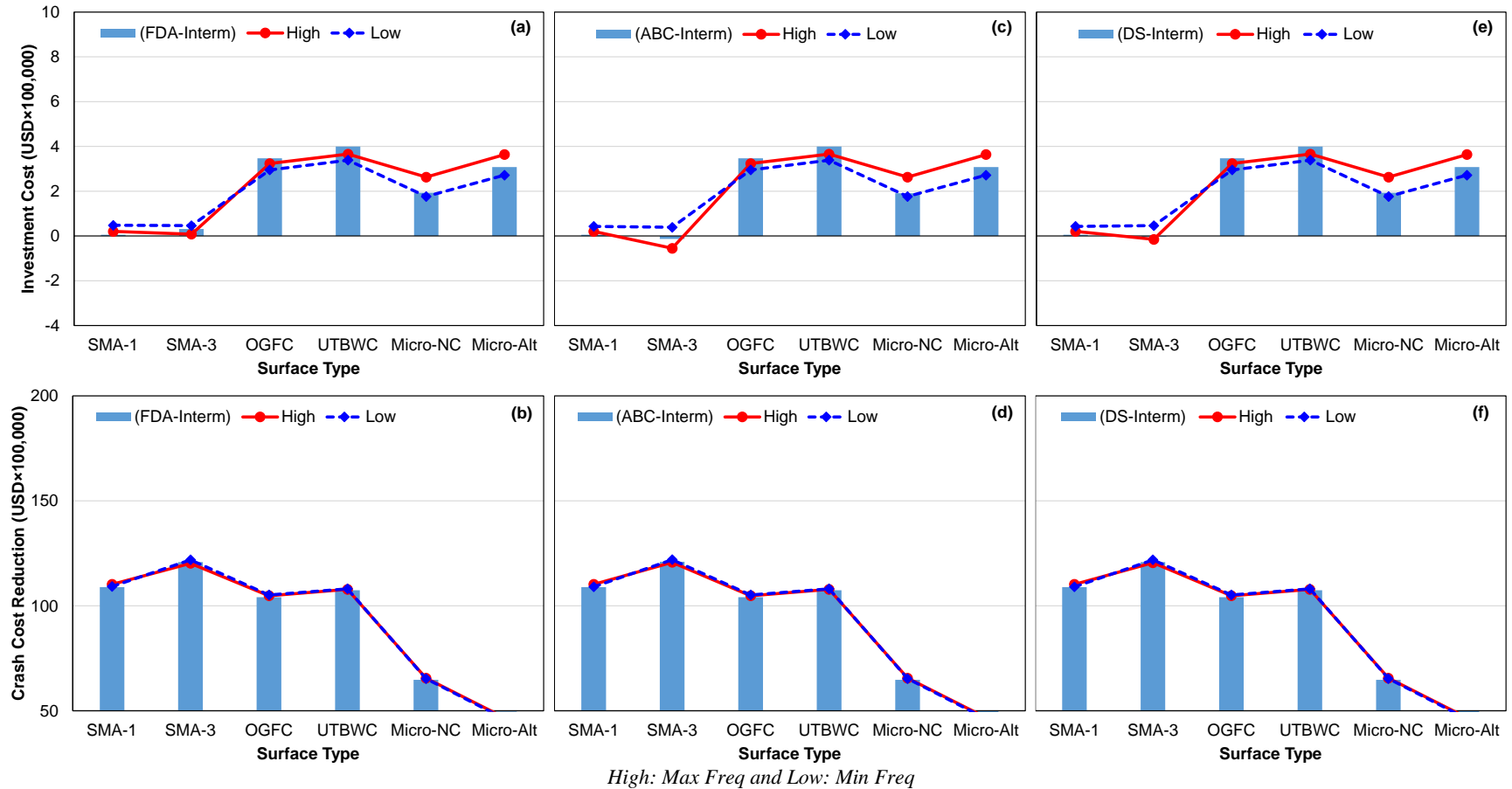


Figure H-13. FDA Intermediate: (a) investment and (b) crash cost reduction. ABC Intermediate: (c) investment and (d) crash cost reduction. DS Intermediate: (e) investment and (f) crash cost reduction.

Thick Structures

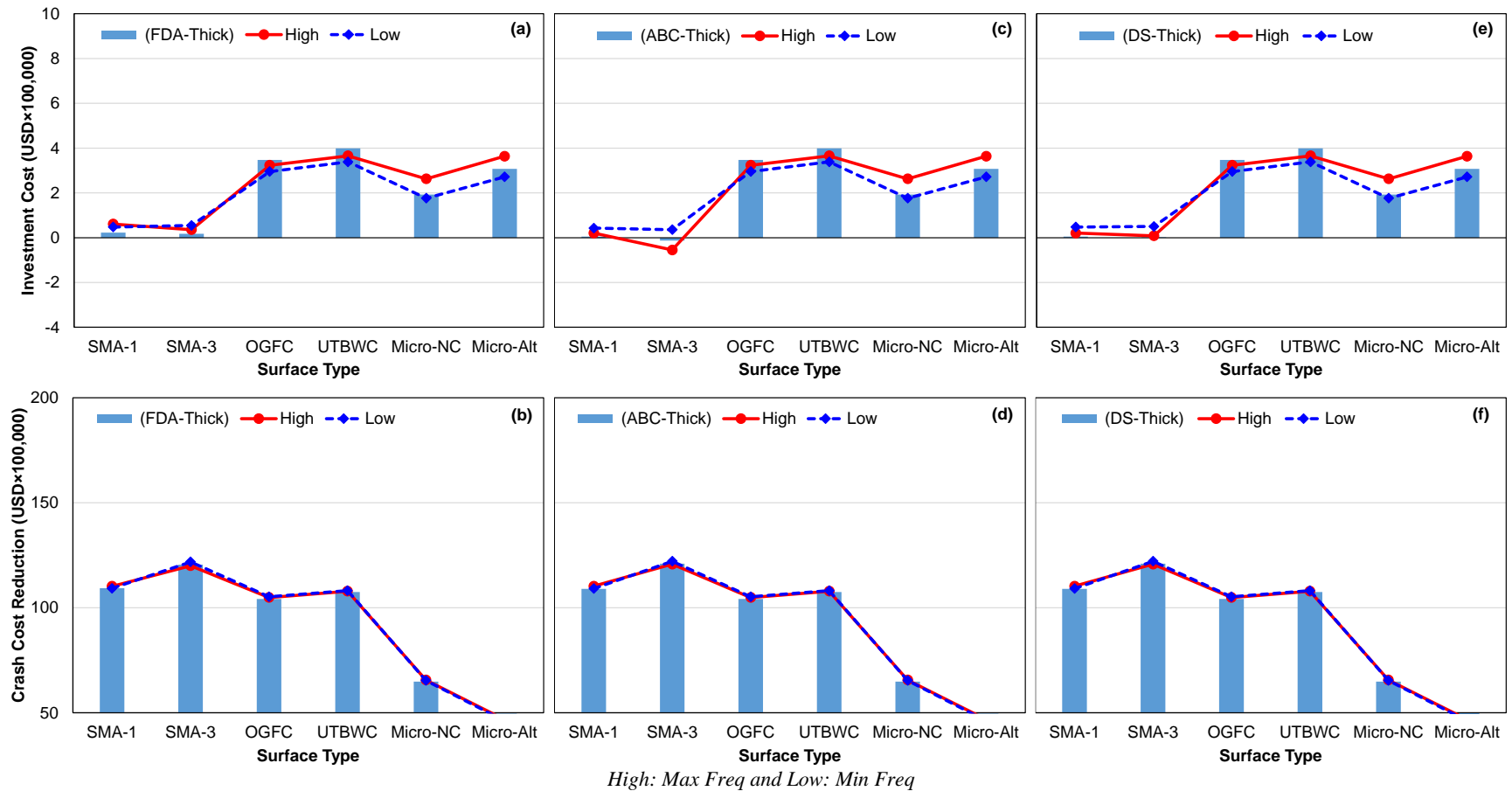


Figure H-14. FDA Thick: (a) investment and (b) crash cost reduction. ABC Thick: (c) investment and (d) crash cost reduction. DS Thick: (e) investment and (f) crash cost reduction.